

**ACOUSTIC EMISSION ANALYSIS OF  
FIBER COMPOSITE FAILURE MECHANISMS**

**Dennis Michael Egan**

Volume 1

DUDLEY ROCK LIBRARY  
NAVAL POSTGRADUATE SCHOOL



ACOUSTIC EMISSION ANALYSIS OF  
FIBER COMPOSITE FAILURE MECHANISMS

by

DENNIS MICHAEL EGAN, LT, USCG  
B.S., United States Coast Guard Academy (1972)

[v.i.]

SUBMITTED IN PARTIAL FULFILLMENT  
OF THE REQUIREMENTS FOR THE  
DEGREES OF

MASTER OF SCIENCE IN MECHANICAL ENGINEERING

and

OCEAN ENGINEER

at the

MASSACHUSETTS INSTITUTE OF TECHNOLOGY

(May 1977)





ACOUSTIC EMISSION ANALYSIS OF  
FIBER COMPOSITE FAILURE MECHANISMS

by

DENNIS MICHAEL EGAN, LT, USCG

Submitted to the Department of Mechanical Engineering and the Department of Ocean Engineering on 13 May 1977 in partial fulfillment of the requirements for the Degrees of Master of Science in Mechanical Engineering and Ocean Engineer, respectively.

i. ABSTRACT

Fracture mechanisms of graphite-polyimide composite material are studied with acoustic emission (AE). Selected for study are four different fiber composite configurations, exhibiting specific predominant fracture mechanisms, as verified under scanning electron microscope. AE counts, AE-RMS, and load versus time are presented from specimen tensile tests.

A wide band (125 kHz - 2 MHz) AE recording system is used to facilitate the spectral analysis of individual AE events. Data analysis techniques are developed which allow for statistical comparison of the similarities between groups of AE spectral energy distributions arising from specimens having different predominant AE generation mechanisms.

Unique group spectral energy distribution characteristics are distinguished in the  $90^\circ$ ,  $10^\circ$  and  $(\pm 45^\circ, \pm 45^\circ)_s$  specimens using the paired-sample t

# ACQUISITION AGREEMENT BETWEEN THE UNIVERSITY OF BRISTOL AND THE BRITISH LIBRARY

THIS AGREEMENT IS MADE THIS 10th DAY OF

1964, between the University of Bristol, hereinafter referred to as the University, and the British Library, hereinafter referred to as the Library, for the purpose of providing for the acquisition of books and other material for the Library by the University.

## 1. DEFINITIONS

In this Agreement the following definitions shall apply:—  
"Acquisition" means the purchase or the acceptance of a book or other material for the Library by the University;  
"Book" means any printed matter, whether in the form of a book, pamphlet, leaflet, or otherwise, and includes any map, chart, or other printed matter;  
"Other material" means any material, whether in the form of a manuscript, drawing, or otherwise, and includes any photograph, film, or other material;  
"University" means the University of Bristol;  
"Library" means the British Library.

2. The University shall acquire for the Library all books and other material which are published in the United Kingdom or in any other country, and which are not already in the collection of the Library, and which are of such a nature as to be of value to the Library for its purposes.  
3. The University shall acquire for the Library all books and other material which are published in the United Kingdom or in any other country, and which are not already in the collection of the Library, and which are of such a nature as to be of value to the Library for its purposes.

4. The University shall acquire for the Library all books and other material which are published in the United Kingdom or in any other country, and which are not already in the collection of the Library, and which are of such a nature as to be of value to the Library for its purposes.



statistical test. However, no unique AE spectral energy distribution characteristics are identified in  $0^\circ$  specimens. Total AE energy and AE spectral energy distribution appear to be dependent upon specimen load.

AE event duration is established as a distinguishing characteristic between AE of  $0^\circ$  and  $10^\circ$  specimens versus AE of  $(\pm 45^\circ, \pm 45^\circ)_s$  and  $90^\circ$  specimens.

AE irreversibility or shakedown with respect to load is observed to generally predominate for unflawed specimens. However, AE irreversibility seems to be violated once an active fatigue crack is generated in the specimen during load cycling.

More rigorous statistical characterization of AE from predominant fracture mechanisms is recommended along with a detailed study of AE dispersion and attenuation properties of the composite material. Finally, it is recommended that AE mean energy-stress constitutive relationships be developed.

Thesis Supervisor: James H. Williams, Jr.  
Title: Associate Professor of Mechanical Engineering





## ii. Table of Contents

	<u>Page</u>
i     Abstract . . . . .	2
ii    Table of Contents . . . . .	4
iii   List of Figures . . . . .	8
iv    List of Tables . . . . .	11
v     Acknowledgements . . . . .	12
I.    Introduction . . . . .	13
A. Background . . . . .	13
1. Definitions . . . . .	13
a. Acoustic Emission (AE) . . . . .	13
b. Fiber Reinforced Composites . . . . .	13
2. AE Applications to Fiber Reinforced Composites . . . . .	14
a. Previous Work . . . . .	14
b. Quantitative Evaluation of Failure Mechanisms With AE . . . . .	16
(1) State of the Art Limitations . . . . .	16
(2) Promising Techniques . . . . .	17
(a) Amplitude Distribution . . . . .	17
(b) Spectral Analysis . . . . .	17
3. Predominant Failure Mechanisms of Fiber Reinforced Composites . . . . .	19
a. General Categorization . . . . .	19
b. Specimen Selections for Failure Mechanism Studies . . . . .	19
(1) 0° Specimen Failure Mechanisms . . . . .	20
(2) 10° Specimen Failure Mechanisms . . . . .	21





## Table of Contents (cont.)

	<u>Page</u>
(3) $(\pm 45^{\circ}, \pm 45^{\circ})_s$ Specimen Failure Mechanisms . . .	21
(4) $90^{\circ}$ Specimen Failure Mechanisms	22
c. Random Characteristics of AE and Statistical Approaches for its Analysis . . .	23
B. Objective of This Work . . . . .	24
II. Discussion . . . . .	25
A. Specimens . . . . .	25
1. Types Selected . . . . .	25
2. Material . . . . .	25
3. Fabrication of Specimens . . . . .	25
4. Specimen Dimensions . . . . .	26
B. Test Equipment and Instrumentation . . . . .	26
C. Test Procedure . . . . .	27
D. Data Analysis Procedure . . . . .	28
1. SEM Evaluation of Fracture Tips . . . . .	28
2. AE Counts, AE-RMS, and Load . . . . .	28
3. Spectral Analysis . . . . .	29
a. AE Just Prior to Specimen Rupture . . . . .	29
b. AE Spectra at Various Loads . . . . .	29
c. Spectral Analysis Procedures . . . . .	29
4. Calculations . . . . .	31
a. Computer Processing and Spectral Density Normalization . . . . .	31



## Table of Contents (cont.)

	<u>Page</u>
b. Calculation of AE Spectral Energy AE Pressure and Normalized Spectral Energy Distribution . . . . .	31
5. Paired-Sample t Statistical Test . . . . .	33
6. AE Shakedown . . . . .	34
III. Results . . . . .	35
A. SEM Results . . . . .	35
B. Time Domain Characteristics of AE . . . . .	36
C. Load, AE Counts, and AE-RMS . . . . .	37
D. Total Spectral Energy per AE and AE Pressure (RMS) Excitation of Transducer . . . . .	38
E. Normalized Spectral Energy Distributions . . . . .	39
1. Individual Spectral Distributions for Each AE Event . . . . .	39
2. Mean Normalized Spectral Energy Distribution . . . . .	40
F. Paired-Sample t Statistic Results . . . . .	42
G. AE Spectra at Various Loads . . . . .	43
H. Observations Concerning AE Shakedown . . . . .	43
IV. Conclusions . . . . .	45
V. Recommendations . . . . .	49
VI. References . . . . .	51
VII. Figures and Tables . . . . .	53
VIII. Appendices . . . . .	105
A. Techniques of Monitoring Acoustic Emission . . . . .	105
B. Computer Program . . . . .	112





## Table of Contents (cont.)

	<u>Page</u>
C. Tabulation of AE Spectral Energy, AE Pressure (RMS) Excitation of the Transducer, and Presentation of Normalized Spectral Energy Distributions for Each AE Event . . . . .	120
D. Paired-Sample t Statistic . . . . .	436
E. AE Spectral Energy, AE Pressure, and Normalized AE Energy Distributions from ( $\pm 45^\circ$ , $\pm 45^\circ$ ) <sub>g</sub> Specimens at Various Ascending Loads . . . . .	446
F. Notes on Operational Procedure for Tests and Data Analysis . . . . .	497





### iii. List of Figures

<u>Figure</u>		<u>Page</u>
1	Insulated Grips, Specimen, and Transducer Attachment. . . . .	54
2	Transducer Response Curve . . . . .	55
3	Transducer Leads and Preamplifier Shielded Against EMI with Aluminum Foil. . . . .	56
4	Test Instrumentation. . . . .	56
5	Typical Fracture Modes of the Four Specimen Types . . . . .	57
6	0° Fracture Surface . . . . .	58
7	Fracture Surfaces of 10° Specimens 180 X . . . .	59
8	Fracture Surfaces of 10° Specimens 1000 X . . . .	59
9	Fracture Surfaces of 90° Specimens Under SEM (300 X and 3000 X). . . . .	60
10	Fracture Surface of ( $\pm 45^\circ$ , $\pm 45^\circ$ ) <sub>s</sub> Specimen. . .	61
11	Typical AE (Ungated) from 0° Specimens. . . . .	62
12	Typical AE (Gated) from 0° Specimens. . . . .	62
13	Typical AE (Gated) from 10° Specimens . . . . .	62
14	Typical AE (Gated) from 10° Specimens . . . . .	62
15	Typical AE (Ungated) from 90° Specimens . . . . .	63
16	Typical AE (Ungated) from 90° Specimens . . . . .	63
17	Typical AE (Gated) from ( $\pm 45^\circ$ , $\pm 45^\circ$ ) <sub>s</sub> Specimens . . . . .	63
18	Load, AE Counts and AE-RMS vs Time: Specimen LV1B . . . . .	65
19	Load, AE Counts and AE-RMS vs Time: Specimen LV4A . . . . .	66



# List of Figures (cont.)

<u>Figure</u>		<u>Page</u>
20	Load, AE Counts and AE-RMS vs Time: Specimen LV4C . . . . .	67
21	Load, AE Counts and AE-RMS vs Time: Specimen LV2B . . . . .	68
22	Load, AE Counts and AE-RMS vs Time: Specimen LV2C . . . . .	69
23	Load, AE Counts and AE-RMS vs Time: Specimen LV2G . . . . .	70
24	Load, AE Counts and AE-RMS vs Time: Specimen LV2H . . . . .	71
25	Load, AE Counts and AE-RMS vs Time: Specimen LV5C . . . . .	72
26	Load, AE Counts and AE-RMS vs Time: Specimen LV5D . . . . .	73
27	Load, AE Counts and AE-RMS vs Time: Specimen LV5G . . . . .	74
28	Load, AE Counts and AE-RMS vs Time: Specimen LV5H . . . . .	75
29	Load, AE Counts and AE-RMS vs Time: Specimen LV5CA . . . . .	76
30	Load, AE Counts and AE-RMS vs Time: Specimen LV5CG . . . . .	77
31	Load, AE Counts and AE-RMS vs Time: Specimen LV5CI . . . . .	78
32	Load, AE Counts and AE-RMS vs Time: Specimen LV5CJ . . . . .	79



## List of Figures (cont.)

<u>Figure</u>		<u>Page</u>
33	Mean Normalized Spectral Energy Distribution LV2B . . . . .	81
34	Mean Normalized Spectral Energy Distribution LV2C . . . . .	82
35	Mean Normalized Spectral Energy Distribution LV2G . . . . .	83
36	Mean Normalized Spectral Energy Distribution LV2H . . . . .	84
37	Mean Normalized Spectral Energy Distribution LV1B . . . . .	85
38	Mean Normalized Spectral Energy Distribution LV4A . . . . .	86
39	Mean Normalized Spectral Energy Distribution LV4C . . . . .	87
40	Mean Normalized Spectral Energy Distribution LV5C . . . . .	88
41	Mean Normalized Spectral Energy Distribution LV5D . . . . .	89
42	Mean Normalized Spectral Energy Distribution LV5G . . . . .	90
43	Mean Normalized Spectral Energy Distribution LV5H . . . . .	91
44	Mean Normalized Spectral Energy Distribution LV5CA . . . . .	92
45	Mean Normalized Spectral Energy Distribution LV5CG . . . . .	93
46	Mean Normalized Spectral Energy Distribution LV5CI . . . . .	94
47	Mean Normalized Spectral Energy Distribution LV5CJ . . . . .	95





#### iv. List of Tables

<u>Table</u>		<u>Page</u>
1	Expected Failure Modes of Specimens . . . . .	96
2	Specimen Identification . . . . .	97
3	Specimen Dimensions . . . . .	98
4	Test Summary: AE Counts . . . . .	99
5	Summary of Mean and Standard Deviation of Failure Loads . . . . .	100
6	Material Parameters . . . . .	101
7	Test Summary: Spectral Analysis . . . . .	103
8	Summary of Paired-Sample t Statistics . . . . .	104
9	Rejection Table for Paired-Sample t Test . . .	442
10	Paired-Sample t Statistic Values for Specimen Pair Comparisons . . . . .	443



## v. Acknowledgements

My personal thanks go to the following people:

- A. The U. S. Coast Guard for allowing my study under active duty at M.I.T.
- B. Professor James H. Williams, Jr. for his guidance and financial support of this thesis.
- C. Mr. Alex Vary of the NASA Lewis Research Center in Cleveland, Ohio for providing the test specimens, material parameters, and specimen grips.
- D. My wife, Margaret, and son, JME, for much support and understanding.
- E. The students of Course 2.30 including:  
Bill Burger, John Stahr, Paul Malchedi, Paola Fano,  
and David Leslie who helped to establish spectral analysis procedures; Angela Chaney for conventional microscope studies; and Cameron Moss, Richard Dana, Michael Gifford, Craig Selvage, Jon Kaplan, and Emeka Okoli for excellent photographic studies with the scanning electron microscope.





## I. INTRODUCTION

### A. Background

#### 1. Definitions

##### a. Acoustic Emission (AE)

"Acoustic emission" (AE) means vibrational energy released from the incremental deterioration of materials subjected to stress. This phenomenon has been seriously studied in materials for the last thirty years. AE has been used successfully to nondestructively test many materials, ranging from metals to nylon rope. It has been applied both as an early warning system of catastrophic failure and as a laboratory tool to study basic material fracture mechanisms. Some of the techniques of monitoring acoustic emission are described in Appendix A.

##### b. Fiber Reinforced Composites

Fiber reinforced composites are generally man-made materials consisting of relatively stiff fibers embedded in a more compliant matrix. The application of such materials is not really new. For instance, papyrus reeds in a pitch matrix were used for small boat construction on the Nile River earlier than 3,000 B.C. Recently, through the combination of graphite or glass fibers with epoxy or polyimide resins, technology has produced new materials having strength to weight ratios over three times that of many structural steels. Consequently there are potentially



many advantages which can be gained by using these new materials in pressure vessels, high performance aircraft, and watercraft.

## 2. AE Applications to Fiber Reinforced Composites

### a. Previous Work

Like many other materials, fiber reinforced composites generally emit sonic and ultrasonic vibrations as they incrementally deteriorate when subjected to stress. The first commercial use of acoustic emission was by Aerojet General Corporation in 1962 (1). They applied it to fiber composite Polaris missile chambers as a safety device to warn of premature failure during hydrostatic proof testing. From 1962 to 1970, little work was done to further qualify acoustic emission applications for composite materials.

AE has been specifically used to study fiber composite failure mechanisms since 1971. Rathbun et al. (2) tested standard tensile specimens, each made of clear epoxy containing a single strand of glass fibers down the center, parallel to the loading axis. Large AE bursts were detected and correlated with the visible appearance of fiber fractures. They observed "cone shaped" fissures in the epoxy resin in the immediate vicinity of the contracted broken fiber tips. Tensile tests of homogeneous epoxy specimens produced no AE which could be detected by their instrumentation. They conducted additional experiments





with glass fiber reinforced spherical pressure vessels, mounting a pair of transducers for AE source location. Their results suggested a significant correlation between the number of AE events occurring in a region and the number of broken strands in that region. However, they found no definite indication in the AE pattern which would allow for a prediction of the burst pressure of a spherical vessel.

Liptai (3) investigated tensile failures of filament wound rings with AE and concluded that a cumulative damage fracture mode governed failure of such material.

Rothwell and Arrington (4) used compression samples composed of a transparent epoxy matrix containing a single carbon fiber aligned parallel to the loading axis. Compression caused the fiber to debond from the epoxy causing a visually detectable defect and releasing AE detectable by their AE counter. Their studies identified two different types of AE patterns. If a debond area initially existed in a specimen, AE count rate would gradually increase with increasing load on the specimen. Undamaged specimens, on the other hand, exhibited suddenly large increases in counts (as a completely bonded specimen would suddenly debond at a certain load). They emphasized, however, that their AE monitoring system could not discriminate between debonding, matrix or fiber fracture mechanisms.



Using amplitude discrimination techniques, Swanson and Hancock (5) correlated one AE count to each filament fracture in boron fiber reinforced aluminum.

Mehan and Mullin (6) attempted to distinguish between AE characteristics of fiber fracture and those of fiber debonding. They suggested that debonding was a much more "gradual" event, resulting in a lower energy AE.

Balderston (7) concluded from tests on notched boron fiber reinforced epoxy specimens that resin failure was characterized by AE bursts of much lower energy content than those arising from fiber failure.

Most of the studies mentioned so far largely reported results of a qualitative nature and, with the possible exception of fiber fracture detection and location, were not too successful in characterizing specific failure mechanisms with AE.

## b. Quantitative Evaluation of Failure Mechanisms with AE

### (1) State of the Art Limitations

Guild and Walton et al. (8) stated that acoustic emission in fiber composites can be broadly related to material degradation but that quantitative relationships rely to a large extent upon successful failure mode identification. These quantitative efforts to further characterize the nature of AE source mechanisms have not been accomplished. This is unfortunate because fiber composite materials usually have several failure





mechanisms, some critical to structural strength and others which are not critical. Since all of these mechanisms are potential AE sources, the development of AE techniques with the capability to distinguish and discriminate between the failure mechanisms becomes imperative. Today there is a flurry of research activity directed towards achieving these ends.

## (2) Promising Techniques

Two of the more promising techniques seem to be amplitude distribution and spectral analysis.

### (a) Amplitude Distribution

Amplitude distribution is the study of the relative population of AE peaks in the time domain. A good discussion of this technique is given by Ono in (9).

### (b) Spectral Analysis

Spectral analysis is the study of the distribution of AE energy in the frequency domain. Carlyle (10) indicated that the energy contained in an AE is a function of the duration and extent of the deformation causing the AE. He stated that the total energy of an AE is directly dependent upon the magnitude of its source deformation mechanism. The AE energy, he stated, is carried in a frequency spectrum which extends up to a frequency which is inversely proportional to the duration



of the source event.

Mehan and Mullin (6) broadly characterized AE spectra from graphite epoxy as having predominant energy below 20 kHz with "different" spectral signatures for different failure mechanisms. They claimed that different AE spectral signatures resulted from fiber fracture, matrix fracture and debonding in boron epoxy composites. Unfortunately, their AE system was of only limited bandwidth capability and operated at frequencies also dominated by natural resonances of the specimens. This may have affected their results.

Pipes et al. (11) reported that the observed spectral content of the AE from boron aluminum composite specimens, which deformed primarily in transverse tension, was unaffected when detected with either of two different transducers, one with a 0.1 - 0.3 MHz band pass filter and the other with a 0.1 MHz high pass filter. Other specimens, which deformed with large in-plane shear, produced quite different spectra of reduced amplitude for the same transducer-filter substitution. These results might be construed to imply that AE due to transverse tension deformation contained substantial spectral energy in the bandwidth 0.1 - 0.3 MHz. AE from in-plane shear deformation mechanisms might have contained significant spectral energy at frequencies outside of the AE system's bandwidth (assuming that the spectral responses



of the two attached transducers were approximately the same).

Speake and Curtis (12) attempted to correlate the spectral content of AE with the fracture modes in graphite epoxy tensile and torsion specimens. Their results were rather qualitative in nature but suggested that fiber breakage mechanisms exhibited spectral energy of significantly lower frequency than matrix cracking mechanisms. They reported that emission spectra were also dependent upon material type, test piece geometry and transducer mounting.

### 3. Predominant Failure Mechanisms of Fiber Reinforced Composites

#### a. General Categorization

Before a successful AE characterization of fiber composite failure mechanisms can be accomplished, it is necessary to establish the expected mechanisms of failure for specific types of specimens. Fiber composite failure mechanisms may be broadly categorized as fiber breakage, tensile failure of the matrix, shear failure of the matrix, delamination between plies, and interface failure between fibers and matrix (such as fiber pullout).

#### b. Specimen Selections for Failure Mechanism Studies

The study of failure mechanisms can be facilitated by





the selection of specimens in which only one to two such mechanisms predominate. Potential specimens for study are unidirectional  $0^\circ$ , unidirectional  $10^\circ$ , unidirectional  $90^\circ$ , and  $(\pm 45^\circ, \pm 45^\circ)_S$ .

#### (1) $0^\circ$ Specimen Failure Mechanisms

$0^\circ$  specimens generally exhibit two predominant failure mechanisms. Rollings (13) studied radiographs of  $0^\circ$  boron aluminum fatigue specimens which had been unloaded just prior to specimen failure (as predicted by a suddenly increasing acoustic emission rate). He observed that many shear cracks had propagated parallel to the filaments prior to specimen rupture. In other specimens loaded to failure he observed multiple fractures of fibers over a very limited length near the crack tip. He believed this to be evidence of a "crazing" failure mechanism.

Berg and Rinsky (14) examined high speed photographs of  $0^\circ$  graphite epoxy specimens. Their results suggested that after one main crack propagated across the fibers near the testing machine grips, longitudinal cracks visibly opened between the fibers and propagated towards the main crack from nucleation sites near the specimen's center. All of their  $0^\circ$  specimens shattered with both longitudinal and transverse fracture surfaces. They proposed that these longitudinal cracks resulted from reverberation of the specimen whereby internal stress wave reflections



created local sites of high transfibrile tension. They also proposed that critical failure in each of the  $0^\circ$  specimens nucleated with the rupture of a small bundle of fibers at or near the edge of the specimen. References (13) and (14) disagree on the order of occurrence of the two fracture mechanisms in  $0^\circ$  specimens. However, they both recognize the presence of both a longitudinal cracking mechanism between fibers and a transverse cracking mechanism across the fibers. Both also specify that it is the transverse fiber breakage mechanism which is critical in  $0^\circ$  specimens.

## (2) $10^\circ$ Specimen Failure Mechanisms

$10^\circ$  specimens exhibit only one predominant failure mechanism, intralaminar shear between fibers along the  $10^\circ$  direction. Chamis (15) gives a good discussion of the stress distribution which leads to this characteristic shear failure in  $10^\circ$  unidirectional fiber composites.

## (3) $(\pm 45^\circ, \pm 45^\circ)_S$ Specimen Failure Mechanisms

$(\pm 45^\circ, \pm 45^\circ)_S$  specimens exhibit several failure mechanisms. Rotem and Hashin (16) reported that the stress-strain curves from such specimens show a plateau of steadily increasing strain under constant stress, similar to plastic yield behavior in ductile materials. They observed that the onset of failure in such specimens





is not due to interlaminar shear, but to lamina cracking, starting just before the plateau on the stress-strain curve. Cracking occurs progressively between fibers at various locations, criss-crossing the whole specimen. The number of cracks increases with continued elongation of the specimen. In the latter stages of failure, interlaminar yielding begins, causing bundles of fibers to move and change orientation with the loading axis prior to specimen failure.

Chang et al. (17) studied failure mechanisms in notched  $(\pm 45^\circ, \pm 45^\circ)_S$  graphite epoxy specimens with a modified X-ray visualization technique. Their observations of incremental damage occurring at the crack tips during ramp loading tensile tests suggested that matrix failures occurred prior to delamination between plies. After delamination started, the failure process accelerated until total specimen rupture occurred.

Both (16) and (17) agree that failure in a  $(\pm 45^\circ, \pm 45^\circ)_S$  specimen is precluded by the nucleation of cracks between fibers and is culminated by final delamination between plies.

#### (4) 90° Specimen Failure Mechanisms

90° specimens fail in the matrix along the direction of the fibers. All reports seem to have concurred that this is due to tensile failure of the matrix and occurs in



a very localized band of the specimen. Liptai (3) suggested the existence of a fatigue mechanism in glass/resin systems whereby small cracks initiate and propagate in the resin phase, where high localized stress concentrations produce small "decohesive" failures. It might be envisioned that the joining up of these smaller cracks into larger cracks of critical length result in specimen failure in the matrix between fibers.

Table 1 summarizes the expected failure modes for  $0^\circ$ ,  $10^\circ$ ,  $(\pm 45^\circ, \pm 45^\circ)_s$ , and  $90^\circ$  specimens, respectively.

c. Random Characteristics of AE and Statistical Approaches for its Analysis

It should be noted that even though a particular specimen type may exhibit a predominant fracture mechanism, there is no guarantee that the vibrational energy released during each incremental fracture will have identical characteristics. Thus it is extremely unlikely that a direct comparison between a single AE event and another AE event will allow for discrimination of fracture mechanisms. However, if a group of such AE events is treated as random data and statistically analyzed, unique group properties may become apparent which allow for the characterization of individual fracture mechanisms.

Amplitude distribution, mentioned previously, uses a statistical approach to characterize group properties of



acoustic emissions. However, statistical approaches have not been used in most spectral analysis studies of AE.

#### B. Objective of This Work

The objective of this work is to study the AE characteristics of graphite fiber reinforced composite specimens that exhibit predominant mechanisms of failure. An attempt is made to establish an AE signature unique to each type of specimen. Primary emphasis is placed on establishing experimental and statistical analysis procedures for obtaining quantitative distinction between the AE spectral energy distributions of specimens exhibiting different predominant failure mechanisms.





## II. DISCUSSION

### A. Specimens

#### 1. Types Selected

Four specimen types were selected for study. They were (as measured relative to the loading axis)  $0^{\circ}$ ,  $10^{\circ}$ , and  $90^{\circ}$  unidirectional and  $(\pm 45^{\circ}, \pm 45^{\circ})_S$  specimens.

#### 2. Material

The specimens were cut from laminates made of AS-1 graphite fiber (Hercules) in a polyimide, PR-288, neat resin (3M). The  $(\pm 45^{\circ}, \pm 45^{\circ})_S$  specimens were cut from a single panel. A portion of this panel was sprayed during layup between its fourth and fifth plies with polyvinyl alcohol, a delaminating agent.

#### 3. Fabrication of Specimens

All panels were die molded and held for two hours under a pressure of 2.17 MPa and a temperature of  $177^{\circ}$  C. The finished laminates were found to be acceptable under both C-scan and amplitude scan ultrasonic examination. Each laminate was cut into a number of specimens using a water cooled diamond wheel. Aluminum tabs were bonded to the ends of each specimen. These tabs were tapered to minimize stress concentrations at the tab-specimen interfaces. Each specimen's tab was inscribed with a particular identification number (see Table 2). Special grips were



fabricated for the specimens. These were bolted onto each of the end tabs and insulated with electrical tape (see Figure 1).

#### 4. Specimen Dimensions

The dimensions for each specimen are given in Table 3.

#### B. Test Equipment and Instrumentation

An EC-500 (Acoustic Emission Technology, Inc. (AET)) wide band transducer, having an exceptionally flat response curve (see Figure 2) over the frequencies 125 kHz to 2 MHz, was used. The transducer's sensitivity over this frequency range was approximately 30.0 microvolts/Pa. The transducer was held onto the specimen with two rubber bands (B.F. Goodrich #12) and coupled with AET-SC6 viscous resin (except as noted in Table 4). The transducer's output was impedance buffered, amplified by 60 dB, and frequency filtered (bandpass) between 125 kHz and 2 MHz (see Figure 3). (Note: The filter had 24 dB/octave roll-off on either side of the passband.) A signal processor (AET Model 201) provided an additional 40 dB amplification, counted the number of signal uncrossings above a pre-set voltage threshold, and measured the root mean square (RMS) of the signal voltage, averaged over 55 msec intervals. (See Appendix A for more details.) The outputs of AE counts and AE-RMS were





recorded on an X-Y recorder (Hewlett Packard Model 7046 A). Amplified AE signals were output from the signal processor to a video tape recorder (AET modified Sony AV-3650) which exhibited a flat reproduction response between 100 kHz and 2 MHz. A spectral analyzer (Hewlett Packard Model 8557 A) was used to monitor the system's background noise.

An Instron tensile testing machine was used to pull the specimens apart. Load versus time was recorded on the audio channel of the video tape recorder and indicated on the Instron machine's chart recorder. The test instrumentation is displayed in Figure 4.

### C. Test Procedure

Detailed experimental procedural notes are presented in Appendix F. Particular care was taken to eliminate electromagnetic interference (EMI) by electrically grounding both specimen and transducer to the AE system's common ground. As previously mentioned, the specimen's grips and loading pins were also electrically insulated from the Instron testing machine. To further reduce EMI, the transducer's leads to the preamplifier, and the preamplifier, itself, were carefully wrapped in aluminum foil (see Figure 3). The specimens were carefully aligned in the Instron machine's loading fixture. This loading fixture was equipped with a universal joint and was also free to rotate in the horizontal plane.



The specimens were extended at a uniform rate of 0.508 mm/min (except as noted in Table 4). Several specimens of each type were ramp loaded to failure in tension while AE was detected, processed, and recorded. Other specimens of each type were loaded, unloaded, and reloaded to allow for the monitoring and study of any AE shakedown behavior which might be displayed. After the specimens had been extended to failure, their fracture surfaces were carefully retained for later examination with the scanning electron microscope (SEM).

#### D. Data Analysis Procedure

##### 1. (SEM) Evaluation of Fracture Tips

The fracture surfaces from various specimen types were examined under SEM. Particular attention was paid towards establishing the specimens' predominant fracture mechanisms and observing any characteristics which might be unique to fractured surfaces from specific types of specimen failure.

##### 2. AE Counts, AE-RMS and Load

AE counts, AE-RMS and load were all normalized with respect to each parameter's maximum value which occurred during the test. This type of presentation facilitated identification of data trends.



### 3. Spectral Analysis

#### a. AE Just Prior to Specimen Rupture

AE generated just prior to each specimen's rupture were spectrally analyzed in an attempt to identify the "spectral signatures" of each of the specimen's critical predominant failure mechanisms.

#### b. AE Spectra at Various Loads

AE from  $(\pm 45^\circ, \pm 45^\circ)_s$  specimens at various loads were also spectrally analyzed, seeking to establish some preliminary evidence of spectral energy distribution trends which might be related to the specimen's load.

#### c. Spectral Analysis Procedures

The taped records of the AE were replayed on the video tape recorder. This recorder offered the facility to slowly scan the test record and locate an individual AE event. The recorder could then be set in a "stop action" mode, replaying the same AE signal sixty times per second. This resulted in an effective transformation of a transient event into a periodic signal. This periodic signal was multiplied by a synchronized time gate. The time gate could be adjusted in width so that it only permitted the signal to pass during the AE event. It is important to note that any AE event was actually superposed upon the system's background noise, similar to





that which existed just prior to the AE event. (see Appendix A for more details)

The resulting signal was input to the spectral analyzer. The spectral analyzer was operated between the frequencies 125 kHz to 2 MHz (swept at 20kHz/sec), with a maximum resolution of 10 kHz. After it became apparent that there was little spectral energy present above 1 MHz, only spectral densities between 125 kHz and 1MHz were recorded. One half of a two sided spectral density was plotted on the X-Y recorder. First the spectral density of the AE signal superposed on background noise was plotted. Then the time gate was adjusted to input an equal time sampling of only the background noise which was present just prior to the AE event. (It was recognized that there was no guarantee that the background noise preceding an AE event was identical to the background noise occurring during the AE event. However, this noise sample was assumed to be a fair estimate of the energy of the background noise which was present during the AE event.) This sample of background noise was input to the spectral analyzer. The spectral density plot of the background noise was then reproduced on the X-Y recorder.



#### 4. Calculations

##### a. Computer Processing and Spectral Density

###### Normalization

Spectral density plots were digitized and computer processed. (The computer program is listed in Appendix B). The computer subtracted the energy spectrum of the background noise from the energy spectrum of the acoustic emission event plus background noise. The resulting spectrum was representative of that arising from only the acoustic emission event itself. This spectrum was normalized with respect to overall energy content. (The area under each 10 kHz increment of the curve was divided by the total area under the curve from 125 kHz to 1 MHz.) Through this normalization procedure, one AE event's spectral energy distribution could be compared to another event's spectral energy distribution, independent of the total spectral energy content of each event.

##### b. Calculation of AE Spectral Energy, AE Pressure and Normalized Spectral Energy Distribution

AE events detected just prior to each specimen's failure were used for statistical energy analysis. The spectral energy, RMS vibrational pressure across the face of the transducer, and normalized spectral energy distribution were calculated for each AE. The total energy (between 125 kHz to 1 MHz) corresponding to each AE



event was approximated by multiplying the square of the event's RMS voltage by the duration of the event (as measured by the time gate) and dividing by the input impedance of the spectral analyzer (50 ohms). The square of the event's RMS voltage, contained within the frequency band of interest, was obtained from the integral of the AE event's spectral density. This mean squared voltage corresponded to the filtered transducer response amplified  $\times 10^5$ . Given that the average transducer sensitivity, over the frequency range 125 - 2000 kHz, was about 30 microvolts/Pa, it was possible to calculate both the amplified spectral energy per AE event and the AE pressure (RMS) excitation of the transducer by use of the following equations:

$$\begin{array}{l} \text{AE event's} \\ \text{energy after} \\ \text{amplification} \\ \text{(Joules)} \end{array} = \frac{2 (\text{sum} \times 10^{-9}) \text{ volts}_{(\text{RMS})}^2 \times (\text{DE}) \text{ sec.}}{50 \text{ ohms}} \quad (1)$$

$$\begin{array}{l} \text{RMS pressure} \\ \text{from AE} \\ \text{excitation} \\ \text{on the face} \\ \text{of the} \\ \text{transducer} \\ \text{(Pa)}_{\text{RMS}} \end{array} = \frac{(2 (\text{sum} \times 10^3))^{\frac{1}{2}} \text{ microvolts}_{\text{RMS}}}{(30) \text{ microvolts/Pa} \times (10^5) \text{ amp}} \quad (2)$$





Where (sum) is output from computer program in Appendix B and is the integral of of the spectrum  $\times 10^{-3}$  from the frequencies 125 kHz to 1 MHz.

$(2 \text{ sum} \times 10^3) = V_{\text{RMS}}^2$  where V is in microvolts.

(DE) = duration of event or time gate width in seconds.

Average transducer sensitivity = 30 microvolts/Pa.

Amplification =  $\times 10^5$

Spectral analyzer input impedance = 50 ohms.

## 5. Paired-Sample t Statistical Test

Groups of AE event normalized spectral energy distributions were used to generate a mean normalized spectral energy distribution for each specimen. Due to the random nature of the AE events, it was decided to use each specimen's mean normalized spectral energy distribution in any tests of the statistical similarities between the AE spectra of different specimens. Each specimen's mean normalized spectral energy distribution would, hopefully, have certain unique characteristics conveyed to it by the group statistics of the specimen's predominant failure mechanisms.

The mean normalized spectral energy distributions were statistically compared for similarity, two at a time, using the paired-sample t test (see Appendix D). This tested the hypothesis that the two specimen spectral distributions actually came from one sample population



and, therefore, had an identical "true" mean spectral energy distribution. Each pair of specimen mean normalized spectral energy distributions was statistically examined at 68 different frequencies from 125 kHz to 800 kHz. A level of significance of 0.74 was used for this evaluation.

#### 6. AE Shakedown

Finally, a brief examination was made concerning any acoustic emission irreversibility or "shakedown" behavior which might be occurring in the specimens. In several of the tensile tests the specimen was loaded, unloaded, then reloaded prior to its rupture. Absence of acoustic emission during reloading would indicate acoustic emission irreversibility with respect to its load.



### III. RESULTS

#### A. SEM Results

Each specimen type failed in a characteristic manner (Figure 5). All of the  $0^{\circ}$  specimens shattered with both transverse cracks propagating across the fibers and longitudinal cracks propagating between the fibers. Scanning electron microscope (SEM) examination showed relatively smooth shear surfaces along the longitudinal cracks with occasional appearance of multiple fissures in the matrix aligned in a "fishscale" pattern along the axis of the fibers. Transverse cracks appeared to be jagged with fractured fibers and holes giving much evidence of a fiber bundle pull-out mechanism. Figure 6 shows typical fracture surfaces of a  $0^{\circ}$  specimen.

Each  $10^{\circ}$  specimen sheared along the fibers' axis. SEM examination showed a fishscale pattern in the matrix between mostly unbroken fibers (See Figures 7 and 8).

The  $90^{\circ}$  specimens visually appeared to have cleanly separated in the matrix between fibers. However, SEM examination indicated a surprising number of broken fibers along the fracture surface suggesting some crack branching through several fiber layers in a relatively narrow fracture zone. The matrix showed many small cracks and scales appearing to have no preferred orientation (see Figure 9).

The  $(\pm 45^{\circ}, \pm 45^{\circ})_2$  specimens failed with separation





between fibers through the specimen's outer plies. Inner plies seemed to have failed in fiber fracture. SEM examination indicated much evidence of fiber fracture and delamination in the fracture zone between the outermost front and back plies and the remainder of the specimen (see Figure 10).

The one uncoated  $(\pm 45^{\circ}, \pm 45^{\circ})_S$  specimen failed in a similar manner as the  $(\pm 45^{\circ}, \pm 45^{\circ})_S$  coated specimens. This was probably due to the fact that the PVA coating was mistakenly applied between the fourth and fifth plies. Since, in this symmetrical laminate, the fourth and fifth ply fiber orientations were identical, a delaminating agent such as PVA would be expected to have little, if any effect upon the failure mode of the specimen.

### B. Time Domain Characteristics of AE

The time domain acoustic emission bursts exhibited some differences among specimen types (see Figures 11 through 17).  $0^{\circ}$  specimen acoustic emissions were typically of large amplitude but very short duration.  $10^{\circ}$  specimen acoustic emissions exhibited similar amplitudes but lasted for somewhat greater durations.  $90^{\circ}$  specimen acoustic emissions were of similar amplitude as the  $10^{\circ}$  and  $0^{\circ}$  specimens. However, the durations of the  $90^{\circ}$  specimen AE bursts were substantially longer.  $(\pm 45^{\circ}, \pm 45^{\circ})_S$  specimen AE bursts were generally greater in both



amplitude and duration than those of any of the other specimen types.

### C. Load, AE Counts, and AE-RMS

Load, AE counts and AE-RMS are each plotted as a function of time in Figures 18 through 32. Table 4 lists ultimate loads, AE counts threshold, total AE counts, and the distance of the failure from the transducer. Table 5 summarizes the mean and standard deviation of each specimen type failure load. The quotient of the standard deviation divided by the mean is presented as an indication of the "degree of scatter" in the rupture strength of the specimen types. The  $0^\circ$  specimens showed the greatest scatter in their failure load as evidenced by a degree of scatter which is greater than eight times that of the  $10^\circ$  or  $(\pm 45^\circ, \pm 45^\circ)_S$  specimens and more than two and a half times that of the  $90^\circ$  specimens. (This large variation in the failure strength of the  $0^\circ$  specimens is similar to that reported for  $0^\circ$  specimens by Pipes et al. (11).)

The  $90^\circ$  and  $0^\circ$  specimen types exhibited highly linear load versus time behavior (at constant crosshead displacement rate). The  $10^\circ$  specimen's load versus time curves became somewhat nonlinear at about 80% of their final failure load. This corresponded to a sudden increase in acoustic emission counts and acoustic emission RMS. The  $(\pm 45^\circ, \pm 45^\circ)_S$  specimens exhibited a



slightly decreasing load plateau with increasing crosshead displacement just prior to failure (somewhat reminiscent of the load versus time behavior of a ductile metal). This coincided with a sharply increased acoustic emission count rate and a large increase in the AE-RMS.

Several specimens, cut from the same panels as the ones used in these tests, were strain gauged and tensile tested in similar grip fixtures at the NASA Lewis Research Center in Cleveland, Ohio. Their measured elastic coefficients and failure stresses are presented in Table 6.

#### D. Total Spectral Energy per AE and AE Pressure (RMS) Excitation of Transducer

The results of equations (1) and (2) applied to each individual AE that was analyzed, are presented in tabular form in Appendix C. The mean results of the AE from each specimen are summarized in Table 7. These results show a surprising variation between specimens of a similar fiber orientation. Other than reflecting a possibly inconsistent operator's bias in choosing the acoustic emission signals to be analyzed, or the limited number of samples which were taken from each specimen, no rational explanation can be given for this somewhat large variation in mean energy or RMS pressure per AE event among similar specimens. (It is possible that extending





the passband of the AE system below 125 kHz might have resulted in more consistent results, but this is sheer conjecture.) This wide variation in the mean energy per AE event emphasized the importance of normalizing a spectrum with respect to the total AE event's energy before making any cross comparisons of two different AE spectral energy distributions.

## F. Normalized Spectral Energy Distributions

### 1. Individual Spectral Distributions for Each AE Event

The normalized spectral energy distributions for each AE event were plotted and appear in Appendix C. These plots are normalized by dividing the area under each 10 kHz increment of the AE spectral energy density curve by the total area under the curve between the frequencies 125 kHz - 1 MHz. Consequently, the units for the Y axis are dimensionless. As mentioned previously, due to the random nature of AE events, any one to one comparison between individual AE event spectra is probably of questionable value. However, these spectra provided the data which allowed for the generation of the mean normalized spectral energy distribution for each specimen. This mean spectral distribution would, hopefully, exhibit certain unique group statistical properties, conveyed to it from the predominant failure mechanisms of the specimen.



## 2. Mean Normalized Spectral Energy Distribution

The mean normalized spectral energy distribution for each specimen was derived from its individual AE event spectral densities. These appear in Figures 33 through 47. (The mean normalized spectral energy distribution is the curve labeled #1.) Each graph also indicates plots which are one standard deviation from the spectral distribution of the mean (curves labeled 2 and 3). As previously mentioned, the Y axis units on these curves are non-dimensional and indicate the group statistics of the mean relative distribution of total AE energy versus frequency. It was very difficult to qualitatively define the differences between one mean normalized spectrum and another. With the exception of the spectrum of specimen IV5CA (Figure 44), all spectra exhibited significant relative energy up to at least 700 kHz. The  $90^{\circ}$  and  $10^{\circ}$  specimens' spectra (Figures 33 to 39) generally showed more uniform energy distribution than the  $0^{\circ}$  and the  $(\pm 45^{\circ}, \pm 45^{\circ})_s$  specimens' spectra (Figures 40 to 47). All four  $90^{\circ}$  specimens exhibited very similar mean normalized spectra (Figures 33 to 36). Of the three  $10^{\circ}$  specimens, IV1B (Figure 37) showed a greater spectral energy content in the frequencies below 250 kHz. This specimen failed somewhat further from the transducer and at a lower load than the other two  $10^{\circ}$  specimens (Note Table 7).



The mean normalized spectra of the  $0^{\circ}$  specimens varied widely from specimen to specimen. Specimen LV5C (Figure 40), which had an extremely high failure load of 32.47 kN, exhibited a very flat and featureless spectral distribution with significant relative energy up to 1 MHz. Specimen LV5H (Figure 43), which had a relatively low failure load of 16.01 kN, exhibited little relative spectral energy above 600 kHz and more energy proportionately in the frequencies below 250 kHz. Specimen LV5D (Figure 41) appeared to have spectra significantly different than any of the other  $0^{\circ}$  specimen spectra, particularly a rather large relative energy component in the frequency range 700 to 1,000 kHz. It should be noted that specimen LV5D was loaded, unloaded, reloaded, partially unloaded and then reloaded to failure. (see Figure 26.) It was the only  $0^{\circ}$  specimen which had such a load history prior to failure.

Three of the four  $(\pm 45^{\circ}, \pm 45^{\circ})_S$  specimens displayed a major proportion of their spectral energy content below 400 kHz. Specimen LV5CI (Figure 46) was the only exception, displaying a significant percentage of spectral energy between the frequencies 400 to 600 kHz. No particular evidence in the loading, failure load, or fracture tips could be found that would account for the apparent difference in the relative spectral energy distribution of specimen LV5CI.





## F. Paired-Sample t Statistic Results

Each mean normalized spectrum was examined statistically using the paired-sample t test. This test calculates the difference between two mean normalized spectra at various frequencies. It either accepts or rejects the hypothesis that "both mean normalized spectra come from the same "master" normalized spectrum." Using the rather high level of significance of 0.74 and examining each pair of mean normalized spectra at 68 different frequencies (between 125 kHz and 800 kHz), the test gave rather promising results. Table 8 gives the percentage of specimen pair comparisons for which the hypothesis that "both specimens had the same spectrum of relative spectral energy distribution" was not rejected. The higher the number on this chart, the more similar are the spectra. With the exception of  $0^{\circ} - 0^{\circ}$  comparisons, like specimen comparisons resulted in a lower percentage of hypotheses rejections than comparisons of unlike specimens. Other inferences relating to the relative similarities of spectra from different specimen types also might be made. For instance the implied similarities resulting from the comparison of  $0^{\circ}$  to the  $(\pm 45^{\circ}, \pm 45^{\circ})_S$  spectra and the  $90^{\circ}$  to the  $(\pm 45^{\circ}, \pm 45^{\circ})_S$  spectra may have some significance relating to the common mechanisms of fiber fracture in the first case and cracking between the fibers in the second case. At any rate, Table 8 shows that the paired-



sample t statistic test can discriminate between various specimen types based upon the mean normalized spectral energy distributions of their AE.

#### G. AE Spectra at Various Loads

Acoustic emissions from the  $(\pm 45^\circ, \pm 45^\circ)_S$  specimens were sampled at various loads of each specimen's tensile test. The spectral energy, pressure, and specimen load is tabulated for each AE and presented along with the respective normalized spectral energy distributions in Appendix F.

It is unlikely that enough acoustic emissions were sampled at each load to establish any statistically valid trends or quantitative conclusions. However, it appeared that the acoustic emission spectral densities shifted from a wide band distribution to a predominantly lower frequency distribution just prior to specimen rupture. More extensive sampling and use of the paired-sample t test would be required to verify this suspected spectral distribution trend.

#### H. Observations Concerning AE Shakedown

Acoustic emission irreversibility was studied in specimens LV5CG, LV5D, LV2H, LV2G, and LV4C. In the last four specimens acoustic emission appeared to be essentially irreversible. (see Figures 26, 24, 23, and 39



respectively.) Once acoustic emissions had been detected in a particular load regime and the specimen had then been unloaded, reloading through the same load regime resulted in detection of very few additional acoustic emissions until the previous "maximum historical load" had been surpassed. However, after the third loading cycle of specimen LV5CG, (see Figure 45) a crack was visually observed extending partially across the specimen. During reloading of the fourth cycle, substantial acoustic emission was detected as occurring well before the previous maximum historical load. Specimen LV5CG ruptured during the fourth cycle at a lower load than its maximum historical load. It failed at the crack which had been observed earlier in the test. Several AE spectra sampled during its fourth loading cycle are presented in Appendix E. LV5CG was the only specimen given cyclic loading in which a crack was visually detected prior to specimen rupture, so it was not possible to establish any repeatable observation of this apparent violation of AE irreversibility.





#### IV. CONCLUSIONS

A. A program to investigate the acoustic emission of graphite fiber polyimide composite failure mechanisms has been conducted.

B. The predominant failure mechanisms of the specimens are as follows:

1.  $0^{\circ}$  unidirectional specimens fail in fiber fracture, fiber pullout, and matrix shear. Small fissures, resulting in a fishscale pattern, are formed in the matrix during the process of fiber pullout and may be the source mechanism of a significant number of lower energy acoustic emissions.
2.  $10^{\circ}$  unidirectional specimens fail in intralaminar shear occurring predominantly in the matrix between the fibers. The fracture surfaces of these specimens are covered with the characteristic fishscales indicating many potential sites for AE generation. The sheared surfaces of the  $10^{\circ}$  specimens seem to be very similar to the longitudinally cracked fracture surfaces of the  $0^{\circ}$  specimens.
3.  $90^{\circ}$  unidirectional specimens exhibit a layered tensile failure of the matrix with some branching between layers causing occasional fiber fracture.
4.  $(\pm 45^{\circ}, \pm 45^{\circ})_S$  specimens fail incrementally with cracks growing in the matrix between fibers from many initiation sites along the edges of the specimen's



surface plies. These cracks appear to propagate gradually towards the center of the specimen during the tensile test, well before specimen rupture. Delamination of the surface plies can be visually detected immediately prior to specimen rupture. Most of the inner plies of the fracture surface fail in fiber fracture.

C. All four specimen types generally exhibit significant increases in normalized acoustic emission count rates at about 80% of the specimen's ultimate load. The AE-RMS generally exhibits characteristics similar to the AE count rate trends. Normalization of the load, AE counts, and AE-RMS aids in establishing general trends of the data, and compensates for some of the experimental variability in such parameters as the AE voltage threshold, specimen failure load, distance from the AE generation site to the transducer, etc.

D. Scatter of the specimen ultimate strength data for similar specimens was reasonably small (see Table 5) with the exception of the  $0^{\circ}$  specimens. It is possible that the  $0^{\circ}$  specimens are particularly sensitive to alignment in the loading fixture such that any slight deviations in alignment greatly effect the specimen's ultimate strength.

E. The mean spectral energy per AE event exhibits inexplicably large variations among specimens of similar fiber orientation (see Table 6). If these values are averaged over each specimen group of similar fiber



orientation, the following comparisons can be made:

1. The average AE event's spectral energy is similar immediately prior to specimen rupture in the  $90^{\circ}$  specimens and the  $(\pm 45^{\circ}, \pm 45^{\circ})_S$  specimens with values of  $22.6 \times 10^{-6}$  joules and  $22.0 \times 10^{-6}$  joules, respectively.

2. The average AE event's spectral energy for the  $10^{\circ}$  and the  $0^{\circ}$  specimens sampled just prior to specimen rupture is of substantially lower magnitude with values of  $1.47 \times 10^{-6}$  joules and  $1.54 \times 10^{-6}$  joules, respectively.

F. Though the AE from different specimen types generally show only minor differences in voltage amplitude, specimen types can be distinguished, with a wide frequency bandwidth AE system, by the characteristic time duration of their AE events. Since spectral energy is a function of both AE voltage amplitude and AE event duration, the similarities of AE voltage amplitude, among all of the specimen types tested, lead to the conclusion that the duration of the AE event has the greatest effect on the total spectral energy of an AE event.

G. The procedure of normalizing the AE spectral energy density with respect to total spectral energy allows for a statistical evaluation of the similarities between spectral energy distributions from different AE events (or groups of events).

H. A paired-sample t statistical comparison of mean





normalized spectral energy distributions can successfully discriminate between AE of  $10^\circ$ ,  $90^\circ$ , and  $(\pm 45^\circ, \pm 45^\circ)_s$  specimens (see Table 8). This test cannot achieve either conclusive distinction or unique recognition of AE from  $0^\circ$  specimens which exhibited wide variations in failure load and relative spectral energy distributions. Refinement of such a statistical approach will require many more unbiased AE samples than could be analyzed in this work.

I. Preliminary results suggest that AE spectra obtained from  $(\pm 45^\circ, \pm 45^\circ)_s$  specimens are not independent of specimen load. In addition, AE occurring at higher loads generally exhibited greater spectral energy content (see Appendix E ). A constitutive relationship between mean AE event energy and specimen load may exist. Other possible implications are the existence of a load dependent spectral dispersion relationship or the relative predominance of different AE generation mechanisms at different loads.

J. In most cases the specimens exhibit AE irreversibility or shakedown with respect to specimen load. However, preliminary observations suggest that this AE irreversibility behavior is violated once a visible crack has formed in the specimen prior to specimen rupture. (see Figure 45.) This conclusion is based upon the test results of specimen IV5CG. (see Appendix E.)



## V. RECOMMENDATIONS

1. More rigorous statistical characterization of the AE spectra from predominant failure mechanisms should be performed. This can be accomplished by analyzing many more AE from each specimen to allow for better estimates of their mean normalized spectral energy distribution. Inducement of certain modes of failure by flaw simulation should also be considered. The paired-sample t statistical test should be used to evaluate the uniqueness of AE spectral characterizations.
2. AE energy vs stress constitutive relationships should be investigated. The best approach to such a study will probably be a statistical one in which the mean AE energy is related to the material's state of stress.
3. AE dispersion relationships and attenuation characteristics in the composite specimens should be studied. Understanding the dependency of the mean AE energy content to the state of stress and proximity of the AE site from the transducer can then be used in conjunction with an AE locator to refine the AE characterization of fracture mechanisms.
4. More scanning electron microscope examination of the specimens' fracture surfaces is recommended. SEM analysis techniques should be established to generate quantitative estimates of the relative predominance of specific fracture mechanisms.



5. AE amplitude distribution characterization of predominant fracture mechanisms should be attempted, using a narrow band, resonant transducer, AE system.
6. AE pulse duration distribution characterization of predominant fracture mechanisms should be attempted, using a wide frequency band, "flat" transducer, AE system.
7. A data interface between the spectral analyzer and a computer compatible hard copy device (magnetic tape, floppy disk, paper tape, etc.) should be designed to enable the rapid data analysis of many AE. Alternatively, the use of the IMLAC X-Y plot reader in the MIT Joint Computer Facility could be programmed for writing spectral data onto floppy disk storage for later processing.
8. Acoustic emission irreversibility or shakedown should be specifically investigated in fiber composites. Such a study should examine the AE characteristics of specimens with known flaws or damage induced after prestressing of the material.





## VI. REFERENCES

1. Green, A. T., Lockman, Haines, "Acoustical Analysis of Filament Wound Polaris Chambers," Aerojet General Corp., Report # 0672-017, (1963).
2. Rathbun, D. K., Beattie, A. G., Hiles, L. A., "Filament Wound Materials Evaluation with Acoustic Emission," SCI-DC-70-260, (22 April 1971).
3. Iiptai, Robert G., "Acoustic Emission from Composite Materials," UCRL-72657, ASTM STP 497, (1972).
4. Rothwell, R., and Arrington, M., "Acoustical Emission and Micromechanical Debond Testing," Nature Physical Science, 233, 163, (1971).
5. Swanson, G. D., and Hancock, J. R., "Off-axis and Transverse Tensile Properties of Boron Fiber Reinforced Aluminum Alloys," Composite Materials: Testing and Design (Second Conference), ASTM STP 497 (1972), pp. 469-482.
6. Mullin, J. V., and Mehan, R. L., "Evaluation of Composite Failures Through Fracture Signature Analysis," Journal of Testing and Evaluation, 1, 3, 215 (1973).
7. Balderston, H. L., "The Broad Range Detection of Incipient Failure Using the Acoustic Emission Phenomenon," Acoustic Emission, ASTM Pub. 505, p. 292 (1972).
8. Guild, F. J., Walton, D., Adams, R. D., and Short, D., "The Application of Acoustic Emission to Fiber Reinforced Composite Materials," Composites, (July 1976) pp. 173-179.
9. Ono, Kanji, "Amplitude Distribution Analysis of Acoustic Emission Signals," Materials Evaluation, (August 1976), p. 122.
10. Carlyle, John M., "Acoustic Emission in Fiber Reinforced Composites," Naval Air Development Center, Warminster, Pa., (May 15, 1975), NADC-75-082-30.



## References. cont.

11. Pipes, R. B., Ballintyn, N. J., and Scott, W. R., "Acoustic Emission Response of Metal Matrix Composites," Naval Air Development Center Report # NADC-76082-30, (January 1976).
12. Speake, J. H., and Curtis, G. J., "Characterization of the Fracture Process in CFRP Using Spectral Analysis of the Acoustic Emissions Arising from the Amplification of Stress," International Conference on Carbon Fibers, Their Place in Modern Technology, (London 1974), paper # 29.
13. Rollins, Fred R., "Acoustic Emission From Boron-Aluminum Composites During Tensile Fracture and Fatigue," AD-731-710, (October 1971).
14. Berg, C. A., Rinsky, A., "Tensile Fracture of Graphite Fiber Reinforced Epoxy Composites," Fibre Science and Technology (3) (1971), Elsevier Publishing Company, Ltd., England.
15. Chamis, C. C., and Sinclair, J. H., "10° Off-Axis Tensile Test for Intralaminar Shear Characterization of Fiber Composites," NASA Technical Note TN D-8215, Lewis Research Center, Cleveland, Ohio 44135, (April 1976).
16. Rotem, Assa, and Hashin, Zvi, "Failure Modes of Angle Ply Laminates," Journal of Composite Materials, Vol. 9, (April 1975), p. 191-206.
17. Chang, F. H., Gordon, D. E., Rodini, B. T., McDaniel, R. H., "Real Time Characterization of Damage Growth in Graphite/Epoxy Laminates," Journal of Composite Materials, Vol. 10, (July 1976), pp. 182-192.
18. Beattie, Alan G., "Energy Analysis in Acoustic Emission," Materials Evaluation, (April 1976), p. 73.
19. Newland, D. E., Random Vibrations and Spectral Analysis, Longman Group, Ltd., London, (1975), pp. 67-73.
20. Miller, Irwin and Freund, John E., Probability and Statistics For Engineers, Prentice Hall, Inc., Englewood Cliffs, New Jersey, (1965), pp. 165-170.



## VII. FIGURES AND TABLES



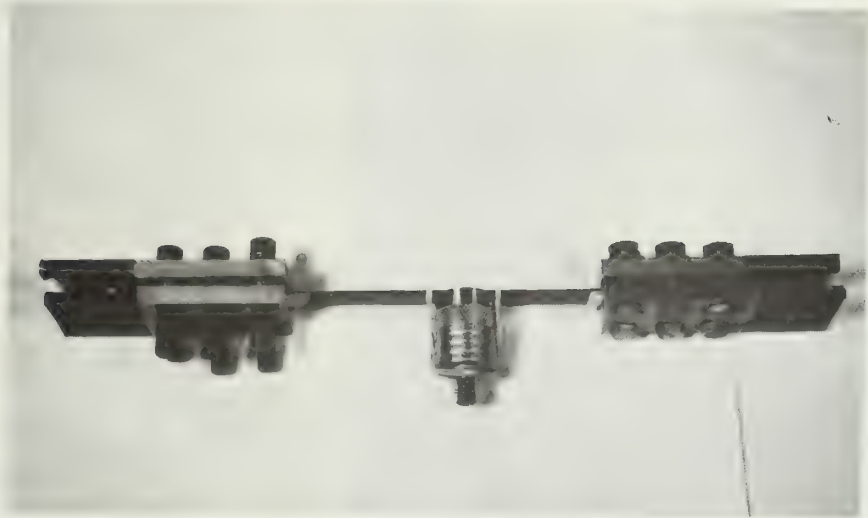


Figure 1 - Insulated grips, specimen, and transducer attachment.



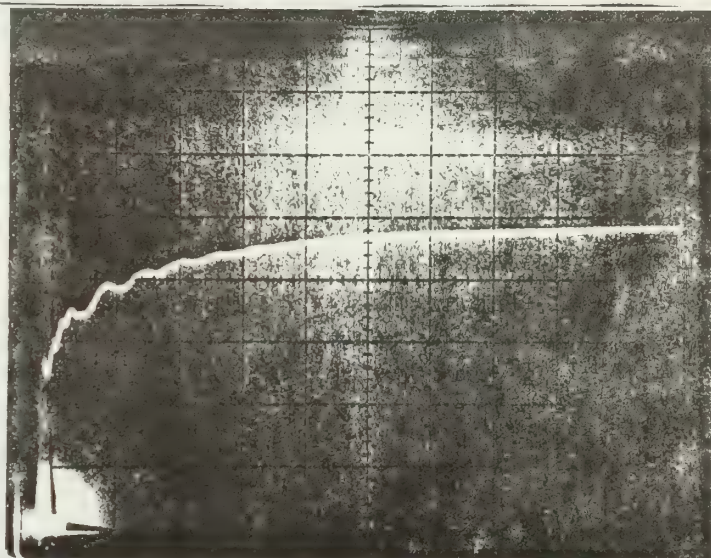


Figure 2 - Transducer Response Curve

Acoustic Emission Technology Transducer No. FC500HD (10375)

Sensitivity  
in dB  
(re  $1\text{V}/\mu\text{Bar}$ )

-50  
-60  
-70  
-80  
-90  
-100  
-110  
-120  
-130



L

.1 .5 .9 1.3 1.7 2.1

Frequency in MHz



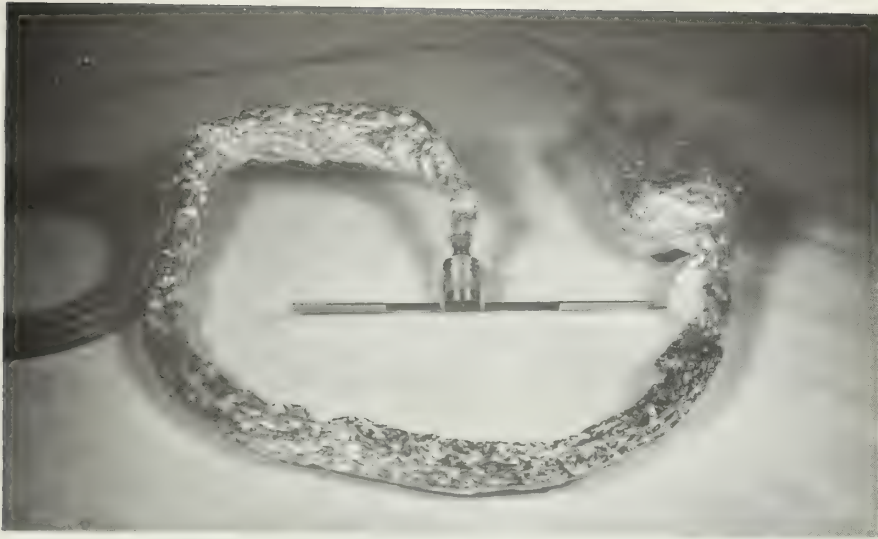


Figure 3 - Transducer leads and preamplifier shielded against EMI with aluminum foil.



Figure 4 - Test instrumentation. From right to left: Spectral analyzer, X-Y recorder, video tape recorder with gate unit, signal processor, and oscilloscope with signal generator (below).





Figure 5 - Typical fracture modes of the four specimen types. From top to bottom:  $90^\circ$ ,  $(\pm 45^\circ, \pm 45^\circ)_s$ ,  $10^\circ$  and  $0^\circ$ .





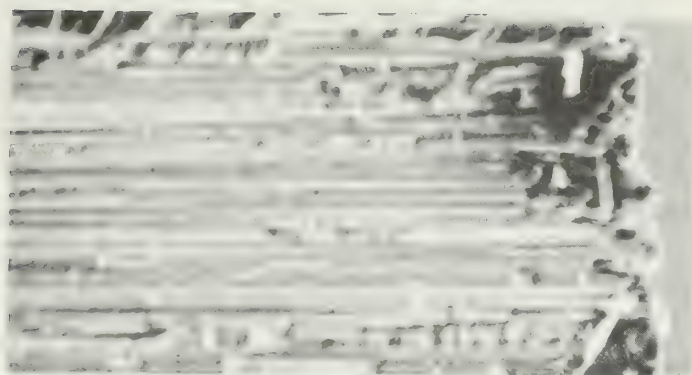


Figure 6 -  $0^{\circ}$  Fracture Surface  
Scanning Electron Microscope  
at 300 X Magnification

These are typical transverse (foreground) and longitudinal (background) fracture surfaces of  $0^{\circ}$  specimens showing evidence of fiber fracture, fiber pullout and matrix shear.

(Note the fishscale pattern in the matrix at top center.)





180 X

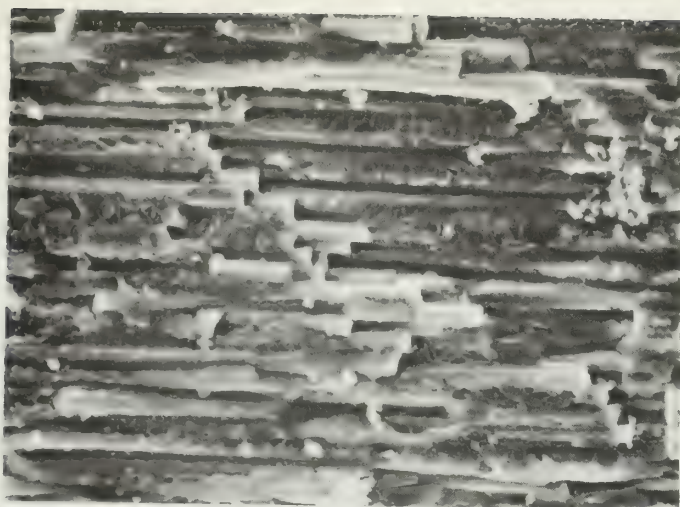
# Figure 7 and 8 - Fracture Surfaces of $10^0$ Specimens

This was the typical appearance of the sheared fracture surface of the  $10^0$  specimens under the scanning electron microscope. Surfaces generally exhibited shear of the matrix with very few fiber fractures. Notice the characteristic fishscale appearance of the matrix.



1000 X





300 X



3000 X

Figure 9 - Fracture Surfaces of  $90^{\circ}$  Specimens Under Scanning Electron Microscope

This is a typical fracture surface of a  $90^{\circ}$  unidirectional specimen. Note the broken fibers and the appearance of multiple fissures near fiber tips. Scales in the matrix follow no distinct pattern.







Figure 10 - Fracture Surface of  $(\pm 45^{\circ}, \pm 45^{\circ})_s$  Specimen  
Scanning Electron Microscope  
at 100 X Magnification

This is the typical fracture surface of the  $(\pm 45^{\circ}, \pm 45^{\circ})_s$  specimens. Notice the first ply at the left hand side which has failed in matrix tension, the delamination of the second and third plies, and the extensive fiber fracture in the remaining plies.





Figures 11 and 12 - Specimen LV5C

0° unidirectional

Y axis = 500 mv/div

X axis = 50 microsec/div

Load = 15.57 kN

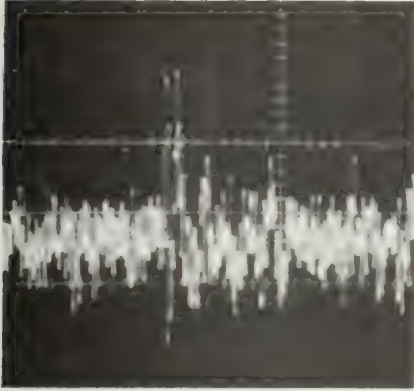


Figure 11 - Ungated Signal

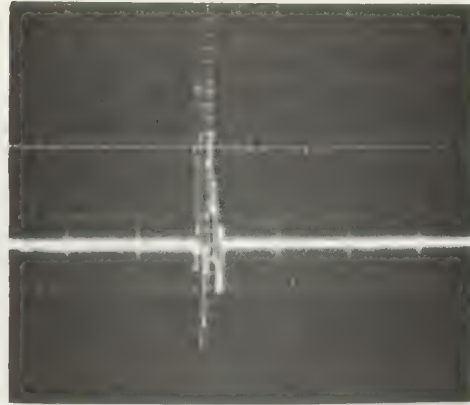


Figure 12 - Gated Signal

Figure 13

Specimen LV4C

10° unidirectional

Y axis = 500 mv/div

X axis = 100 microsec/div

Load = 6.89 kN just prior  
to specimen failure

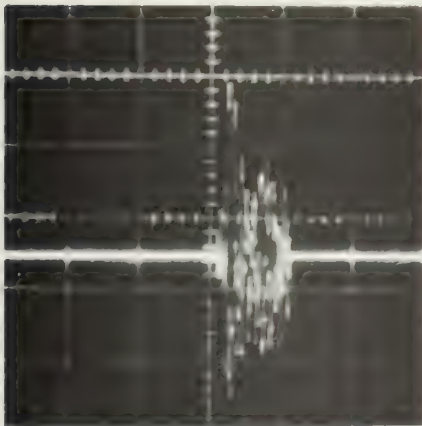


Figure 13 - Gated Signal

Figure 14

Specimen LV1B

10° unidirectional

Y axis = 500 mv/div

X axis = 70 microsec/div

Load = 6.4 kN just prior  
to specimen  
failure

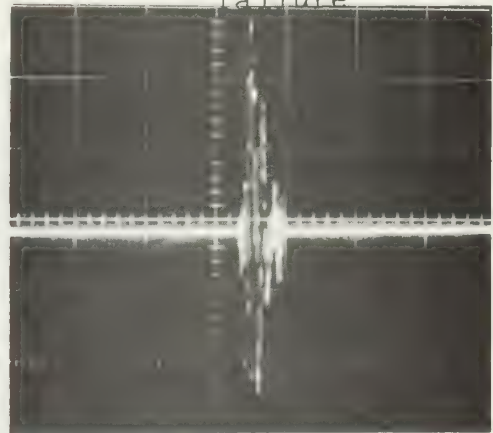


Figure 14 - Gated Signal



Figure 15

Specimen LV2G (ungated)  
90° unidirectional  
Y axis = 500 mv/div  
X axis = 100 microsec/div  
Load = 0.80 kN

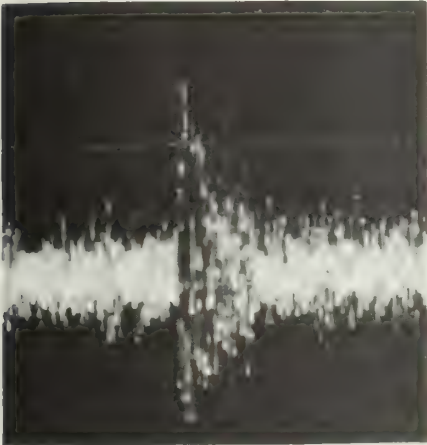


Figure 16

Specimen LV2B (ungated)  
90° unidirectional  
Multiple Emission  
Y axis = 500 mv/div  
X axis = 200 microsec/div  
Load = 0.85 kN

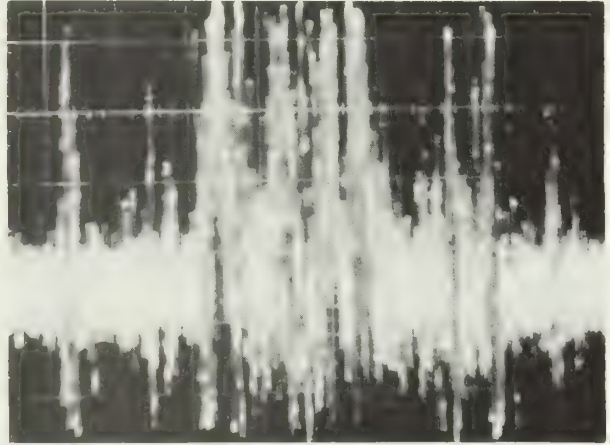
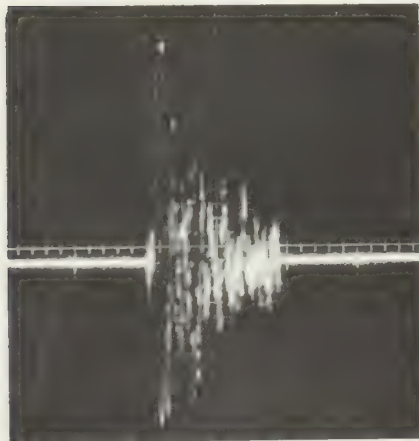


Figure 17

Specimen LV5CI (gated)  
( $\pm 45^\circ$ ,  $\pm 45^\circ$ )<sub>s</sub>  
Y axis = 500 mv/div  
X axis = 200 msec/div  
Load = 2.22 kN





Figures 18 - 32

Load, Acoustic Emission Counts, and Acoustic Emission RMS versus Time.

Note: To facilitate data presentation, each parameter is normalized with respect to its maximum value occurring during the test. To obtain actual parameter values, multiply the normalized value by its respective normalizing factor which is given on each graph.





Figure 18  
 Specimen LVIB ( $10^0$ )  
 Load, AE Counts, and RMS vs Time  
 AE Counts Threshold = 0.8 volts @ 100 dB

Parameter	Legend	Normalizing Factor
Load	-X-X-	6,405 kN
AE Counts	-O-O-	105,000
RMS	-Δ-Δ-	52.5 mv
Time	X Axis	873.0 sec.

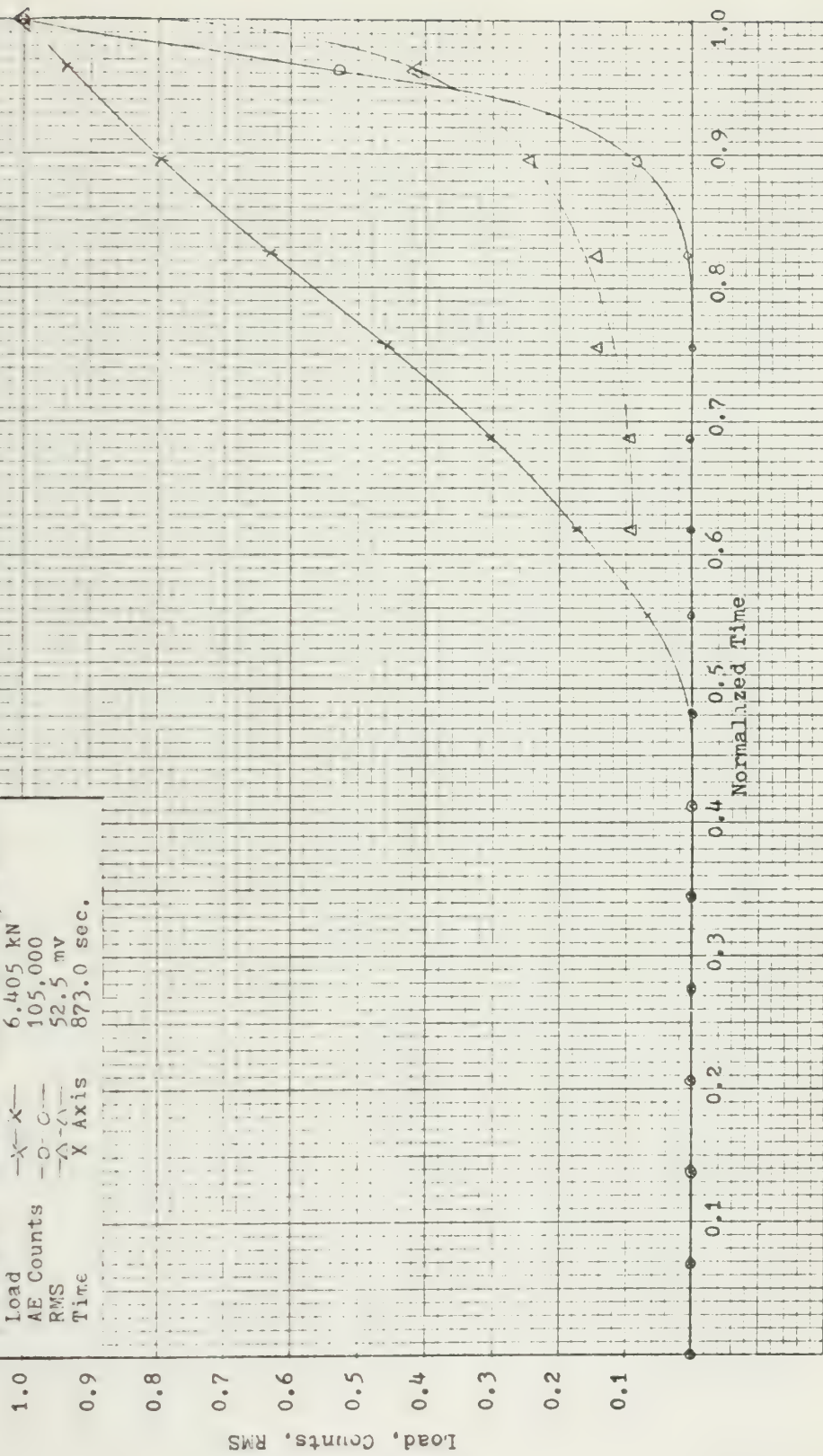
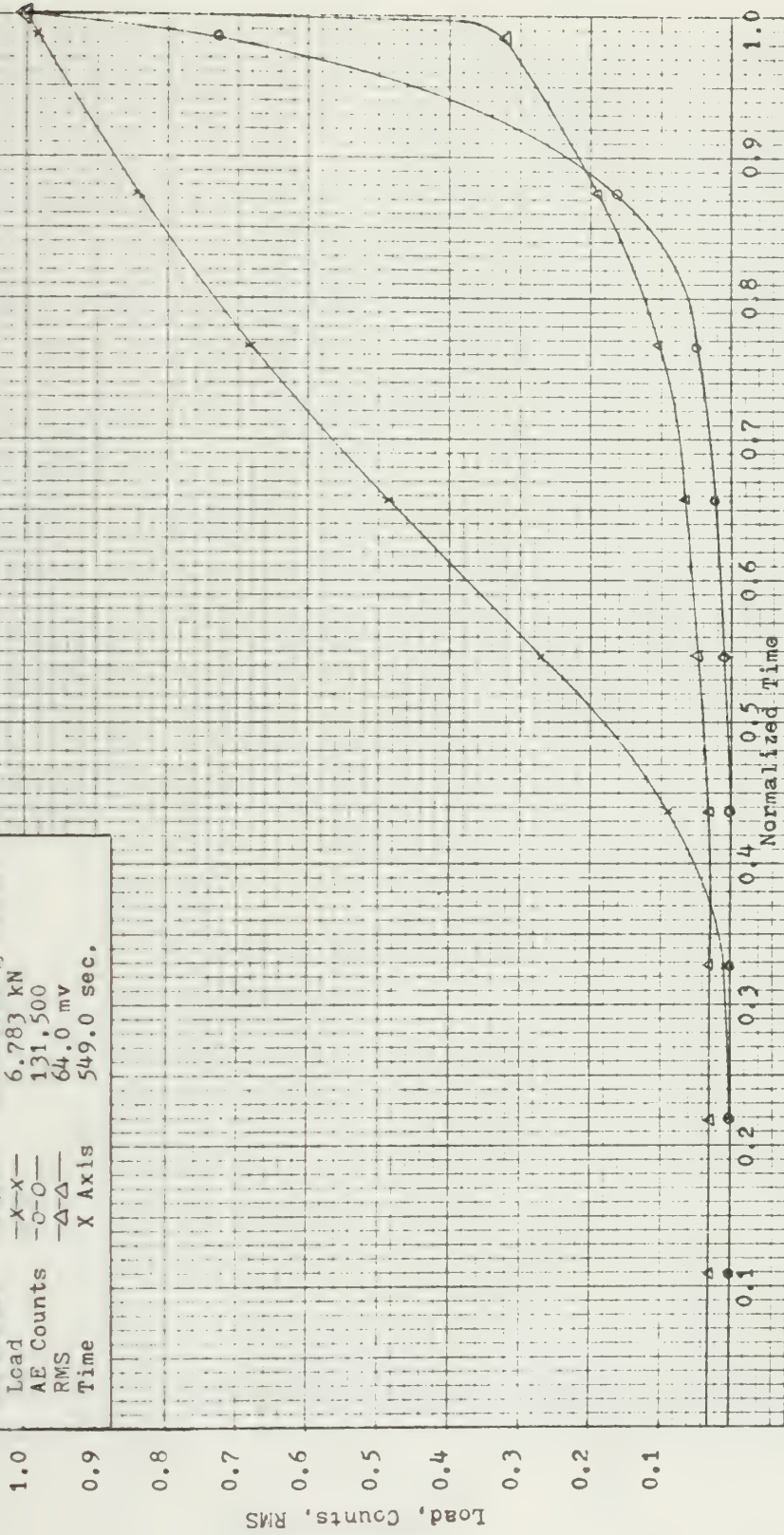




Figure 19

Specimen LV4A ( $10^0$ )  
 Load, AE Counts, and RMS vs Time  
 AF Counts Threshold = 0.7 volts @ 100 dB

Parameter	Legend	Normalizing Factor
Load	-X-X-	6,783 kN
AE Counts	-O-O-	131,500
RMS	-Δ-Δ-	64.0 mv
Time	X Axis	549.0 sec.

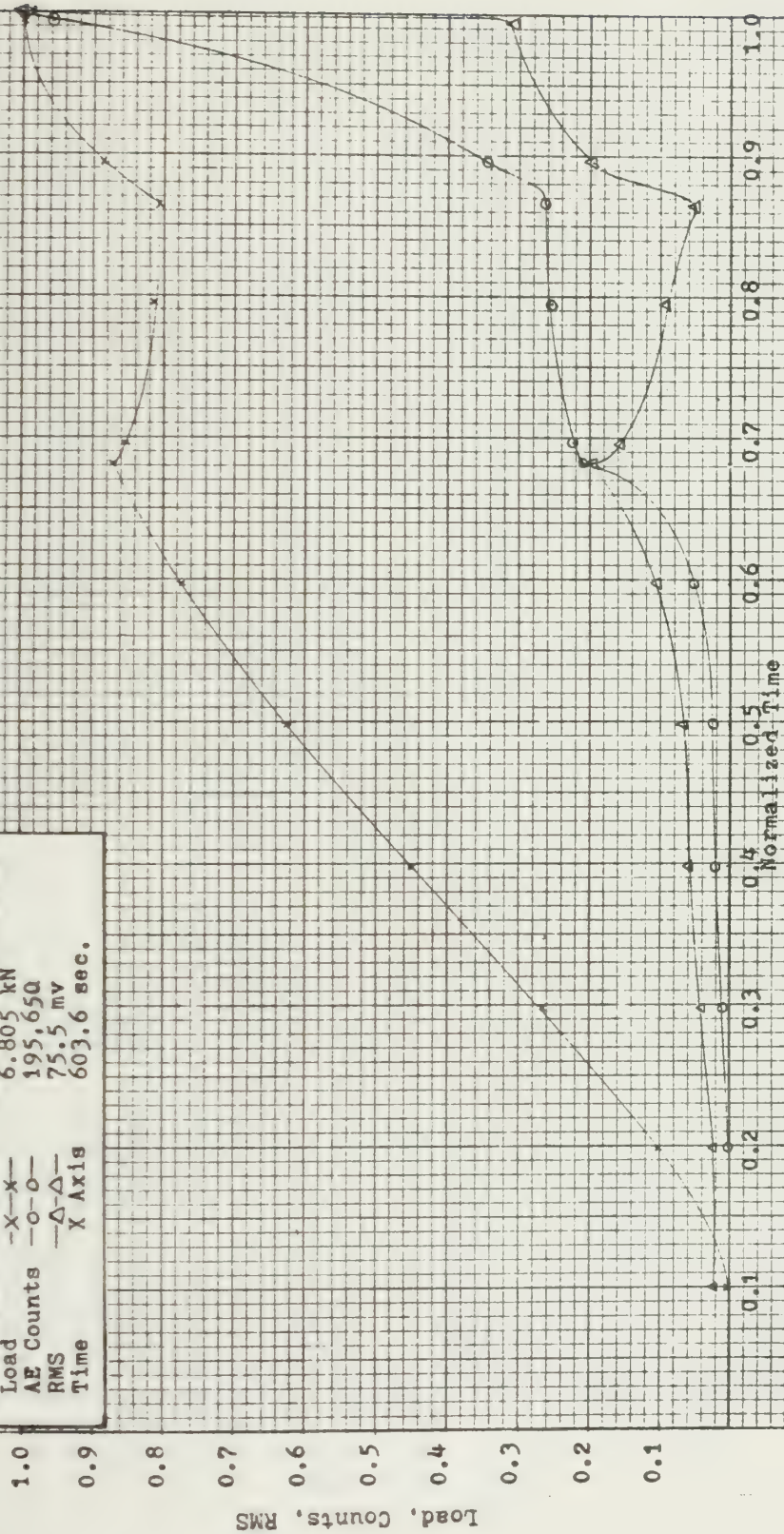






**Figure 20**  
 Specimen LV4C ( $10^0$ )  
 Load, AE Counts, and RMS vs Time  
 AE Counts Threshold = 0.7 volts @ 100 dB

Parameter	Legend	Normalizing Factor
Load	-X-X-	6.805 kN
AE Counts	-O-O-	195,650
RMS	-Δ-Δ-	75.5 mv
Time	X Axis	603.6 sec.





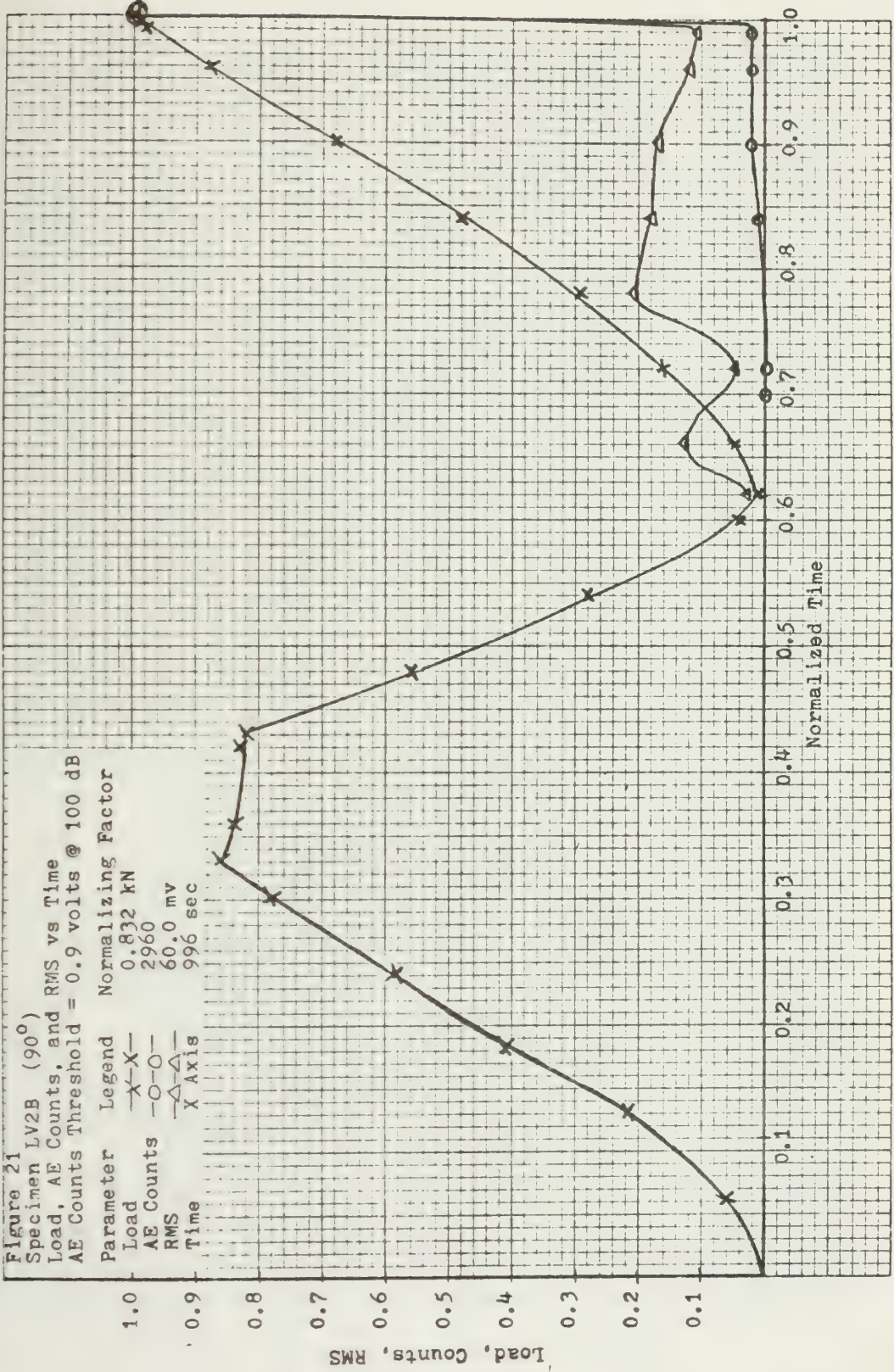


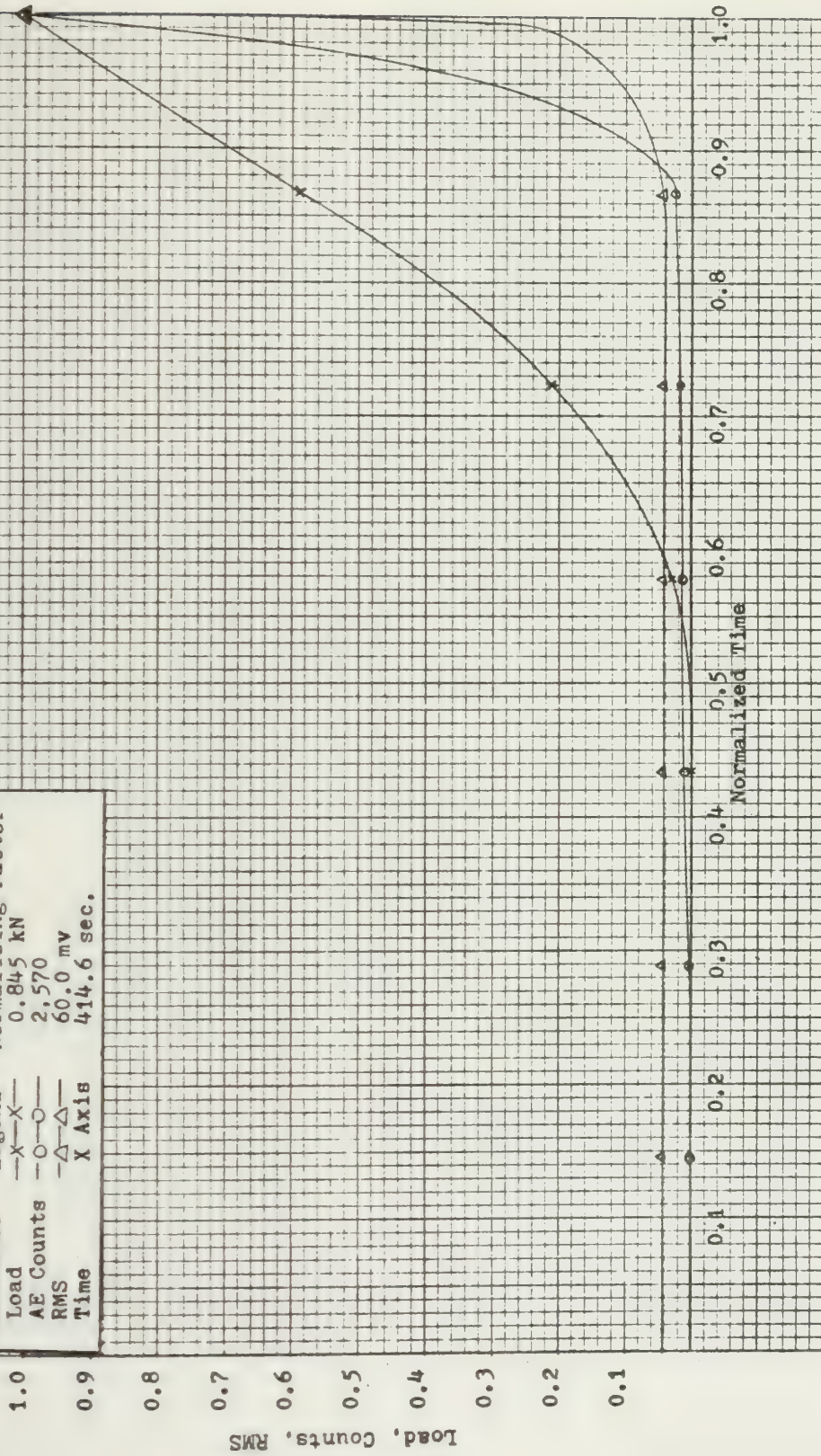




Figure 22

Specimen LV2C (90°)  
 Load, AE Counts, and RMS vs Time  
 AE Counts Threshold = 0.8 volts @ 100 dB

Parameter	Legend	Normalizing Factor
Load	-X-X-	0.845 kN
AE Counts	-O-O-	2,570
RMS	-Δ-Δ-	60.0 mV
Time	X Axis	414.6 sec.





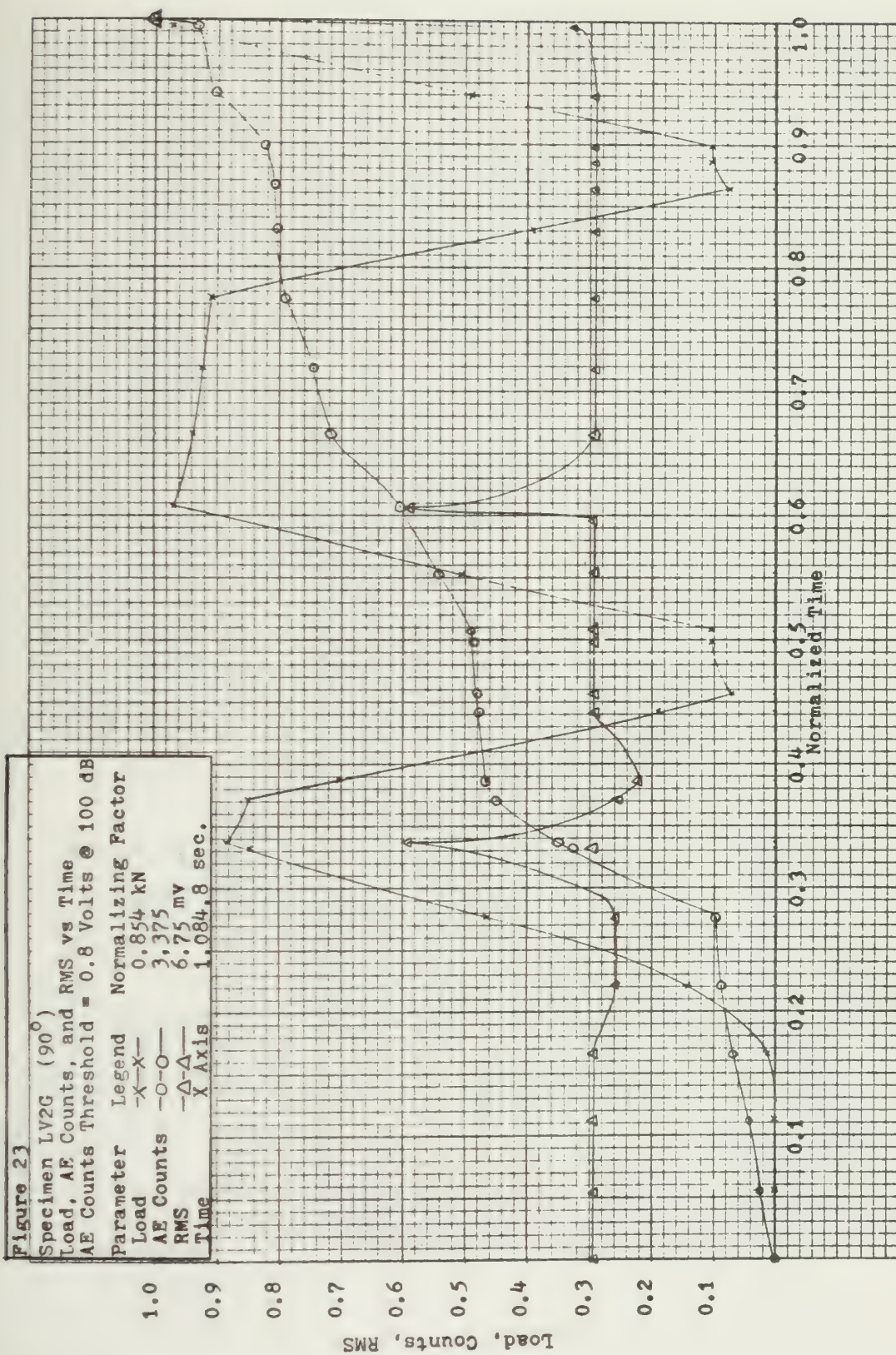






Figure 24

Specimen LV2H (90°)  
 Load, AE Counts, and RMS vs Time  
 AE Counts Threshold = 0.8 volts @ 100 dB

Parameter	Legend	Normalizing Factor
Load	-X-X-	0.934 kN
AE Counts	-O-O-	8,750
RMS	-Δ-Δ-	no data
Time	X Axis	636.0 sec.

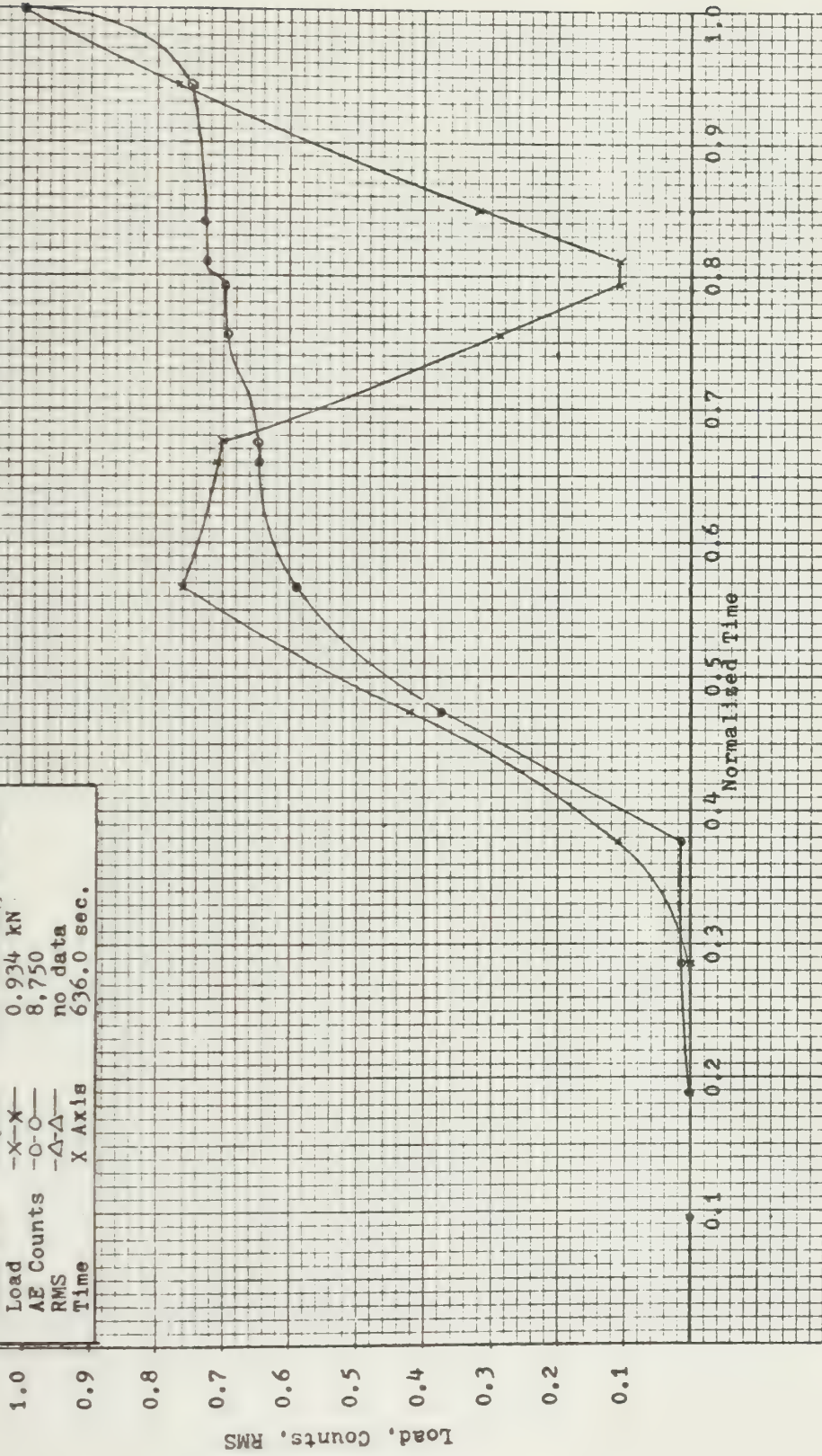






Figure 25

Specimen LV5C (0°)  
 Load, AE Counts, and RMS vs Time  
 AE Counts Threshold = 0.7 volts @ 100 dB

Parameter	Legend	Normalizing Factor
Load	-X-X-	32.47 kN
AE Counts	-O-O-	41,550
RMS	-Δ-Δ-	50.5 mv
Time	X Axis	1.254.0 sec.

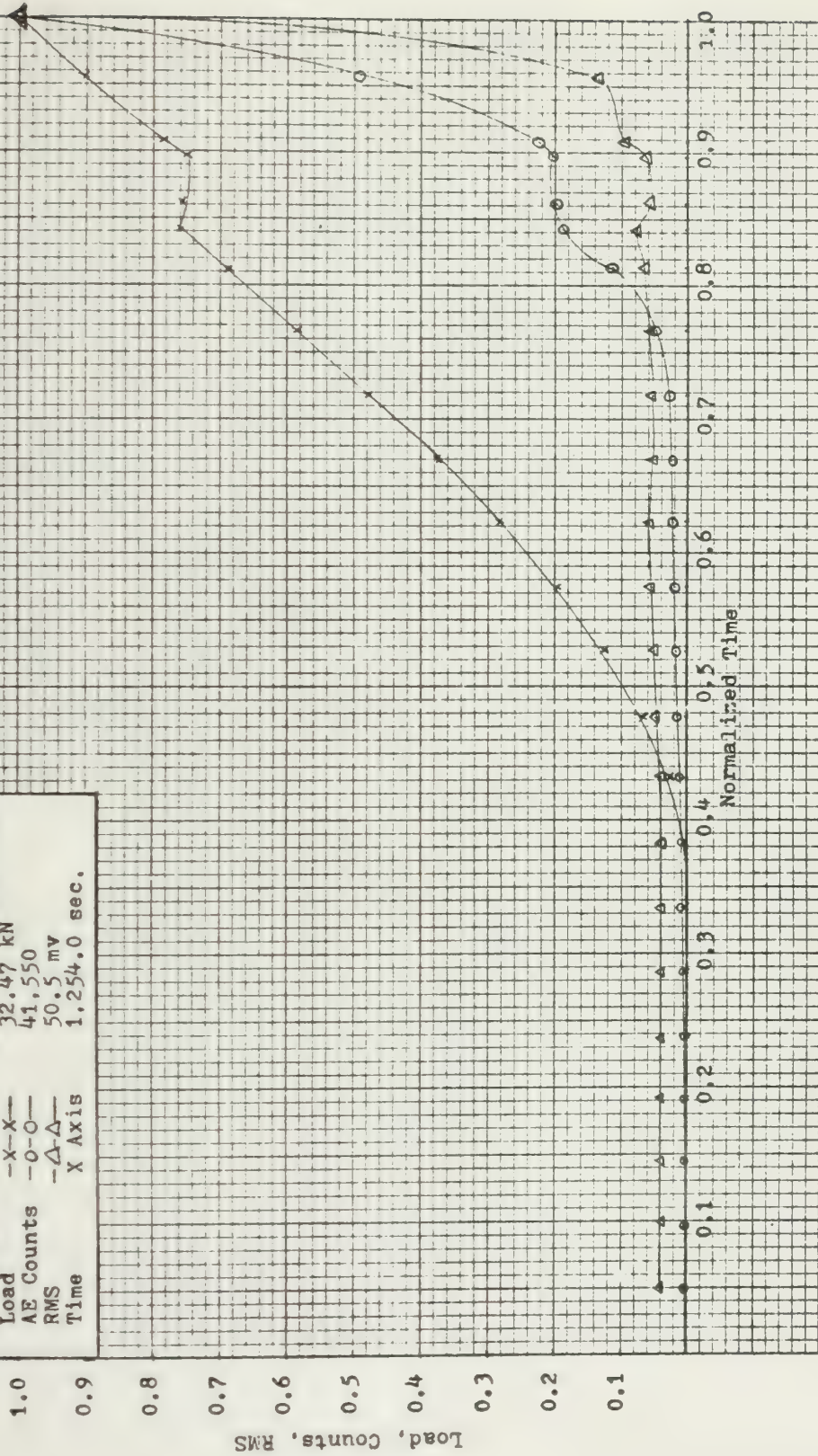




Figure 26

Specimen LV5D (0°)  
 Load, AE Counts, and RMS vs Time  
 AE Counts Threshold = 0.6 volts @ 100 dB

Parameter	Legend	Normalizing Factor
Load	-x-x-	18.95 kN
AE Counts	-o-o-	116,275
RMS	-Δ-Δ-	53.5 mv
Time	X Axis	1,447.2 sec.

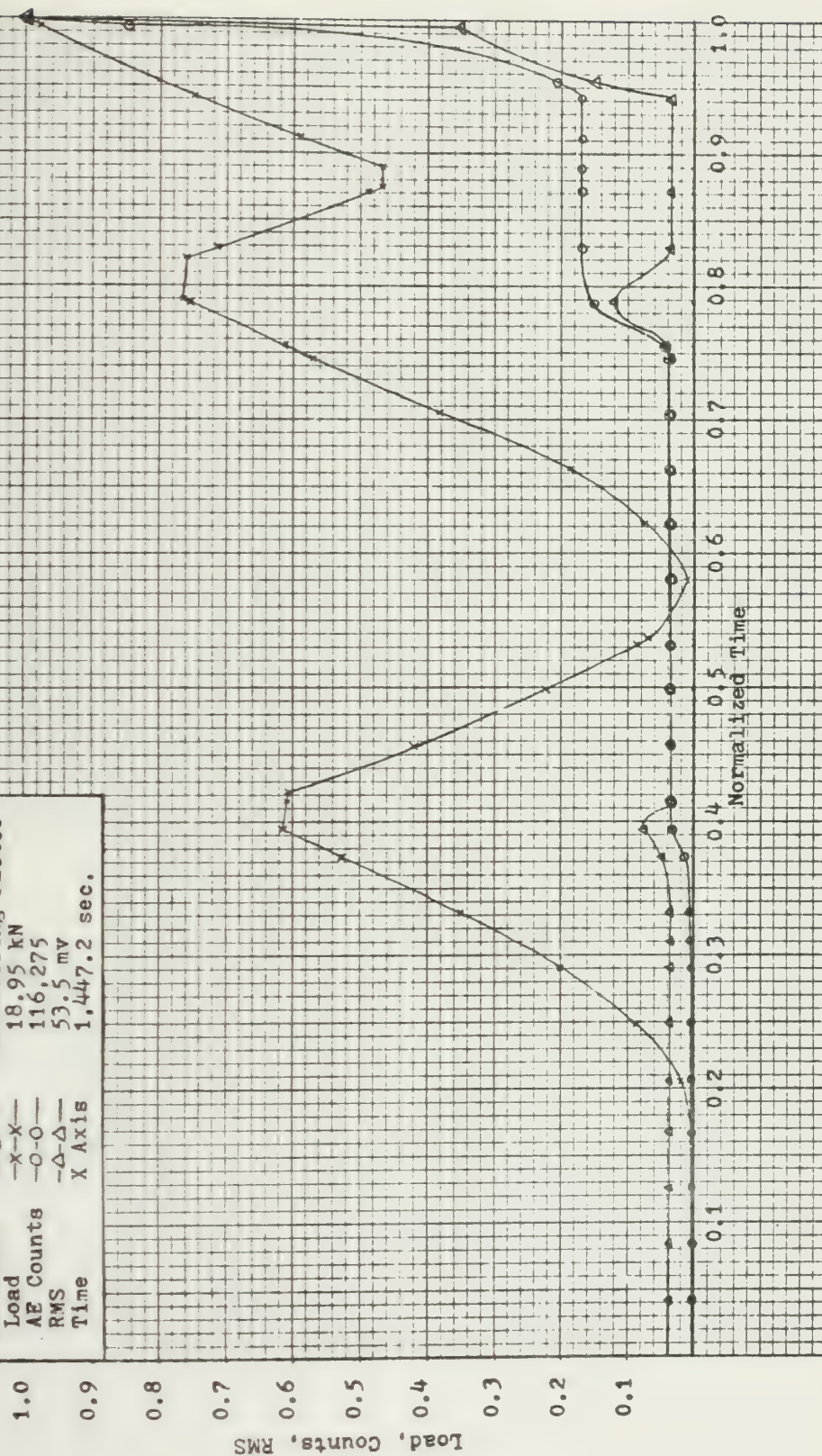






Figure 27

Specimen LV5G ( $0^{\circ}$ )  
 Load, AE Counts, and RMS vs Time  
 AE Counts Threshold = 0.7 volts @ 100 dB

Parameter	Legend	Normalizing Factor
Load	-X-X-	15.90 kN
AE Counts	-O-O-	2,800
RMS	-Δ-Δ-	no data
Time	X Axis	537.0

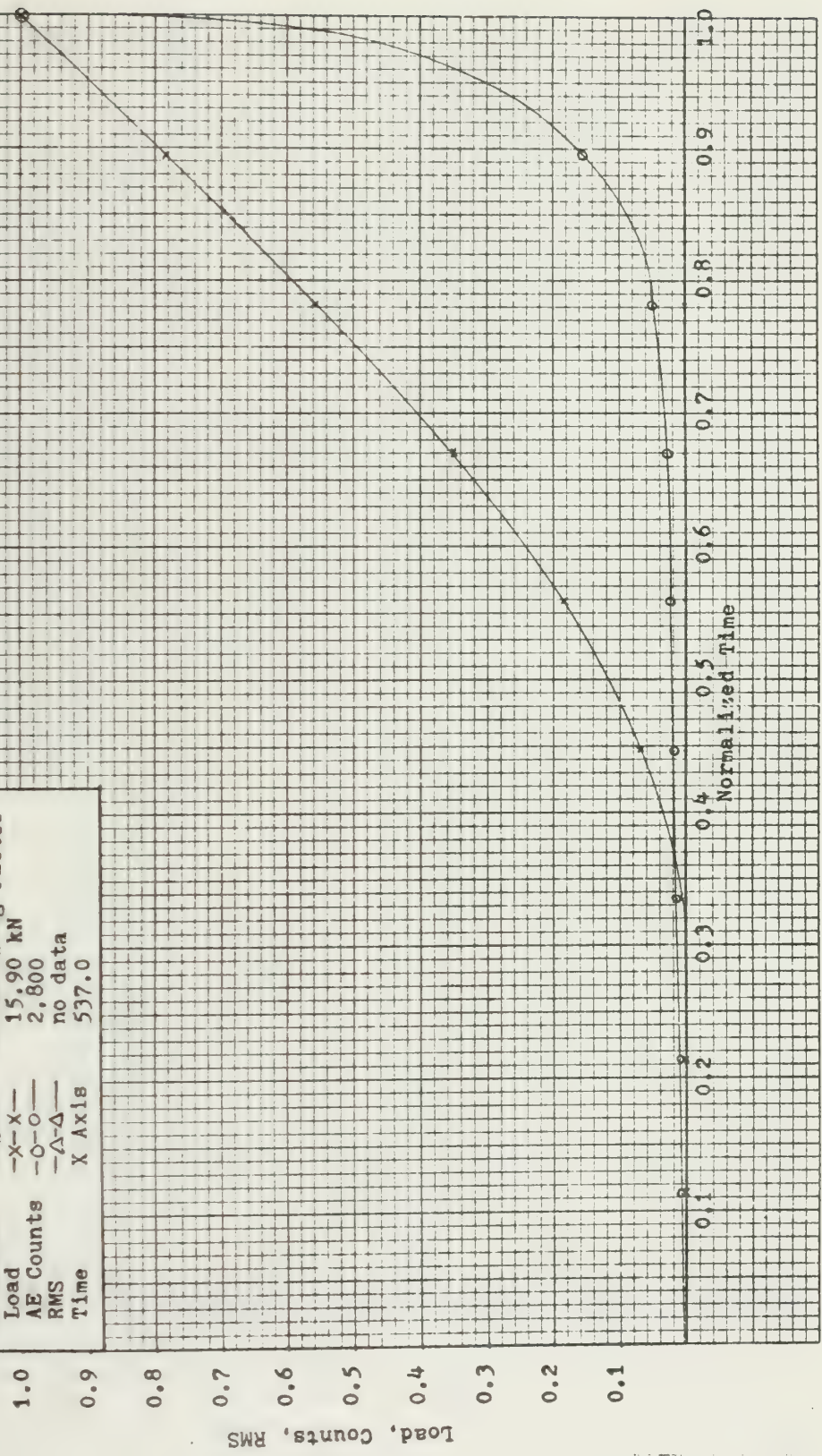




Figure 28

Specimen LV5H (0°)  
 Load, AE Counts, and RMS vs Time  
 AE Counts Threshold = 0.7 volts @ 100 dB

Parameter	Legend	Normalizing Factor
Load	x-x-	16.01 kN
AE Counts	-o-o-	13,850
RMS	-Δ-Δ-	59.6 mv
Time	X Axis	591.0 sec.

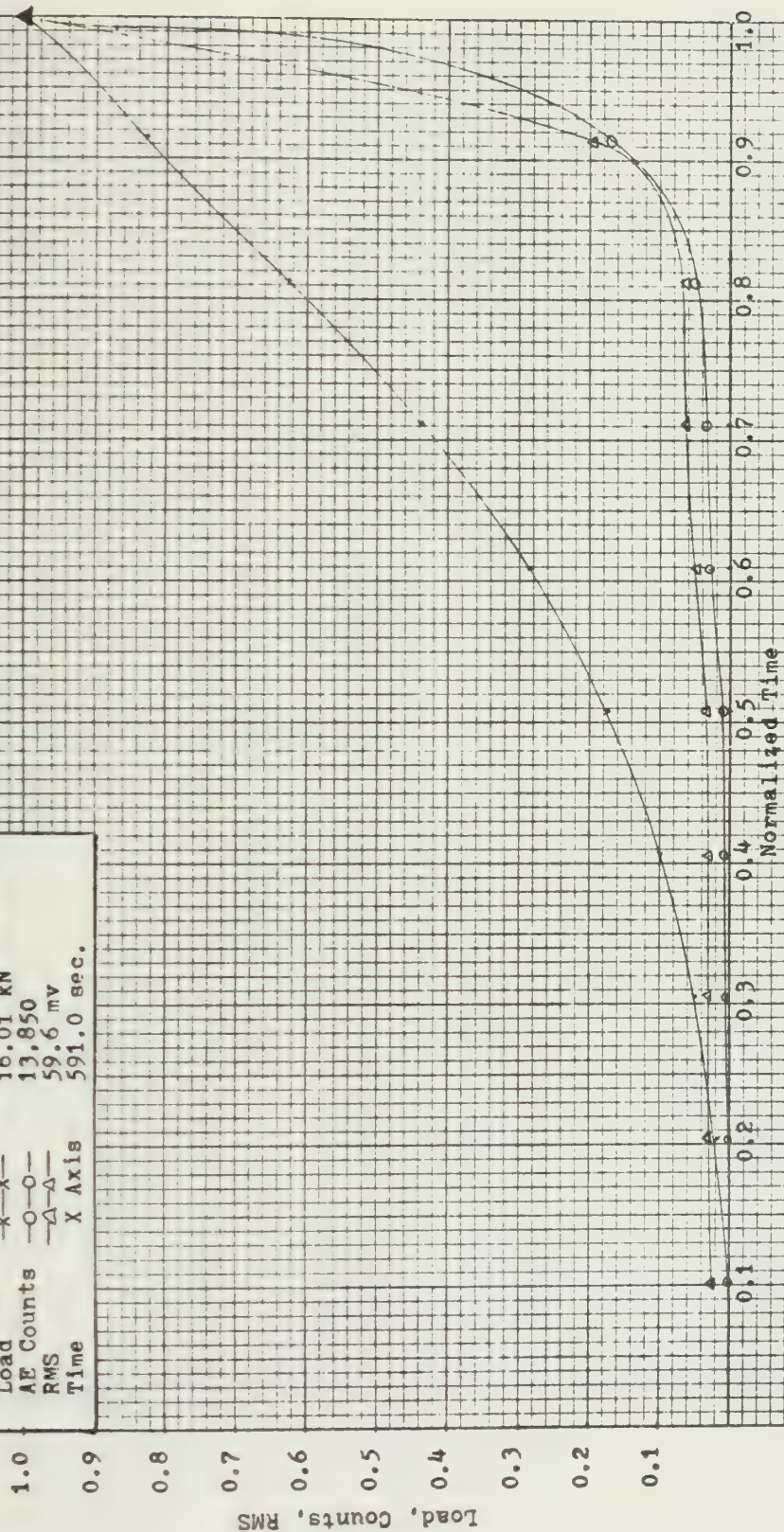


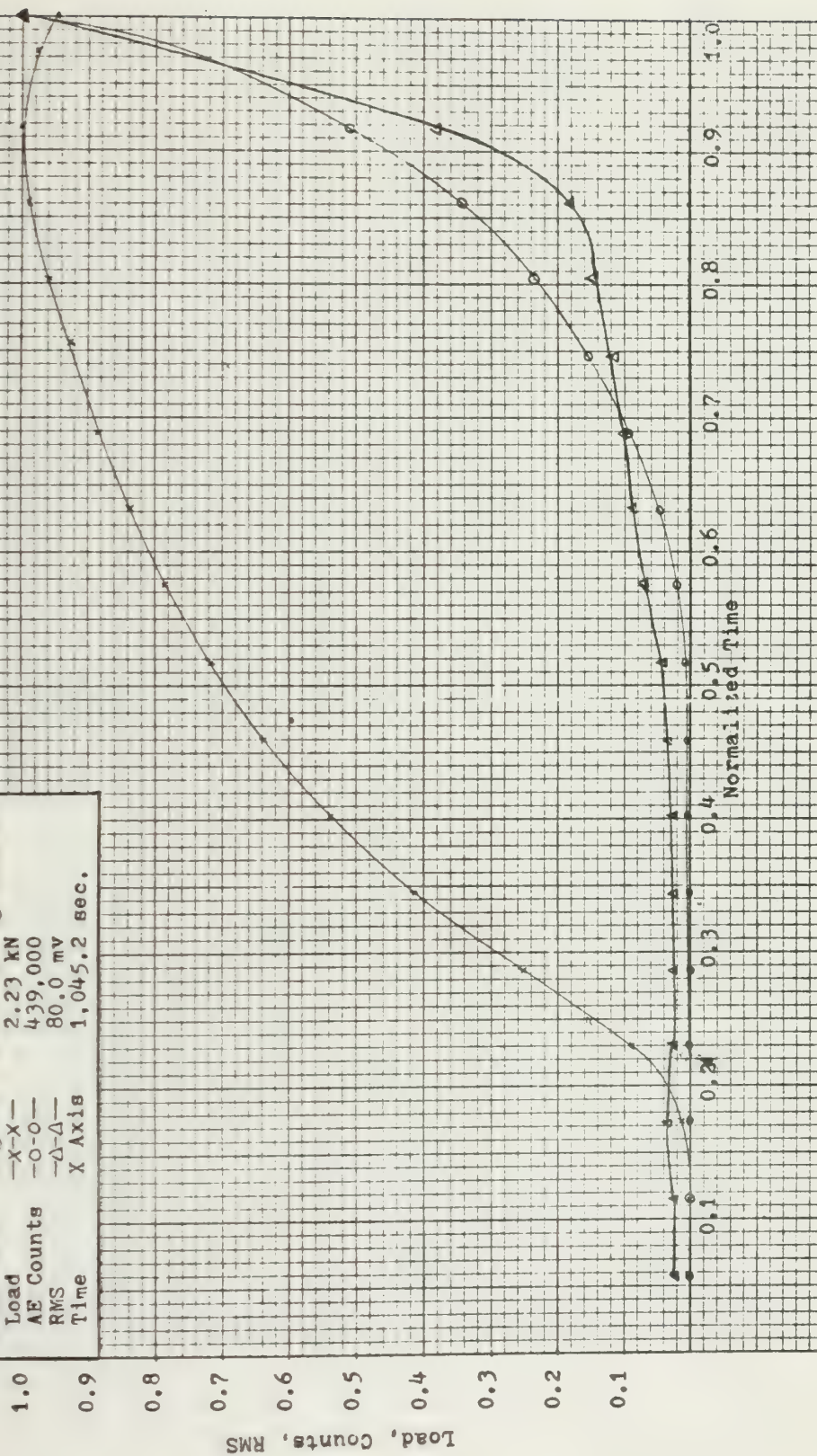




Figure 29

Specimen LV5CA ( $\pm 45^\circ$ )  
 Load, AE Counts, and RMS vs Time  
 AE Counts Threshold = 0.7 volts @ 100 dB

Parameter	Legend	Normalizing Factor
Load	-X-X-	2.23 kN
AE Counts	-O-O-	439,000
RMS	-Δ-Δ-	80.0 mv
Time	X Axis	1,045.2 sec.





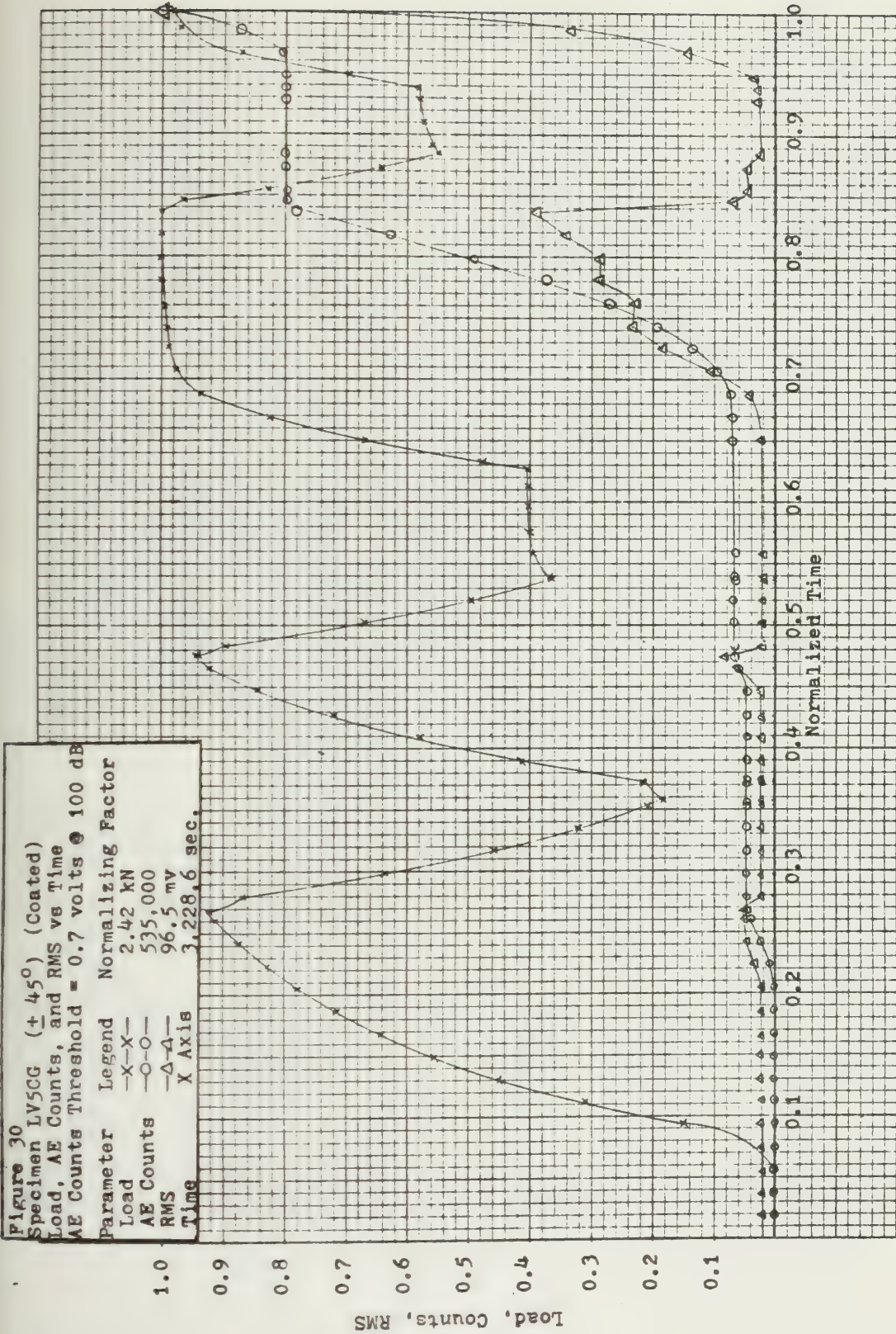






Figure 31

Specimen LV5C1 ( $\pm 45^\circ$ ) (Coated)  
 Load, AE Counts, and RMS vs Time  
 AE Counts Threshold = 0.7 volts @ 100 dB

Parameter	Legend	Normalizing Factor
Load	-x-x-	2.30 kN
AE Counts	-o-o-	412,500
RMS	-Δ-Δ-	91.0 mV
Time	X Axis	966.0 sec.

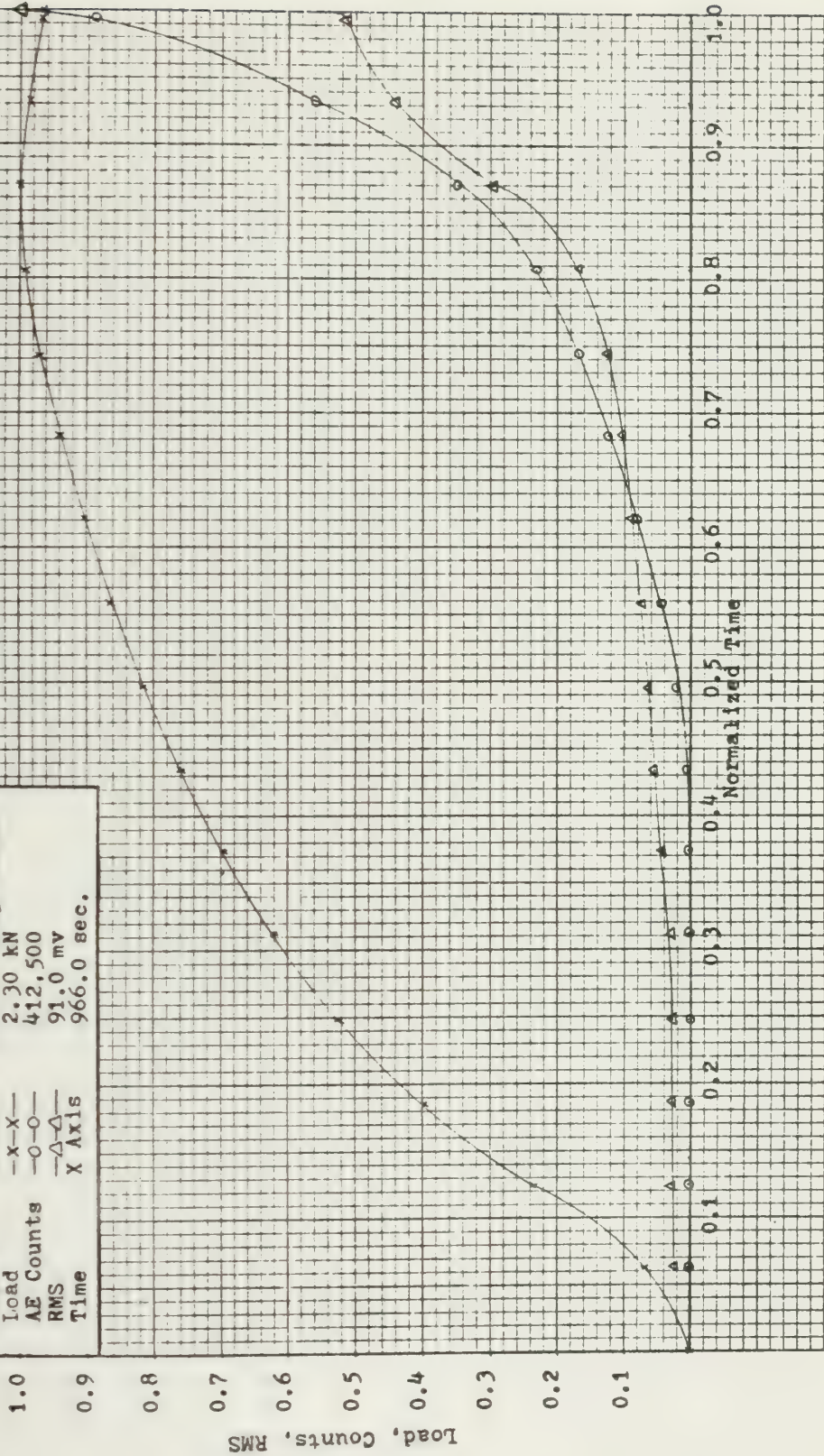






Figure 32

Specimen LV50J ( $\pm 45^\circ$ ) (Coated)

Load, AE Counts, and RMS vs Time

AE Counts Threshold = 0.7 volts @ 100 dB

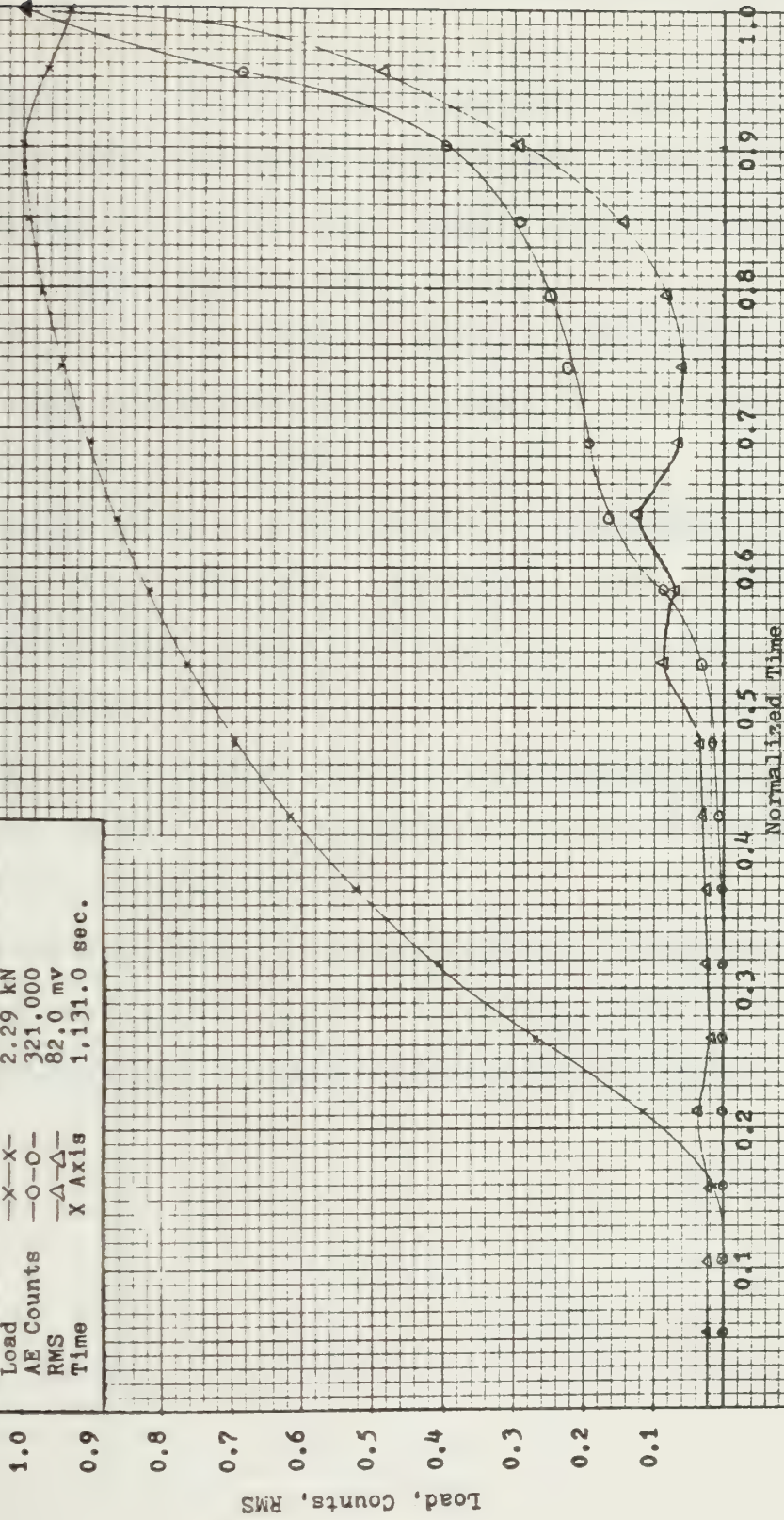
Parameter Legend Normalizing Factor

Load -x-x- 2.29 kN

AE Counts -o-o- 321,000

RMS -Δ-Δ- 82.0 mV

Time X Axis 1,131.0 sec.



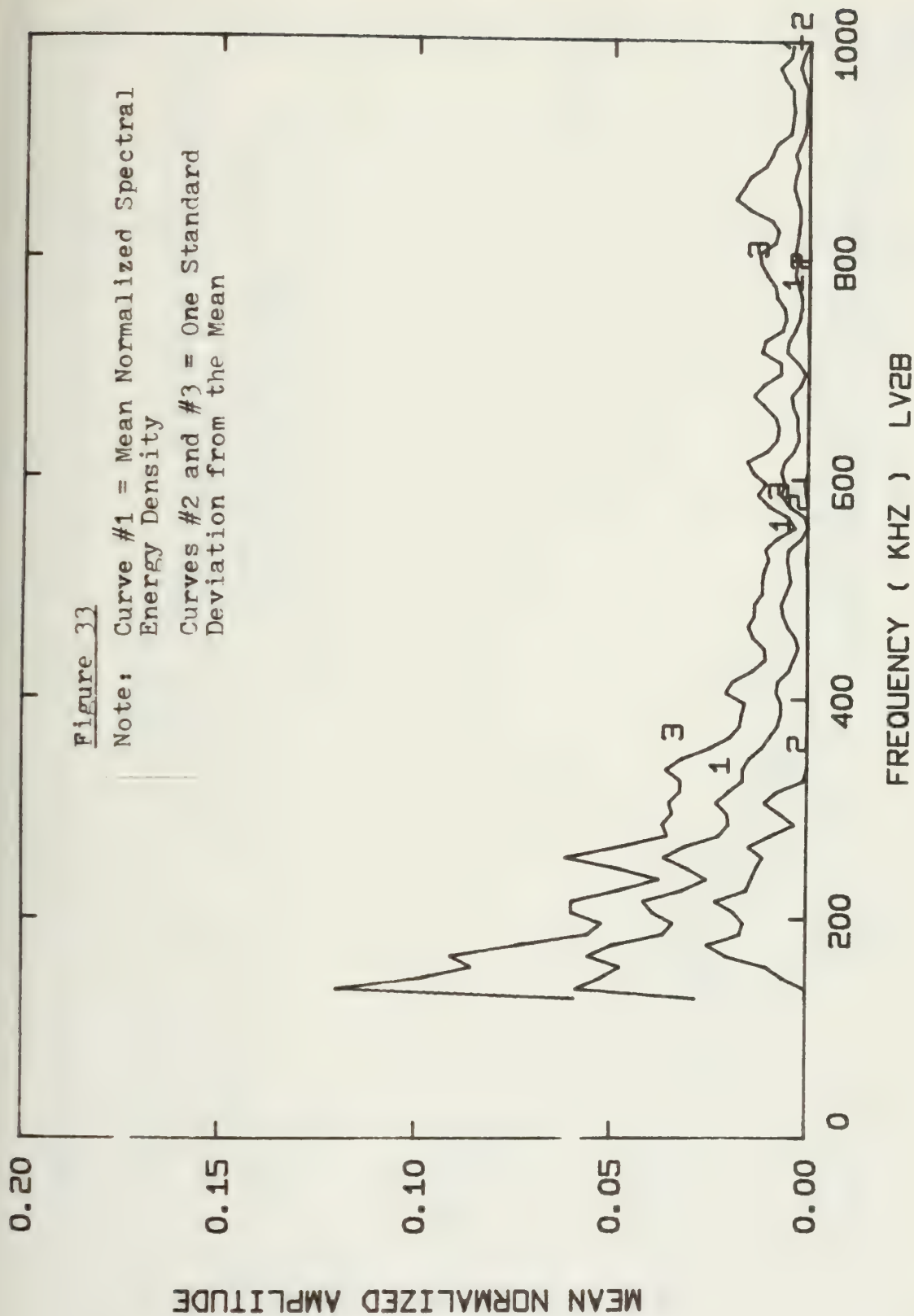


## Figures 33 - 47

### Mean Normalized Spectral Energy Distributions

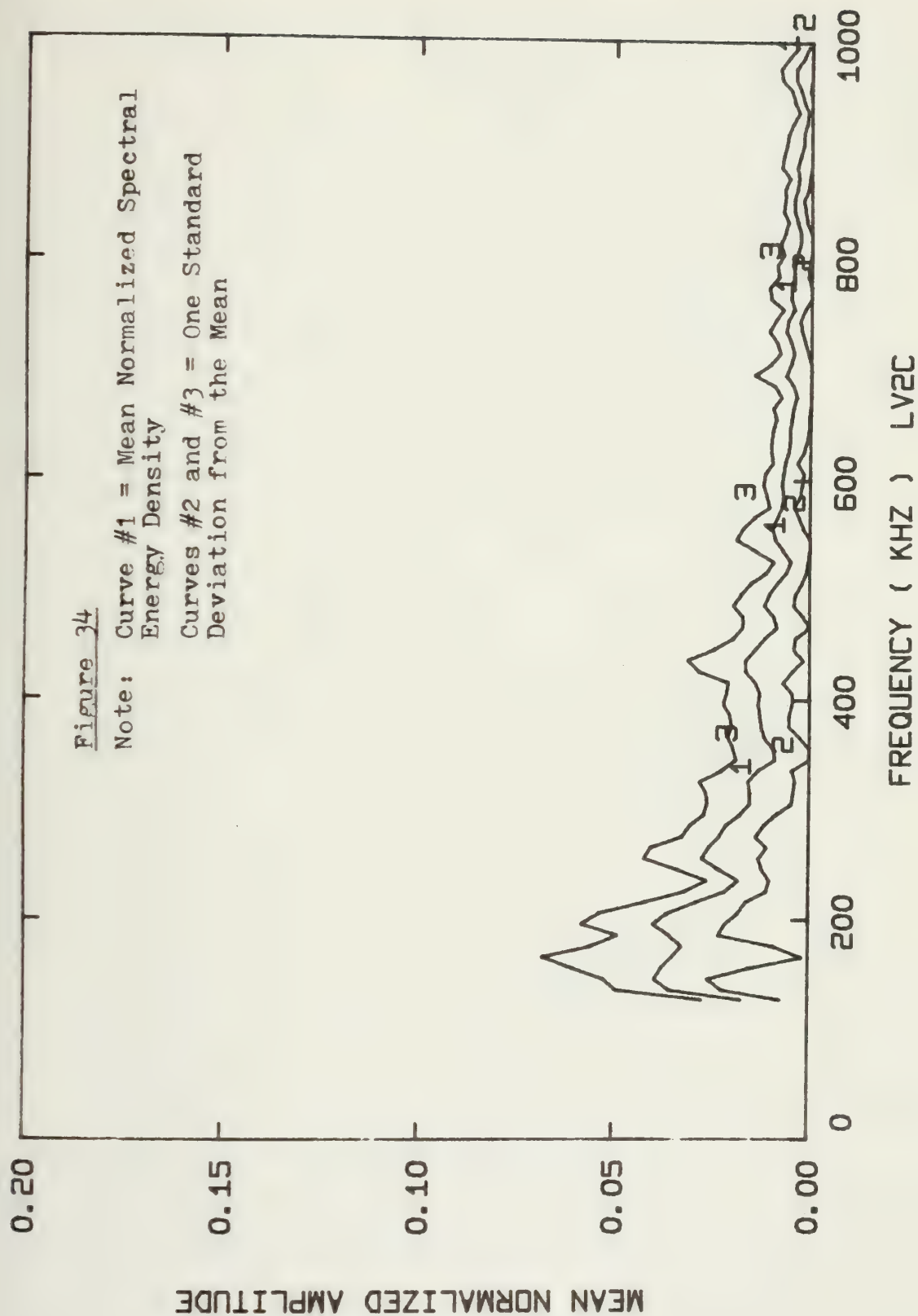
1. Curve #1 of each of the following figures represents the mean of all AE normalized spectral energy distributions (see Appendix C) which were analyzed for the particular specimen identified on the X axis.
2. The AE whose normalized spectra were used to generate these mean statistics were all sampled just prior to the rupture of each specimen.
3. Curves #2 and #3 are plotted one standard deviation from the mean (curve #1). (However, Curve #2 is somewhat distorted because negative values were plotted as zero on the graph.)
4. The units of the Y axis are non-dimensional.
5. See Appendix C for more details on the energy normalization procedure.
6. Also see Table 6 which summarizes the number of AE spectra used in the generation of each figure and the total energy used in the normalization procedure.



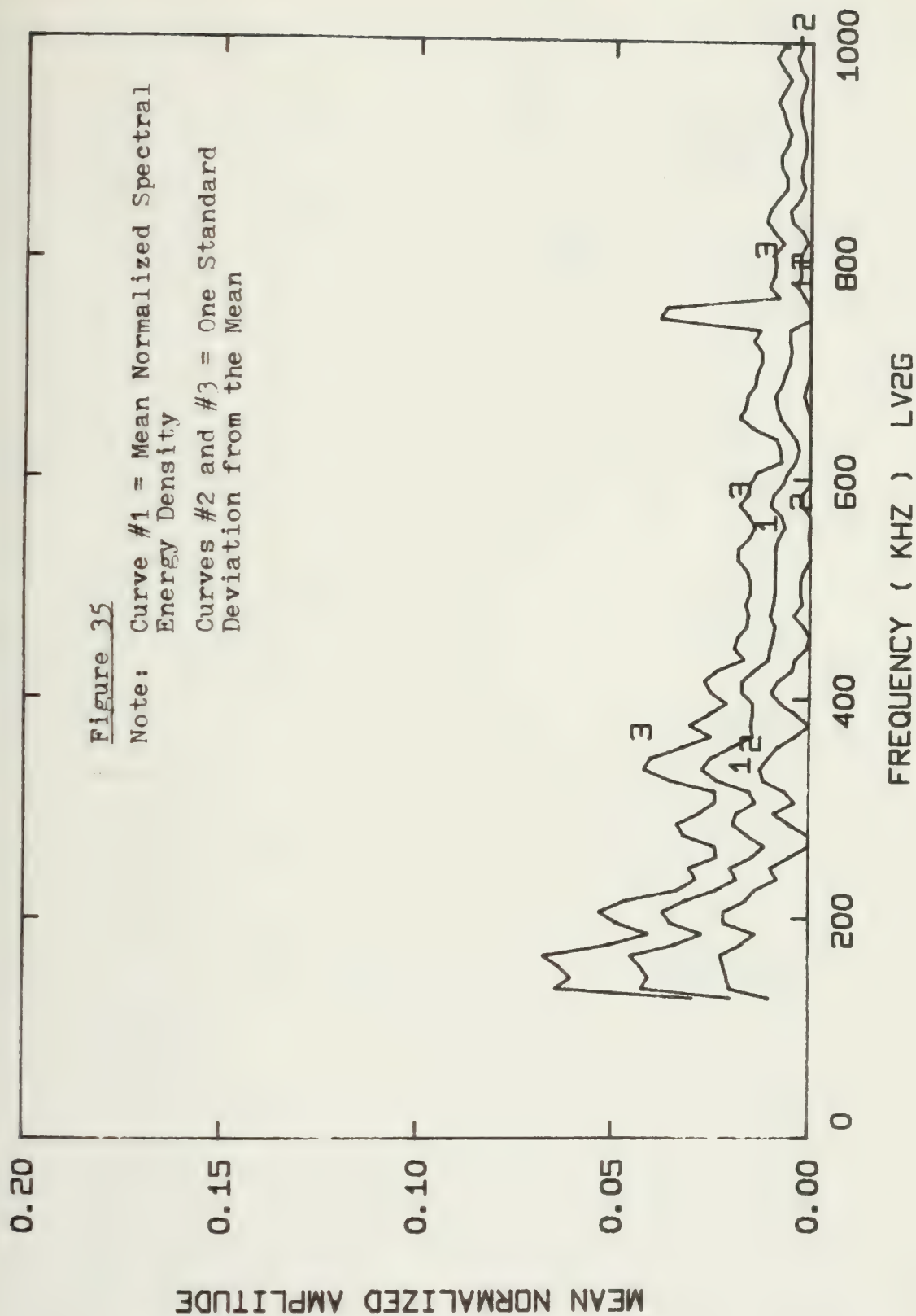




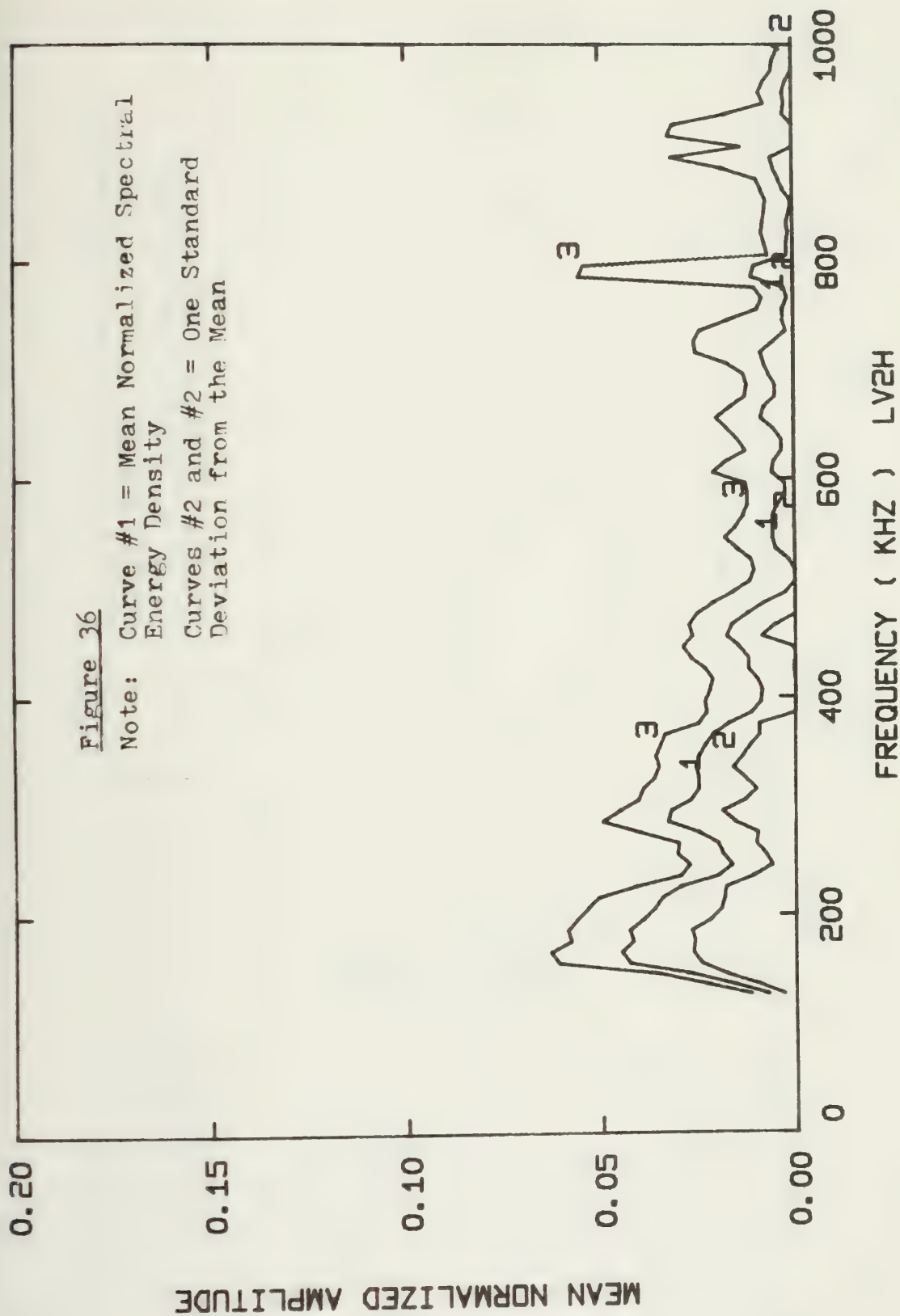






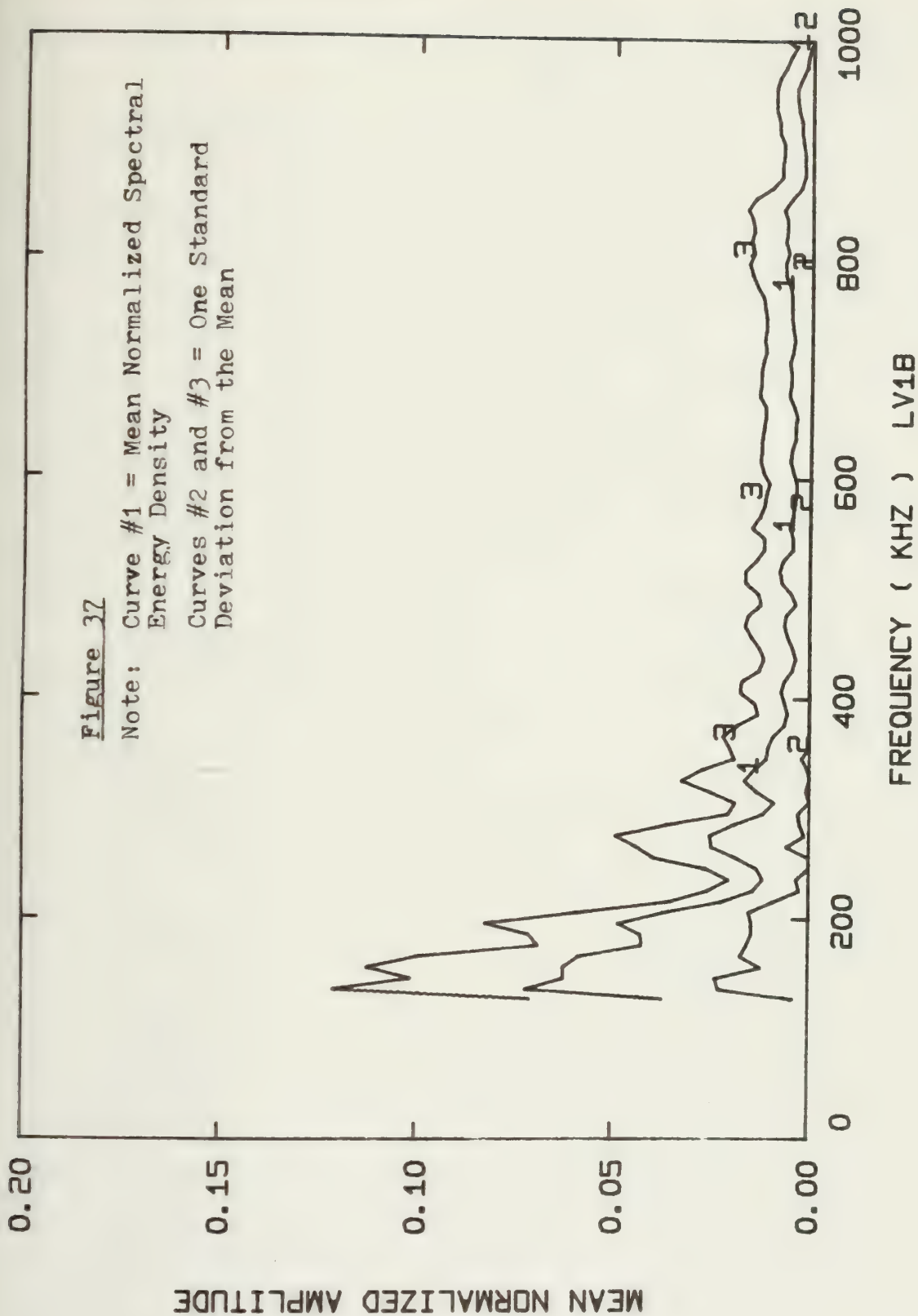




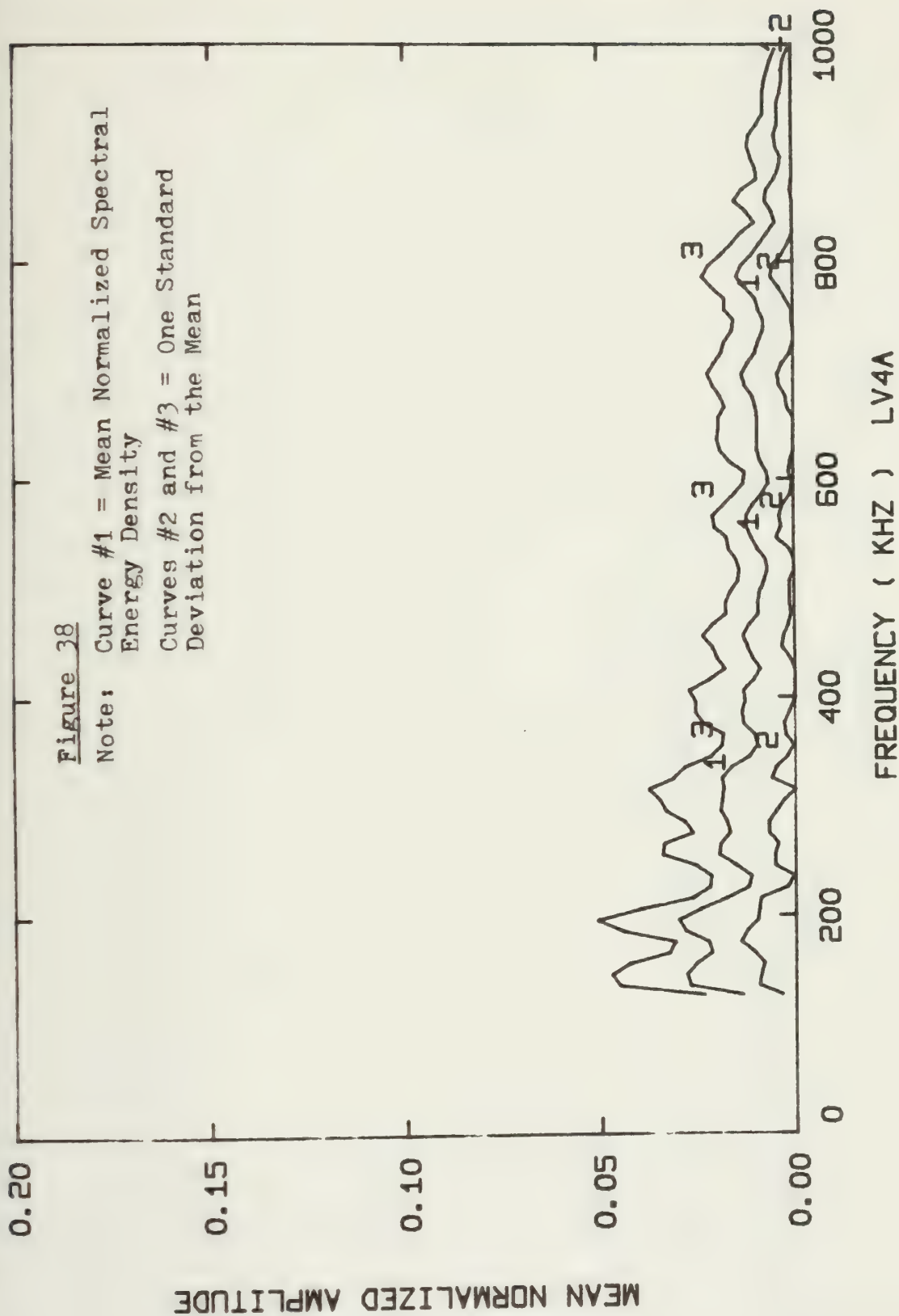




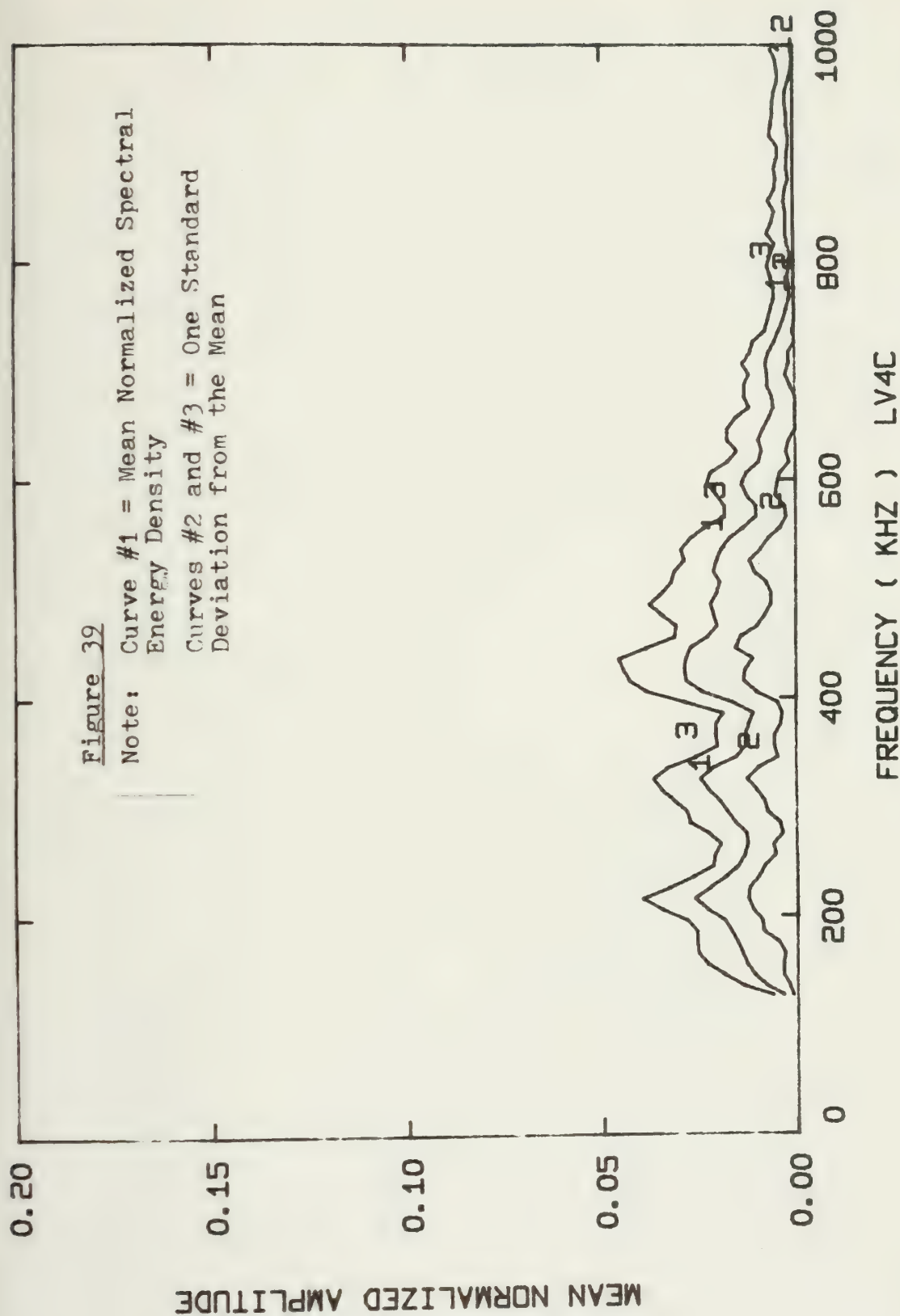






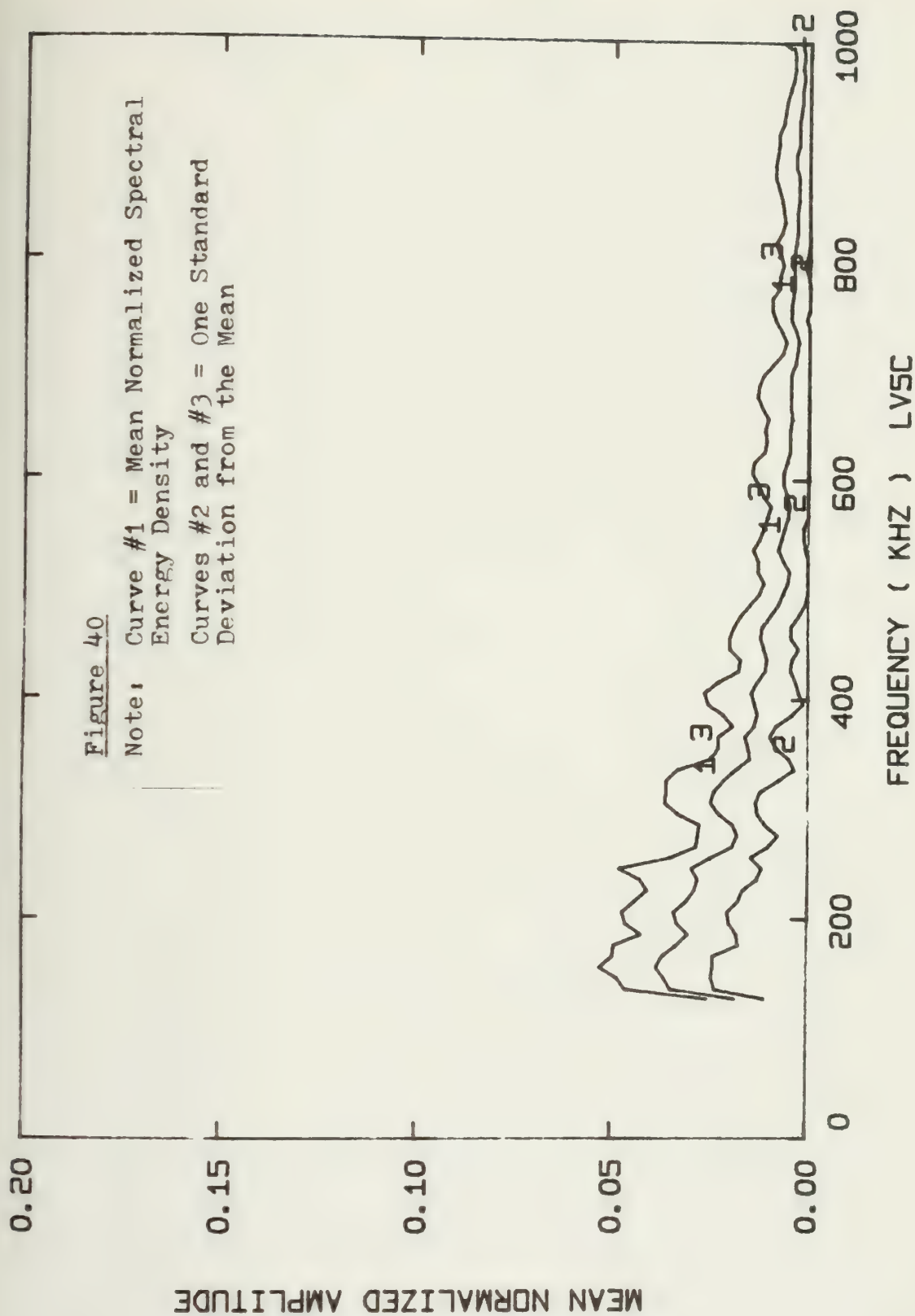




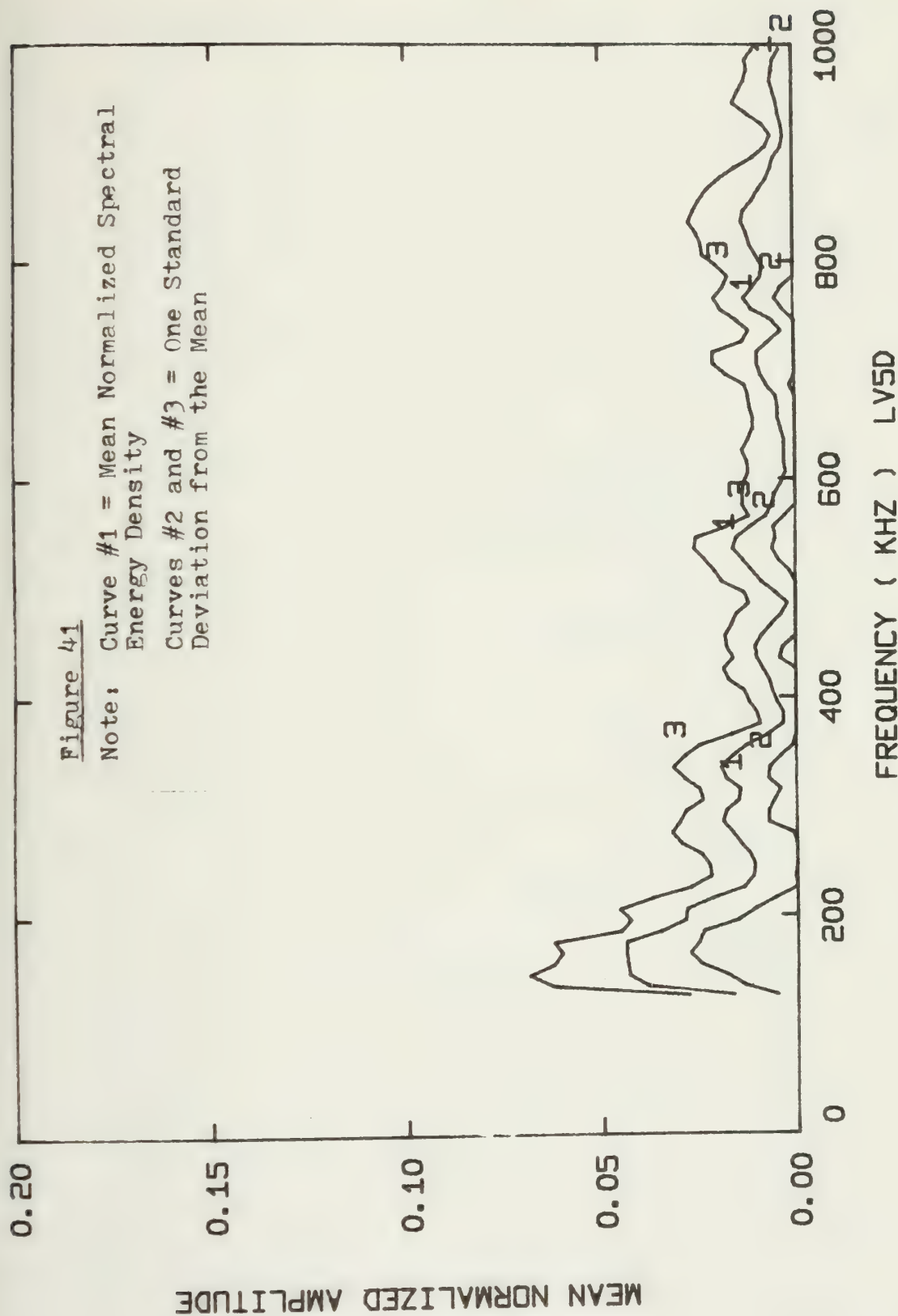




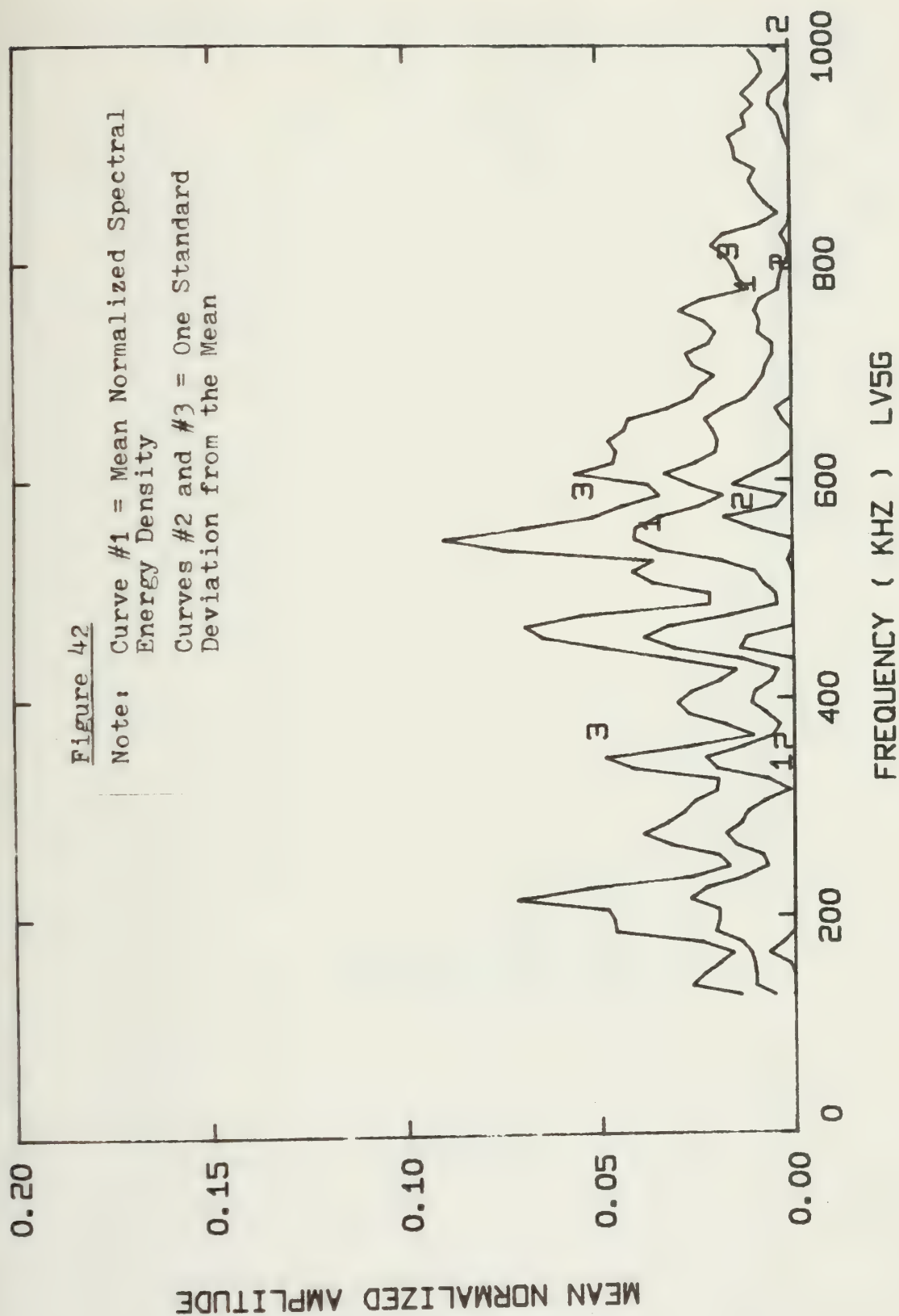






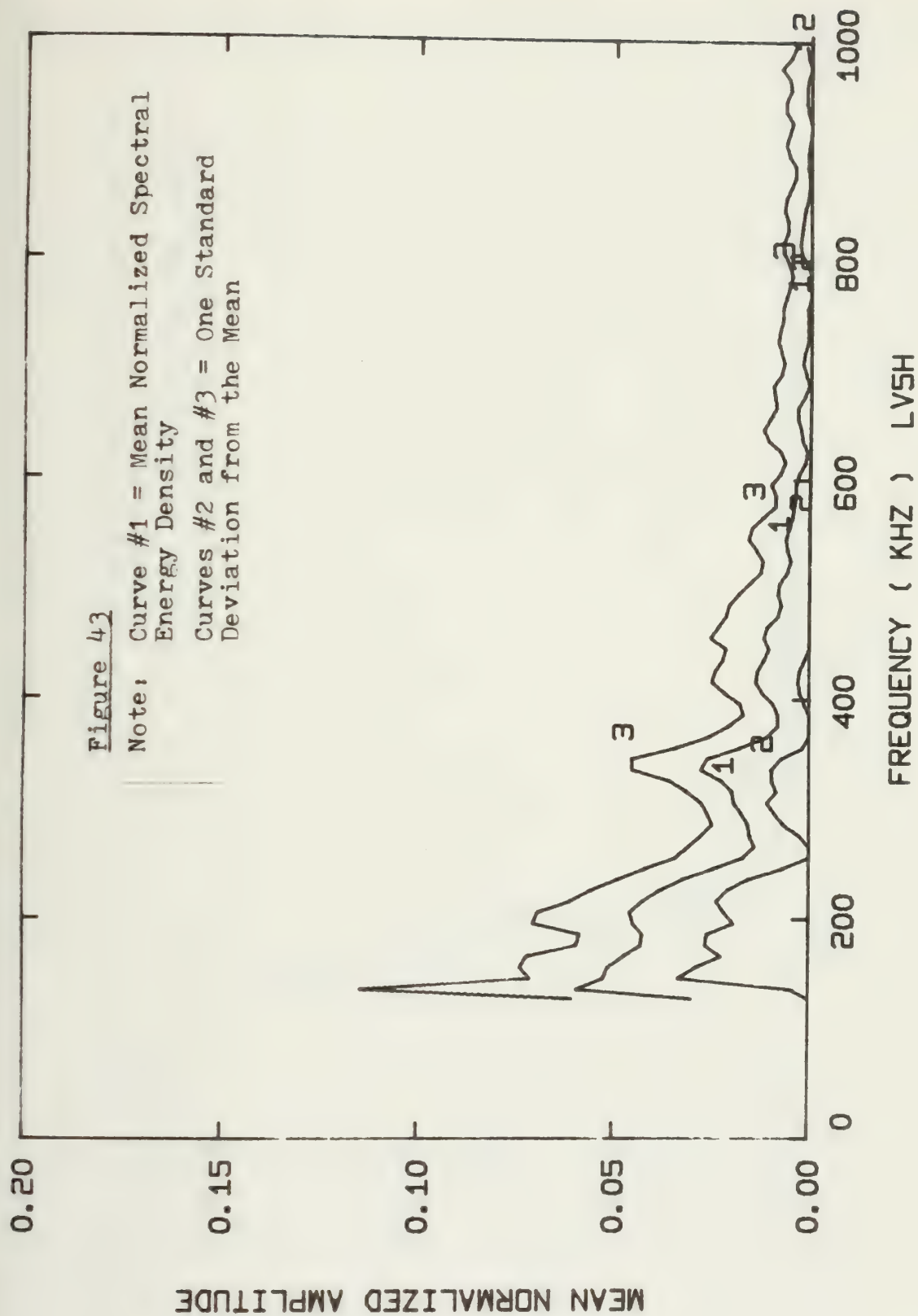




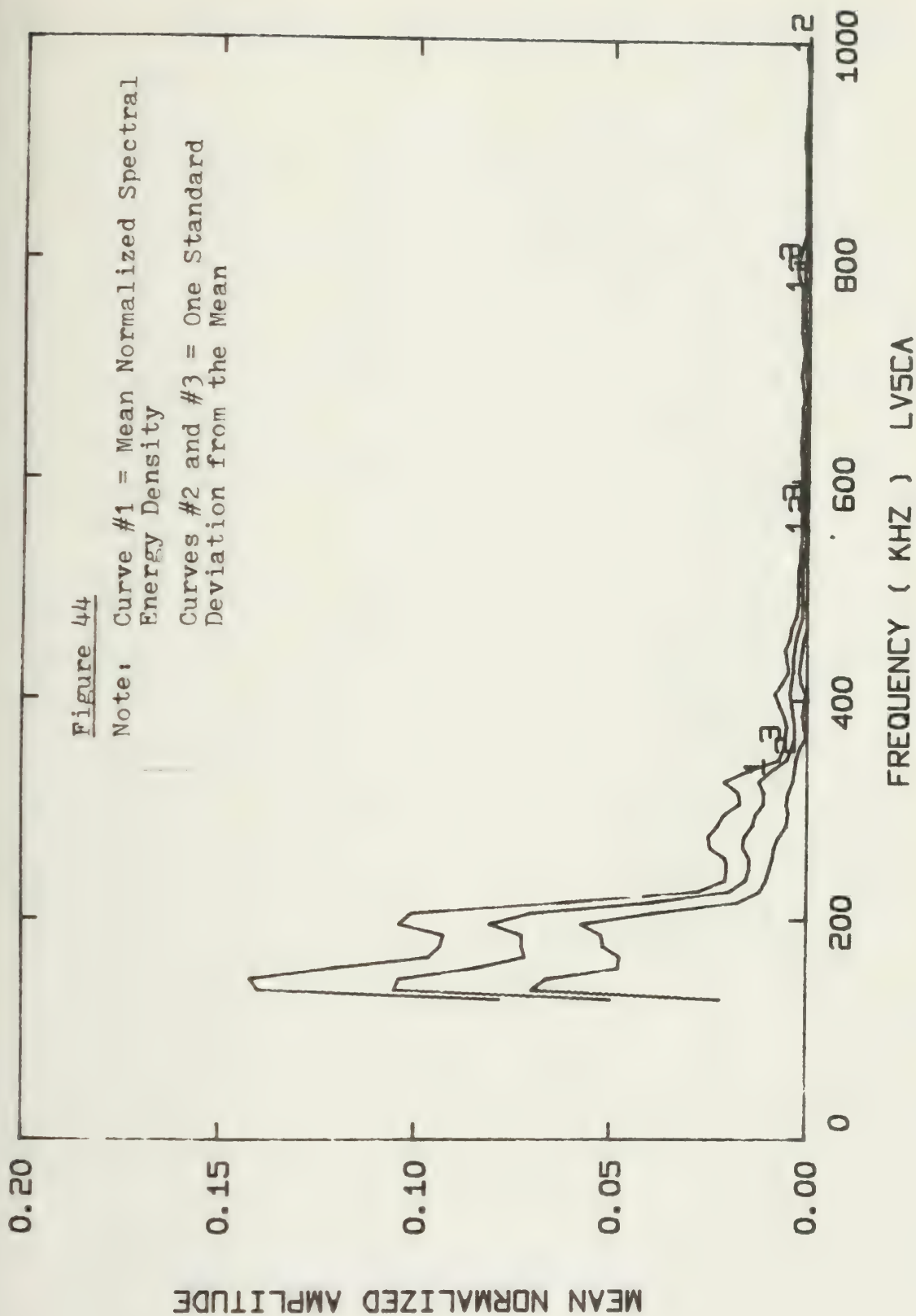




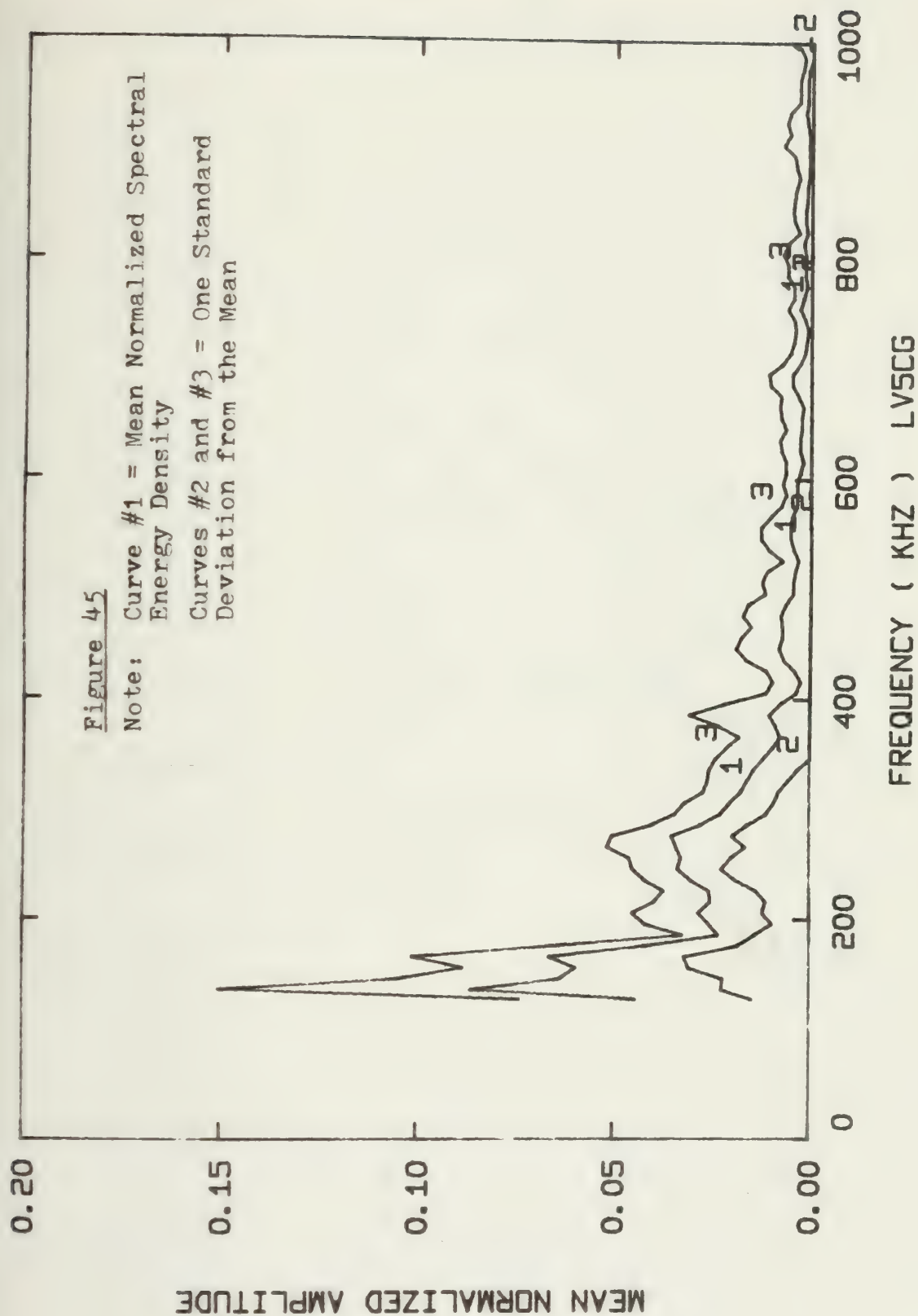




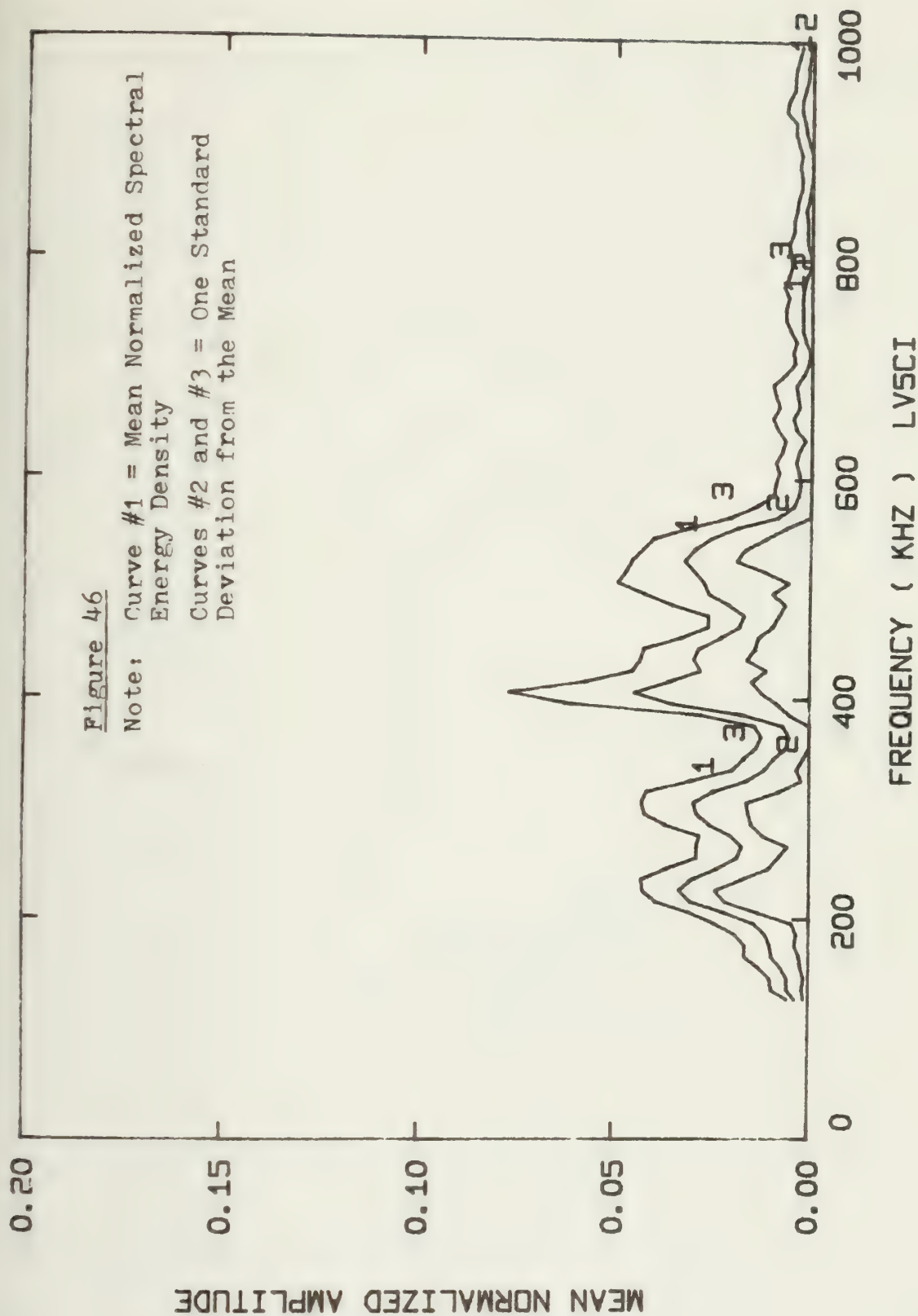
















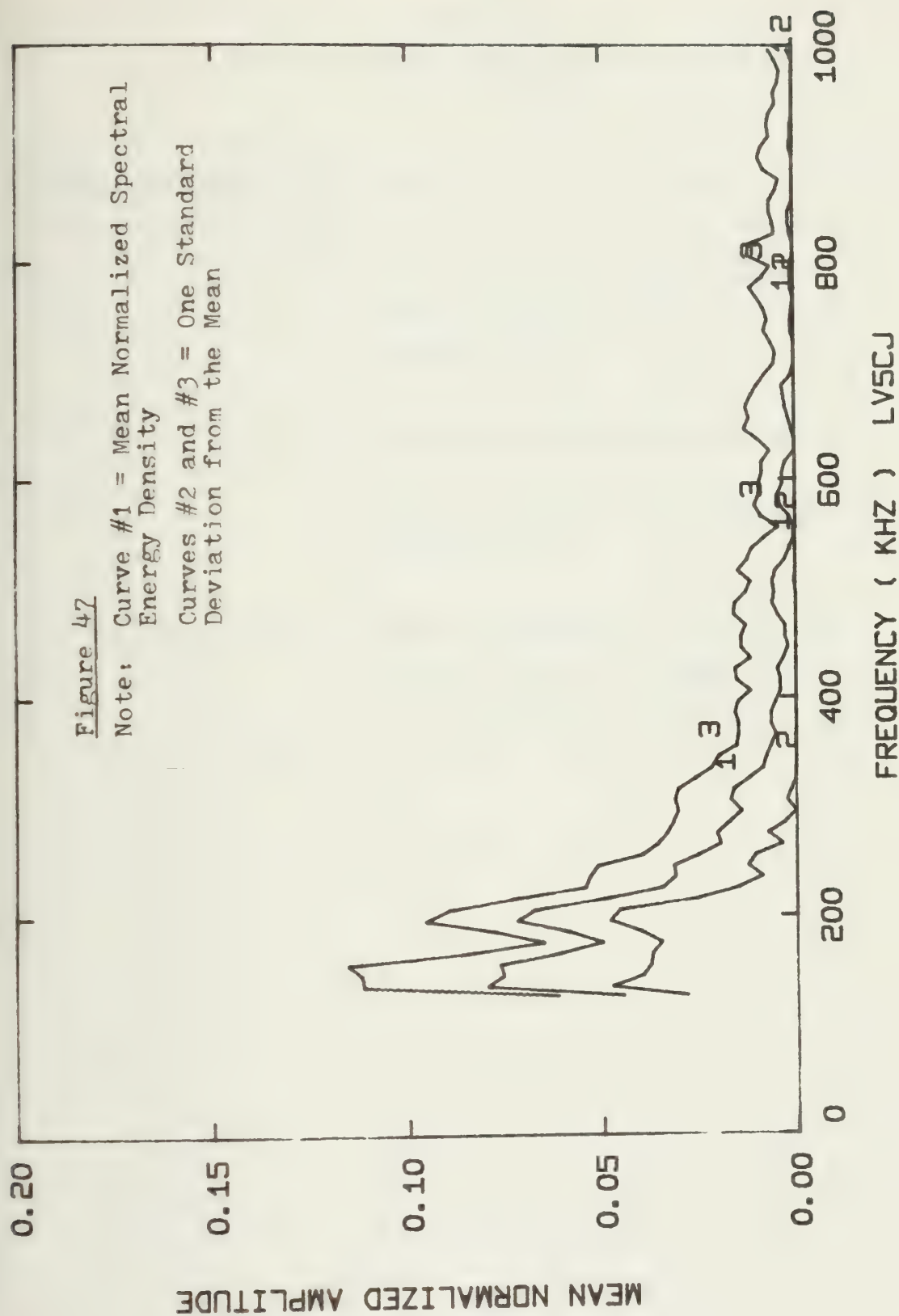




Table 1  
Expected Failure Modes of Specimens

Specimen Type	Expected Failure Modes
$0^\circ$	Fiber fracture, shear and/or tensile fracture of the matrix between fibers.
$10^\circ$	Intralaminar matrix cracking.
$90^\circ$	Tensile failure of the matrix between fibers.
$(\pm 45^\circ, \pm 45^\circ)_S$	Tensile cracking in the matrix between fibers followed by delamination and fiber fracture.



Table 2  
Specimen Identification

LV1B: Unidirectional,  $10^{\circ}$  off-axis

LV4A and LV4C: Unidirectional,  $10^{\circ}$  off-axis

LV2B, LV2C, LV2G, LV2H: Unidirectional,  $90^{\circ}$

LV5C, LV5D, LV5G, LV5H: Unidirectional,  $0^{\circ}$

LV5CA:  $(\pm 45^{\circ}, \pm 45^{\circ})_S$  (uncoated)

LV5CG, LV5CJ, LV5CI:  $(\pm 45^{\circ}, \pm 45^{\circ})_S$  with polyvinyl  
alcohol coated between 4th and  
5th plies.





Table 3  
Specimen Dimensions

	Specimen	Overall Length	Gauge Length	Width	Thickness
10°	LV1B	301.6 mm	174.6 mm	12.7 mm	1.029 mm
	LV4A	301.6 mm	174.6 mm	12.7 mm	1.041 mm
	LV4C	301.6 mm	174.6 mm	12.7 mm	1.035 mm
90°	LV2B	254.0 mm	120.6 mm	12.7 mm	0.978 mm
	LV2C	254.0 mm	120.6 mm	12.7 mm	0.991 mm
	LV2G	254.0 mm	120.6 mm	12.7 mm	0.991 mm
	LV2H	254.0 mm	120.6 mm	12.7 mm	0.991 mm
0°	LV5C	254.0 mm	120.6 mm	12.7 mm	1.016 mm
	LV5D	254.0 mm	120.6 mm	12.7 mm	1.041 mm
	LV5G	254.0 mm	120.6 mm	12.7 mm	1.041 mm
	LV5H	254.0 mm	120.6 mm	12.7 mm	1.016 mm
± 45°	LV5CA	254.0 mm	120.6 mm	12.7 mm	0.975 mm
	LV5CG	254.0 mm	120.6 mm	12.7 mm	0.978 mm
	LV5CI	254.0 mm	120.6 mm	12.7 mm	0.970 mm
	LV5CJ	254.0 mm	120.6 mm	12.7 mm	0.978 mm



Table 4  
Test Summary: AE Counts

Specimen	Crosshead Velocity mm/min	Failure Load (kN)	Distance from Transducer to Point of Failure (mm)	AE Counts Threshold (volts)	Total AE Count	Test Duration (sec)	Couplant
LV2B	.508	.832	51	0.9	2960	186.0	SC6+2RB
LV2C	.508	.845	67	0.8	2570	414.6	DEVCON 5***
LV2G	.508	.854	64	0.8	3375	1084.8	SC6+2RB
LV2H	.508	.934	57*	0.8	8750	636.0	DEVCON 5***
LV1B	.508	6.405	60*	0.8	105000	873.0	SC6+2RB
LV4A	.508	6.783	46*	0.7	131500	549.0	SC6+2RB
LV4C	.254	6.805	54*	0.7	195650	603.6	SC6+2RB
LV5C	.254	32.47	**	0.7	41550	1254.0	SC6+2RB
LV5D	.508	18.95	**	0.6	116275	1447.2	SC6+2RB
LV5G	.508	15.90	**	0.7	2800	537.0	SC6+2RB
LV5H	.508	16.01	**	0.8	13850	591.0	SC6+2RB
LV5CA	.508	2.23	89	0.7	439000	1045.2	DEVCON 5***
LV5CG	.508	2.42	86	0.7	535000	3228.6	SC6+2RB
LV5CI	.508	2.30	57	0.7	412500	966.0	SC6+2RB
LV5CJ	.508	2.29	44	0.7	321000	1131.0	DEVCON 5***

Notes: \* Average      \*\* Shattered      \*\*\* Epoxy couplant with thickness  
 $= 5.1 \times 10^{-2} \text{ mm} \pm 1.3 \times 10^{-2} \text{ mm}$



Table 5

## Summary of Mean and Standard Deviation of Failure Loads

Specimen Type	Mean Failure Load (kN)	Standard Deviation (kN)	Parameter of Scatter *
90°	0.831	0.0887	0.1068
10°	6.664	0.2249	0.0337
0°	20.672	6.1170	0.2959
(± 45°, ± 45°) <sub>s</sub>	2.310	0.0796	0.0345

\* Parameter of Scatter = Standard Deviation/Mean



Notes for Table 6

AS-1 graphite fiber (Hercules) had a tensile modulus (secant) of  $237.9 \times 10^{+3}$  MPa. The ultimate axial strength was 2.83 to  $3.10 \times 10^{+3}$  MPa.

PR-288 neat resin (3M) had a tensile modulus (secant) of  $3.45 \times 10^{+3}$  MPa. The ultimate axial strength was 57.92 MPa.

All specimens had a fiber volume fraction of 0.52.





Table 6  
Material Parameters

Specm.	Fiber Angle	Shear Modulus (secant) $\times 10^{-3}$ MPa	Tensile Modulus (secant) $\times 10^{-3}$ MPa	Poissons Ratio	Ultimate Axial MPa	Strength Shear MPa
LV1E	10°	3.97 $\pm$ .66	54.61 $\pm$ .28	.405 $\pm$ .23	436.4	74.47
LV1F	10°	1.50 $\pm$ .01	37.79 $\pm$ .55	.799 $\pm$ .07	464.0	79.29
LV1G	10°	2.07 $\pm$ .03	32.96 $\pm$ 1.45	.652 $\pm$ .06	489.6	84.12
LV2I	90°		10.89 $\pm$ .07	.0339 $\pm$ .0016	65.16	
LV2J	90°		11.24 $\pm$ .14	.0230 $\pm$ .0037	51.37	
LV2K	90°		10.62 $\pm$ .41	.0305 $\pm$ .0006	58.68	
LV4E	10°	1.33 $\pm$ .02	31.65 $\pm$ .90	.267 $\pm$ .018	473.0	80.67
LV4F	10°	1.23 $\pm$ .01	30.41 $\pm$ .28	.579 $\pm$ .026	477.8	81.36
LV4G	10°	1.70 $\pm$ .07	29.44 $\pm$ 1.10	.699 $\pm$ .125	470.2	80.67
LV5I	0°		127.6 $\pm$ 0	.304 $\pm$ .007	1262	
LV5J	0°		135.8 $\pm$ 1.4	.317 $\pm$ .007	1496	
LV5K	0°		124.1 $\pm$ 2.1	.286 $\pm$ .004	1468	



Table 7  
Test Summary: Spectral Analysis

Specimen (# of AE Spectra)	Crosshead Velocity (mm/min)	Failure Load (kN)	Mean Energy per AE from Amplifier (Joules x 10 <sup>+6</sup> )	RMS Pressure per AE at Transducer (Pa x 10 <sup>+5</sup> )	Distance from Transducer to Point of Failure (mm)
LV2B (14)	.508	.832	21.52	168.89	51
LV2C (10)	.508	.845	2.583	131.13	67
LV2G (14)	.508	.854	0.3198	92.63	64
LV2H (29)	.508	.934	65.80	116.52	57*
LV1B (33)	.508	6.405	3.916	107.85	60*
LV4A (20)	.508	6.783	0.1393	74.84	46*
LV4C (26)	.254	6.805	0.3648	88.68	54
LV5C (16)	.254	32.47	5.9811	83.41	**
LV5D (19)	.508	18.95	0.07143	57.58	**
LV5G (12)	.508	15.90	0.09315	56.03	**
LV5H (23)	.508	16.01	0.02684	52.25	**
LV5CA (19)	.508	2.23	18.61	476.68	89
LV5CG (19)	.508	2.42	68.38	444.81	86
LV5CI (15)	.508	2.3	0.4009	91.74	57
LV5CJ (22)	.508	2.29	0.4399	93.18	44

Notes:      \*Average      \*\*Shattered



Table 8  
Summary of Paired-Sample t Statistics  
over Frequencies 125 kHz to 800 kHz

	0°	10°	90°	± 45
0°	16.7	25.0	31.2	56.2
10°	25.0	66.7	50.0	50.0
90°	31.2	50.0	66.7	56.2
± 45°	56.2	50.0	56.2	83.3

Level of significance = 0.74

Degrees of freedom = 67

This Table gives the percentage of specimen comparisons for which the hypothesis that "both specimens had the same mean normalized spectral energy distribution" was not rejected. (The higher the number, the more similar are the spectra)





## VIII. APPENDICES

### Appendix A. Techniques of Monitoring Acoustic Emission

Of several techniques of monitoring acoustic emission, (AE) the more popular measure AE event count, AE event rate count, ring down or upcrossing AE count, ring down AE count rate, AE-RMS, AE amplitude distribution and spectral analysis. Without exception, these techniques depend upon some type of transducer that will convert vibrational energy into an electric analog signal. Most transducers respond to acoustic emission at their natural resonant frequency. After necessary amplification, event counters are triggered each time the transducer is excited by a transient acoustic emission event. Event rate devices simply differentiate the accumulative AE event counting registers. Since most transducers are not critically damped, they will resonate or ring for a certain period after excitation. Most event counting devices will not count faster than this required damping period. Consequently, such devices are not as useful for applications where multiple acoustic emissions or continuous acoustic emissions are to be monitored.

Ring down or upcrossing counting devices trigger each time the signal voltage rises above a pre-set voltage threshold. Consequently, a single acoustic emission can register as several counts, as the transducer's response resonates above the threshold voltage several times.



Also, intermittent excursions of the system's background noise above the voltage threshold will also register as counts. The procedure is generally to set the threshold level such that the system is predominantly triggered by acoustic emission excitation and only infrequently by system background noise. For narrow band, resonant transducers, where the damping is independent of amplitude and frequency, Beattie (18) shows that the ring-down count is related to the energy of the acoustic emission signals. Ring-down count rate devices simply differentiate the accumulative count registers.

RMS devices sample the amplified signals from the system and transducer and measure the root mean square of the total resulting signal voltage over prescribed time intervals. Such devices are especially useful in measuring multiple or continuous acoustic emissions which might saturate other devices.

Amplitude distribution devices generally measure the voltage amplitude of all AE or noise source events that rise above a pre-set minimum voltage threshold or in some cases fall within a pre-set voltage acceptance window. The numbers of events having particular amplitudes are stored in designated registers for later generation of an amplitude distribution output after many samples have been accumulated.



The same transient acoustic emission event must be input many times into a spectral analysis device to enable sufficient samples to be taken for the generation of the AE event's spectral energy distribution. This is made possible either by playing a loop of tape which contains only the AE event over and over again, or alternatively displaying one frame of a video tape recording, which contains the AE event, in stop action mode. A very wide band frequency response is easily obtainable with the latter technique. The additional utilization of a signal time-gate, synchronized to open during the AE event and to close at all other times, enhances the signal to noise ratio input to the spectral analyzer. The spectral analyzer is essentially a variable frequency, narrow-band filter with an RMS meter or scope to display the filter output. The filter's center frequency is continuously varied across a selected bandwidth at a pre-set scan rate. A long averaging time (low scan rate) and a sharp filter with a very narrow bandwidth will enhance the accuracy and the resolution of the measured spectral density.

One of the minor difficulties encountered in spectral analysis is separating the spectrum of the AE event from the spectrum of the system background noise upon which the AE spectrum is superposed. Newland (19) addresses such a problem in his discussion of the output spectral density





resulting from the input of two random process sample functions. Assuming that an AE event and the system background noise are independent random events with no correlation, the output spectral density is given by:

$$S_y(f) = \left| H_1(f) \right|^2 S_{x_1}(f) + \left| H_2(f) \right|^2 S_{x_2}(f)$$

where  $S_y(f)$  = mean square voltage spectral density which is output from the spectral analyzer due to the input of the AE event superposed upon system background noise.

$S_{x_1}(f)$  = mean square voltage spectral density of the acoustic emission event which is input into the spectral analyzer.

$S_{x_2}(f)$  = mean square voltage spectral density of the system's background noise which is input into the spectral analyzer.

$H_1(f)$  = the transfer function which yields the measured spectral density of the AE event. This measured spectral density, when averaged, is directly proportional to the spectral density of the AE event input.





$H_2(f)$  = the transfer function which yields the measured spectral density of the system's background noise. This measured spectral density, when averaged, is directly proportional to the spectral density of the system's background noise.

The assumption of independent random processes allows for the separation of the AE event's spectrum from the system background noise spectrum by a very simple process. First, a sample is obtained of system background noise occurring over an equal time duration as the AE event. This noise sample should be taken just prior to the AE event to insure independence. The mean square voltage spectral density of the system background noise is generated, maintaining the control settings on the spectral analyzer just like those used for processing the AE event itself. The mean square spectral density of the AE event can then be obtained by subtracting the system background noise spectrum from the spectrum which was measured due to input of the AE event superposed on background noise. Because the durations of the AE event and the sample of the system background noise are identical, the spectral energy density of the AE event may be obtained by dividing its mean square voltage spectral density by the 50 ohm input impedance of the spectral analyzer and then multiplying this quotient by the duration of the acoustic



emission event. If a presentation of normalized spectral energy distribution is desired, where normalization is done with respect to the total energy under the spectrum, the following procedure may be used:

The spectra can be divided up into incremental areas. The width of each area can be governed by the maximum resolution of the spectral analyzer. ( In this work this resolution was 10 kHz.) The height of each incremental area is governed by the ordinate of the mean square voltage spectral distribution multiplied by the duration of the AE event and divided by the 50 ohm input impedance of the spectral analyzer. The area in each increment represents ( for a two sided spectrum ) one half of the AE event's energy which exists within that particular incremental band of frequency. This incremental area is divided by the total area under the energy spectrum within the bandwidth of the AE system. This total area is simply the total area under the mean square voltage spectral distribution times the AE event's duration, divided by the 50 ohm input impedance. Conveniently, the AE event's duration and the input impedance cancel out in the normalization procedure. To economize on computer time the normalized spectral energy distribution is obtained by simply normalizing the mean square voltage spectrum with respect to  $\overline{v}_{RMS}^2$ . A spectral energy distribution which is



normalized with respect to total AE event energy, is potentially desirable because it allows for direct spectral energy distribution comparisons between two different AE events, independent of each individual event's total energy.





## Appendix B. Computer Program

The following computer program was written to accept digitized RMS voltage spectra (linear scale), generate and plot the normalized spectral energy distribution for each AE, compute and plot mean normalized spectral energy distributions for each specimen, and statistically compare one specimen's mean spectrum to another specimen's mean spectrum using the paired-sample t test.



# A.E. SPECTRA NORMALIZATION, PLOT, AND PAIRED T STATISTIC

```

INTEGER J
INTEGER*2 XLAB(40)
REAL ARRAY (4,88),XSCL(4)
REAL ARAY(2,88)
DIMENSION IA(89),P(89),R(89),C(89),D(88),E(88),F(88),G(88),FREQ(89
*),FMEAN(89),TMEAN(15,88),TSTD(15,88),STD(88)
DIMENSION IB(89)
DELTA =10.
FREQ(1)=127.5
FREQ(2)=135.
Q=0
DO 1 I=3,88
  FREQ(I)=FREQ(I-1)+10.
1 CONTINUE
NIKE =0
READ (6,3) NARGE
2 CALL FINIT(F,S,FMEAN,STD,P,88)
3 FORMAT (15)
5 DO 8 I=1,89
  IA(I)=0
  A(I)=0.
  IB(I)=0
  R(I)=0.
  C(I)=0.
  IF(I.LT.88) GO TO 8
  D(I)=0.
  E(I)=0.
8 CONTINUE
9 READ(8,307) IA
300 FORMAT(15I5,I4)
DO 10 I=1,89
  A(I)=FLOAT(IA(I))

```



# A.E. SPECTRA NORMALIZATION, PLOT, AND PAIRED T STATISTIC

```

10 CONTINUE
  READ(2,300) TB
  DO 20 I=1,89
    B(I)=FLOAT(IP(I))
    C(I)= A(I)**2.-B(I)**2.0
20 CONTINUE
  D(1)=(C(1)+C(2))*DELTA/4.
  SUM=D(1)
  DO 40 I=2,88
    J=I+1
    D(I)=((C(I)+C(J))*DELTA)/2.
    SUM=D(I)+SUM
40 CONTINUE
  READ(3,718) XLAB
  WRITE(5,718) XLAB
  WRITE (5,301) SUM
301 FORMAT(' SUM= ',E18.7)
  IF(SUM.LT.0.) GO TO 42
  GO TO 44
42 READ(9,400) M
  IF(M.LT.0) GO TO 498
  GO TO 5
44 DO 50 I=1,88
  E(I)=D(I)/SUM
45 ARAY(1,I)=E(I)
  IF (ARAY(1,I).GT.0.) GO TO 46
  ARAY(1,I)=0.000001
46 ARAY(2,I)=FREQ(I)
50 CONTINUE
  NVAR=2
  NPIS=98
  LABEL=-4
  ISCL=-2

```



# A.E. SPECTRA NORMALIZATION, PLOT, AND PAIRED T STATISTIC

```

      FTIME=0.
      LOOK=2
      MOVE = 1
      NROW=2
      NX=2
      DATA XSCL/100.,1000.,0.,.2/
      IF(MIKE.LP.MARGE)GO TO 59
      CALL PICTR(ARAY,NROW,XLAB,XSCL,NVAPS,NPTS,NX,MOVE,LABEL,ISCL,FTIME
*,LOOK)
59  CONTINUE
      DO 60 I=1,98
      F(I)=(E(I)+F(I))
      G(I)=(E(I)**2.0)+G(I)
60  CONTINUE
C    NOW READ EITHER A TITLE CARD CONTAINING A POSITIVE INTEGER IN
C    COLUMNS ONE AND TWO OR A NEGATIVE NUMBER IN COLUMNS ONE AND TWO.
C    A POSITIVE NUMBER INDICATES THAT A NEW SPECTRA FROM THE SAME
C    SPECIMEN IS TO BE PROCESSED. A NEGATIVE NUMBER SIGNALS THE END OF
C    SPECTRA TO BE PROCESSED FOR ANY ONE SPECIMEN AND ALLOWS THE
C    PROGRAM TO GO ON.
      READ(9,400)M
400  FORMAT(I2)
      MIKE = 1 + MIKE
      IF(M.LT.0)GO TO 500
      P=P+1.
      GO TO 5
C    IT IS IMPORTANT TO INCLUDE A NEGATIVE NUMBER IN COLUMNS 1 & 2
C    AFTER ALL OF THE SPECTRAL DATA OF ANY ONE SPECIMEN.
498  P=P-1.
500  P=P+1.0
C    P INDICATES HOW MANY SPECTRA WERE READ IN FOR EACH SPECIMEN
C    NOW CALCULATE THE MEAN SPECTRAL SIGNATURE WITH ITS STANDARD
C    DEVIATION FOR EACH SPECIMEN.

```





# A.E. SPECTRA NORMALIZATION, PLOT, AND PAIRED T STATISTIC

```

DO 550 I=1,88
STD(I)=SQRT(ABS((P*G(I)-F(I)**2.)/(P*(P-1.))))
FMEAN(I)= F(I)/P
550 CONTINUE
Q=Q+1
C Q COUNTS THE NUMBER OF SPECIMENS AND IS AN INTEGER
DO 620 I=1,88
TMEAN(Q,I)=FMEAN(I)
TSTD(Q,I)=STD(I)
620 CONTINUE
READ(9,400)K
C FOLLOWING THE NEGATIVE INTEGER PLACED AT THE END OF A SPECIMEN'S
C DATA SET, ADD AN ADDITIONAL K CARD. A BLANK CARD OR POSITIVE NO.
C IN COL. 1 & 2 INDICATES THAT MORE SPECIMENS ARE TO BE READ.
C A NEGATIVE NUMBER IN COLUMNS 1&2 INDICATES THAT ALL DATA HAS
C BEEN READ FROM ALL OF THE SAMPLES.
IF(K.LT.0) GO TO 700
GO TO 2
700 CONTINUE
C THE FOLLOWING PLOT ROUTINE REQUIRES Q TITLE CARDS, ONE FOR EACH
C SPECIMEN THAT WAS ANALYZED. THESE CARDS FOLLOW TWO MINUS INTEGER
C CARDS WHICH INDICATED THAT ALL SPECIMENS' DATA HAD BEEN READ IN.
C THE FIRST FORTY COLUMNS WILL BE USED TO LABEL THE X AXIS AND THE
C SECOND FORTY COLUMNS WILL BE USED TO LABEL THE Y AXIS.
NVAR=3
LABEL=4
NROW=4
NX=4
NROW=-1
DO 720 J=1,Q
DO 715 I=1,88
ARRAY(I,I)=TMEAN (J,I)
IF(ARRAY(I,I).GT.0.) GO TO 710

```



# A.E. SPECTRA NORMALIZATION, PLOT, AND PAIRED T STATISTIC

```

      ARRAY(1,I)=0.000001
710  ARRAY(2,I)=TMEAN(J,I)-ISTD(J,I)
      IF(ARRAY(2,I).GT.0.) GO TO 712
      ARRAY(2,I)=0.000001
712  ARRAY(3,I)=TMEAN(J,I)+ISTD(J,I)
      IF(ARRAY(3,I).GT.0.) GO TO 714
      ARRAY(3,I)=0.000001
714  ARRAY(4,I)=FREQ(I)
716  CONTINUE
      READ(9,719)XLAB
      WRITE(5,718)XLAB
718  FORMAT (40A2)
      PAUSE 2
      CALL PICTR(ARRAY,NROW,XLAB,XSCL,NVARS,NPTS,NX,MOVE,LABEL,ISCL,FTIM
•E,LOOK)
720  CONTINUE
C    THIS NEXT ROUTINE COMMENCES A PAIRED SAMPLE T STATISTICAL TEST OF
C    67 DEGREES OF FREEDOM. IT TESTS THE NULL HYPOTHESIS THAT ONE
C    SPECIMEN'S MEAN NORMALIZED SPECTRAL SIGNATURE IS FROM THE SAME
C    ENSEMBLE AS ANOTHER SPECIMEN'S MEAN NORMALIZED SIGNATURE. THIS
C    TEST ASSUMES THAT EACH SPECIMEN'S SIGNATURE COMES FROM A NORMAL
C    POPULATION OF SAMPLE SPACE MEAN SPECTRAL SIGNATURES. THEN THE
C    PAIRED T STATISTIC MAY BE USED REGARDLESS OF WHETHER THE SAMPLES
C    ARE INDEPENDENT ( SAMPLES MAY BE DEPENDENT UPON FREQUENCY ) OR
C    WHETHER THE POPULATION VARIANCES ARE EQUAL ( THEY PROBABLY ARE
C    NOT )
C    THIS SECTION OF THE PROGRAM REQUIRES THAT AT LEAST TWO SPECIMENS
C    BE AVAILABLE FOR ANALYSIS. (Q MUST BE GREATER THAN ONE )
      IF(Q.LT.2) GO TO 730
      L=Q-1
      DO 730 K=1,L
      DO 730 J=1,Q
      IF(J.GT.Q-K) GO TO 730

```



A.E. SPECTRA NORMALIZATION, PLOT, AND PAIRED T STATISTIC

```
NO =J+K
DO 725 I=1,88
F(I)=TMEAN(J,I)
G(I)=TMEAN(NO,I)
725 CONTINUE
T=0.
CALL PAIRT(F,G,T)
WRITE(5,740) T,J,NO
730 CONTINUE
740 FORMAT(' PAIRED T STATISTIC IS ',E14.7,' FOR SPECIMEN ', I2,' AND
*SPECIMEN ', I2)
STOP
END
*MAIN* HAS      NO ERRORS
```





# A.E. SPECTRA NORMALIZATION, PLOT, AND PAIRED T STATISTIC

```

SUBROUTINE PAIRT(A,B,T)
DIMENSION A(68),B(68),A1(68),A2(68)
D=0.
C=0.
DO 800 I=1,68
A1(I) = A(I)-B(I)
A2(I) = A1(I)**2.
C=A1(I) +C
D= A2(I) +D
900 CONTINUE
E=C/68.
SD=((D-(C**2.)/68.)/4556. )**0.5
T=E/SD
RETURN
END

SUBROUTINE FINIT(A,B,C,D,E,N)
DIMENSION A(88),B(88),C(88),D(88)
DO 850 I=1,N
A(I)=0.
B(I)=0.
C(I)=0.
D(I)=0.
850 CONTINUE
E=0.
RETURN
END

```

C



Appendix C. Tabulation of AE Spectral Energy, AE Pressure (RMS) Excitation of the Transducer, and Presentation of Normalized Spectral Energy Distributions for Each AE Event

1. Normalized AE spectral energy distributions are presented for each AE sampled just prior to specimen rupture.
2. The group of normalized AE spectral energy distribution graphs for each specimen are preceded by a tabulation sheet containing the graph identification code numbers (from the X axis on each respective graph), AE energies used to normalize each of the graphs, and their AE pressure (RMS) excitation respectively.
3. The units on the Y axis of each graph are non-dimensional. The procedure used to normalize the AE spectral energy distributions is accomplished as follows:
  - a. The spectral energy distribution of an AE is divided into 10 kHz wide increments between 130 kHz and 1 MHz.
  - b. Each incremental area is divided by the summation of all of the incremental areas. (This is energy divided by energy.)
  - c. The resulting value represents the fraction of total detected AE energy contained in each 10 kHz wide band-



width (frequency increment). Each of these values is plotted at the mid-frequency of their incremental bandwidth to generate a "normalized spectral energy distribution " .

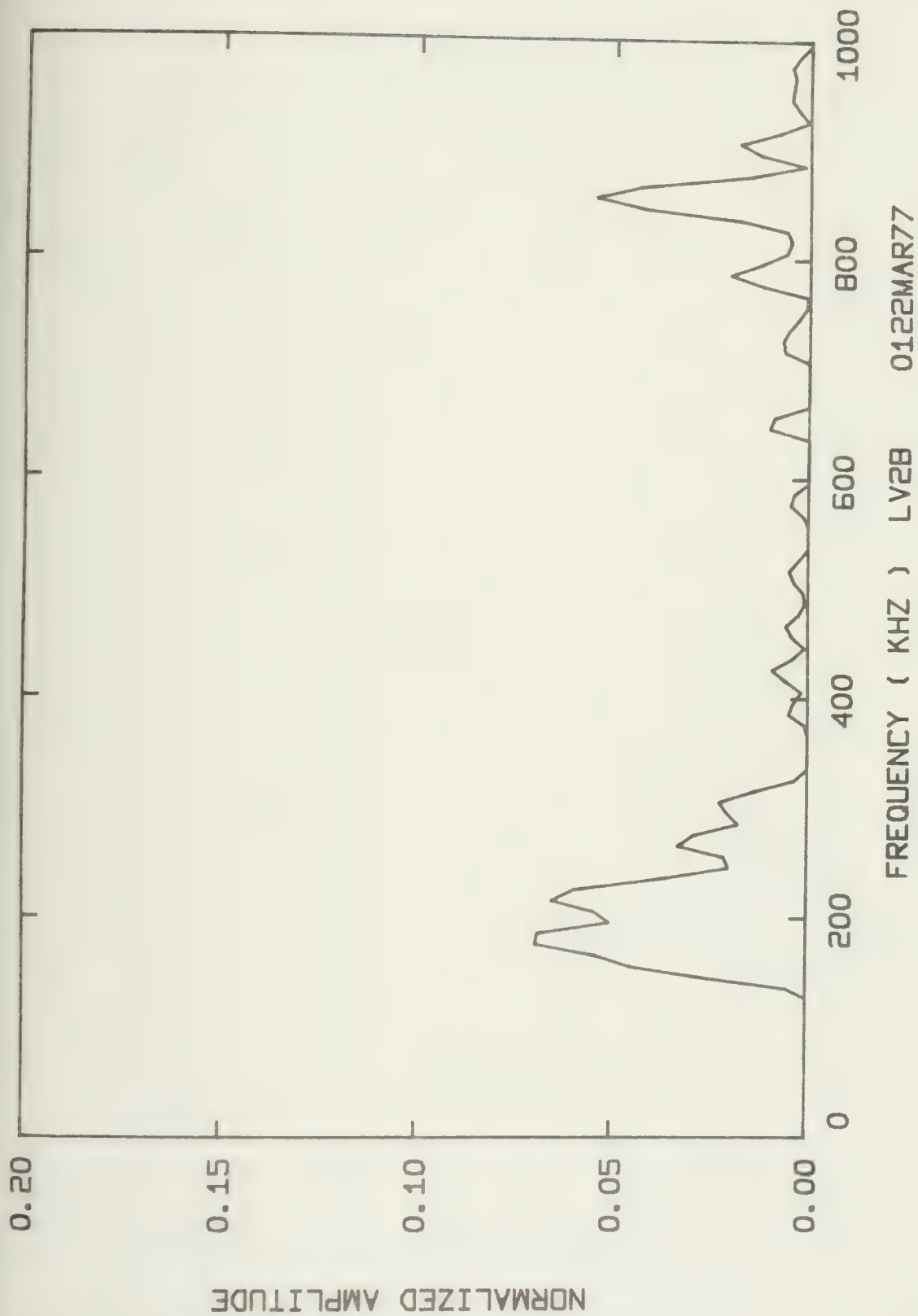


Summary of Energy per Acoustic Emission and RMS Pressure  
Across the Transducer's Face for Each Spectra

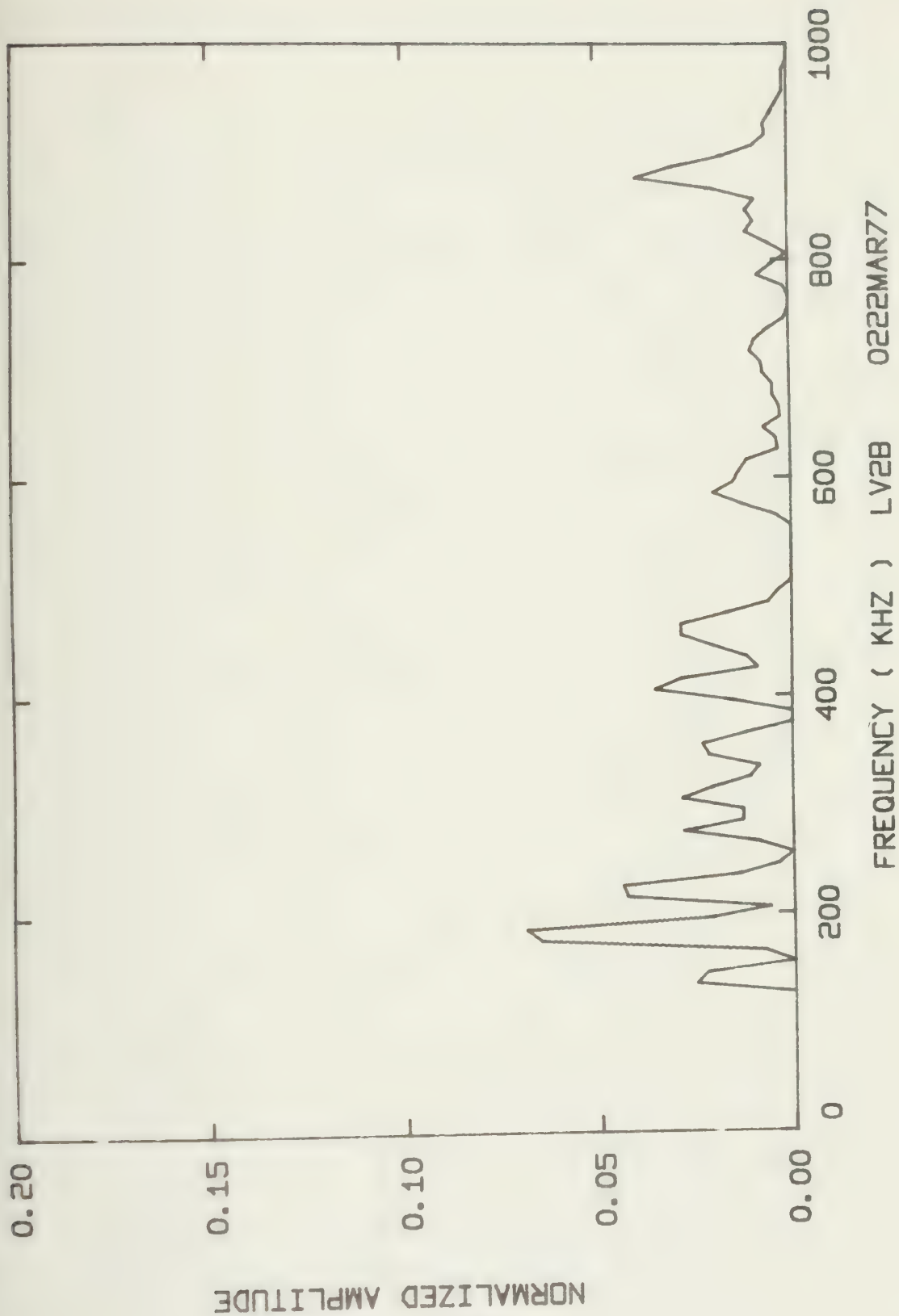
Spectral Distrib. Graph Code Number	Energy per AE (Joules)	RMS Pressure Across Face of Transducer (Pa x 10 <sup>5</sup> )
LV2B 0122MAR77	54.366 x 10 <sup>-9</sup>	59.58
0222MAR77	67.899 x 10 <sup>-9</sup>	63.95
0322MAR77	144.03 x 10 <sup>-9</sup>	85.26
0422MAR77	434.33 x 10 <sup>-9</sup>	116.1
0522MAR77	64.097 x 10 <sup>-9</sup>	69.47
0622MAR77	918.29 x 10 <sup>-9</sup>	153.06
0123MAR77	323.18 x 10 <sup>-9</sup>	108.78
0223MAR77	85.526 x 10 <sup>-9</sup>	65.52
0323MAR77	30.386 x 10 <sup>-6</sup>	49.24
0423MAR77	218.24 x 10 <sup>-9</sup>	72.94
0523MAR77	478.56 x 10 <sup>-9</sup>	122.04
0623MAR77	99.568 x 10 <sup>-9</sup>	61.225
0823MAR77	16.060 x 10 <sup>-6</sup>	414.45
0923MAR77	230.46 x 10 <sup>-6</sup>	922.78



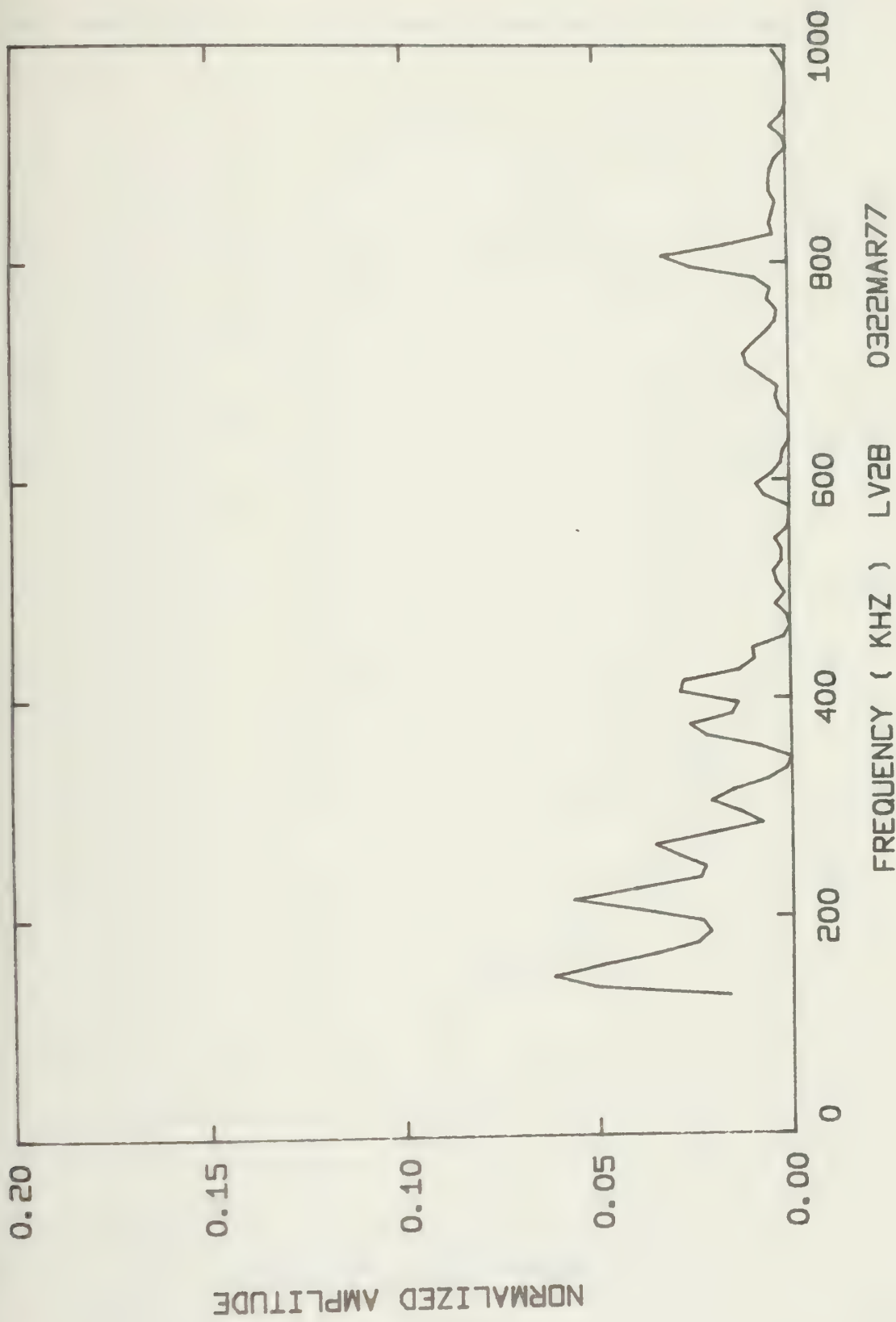






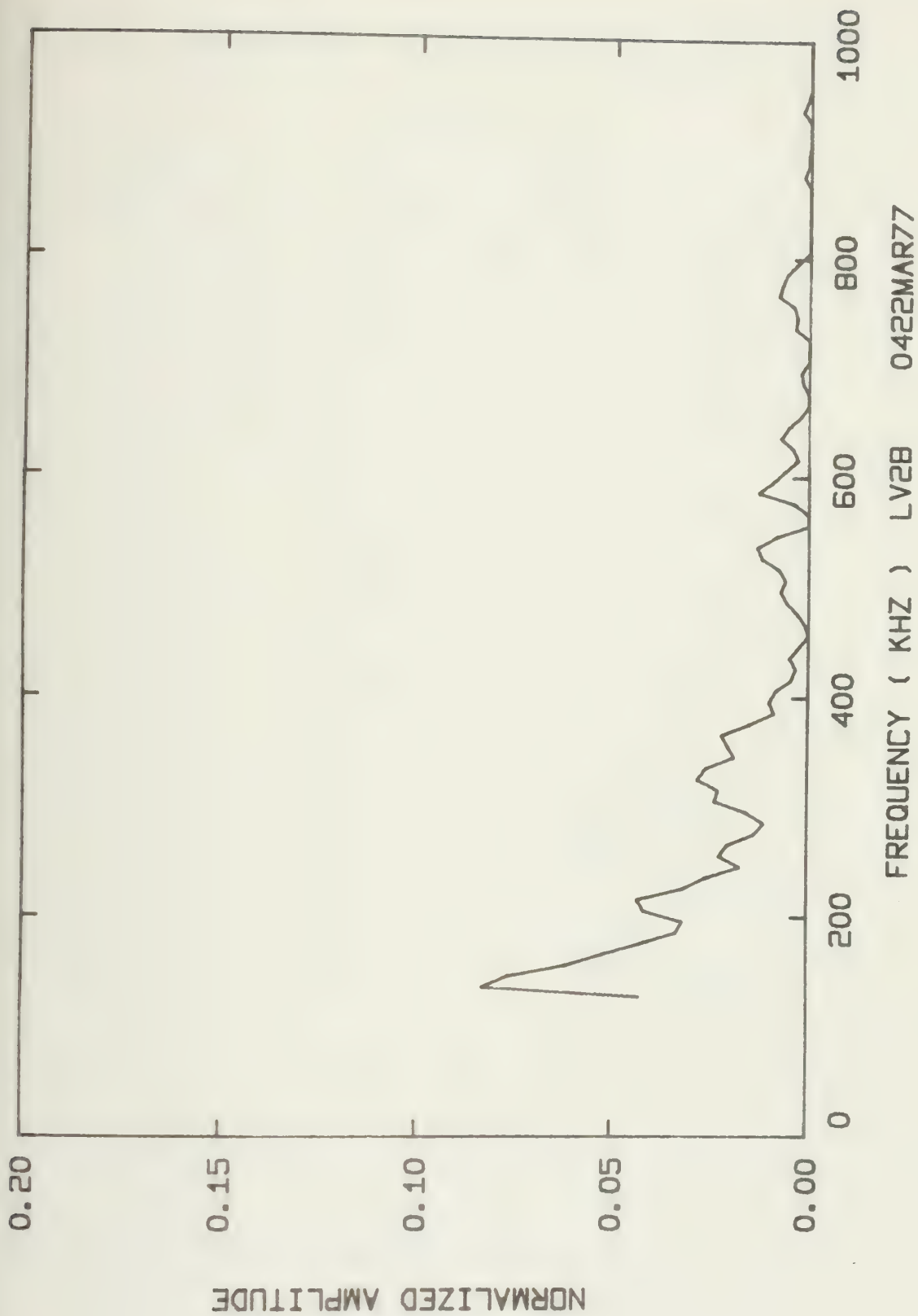




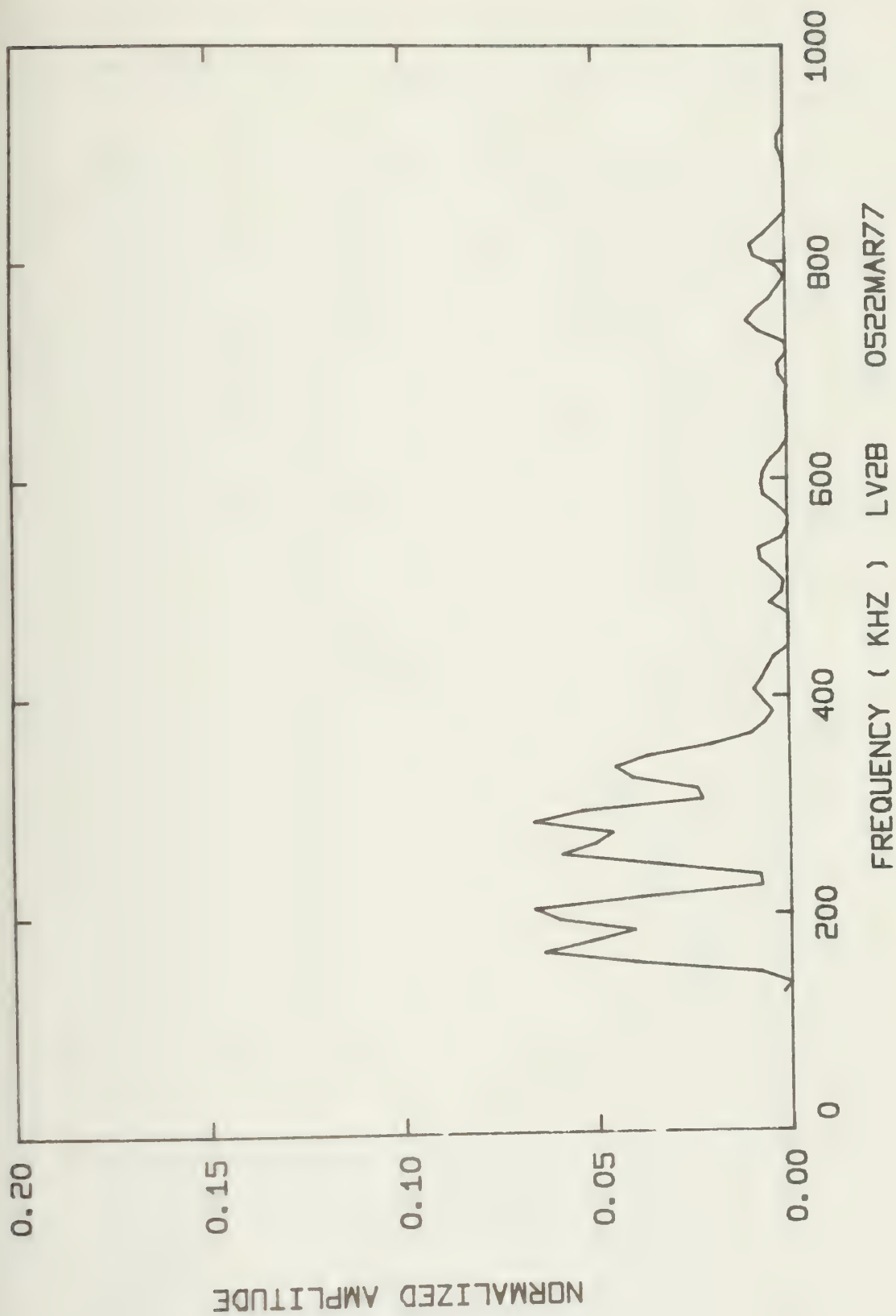




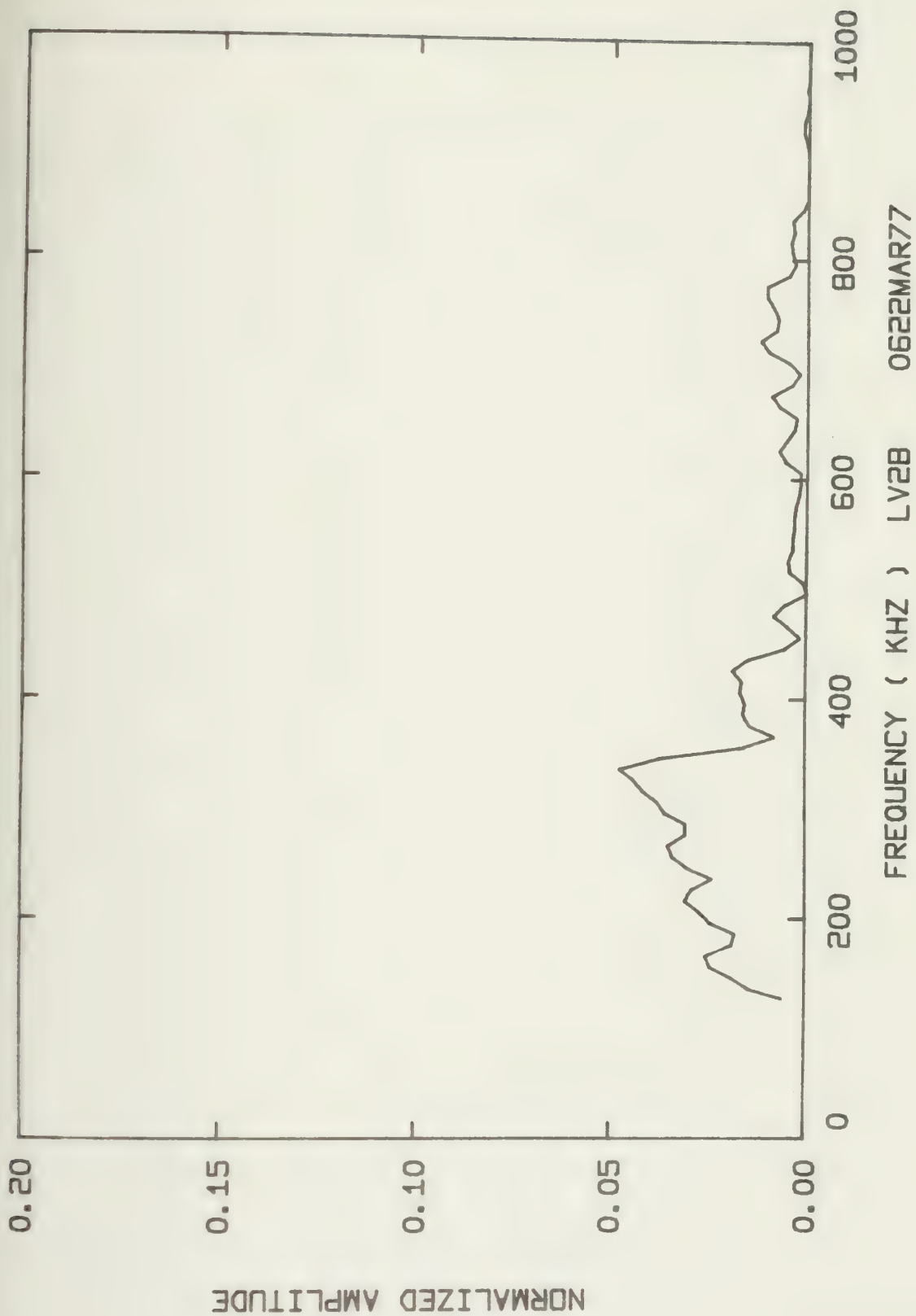




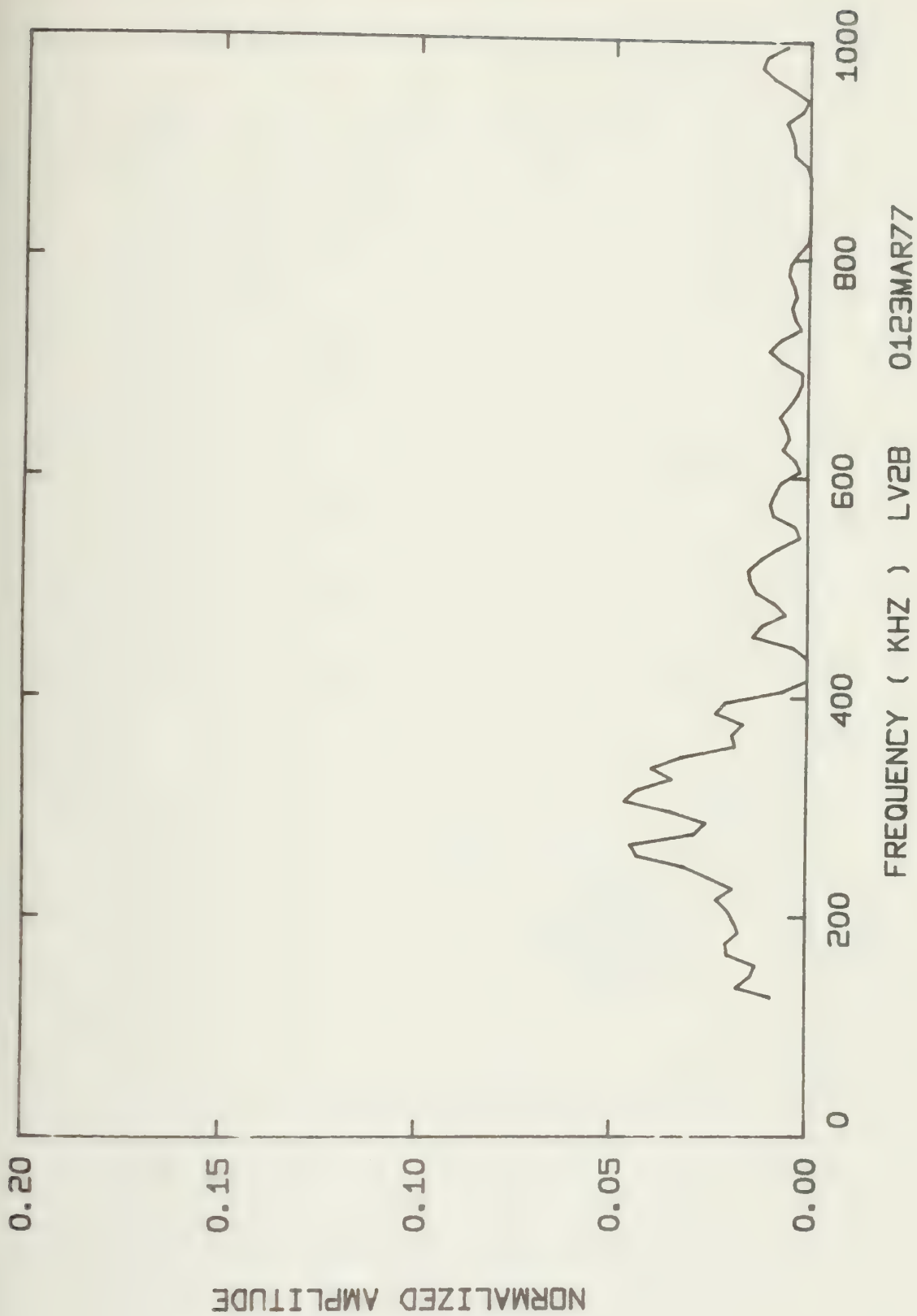






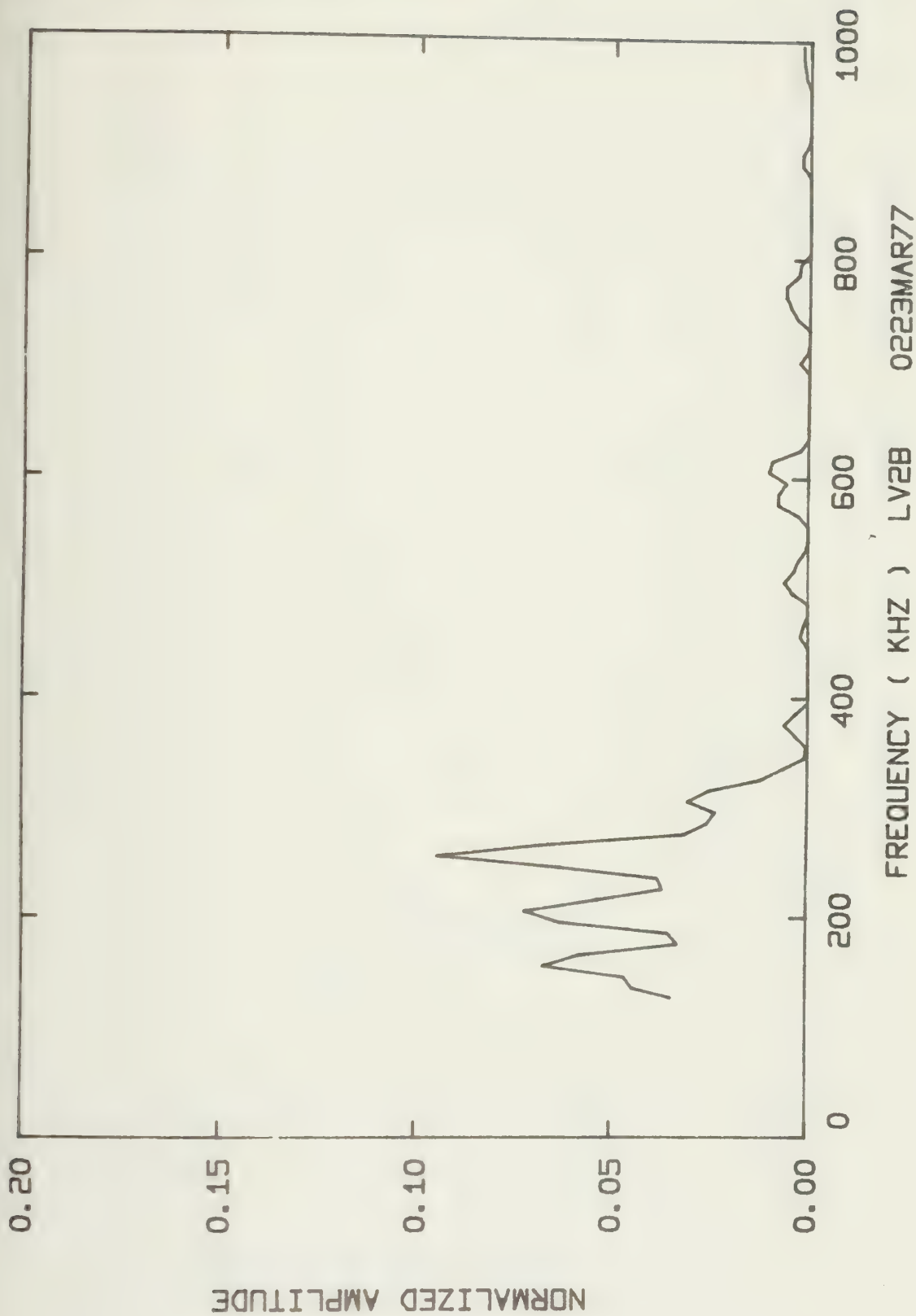




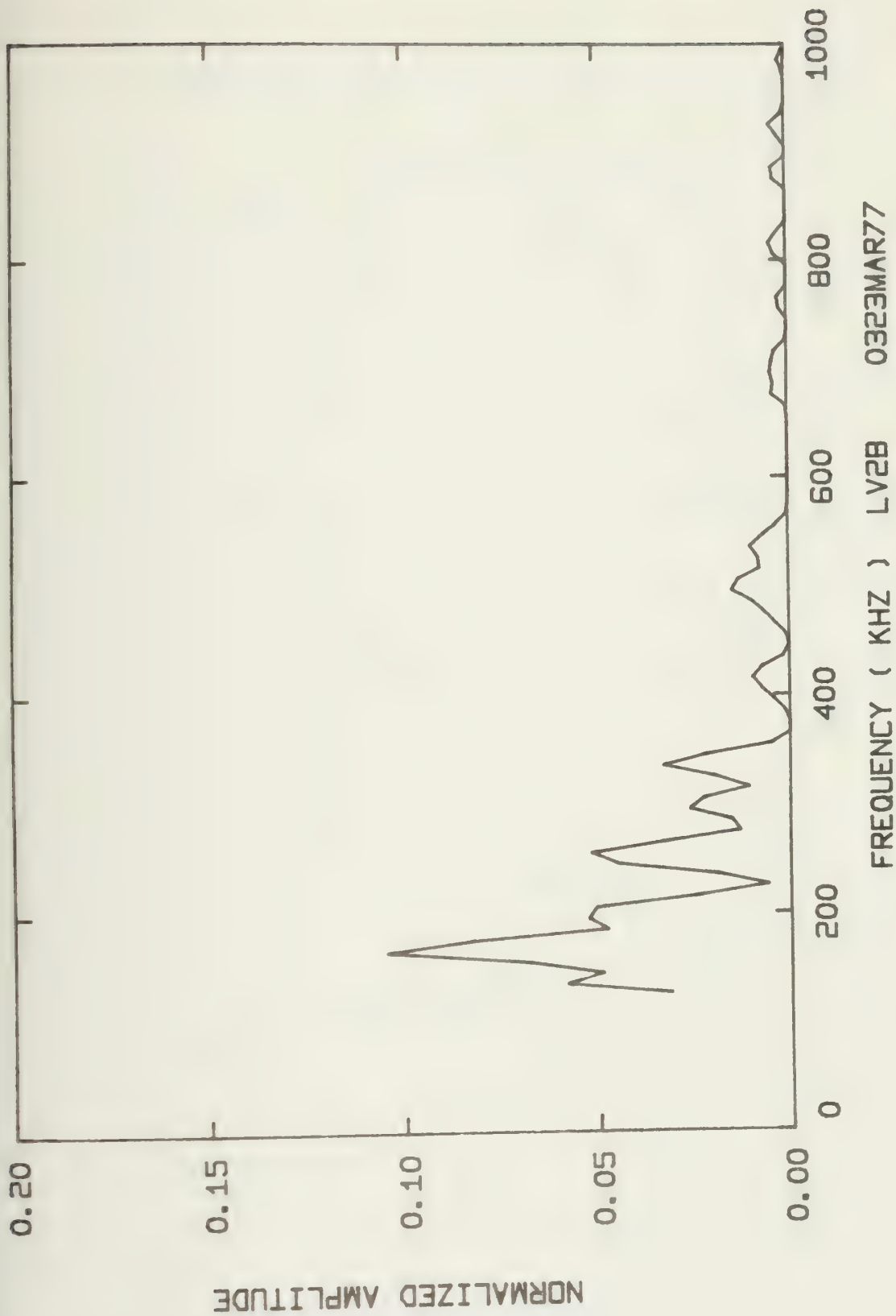




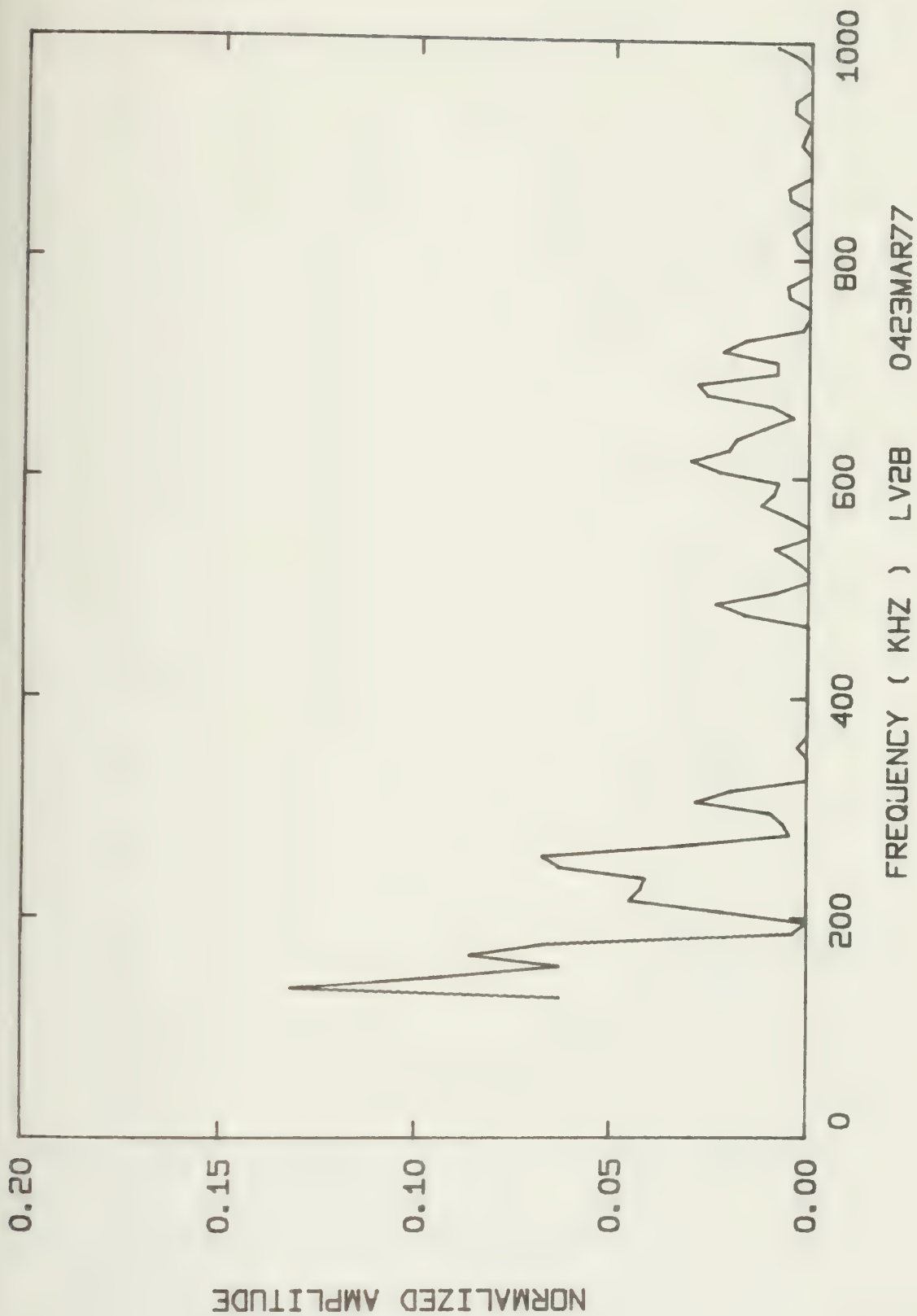






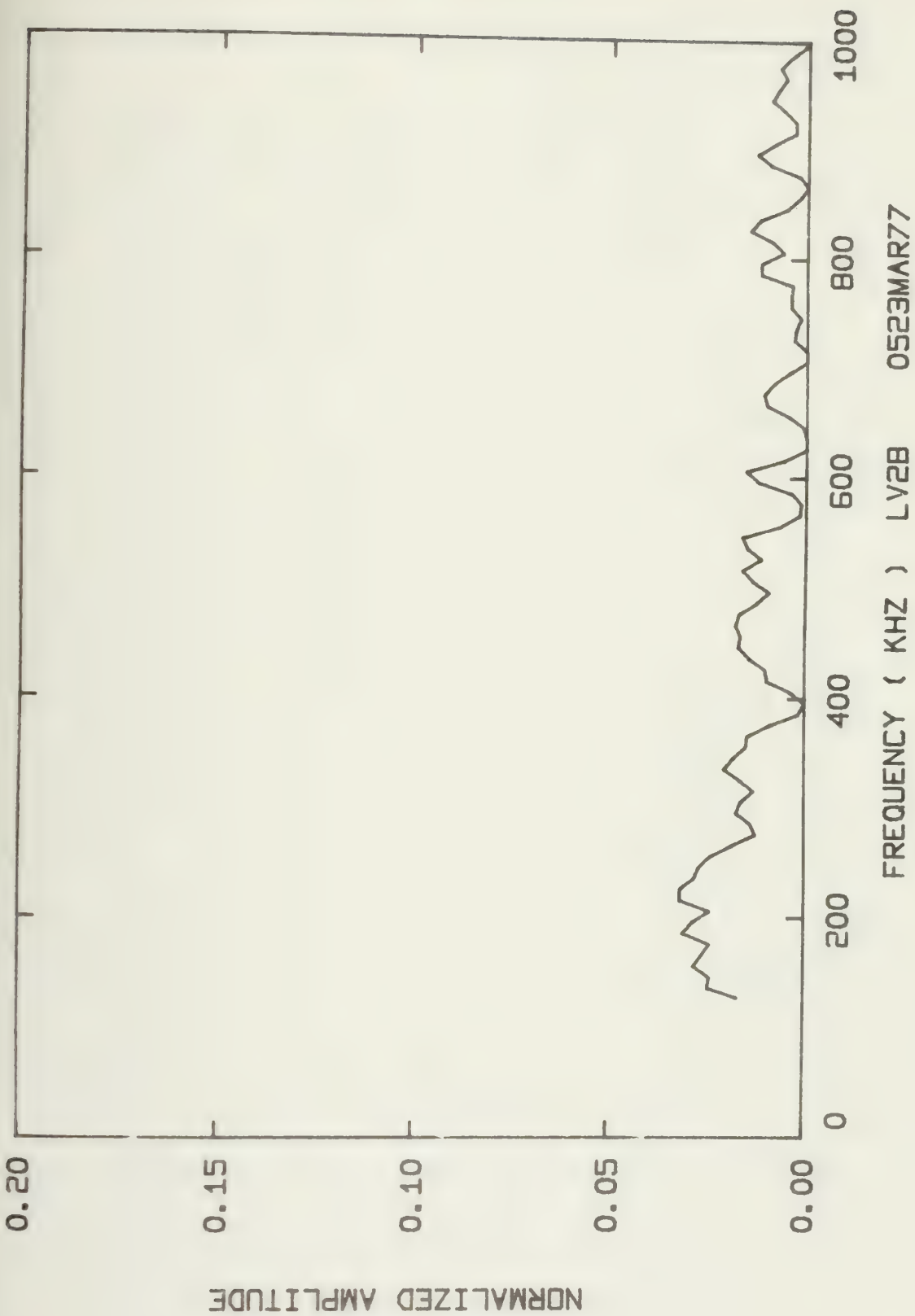




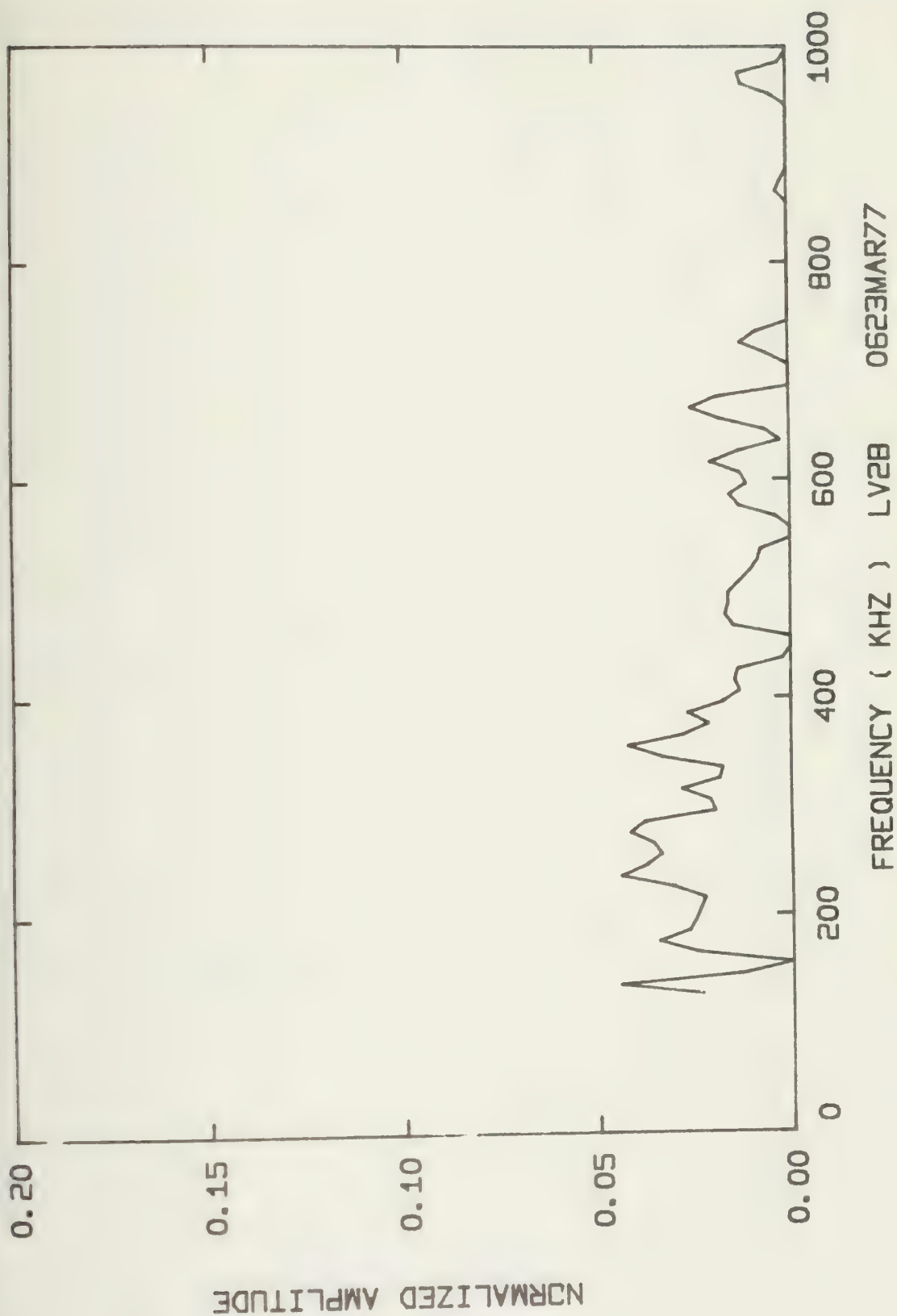




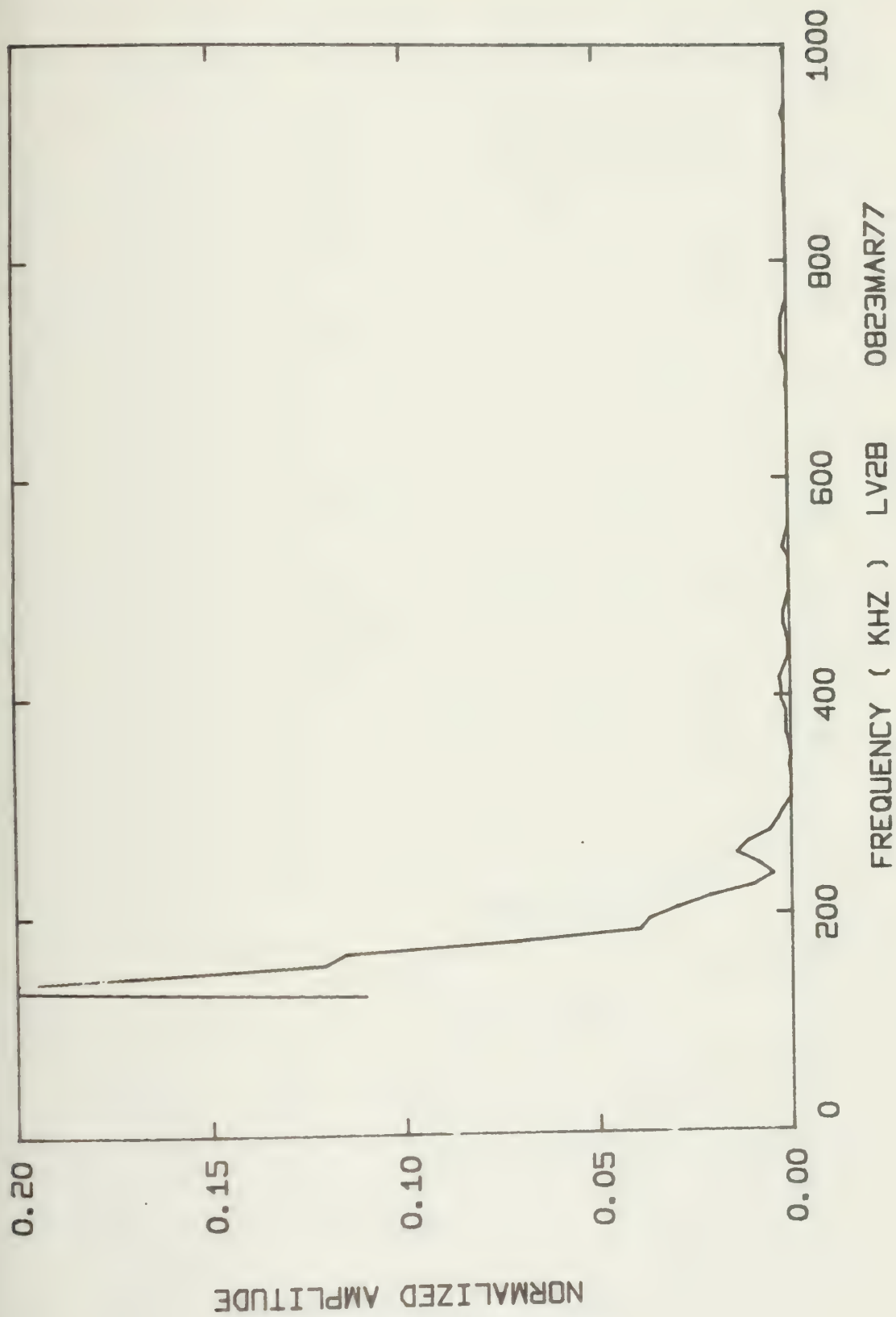




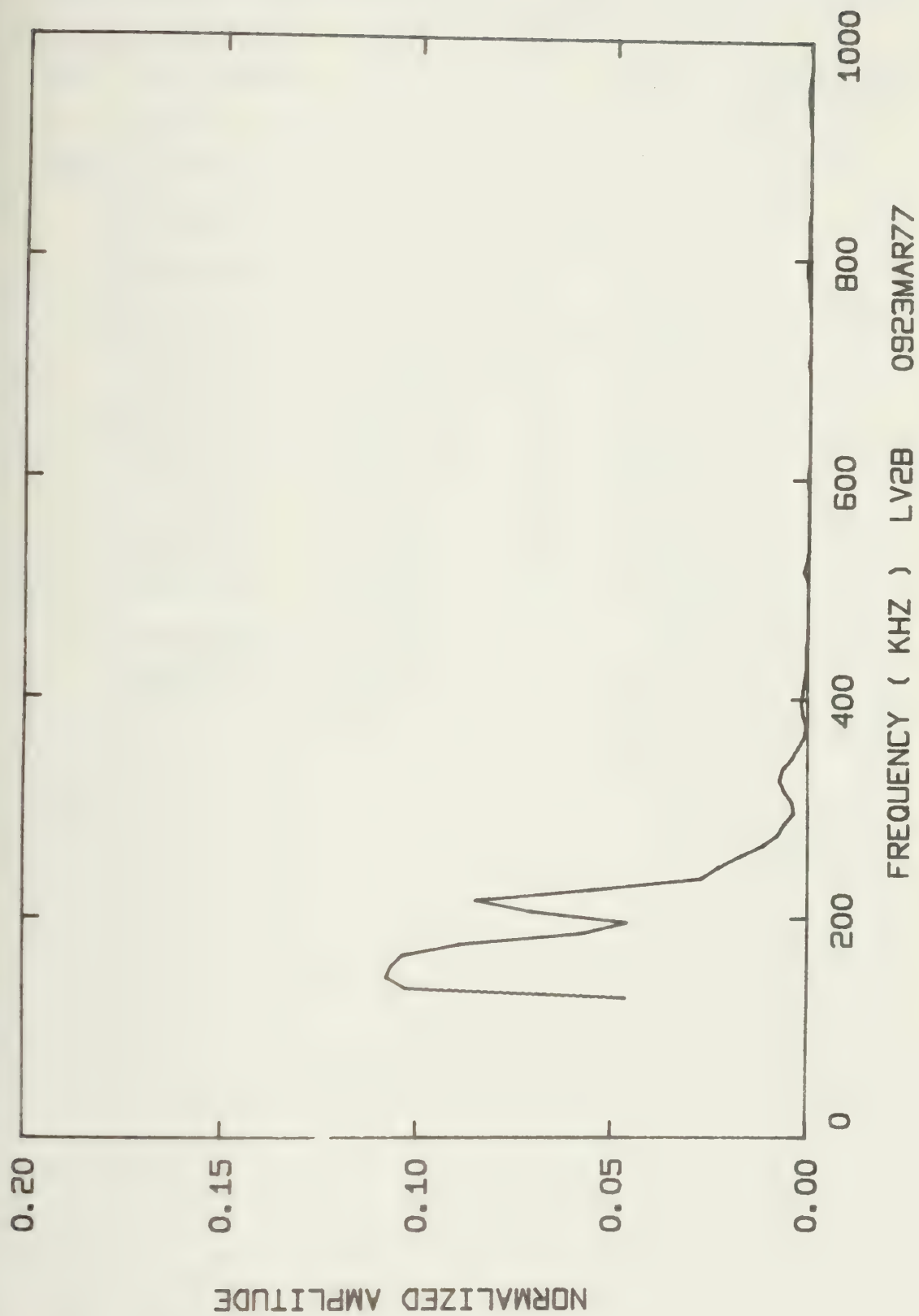












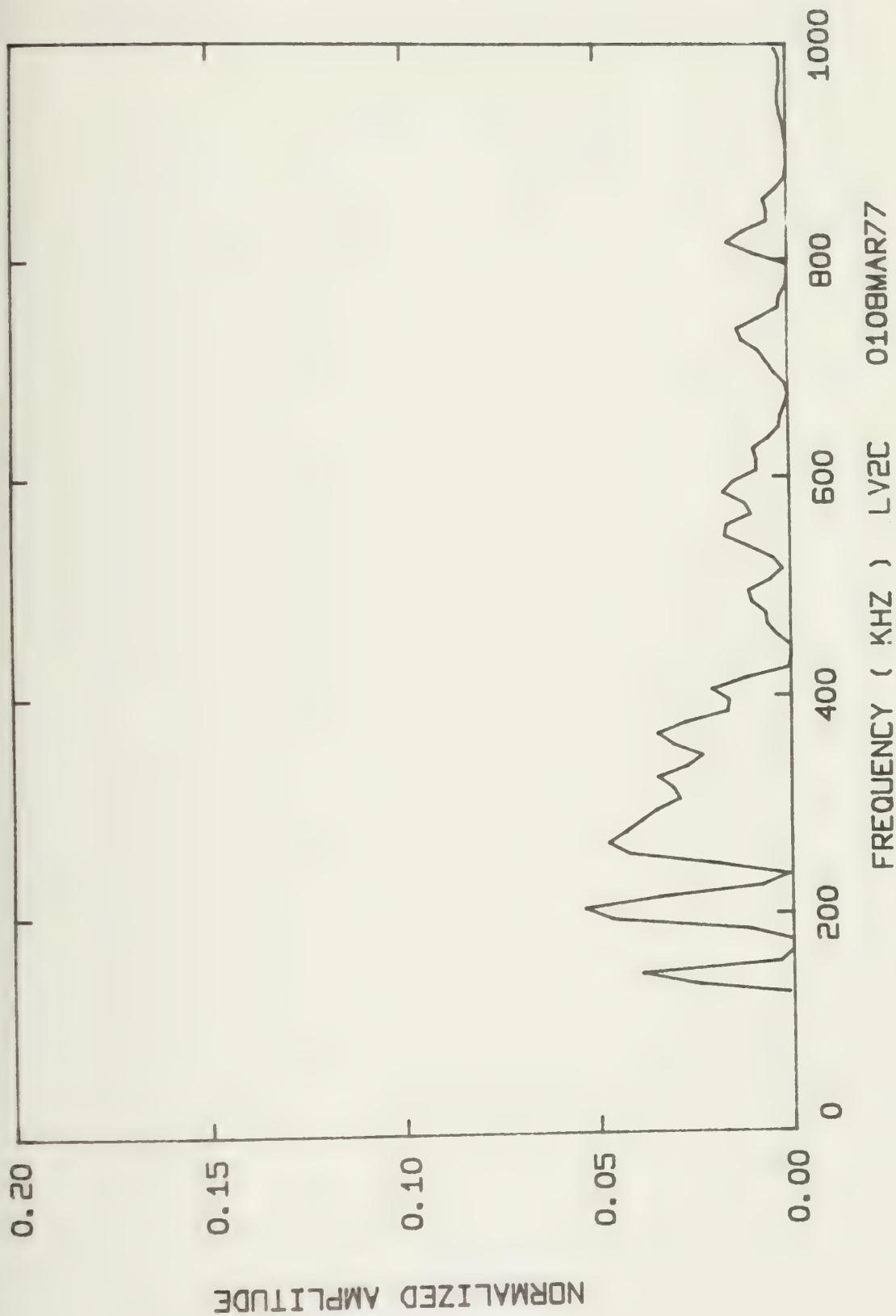




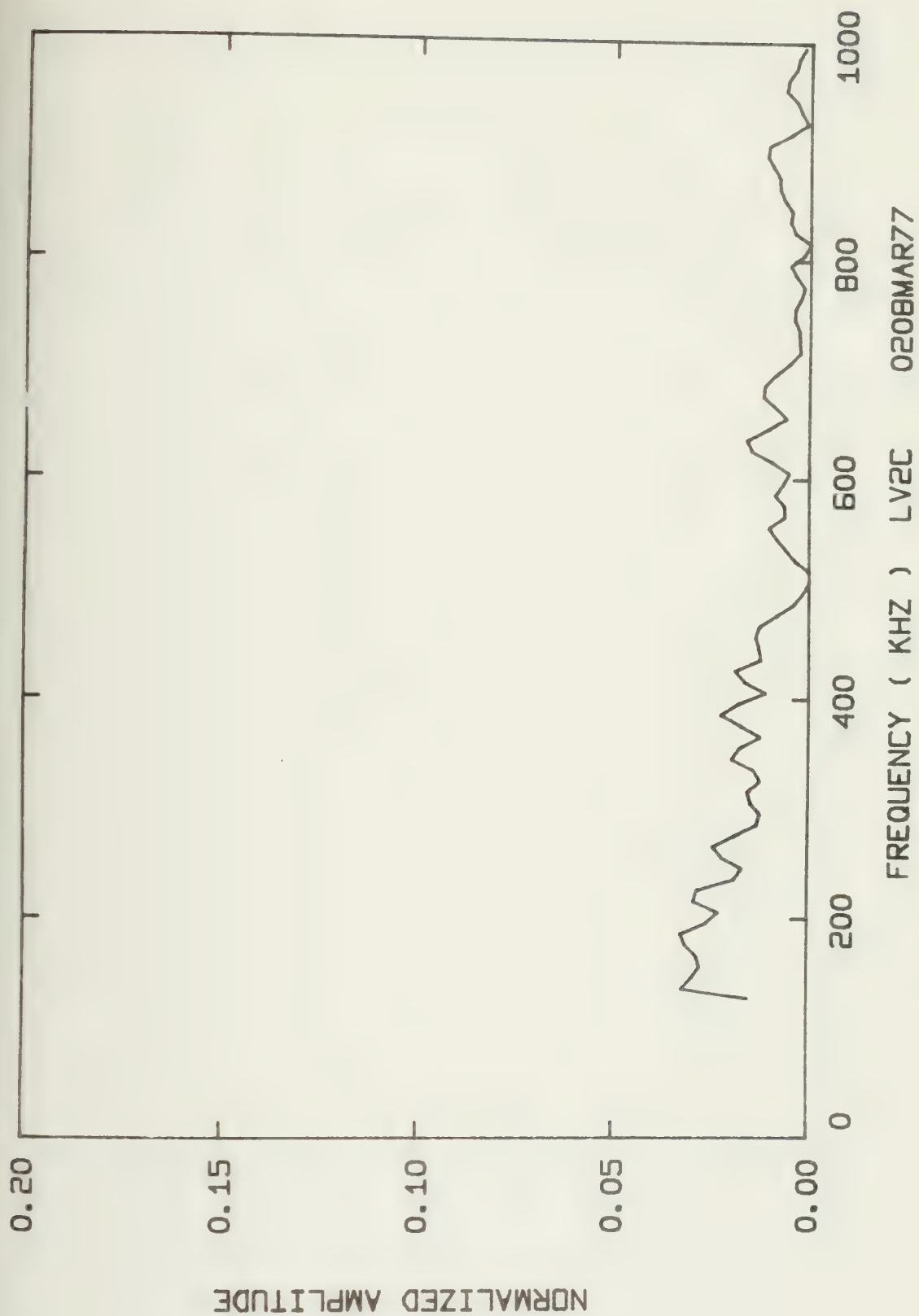
Summary of Energy per Acoustic Emission and RMS Pressure  
Across the Transducer's Face for Each Spectra

Spectral Distrib. Graph Code Number	Energy per AE (Joules)	RMS Pressure Across Face of Transducer (Pa x 10 <sup>5</sup> )
LV2C 0108MAR77	50.520 x 10 <sup>-9</sup>	67.024
0208MAR77	600.69 x 10 <sup>-9</sup>	140.84
0308MAR77	247.07 x 10 <sup>-9</sup>	104.81
0408MAR77	22.939 x 10 <sup>-9</sup>	55.32
0508MAR77	10.406 x 10 <sup>-9</sup>	45.47
0608MAR77	24.446 x 10 <sup>-6</sup>	605.29
0708MAR77	220.73 x 10 <sup>-9</sup>	94.87
0908MAR77	100.75 x 10 <sup>-9</sup>	71.12
1008MAR77	99.711 x 10 <sup>-9</sup>	70.56
1108MAR77	32.859 x 10 <sup>-9</sup>	56.83
0808MAR77	100.75 x 10 <sup>-9</sup>	71.11

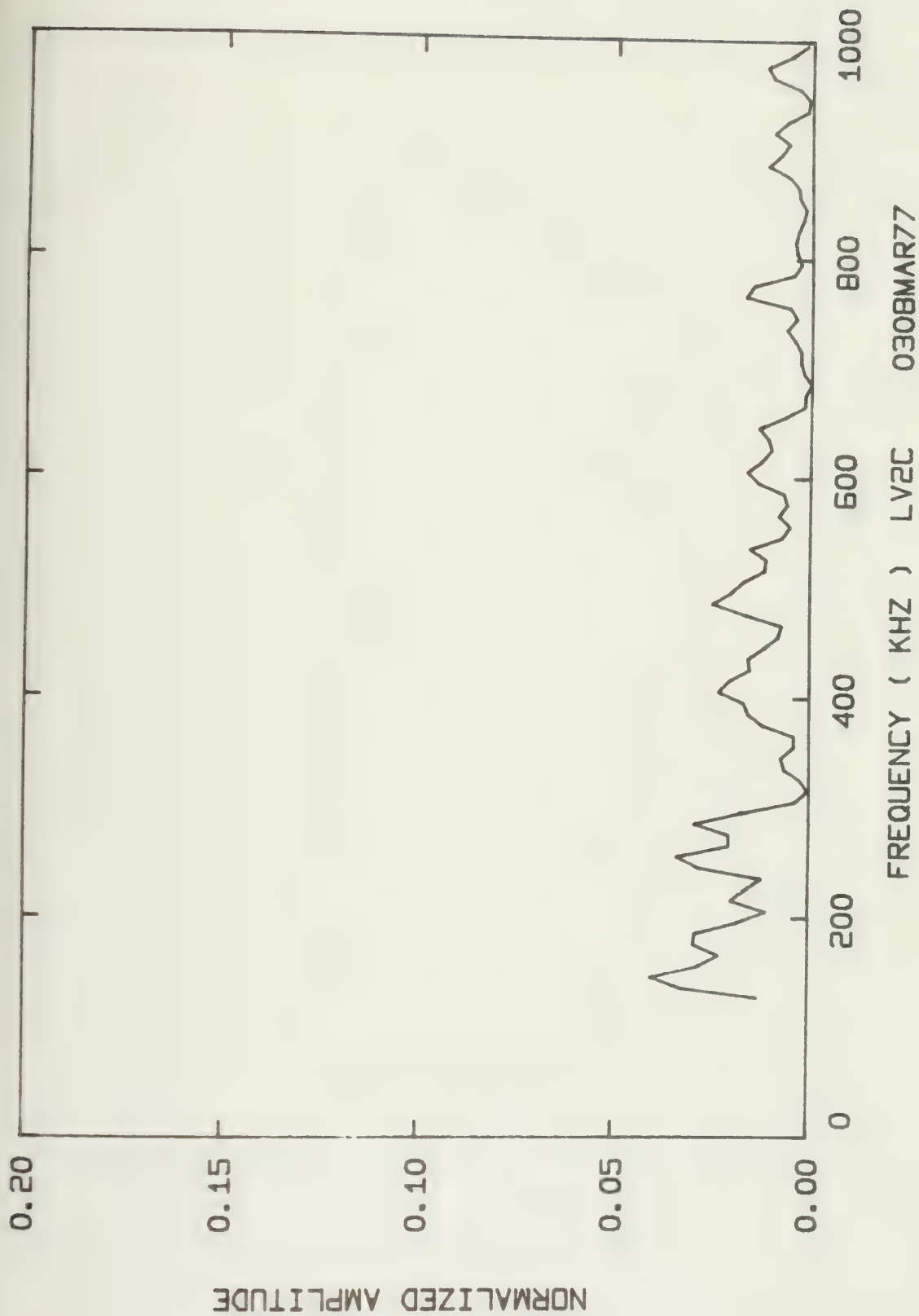






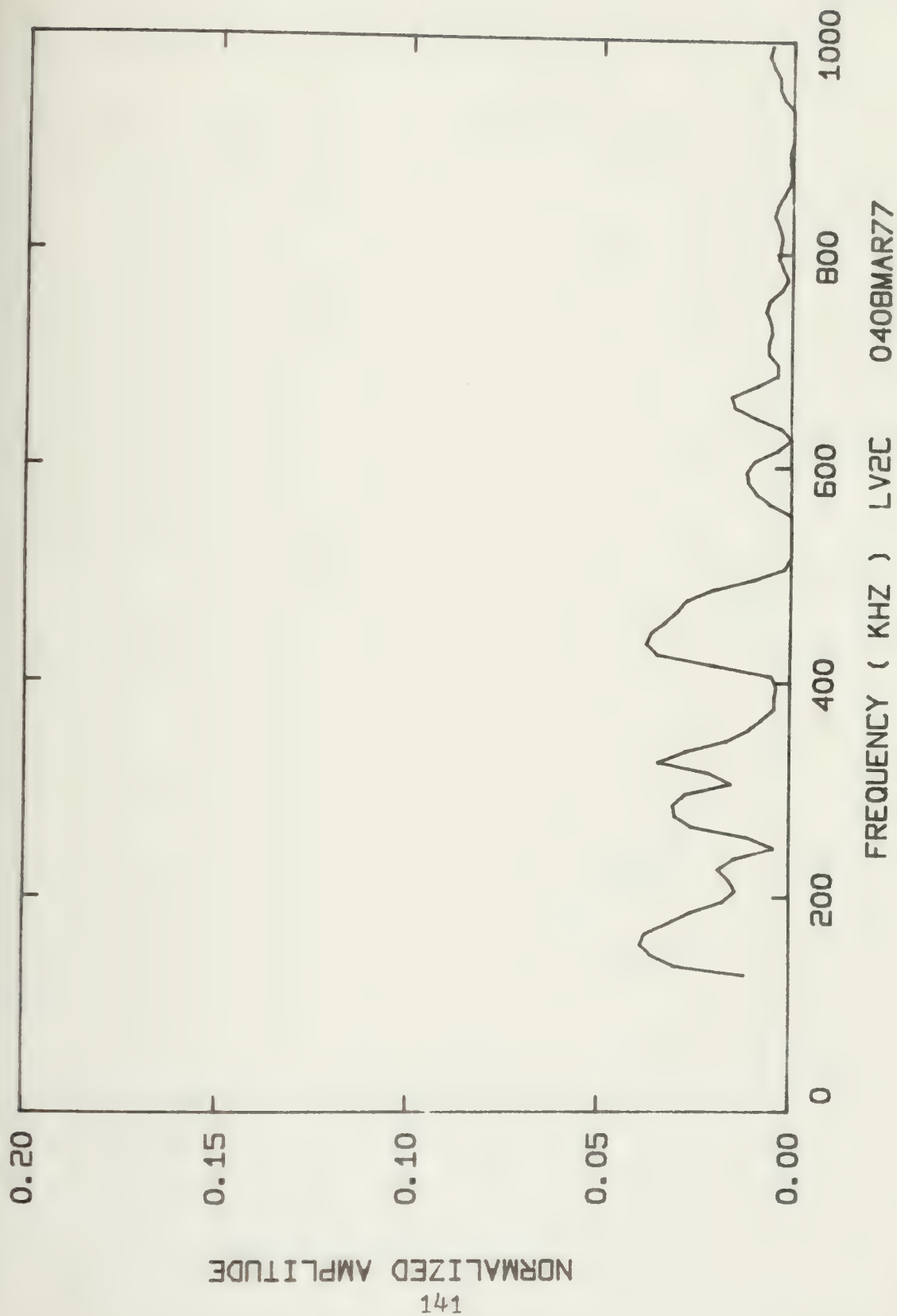




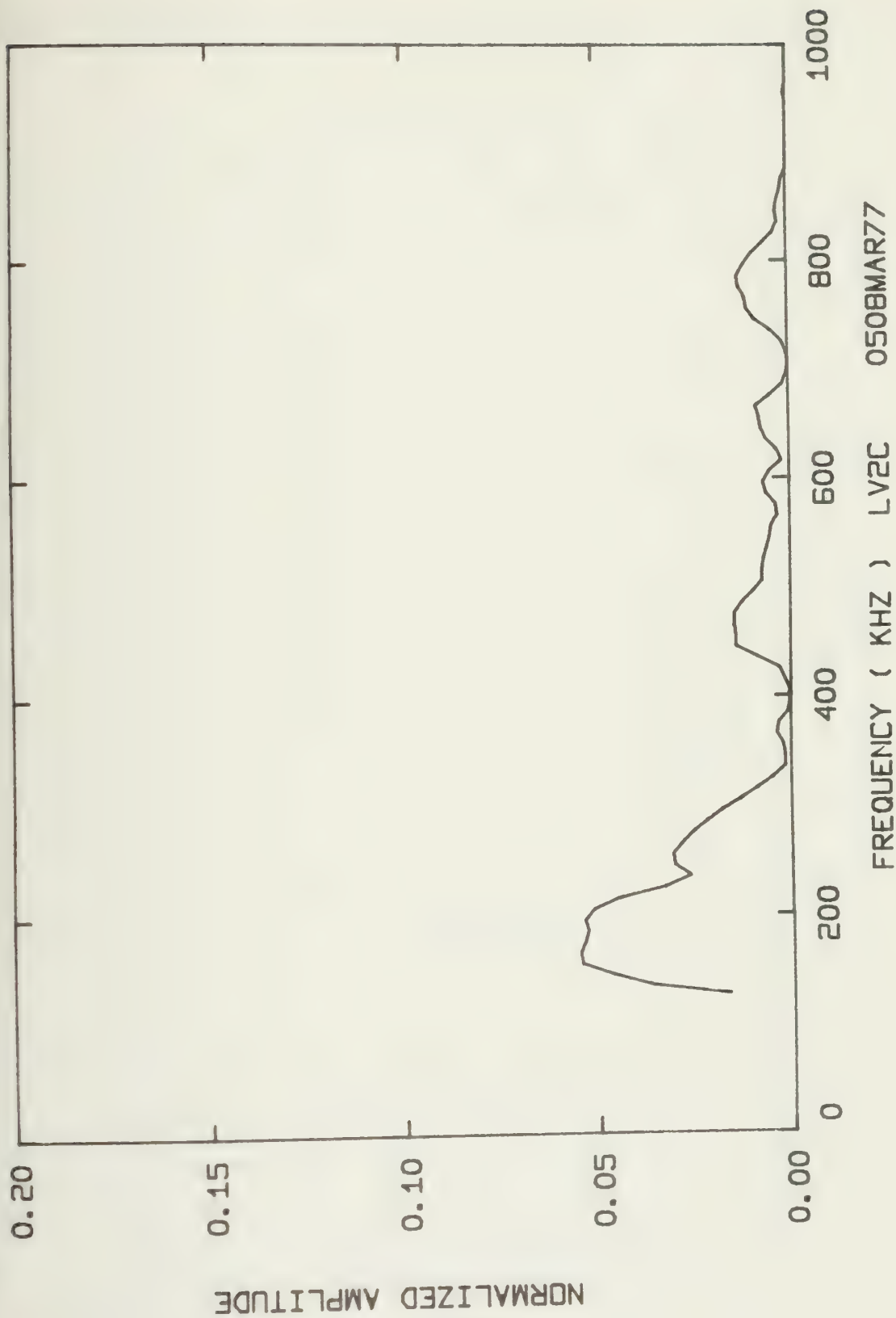




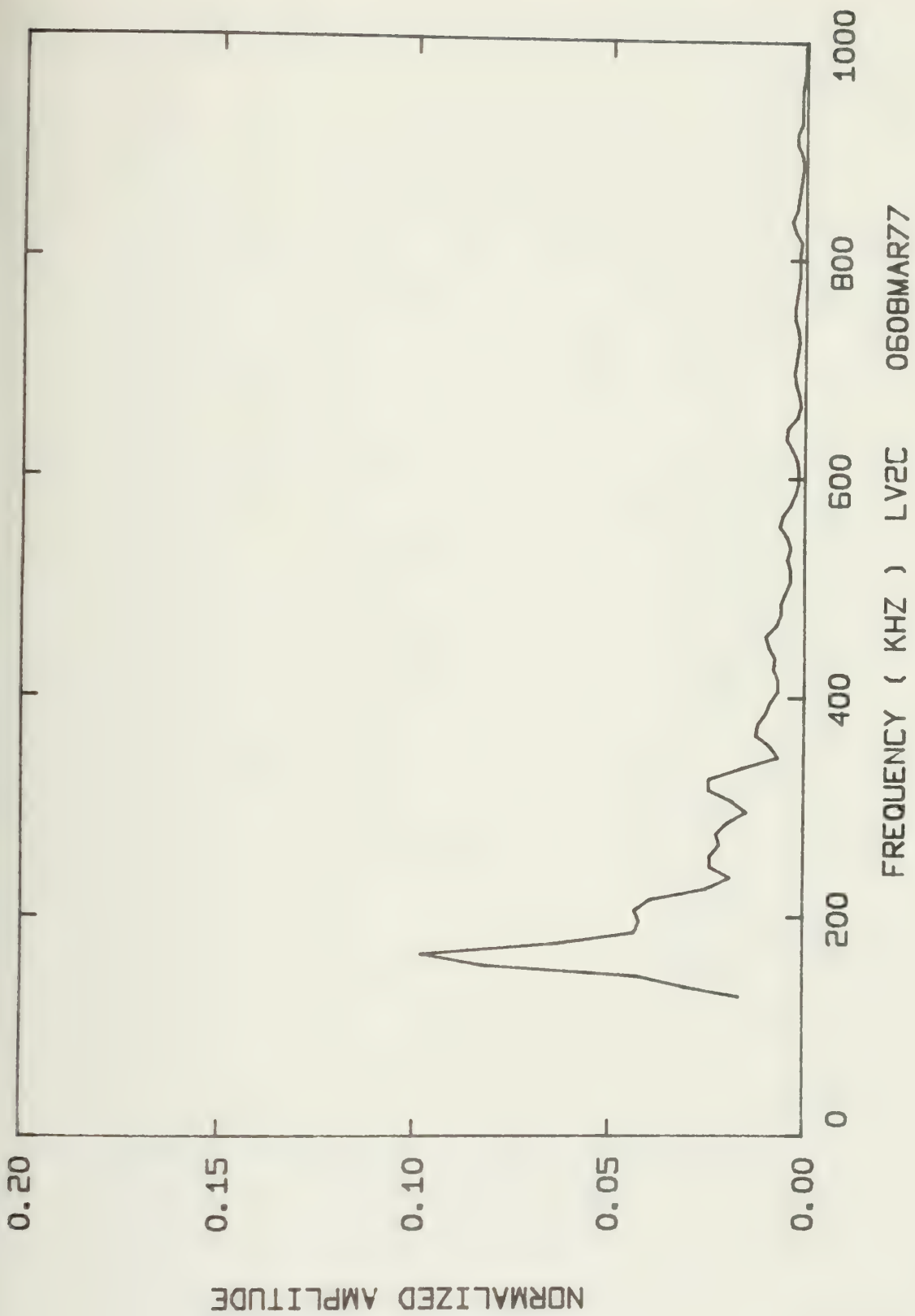




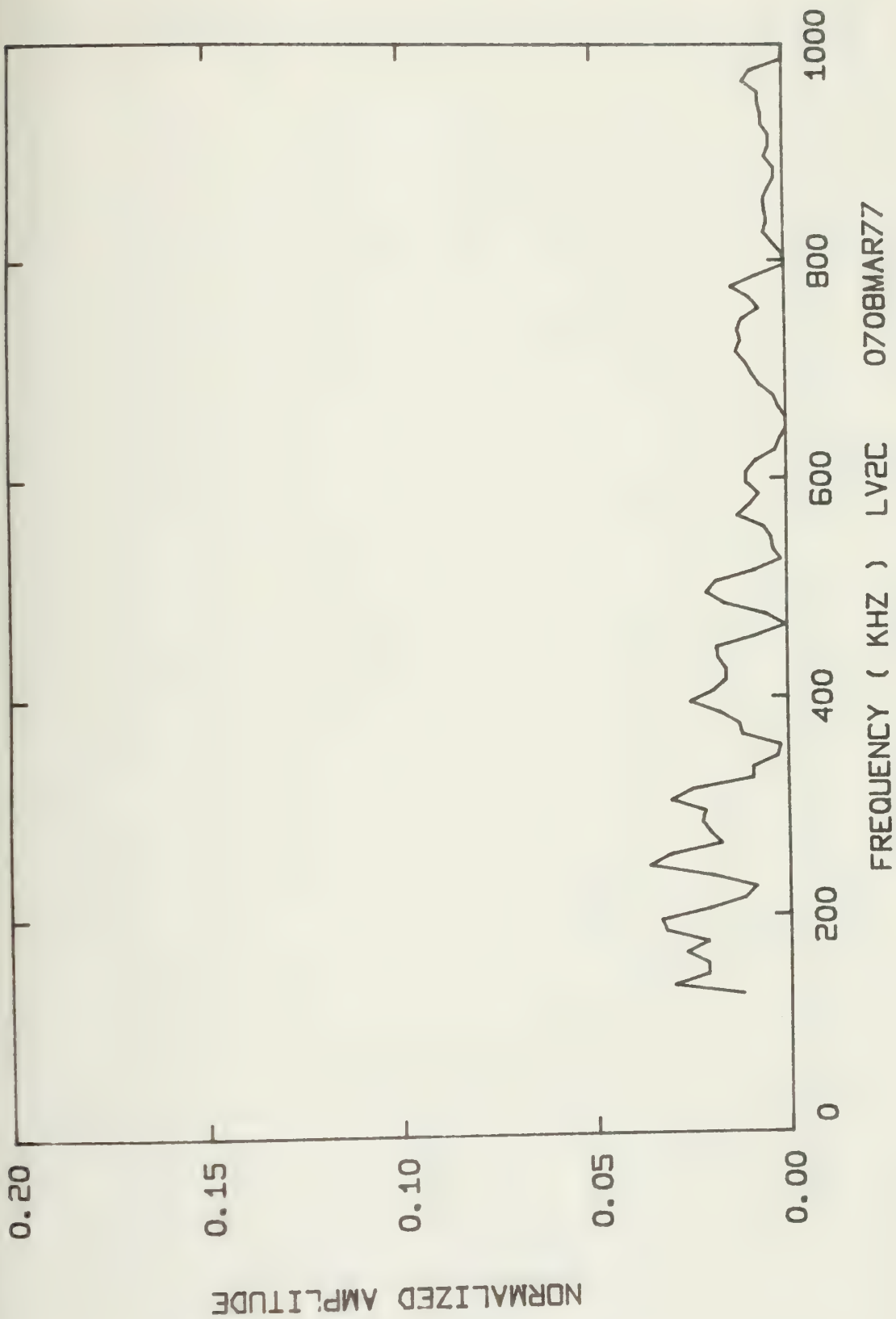






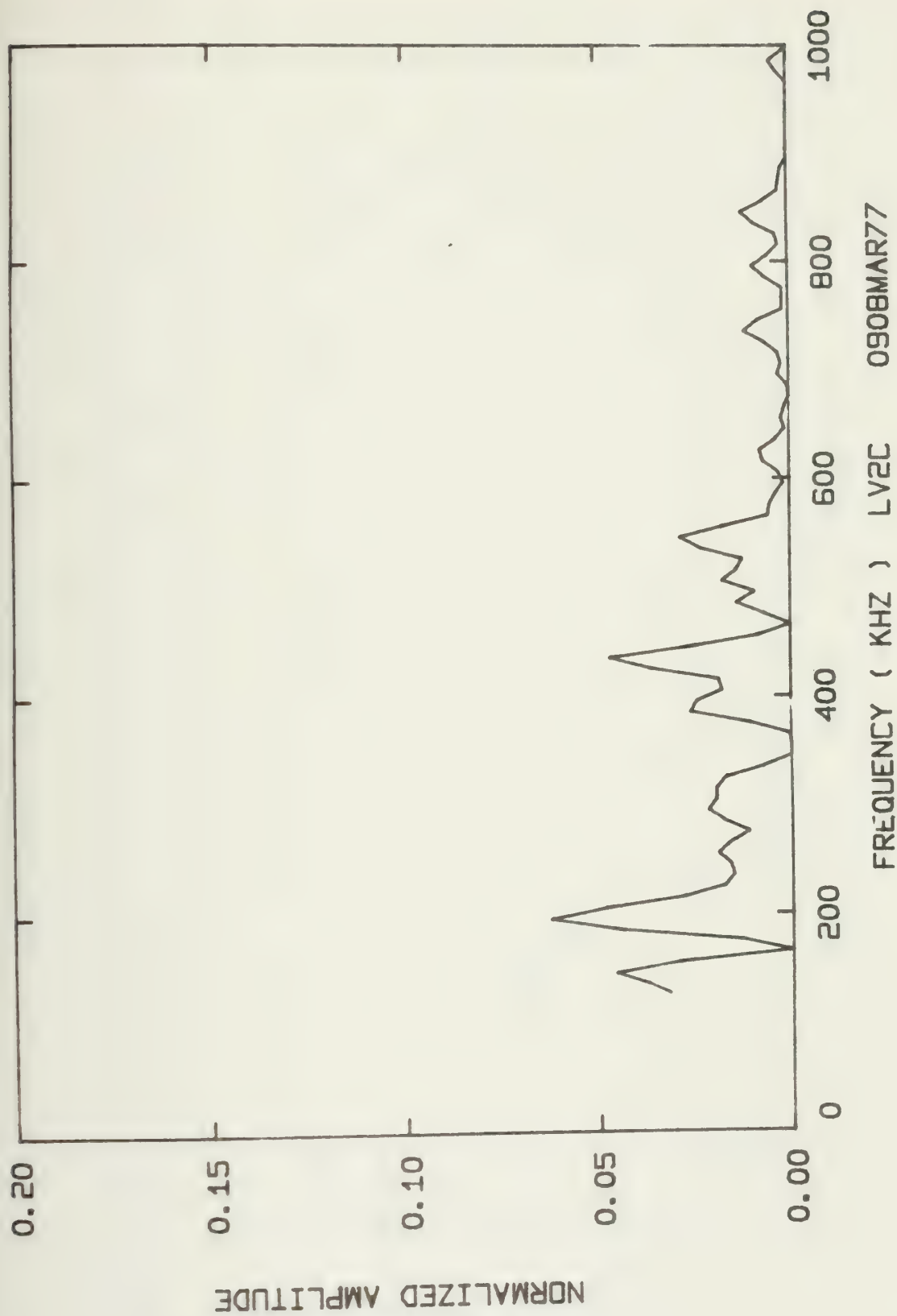




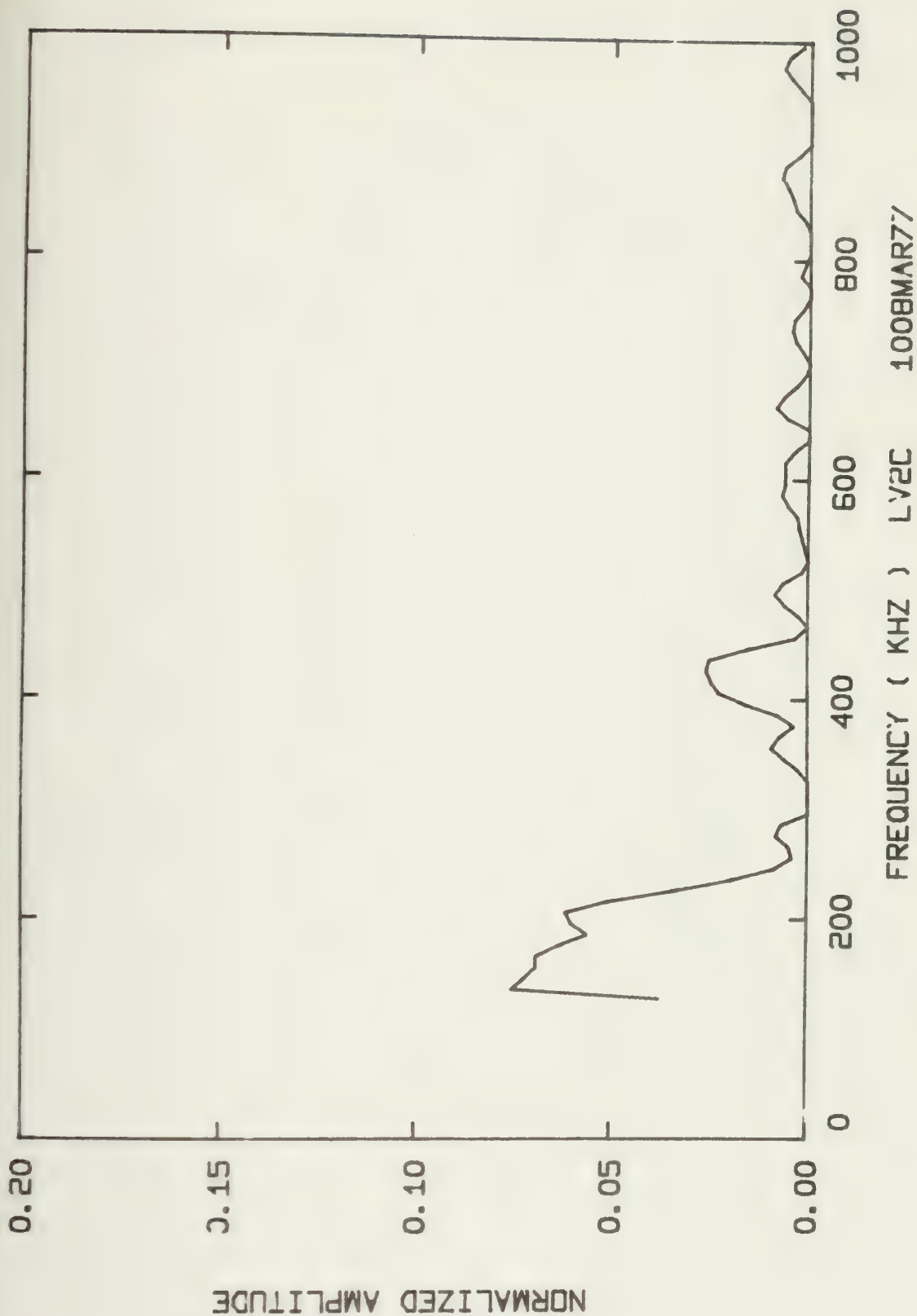




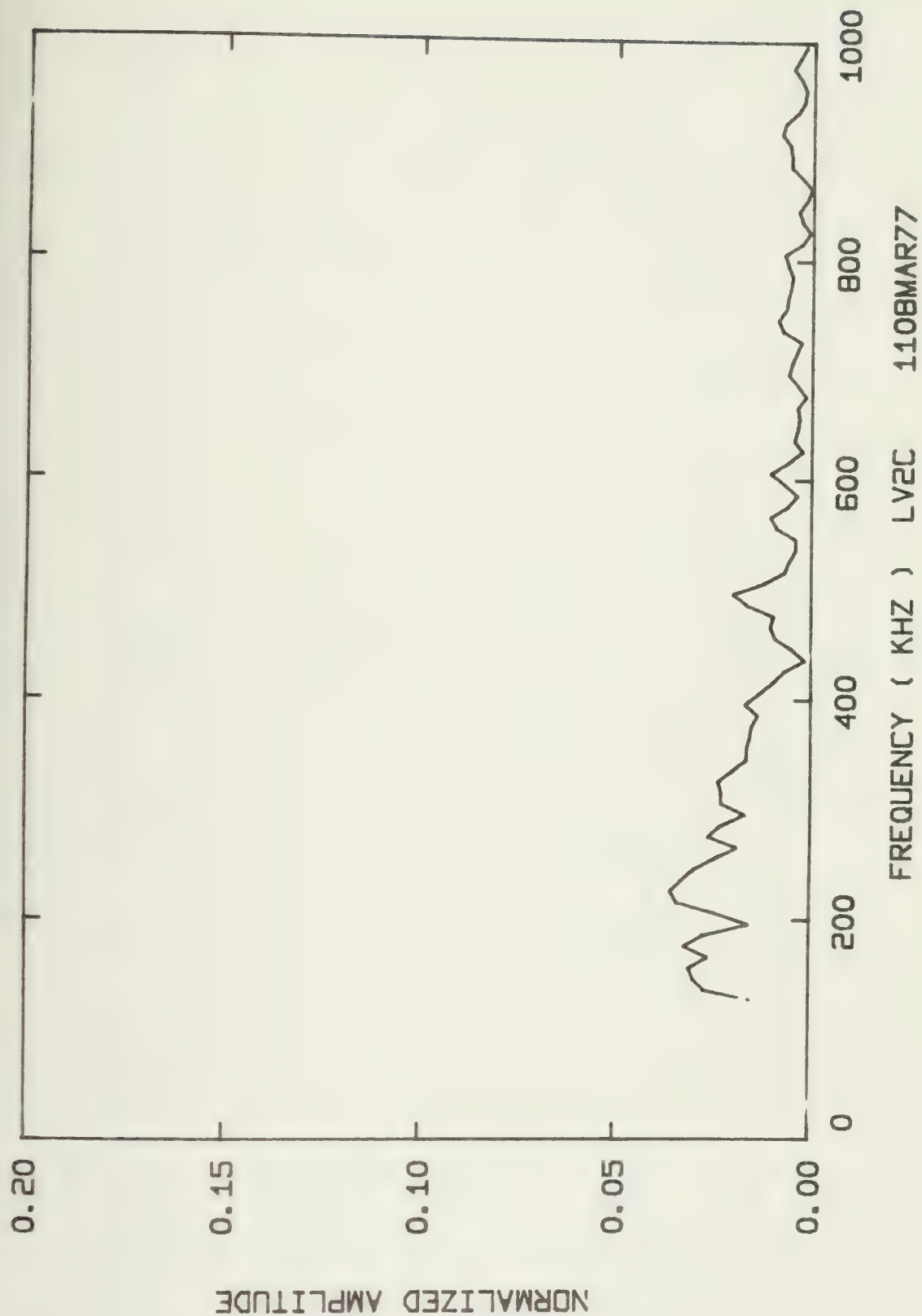




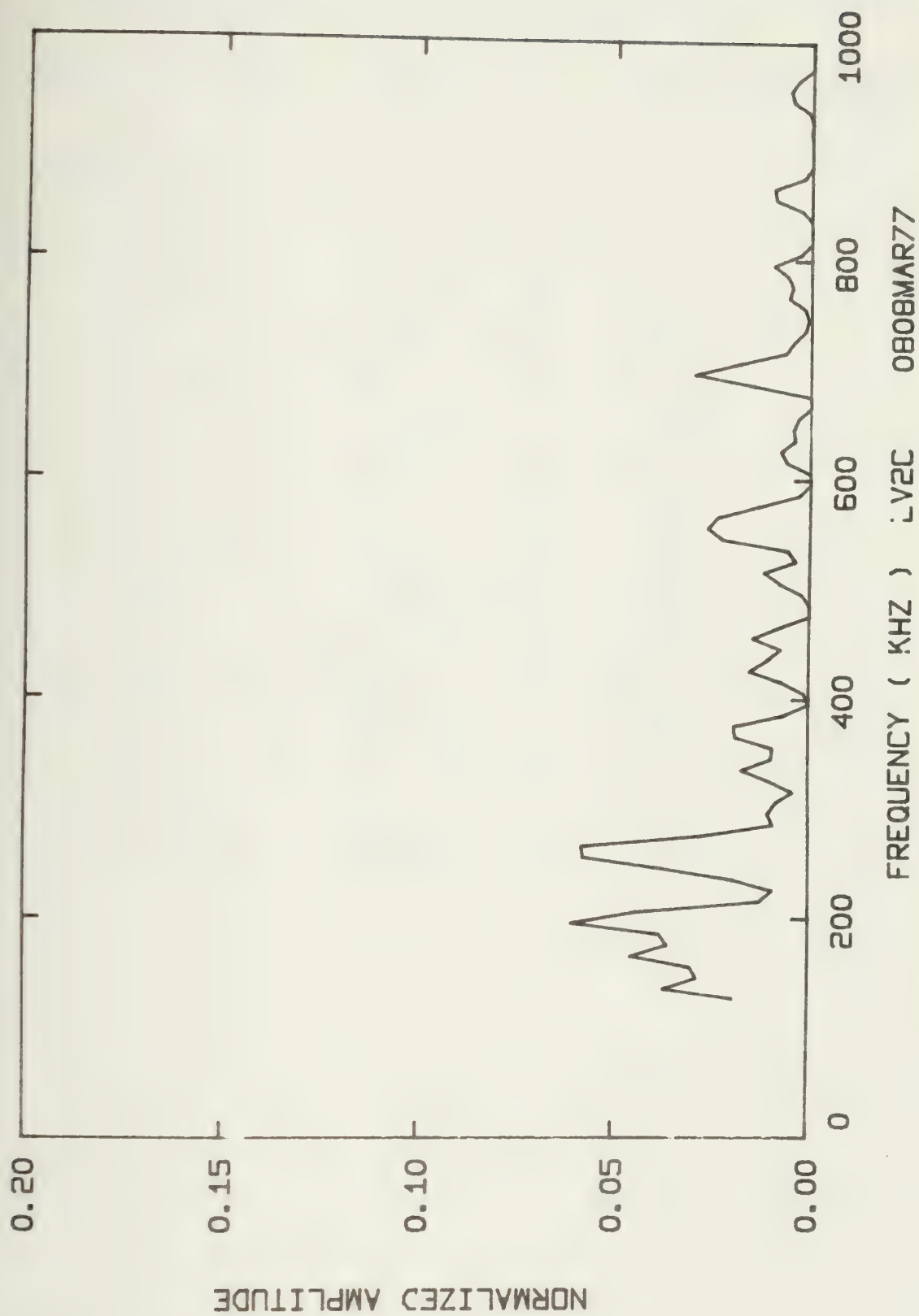












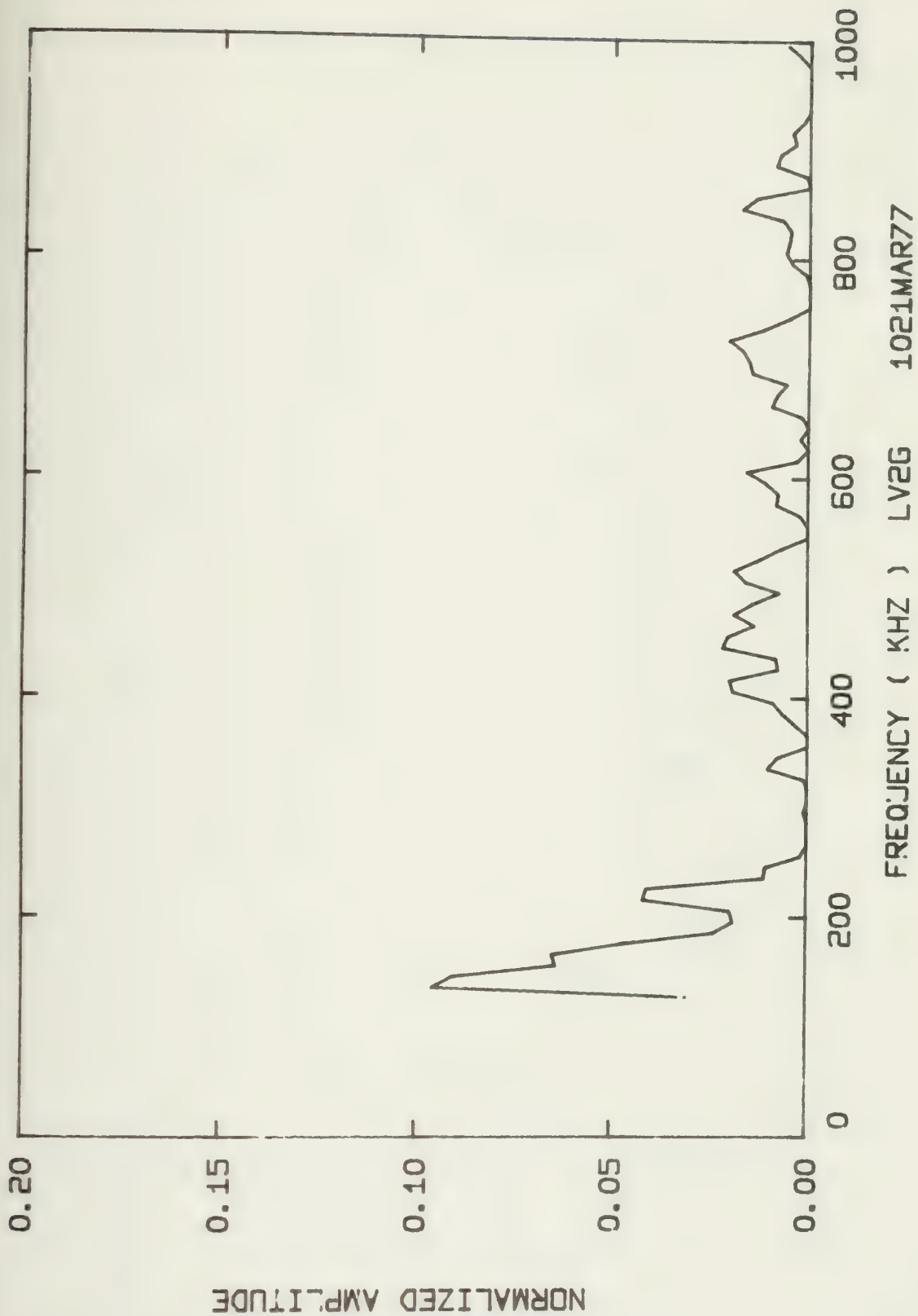




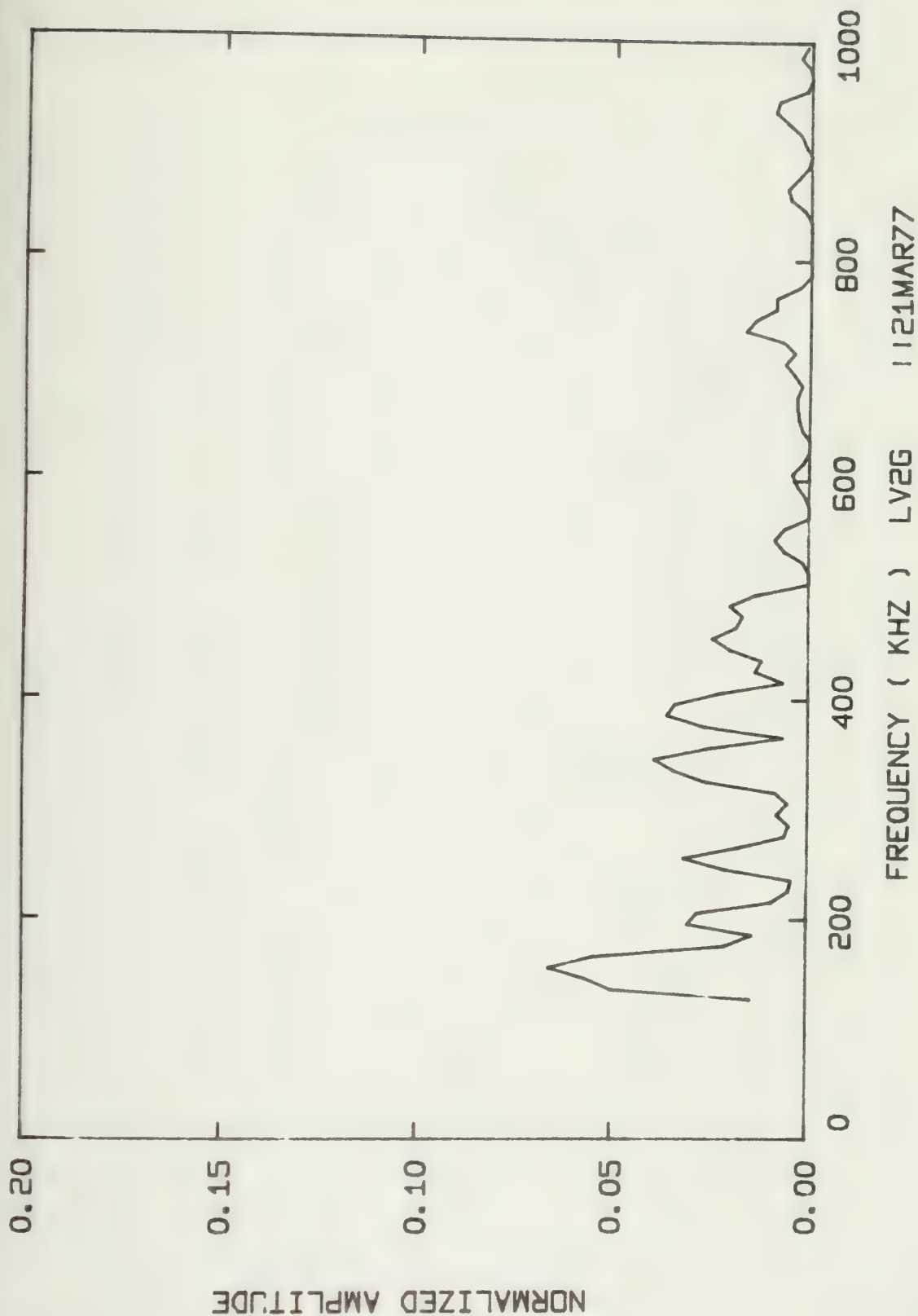
Summary of Energy per Acoustic Emission and RMS Pressure  
Across the Transducer's Face for Each Spectra

Spectral Distrib. Graph Code Number	Energy per AE (Joules)	RMS Pressure Across Face of Transducer (Pa x 10 <sup>5</sup> )
LV2G 1021MAR77	91.164 x 10 <sup>-9</sup>	66.93
1121MAR77	126.25 x 10 <sup>-9</sup>	76.20
1221MAR77	63.196 x 10 <sup>-9</sup>	62.72
1321MAR77	56.881 x 10 <sup>-9</sup>	69.48
1421MAR77	80.437 x 10 <sup>-9</sup>	64.96
1521MAR77	1.4880 x 10 <sup>-6</sup>	183.64
1621MAR77	91.072 x 10 <sup>-9</sup>	76.06
1721MAR77	60.676 x 10 <sup>-9</sup>	61.46
1821MAR77	159.60 x 10 <sup>-9</sup>	82.87
1921MAR77	190.72 x 10 <sup>-9</sup>	82.76
2021MAR77	269.14 x 10 <sup>-9</sup>	100.66
2121MAR77	487.21 x 10 <sup>-9</sup>	116.71
2221MAR77	414.73 x 10 <sup>-9</sup>	103.71
2321MAR77	898.88 x 10 <sup>-9</sup>	148.61



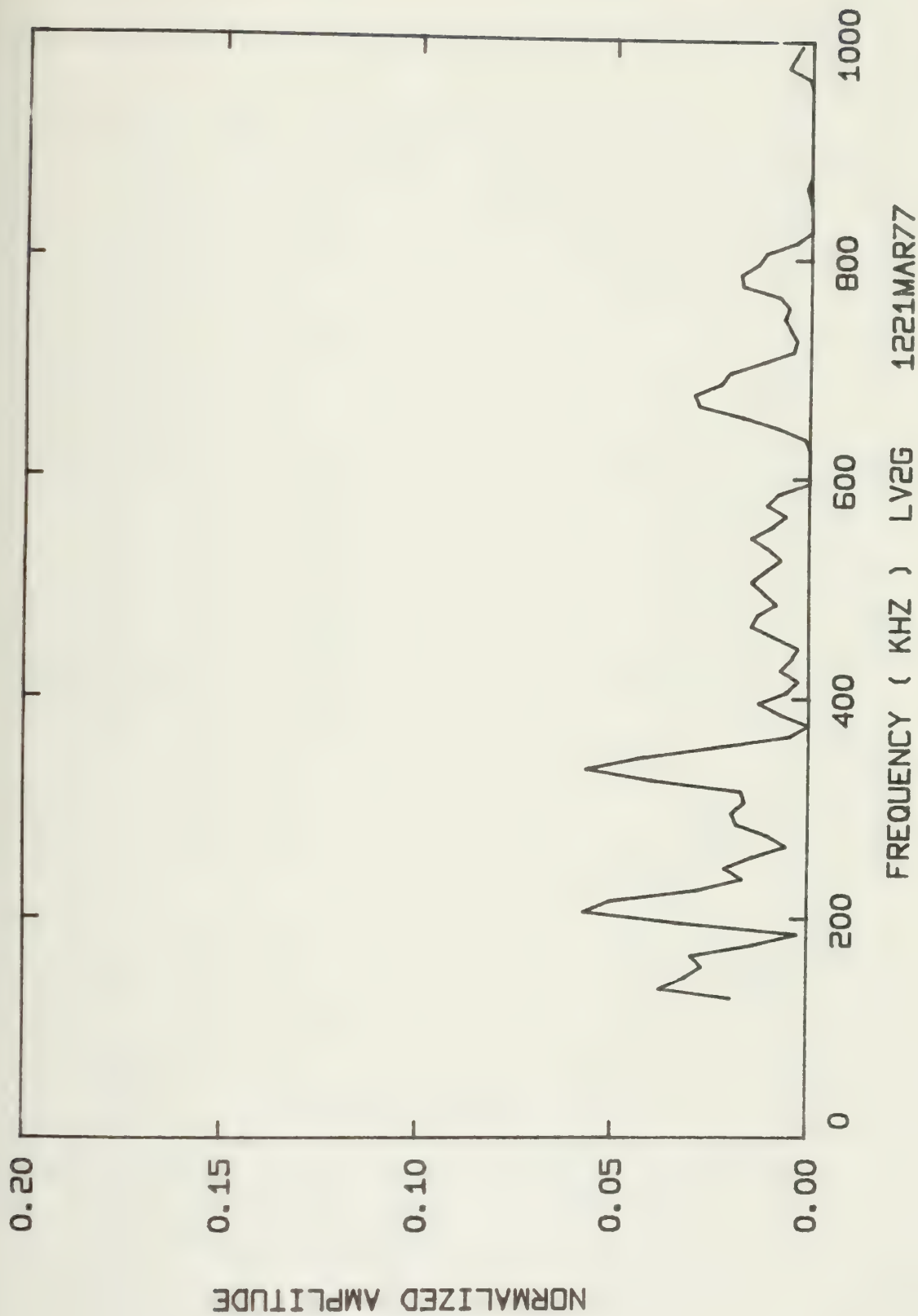






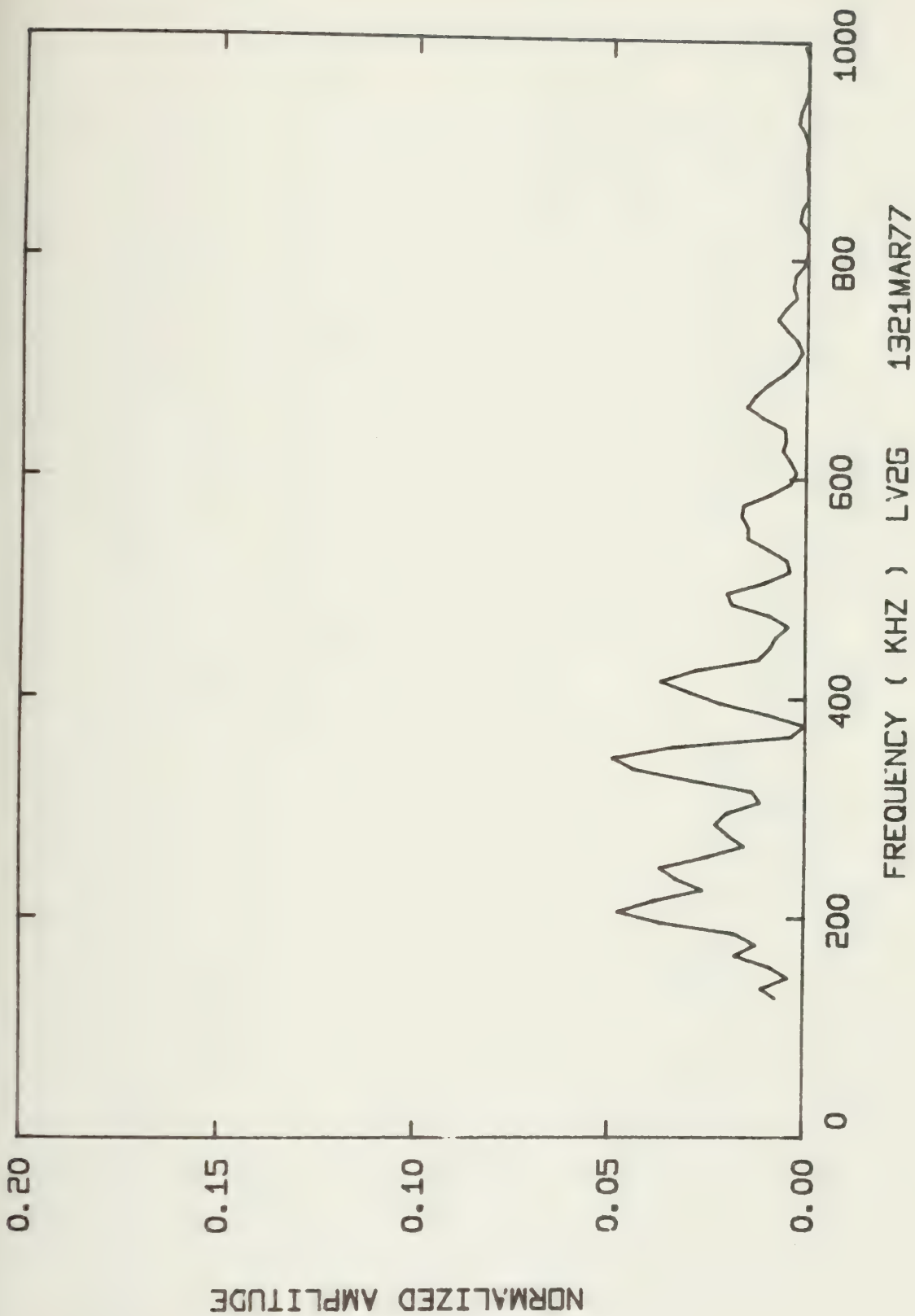
1121MAR77



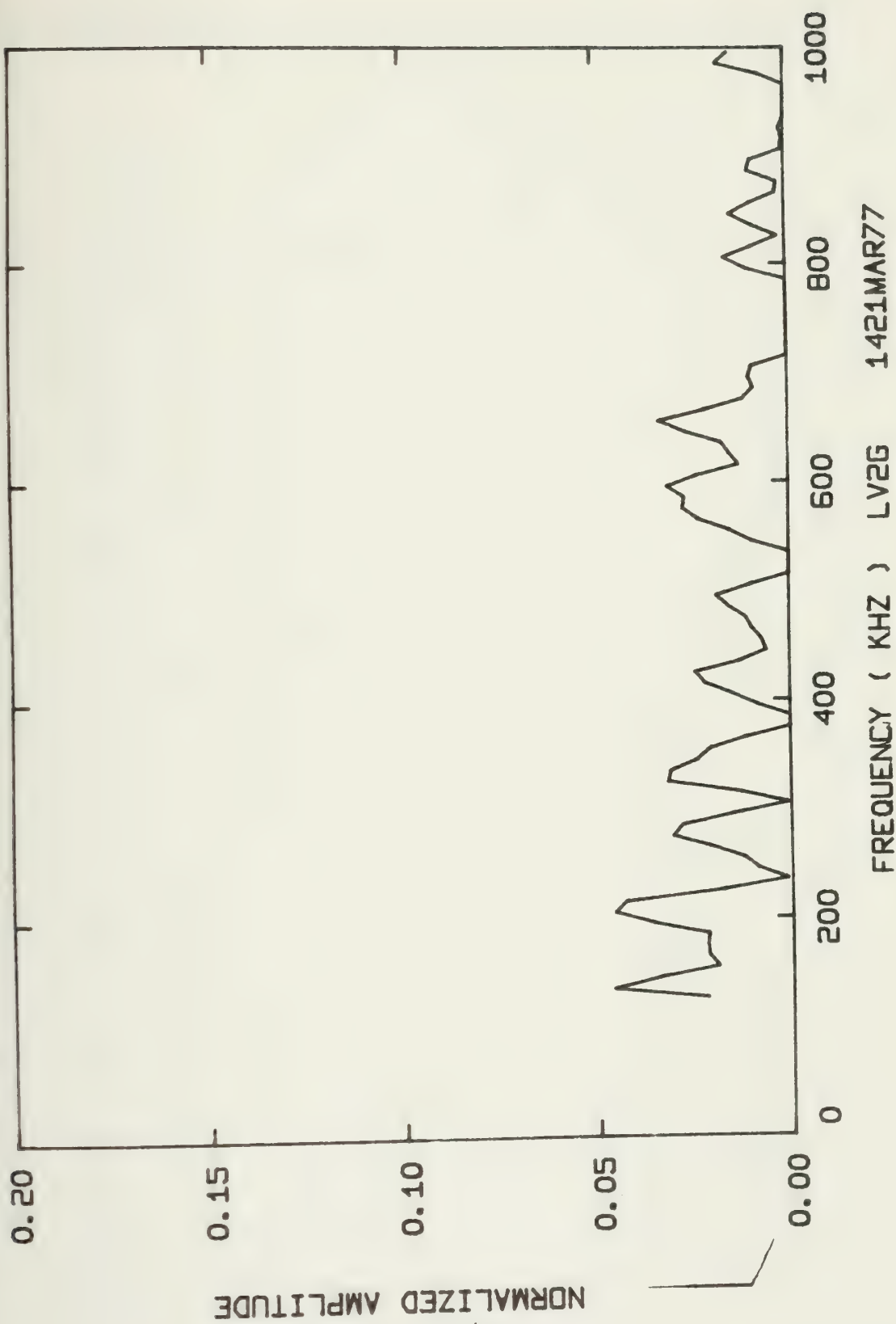




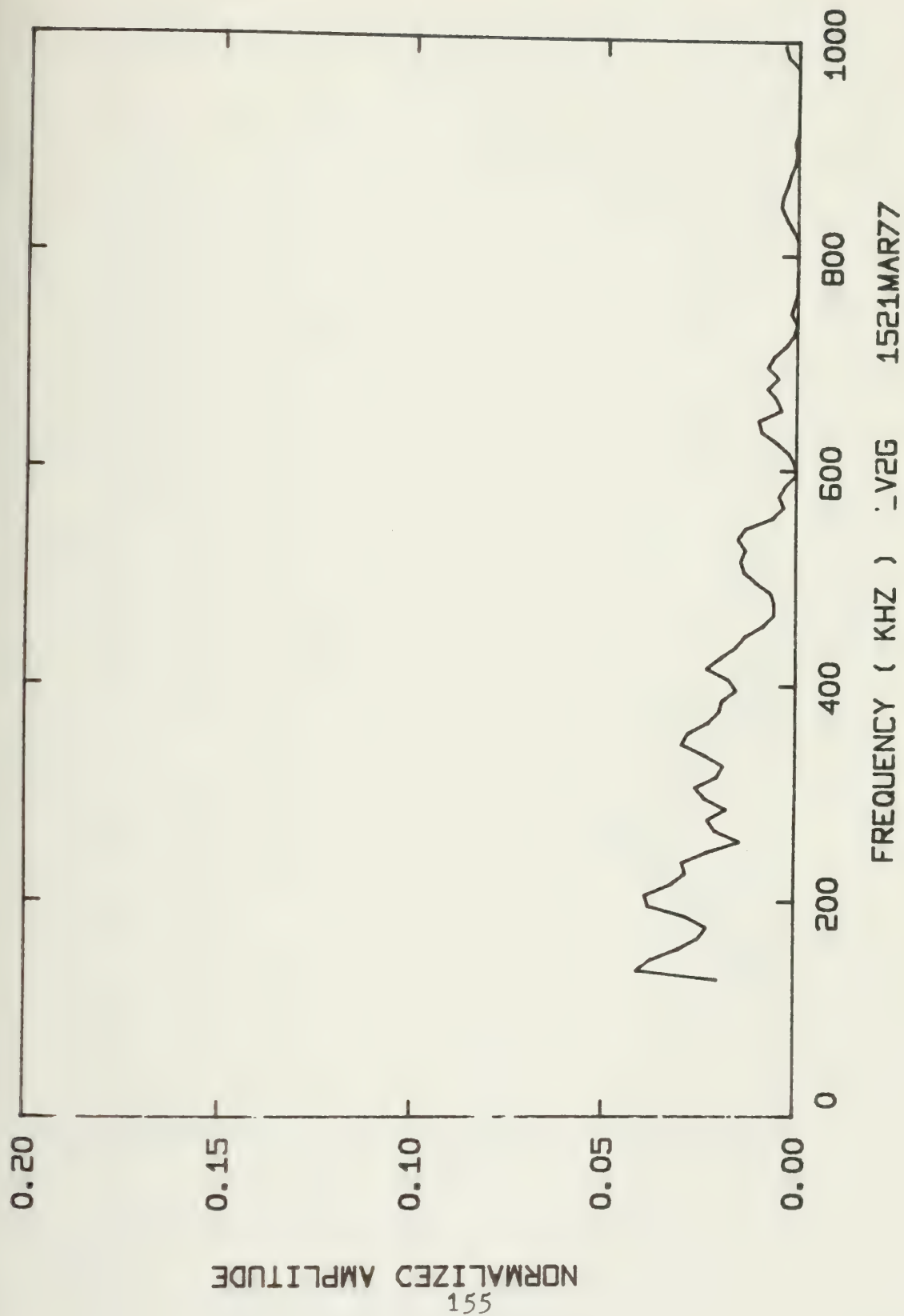




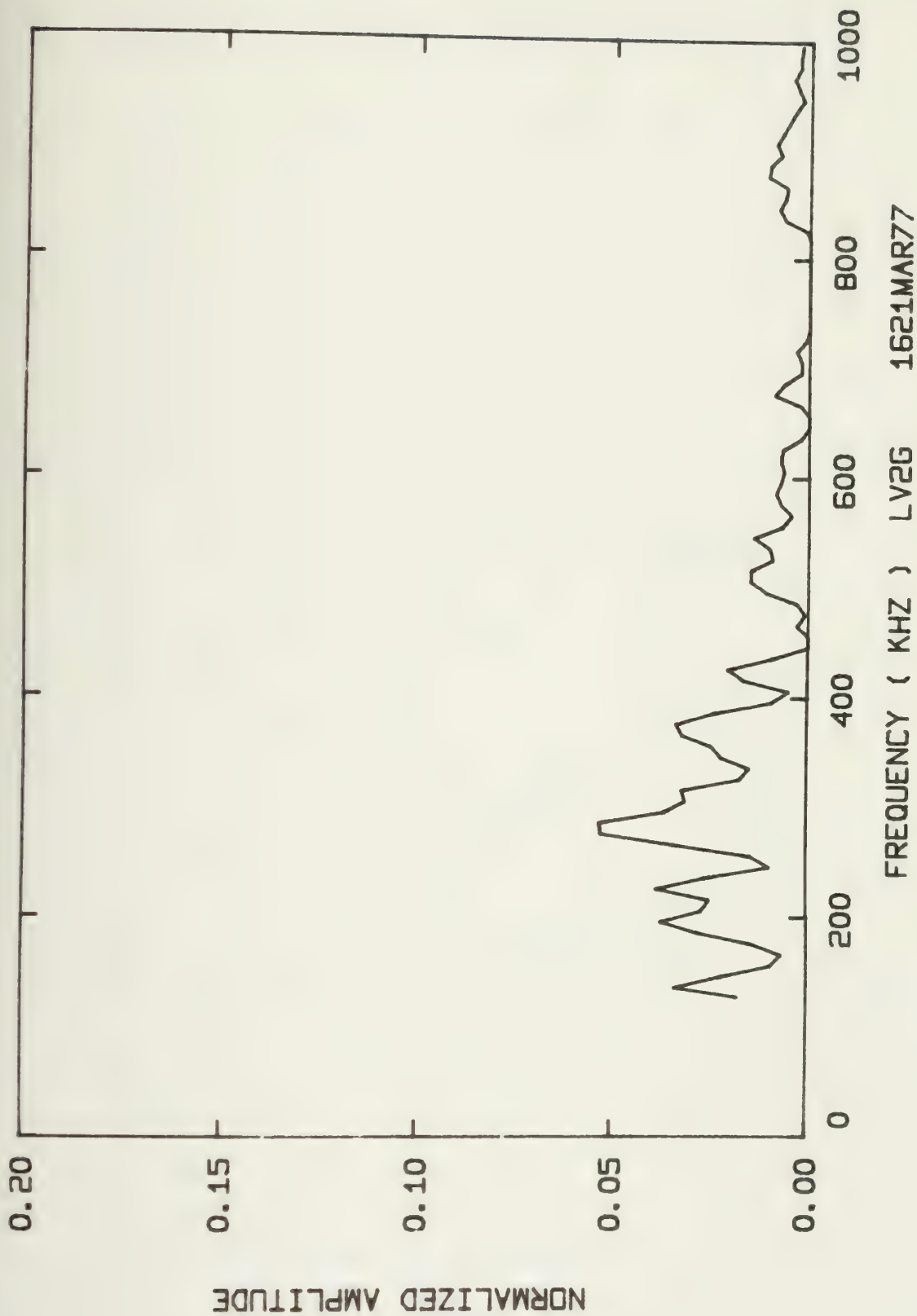






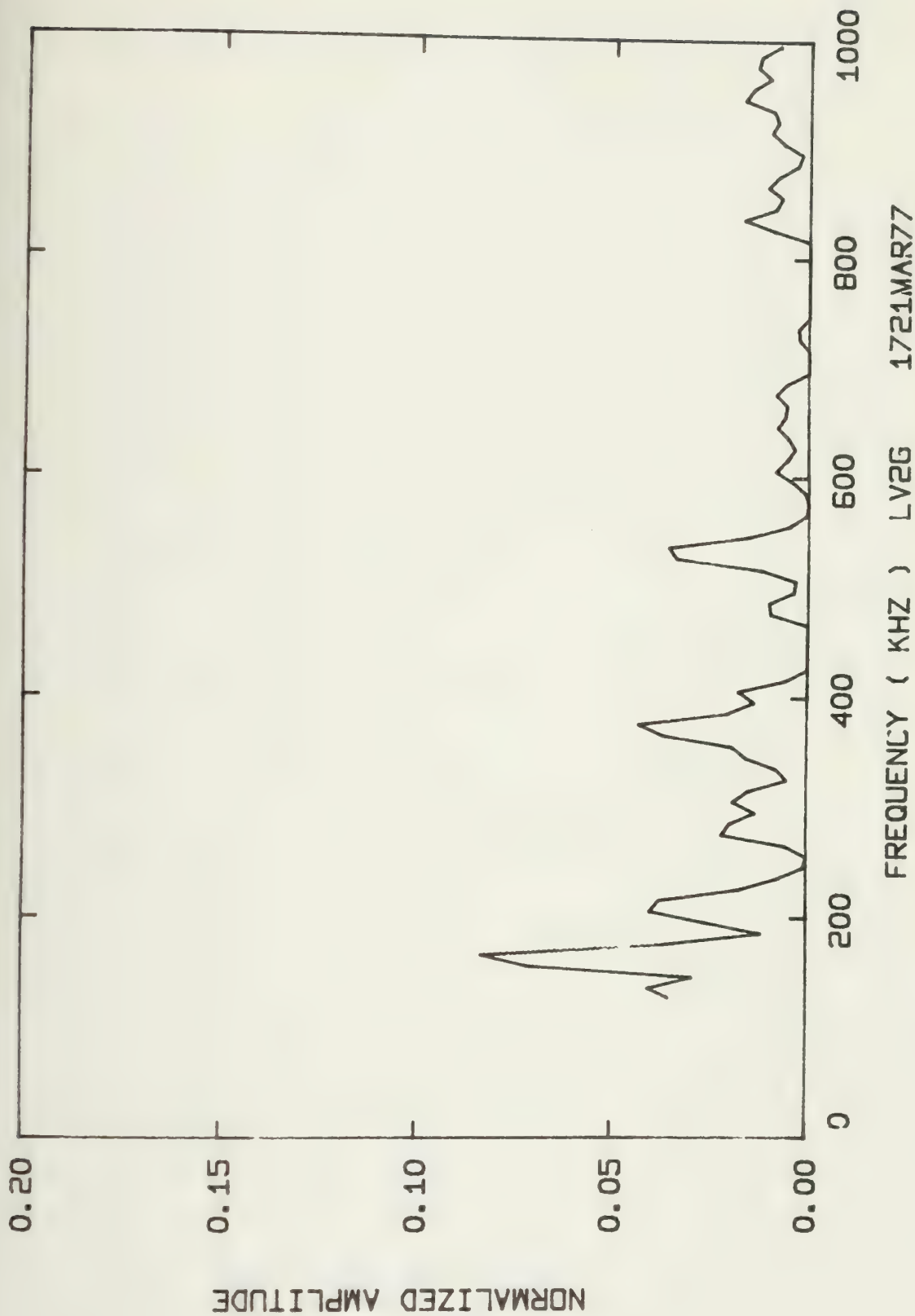




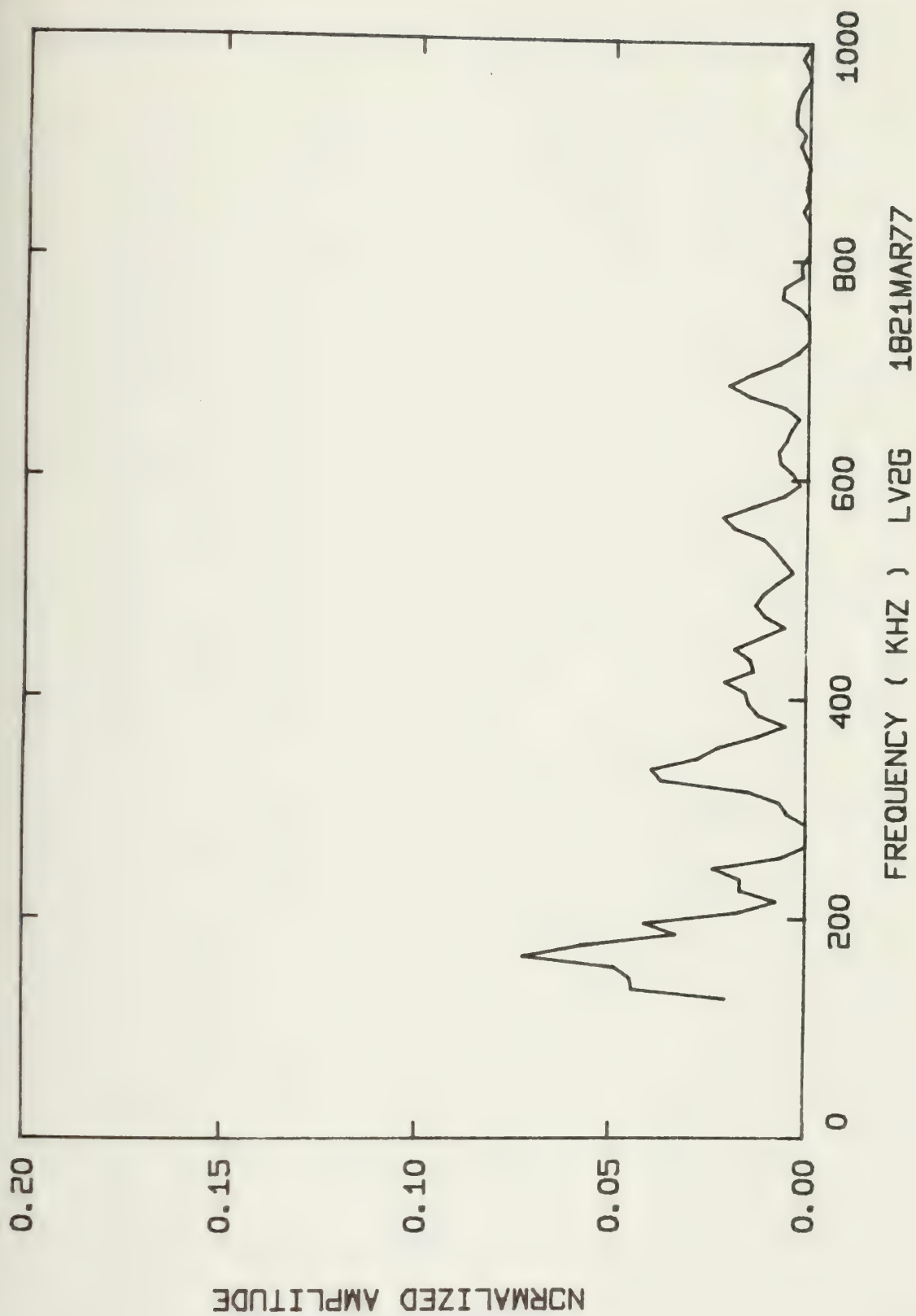




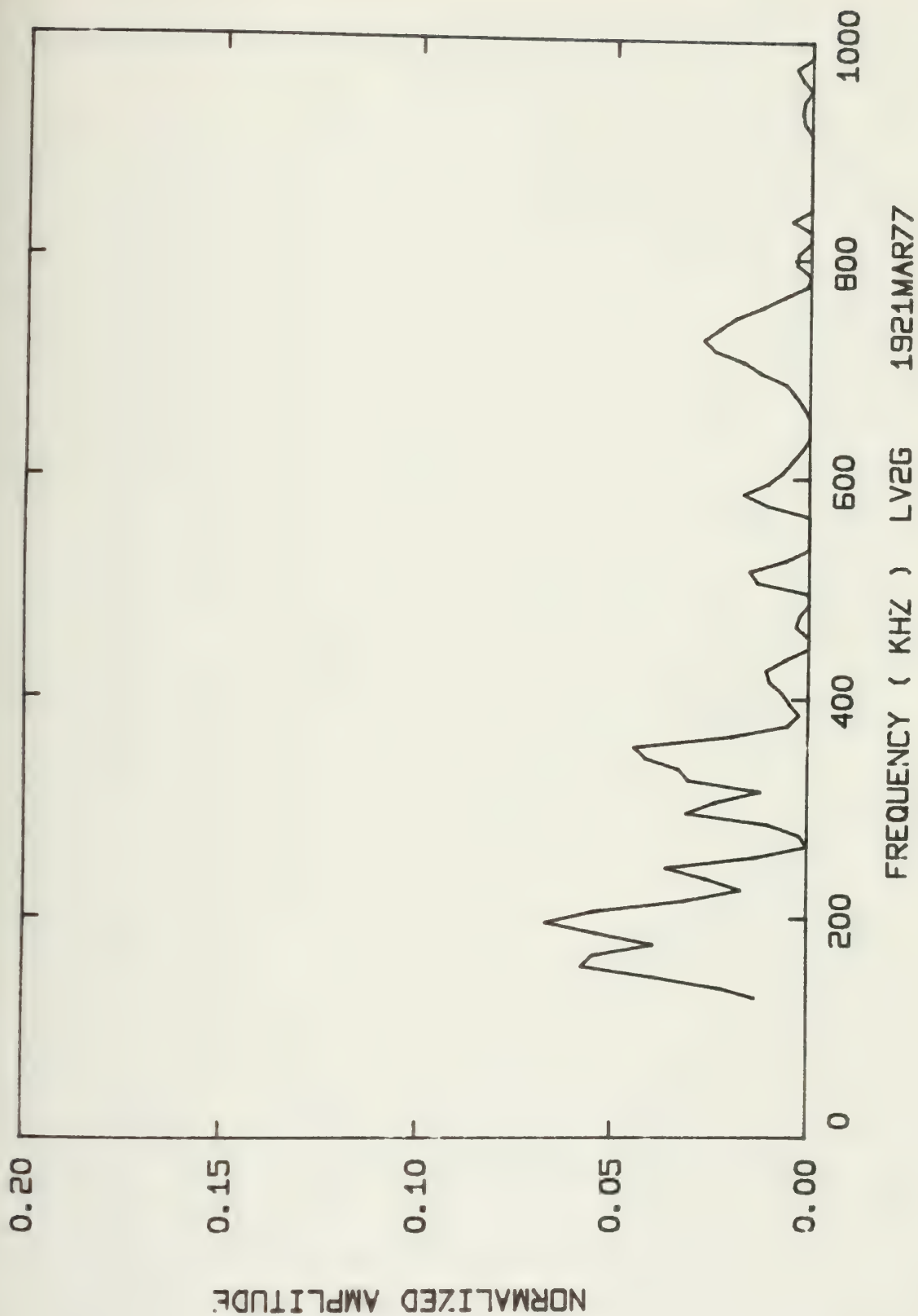




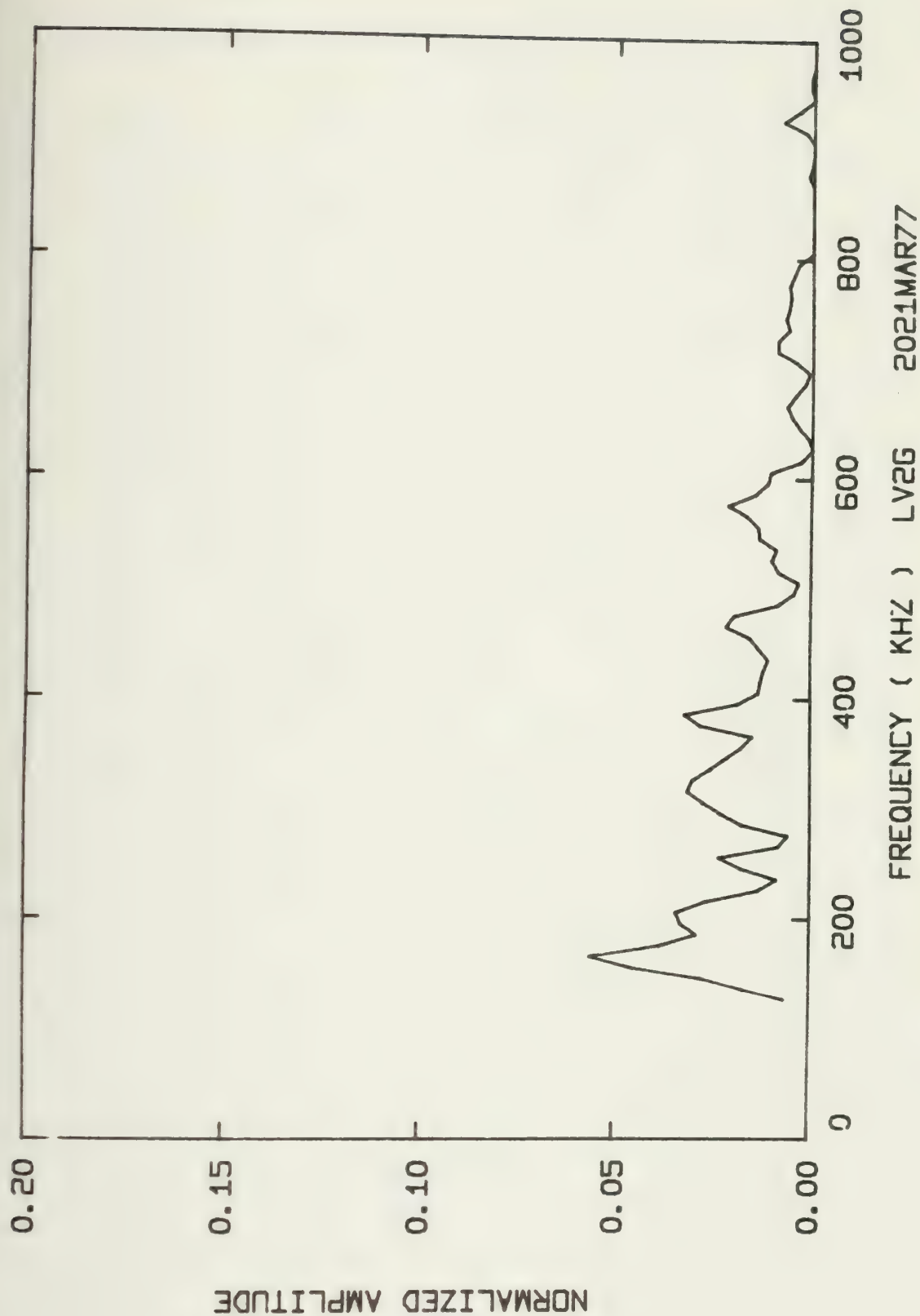






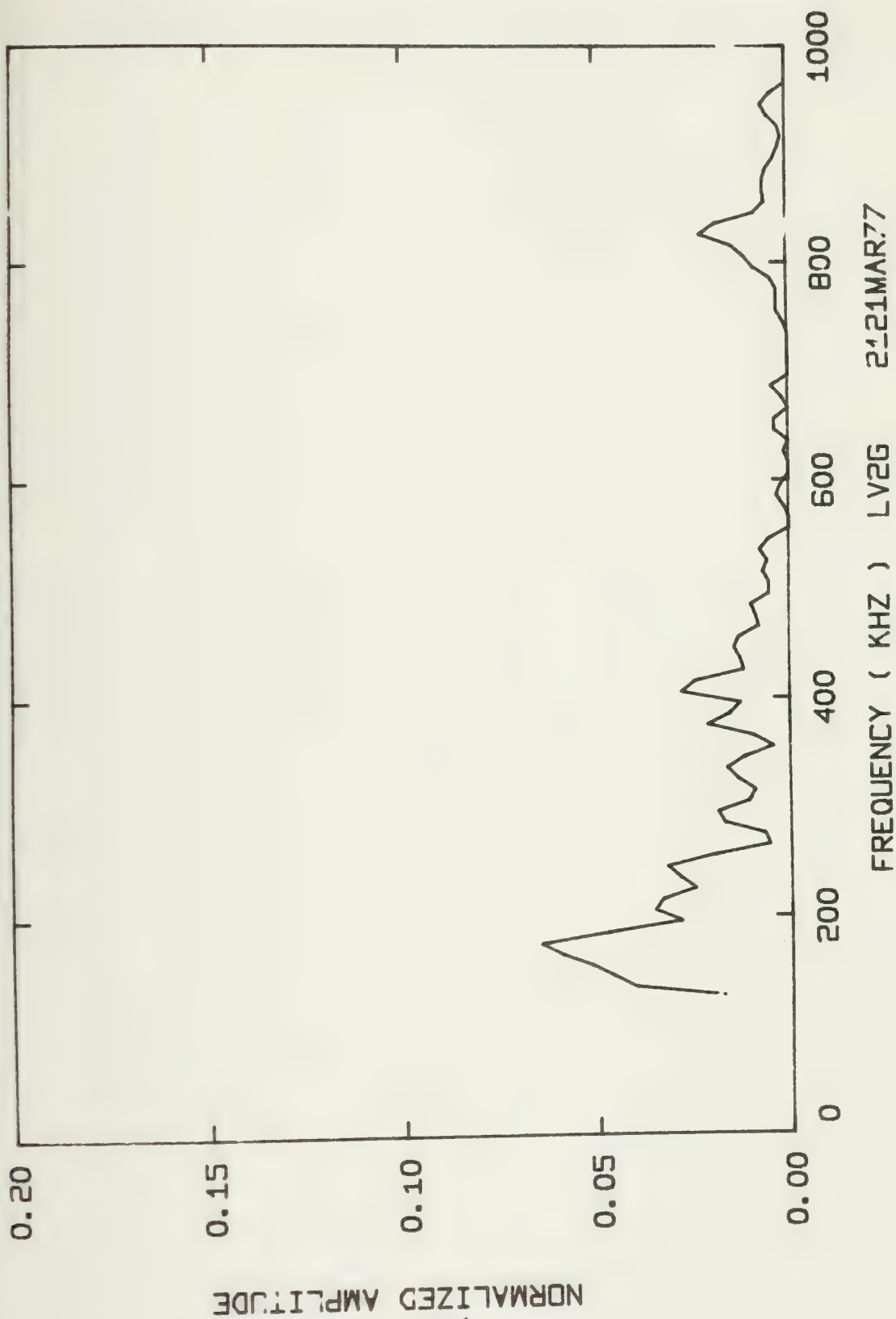




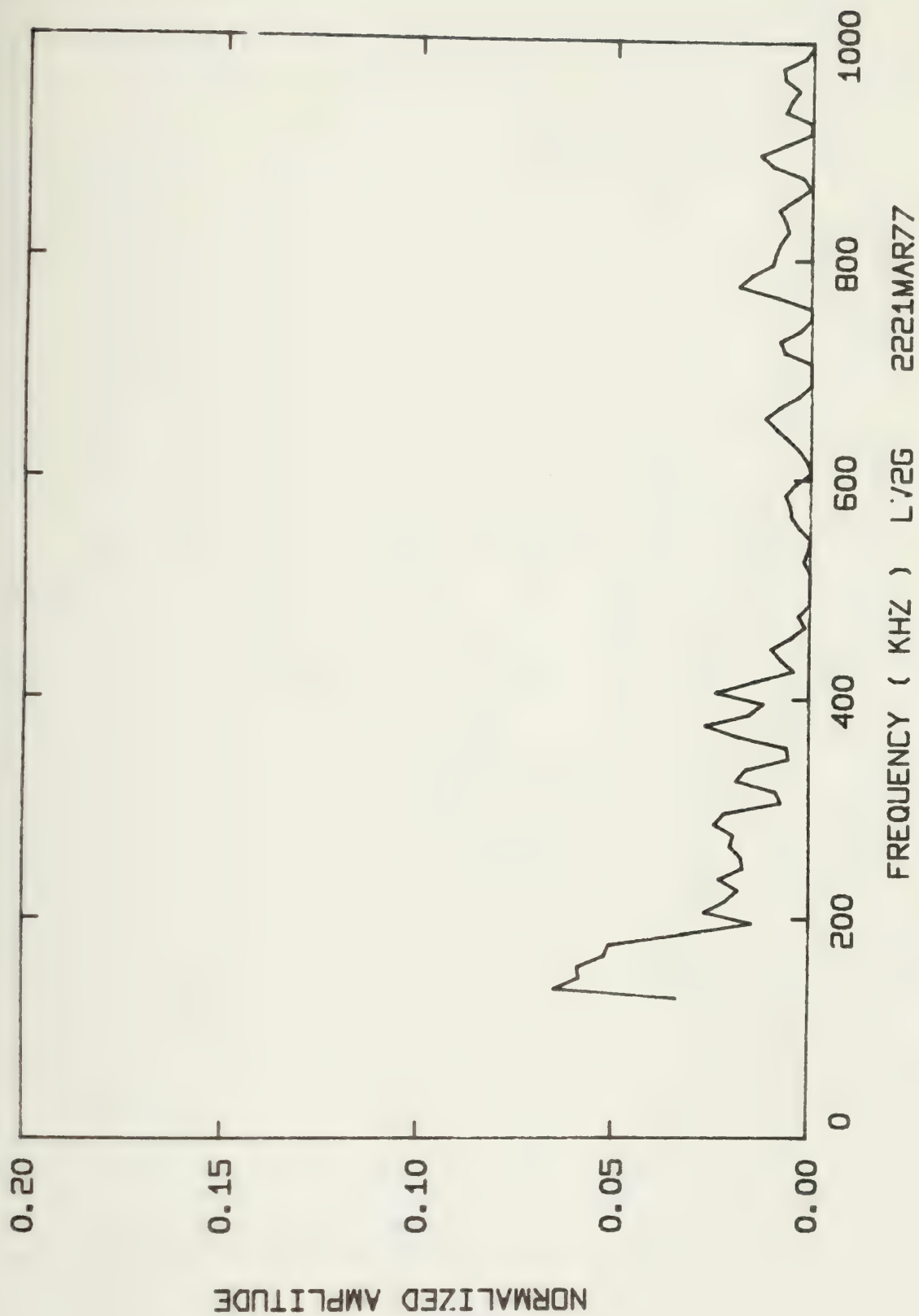




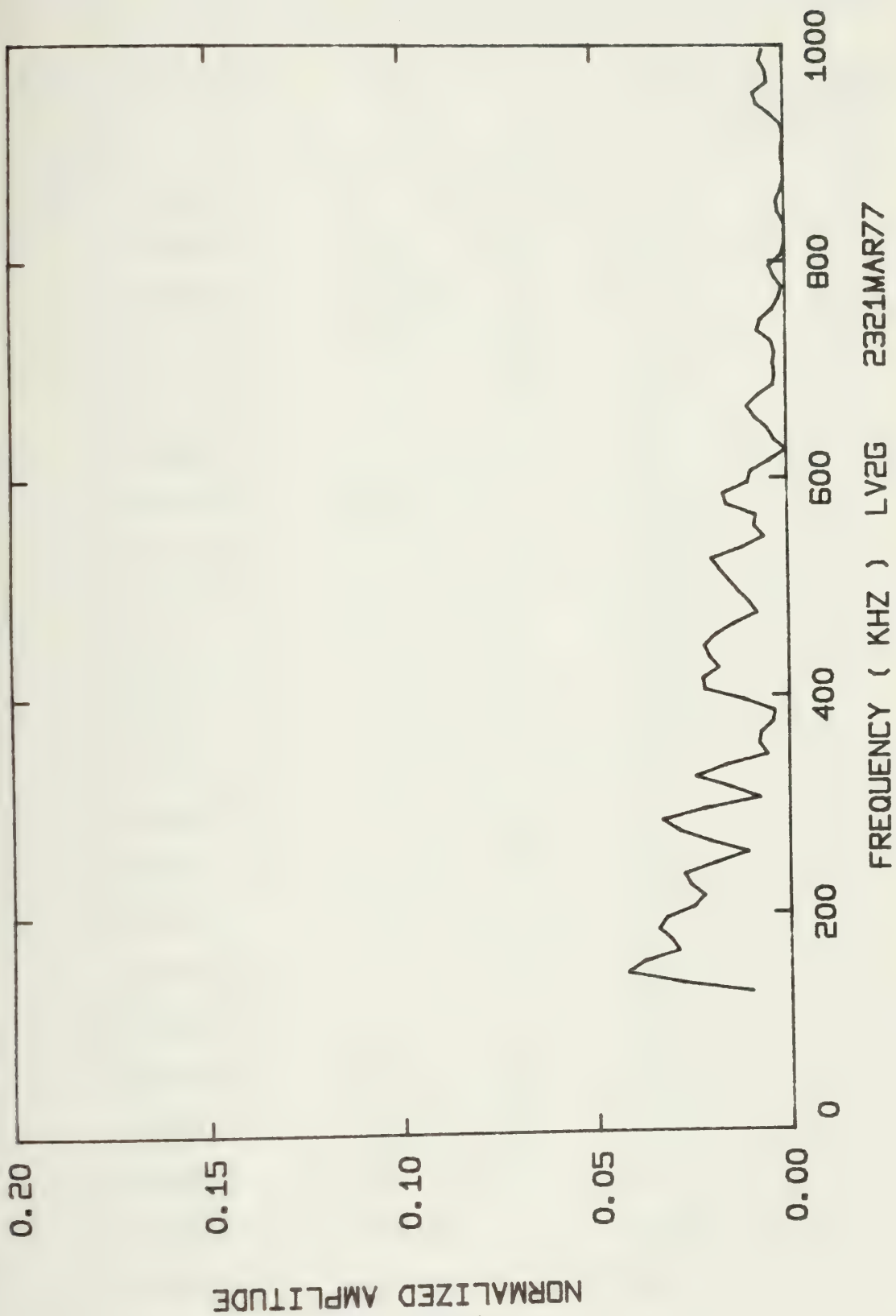














Summary of Energy per Acoustic Emission and RMS Pressure  
Across the Transducer's Face for Each Spectra

Spectral Distrib. Graph Code Number	Energy per AE (Joules)	RMS Pressure Across Face of Transducer (Pa x 10 <sup>5</sup> )
LV2H 0118MAR77	135.25 x 10 <sup>-9</sup>	63.82
0218MAR77	306.51 x 10 <sup>-9</sup>	87.01
0318MAR77	280.24 x 10 <sup>-9</sup>	74.22
0418MAR77	410.84 x 10 <sup>-9</sup>	123.14
0518MAR77	1.0054 x 10 <sup>-6</sup>	135.67
0618MAR77	179.95 x 10 <sup>-9</sup>	74.22
0718MAR77	388.96 x 10 <sup>-9</sup>	101.15
0818MAR77	119.82 x 10 <sup>-6</sup>	72.13
0918MAR77	2.1332 x 10 <sup>-6</sup>	175.05
1018MAR77	1.3396 x 10 <sup>-6</sup>	148.13
1118MAR77	1.4000 x 10 <sup>-6</sup>	151.44
1218MAR77	1.7662 x 10 <sup>-6</sup>	170.09
0119MAR77	116.28 x 10 <sup>-9</sup>	71.06
0219MAR77	241.21 x 10 <sup>-9</sup>	89.69
0319MAR77	125.80 x 10 <sup>-9</sup>	81.93
0121MAR77	265.88 x 10 <sup>-9</sup>	100.25
0221MAR77	771.25 x 10 <sup>-9</sup>	121.73
0321MAR77	506.68 x 10 <sup>-9</sup>	106.51
0421MAR77	2.1499 x 10 <sup>-6</sup>	180.96
0521MAR77	158.70 x 10 <sup>-9</sup>	67.63
0621MAR77	1.2939 x 10 <sup>-6</sup>	126.92
0721MAR77	2.1031 x 10 <sup>-6</sup>	166.31

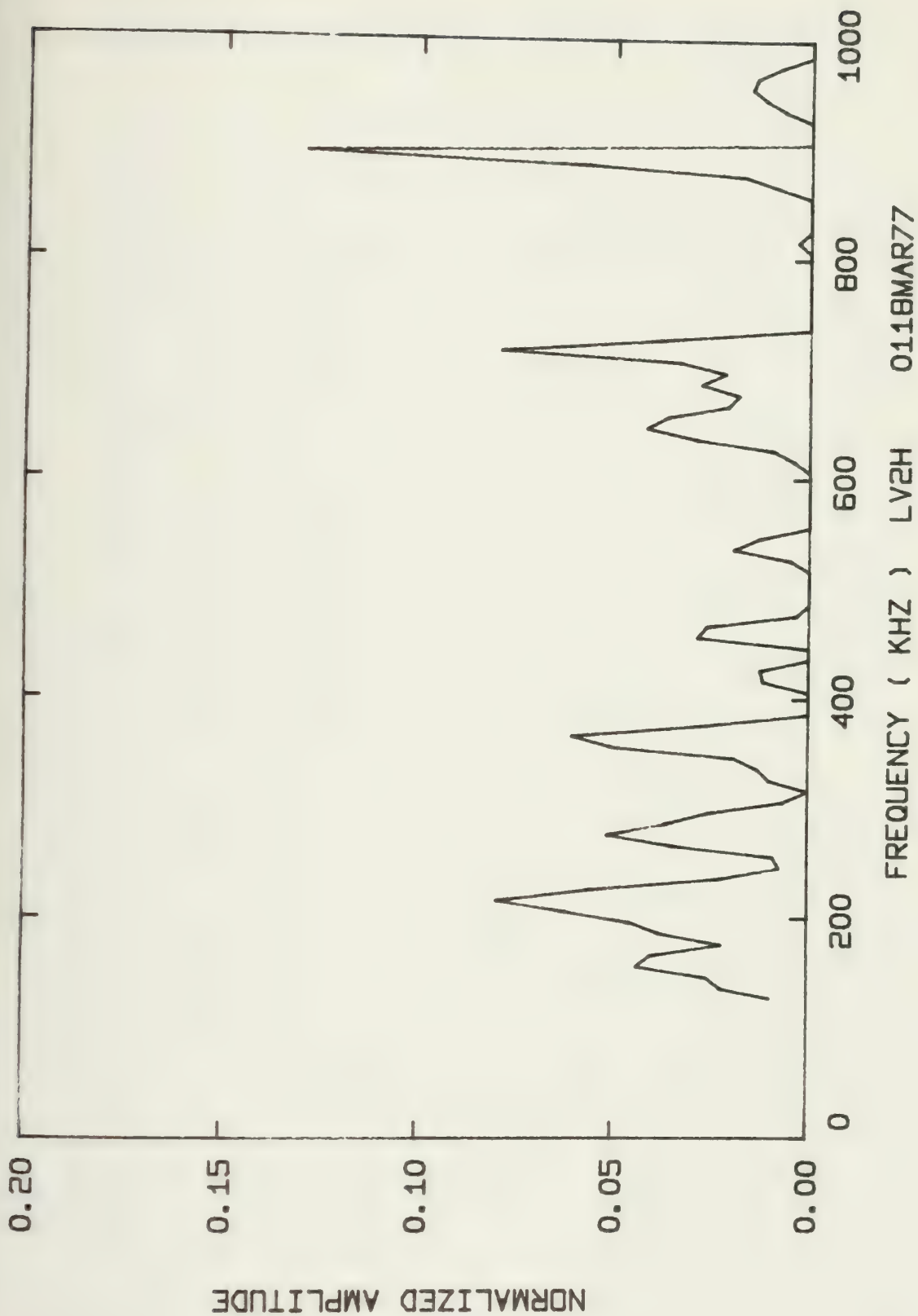




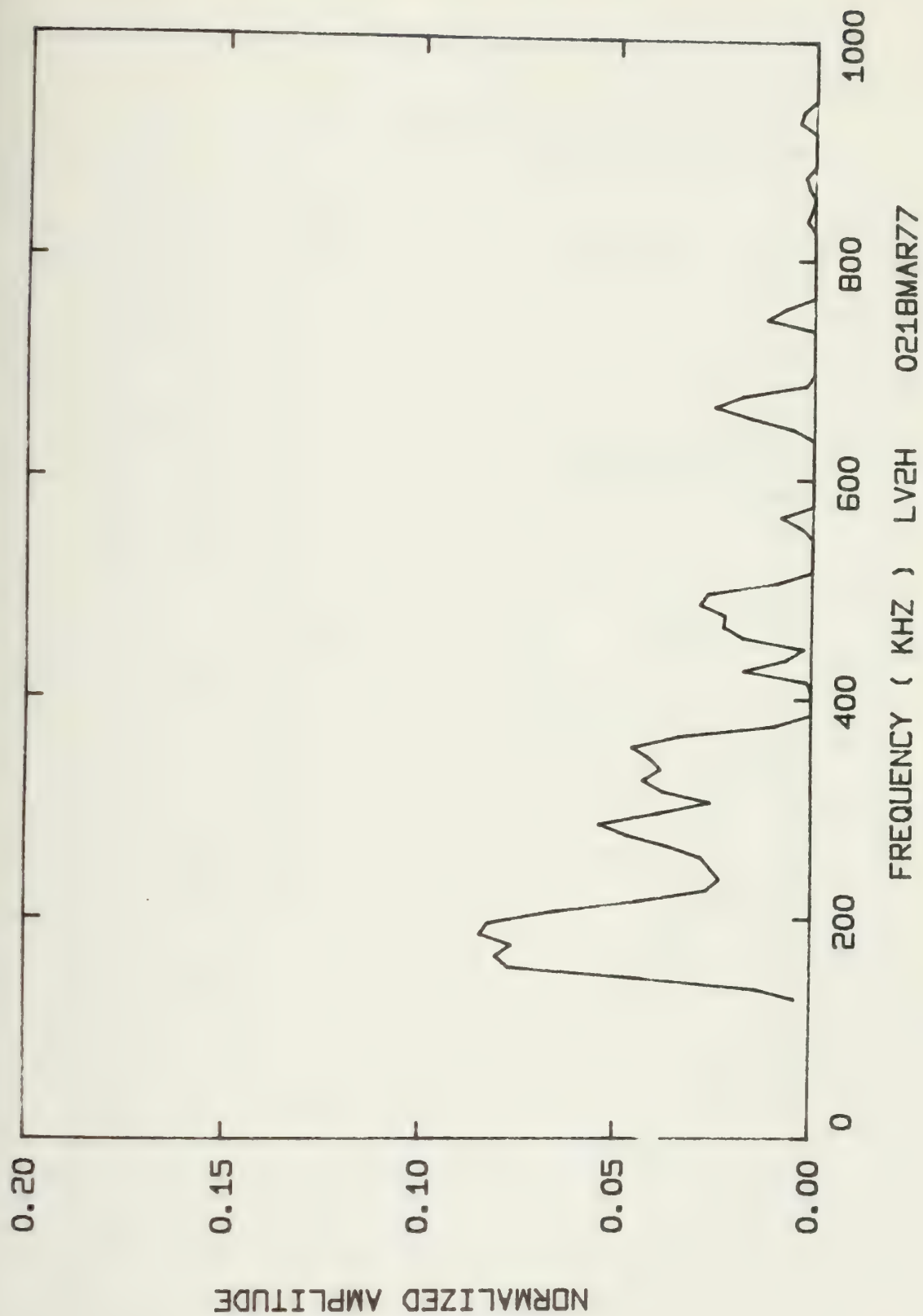
Summary of Energy per Acoustic Emission and RMS Pressure  
Across the Transducer's Face for Each Spectra

Spectral Distrib. Graph Code Number	Energy per AE (Joules)	RMS Pressure Across Face of Transducer (Pa x 10 <sup>5</sup> )
LV2H 0821MAR77	1.0554 x 10 <sup>-6</sup>	147.98
0921MAR77	673.47 x 10 <sup>-9</sup>	113.28
0110MAR77	2.3945 x 10 <sup>-6</sup>	193.03
0210MAR77	848.16 x 10 <sup>-9</sup>	122.82
0310MAR77	1.5972 x 10 <sup>-6</sup>	156.87
0410MAR77	132.91 x 10 <sup>-9</sup>	72.98
0510MAR77	261.59 x 10 <sup>-9</sup>	82.95

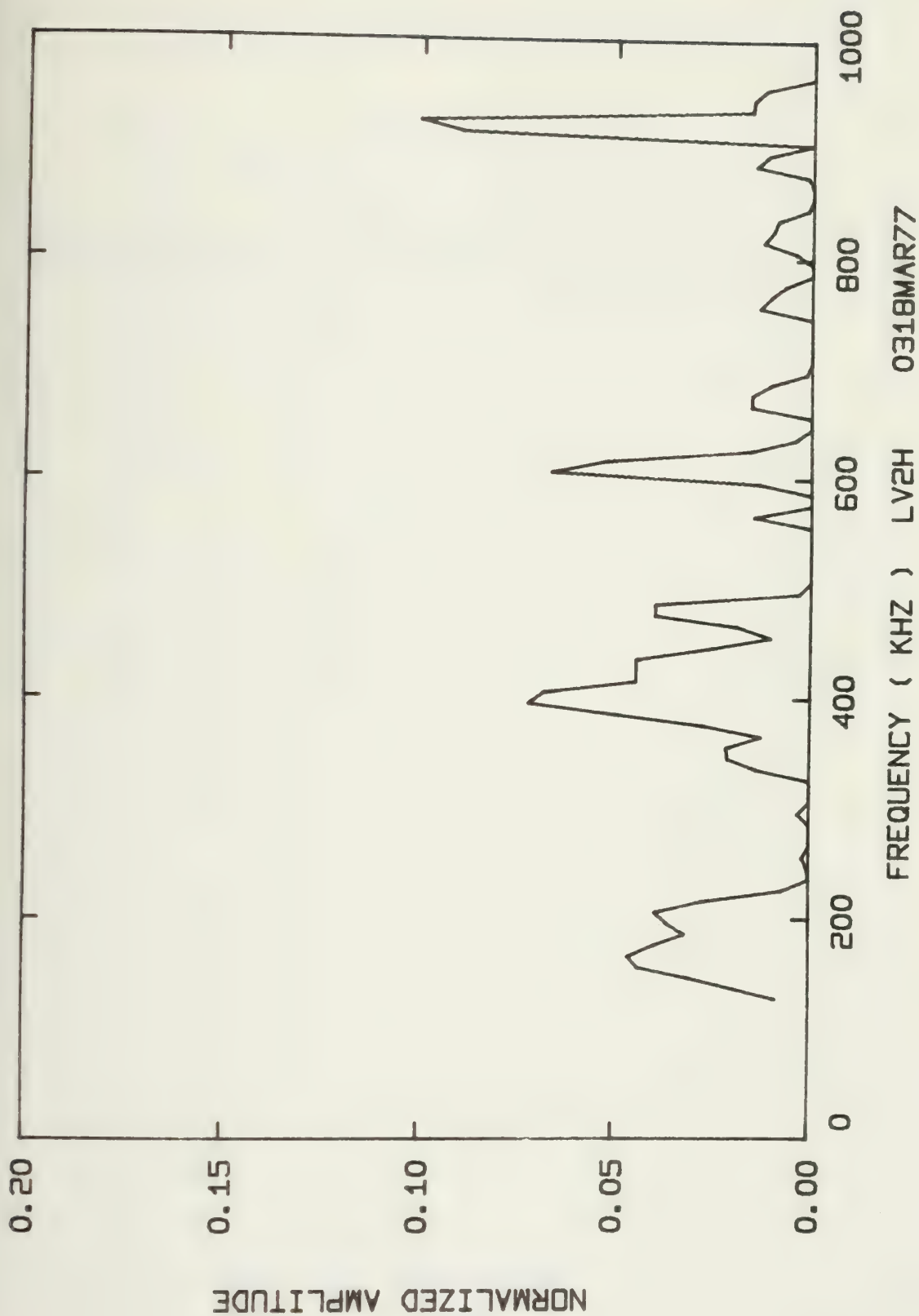






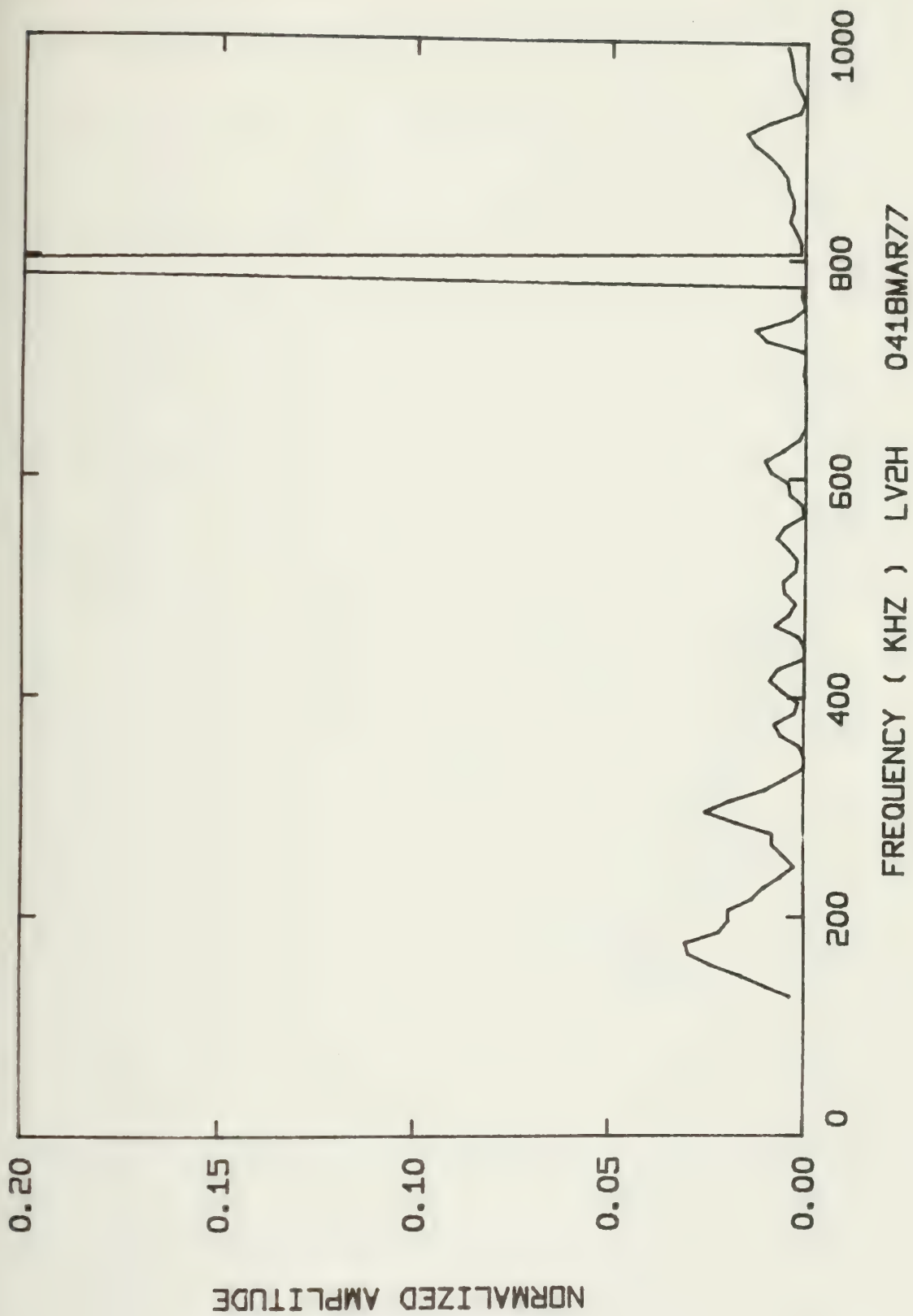




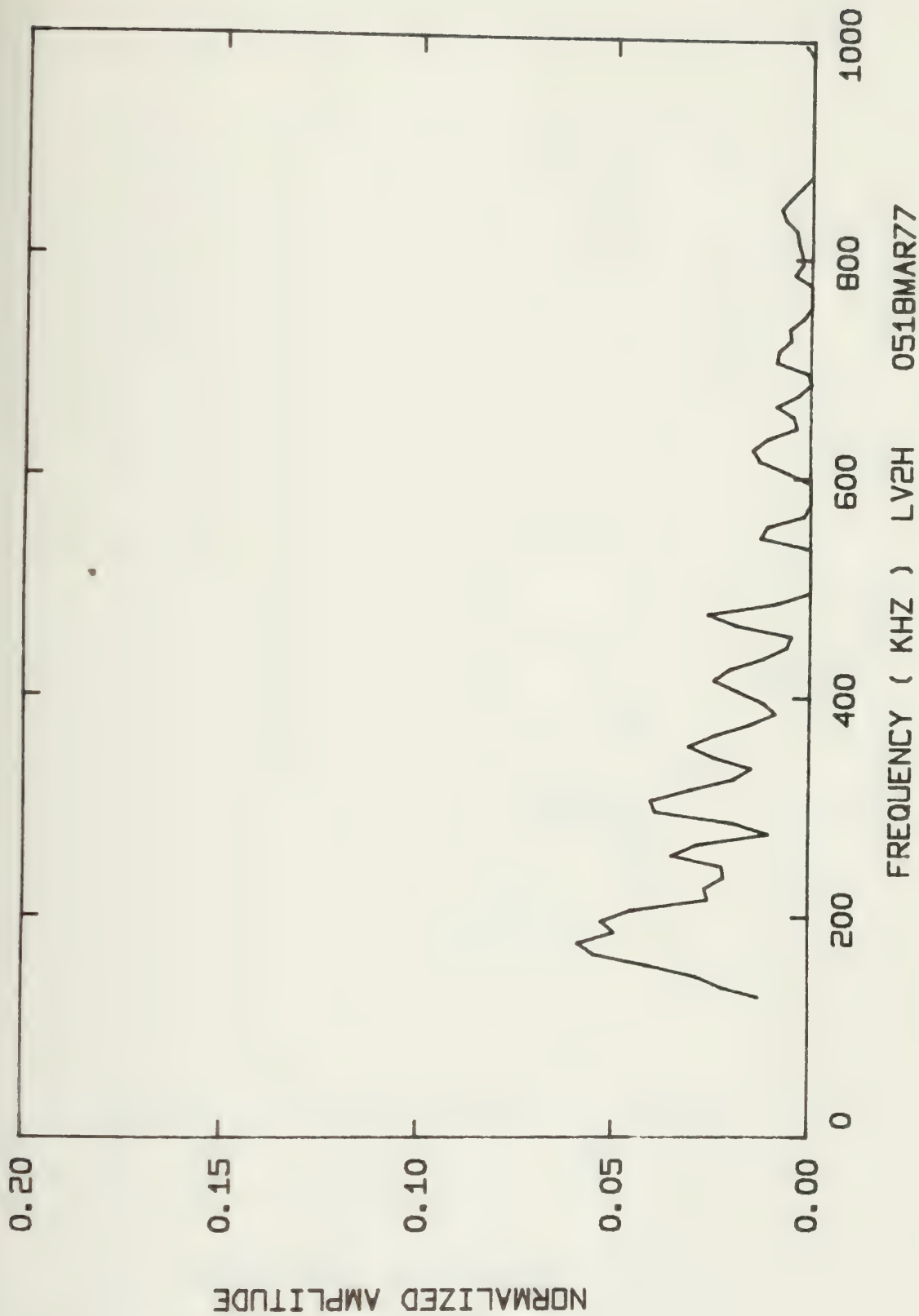


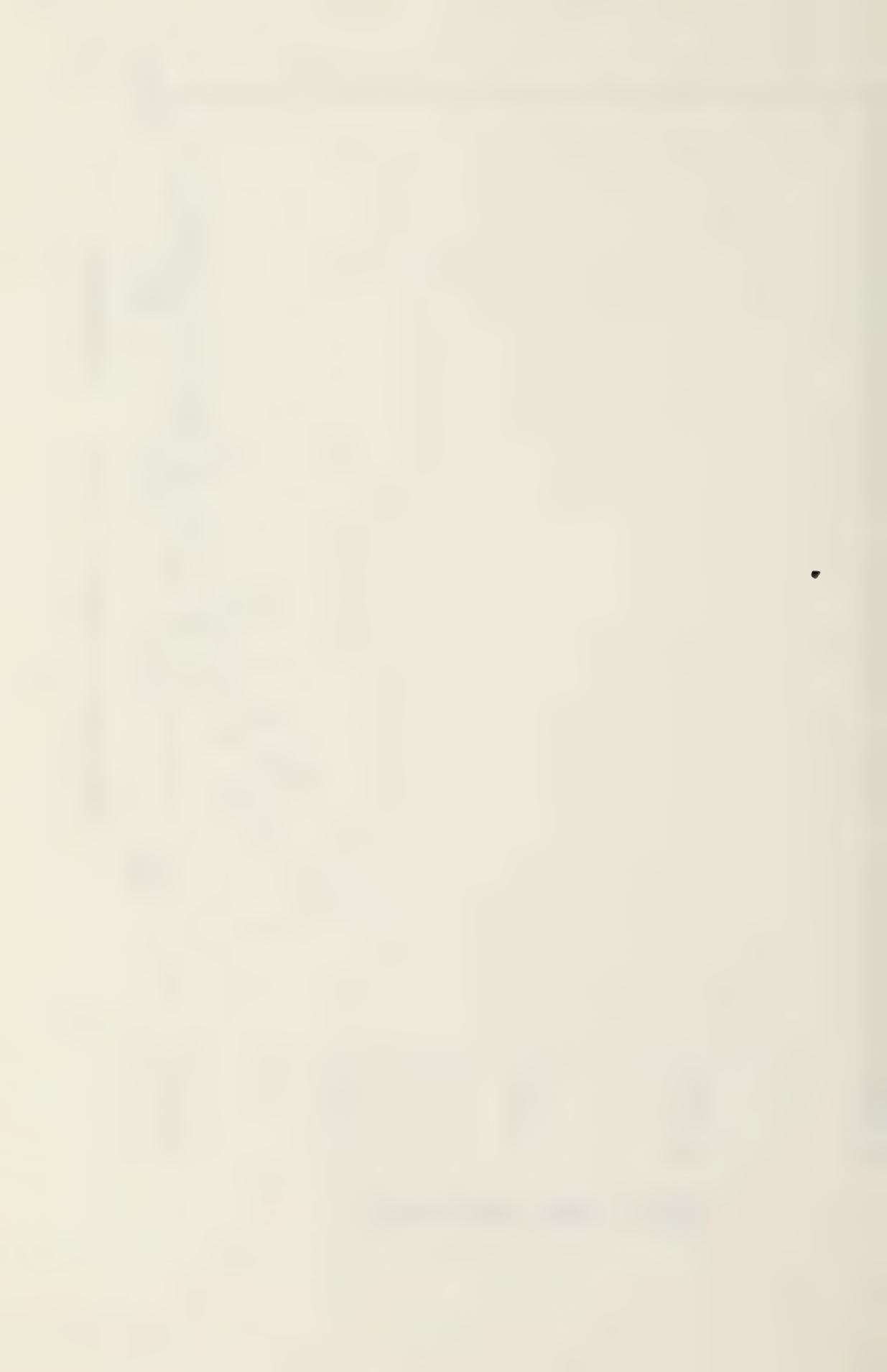


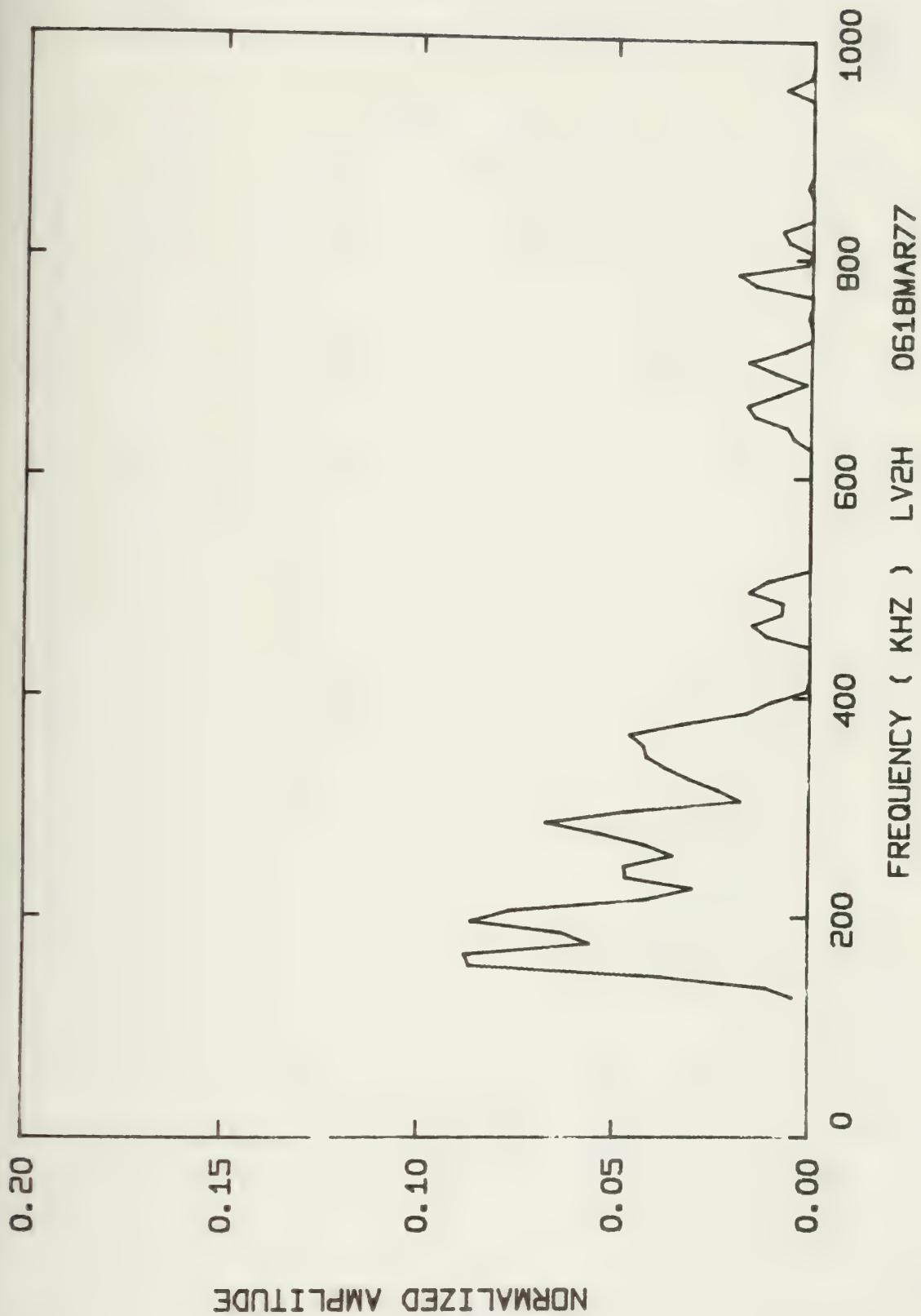




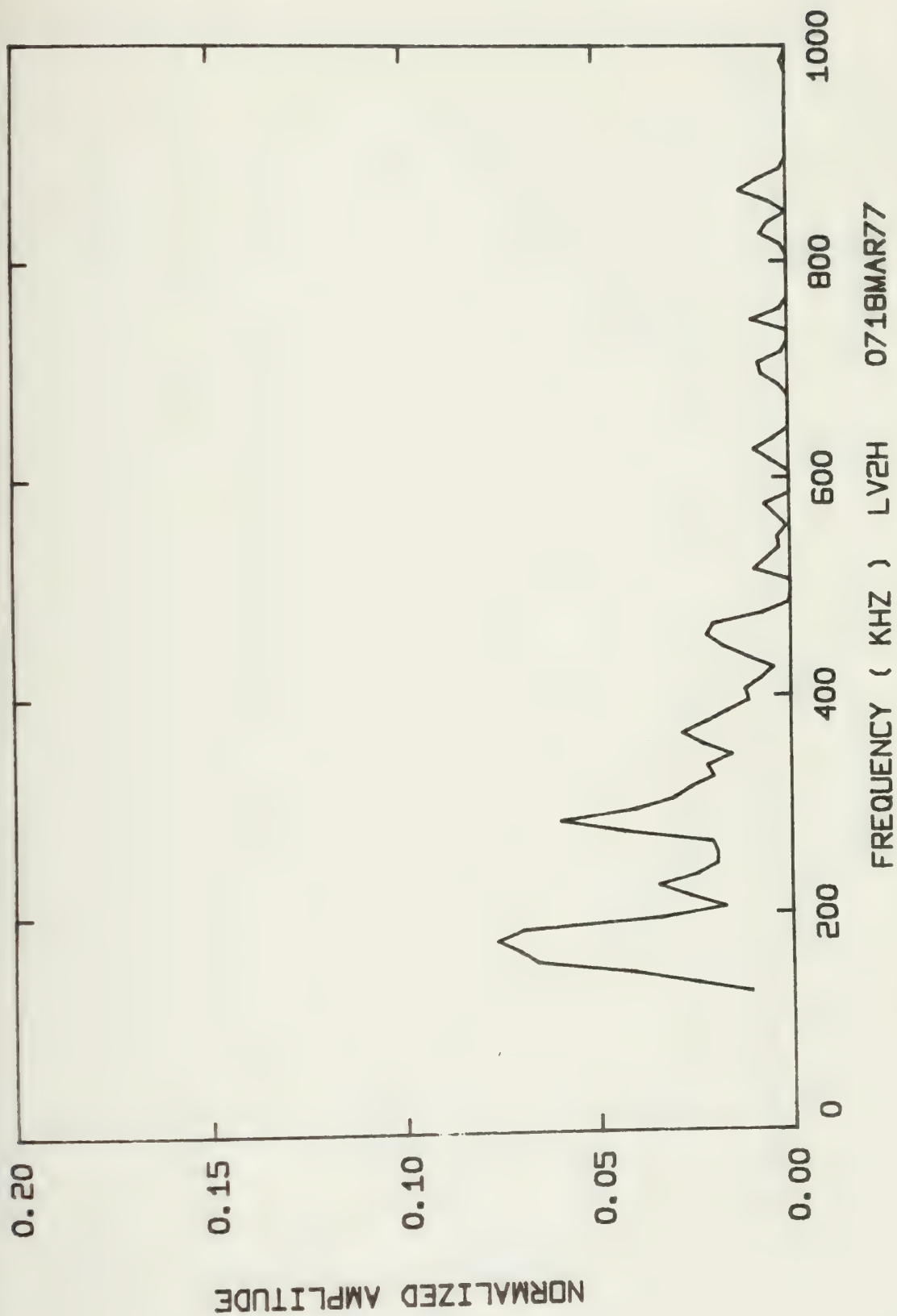






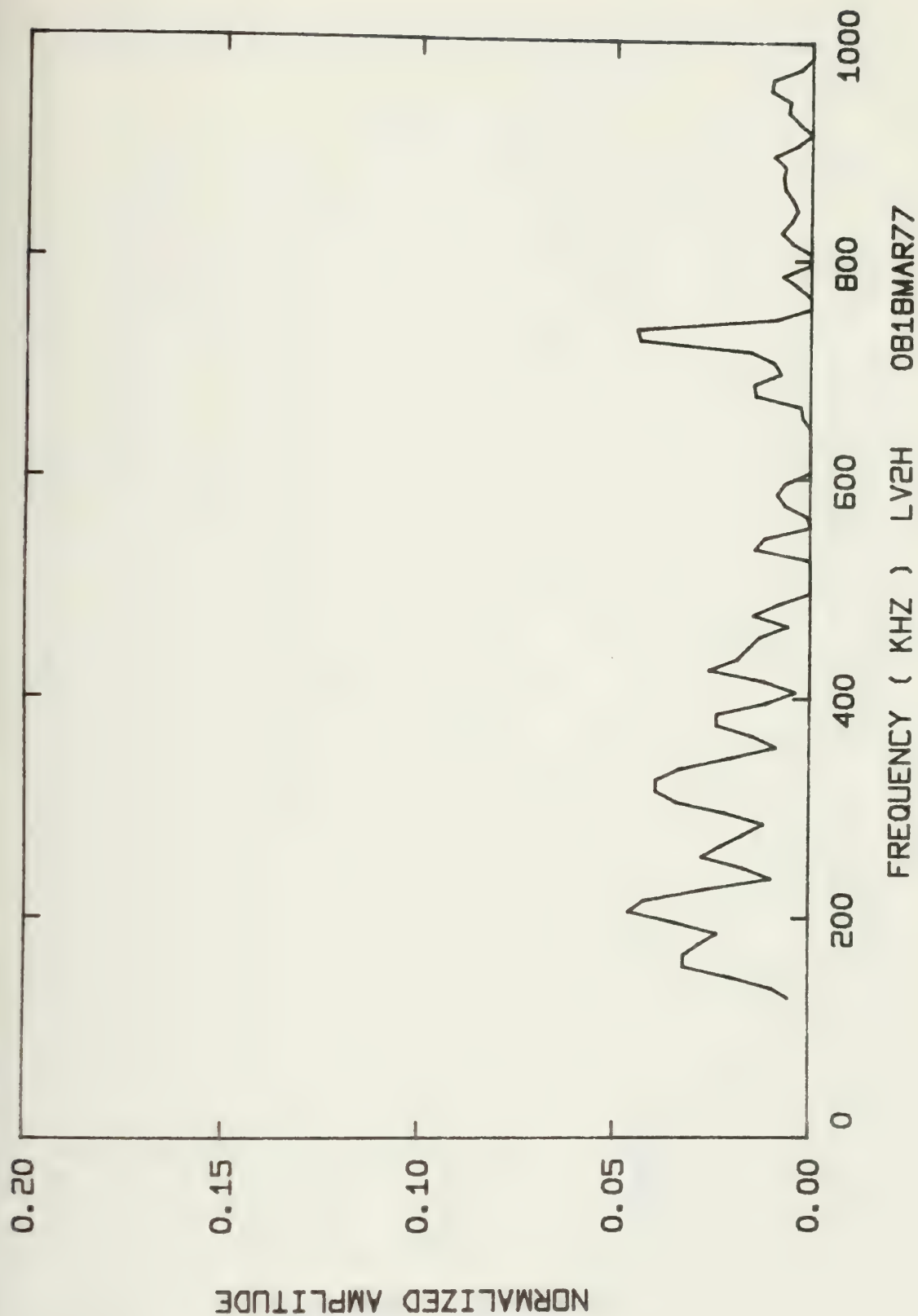




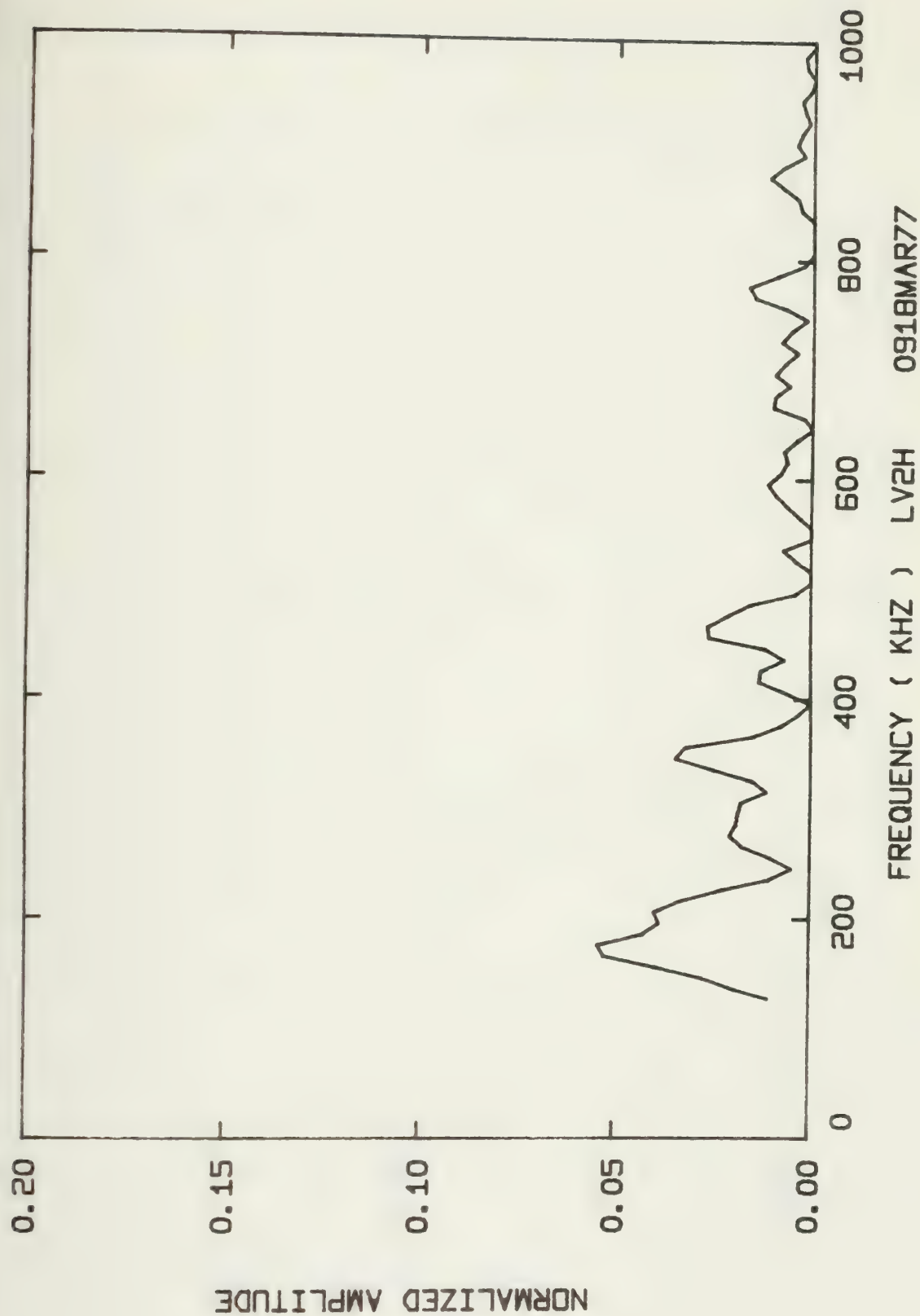




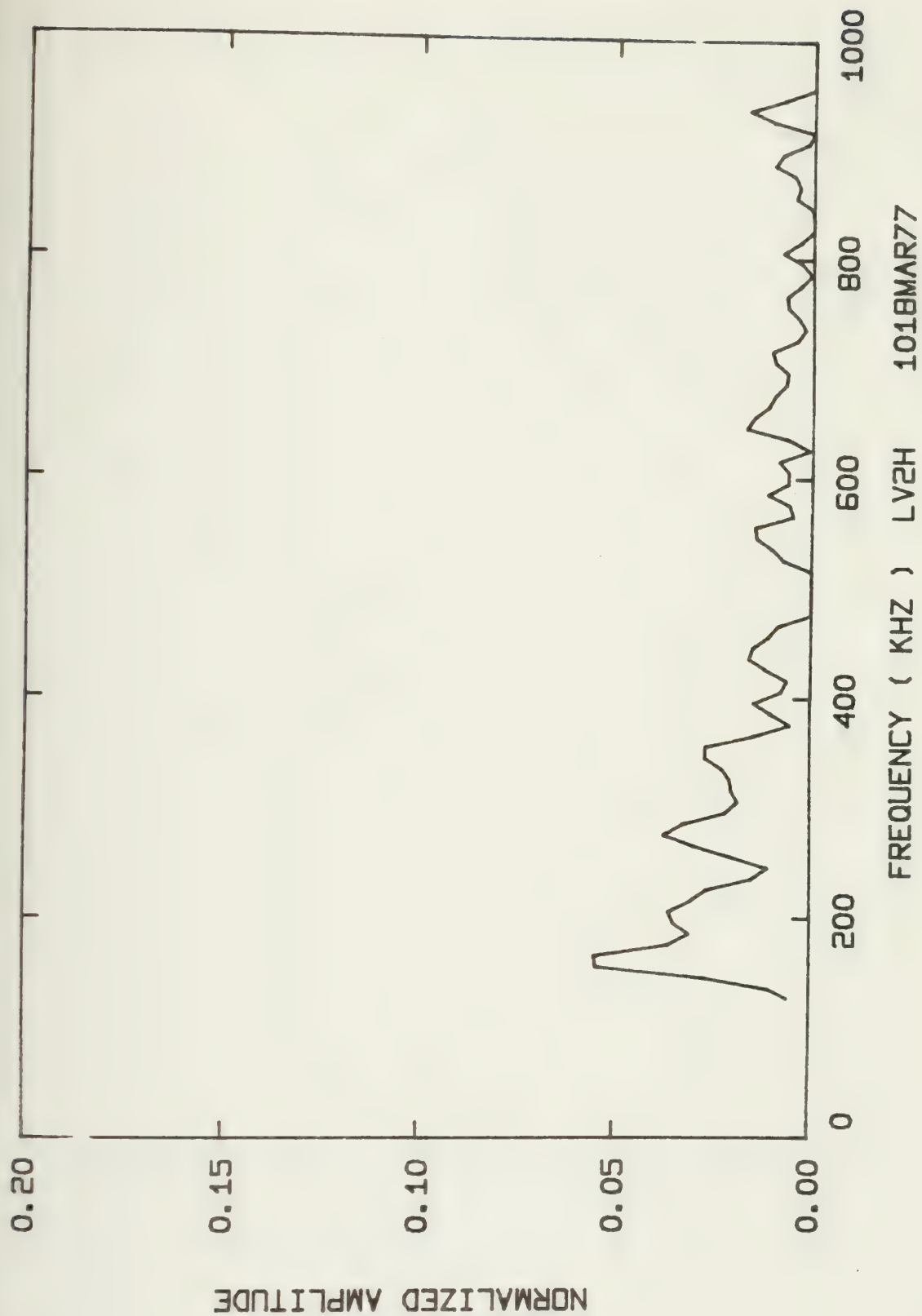




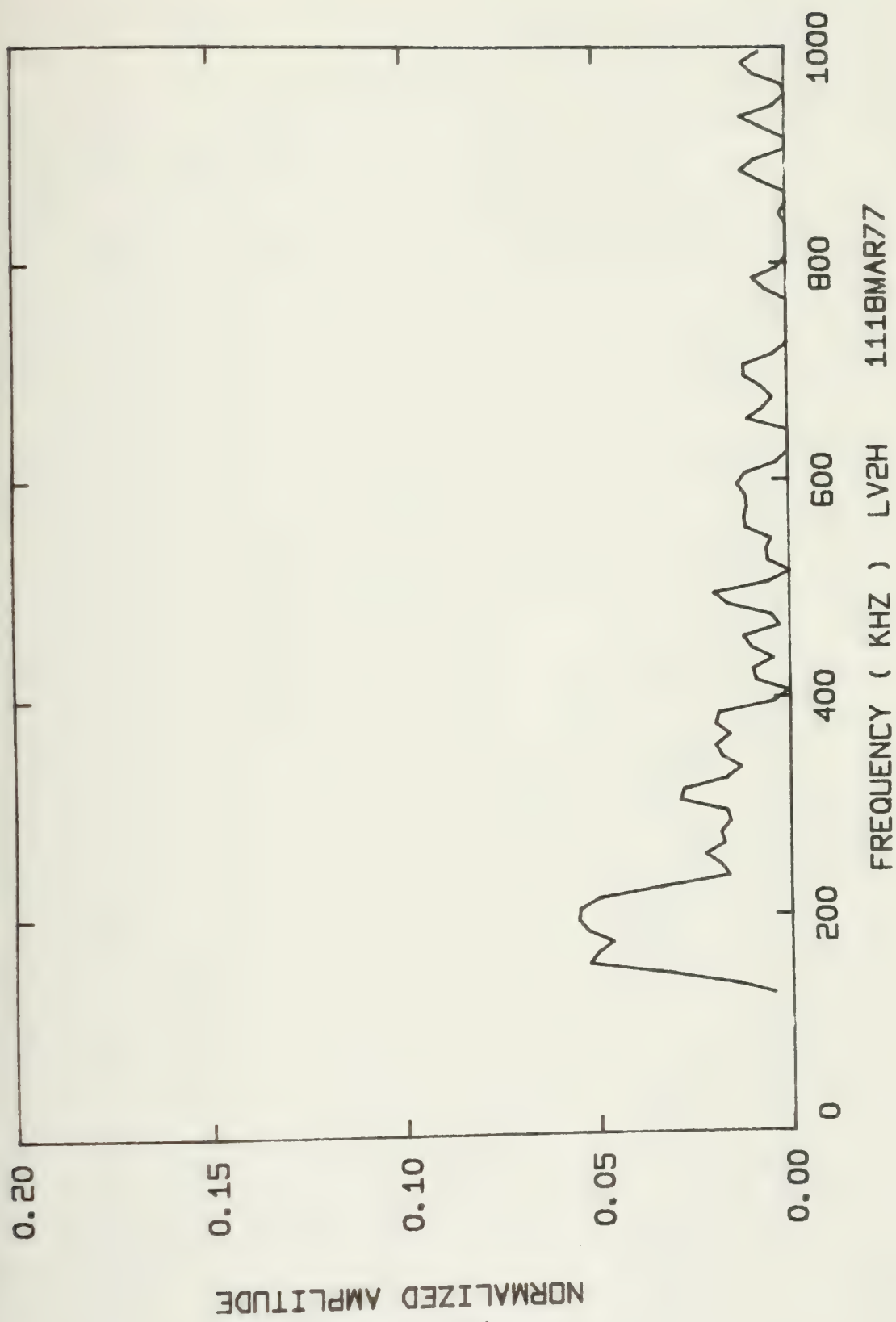






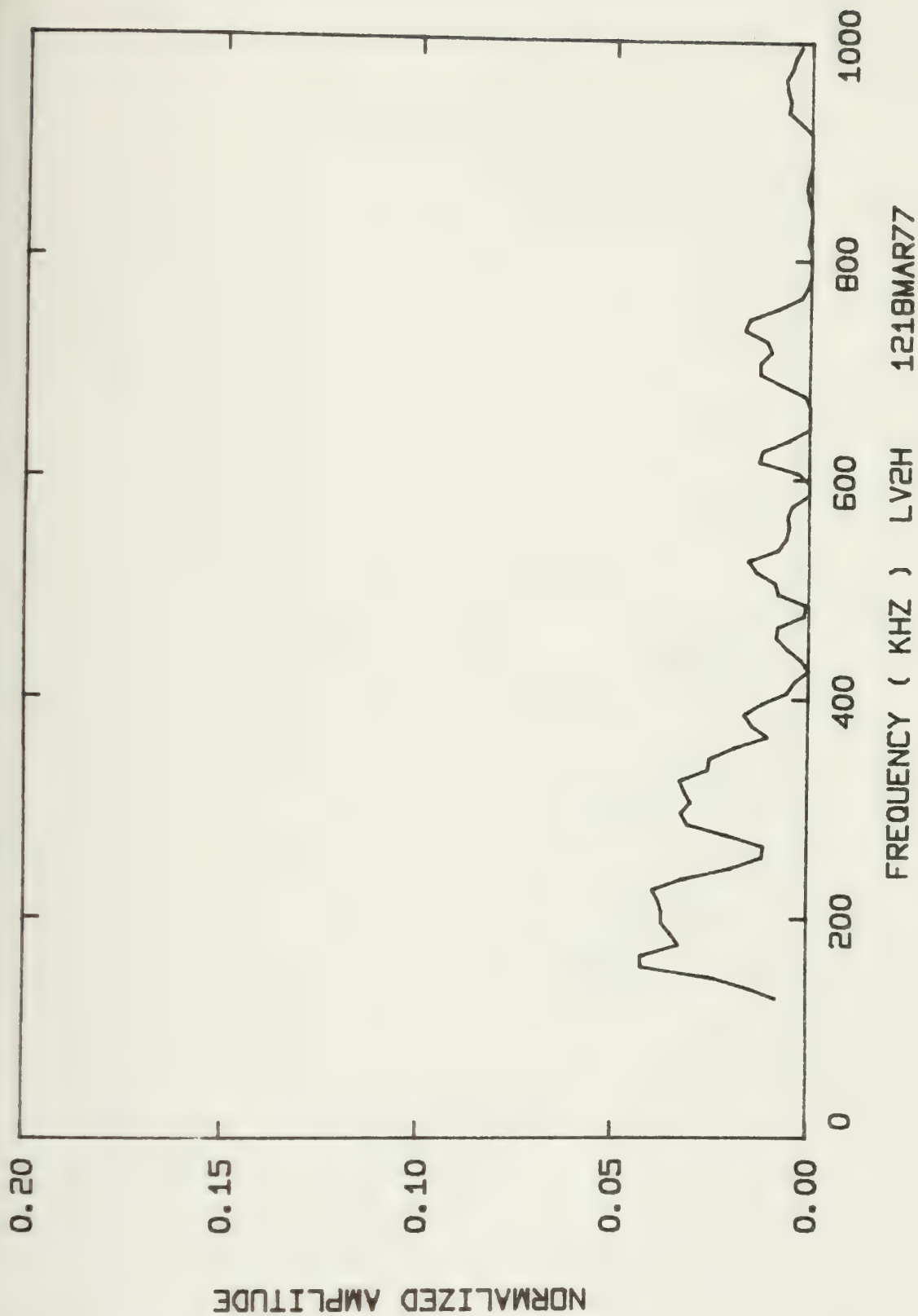




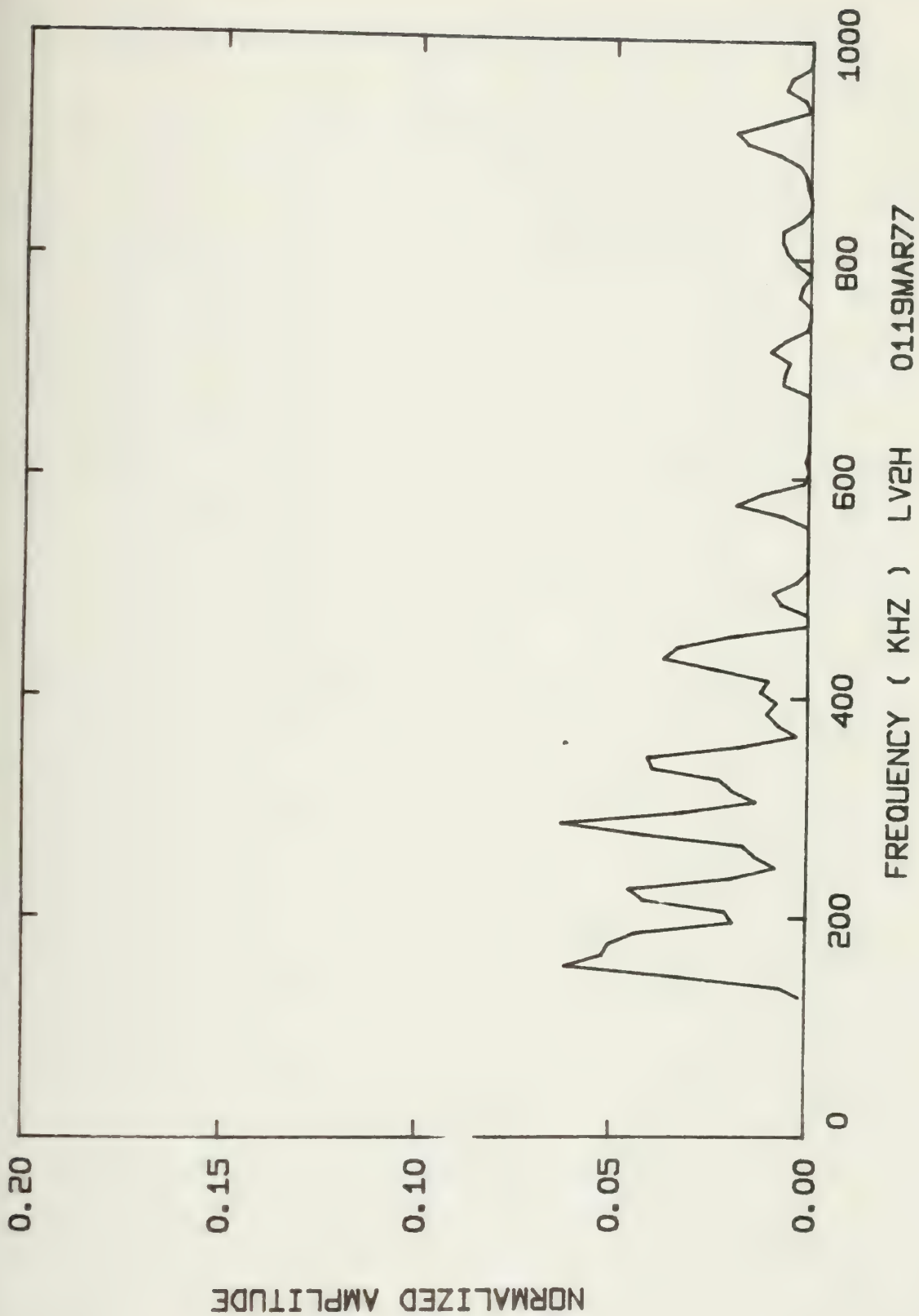




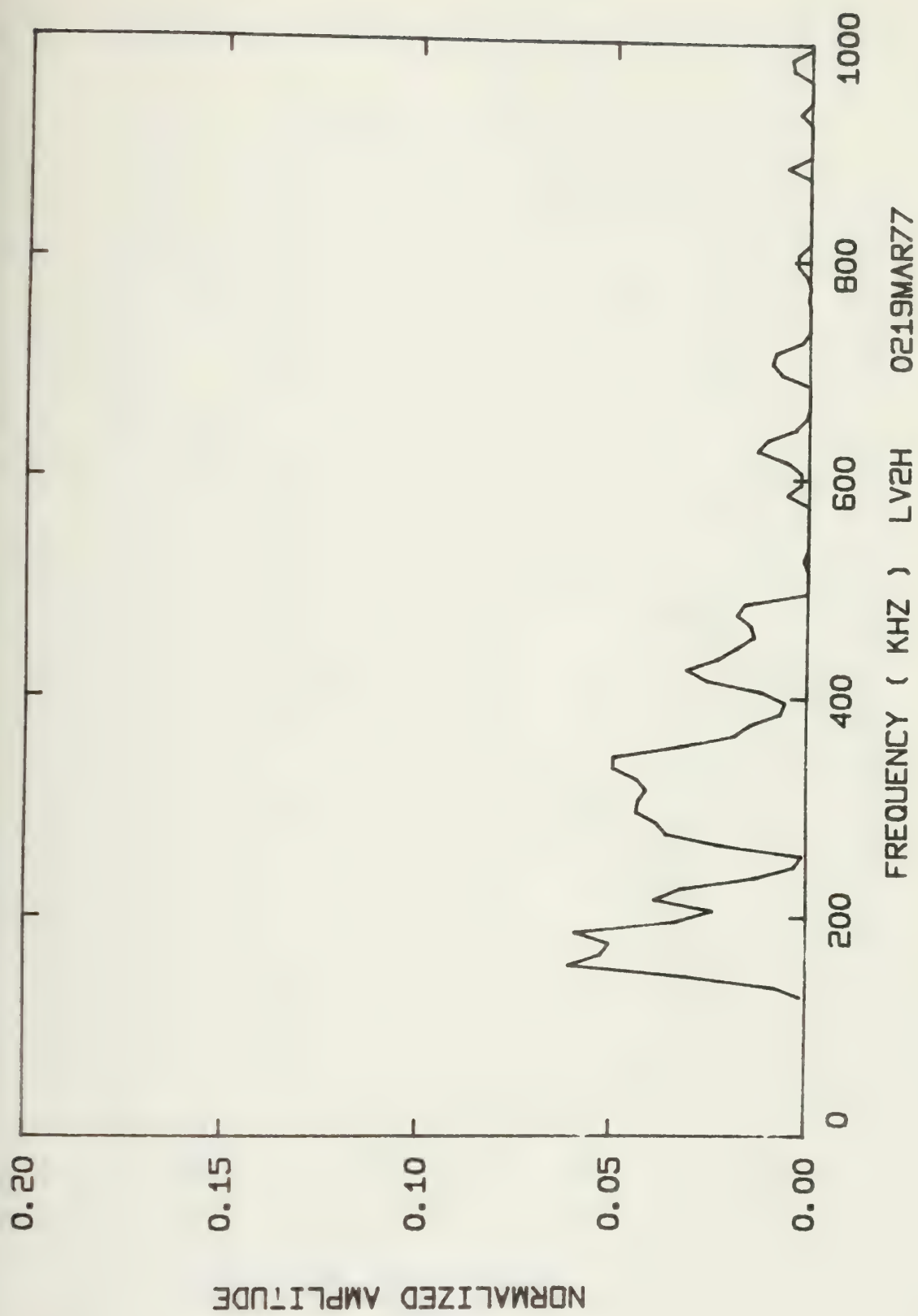




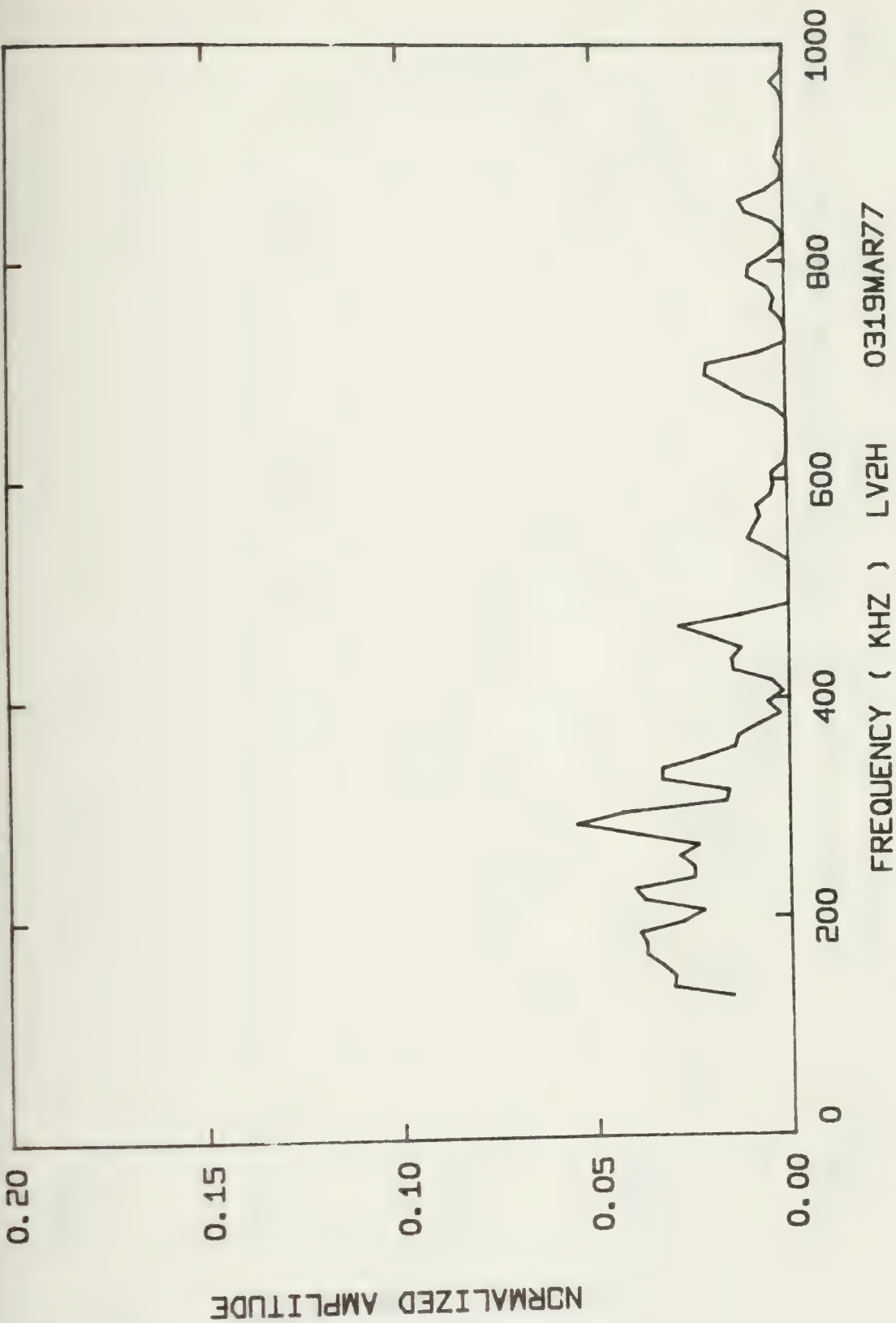






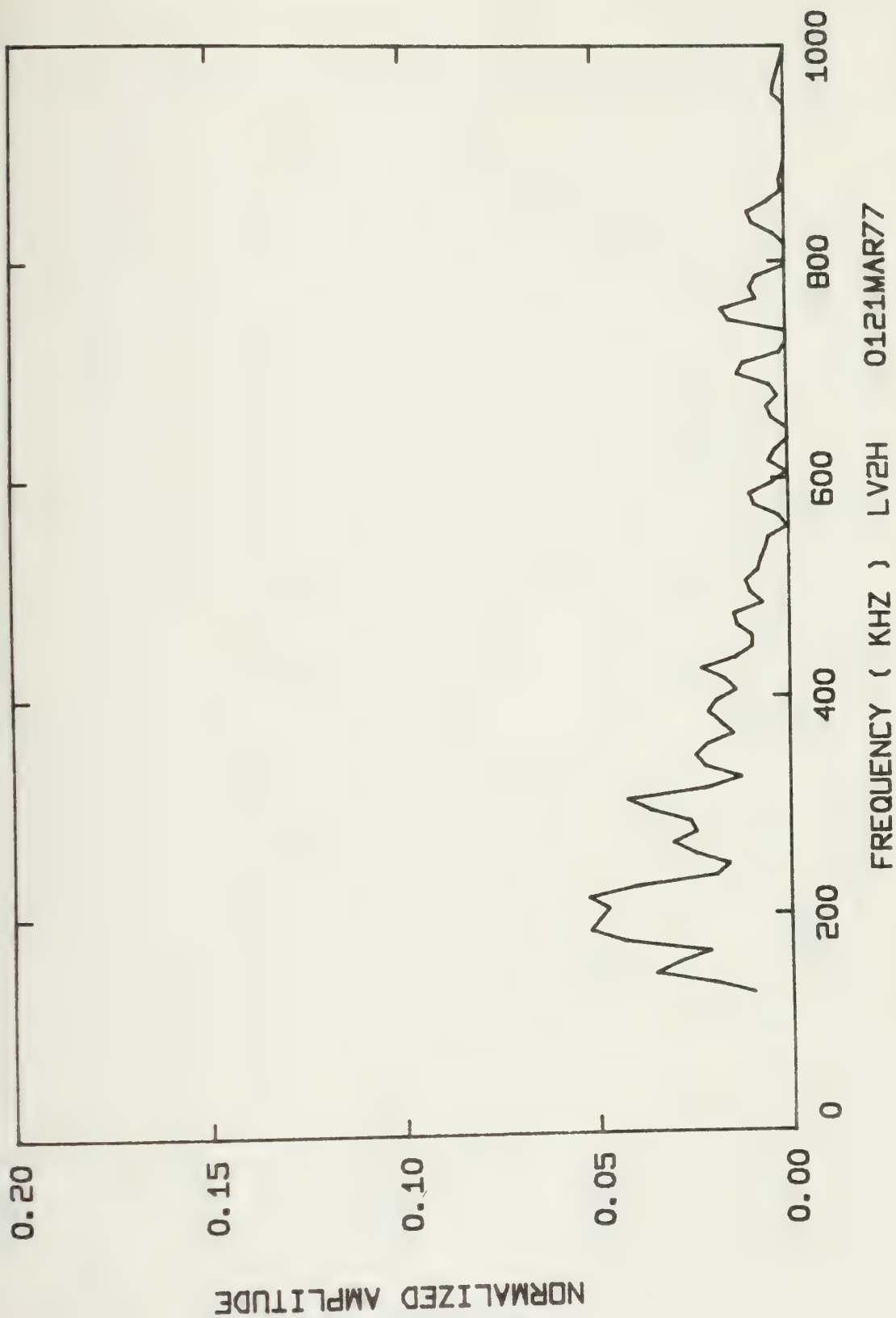




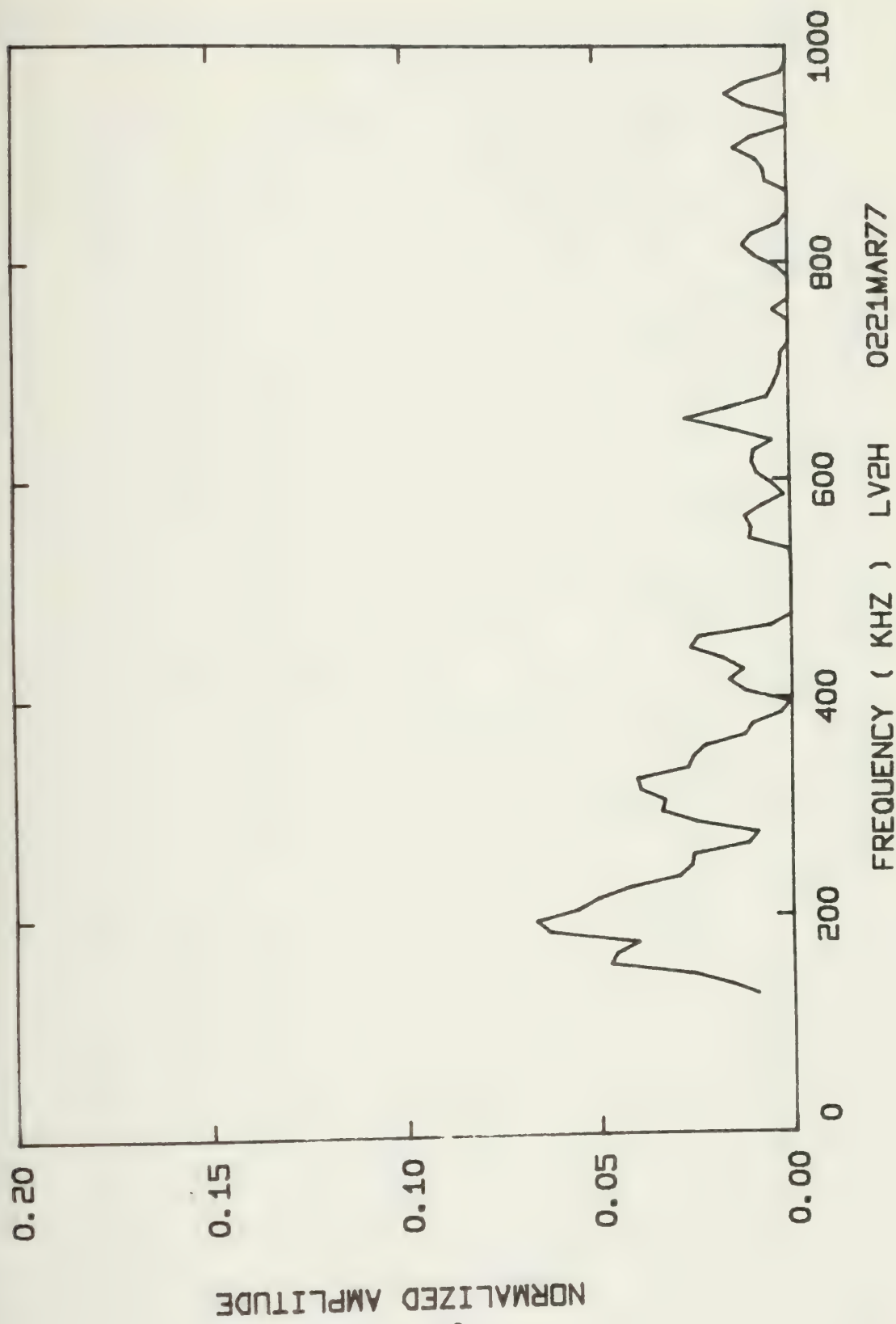




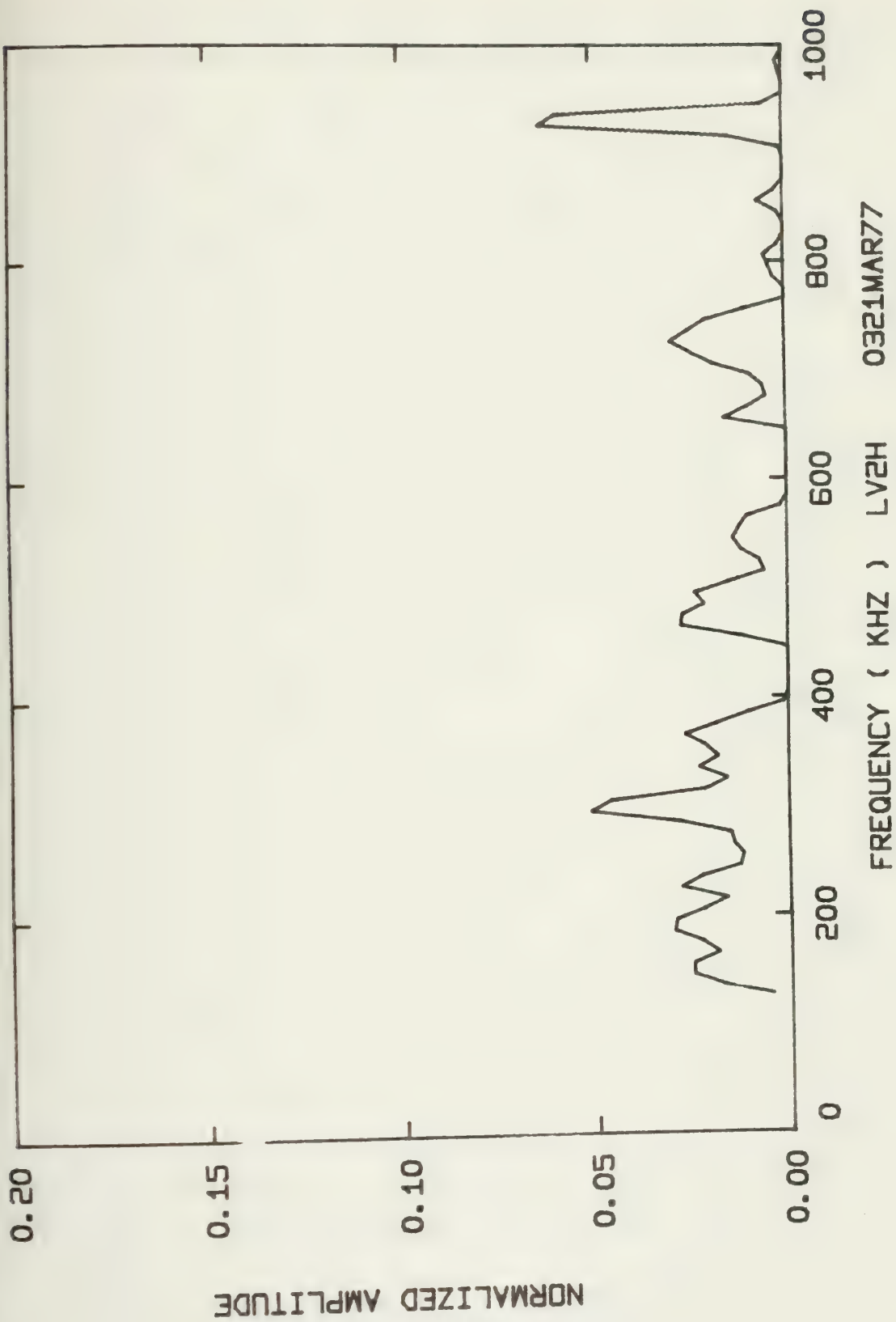




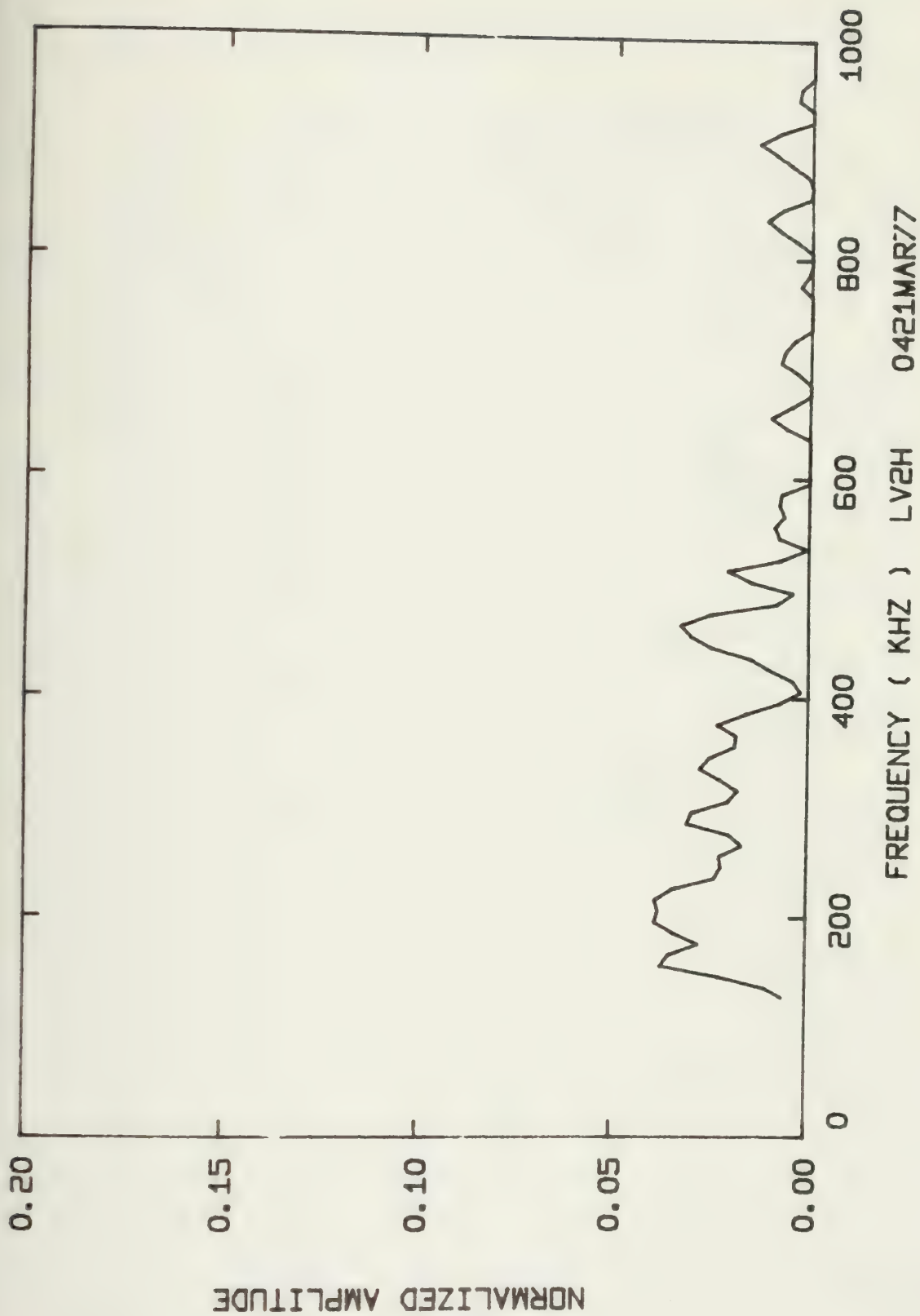






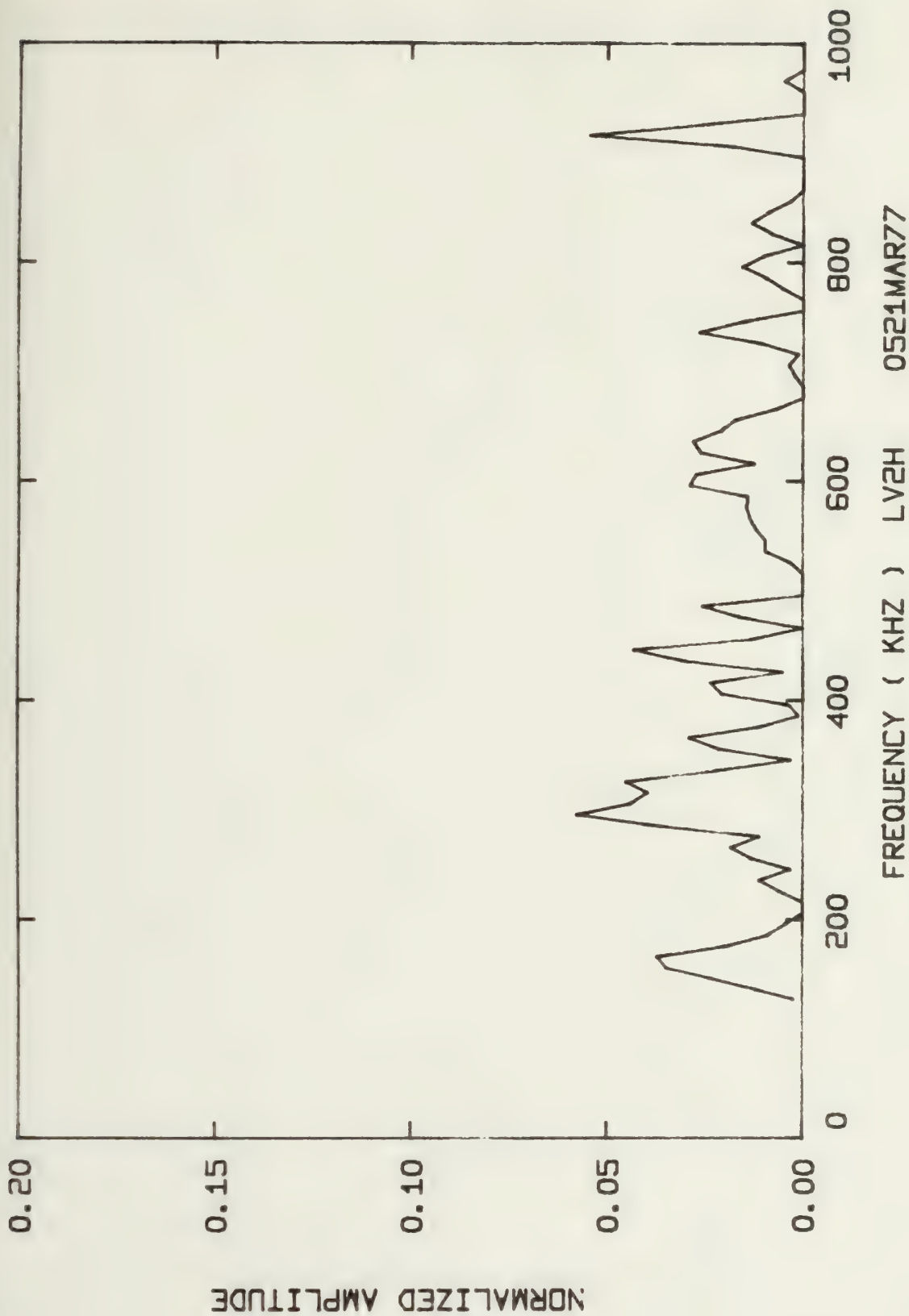




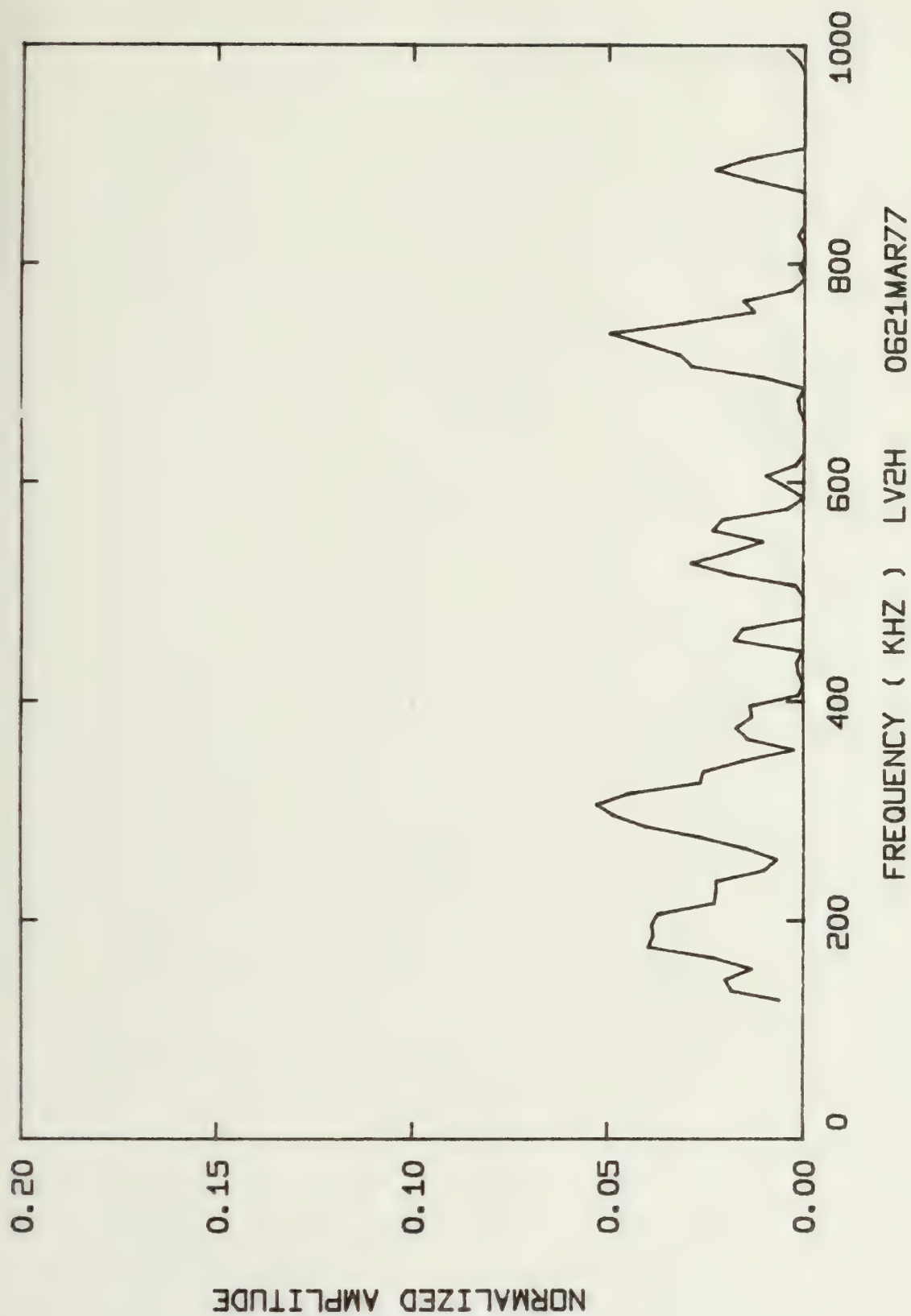




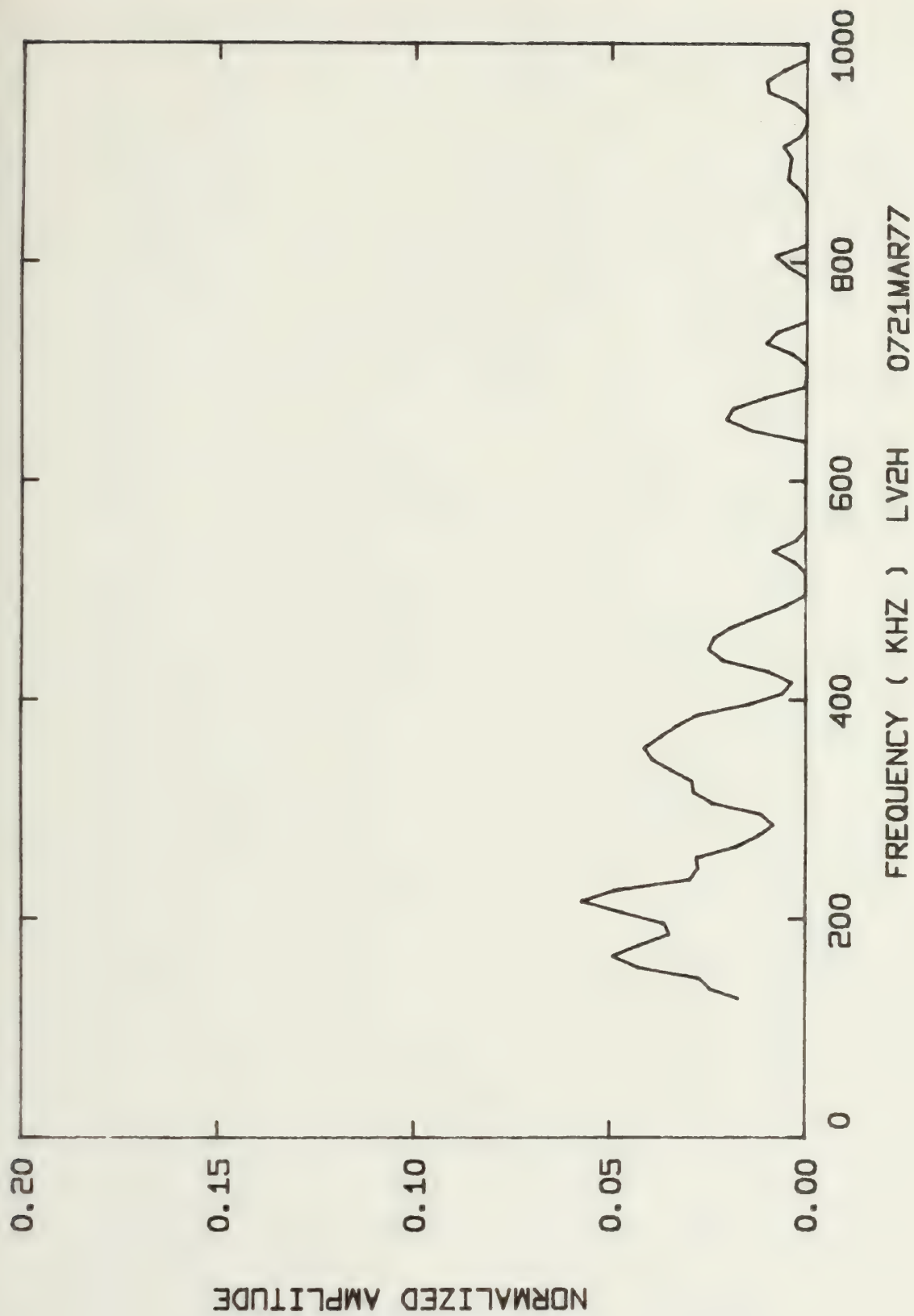




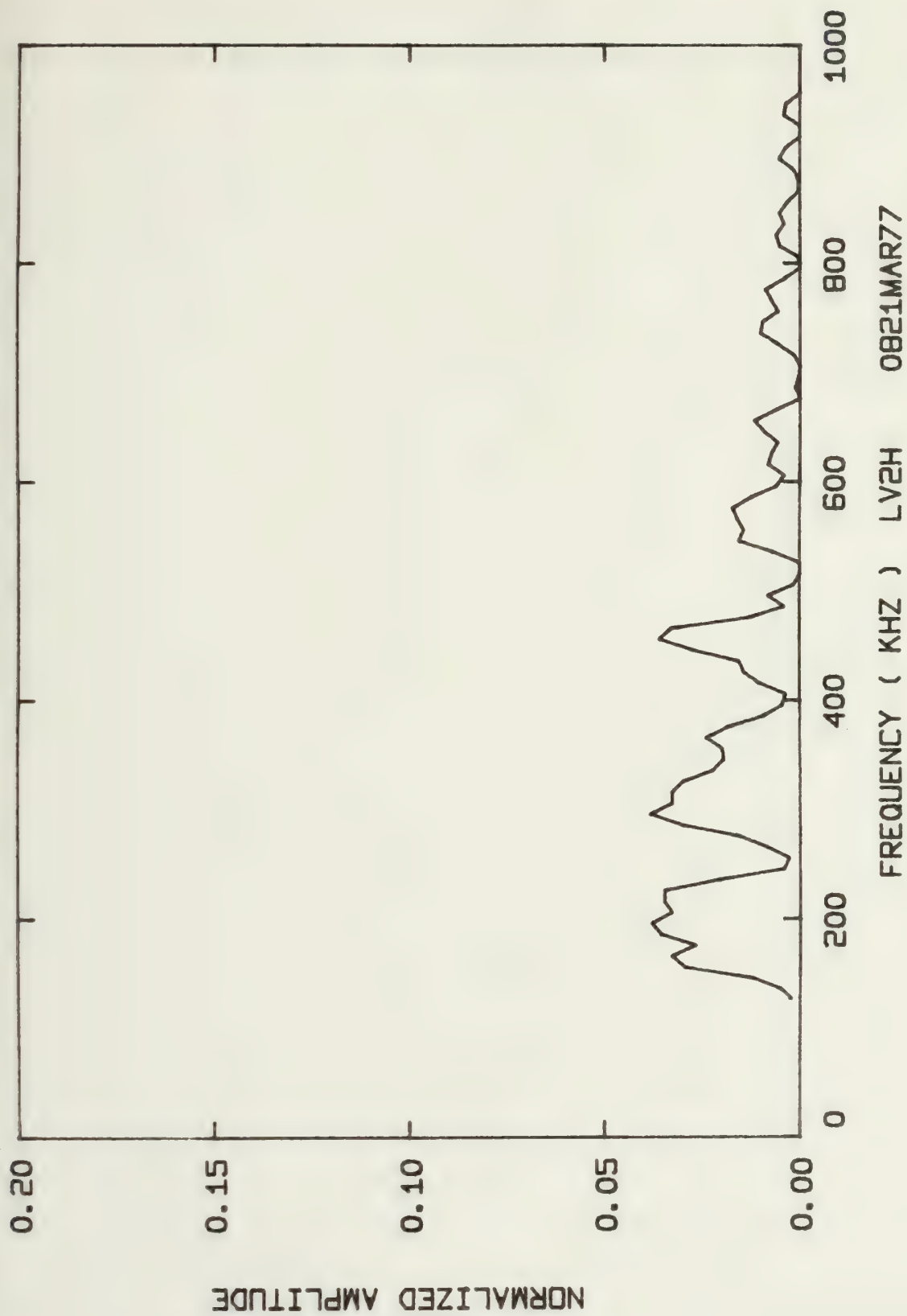






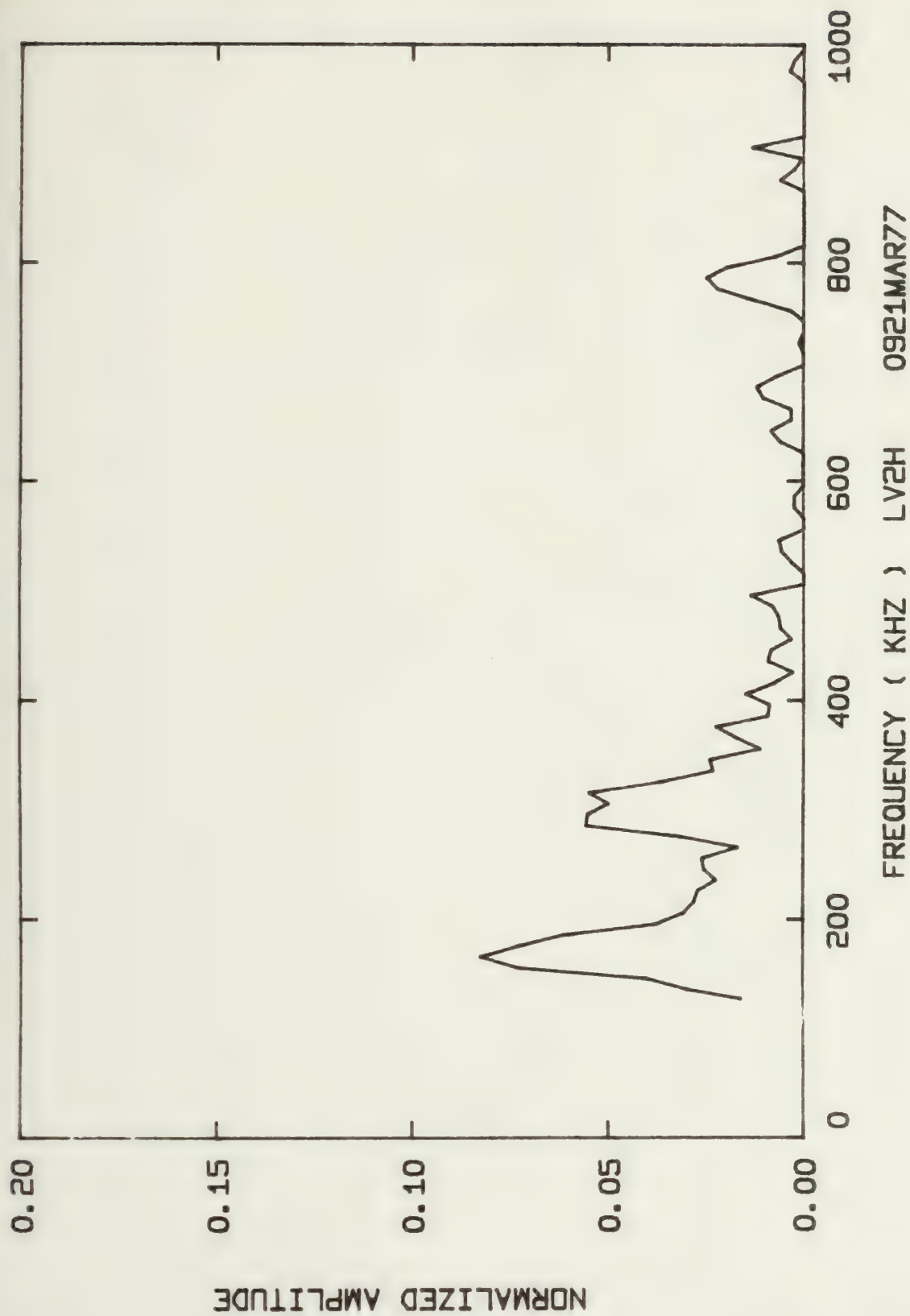




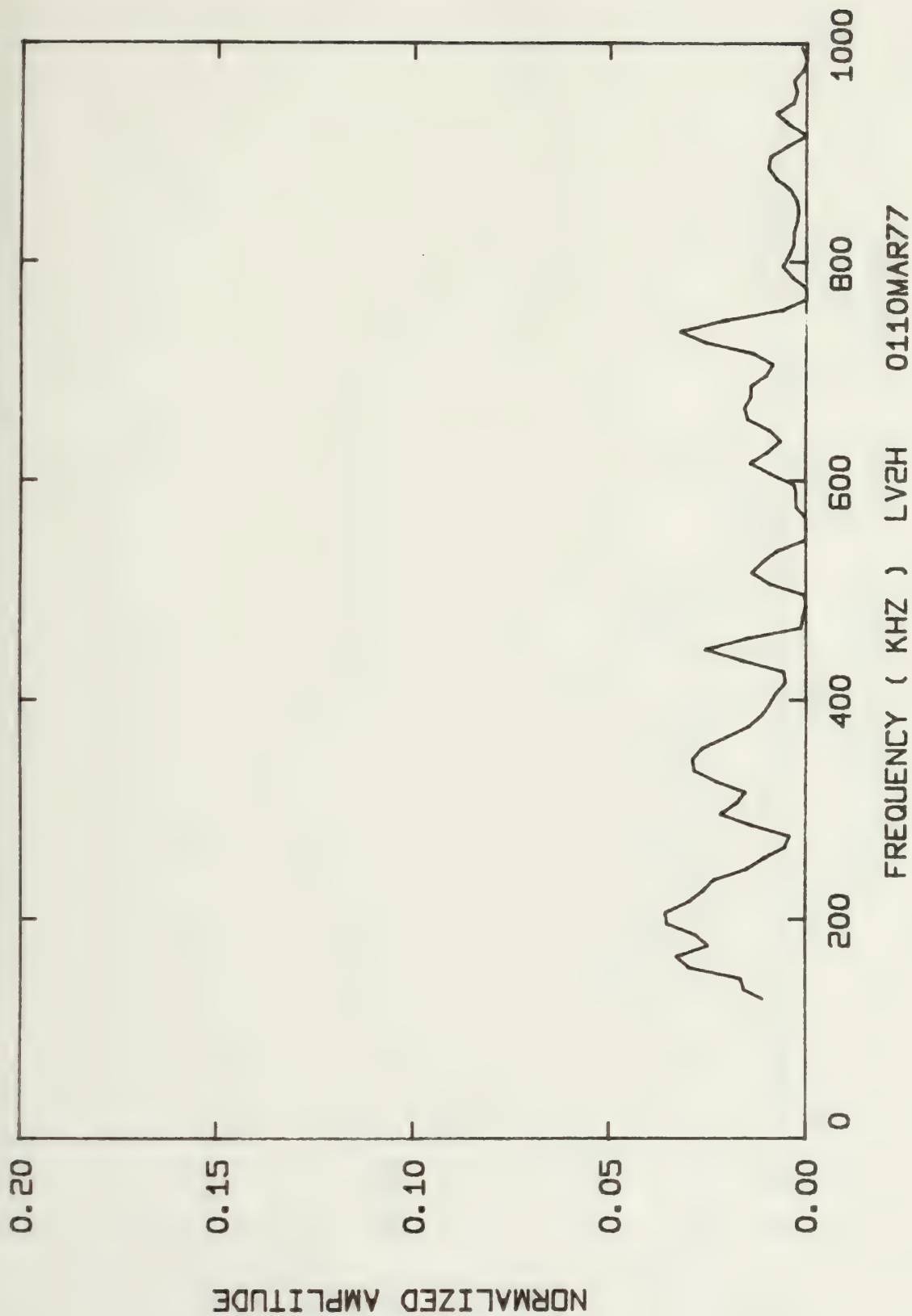




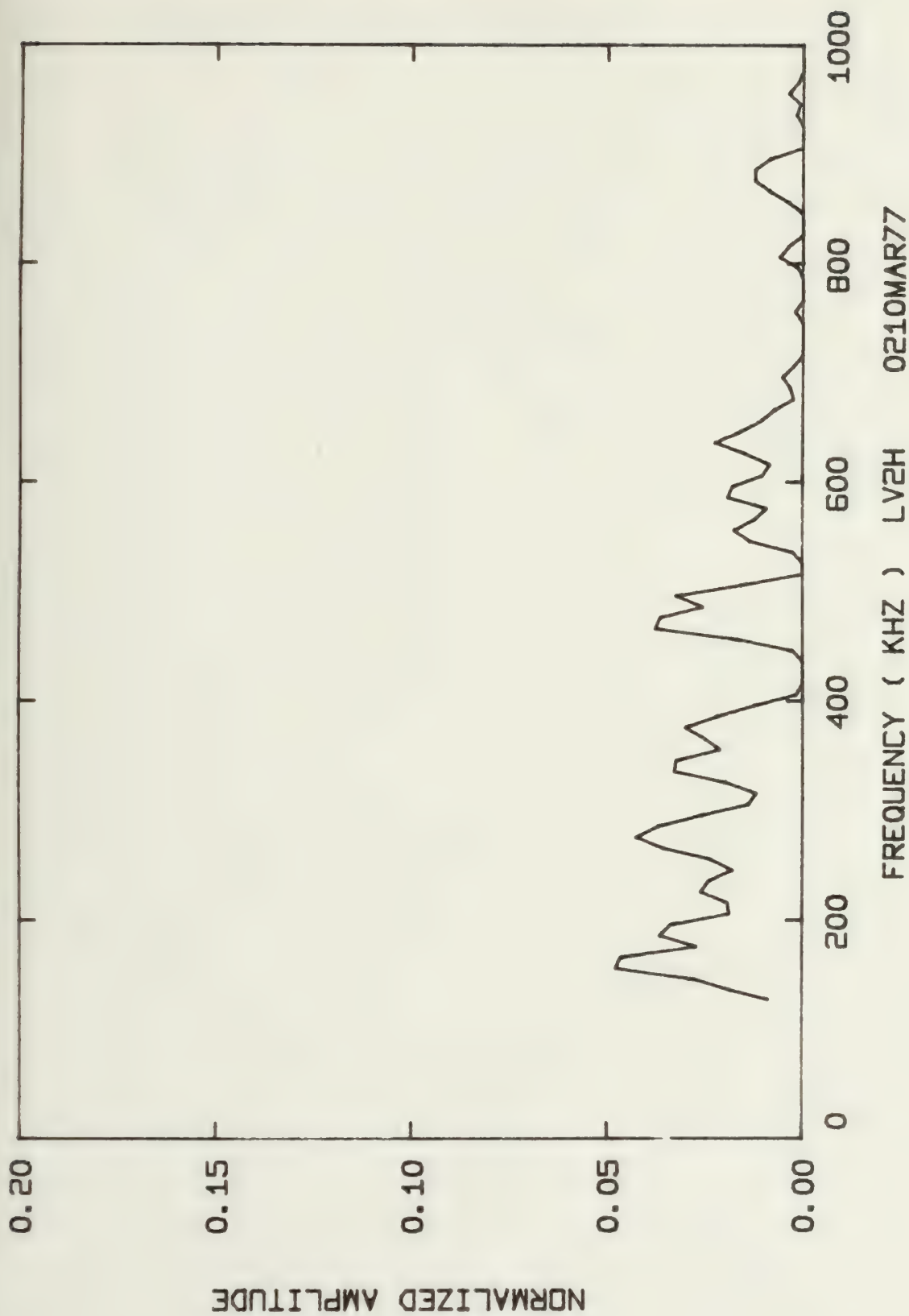




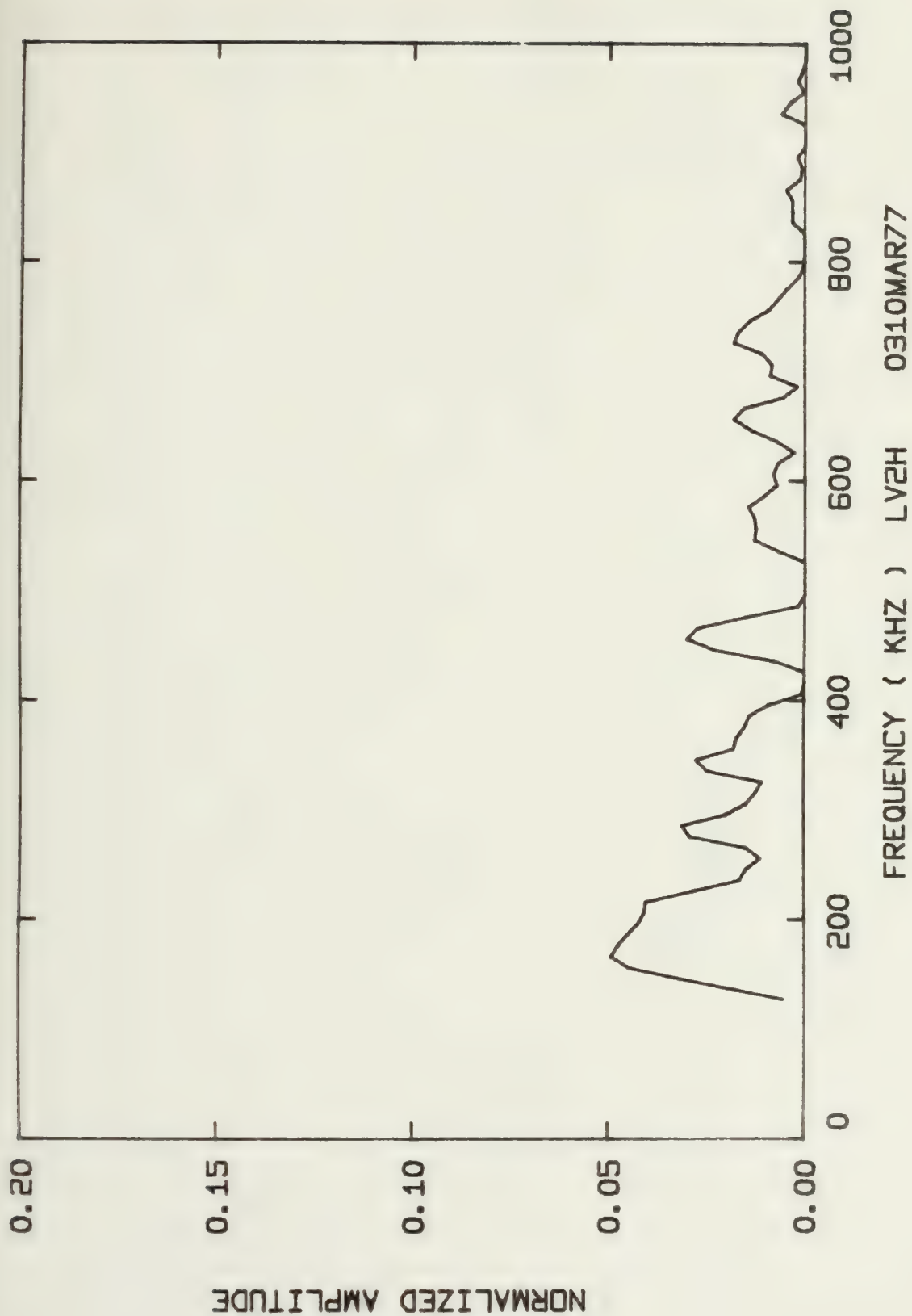






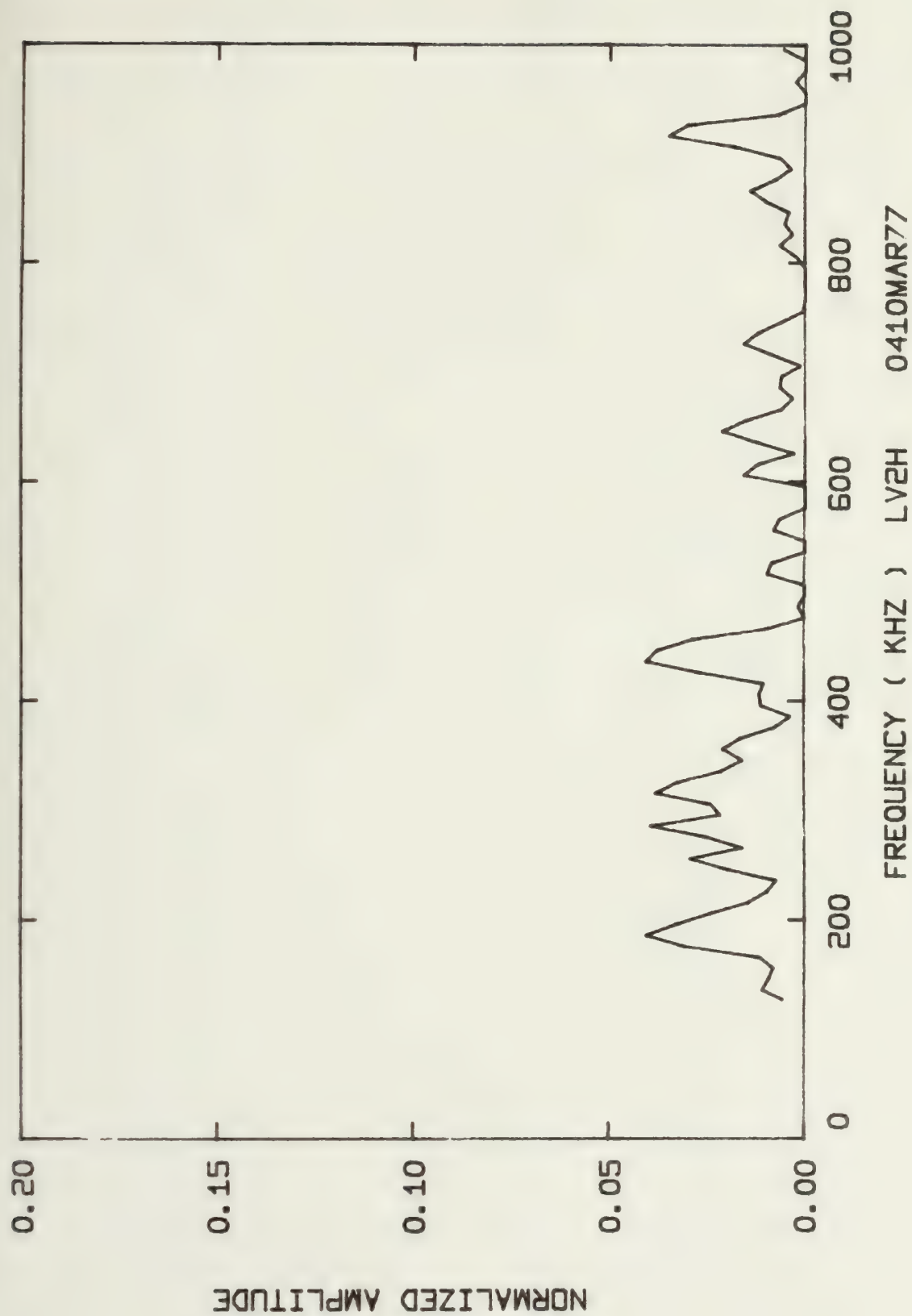




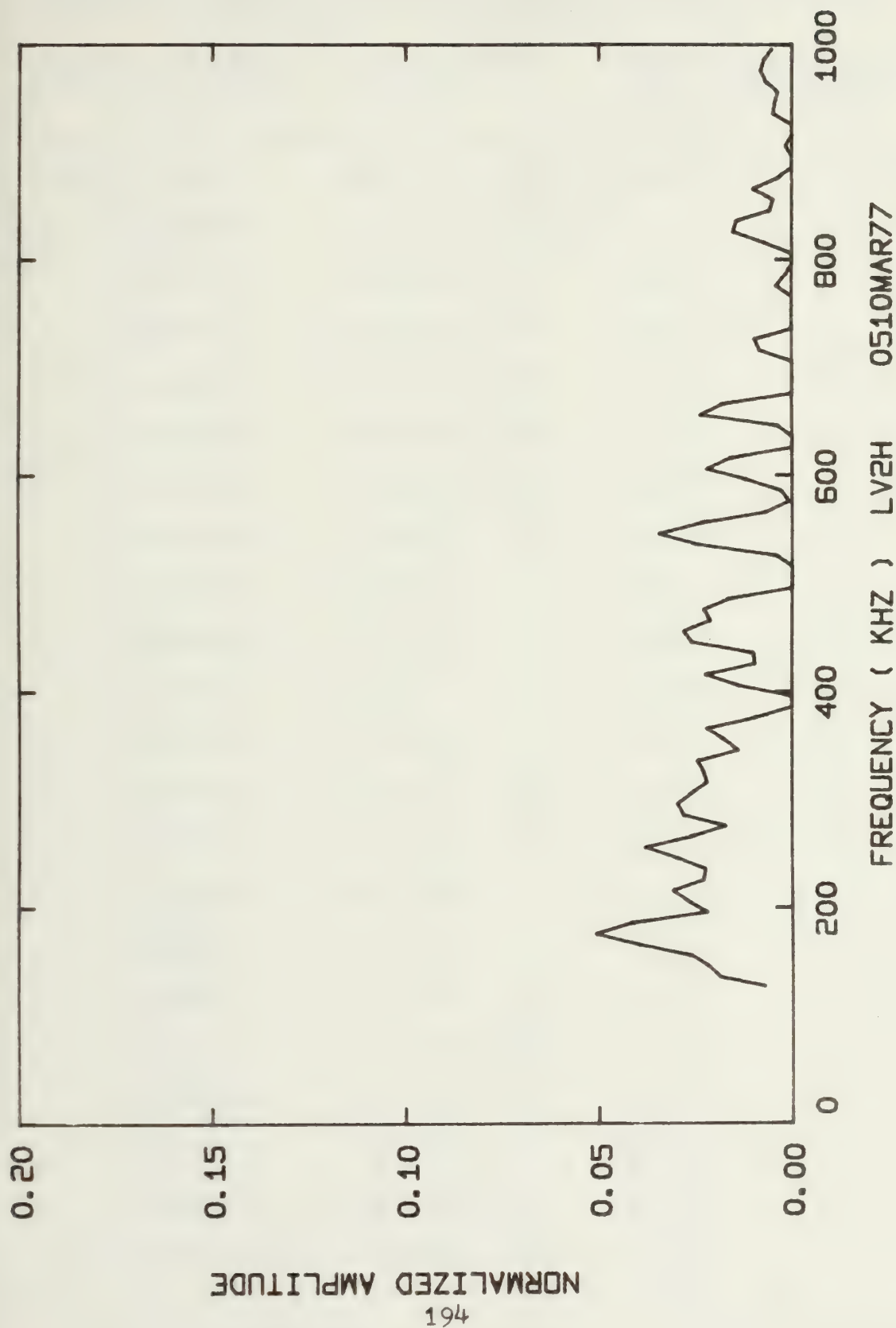














Summary of Energy per Acoustic Emission and RMS Pressure  
Across the Transducer's Face for Each Spectra

Spectral Distrib. Graph Code Number	Energy per AE (Joules)	RMS Pressure Across Face of Transducer (Pa x 10 <sup>5</sup> )
LV1B 0122FEB77	284.06 x 10 <sup>-9</sup>	103.00
0222FEB77	140.27 x 10 <sup>-9</sup>	72.38
0322FEB77	21.626 x 10 <sup>-9</sup>	44.94
0422FEB77	102.54 x 10 <sup>-9</sup>	70.07
0123FEB77	17.952 x 10 <sup>-9</sup>	45.21
0223FEB77	47.606 x 10 <sup>-9</sup>	53.38
0323FEB77	22.855 x 10 <sup>-9</sup>	42.89
0423FEB77	125.98 x 10 <sup>-9</sup>	78.68
0523FEB77	73.631 x 10 <sup>-9</sup>	52.44
0623FEB77	145.89 x 10 <sup>-9</sup>	80.16
0723FEB77	53.872 x 10 <sup>-9</sup>	60.59
0823FEB77	116.46 x 10 <sup>-9</sup>	75.26
0923FEB77	259.37 x 10 <sup>-9</sup>	91.07
1023FEB77	110.16 x 10 <sup>-9</sup>	69.00
1123FEB77	27.308 x 10 <sup>-9</sup>	53.23
1223FEB77	15.637 x 10 <sup>-9</sup>	49.33
1323FEB77	32.859 x 10 <sup>-9</sup>	52.81
1423FEB77	48.236 x 10 <sup>-9</sup>	55.17
1523FEB77	34.290 x 10 <sup>-9</sup>	50.61
1623FEB77	65.353 x 10 <sup>-9</sup>	62.34
1723FEB77	20.274 x 10 <sup>-9</sup>	53.56
1823FEB77	130.48 x 10 <sup>-9</sup>	76.90

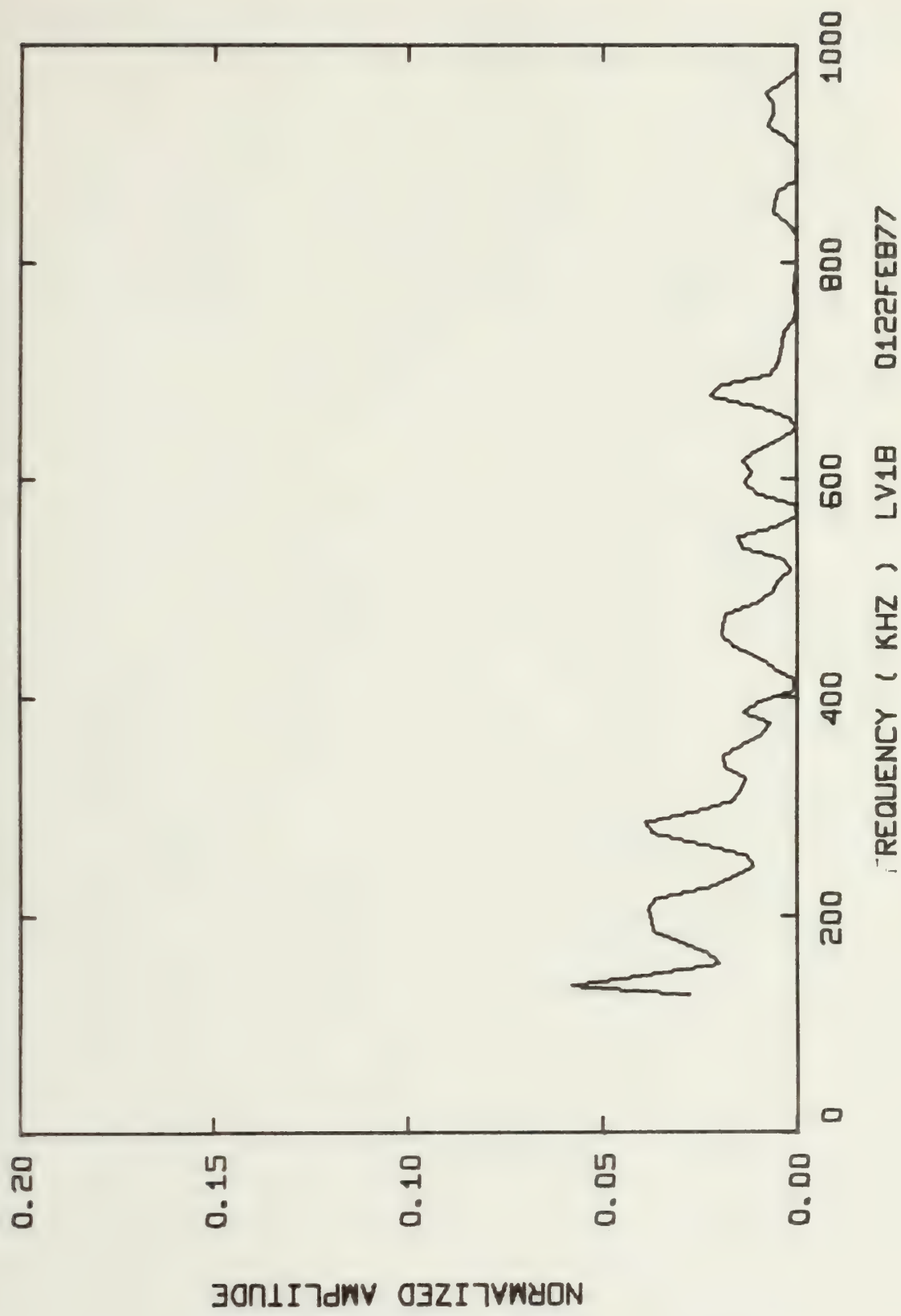


Summary of Energy per Acoustic Emission and RMS Pressure  
Across the Transducer's Face for Each Spectra

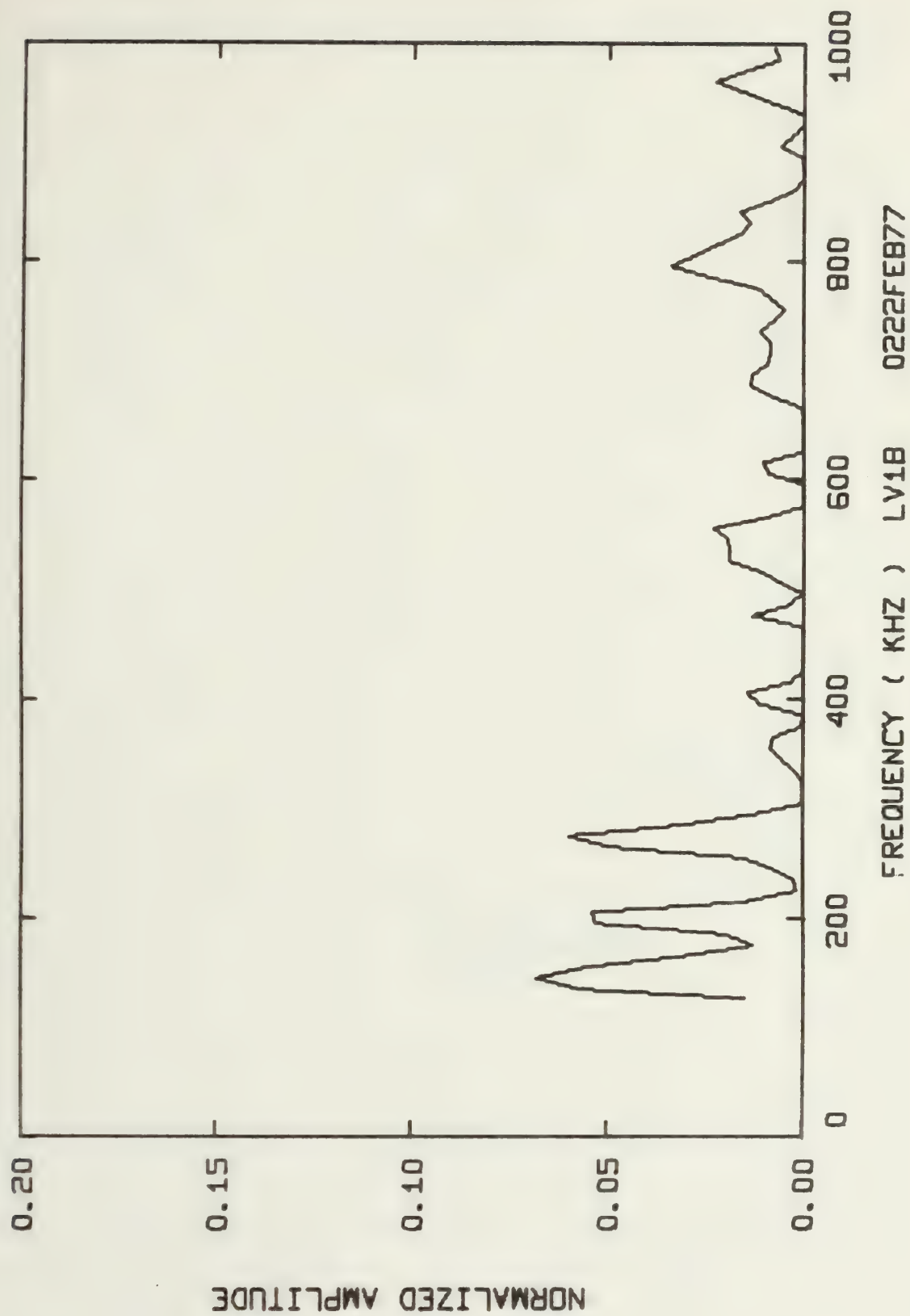
Spectral Distrib. Graph Code Number	Energy per AE (Joules)	RMS Pressure Across Face of Transducer (Pa x 10 <sup>5</sup> )
LV1B 1023MAR77	238.82 x 10 <sup>-9</sup>	117.32
1123MAR77	2.4299 x 10 <sup>-6</sup>	230.51
1223MAR77	159.98 x 10 <sup>-9</sup>	123.77
1323MAR77	535.20 x 10 <sup>-9</sup>	175.63
1423MAR77	216.33 x 10 <sup>-9</sup>	104.21
1523MAR77	2.5170 x 10 <sup>-6</sup>	267.27
1623MAR77	285.55 x 10 <sup>-9</sup>	110.09
1723MAR77	202.23 x 10 <sup>-9</sup>	125.70
1823MAR77	197.65 x 10 <sup>-9</sup>	76.06
1923MAR77	949.71 x 10 <sup>-9</sup>	127.15
2023MAR77	119.61 x 10 <sup>-6</sup>	708.26



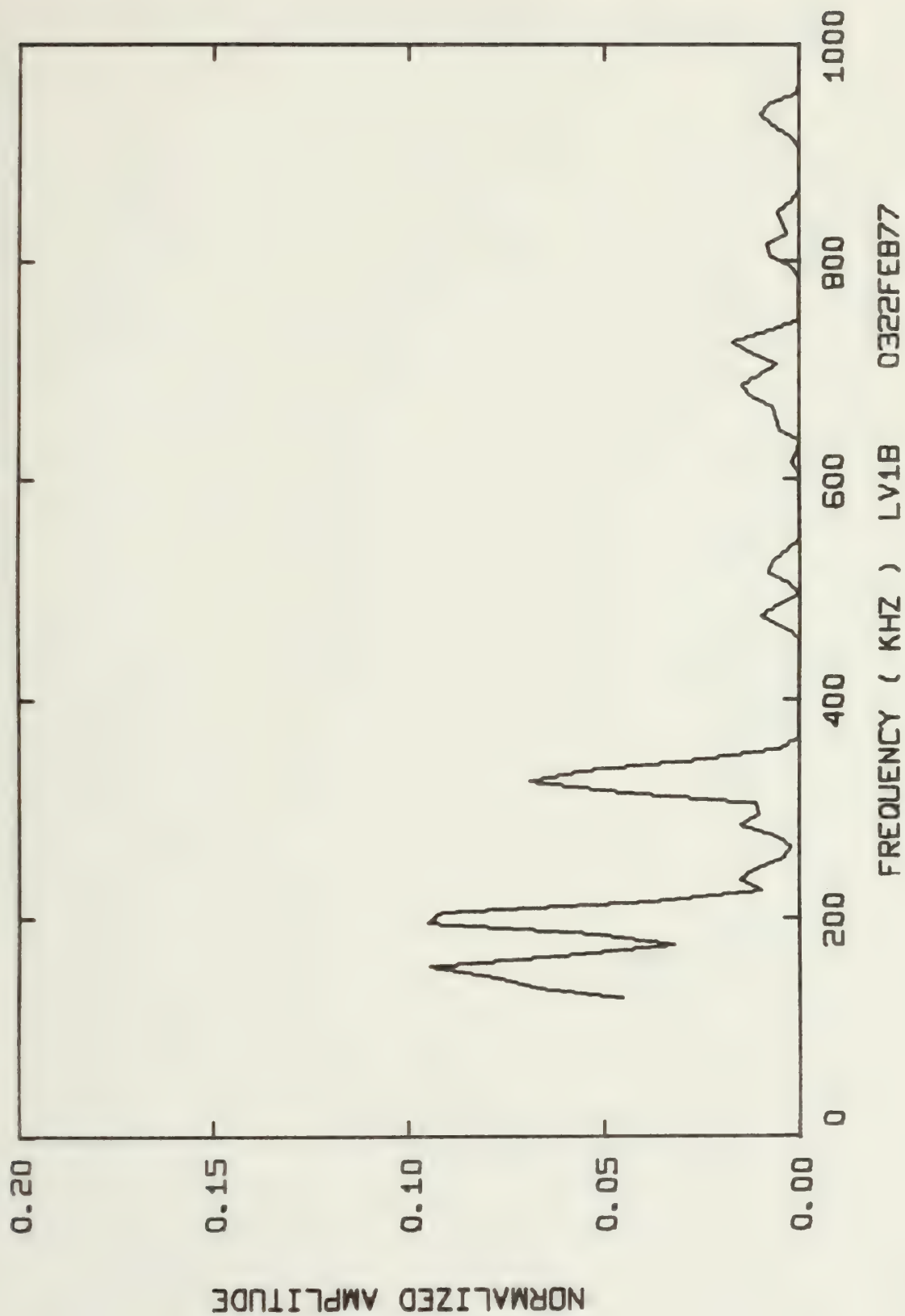




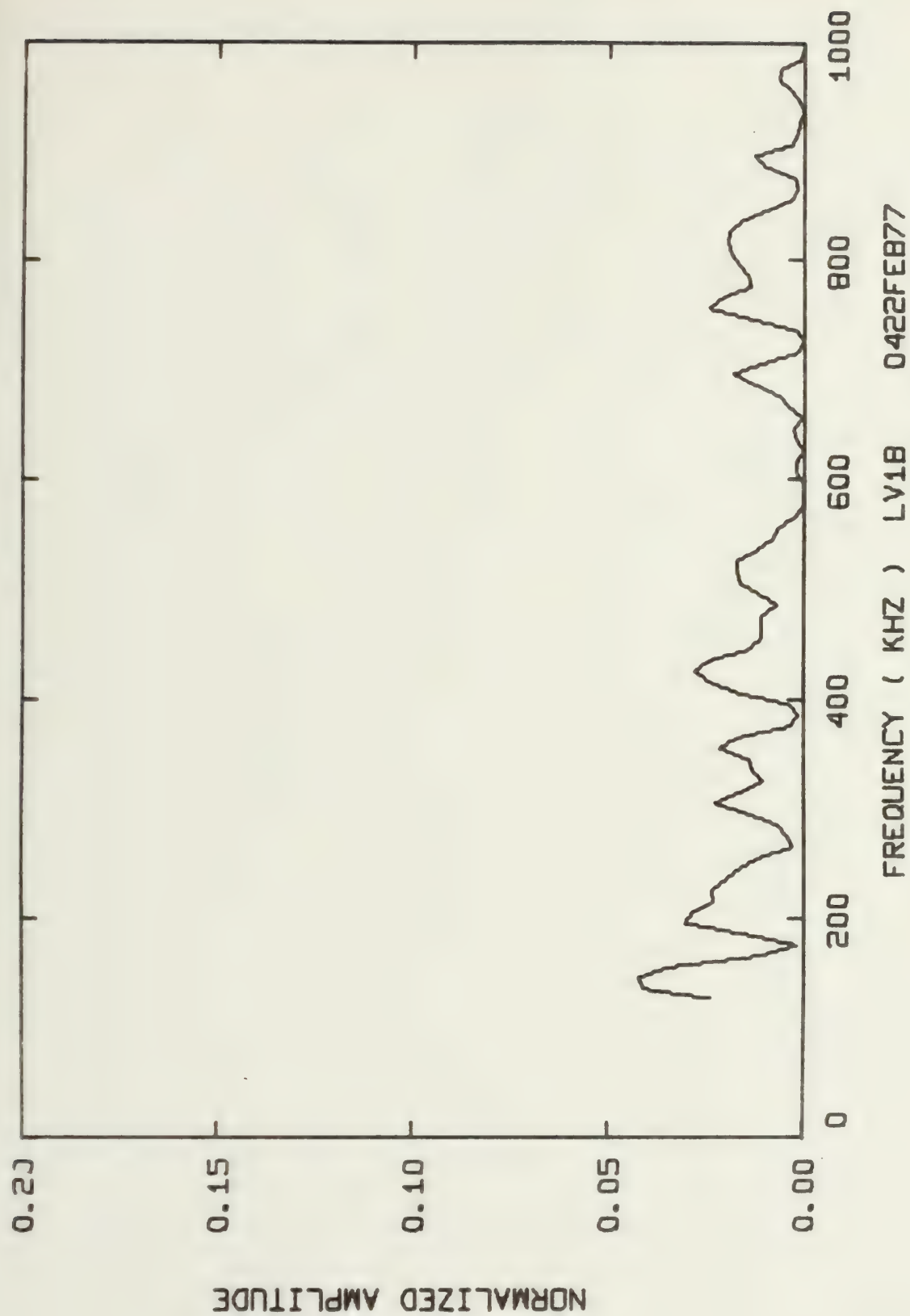






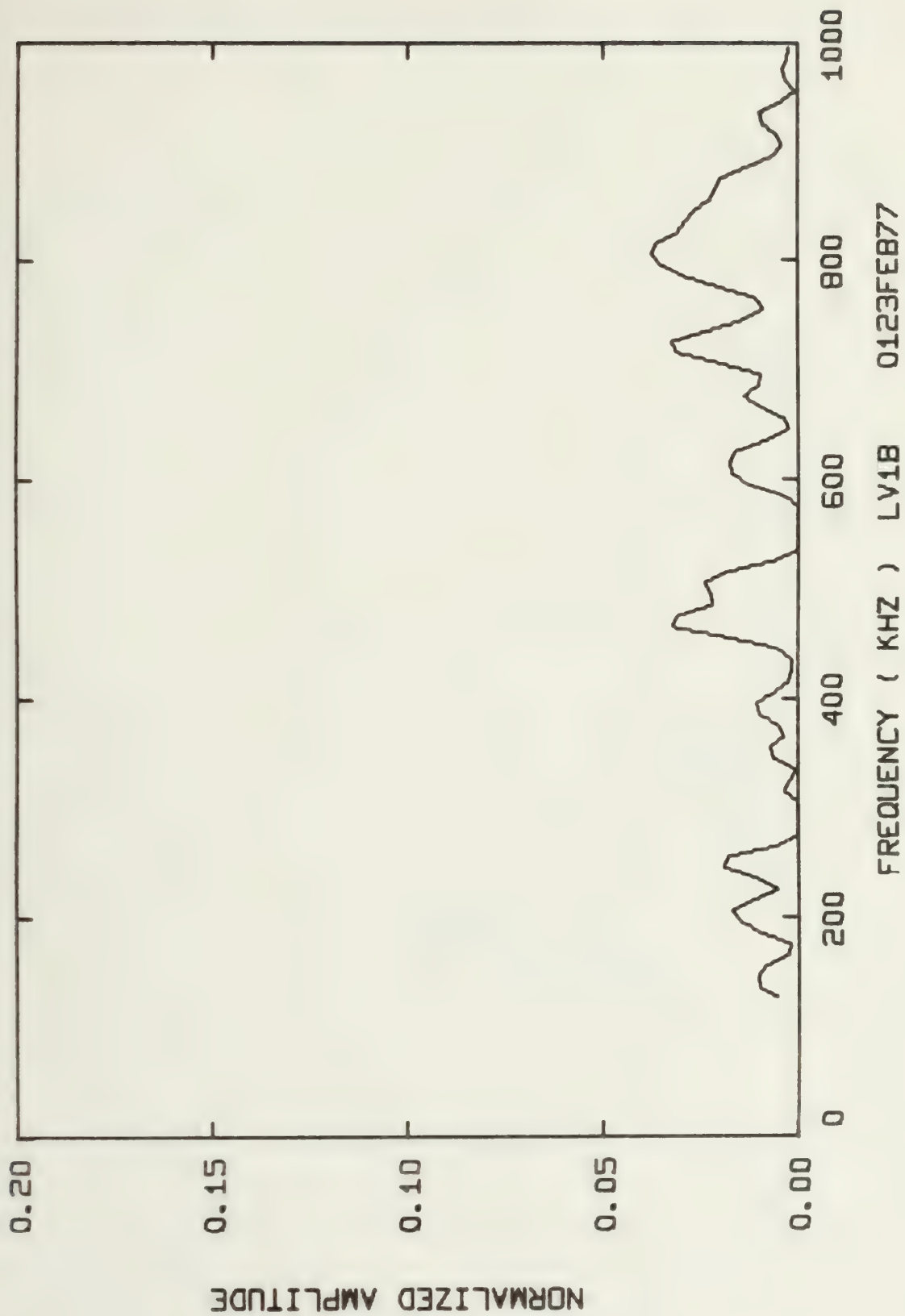




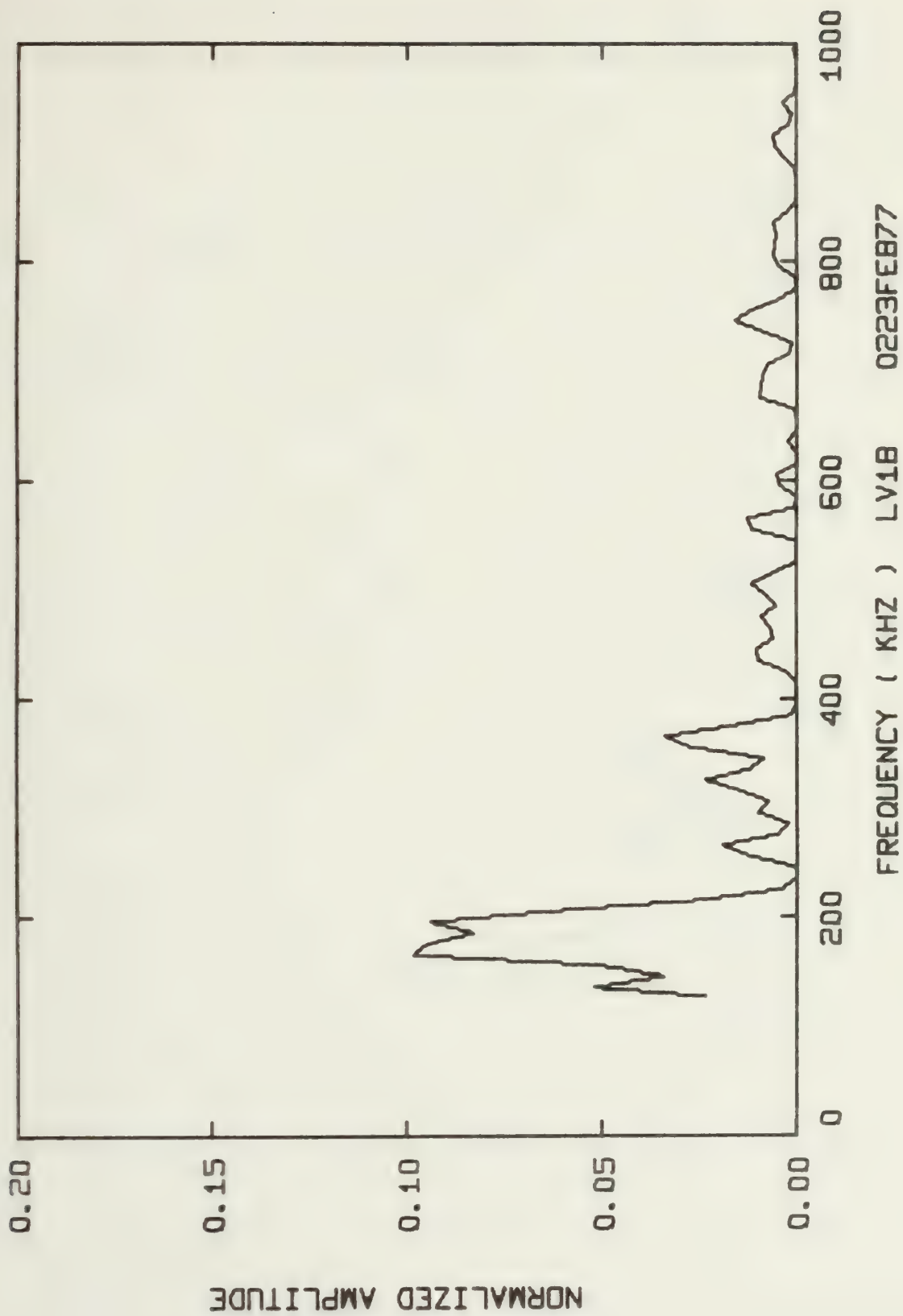




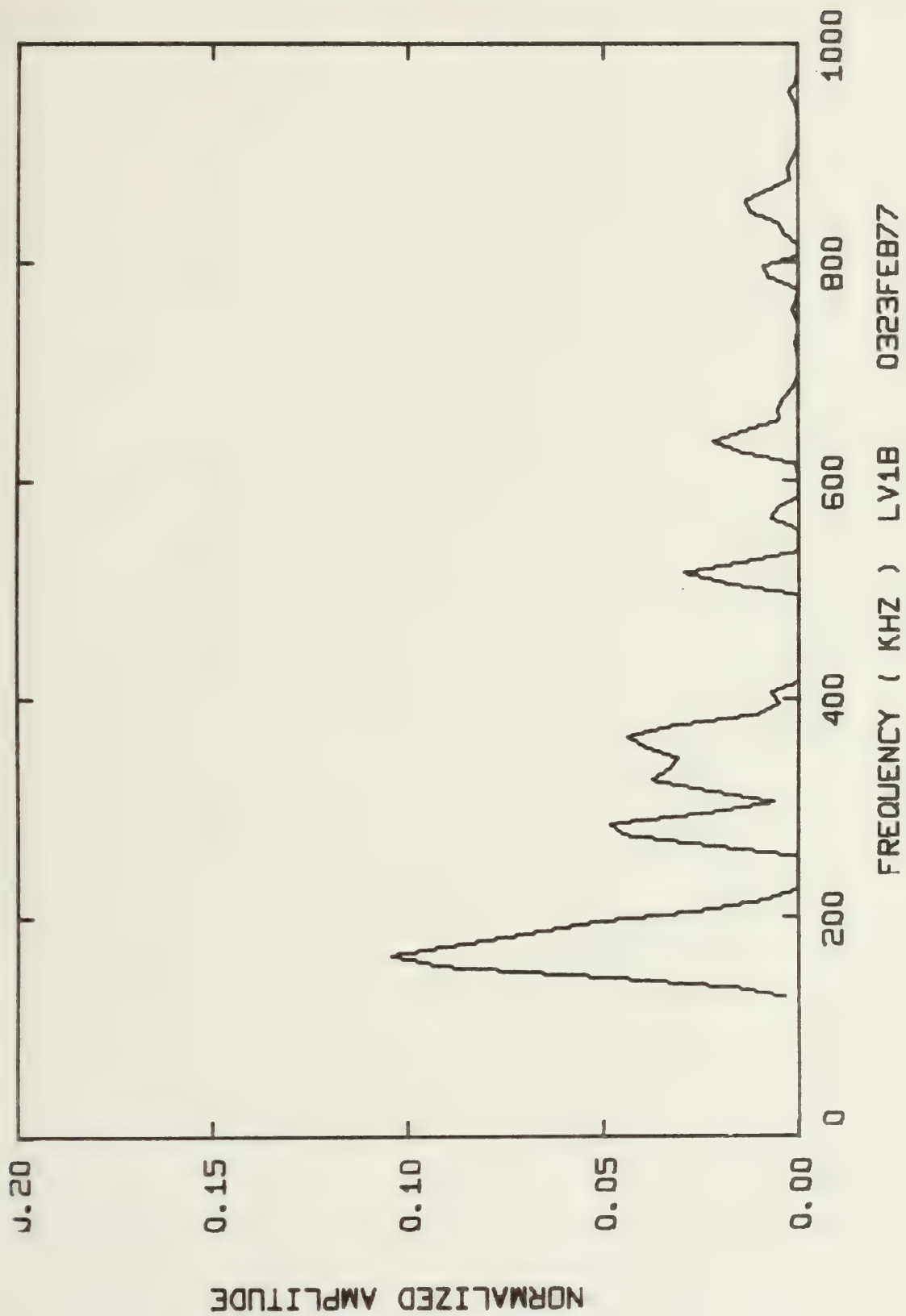




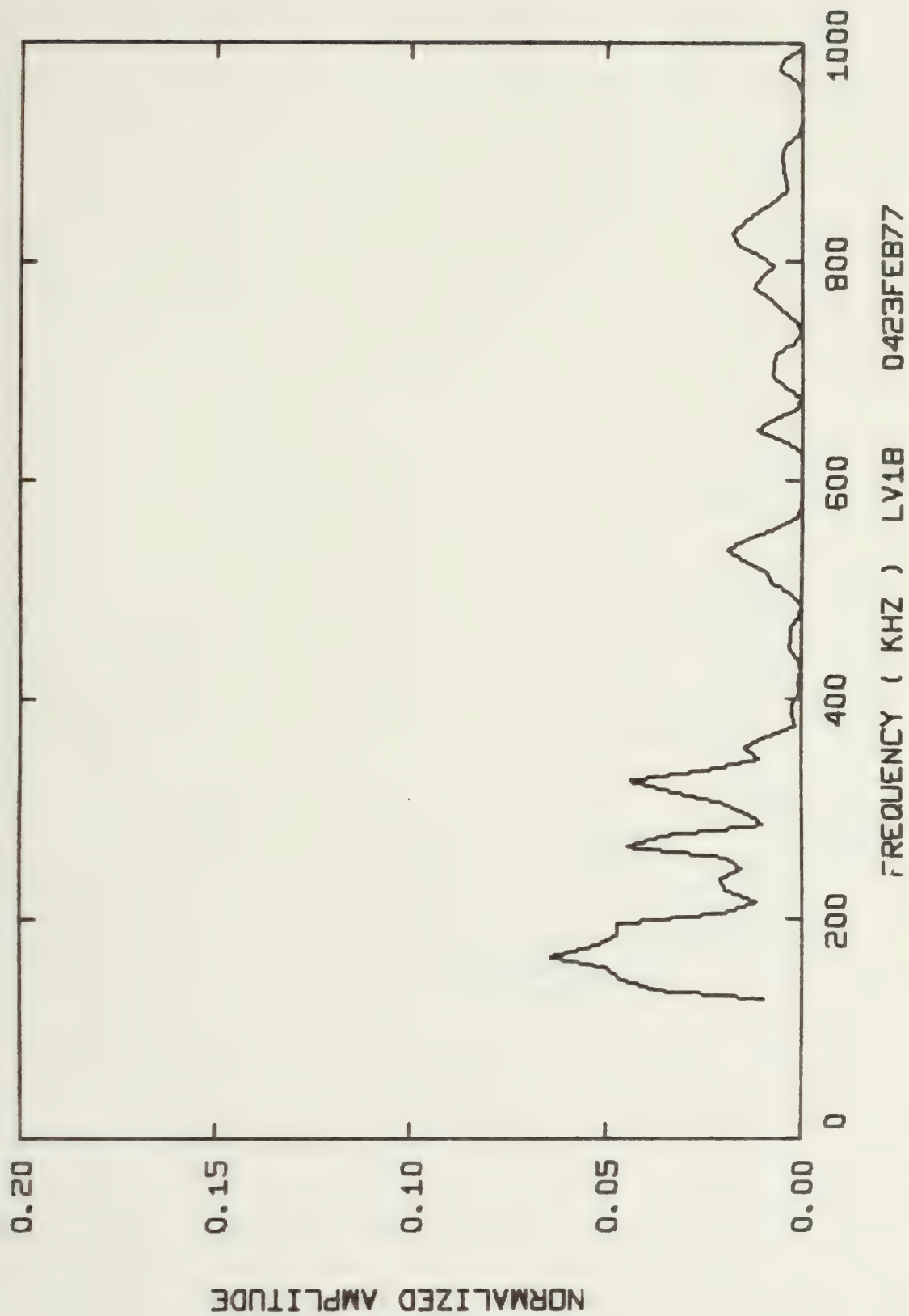






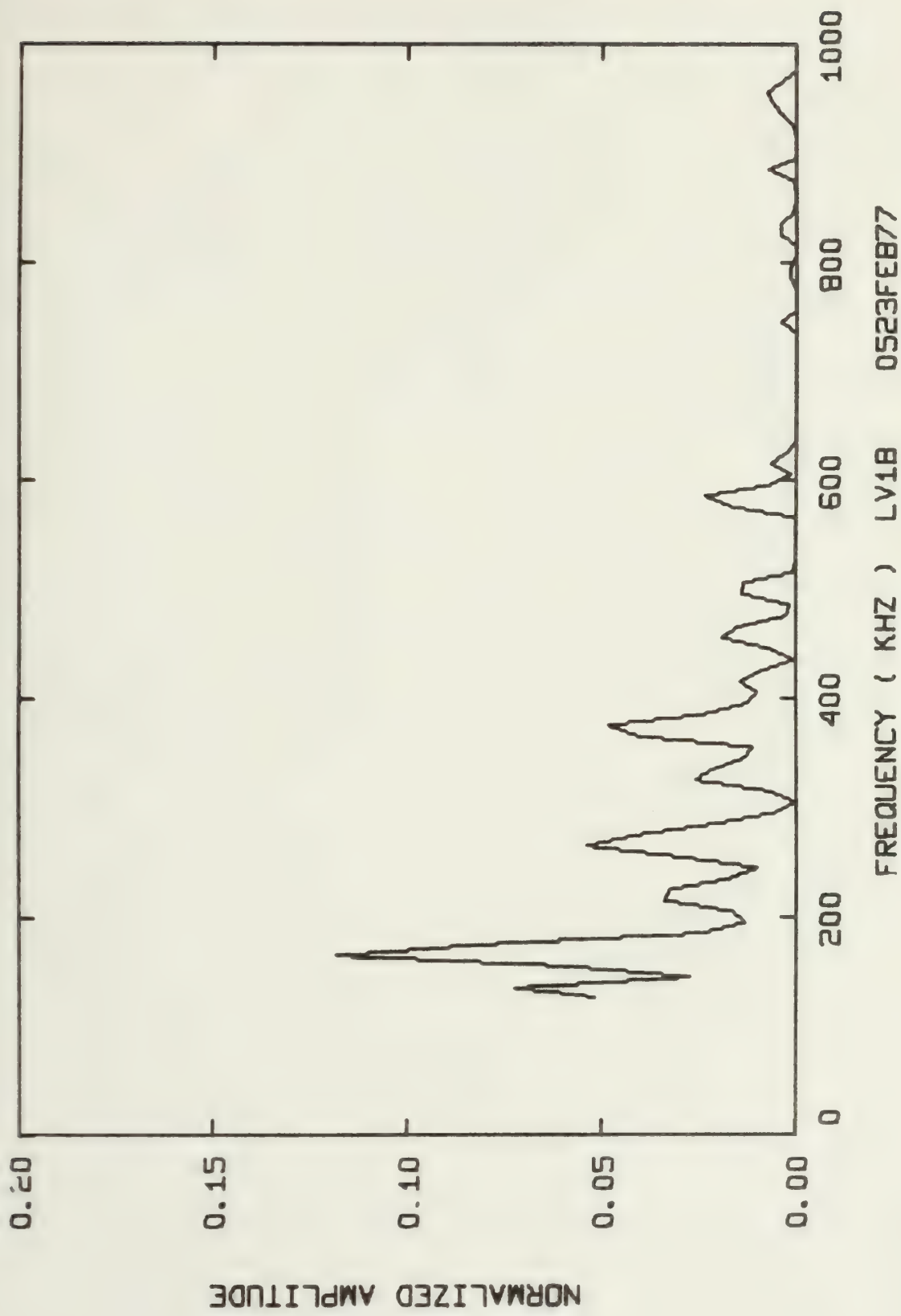




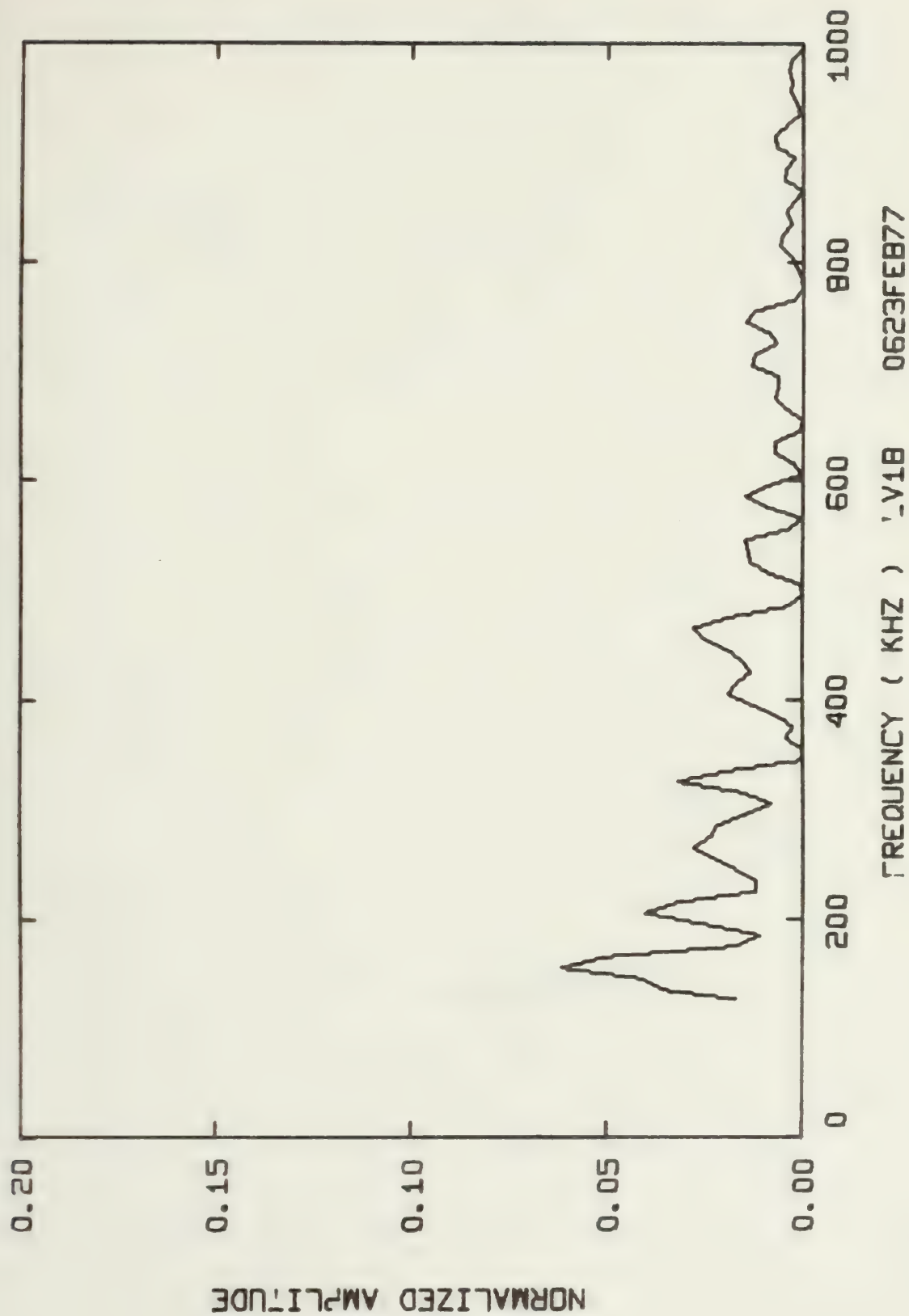




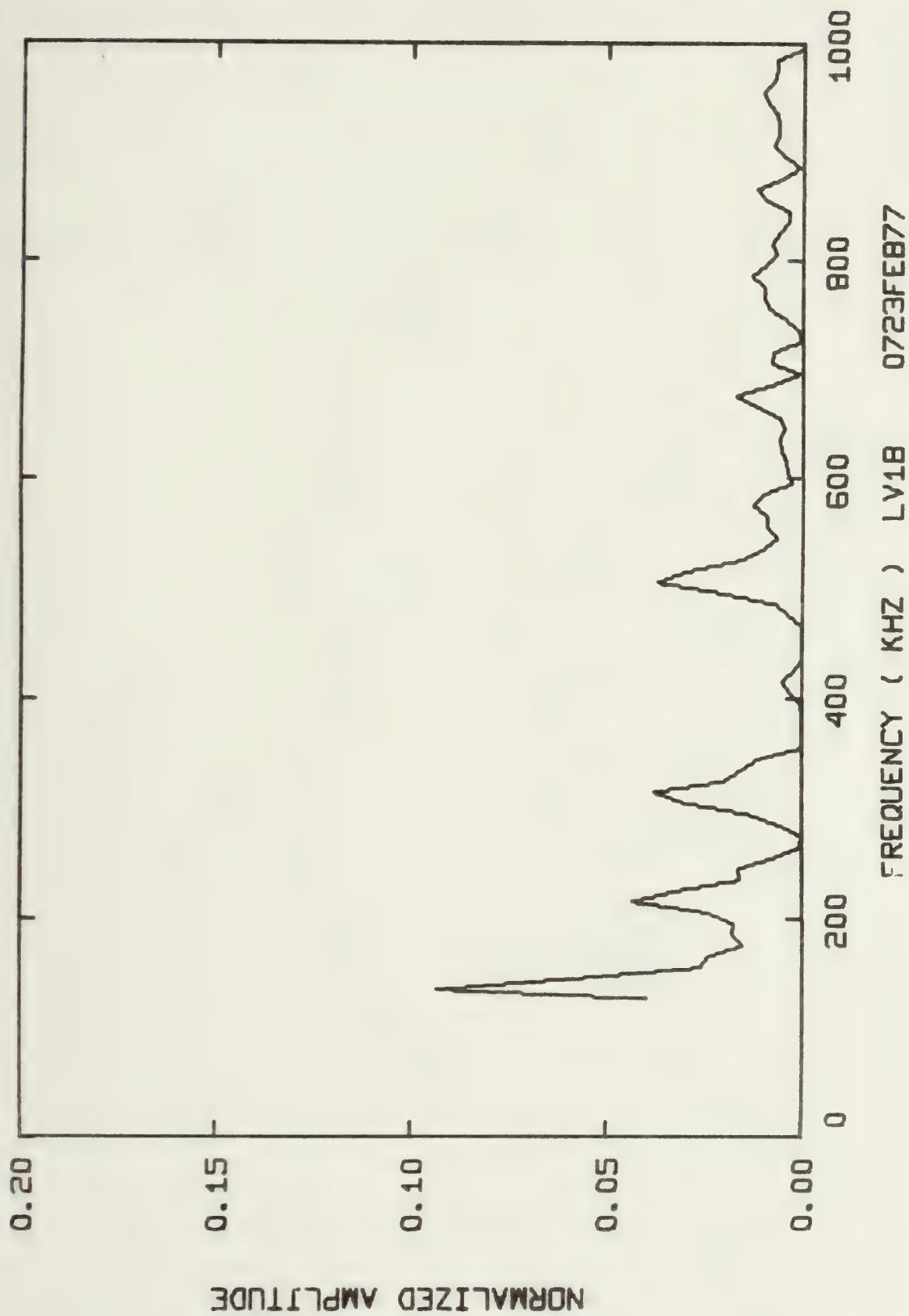




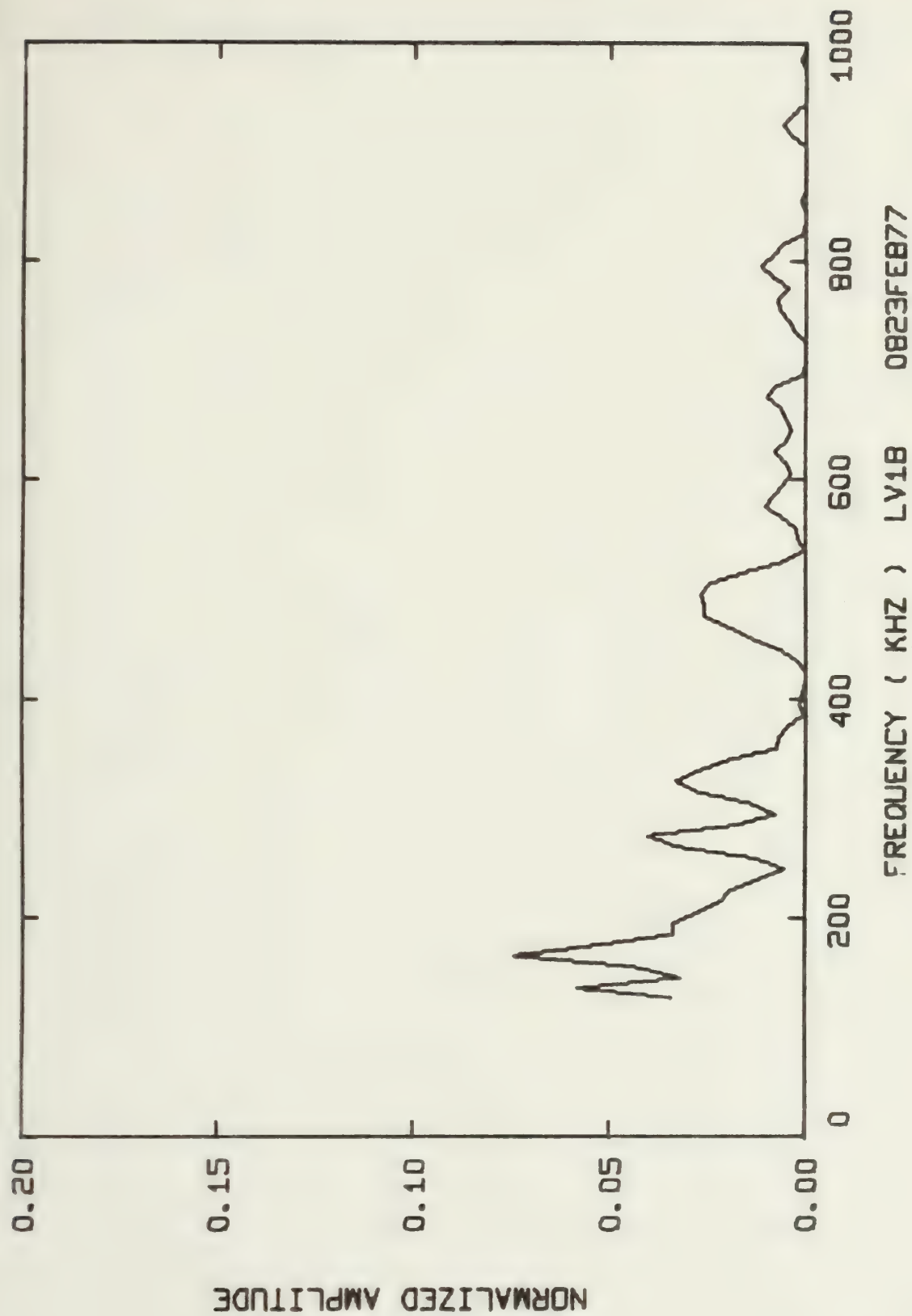






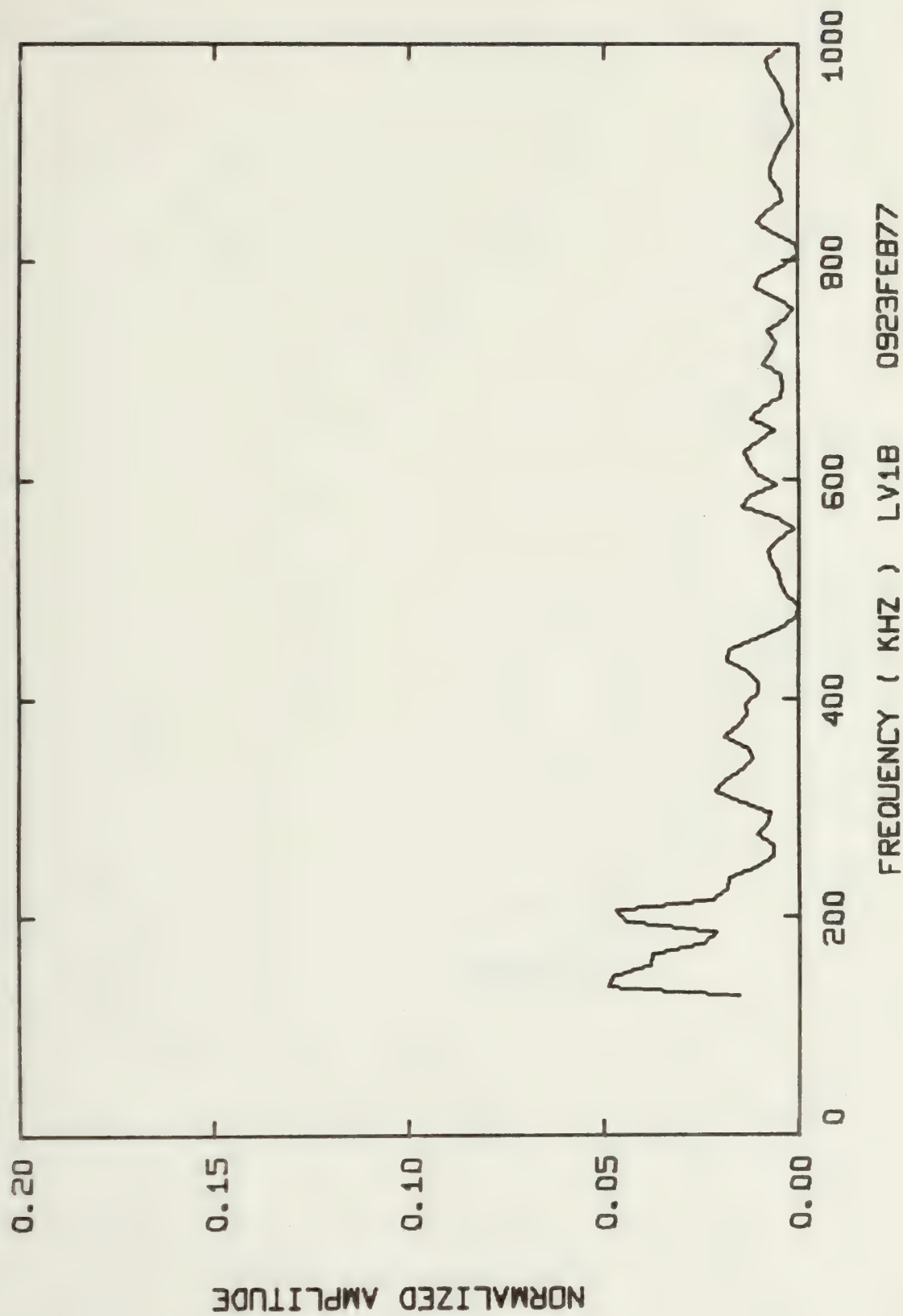




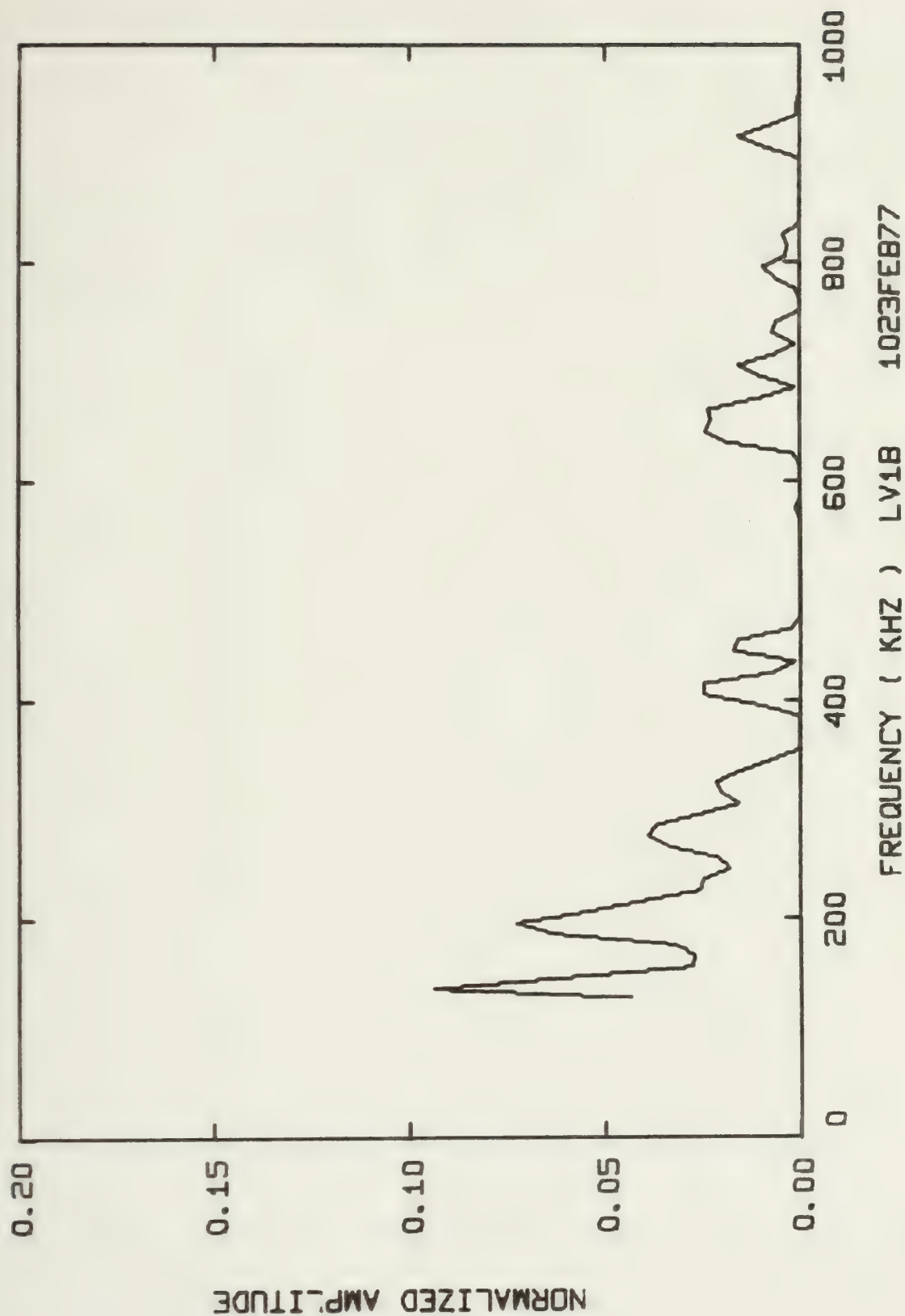




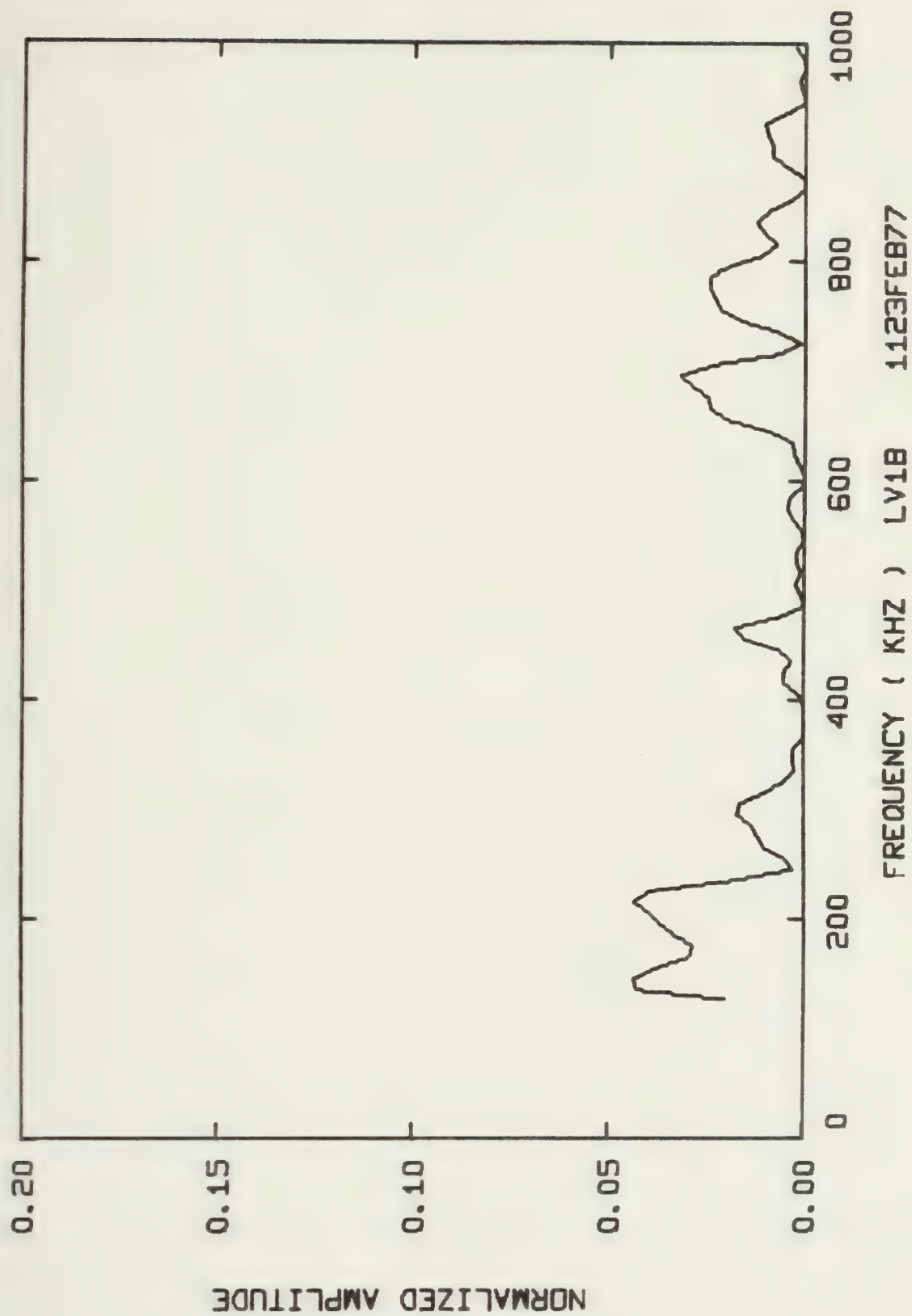




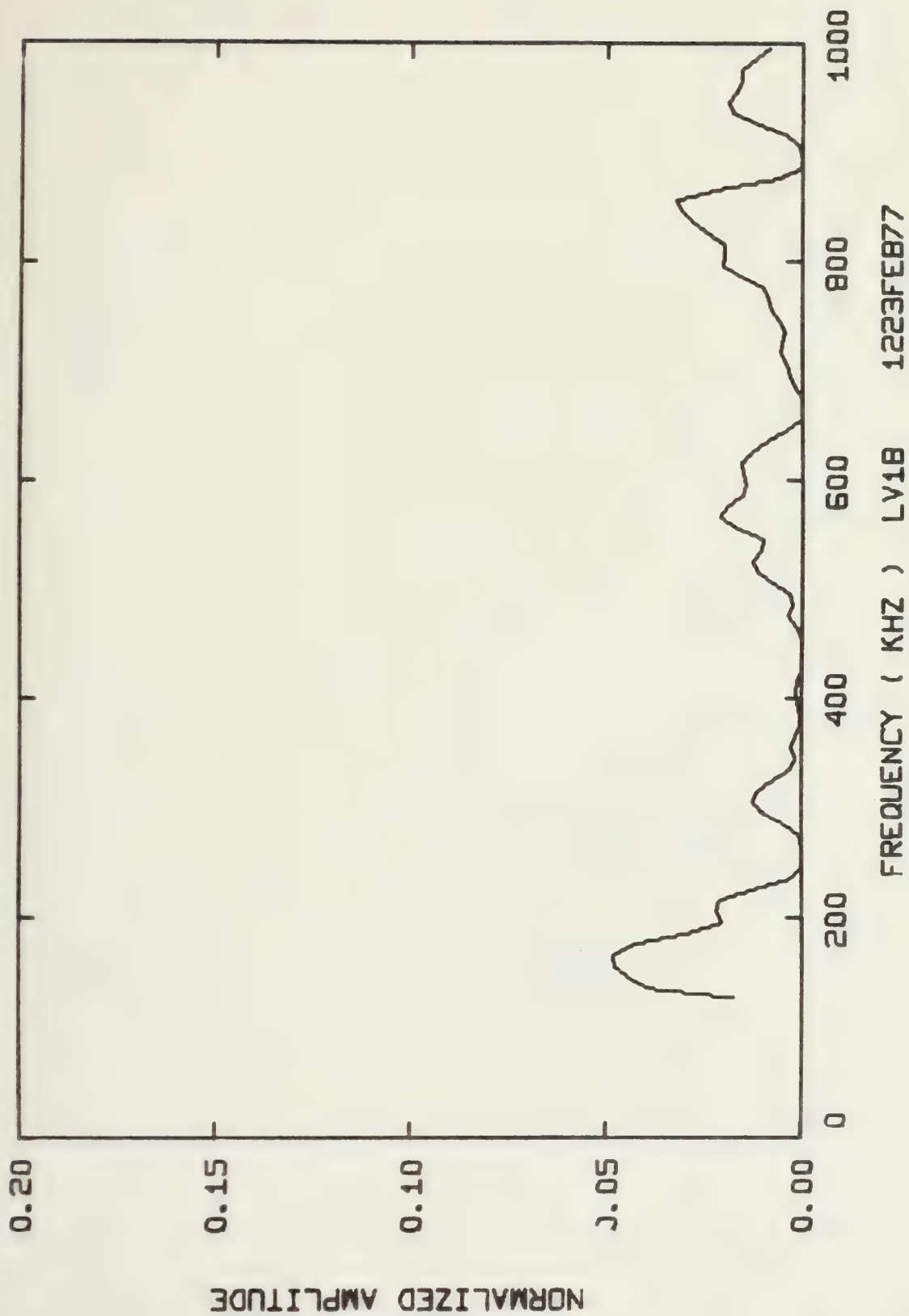






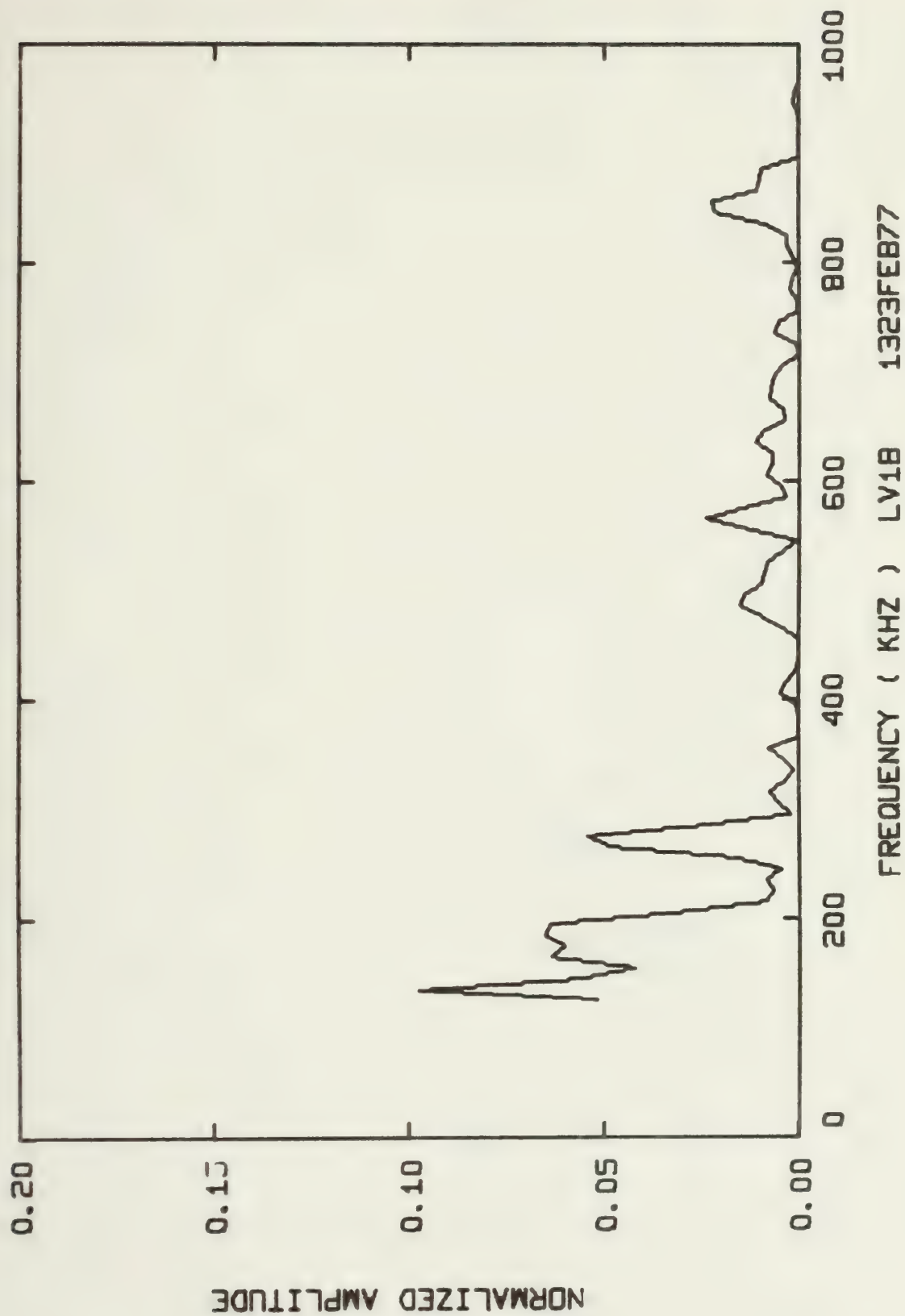




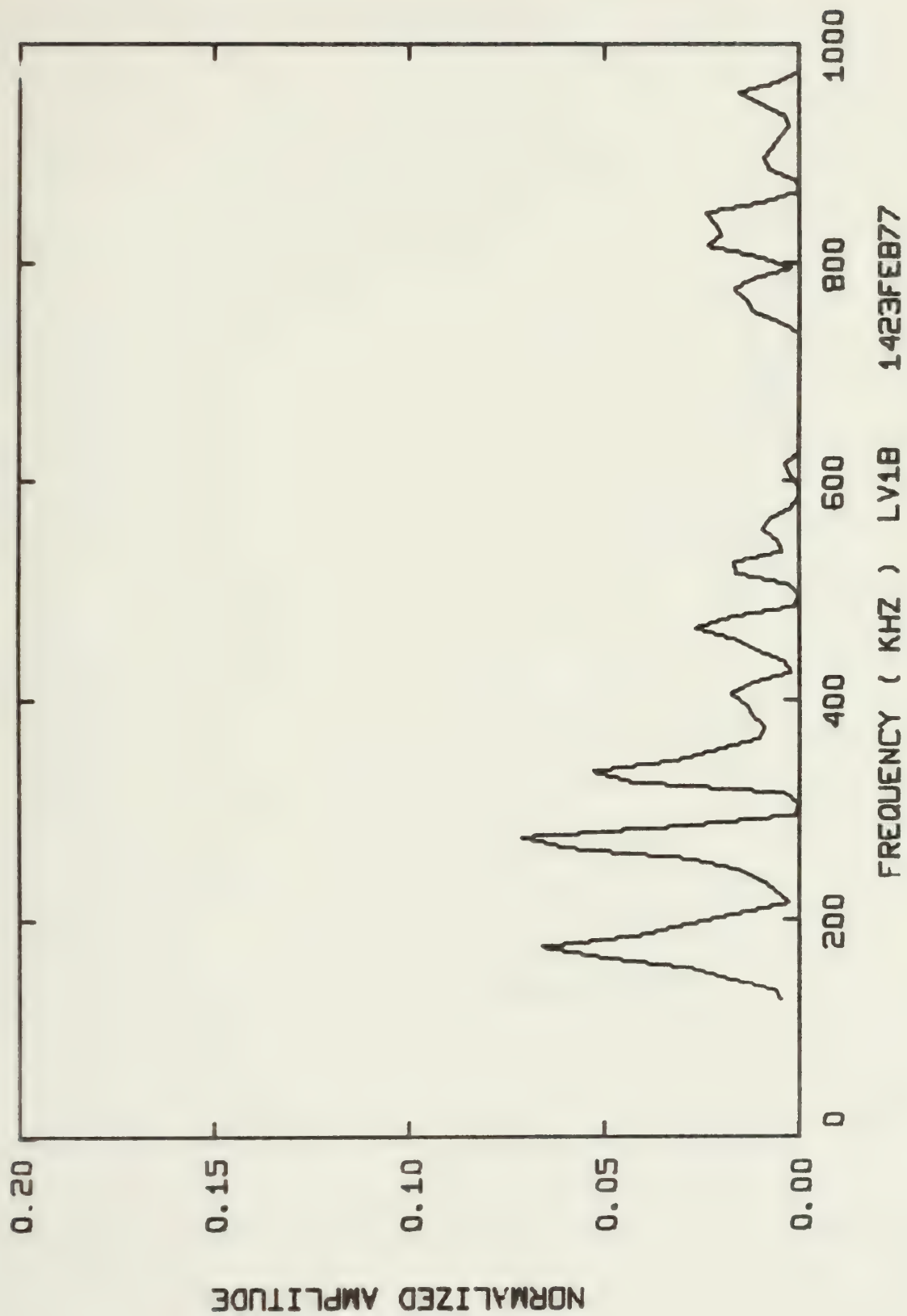




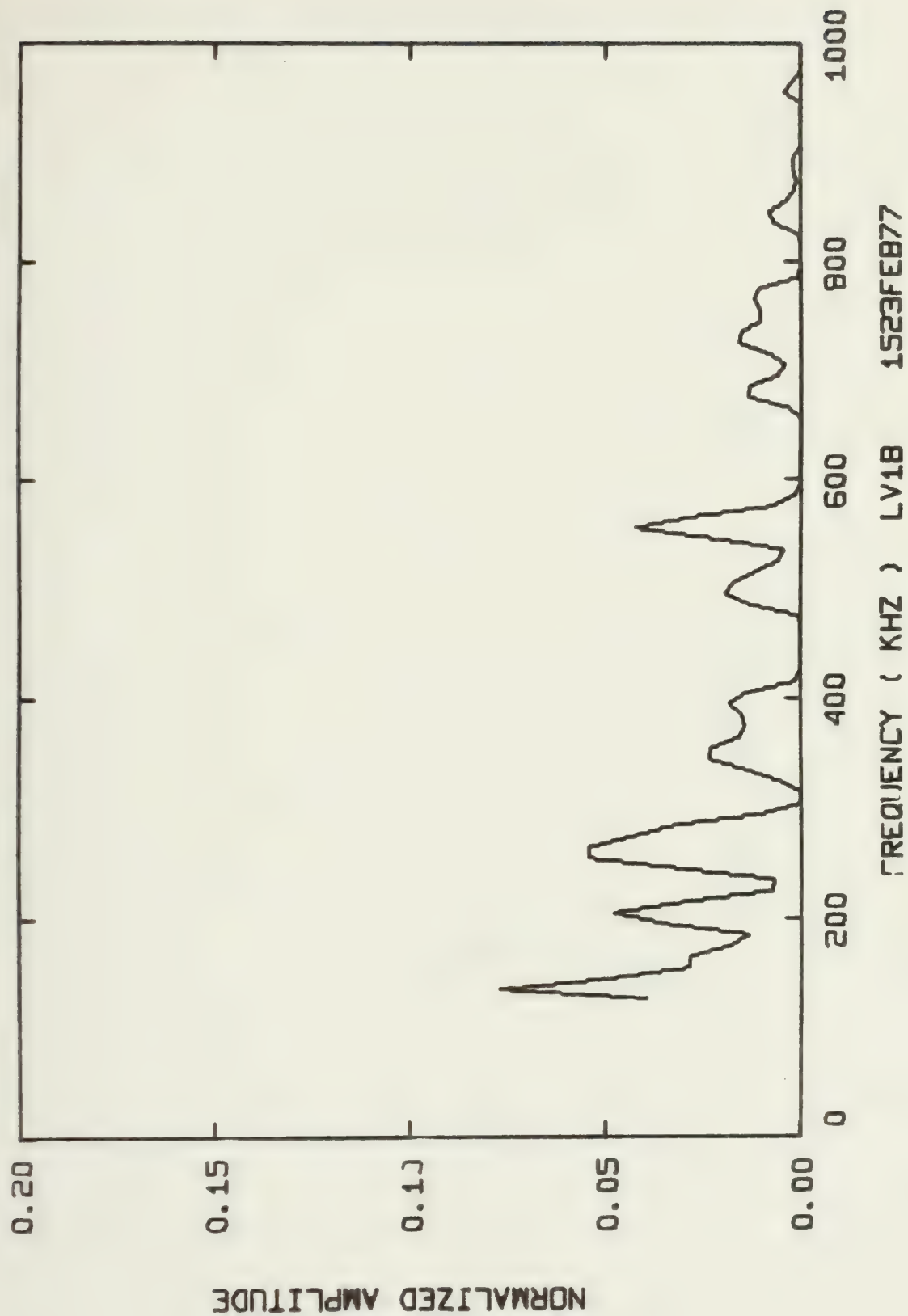




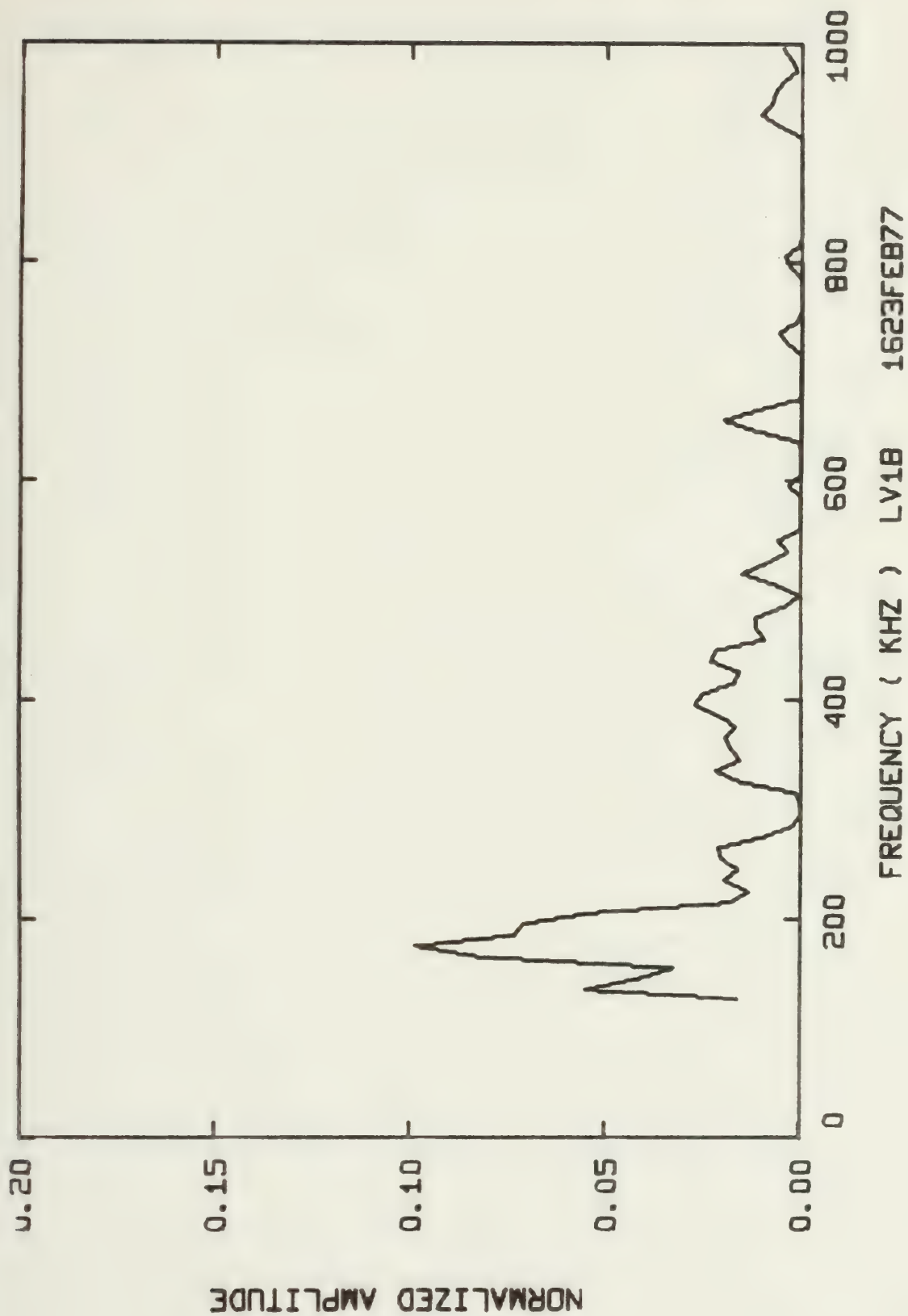






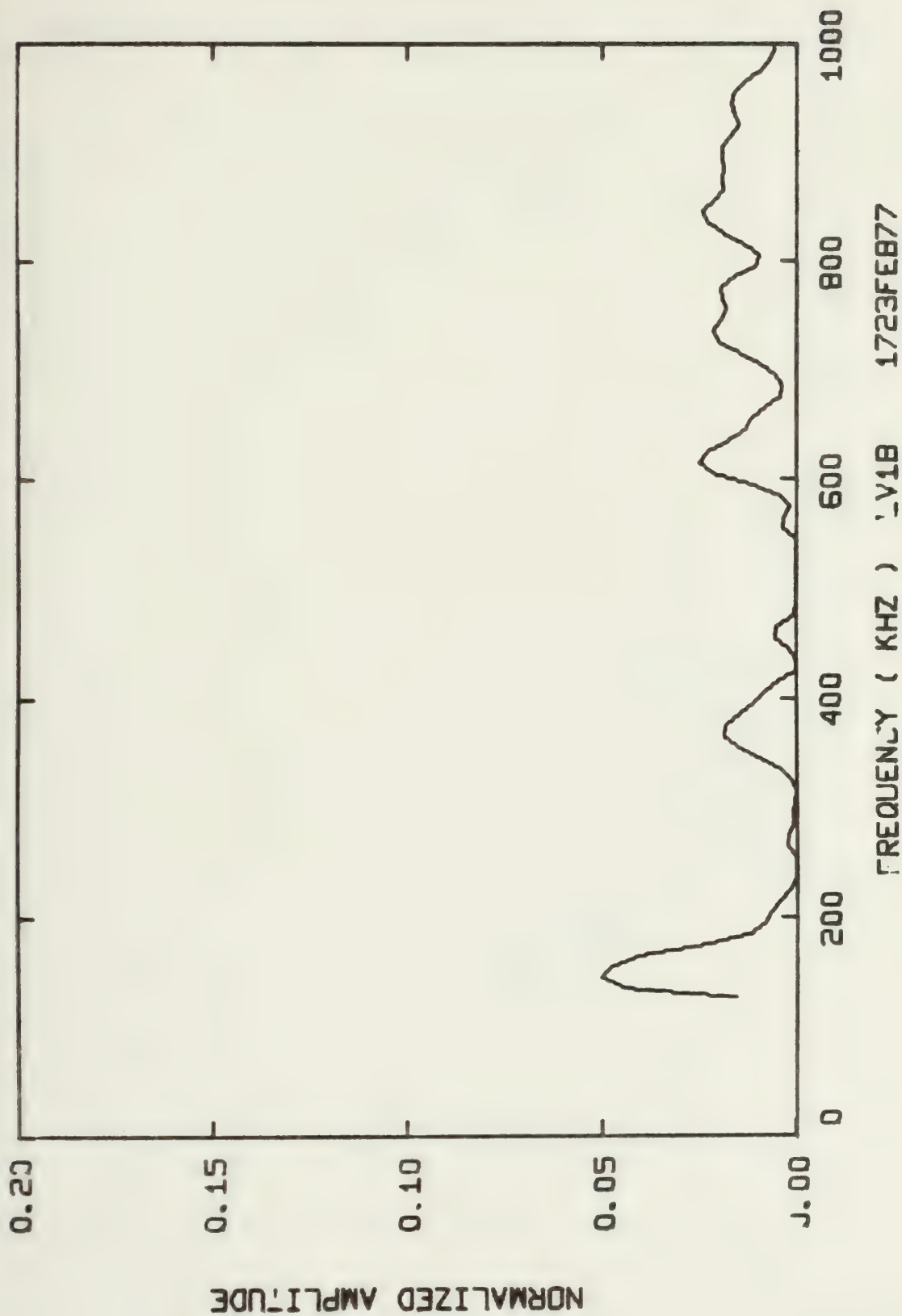




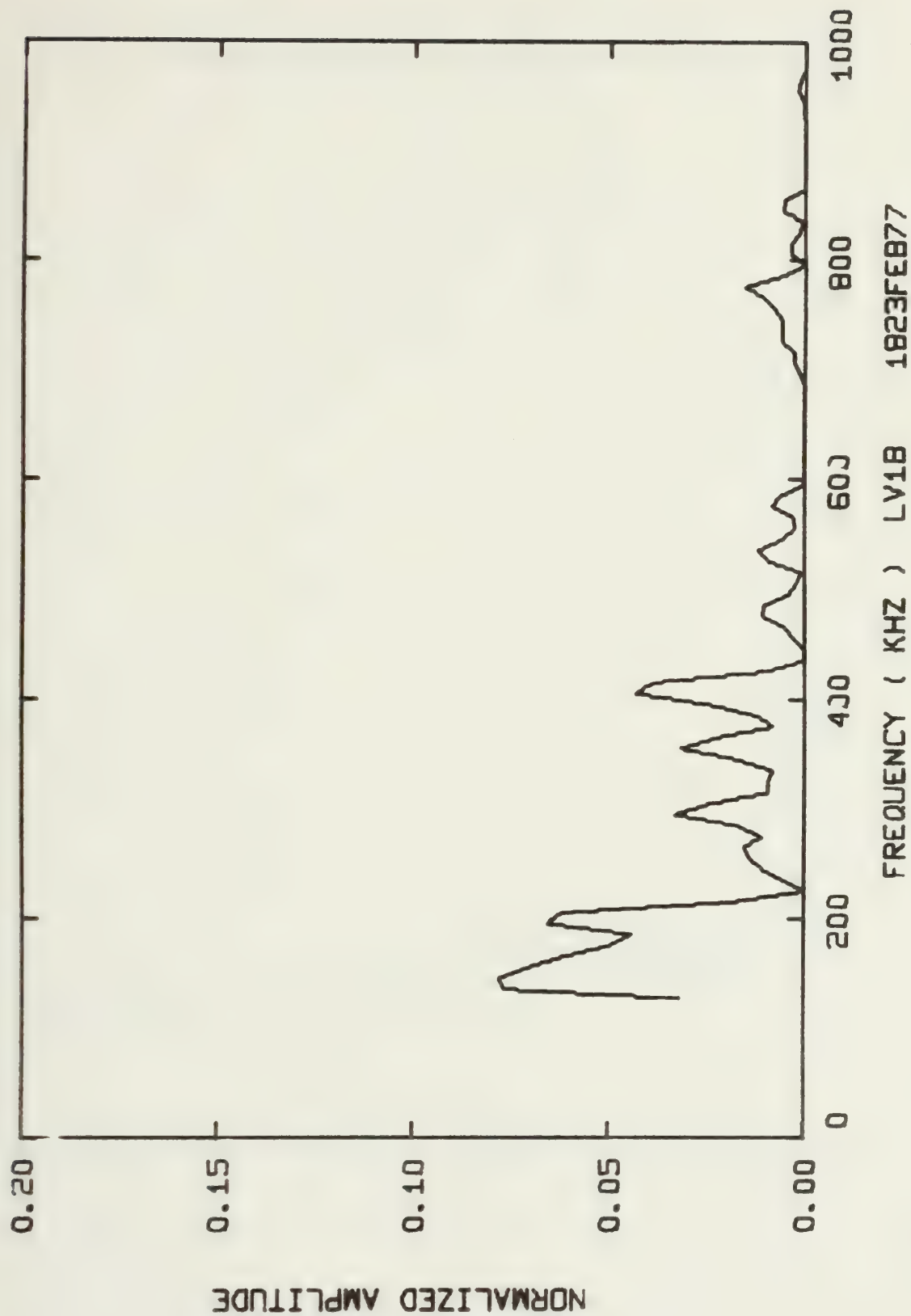




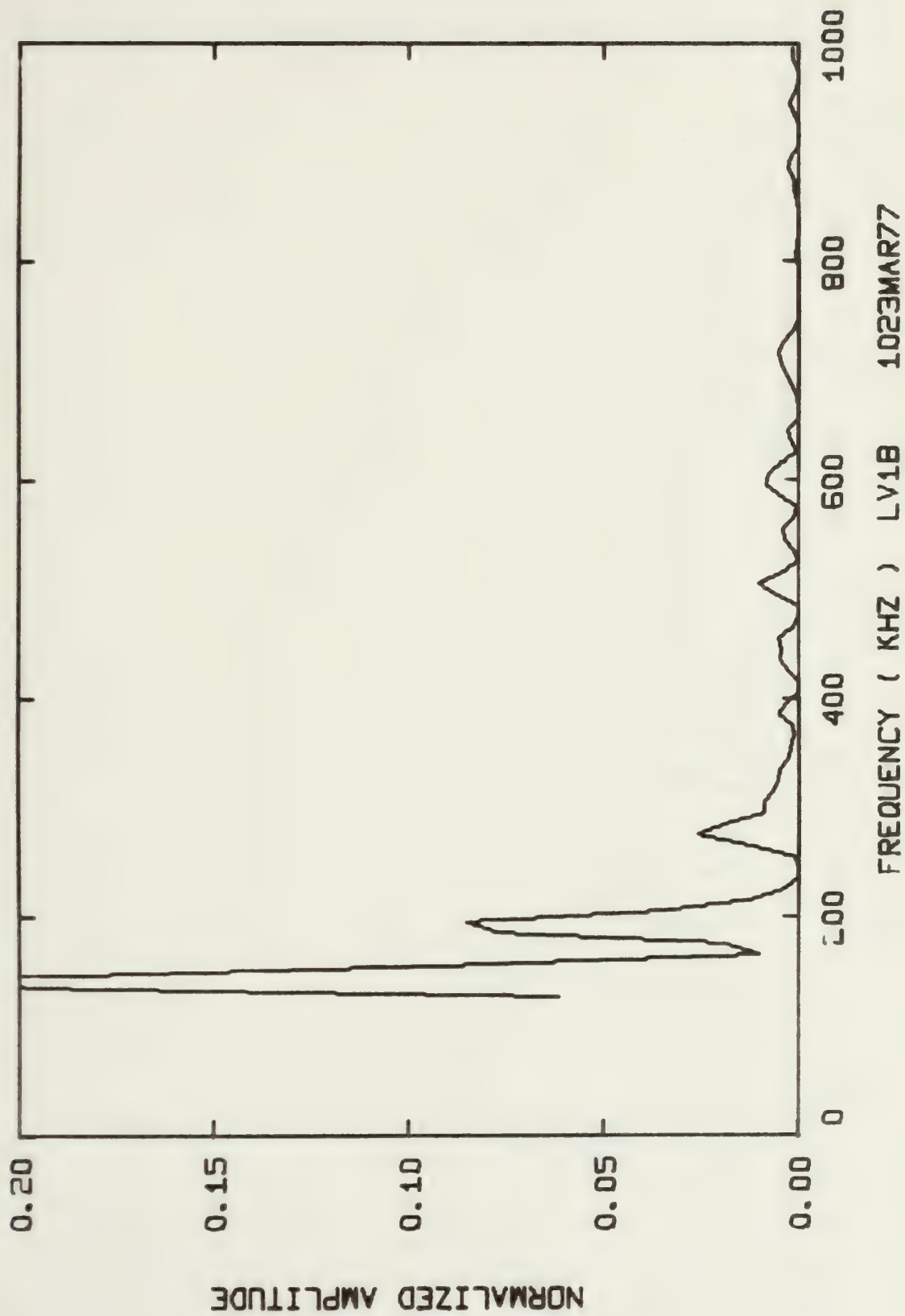




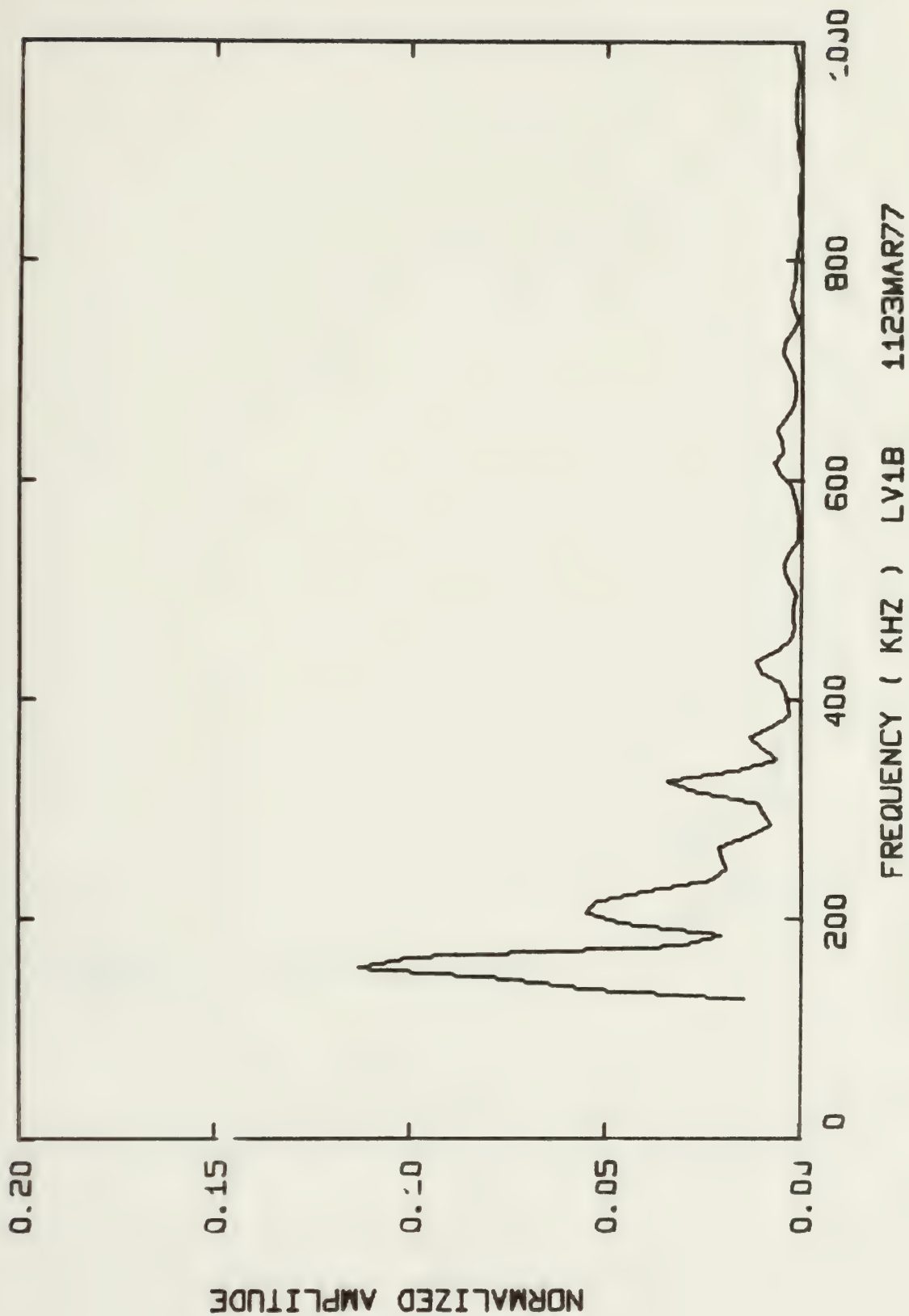






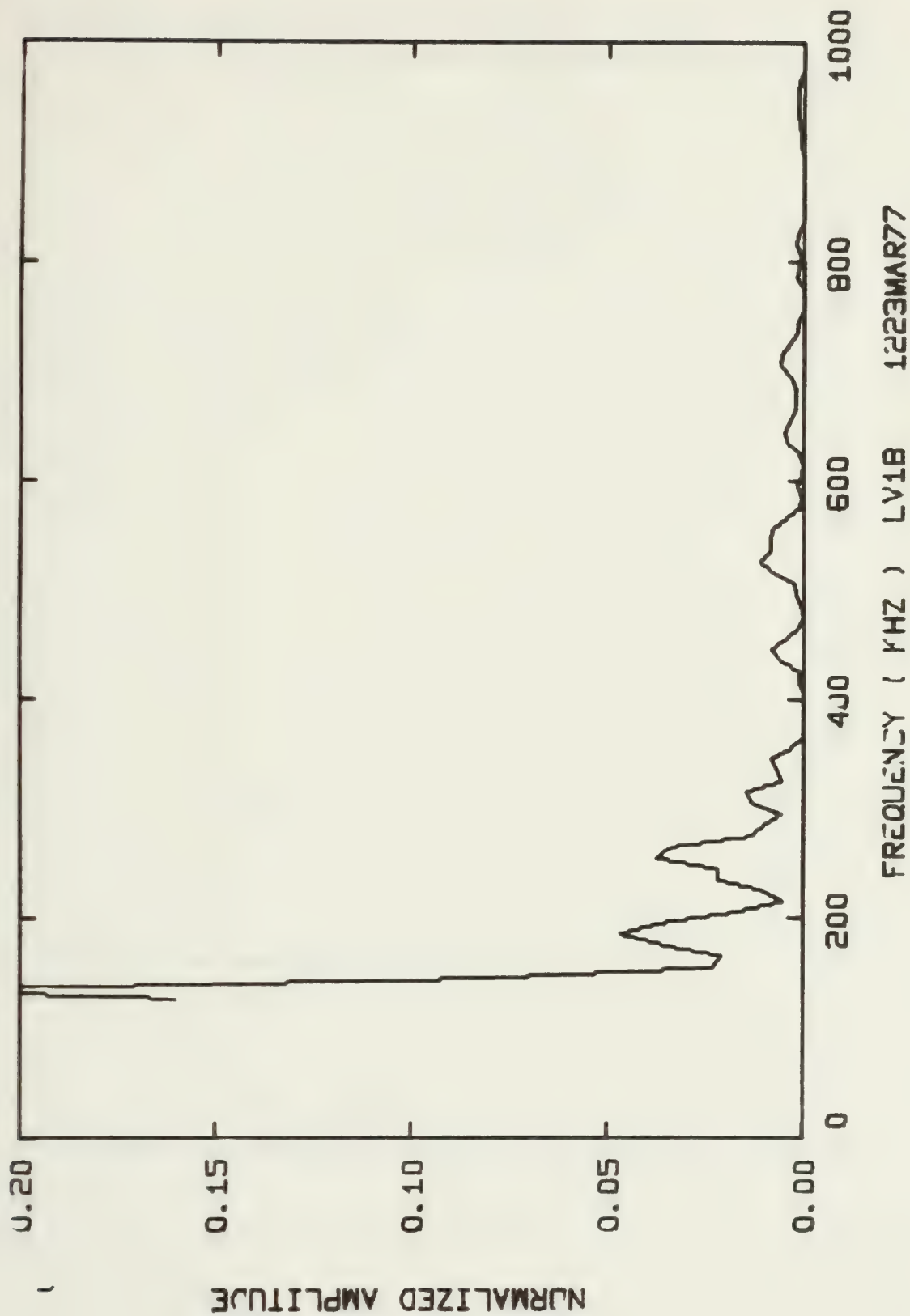




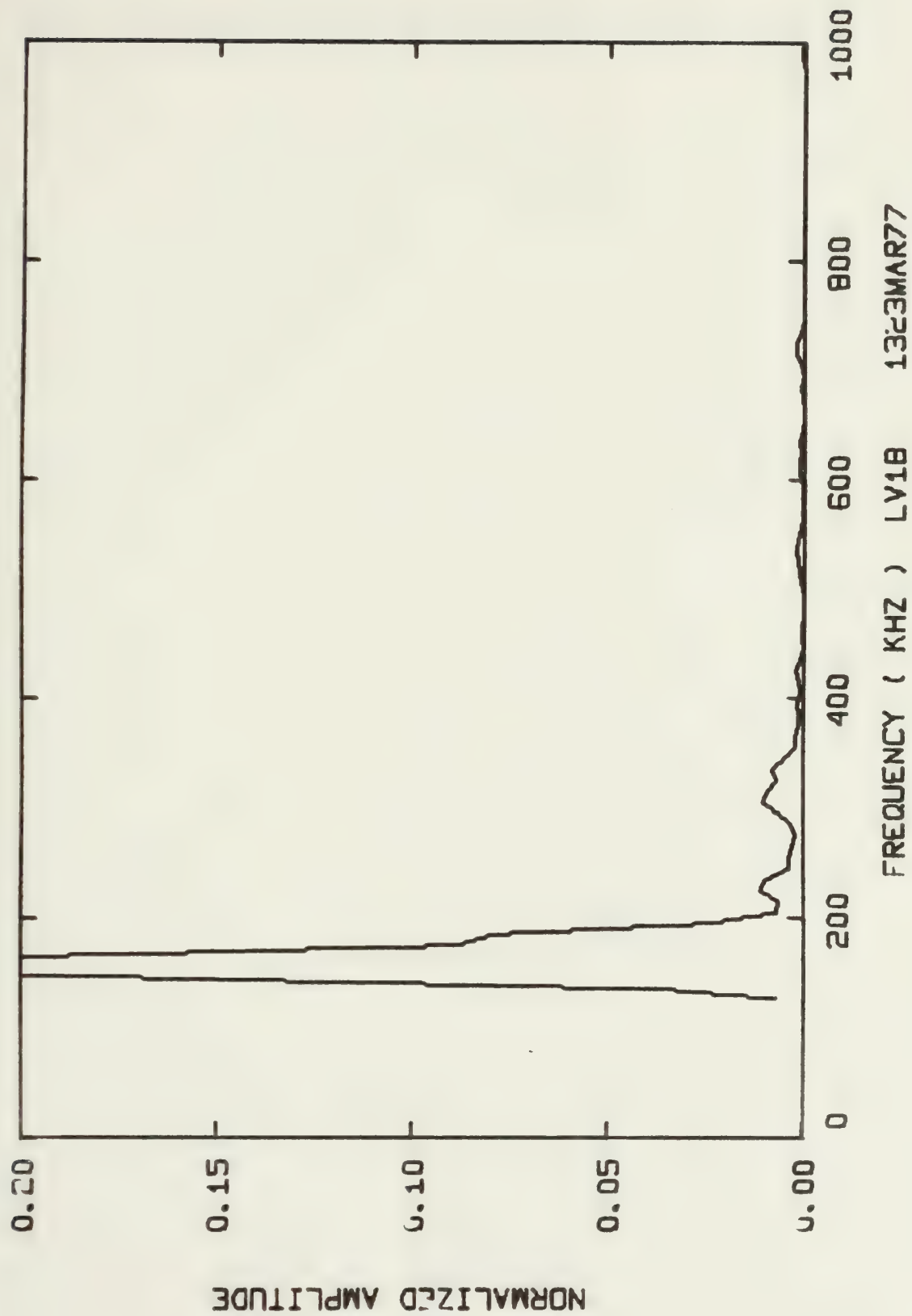




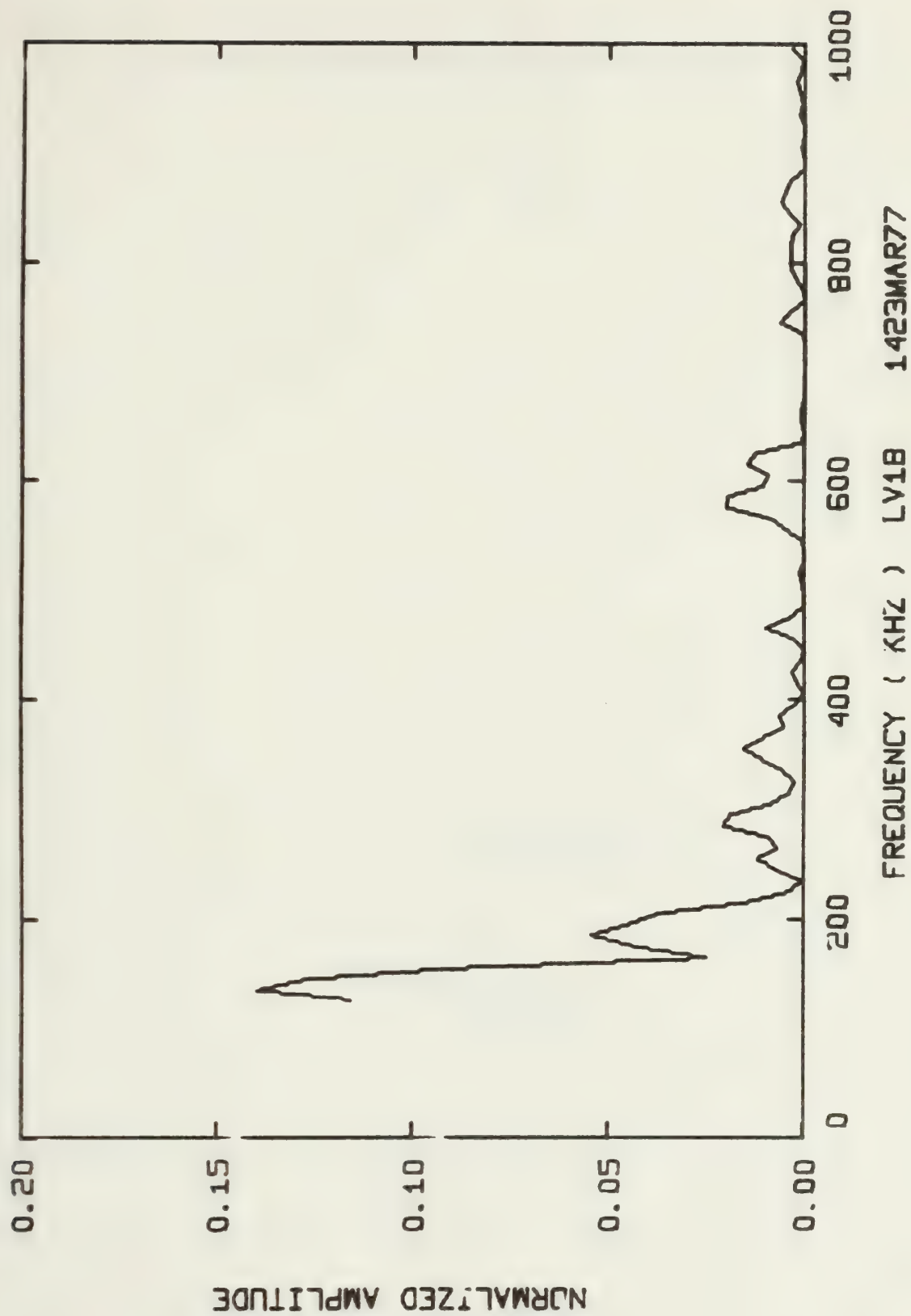




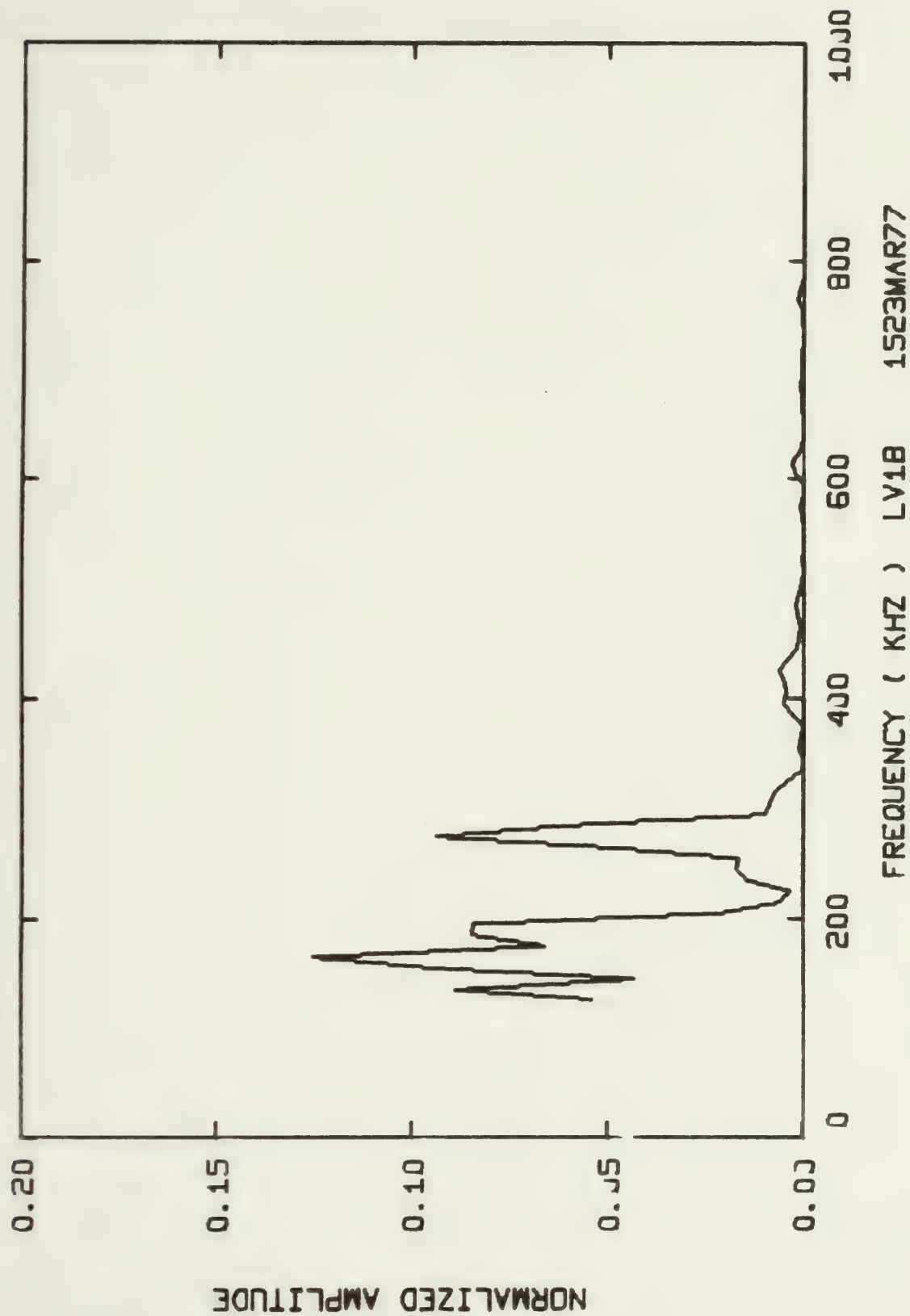






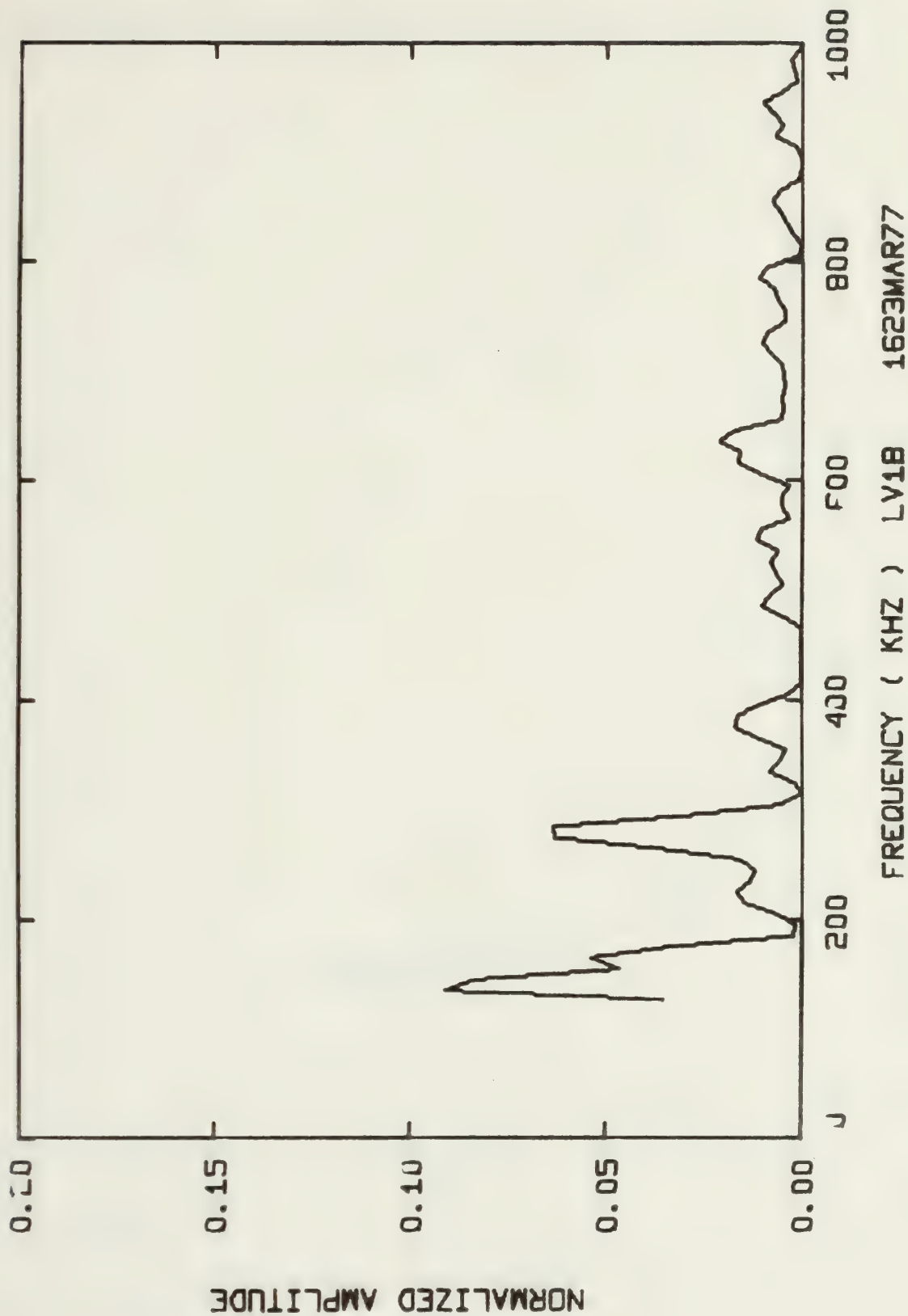




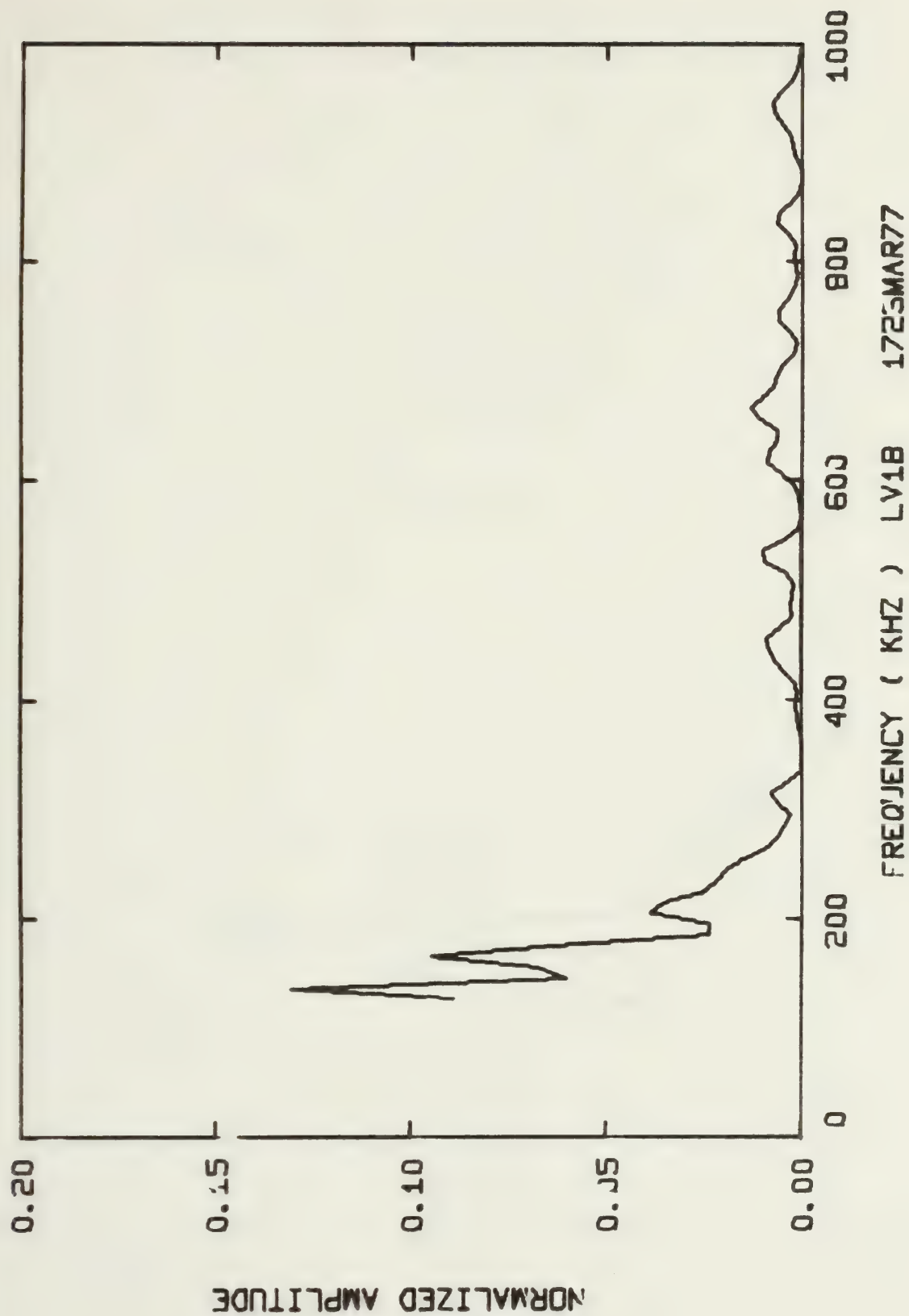




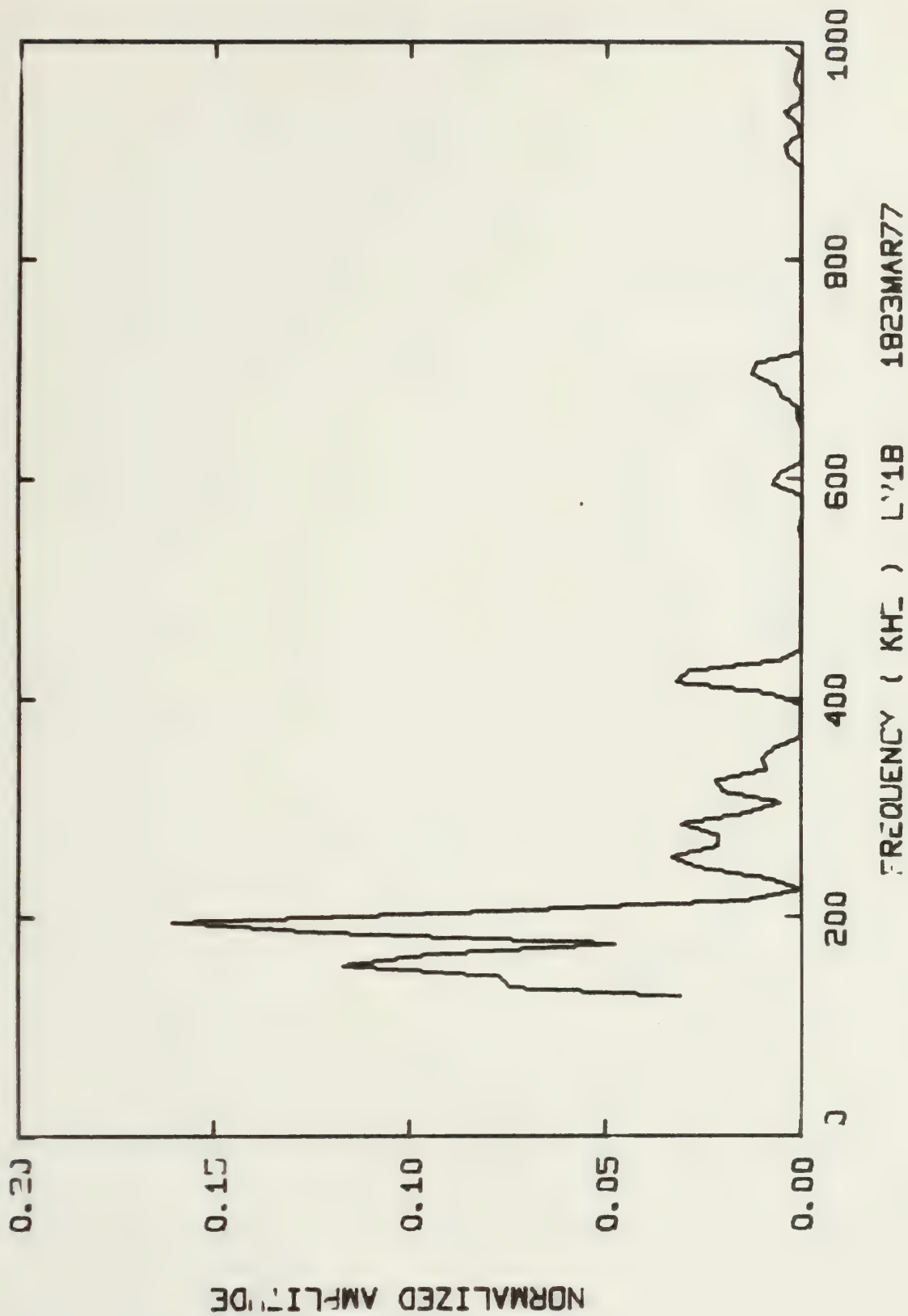




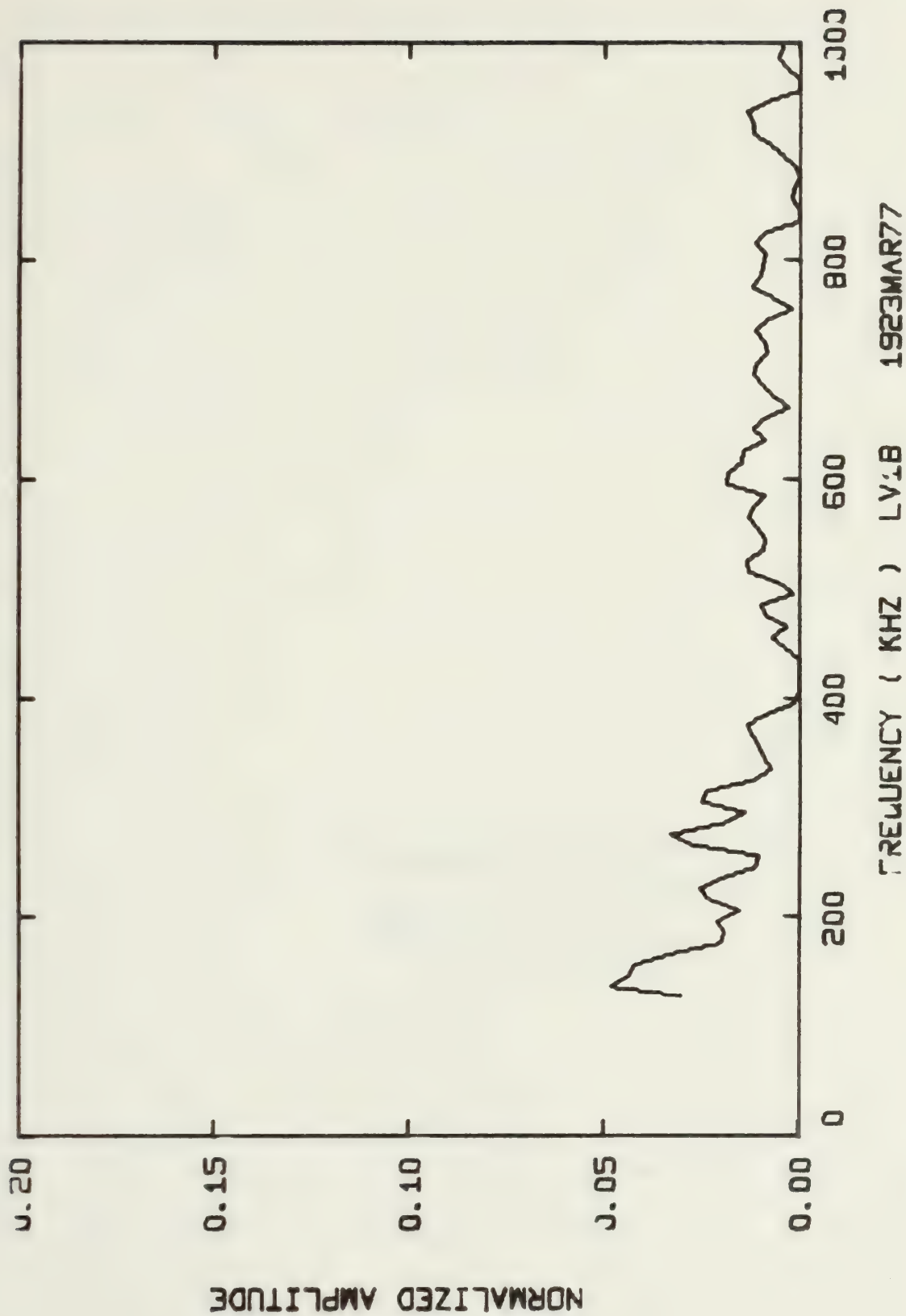






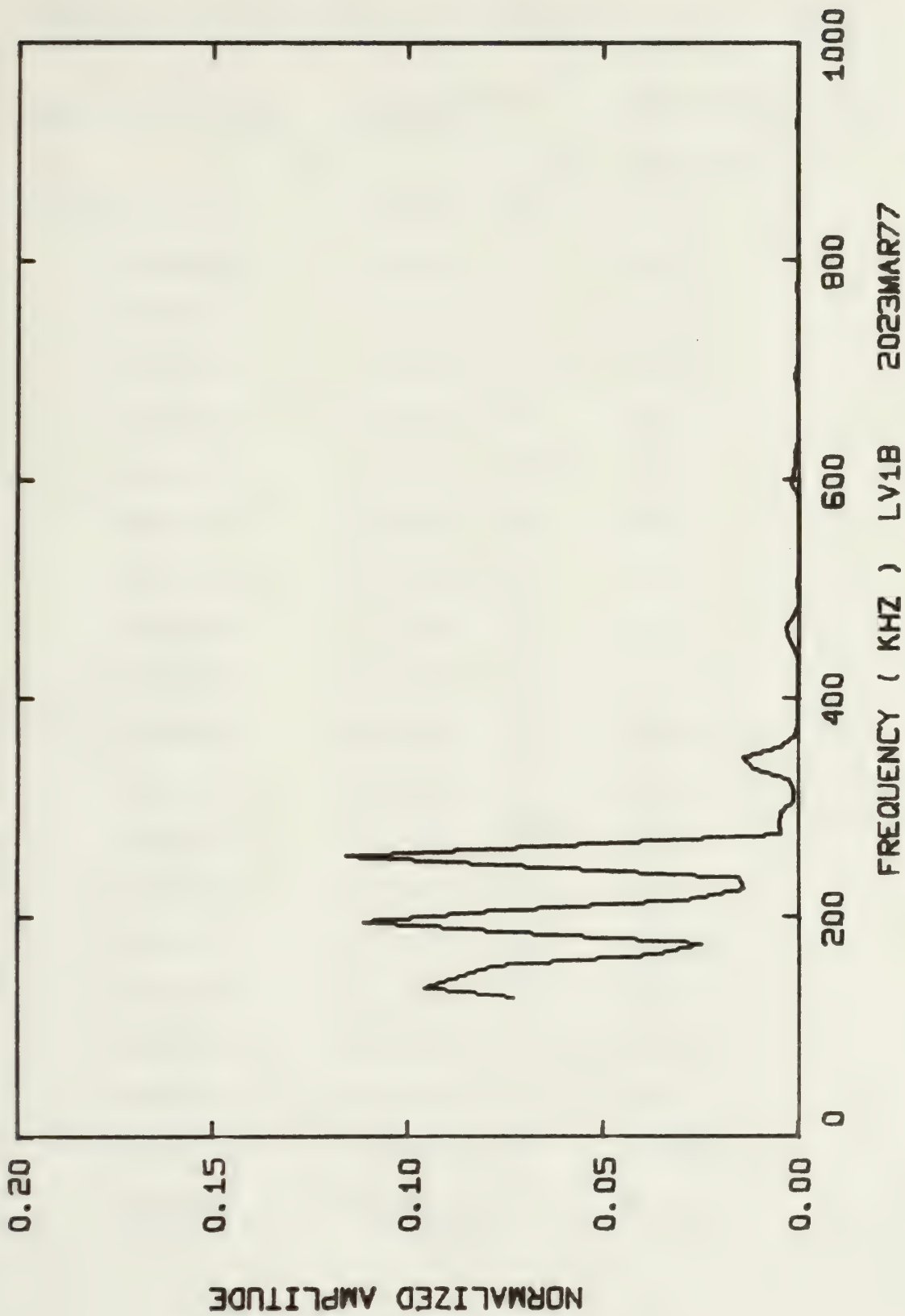










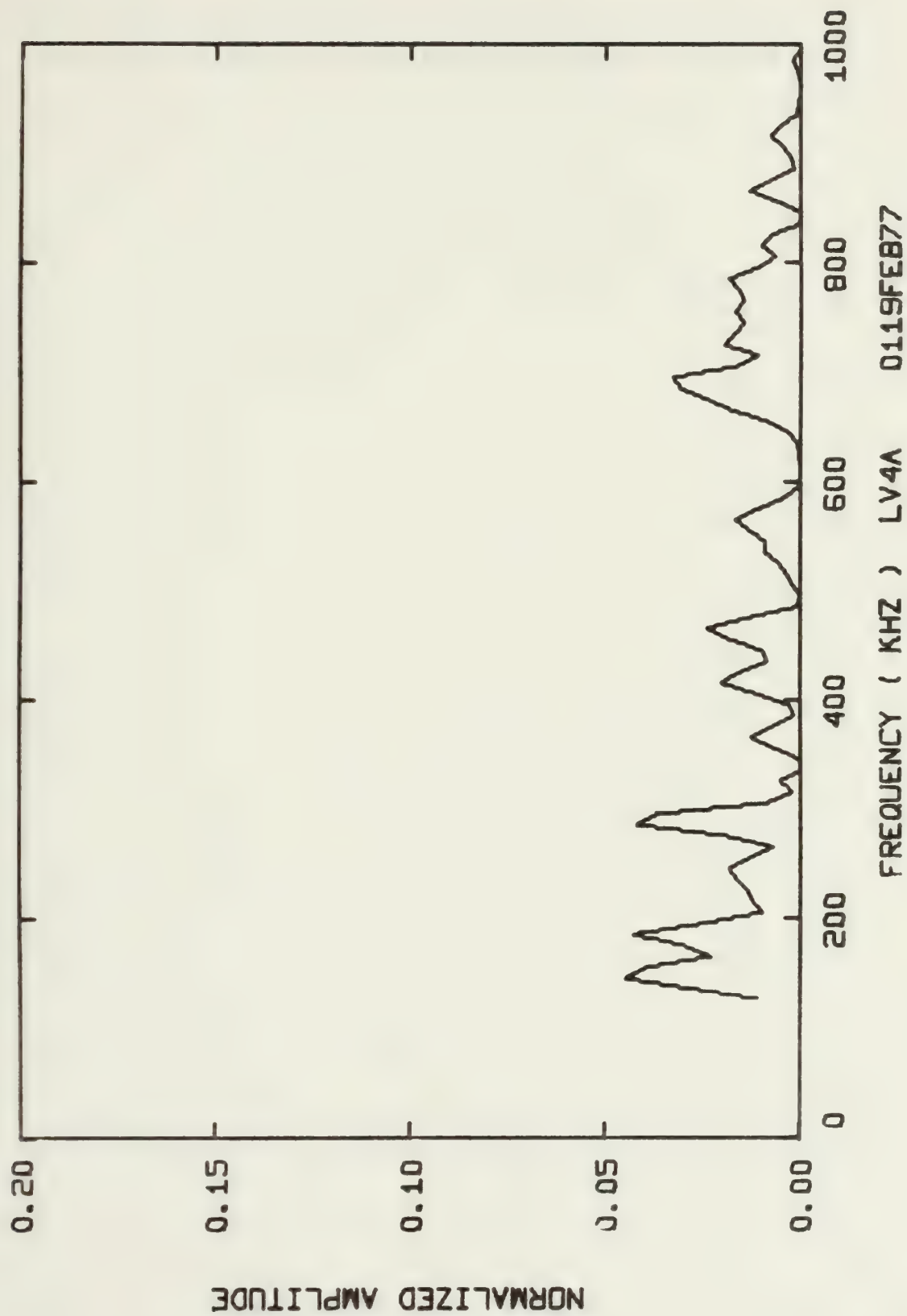




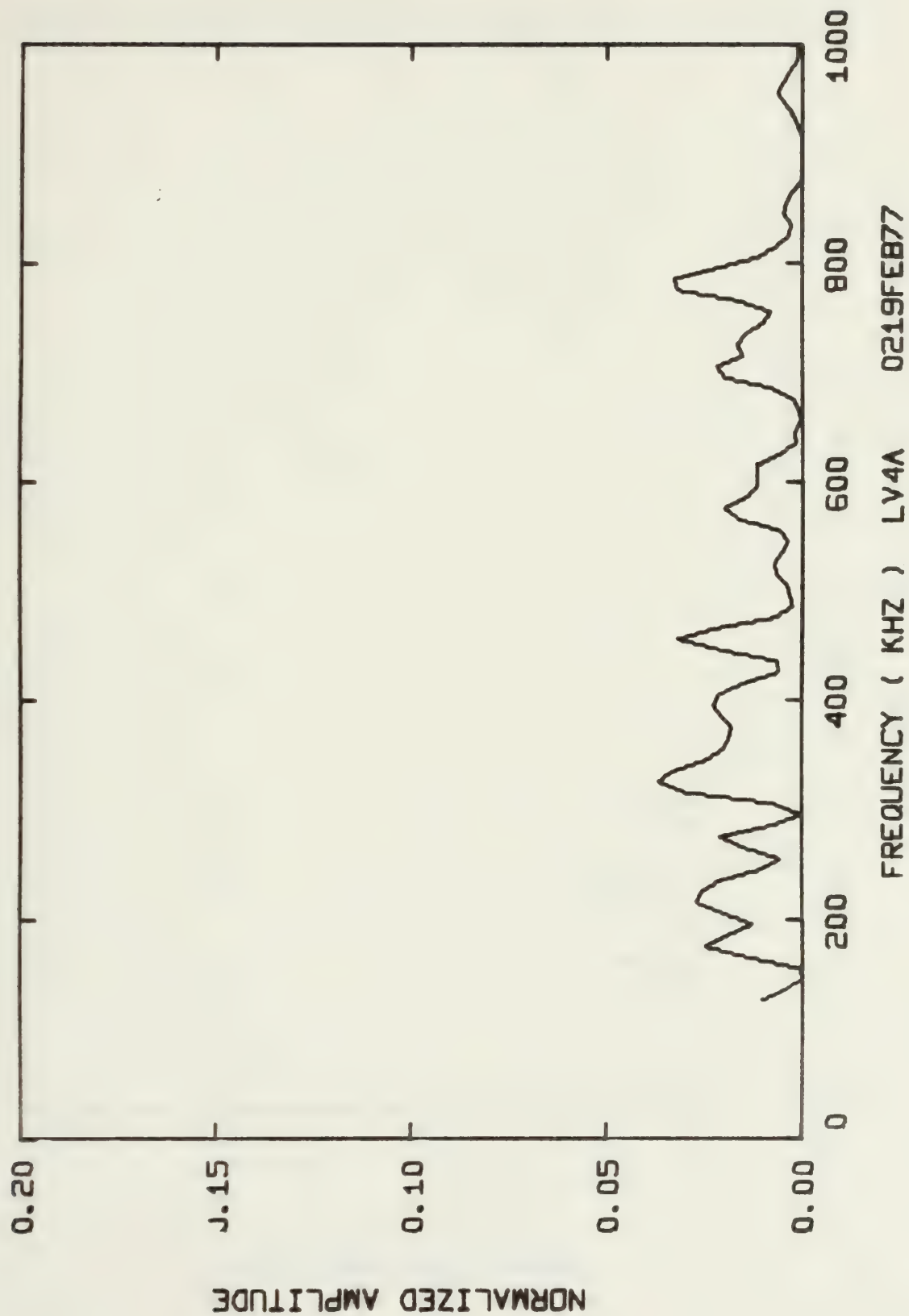
Summary of Energy per Acoustic Emission and RMS Pressure  
Across the Transducer's Face for Each Spectra

Spectral Distrib. Graph Code Number	Energy per AE (Joules)	RMS Pressure Across Face of Transducer (Pa x 10 <sup>5</sup> )
LV4A 0119FEB77	93.634 x 10 <sup>-9</sup>	75.10
0219FEB77	94.549 x 10 <sup>-9</sup>	75.47
0319FEB77	67.462 x 10 <sup>-9</sup>	69.61
0419FEB77	58.222 x 10 <sup>-9</sup>	71.95
0519FEB77	47.261 x 10 <sup>-9</sup>	64.83
0619FEB77	87.986 x 10 <sup>-9</sup>	72.80
0719FEB77	69.420 x 10 <sup>-9</sup>	64.67
0819FEB77	80.749 x 10 <sup>-9</sup>	69.74
0919FEB77	77.356 x 10 <sup>-9</sup>	68.04
1019FEB77	60.352 x 10 <sup>-9</sup>	75.07
1119FEB77	224.96 x 10 <sup>-9</sup>	94.34
1219FEB77	74.454 x 10 <sup>-9</sup>	65.91
1319FEB77	35.989 x 10 <sup>-9</sup>	62.88
1419FEB77	19.971 x 10 <sup>-9</sup>	46.84
1519FEB77	529.30 x 10 <sup>-9</sup>	120.03
1619FEB77	25.163 x 10 <sup>-9</sup>	57.94
1719FEB77	48.637 x 10 <sup>-9</sup>	59.80
1819FEB77	19.216 x 10 <sup>-9</sup>	50.63
1919FEB77	1.0218 x 10 <sup>-6</sup>	162.79
2019FEB77	49.909 x 10 <sup>-9</sup>	68.26



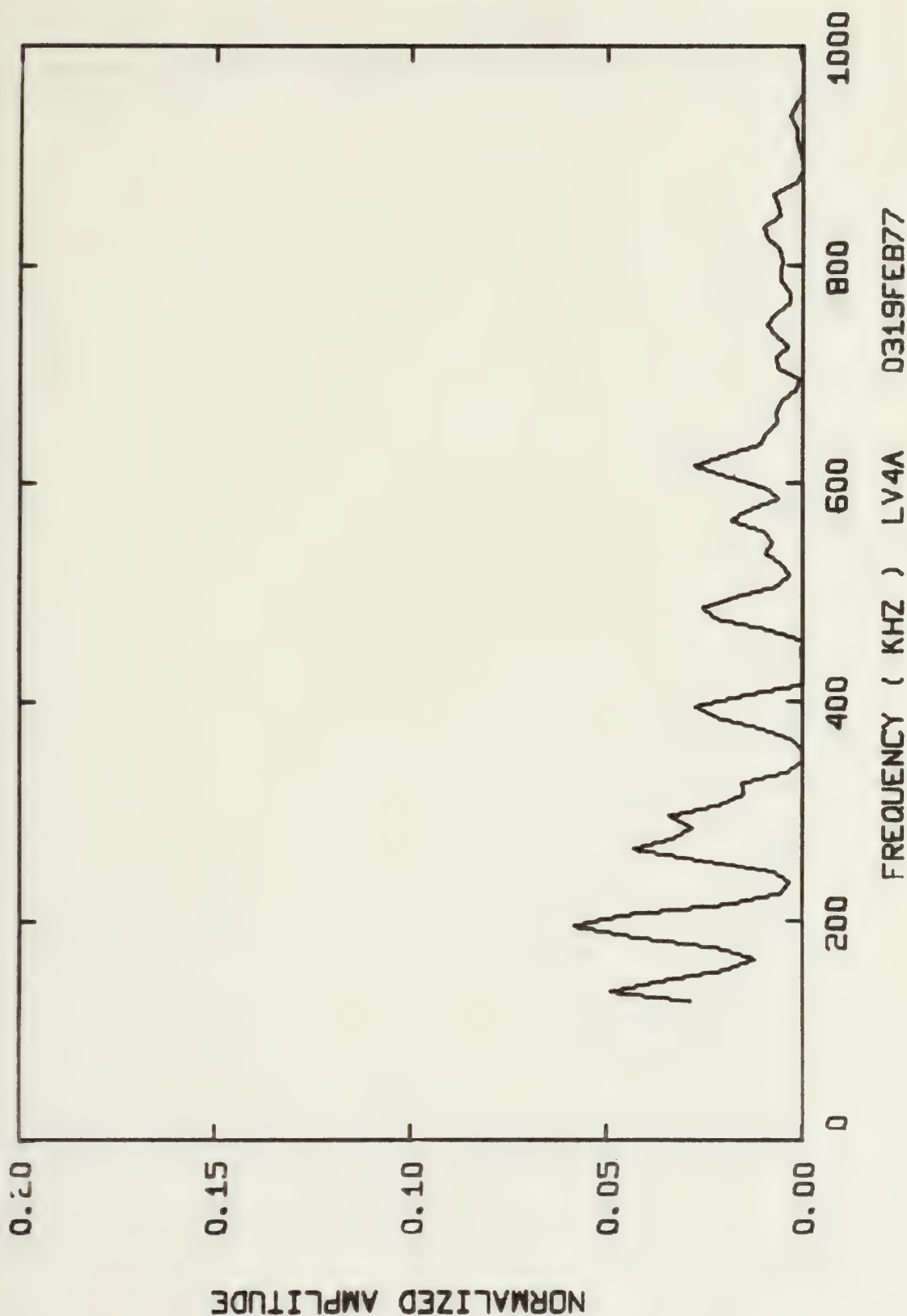




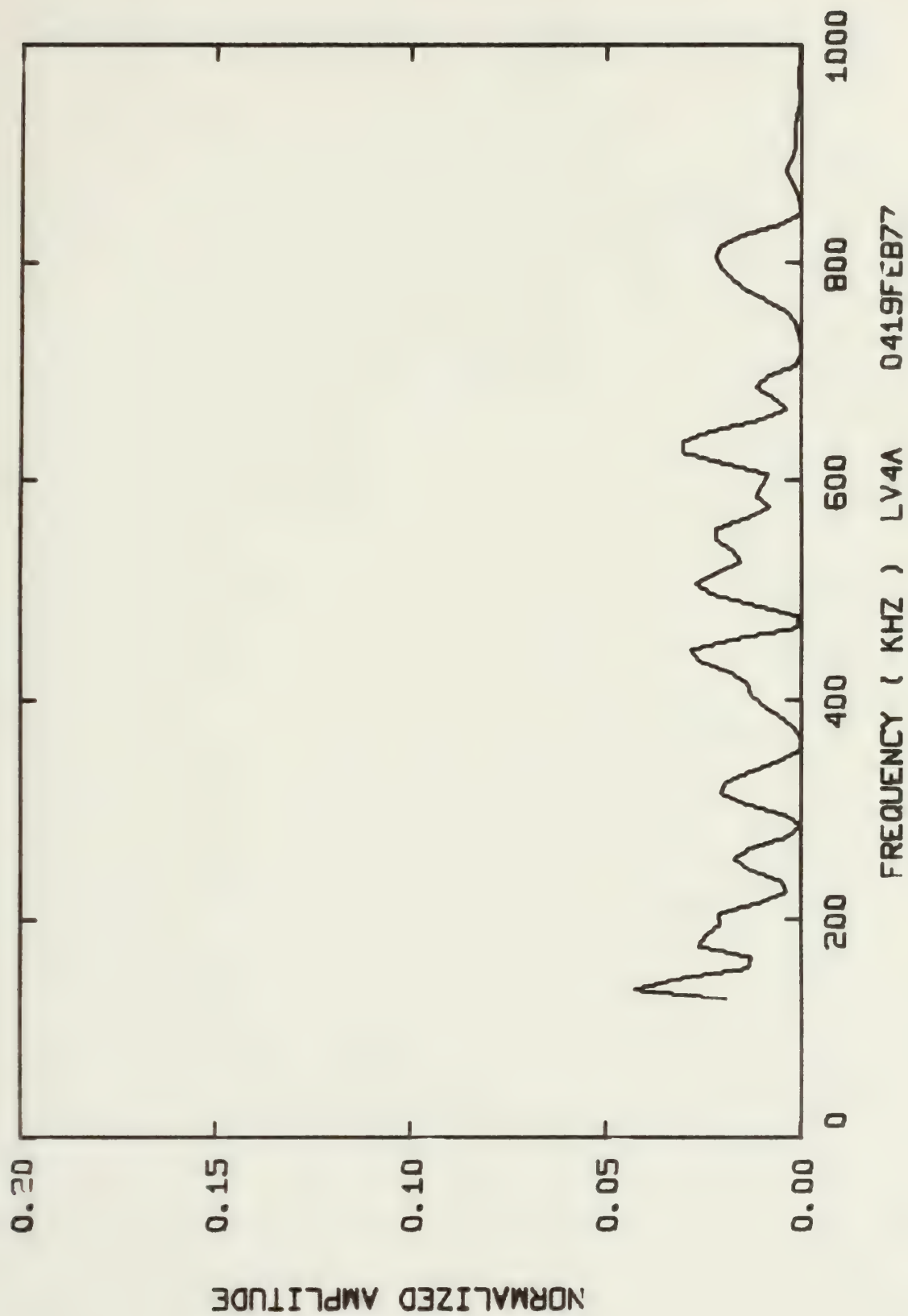




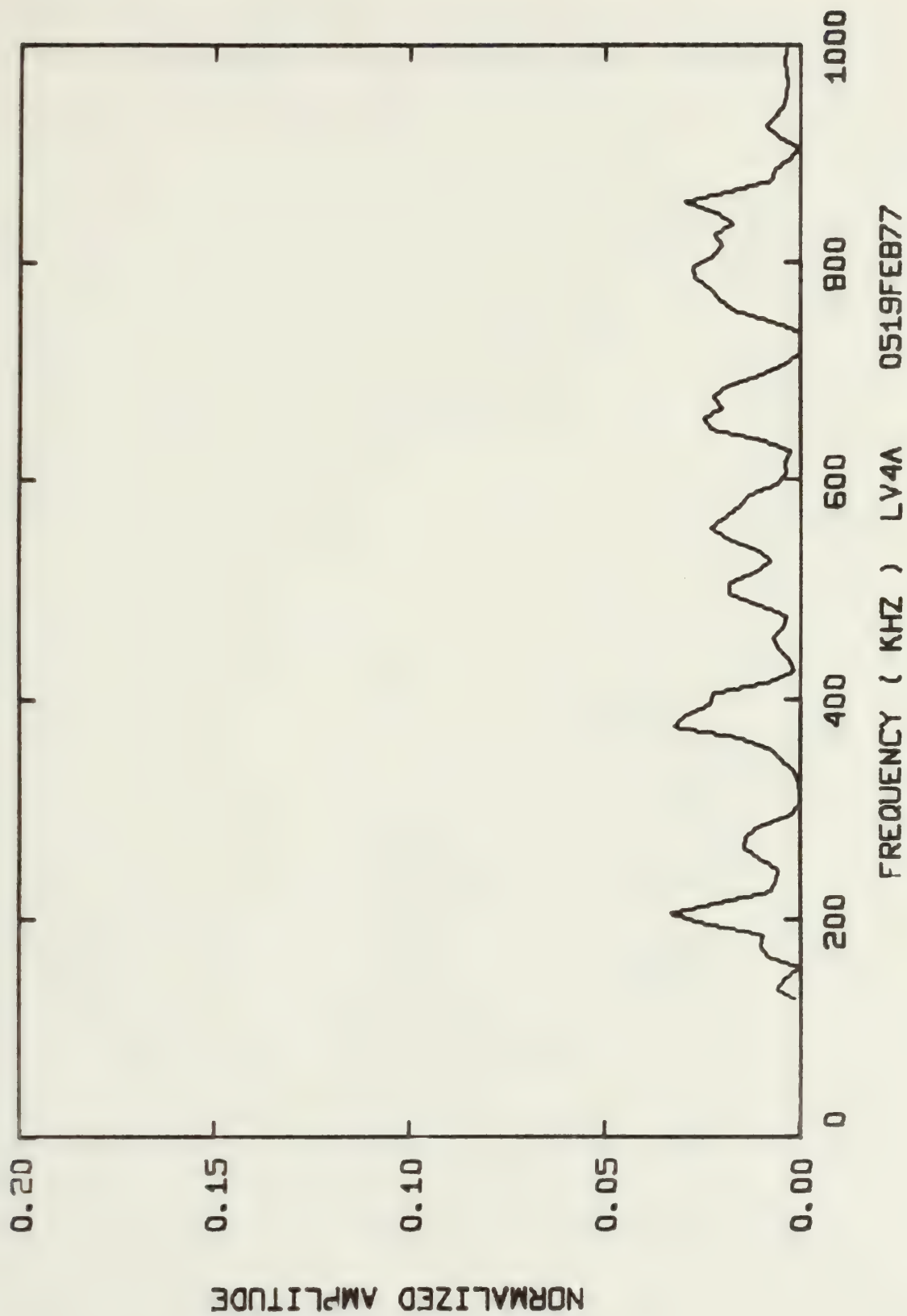




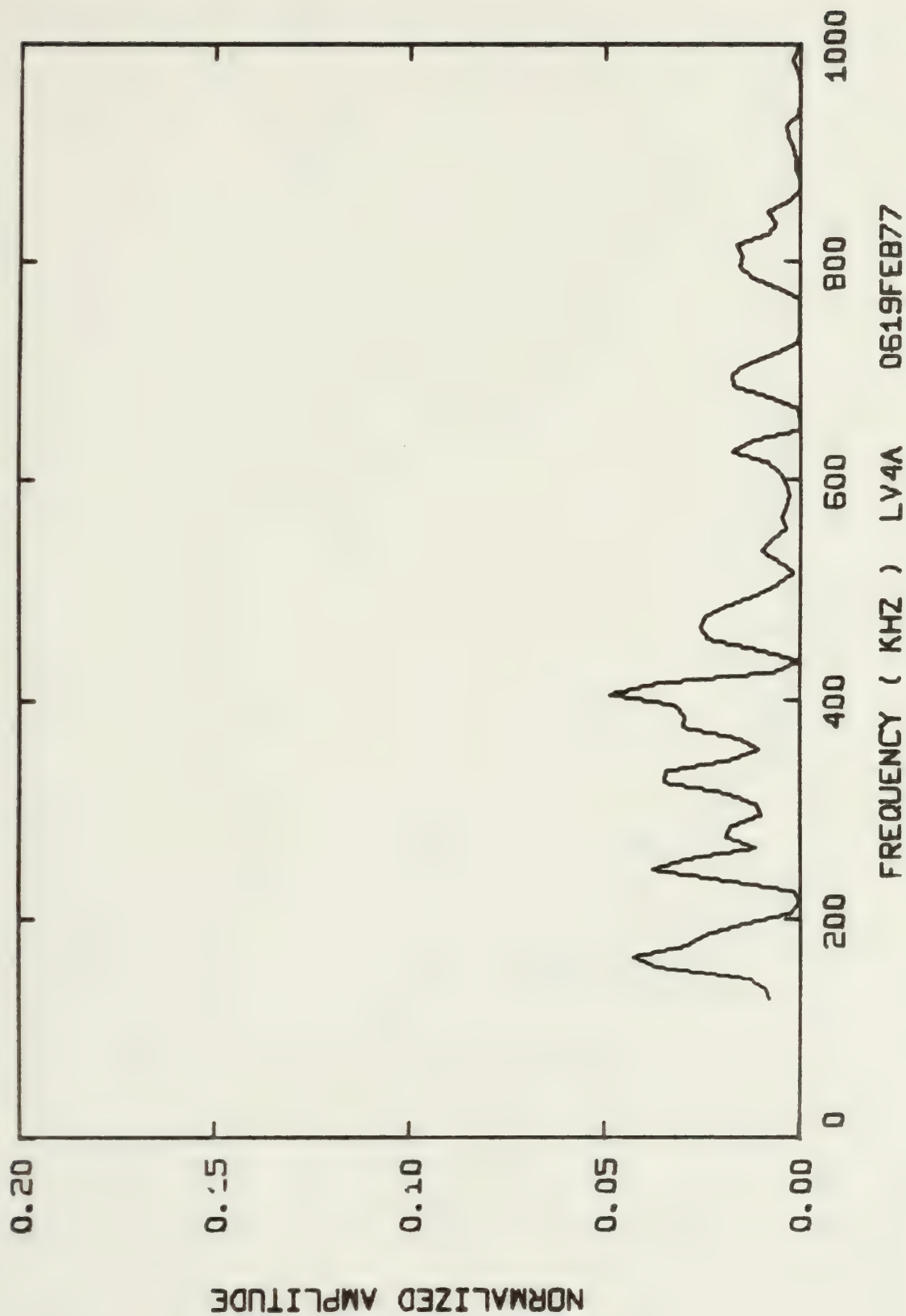






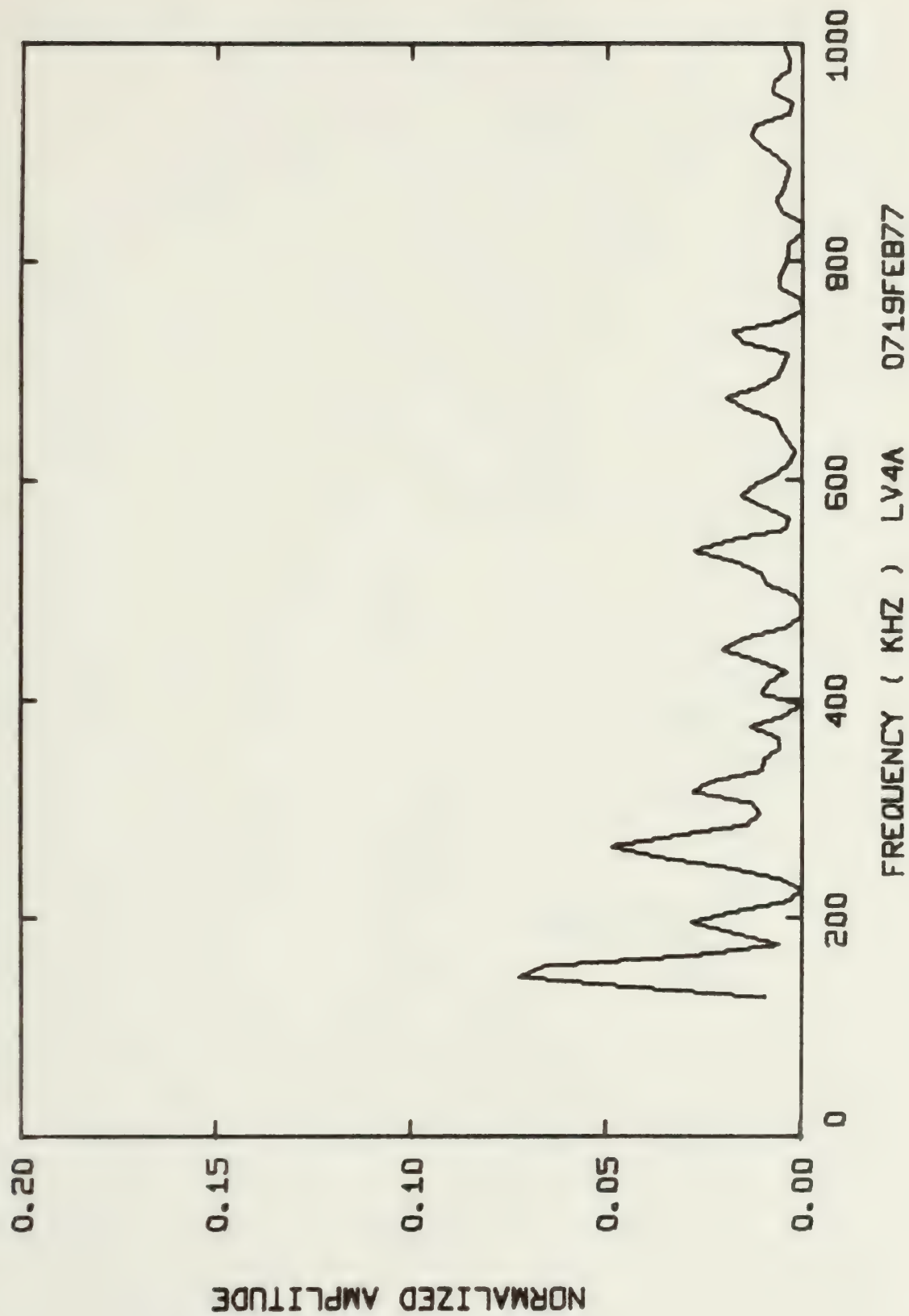




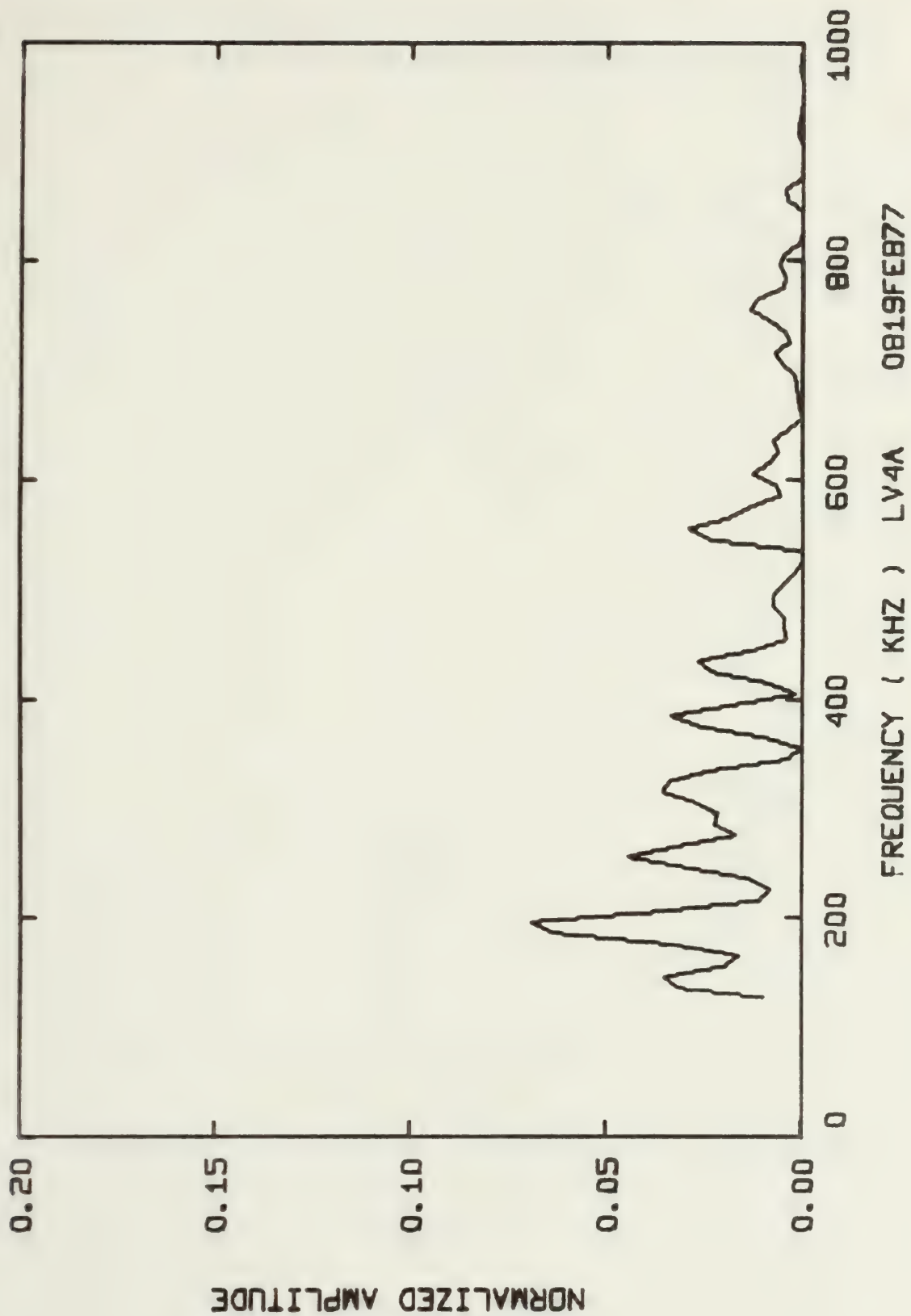




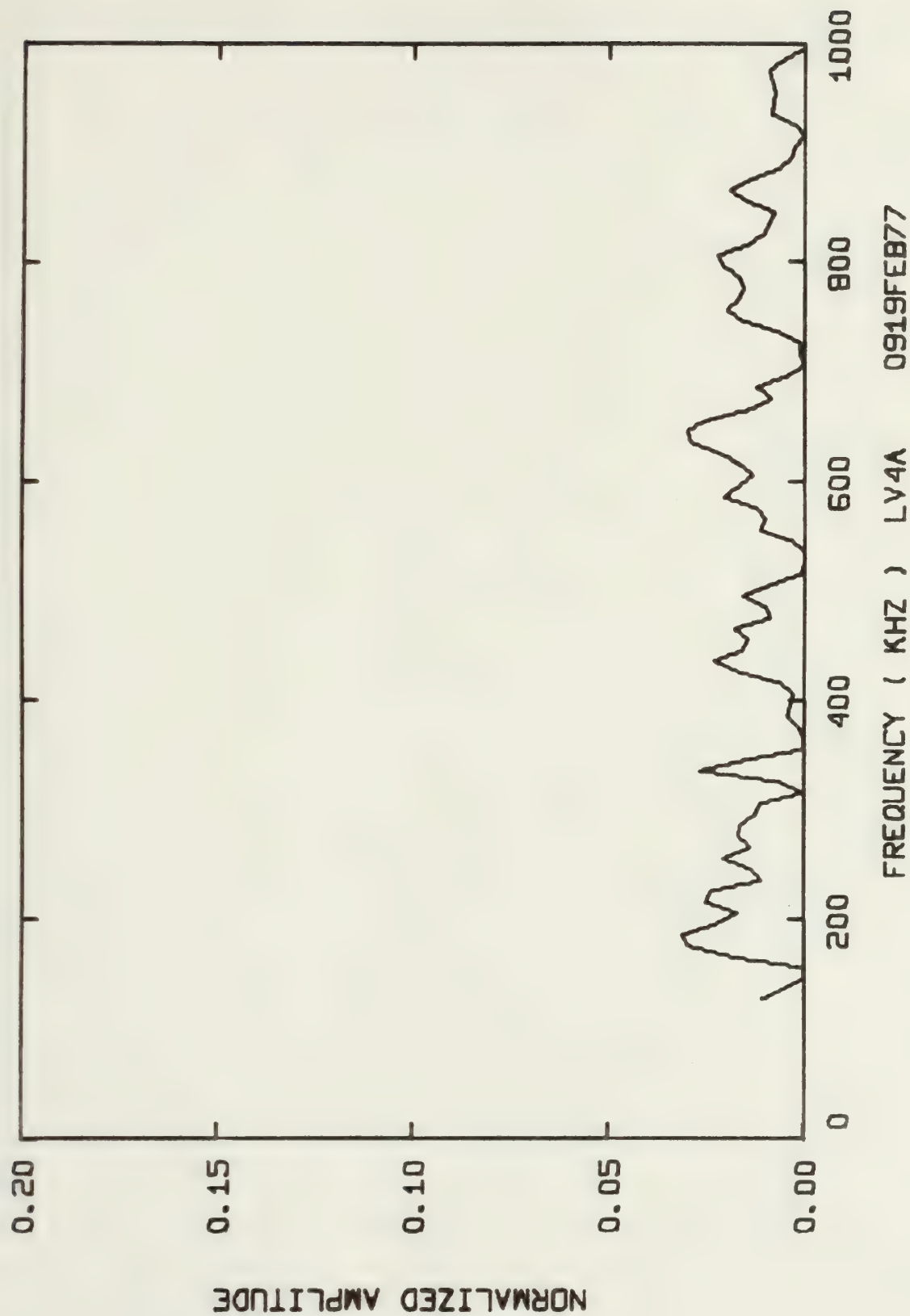




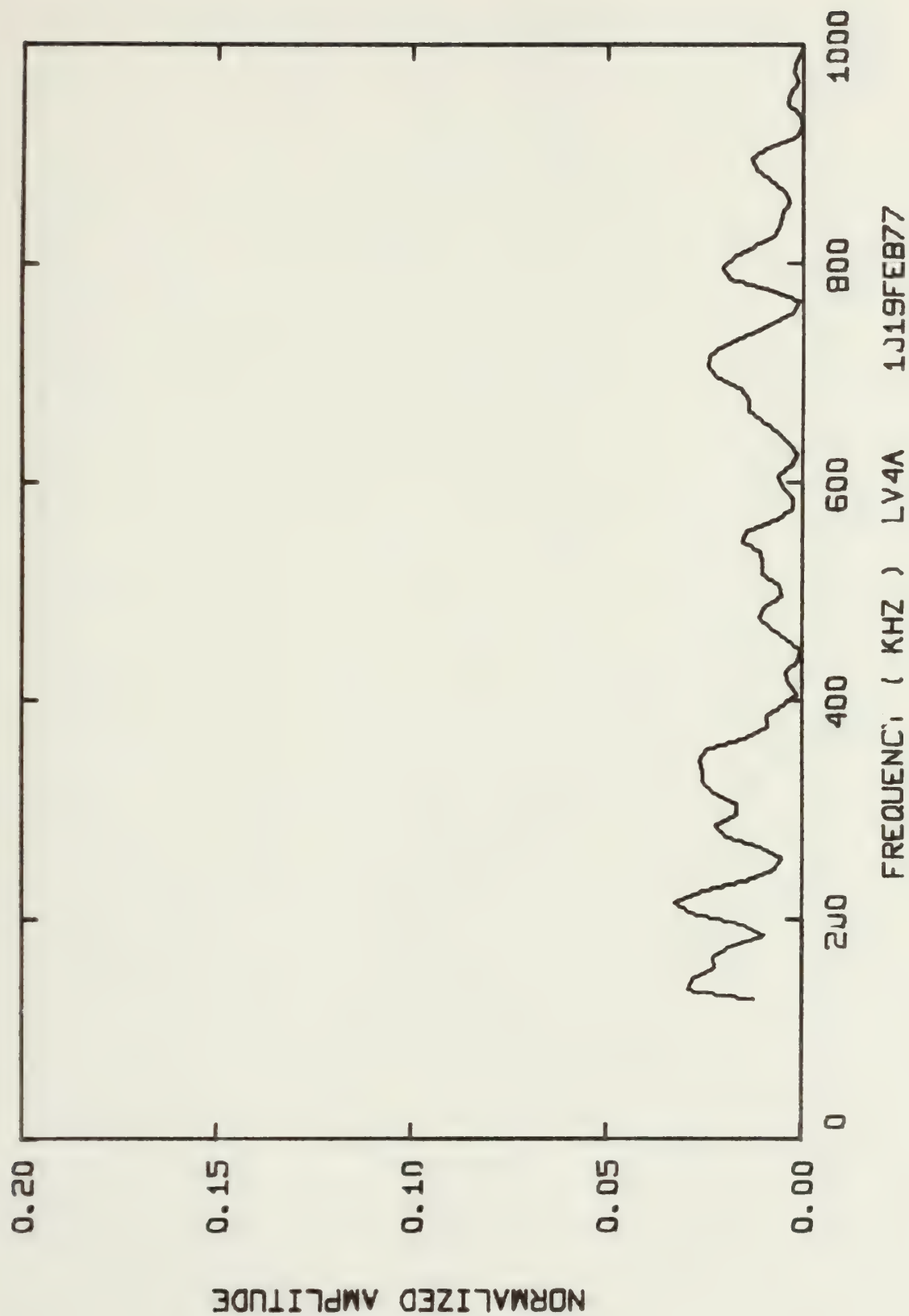






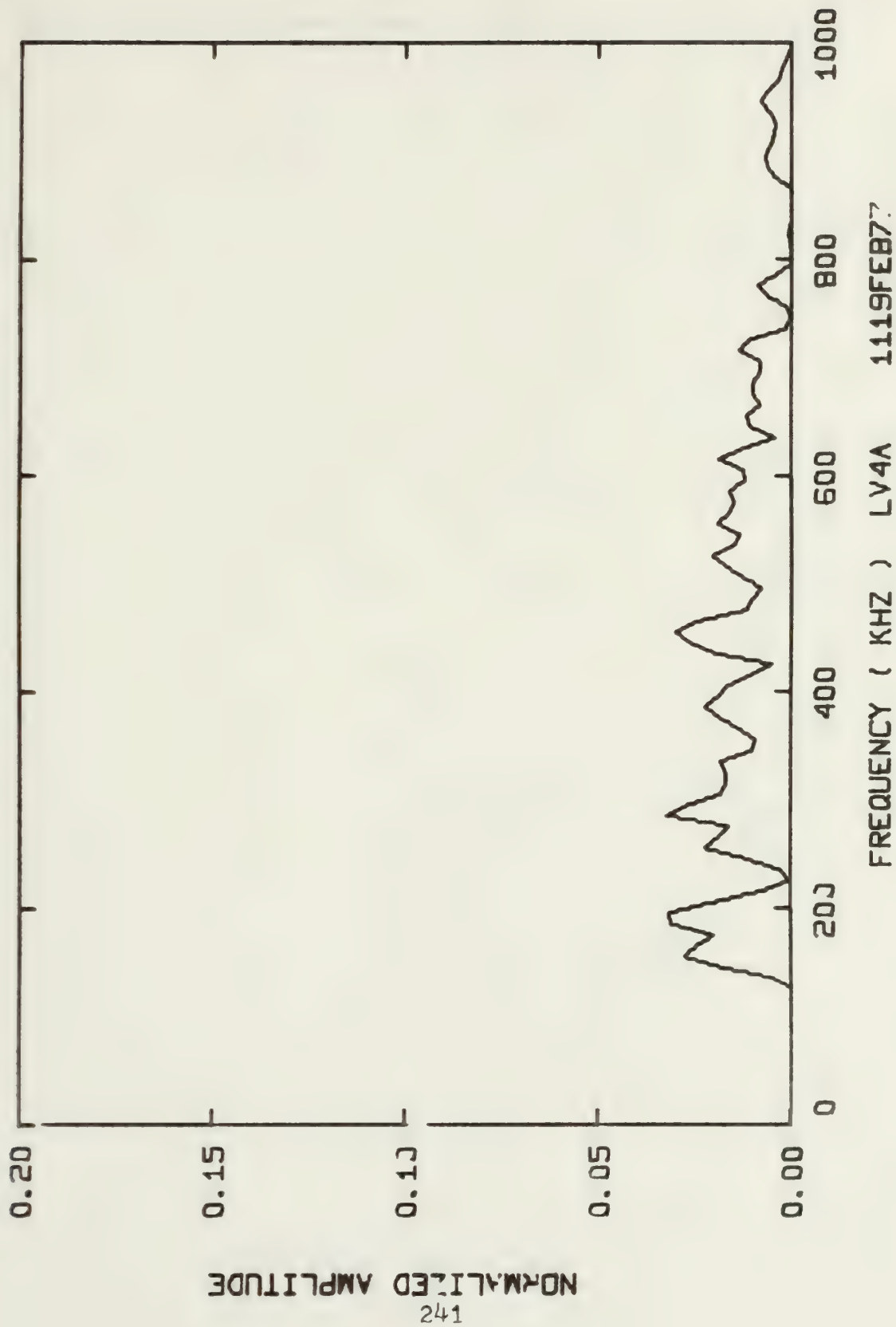




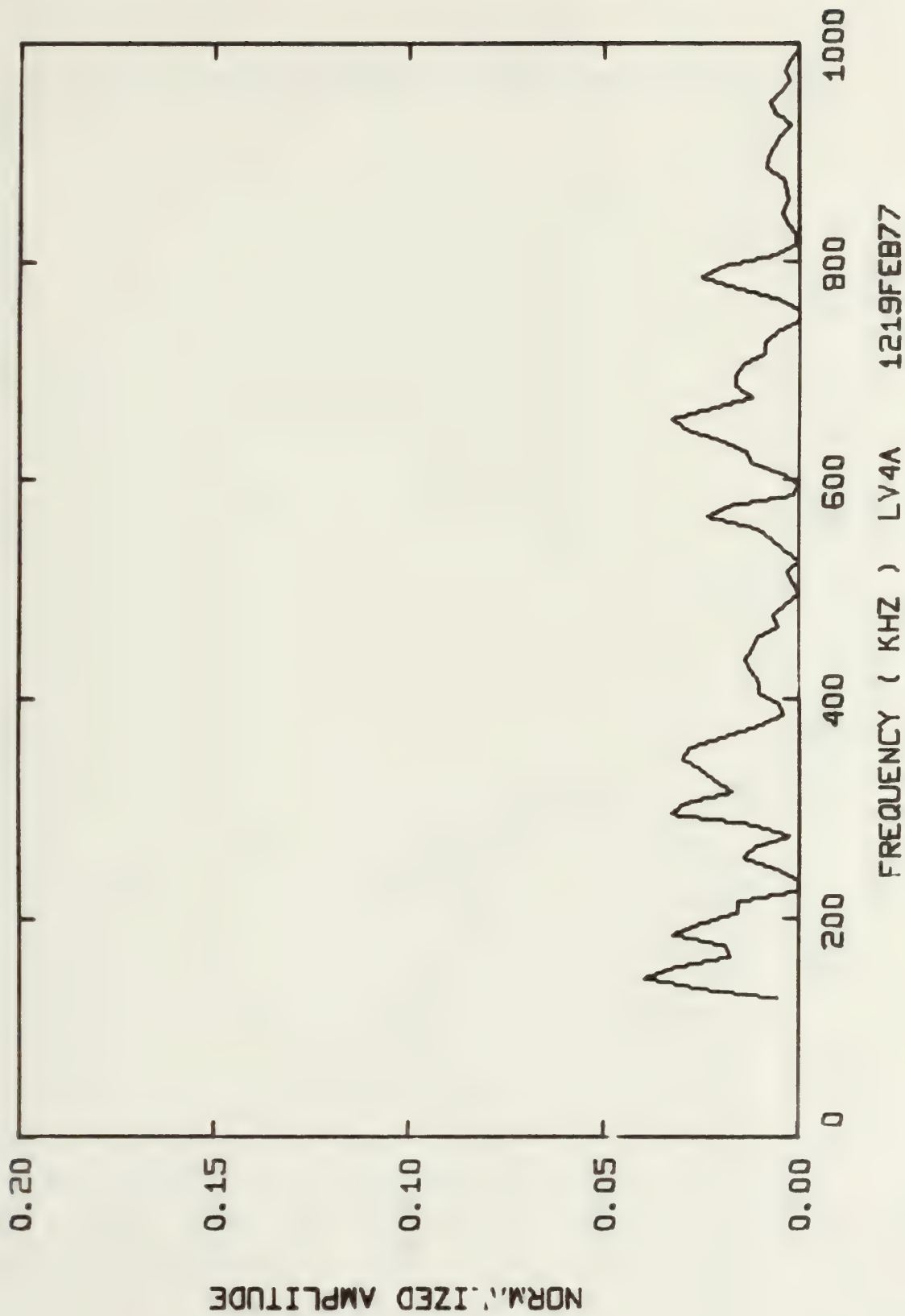




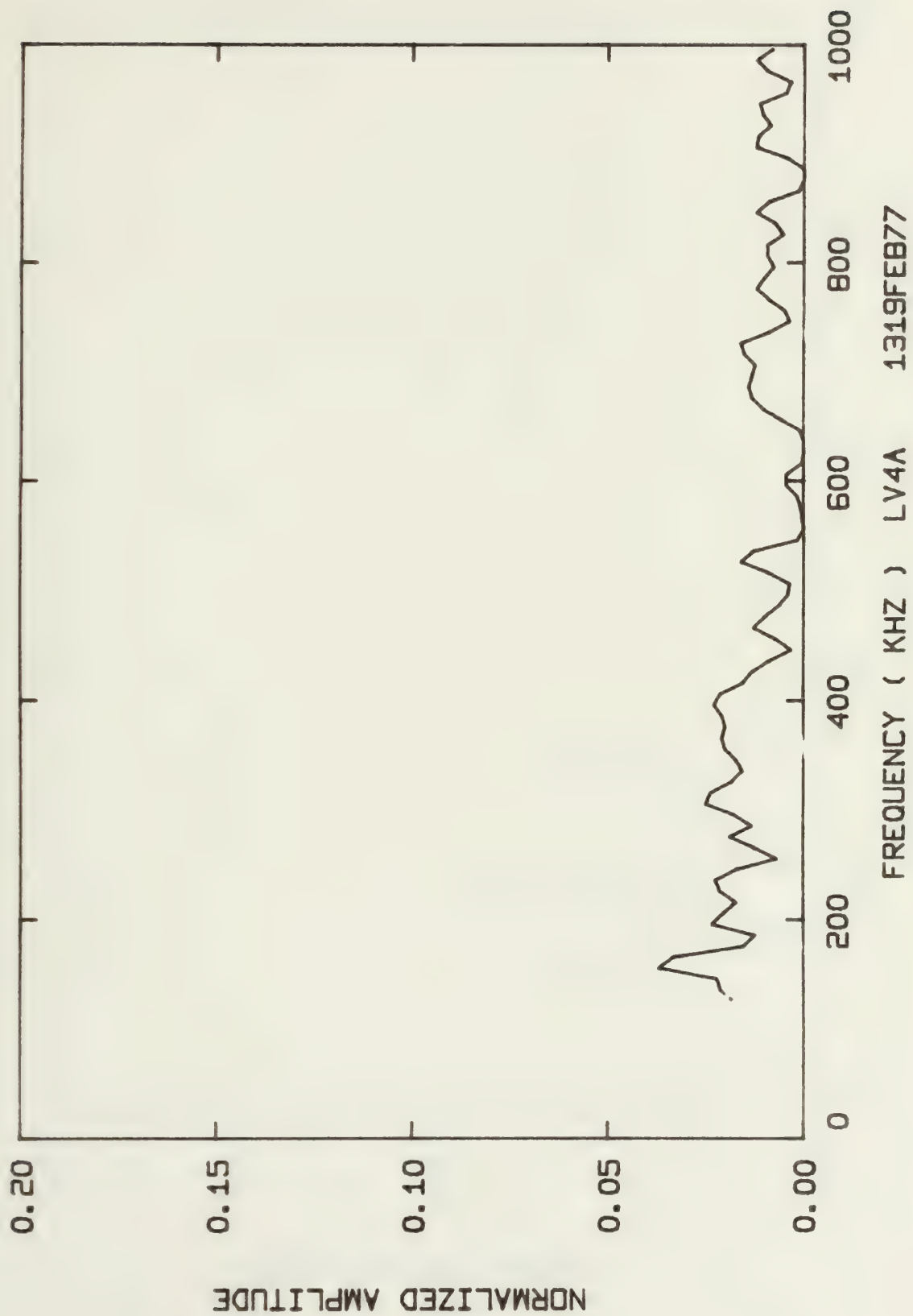




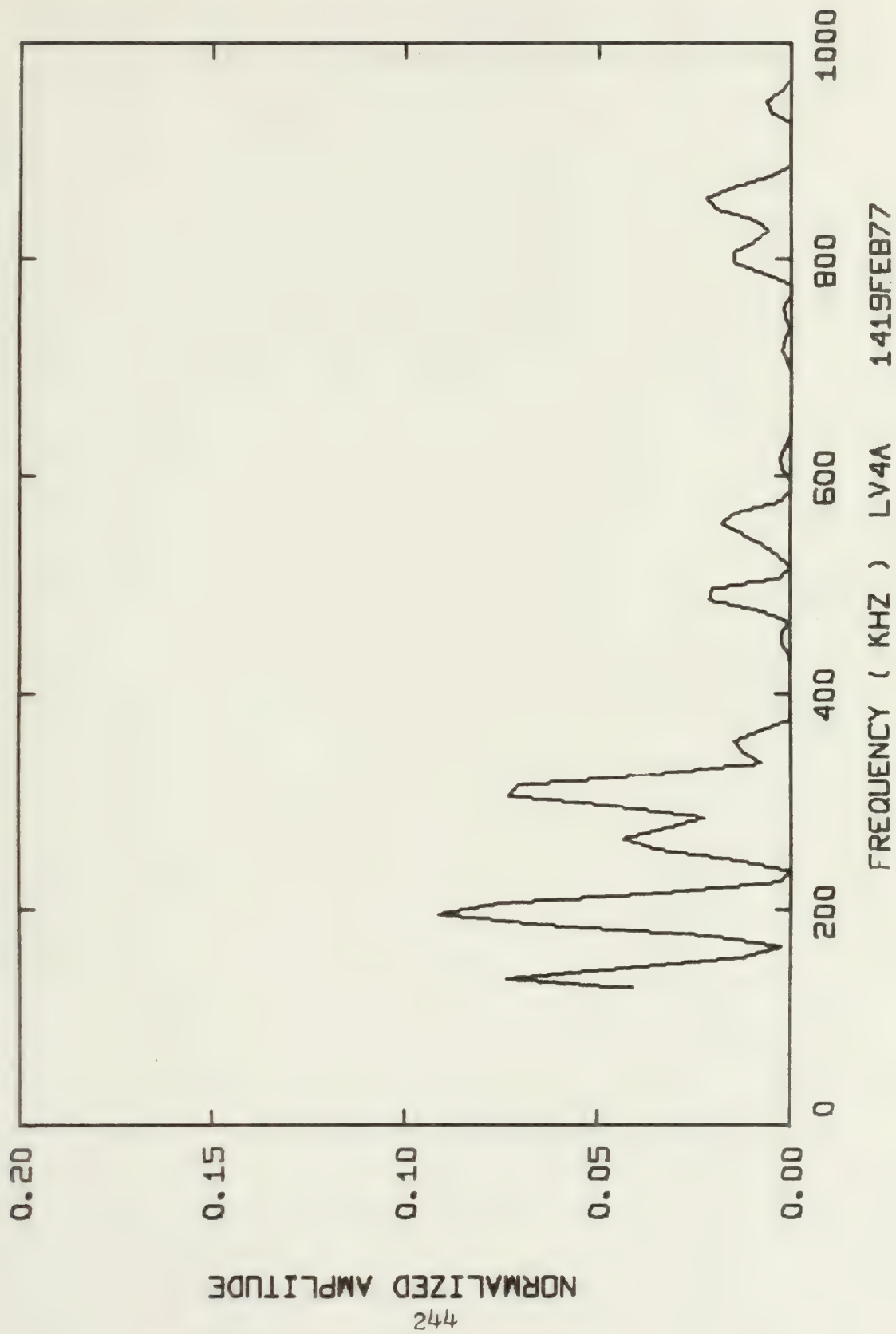






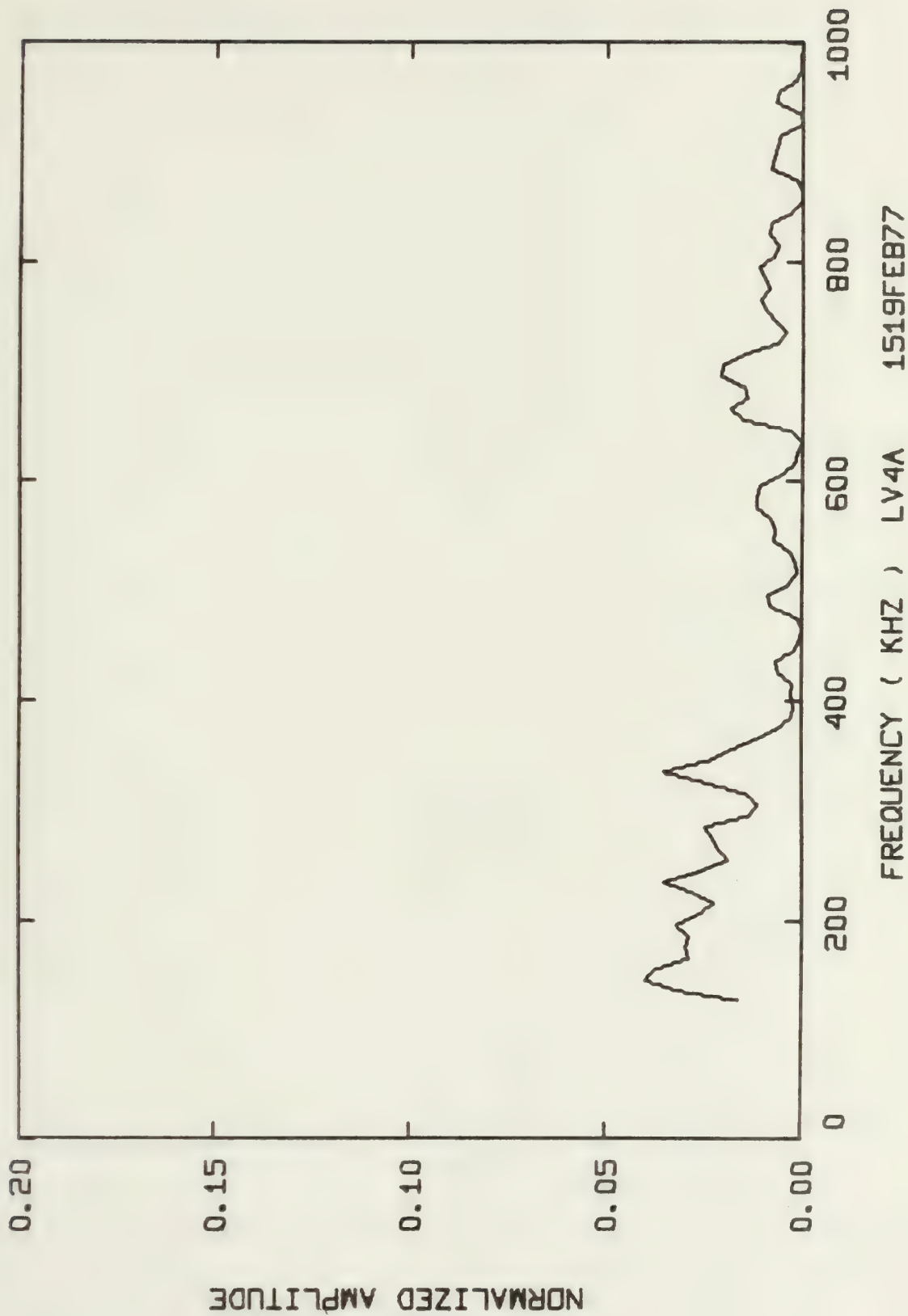




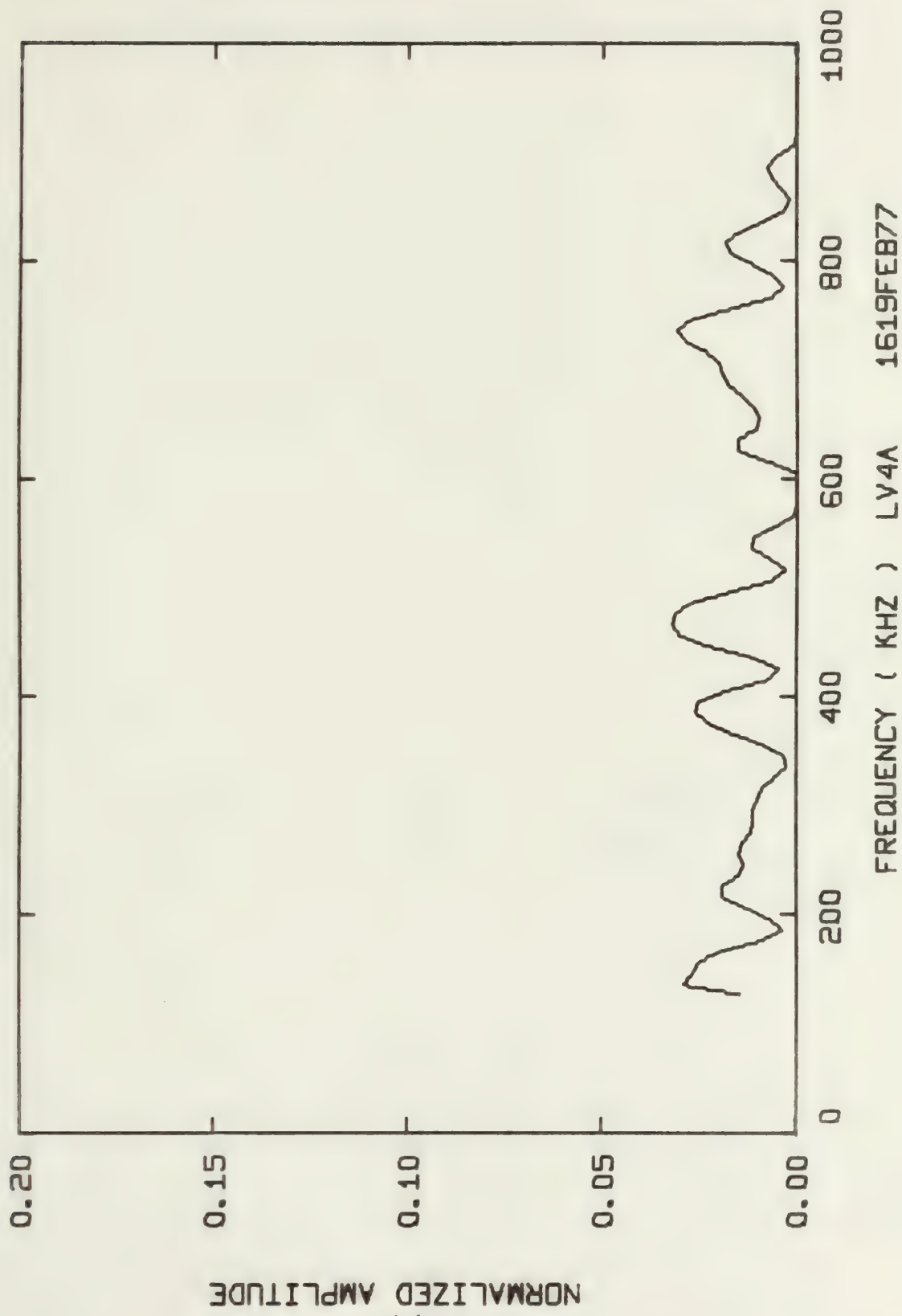




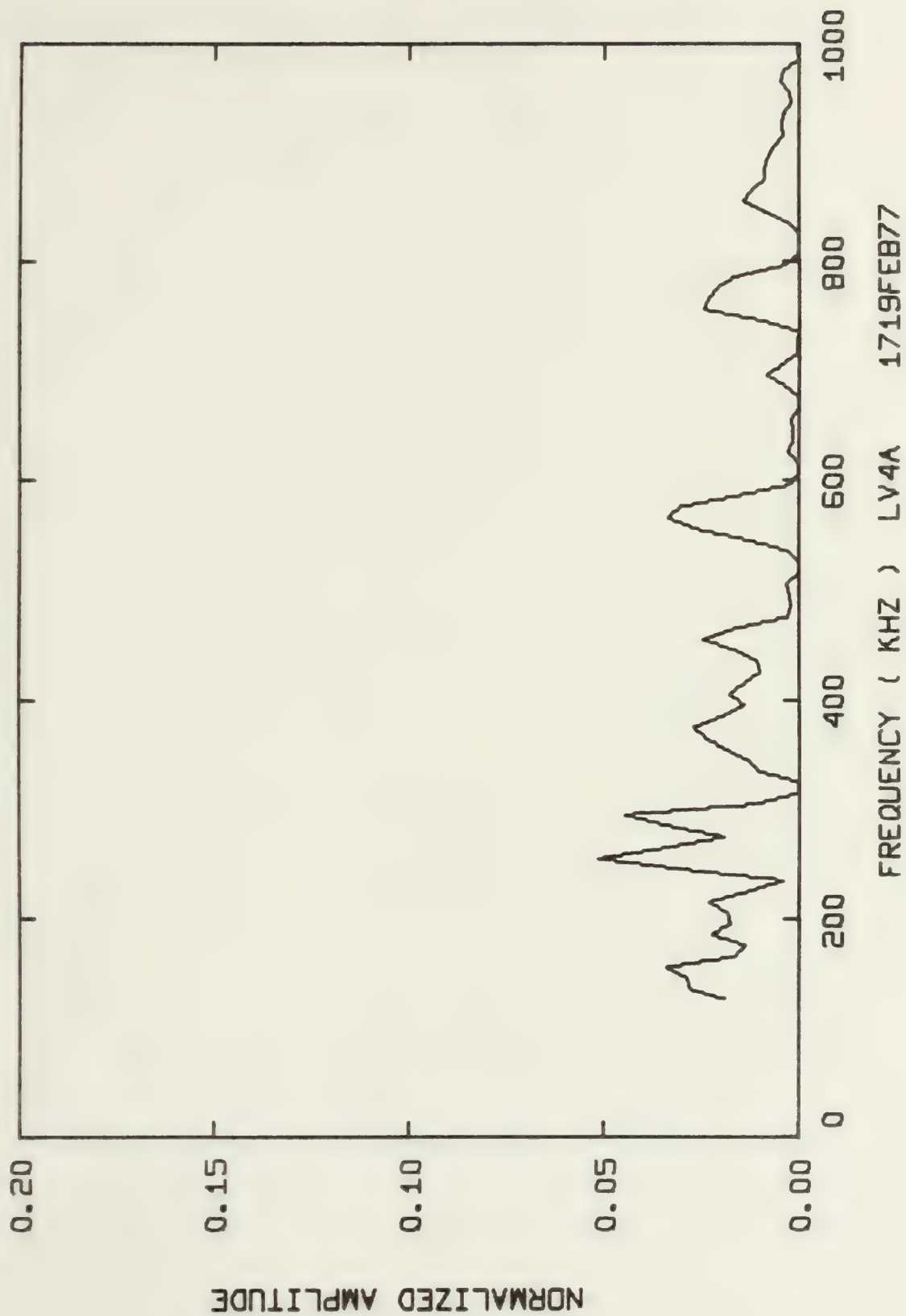




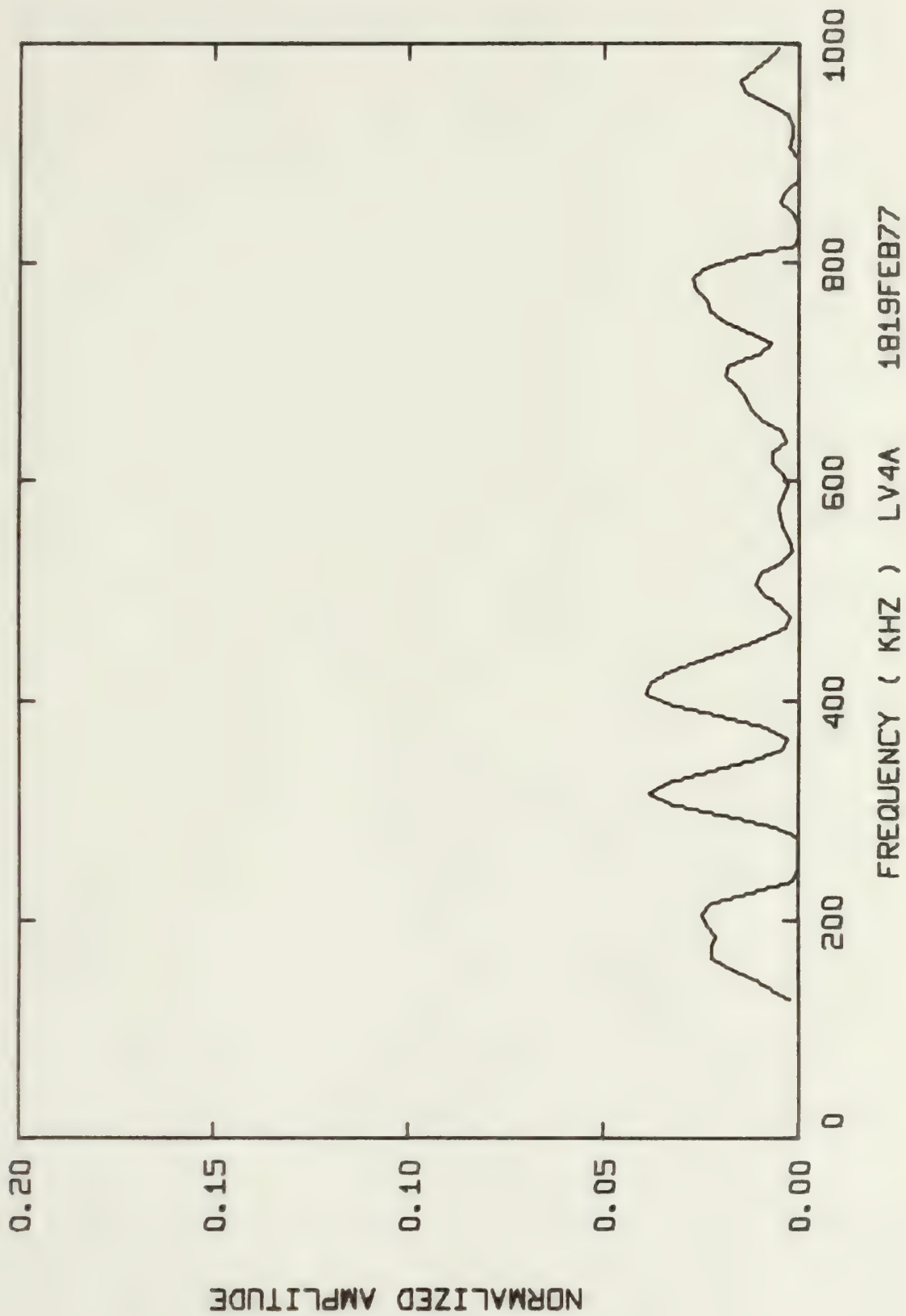






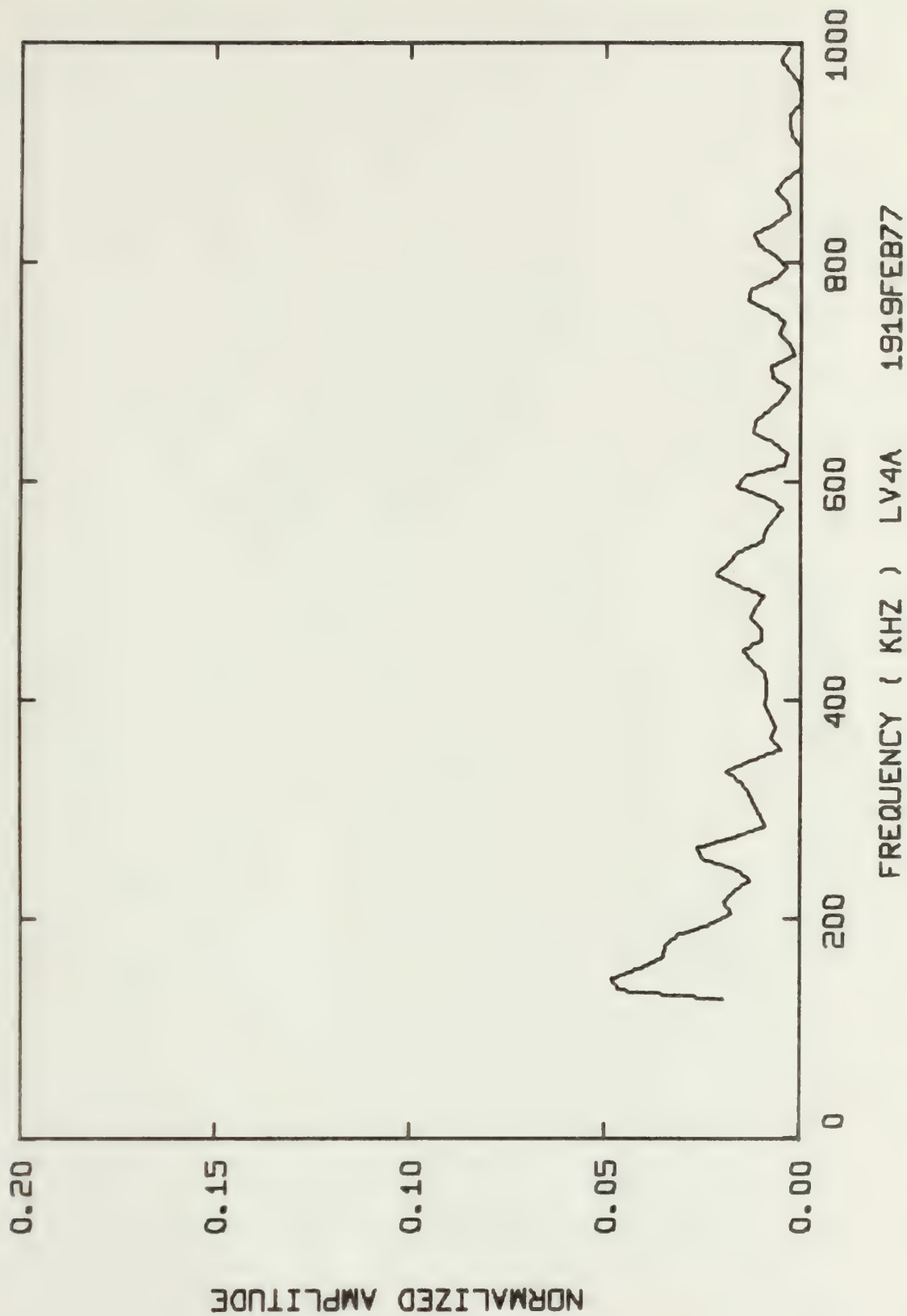




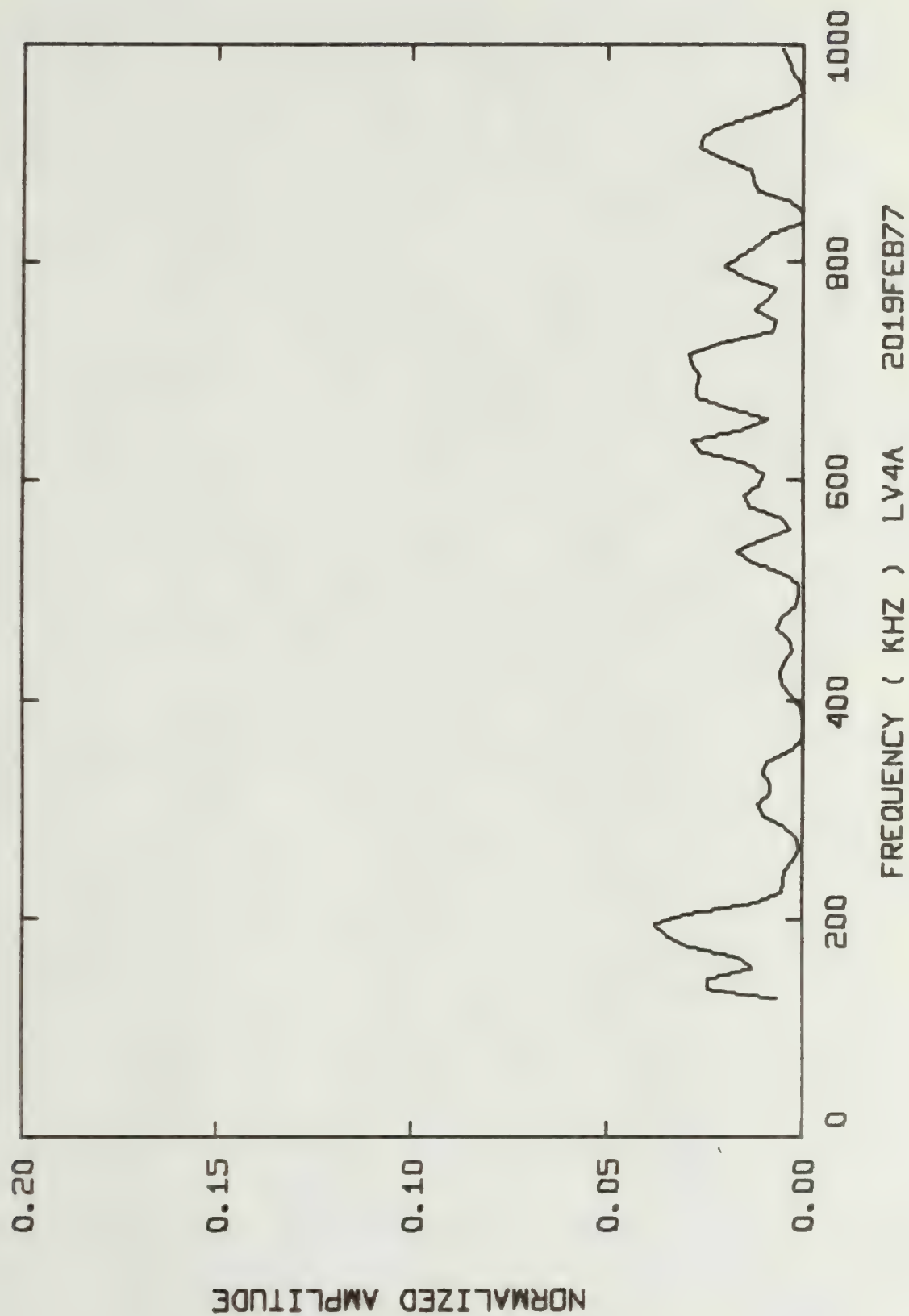














Thesis  
E263  
v.1

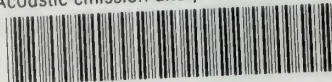
Egan

Acoustic emission  
analysis of fiber  
composite failure  
mechanisms.

171166

thesE263v.1

Acoustic emission analysis of fiber comp

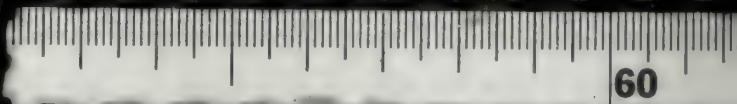


3 2768 001 90359 4

DUDLEY KNOX LIBRARY







**ACOUSTIC EMISSION ANALYSIS OF  
FIBER COMPOSITE FAILURE MECHANISMS**

**Dennis Michael Egan**

Volume 2



ACOUSTIC EMISSION ANALYSIS OF  
FIBER COMPOSITE FAILURE MECHANISMS

by

DENNIS MICHAEL EGAN, LT, USCG  
B.S., United States Coast Guard Academy (1972)

[v.v]

SUBMITTED IN PARTIAL FULFILLMENT  
OF THE REQUIREMENTS FOR THE  
DEGREES OF

MASTER OF SCIENCE IN MECHANICAL ENGINEERING

and

OCEAN ENGINEER

at the

MASSACHUSETTS INSTITUTE OF TECHNOLOGY

(May 1977)



Summary of Energy per Acoustic Emission and RMS Pressure  
Across the Transducer's Face for Each Spectra

Spectral Distrib. Graph Code Number	Energy per AE (Joules)	RMS Pressure Across Face of Transducer (Pa x 10 <sup>5</sup> )
LV4C 0105FEB77	30.114 x 10 <sup>-9</sup>	47.62
0205FEB77	136.38 x 10 <sup>-9</sup>	83.65
0117FEB77	60.006 x 10 <sup>-9</sup>	52.03
0217FEB77	1.2944 x 10 <sup>-6</sup>	131.87
0317FEB77	76.303 x 10 <sup>-9</sup>	71.72
0417FEB77	26.521 x 10 <sup>-9</sup>	55.64
0517FEB77	40.270 x 10 <sup>-9</sup>	67.92
0617FEB77	95.416 x 10 <sup>-9</sup>	71.35
0717FEB77	270.46 x 10 <sup>-9</sup>	84.46
0817FEB77	208.88 x 10 <sup>-9</sup>	82.72
0917FEB77	78.044 x 10 <sup>-9</sup>	72.40
1017FEB77	293.95 x 10 <sup>-9</sup>	88.11
1117FEB77	1.0465 x 10 <sup>-6</sup>	145.59
1217FEB77	116.92 x 10 <sup>-9</sup>	21.599
1317FEB77	211.88 x 10 <sup>-9</sup>	68.30
1417FEB77	180.45 x 10 <sup>-9</sup>	86.73
1517FEB77	2.0712 x 10 <sup>-6</sup>	162.99
0118FEB77	111.34 x 10 <sup>-9</sup>	59.57
0218FEB77	525.35 x 10 <sup>-9</sup>	121.00
0120FEB77	838.43 x 10 <sup>-9</sup>	128.85
0220FEB77	79.977 x 10 <sup>-9</sup>	79.72
0320FEB77	61.196 x 10 <sup>-9</sup>	56.90



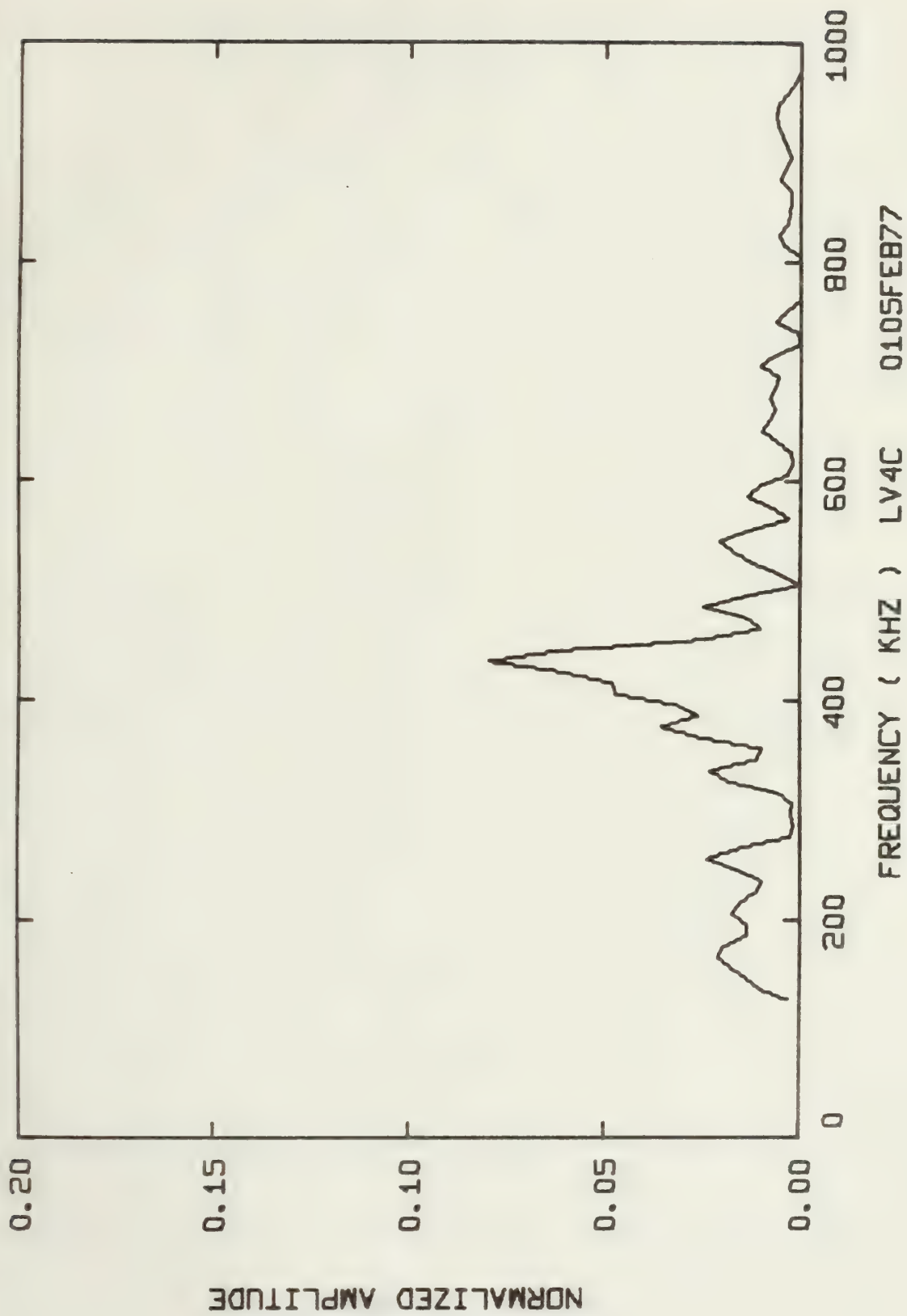


Summary of Energy per Acoustic Emission and RMS Pressure  
Across the Transducer's Face for Each Spectra

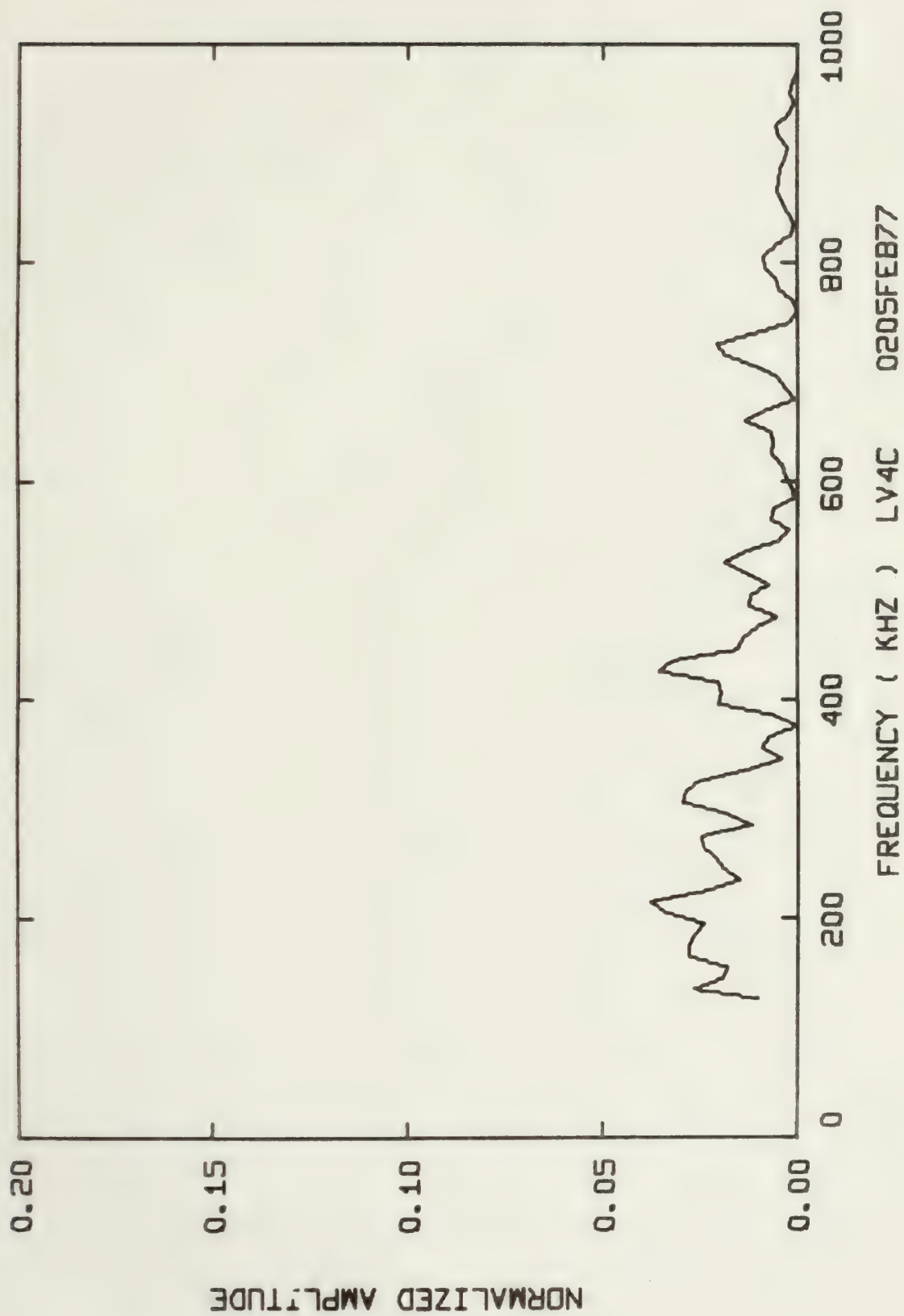
Spectral Distrib. Graph Code Number	Energy per AE (Joules)	RMS Pressure Across Face of Transducer (Pa x 10 <sup>5</sup> )
LV4C 0420FEB77	151.62 x 10 <sup>-9</sup>	86.78
0520FEB77	295.07 x 10 <sup>-9</sup>	90.82
0620FEB77	1.1095 x 10 <sup>-6</sup>	142.53
0720FEB77	73.870 x 10 <sup>-9</sup>	75.19
0216FEB77	136.38 x 10 <sup>-9</sup>	83.64



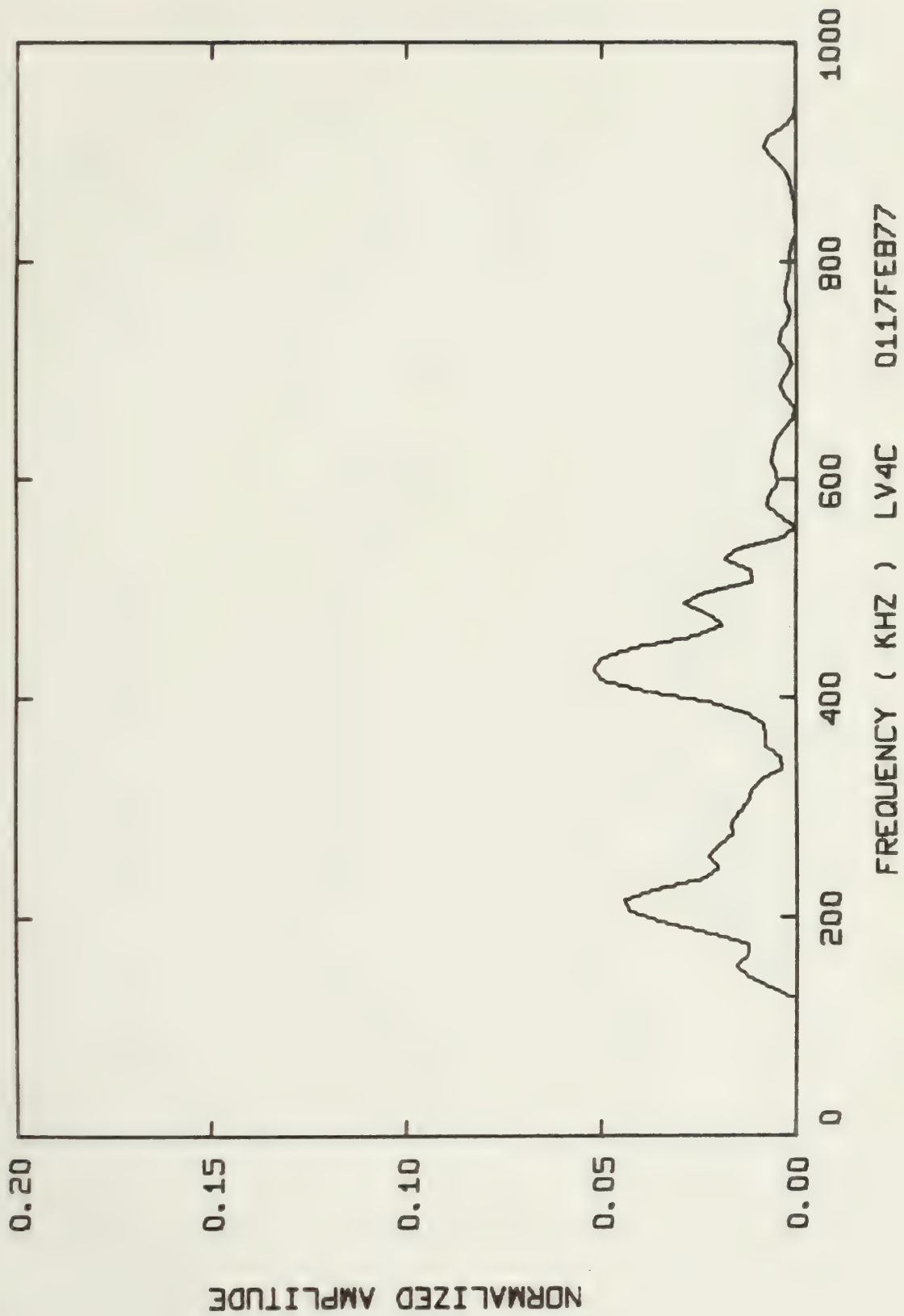




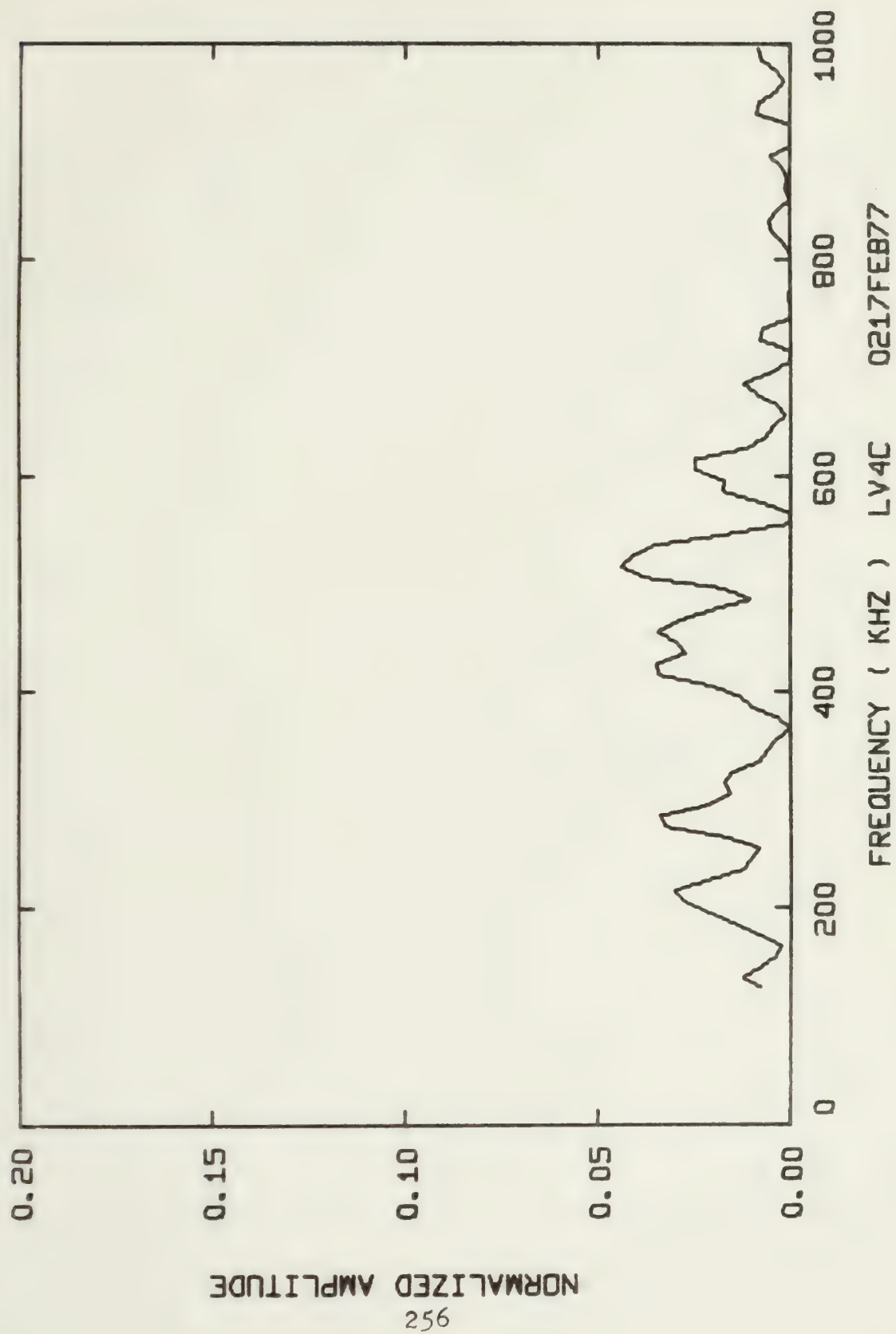






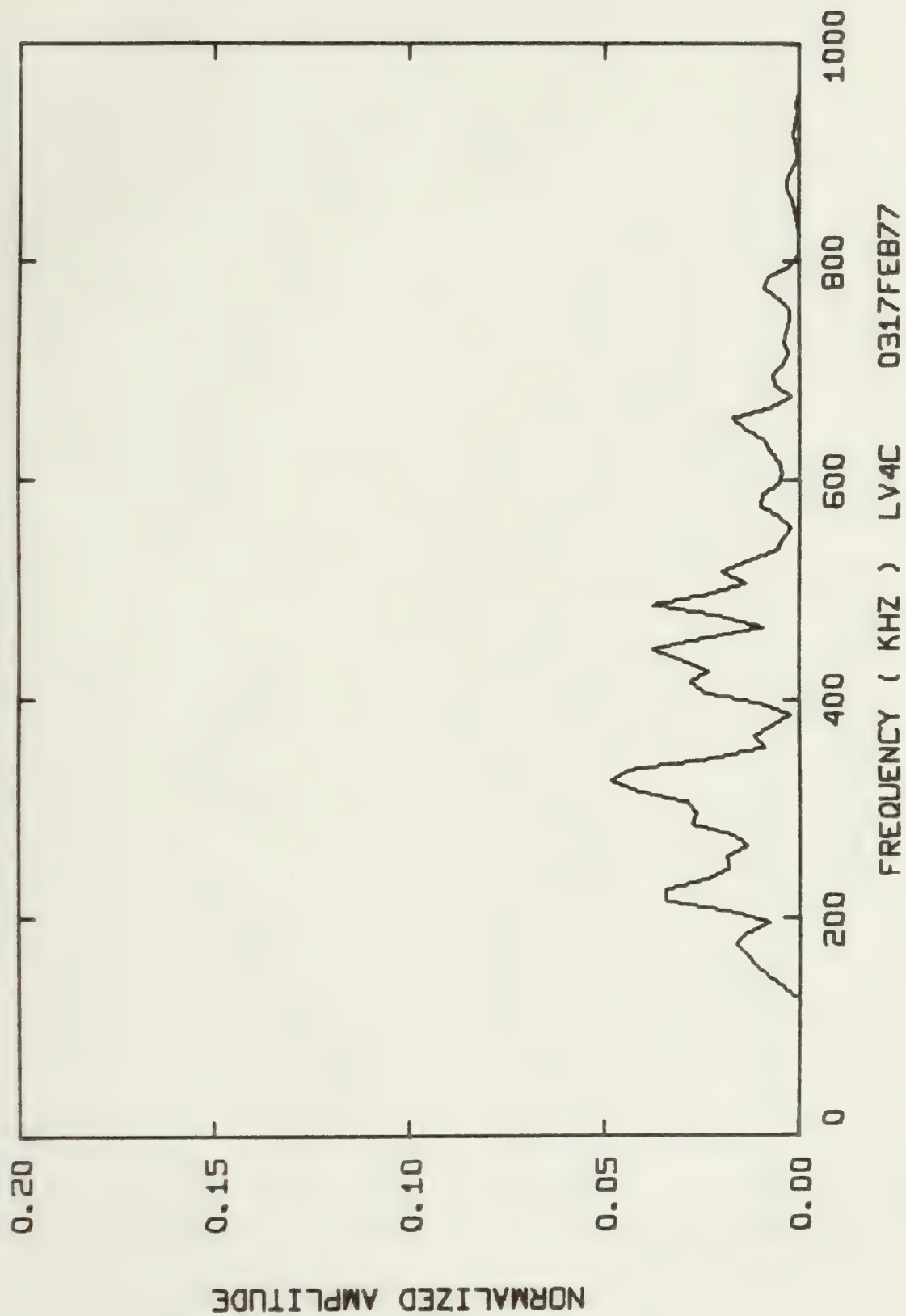




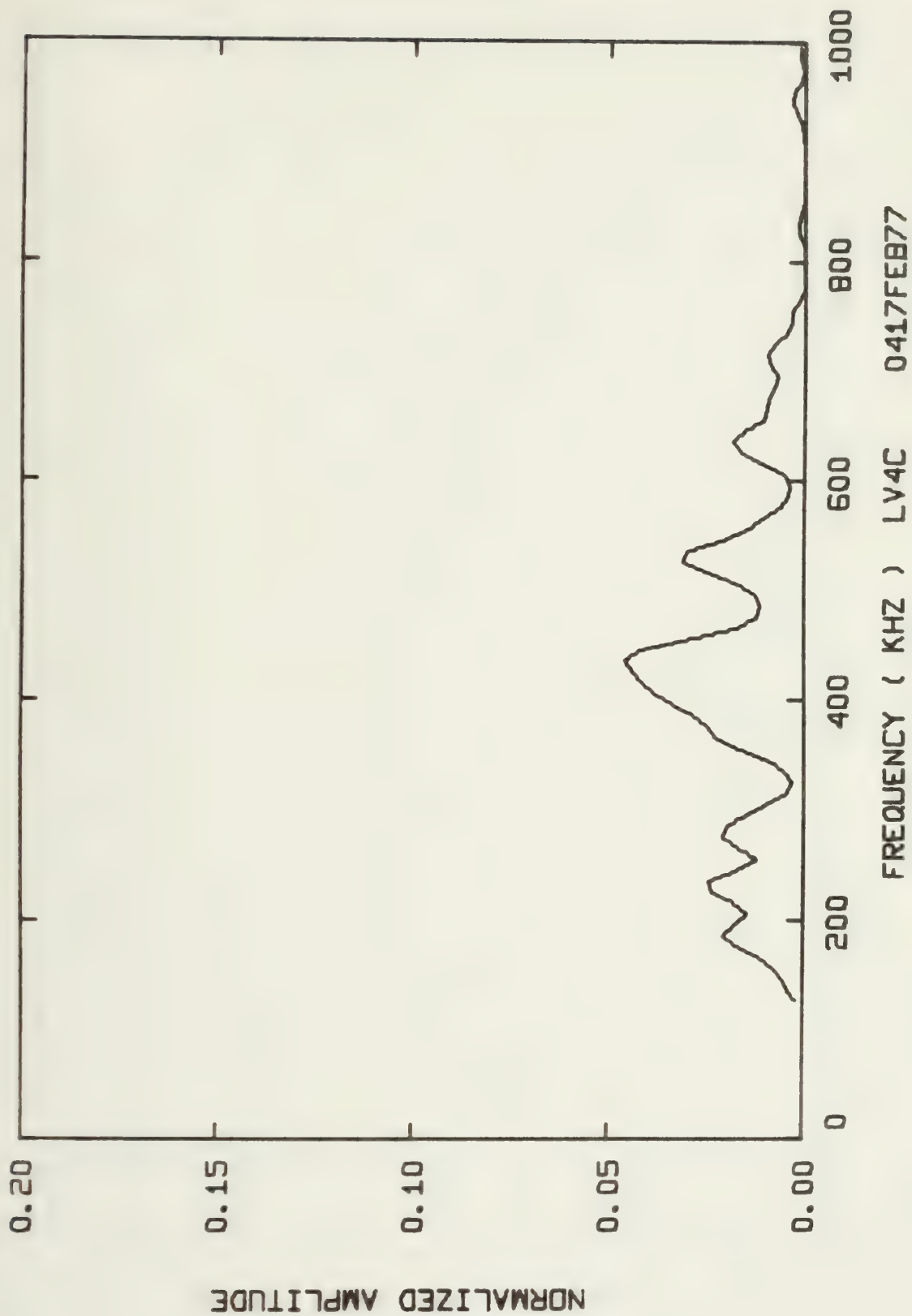




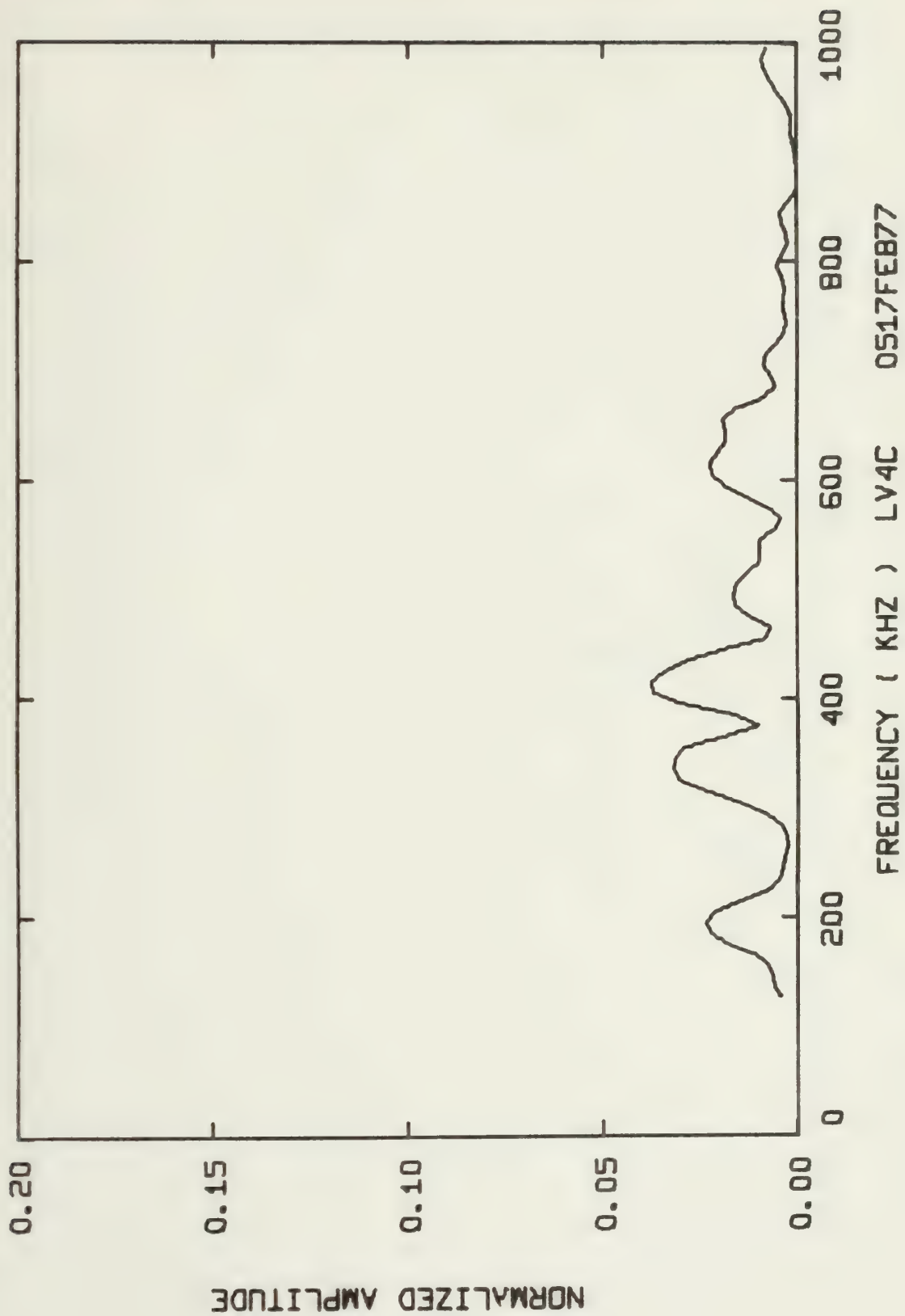




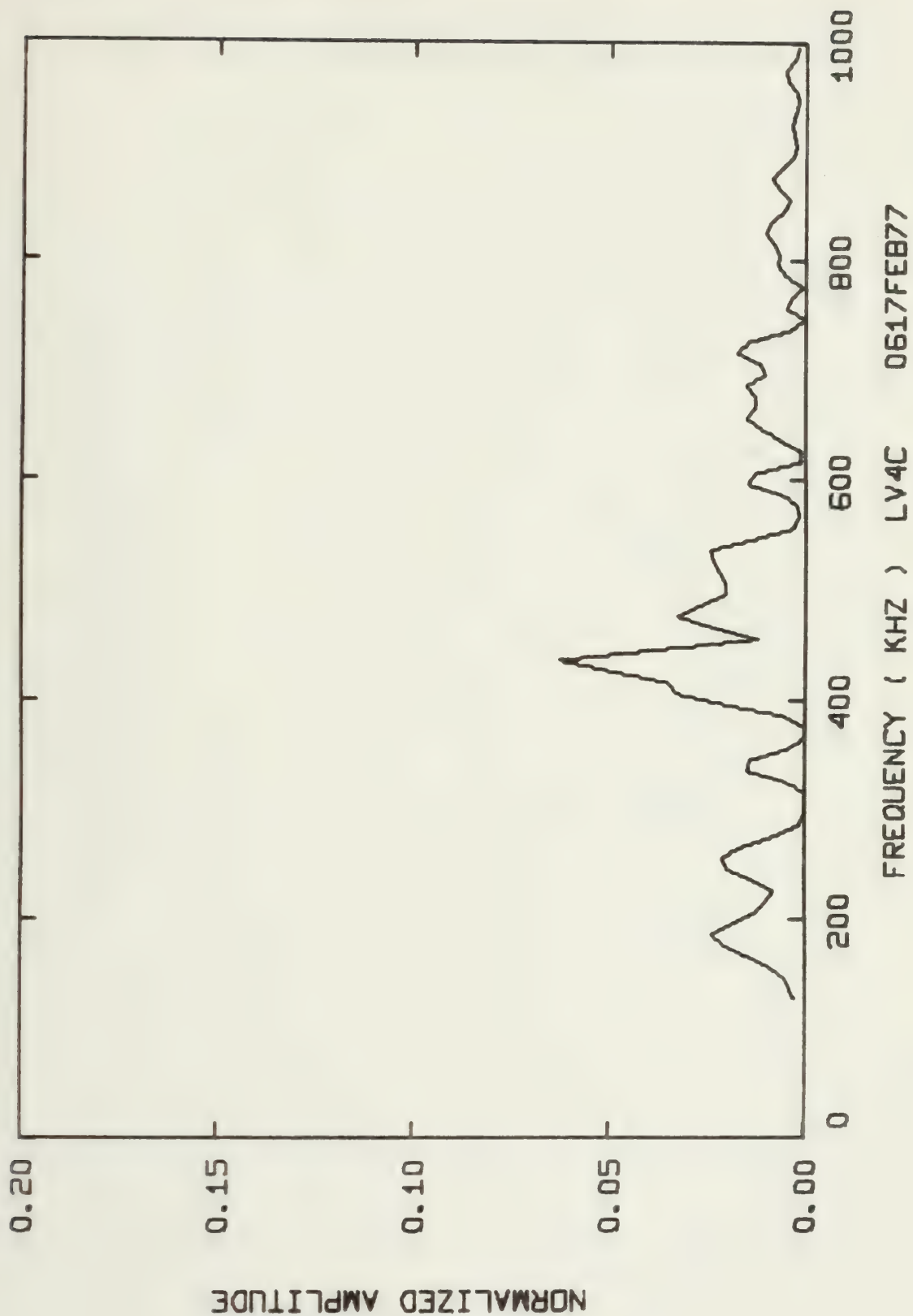






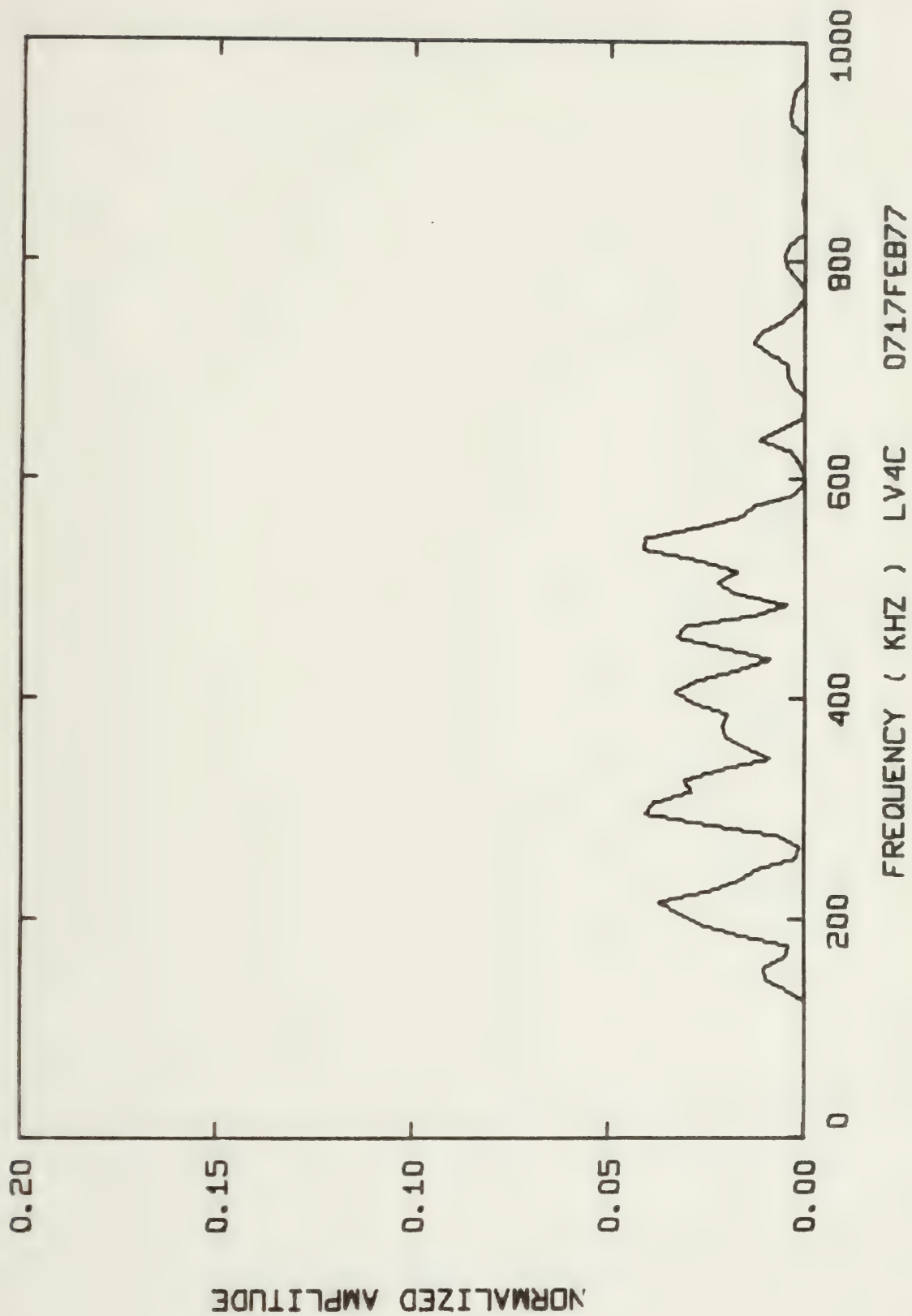




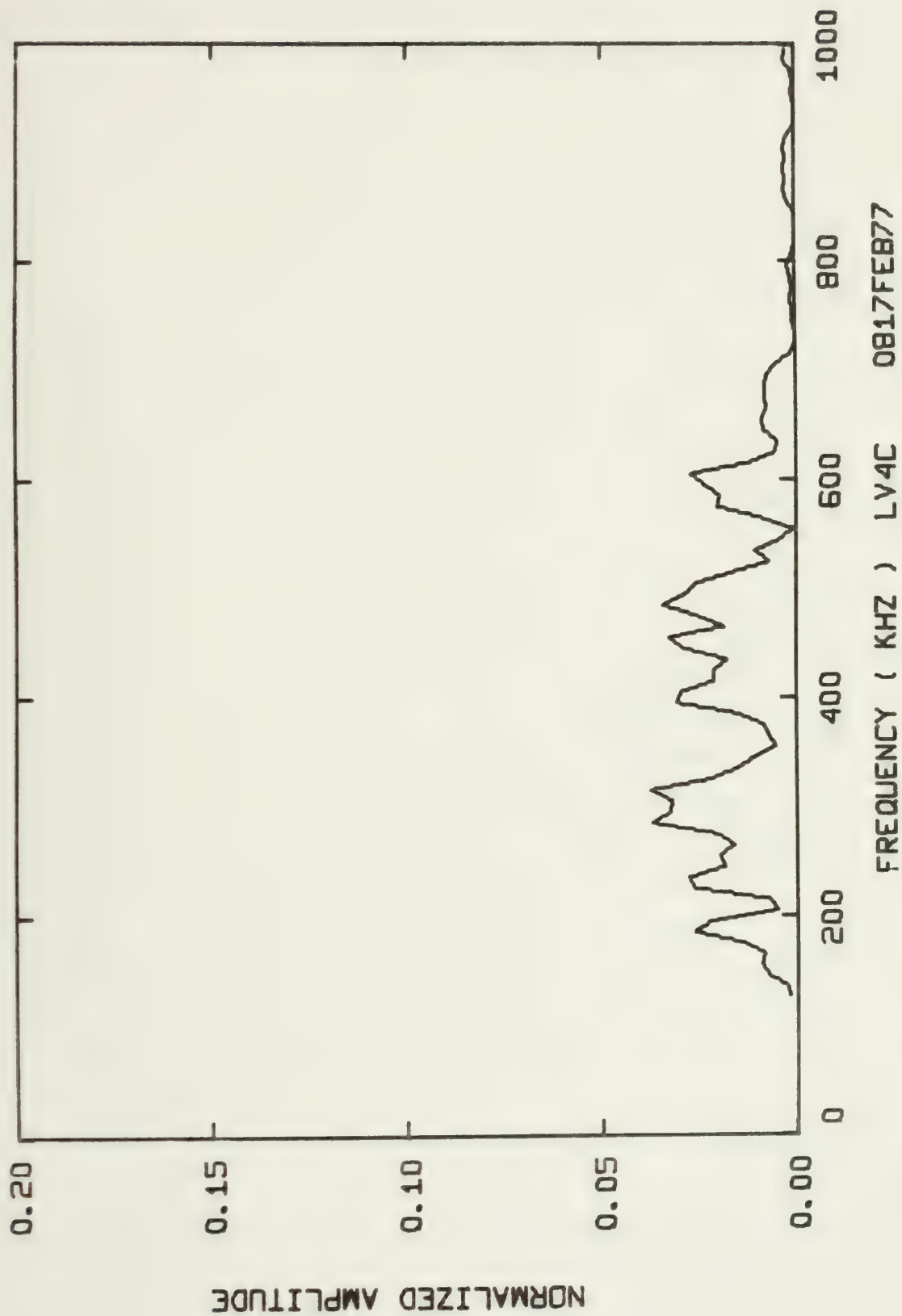




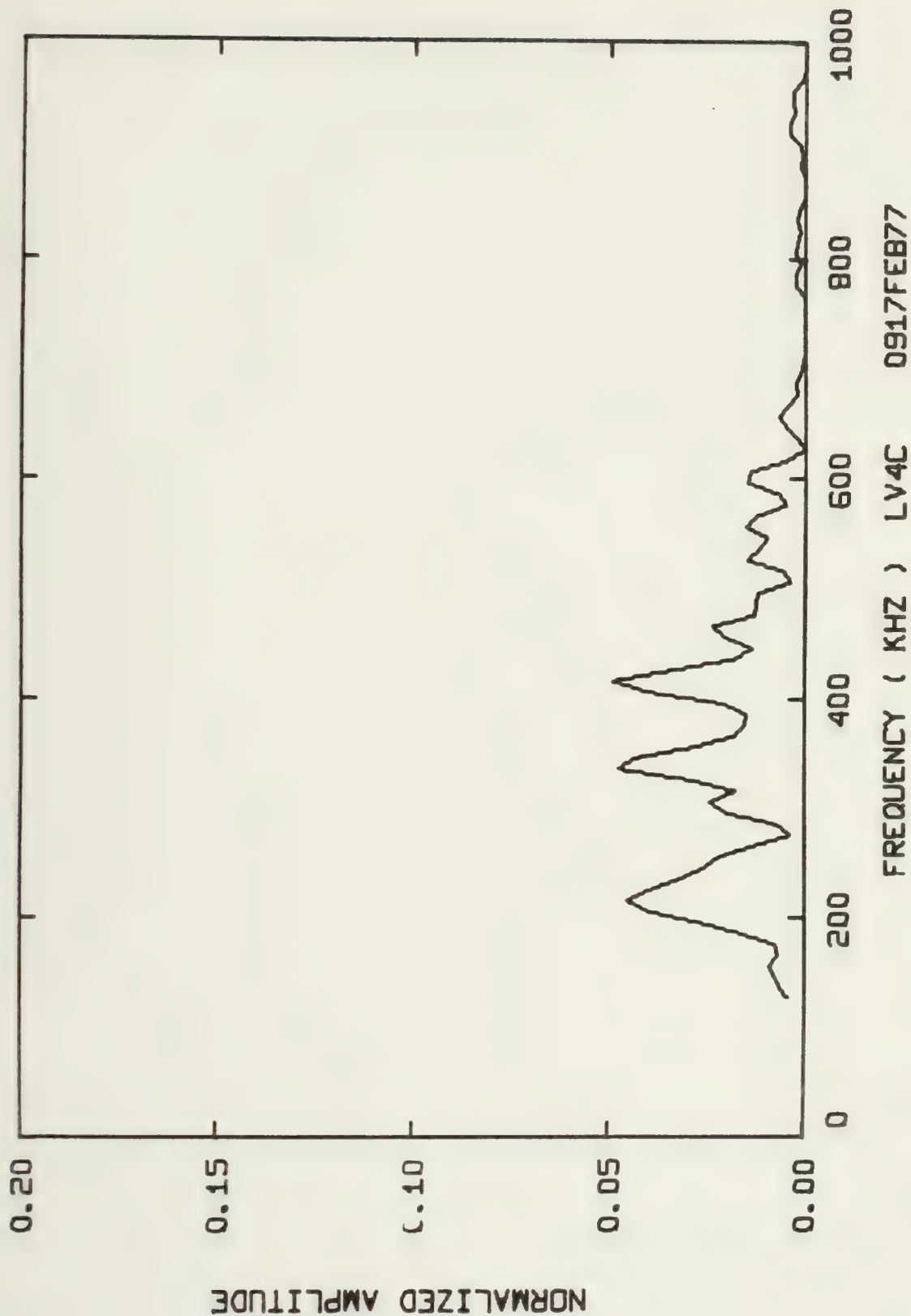




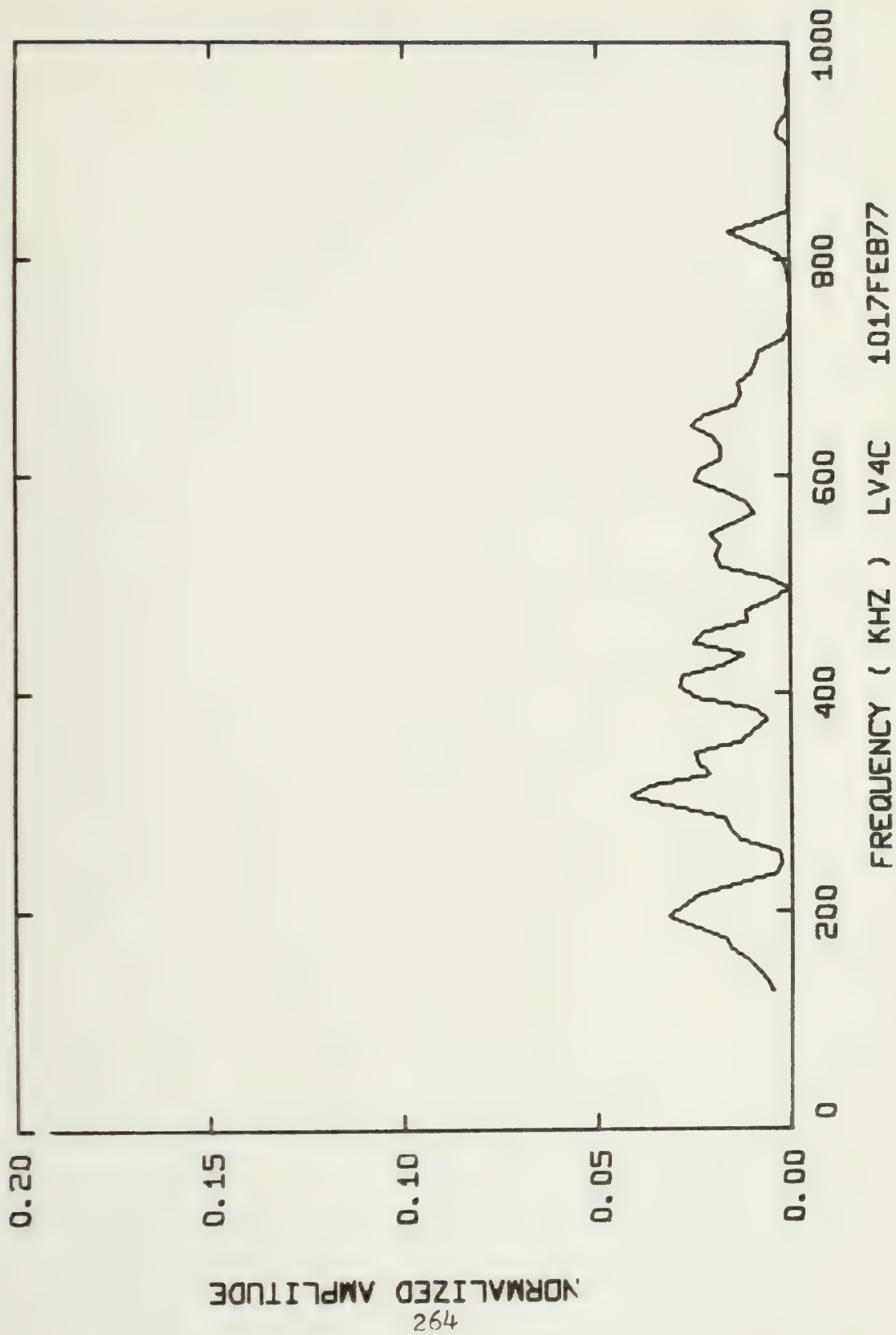






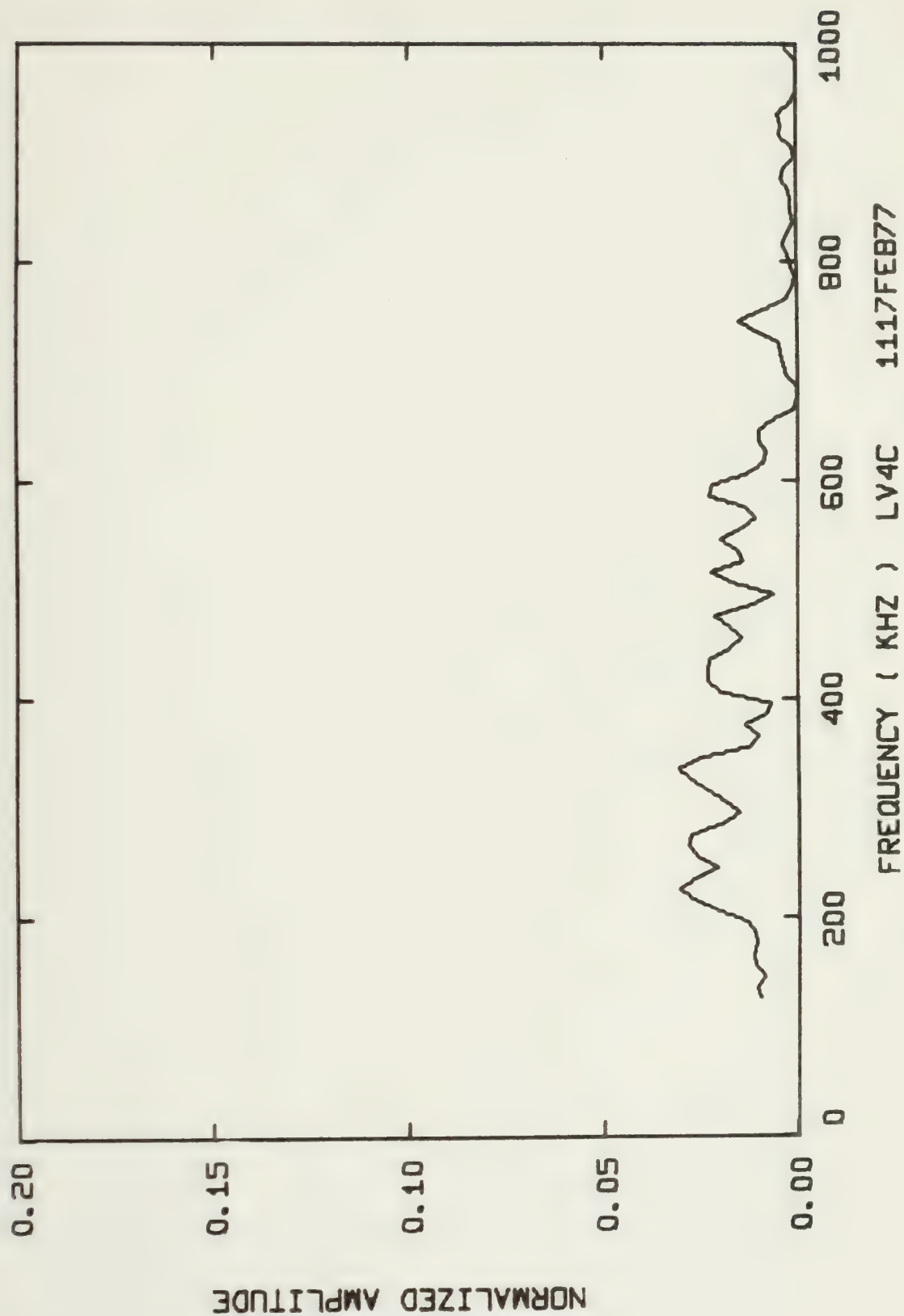




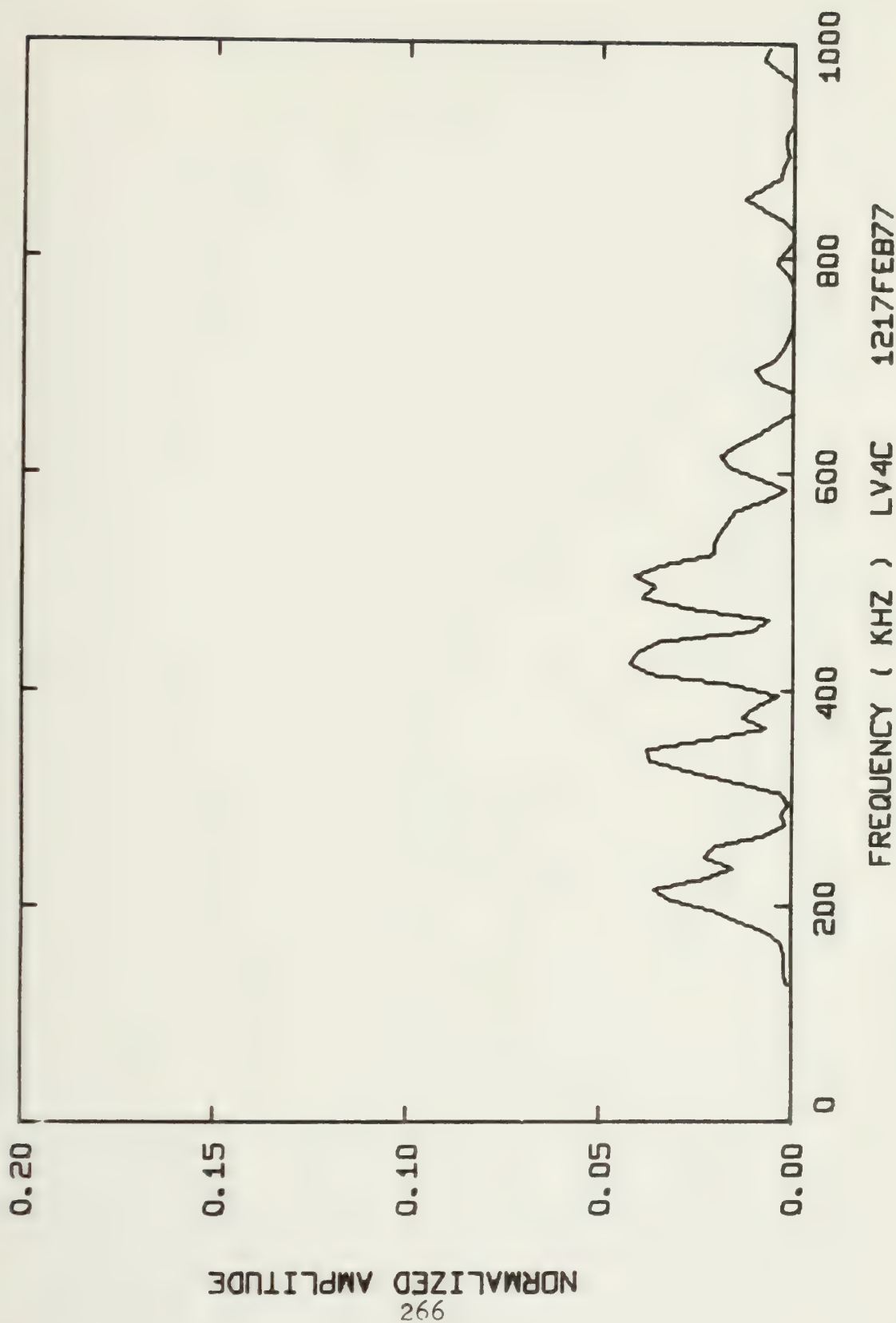




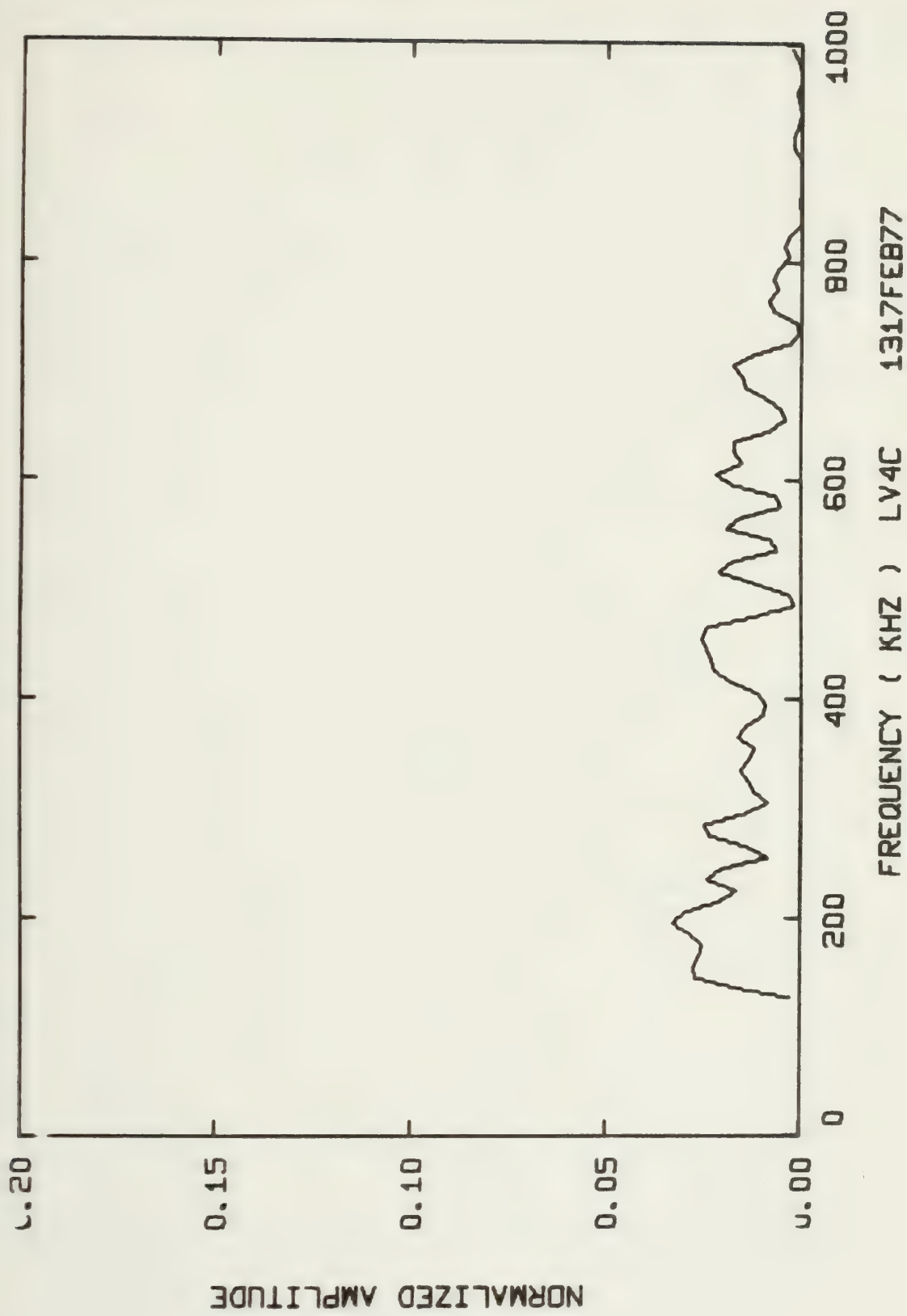




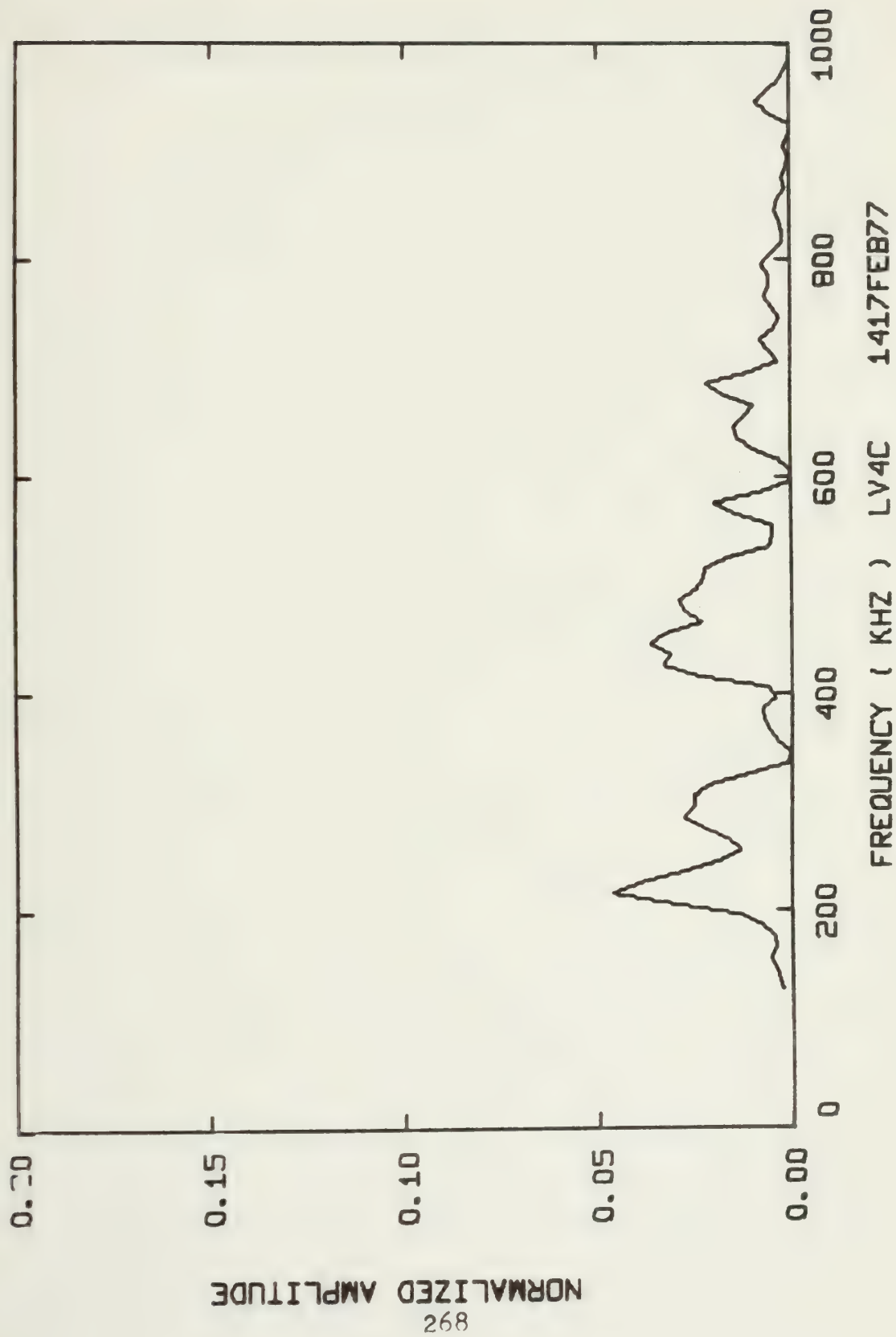






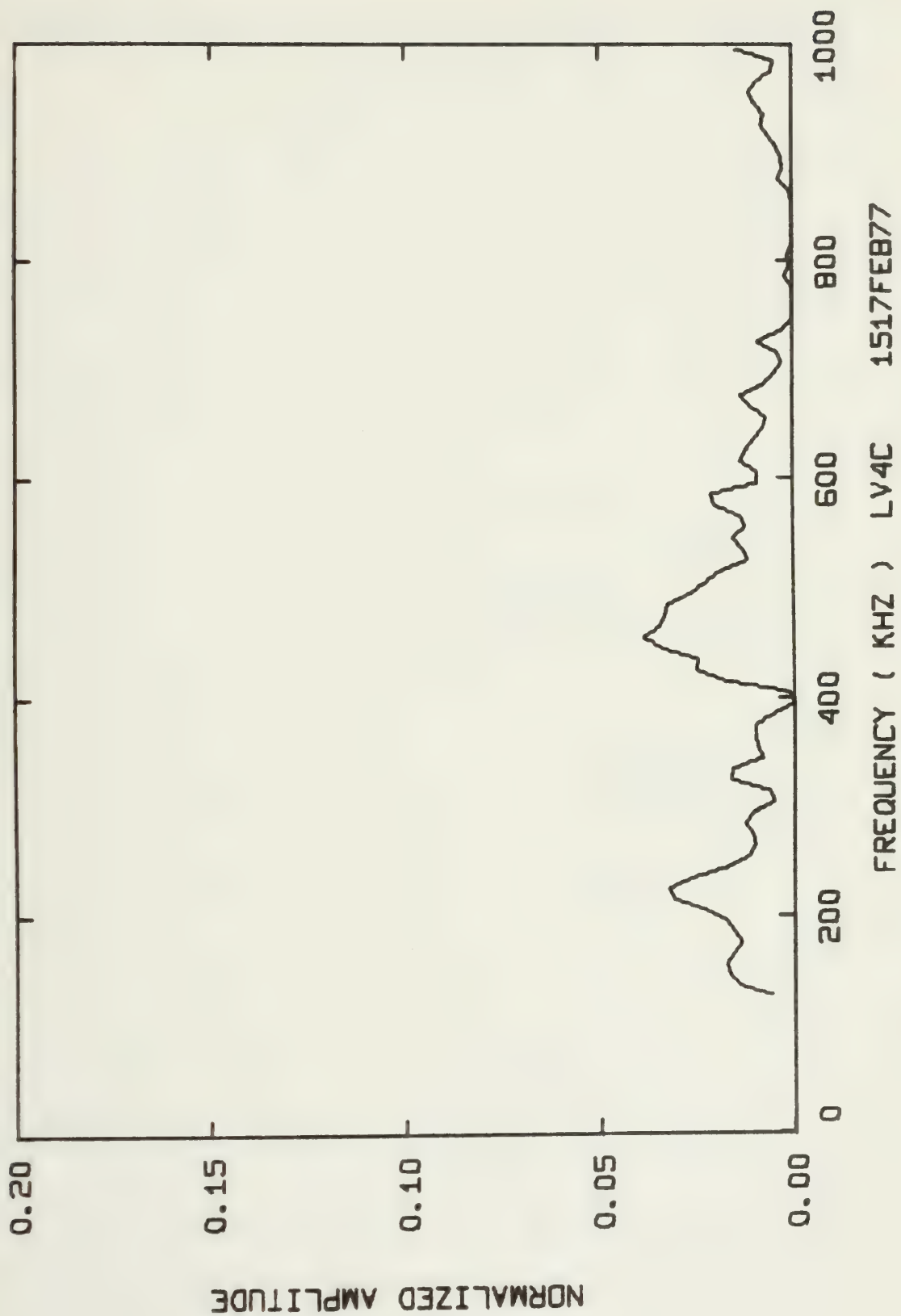




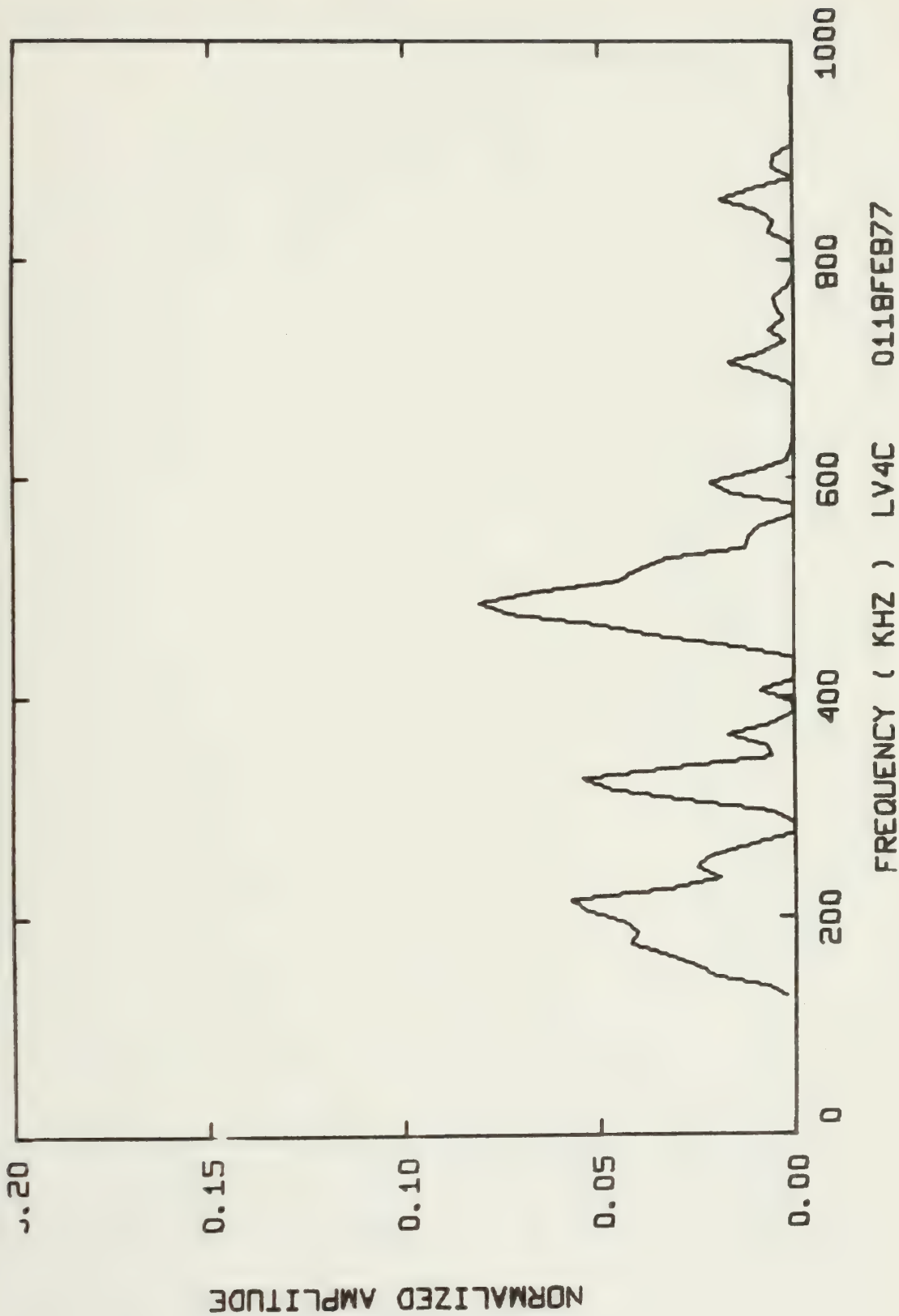




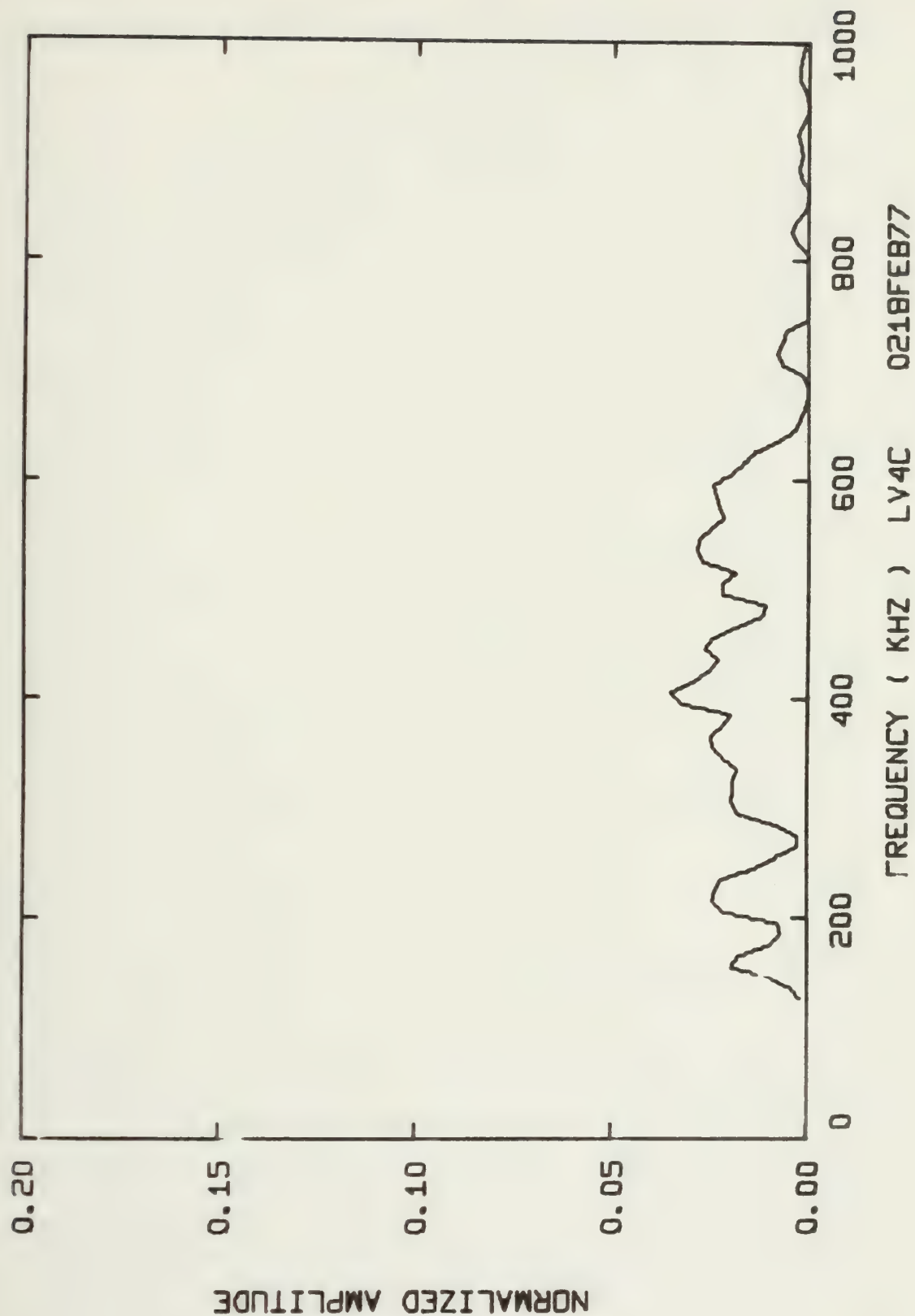




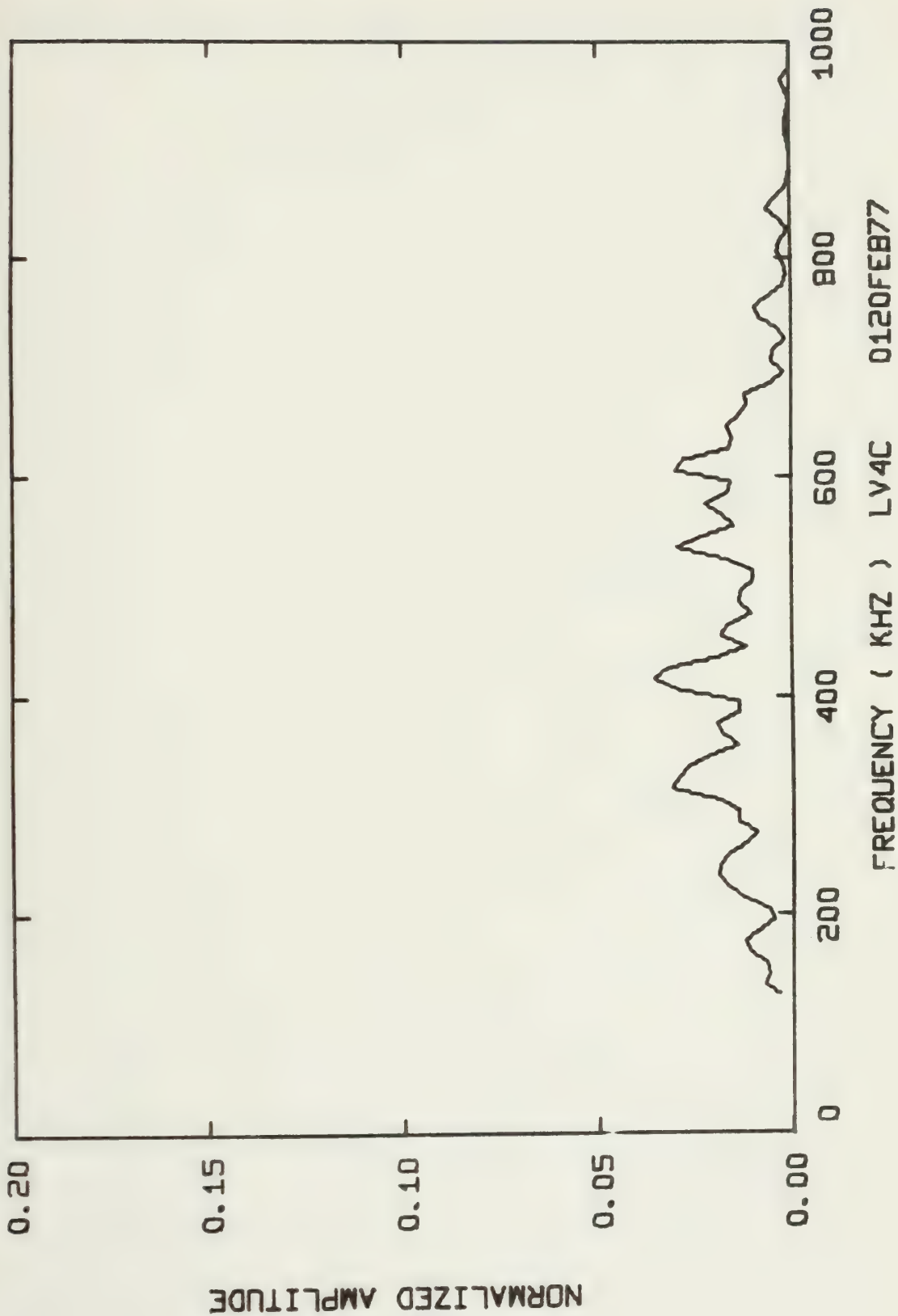






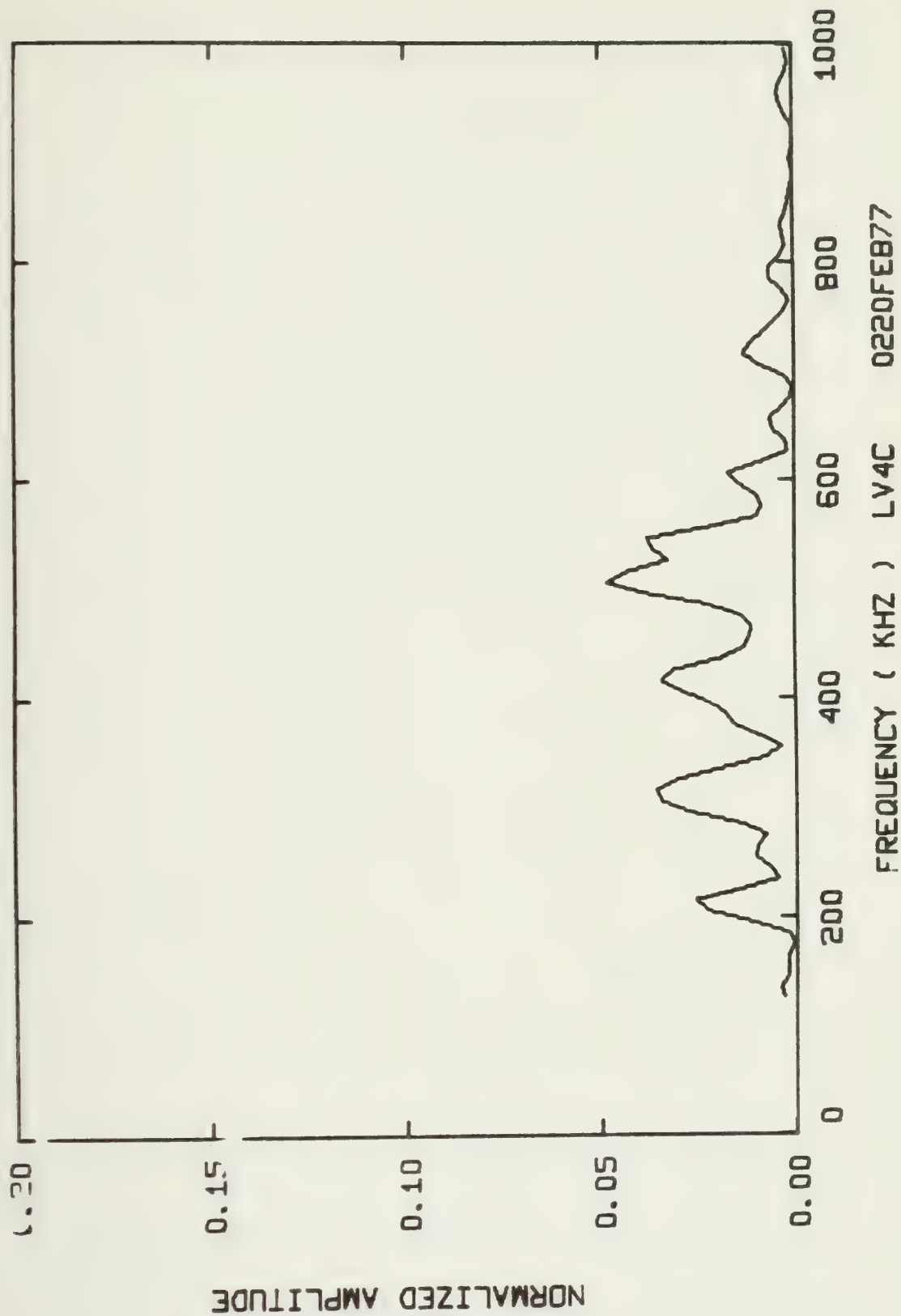




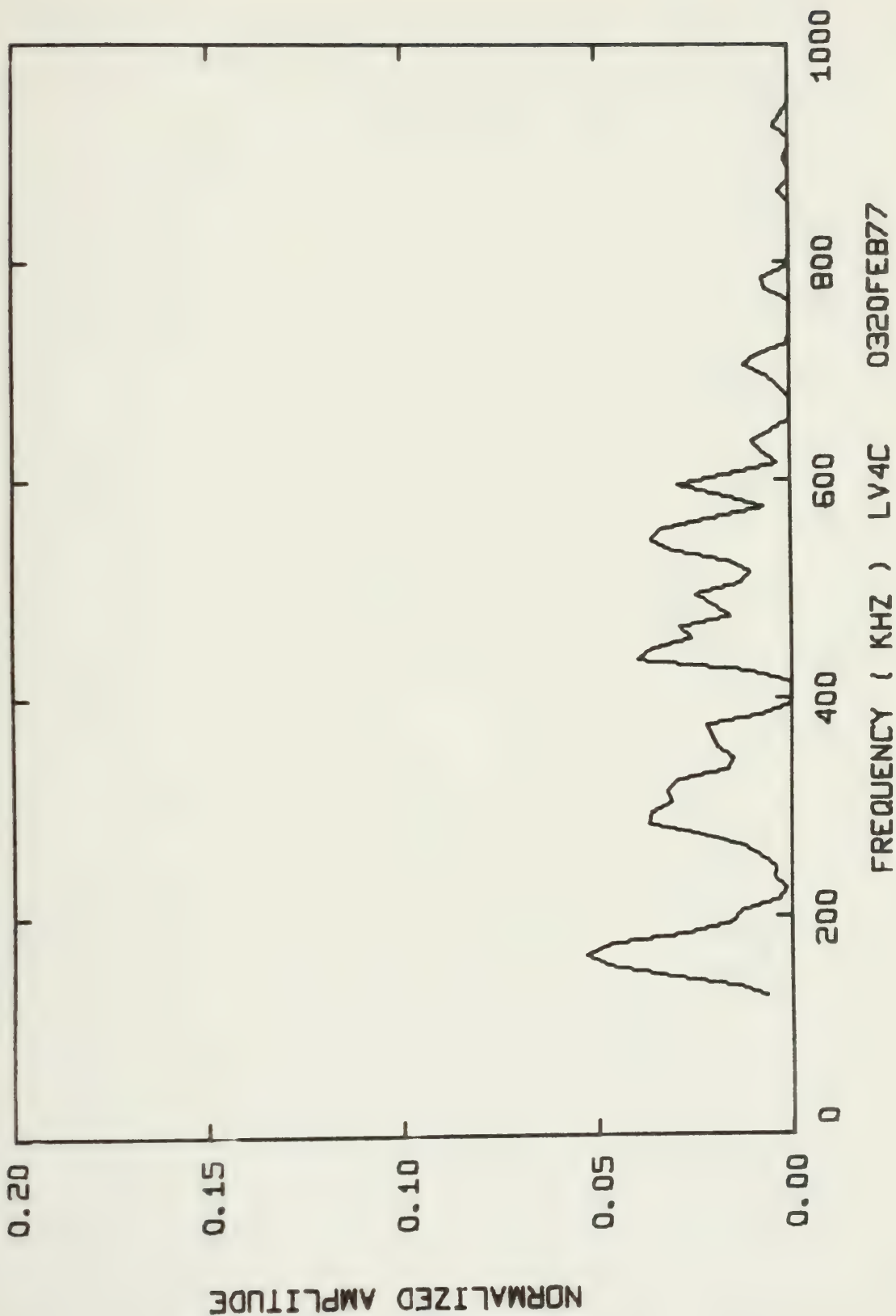




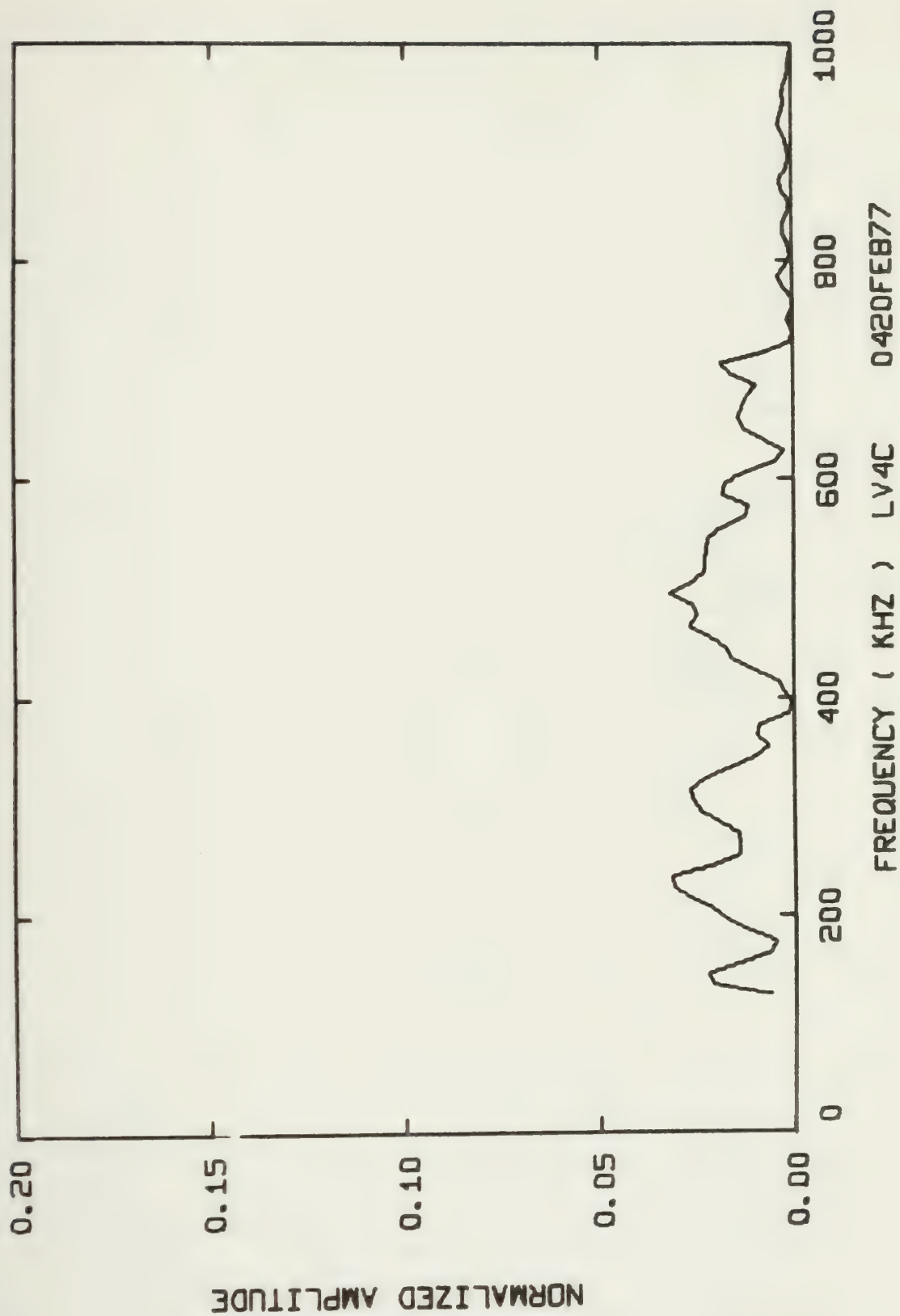




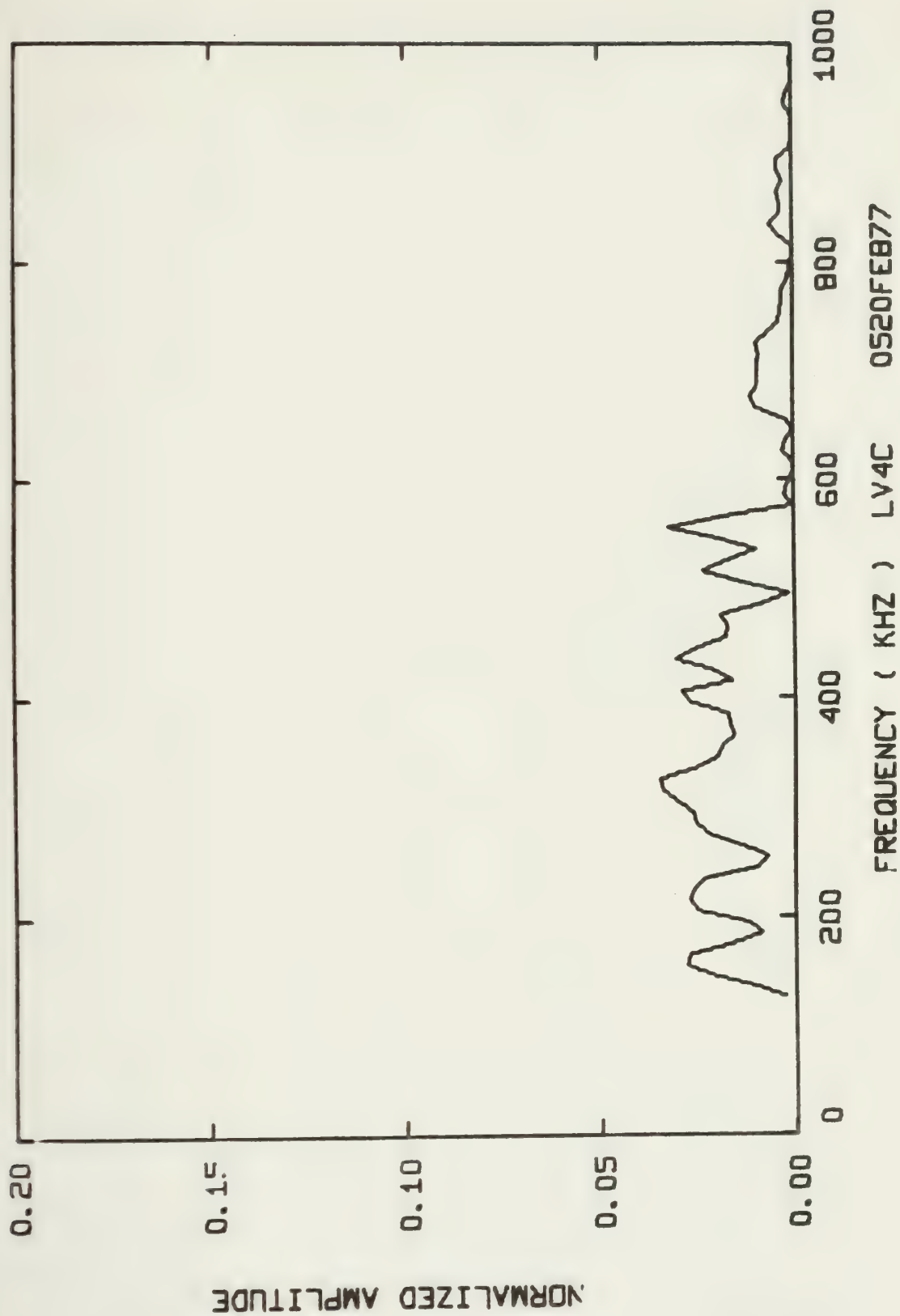






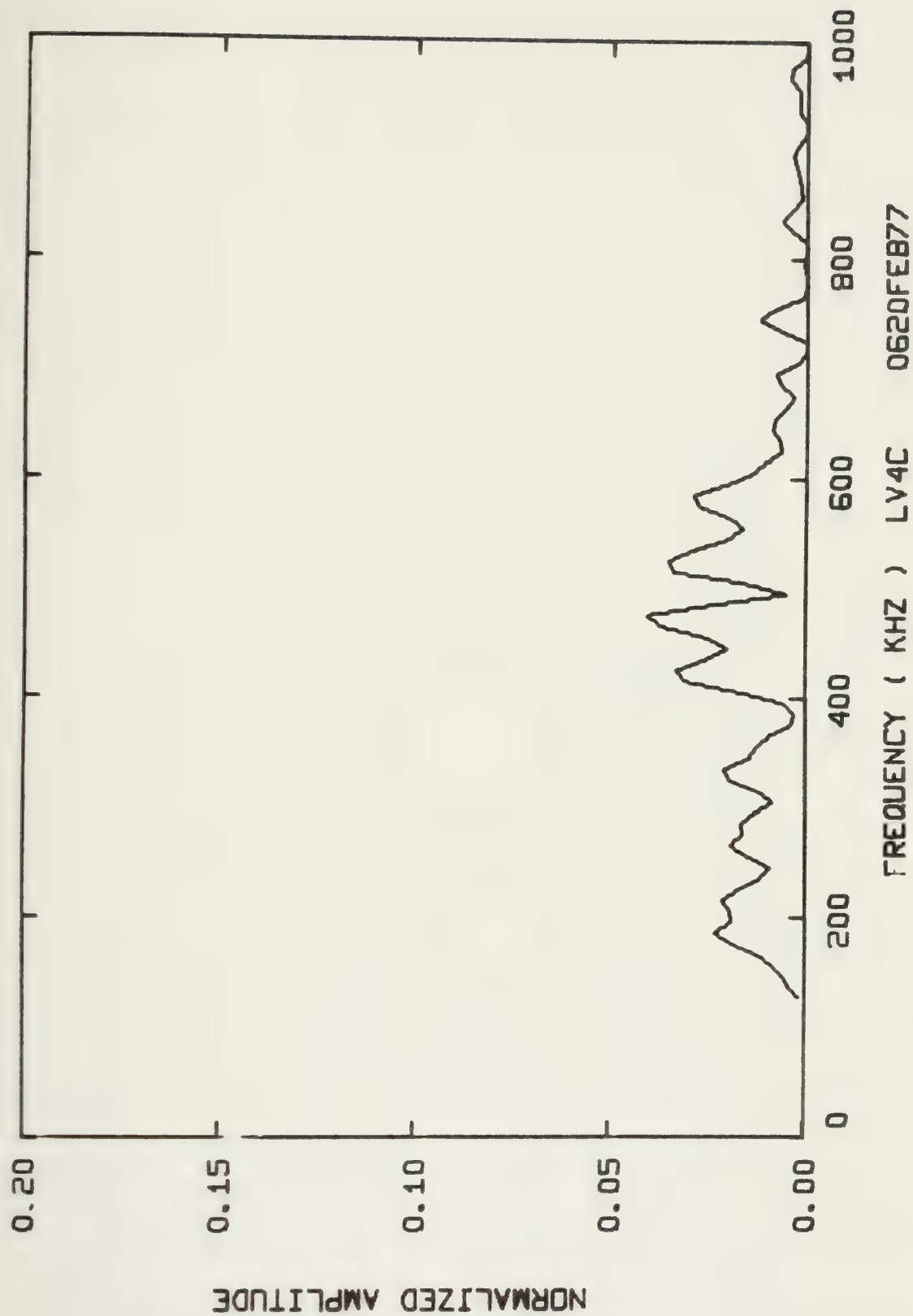




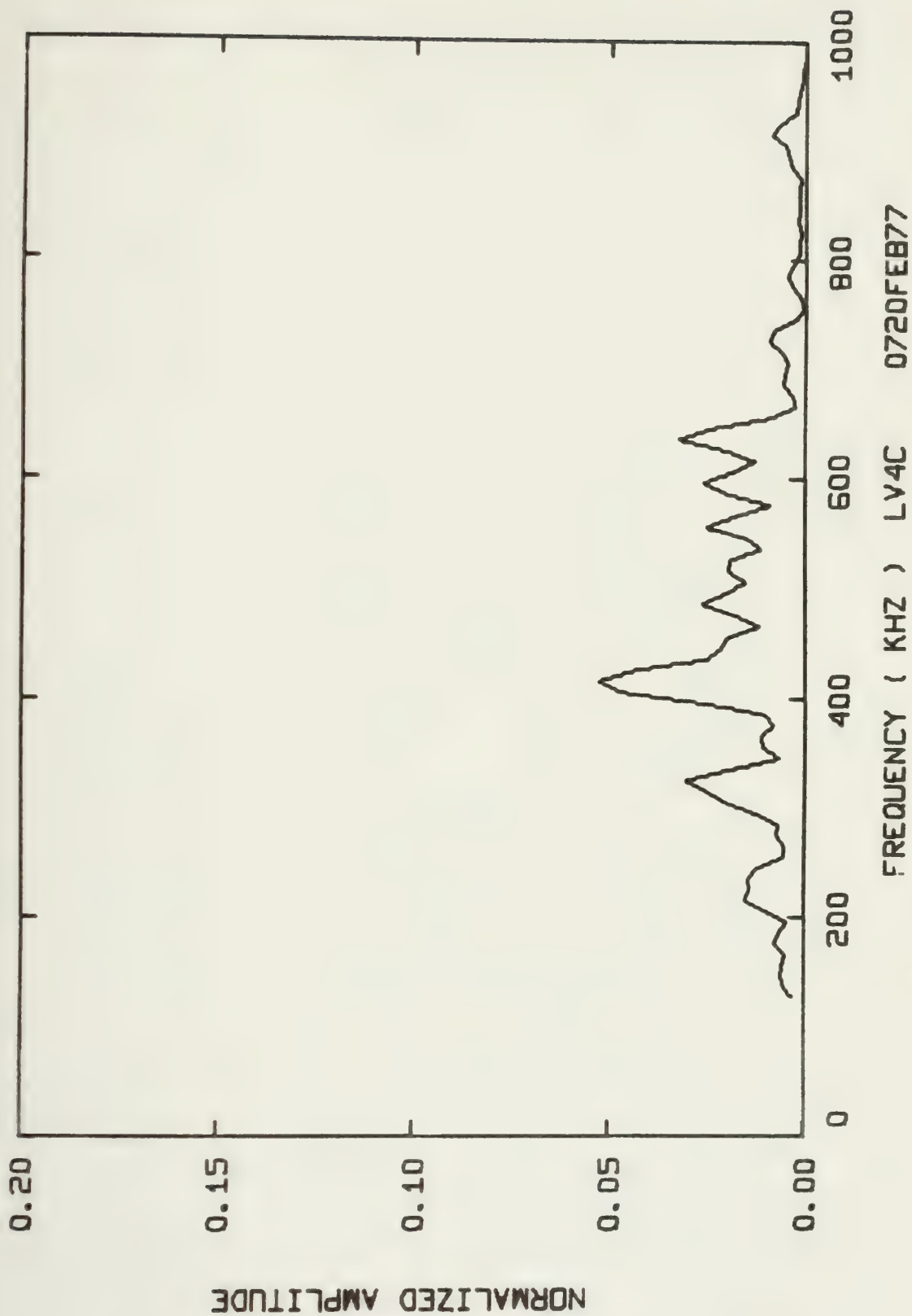




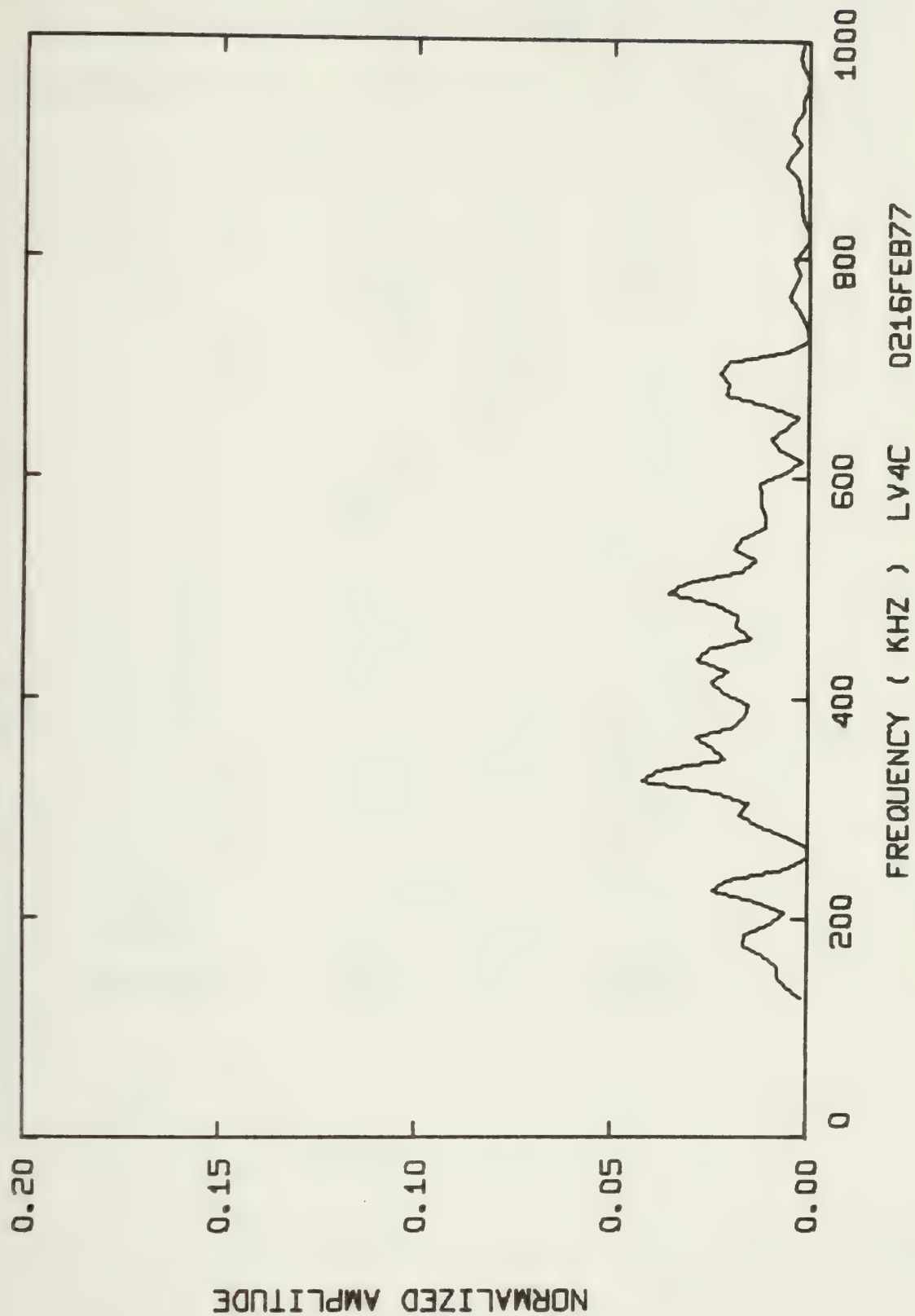












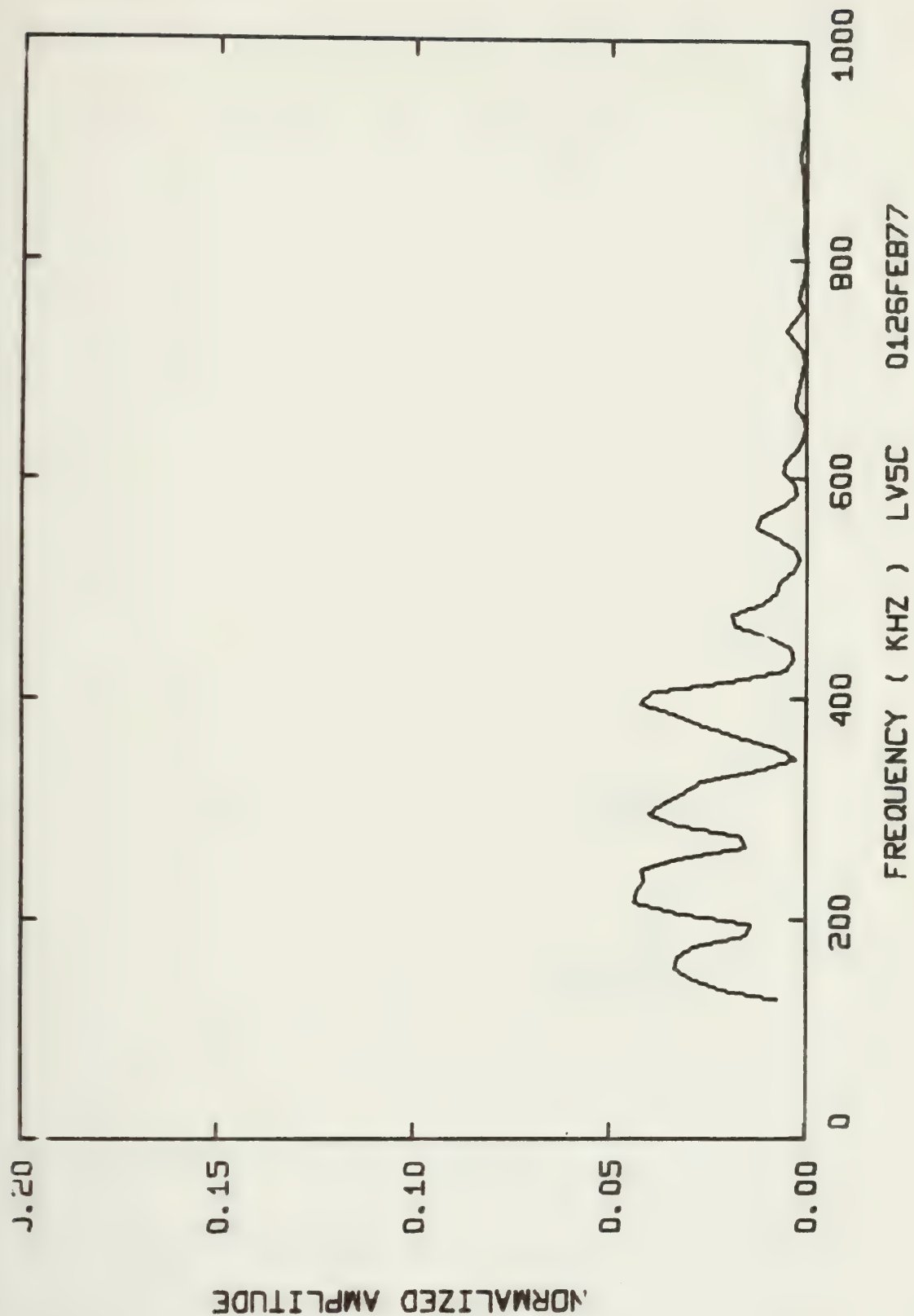


Summary of Energy per Acoustic Emission and RMS Pressure  
Across the Transducer's Face for Each Spectra

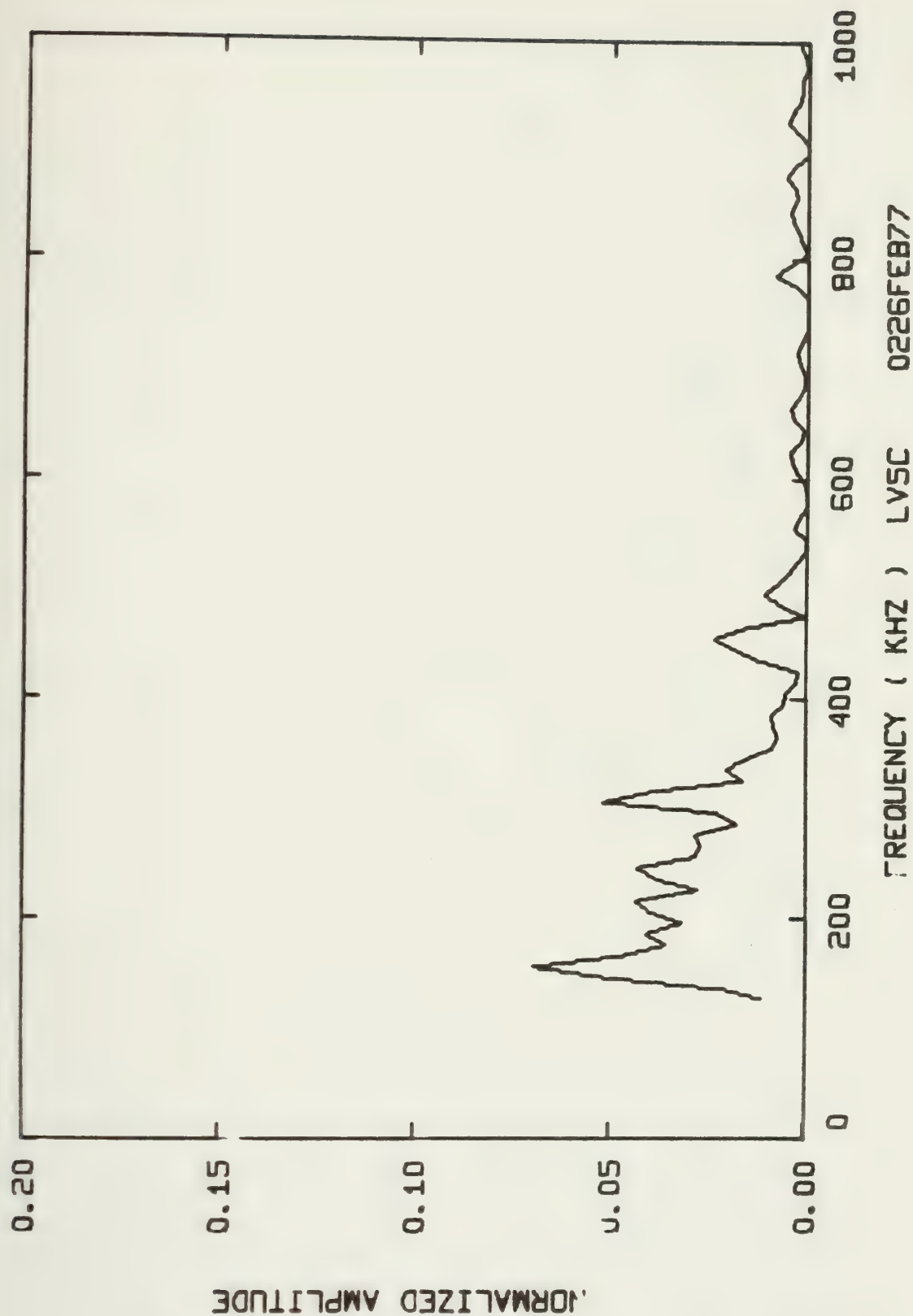
Spectral Distrib. Graph Code Number	Energy per AE (Joules)	RMS Pressure Across Face of Transducer (Pa x 10 <sup>5</sup> )
LV5C 0126FEB77	49.645 x 10 <sup>-9</sup>	69.85
0226FEB77	92.405 x 10 <sup>-9</sup>	70.22
0326FEB77	9.6739 x 10 <sup>-9</sup>	40.52
0426FEB77	34.964 x 10 <sup>-9</sup>	61.97
0526FEB77	101.82 x 10 <sup>-9</sup>	83.00
0626FEB77	44.544 x 10 <sup>-9</sup>	67.61
0726FEB77	179.37 x 10 <sup>-9</sup>	83.53
0826FEB77	932.57 x 10 <sup>-9</sup>	142.30
0926FEB77	165.52 x 10 <sup>-9</sup>	79.42
1026FEB77	130.91 x 10 <sup>-9</sup>	73.87
0127FEB77	747.99 x 10 <sup>-9</sup>	140.06
0227FEB77	147.70 x 10 <sup>-9</sup>	82.02
0327FEB77	169.17 x 10 <sup>-9</sup>	87.78
0427FEB77	80.192 x 10 <sup>-9</sup>	63.62
0527FEB77	230.10 x 10 <sup>-9</sup>	93.27
0627FEB77	268.44 x 10 <sup>-9</sup>	95.47



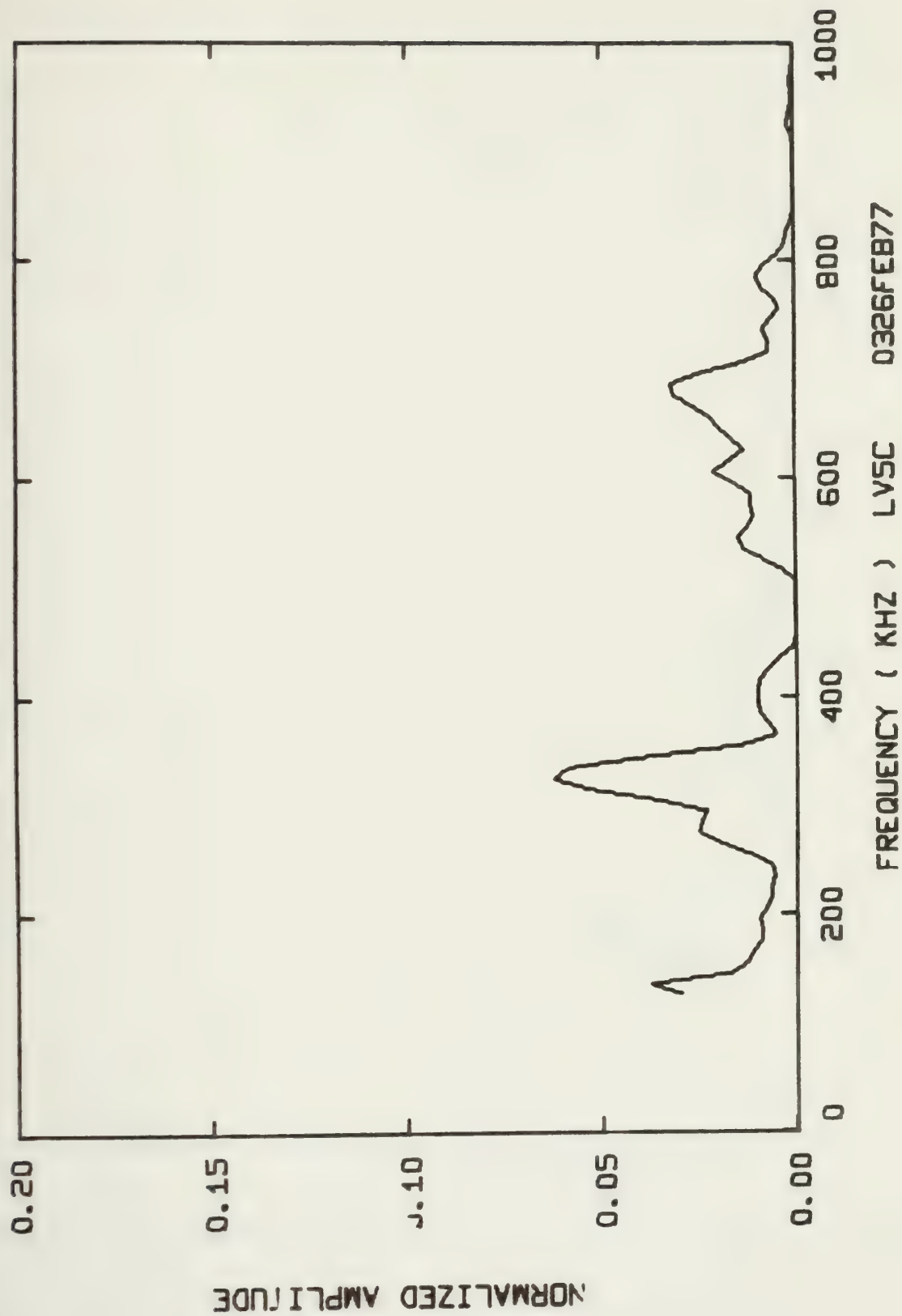




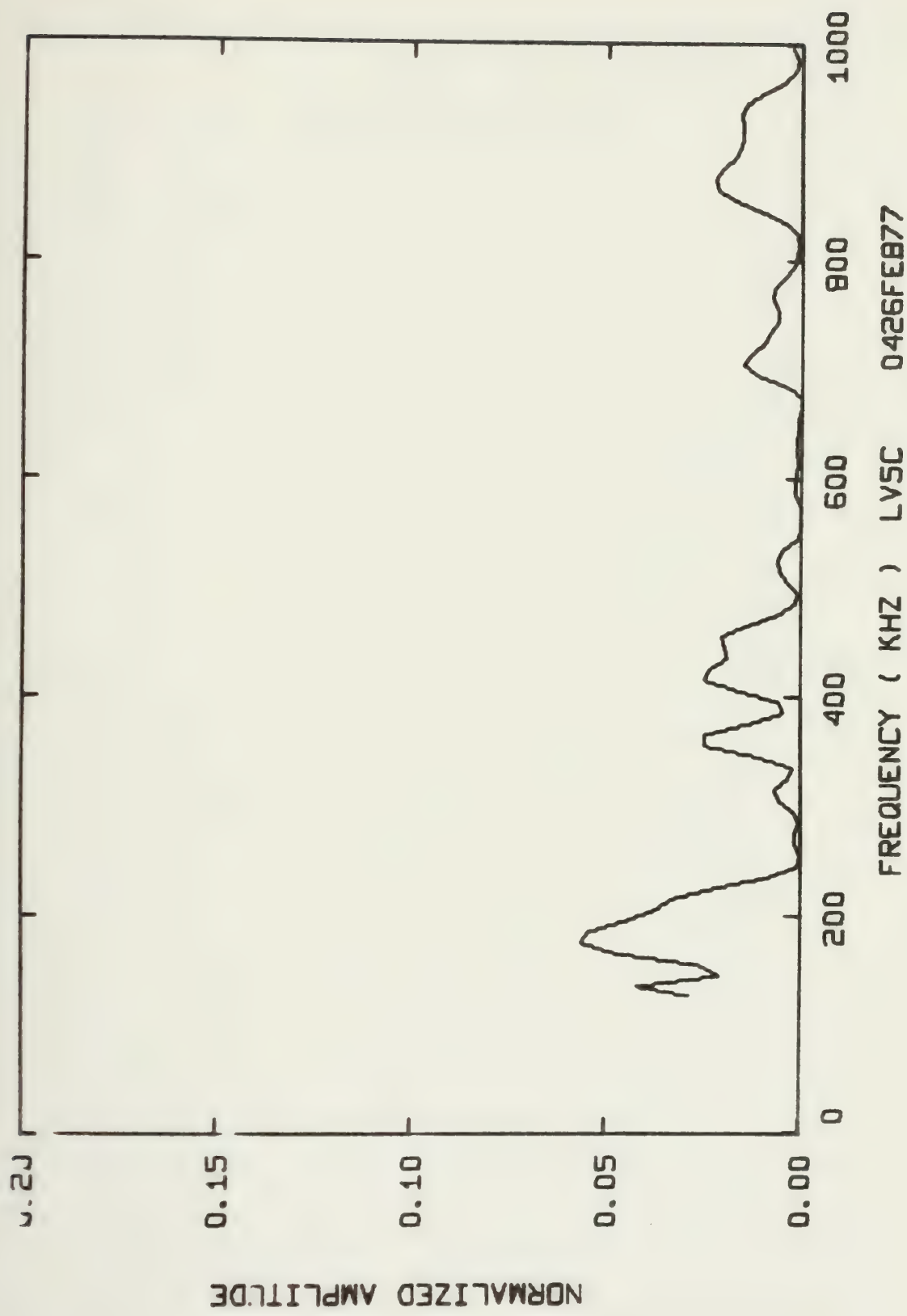






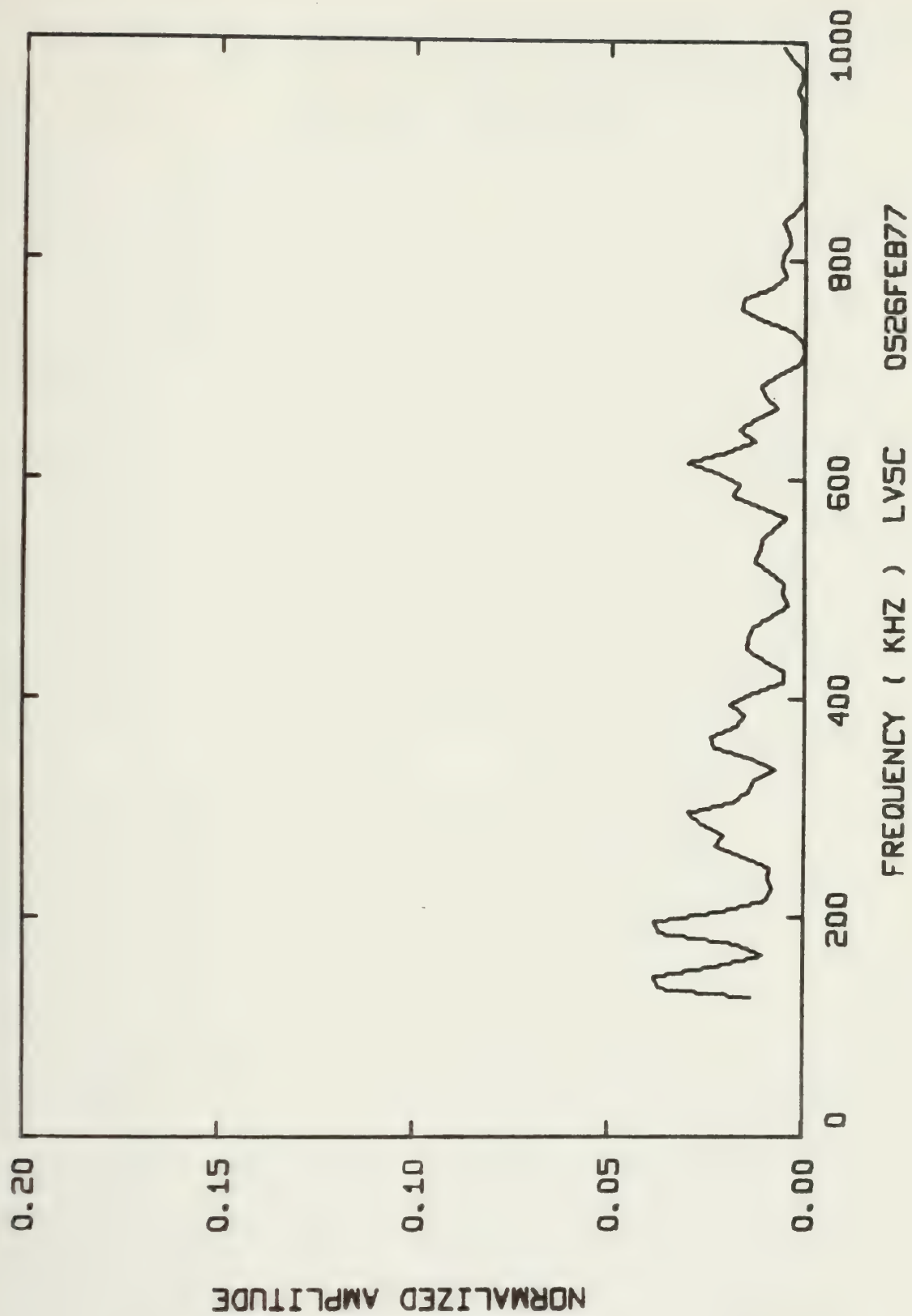




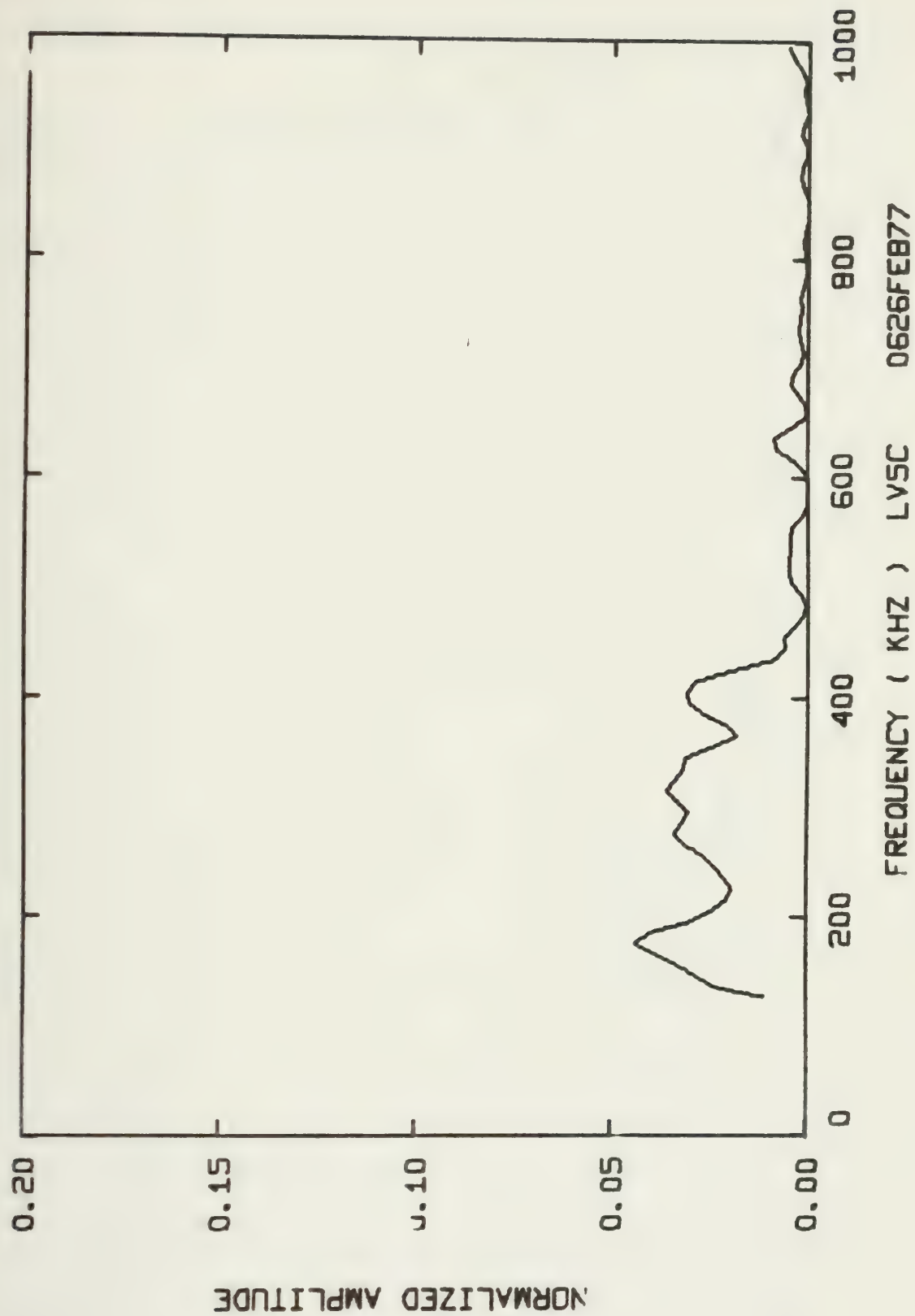




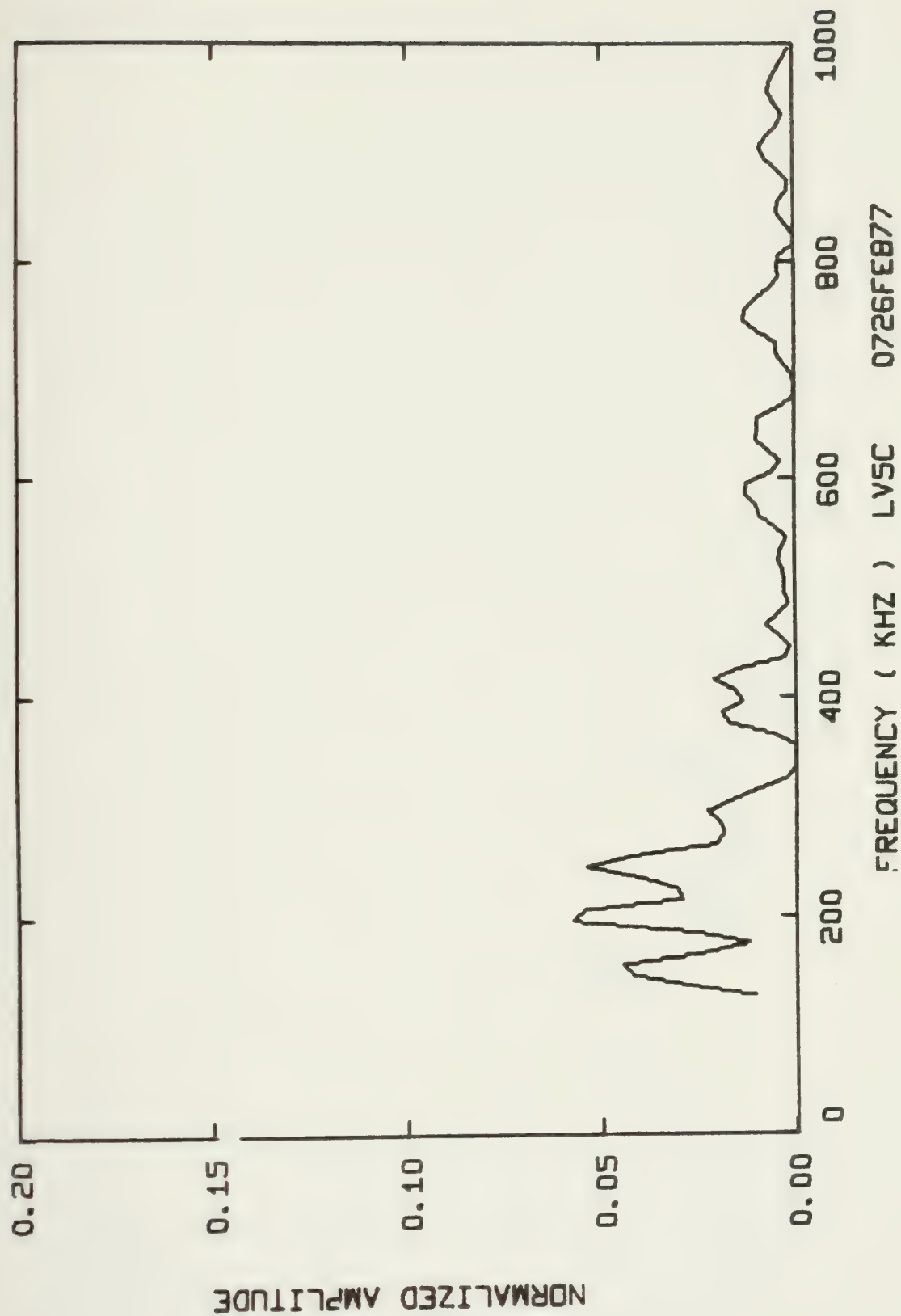




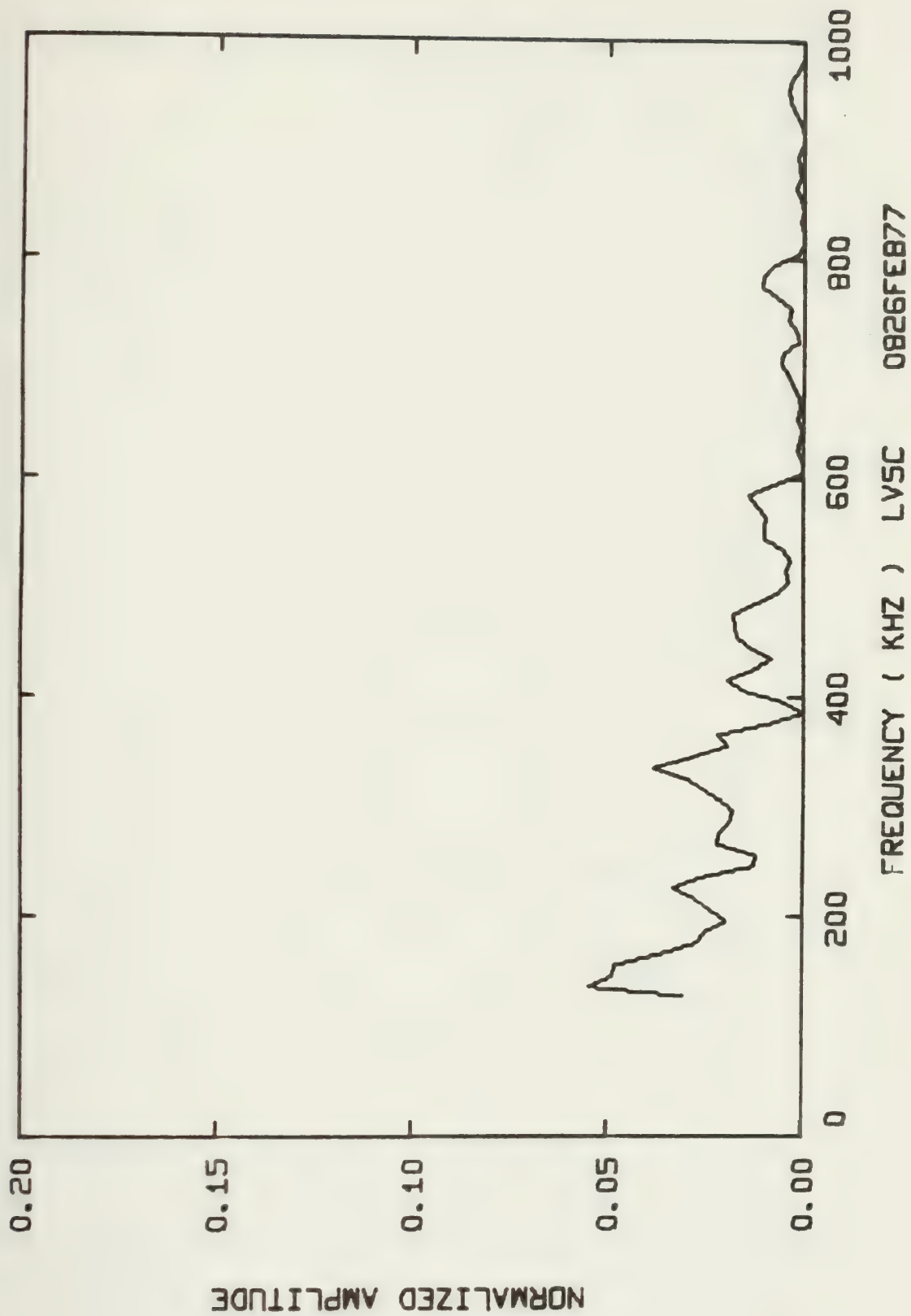






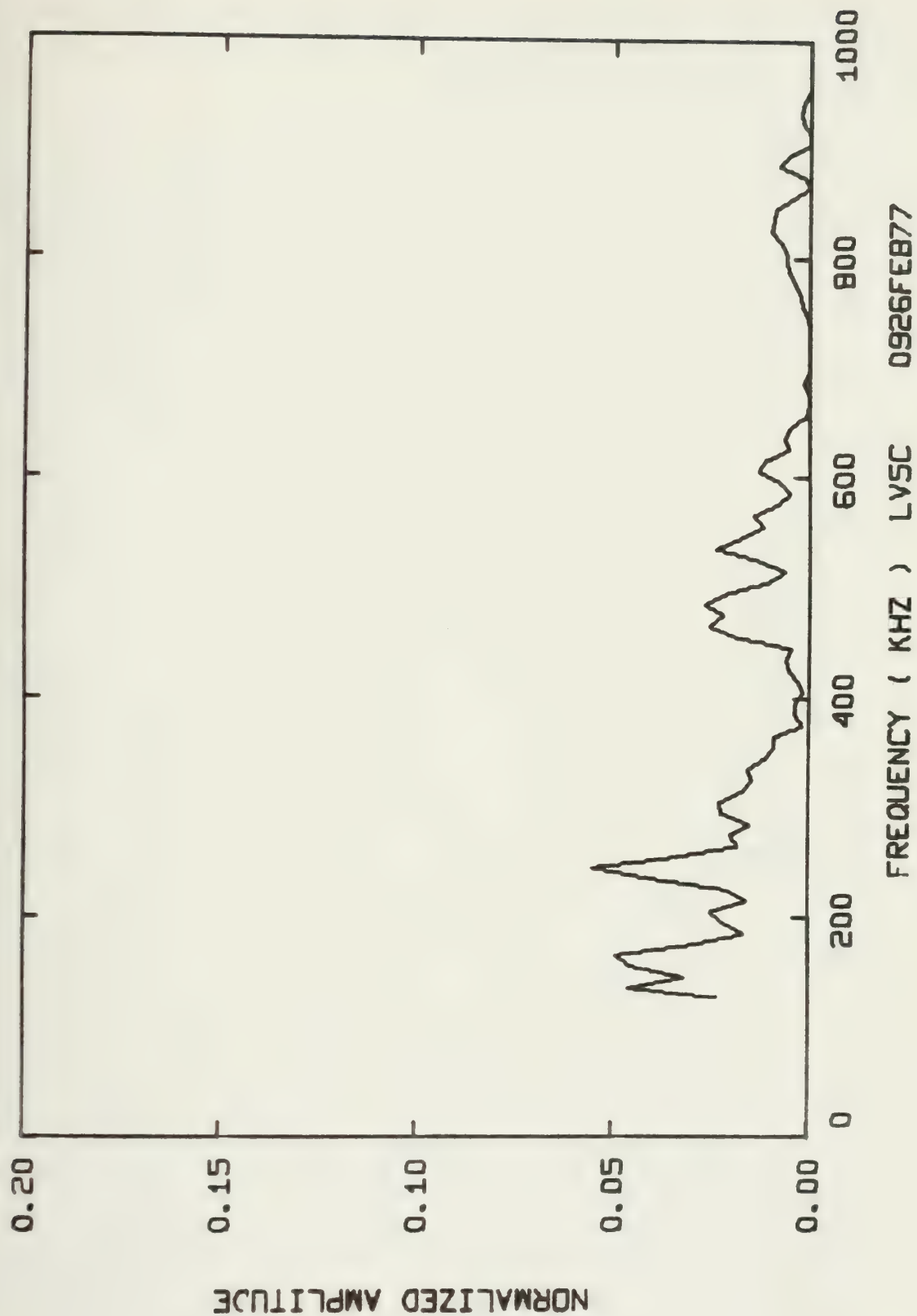




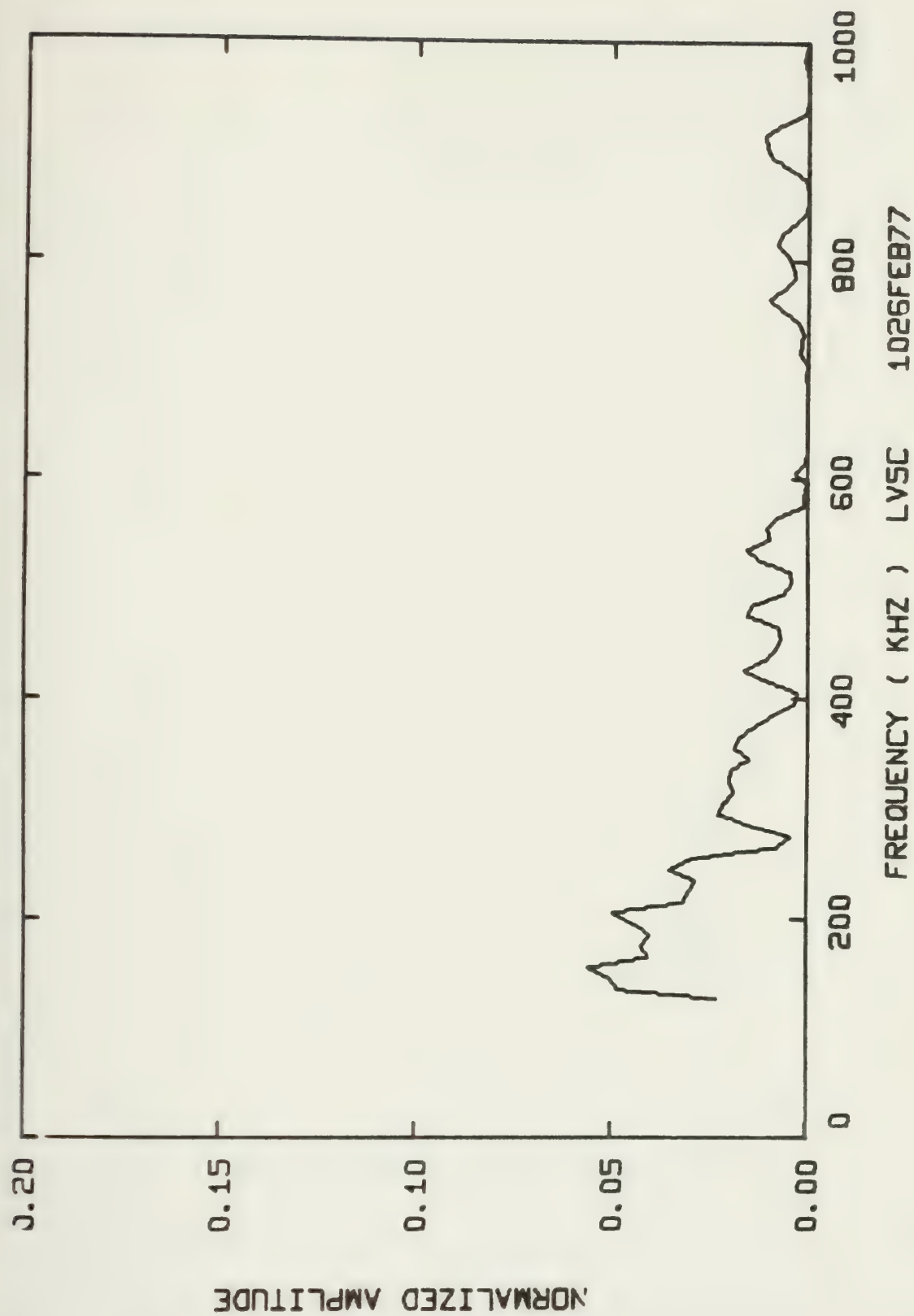




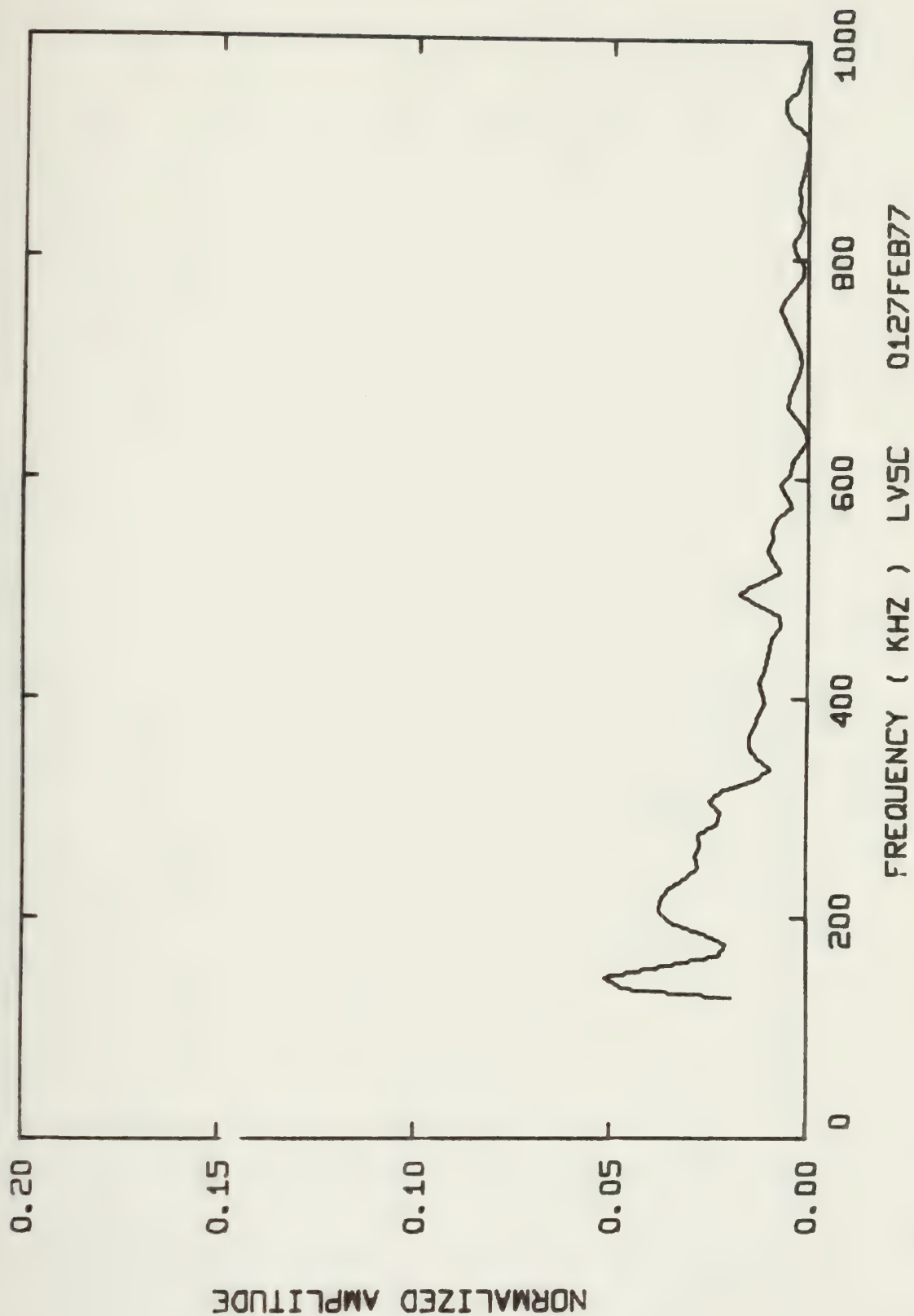




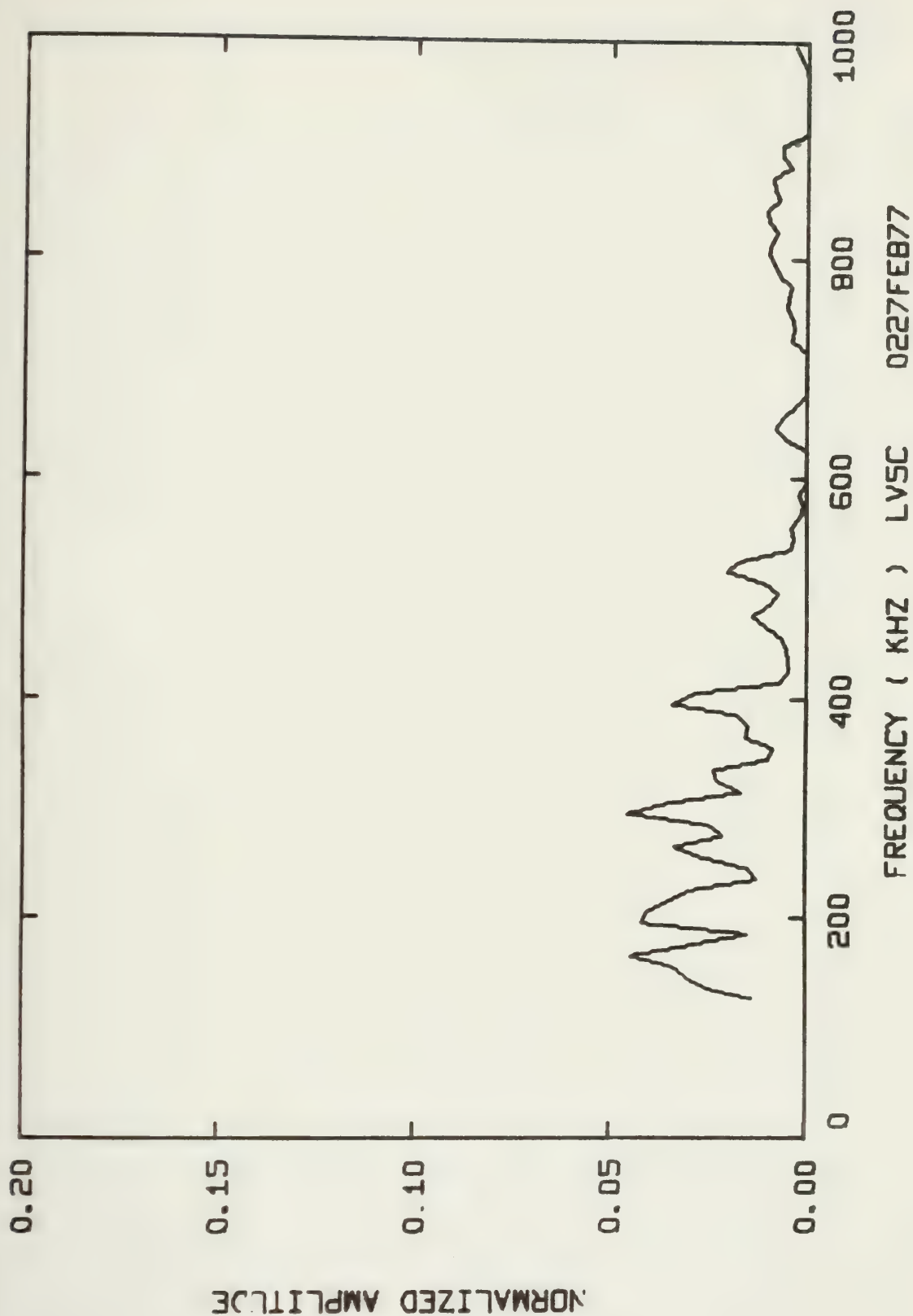






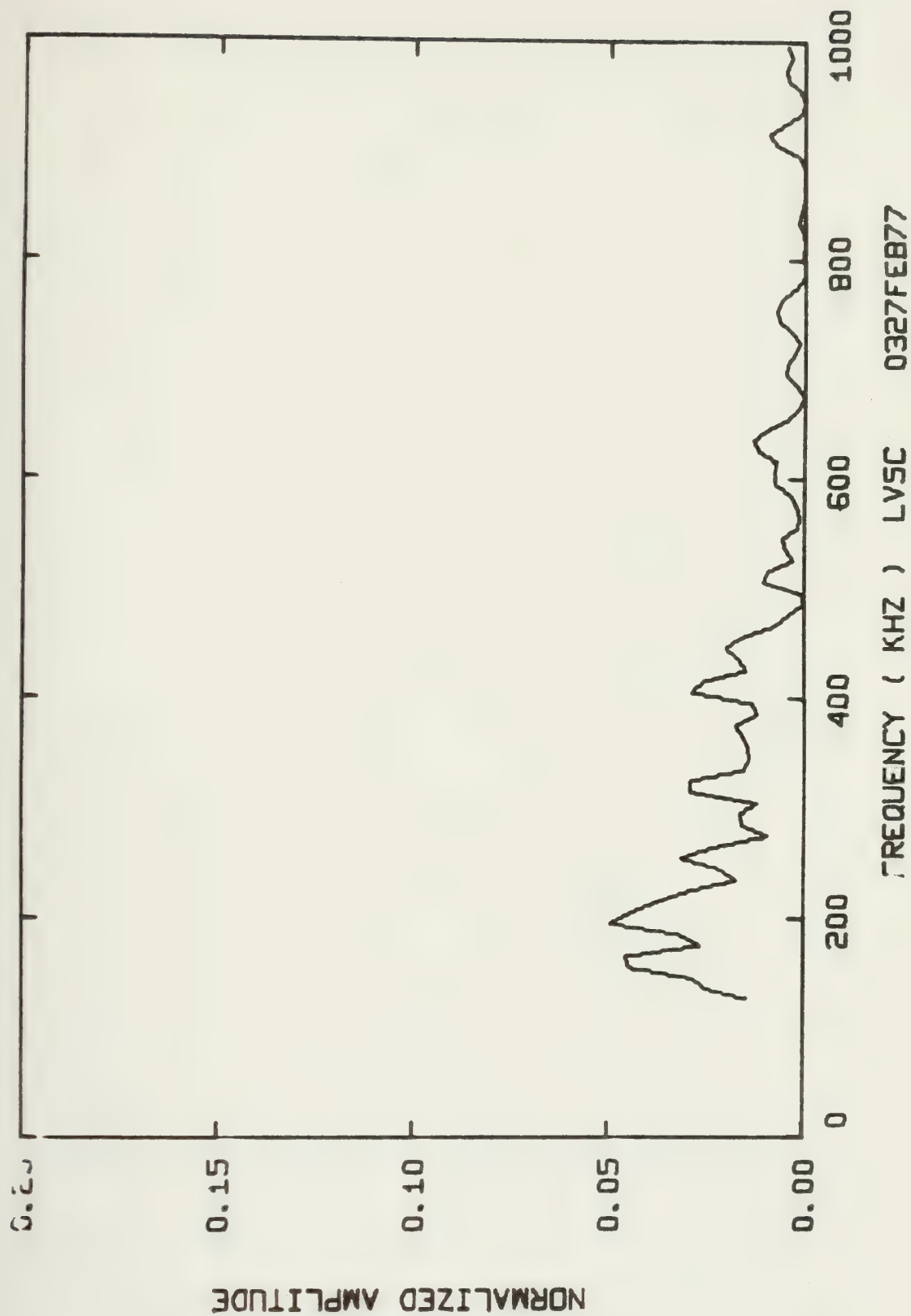




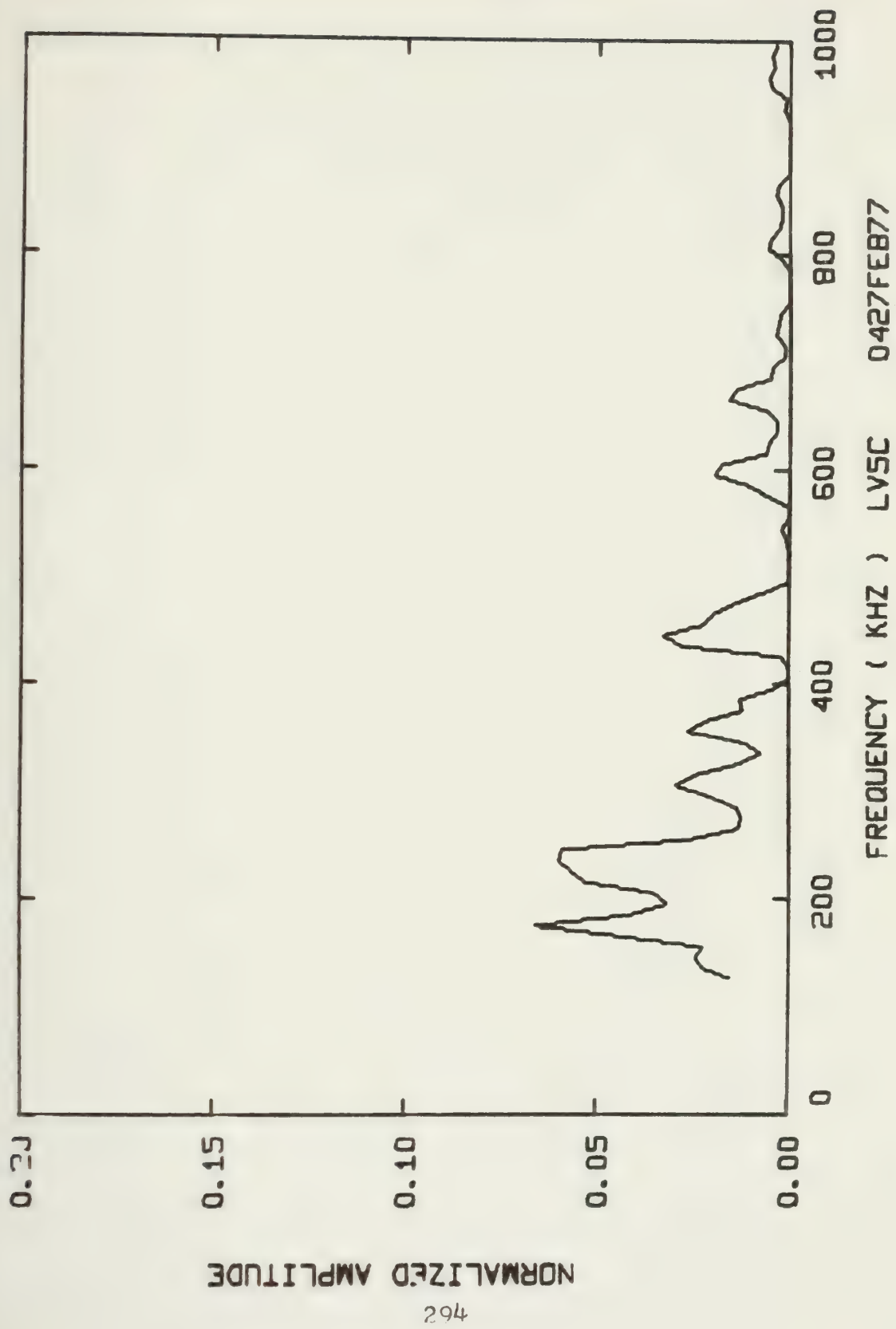




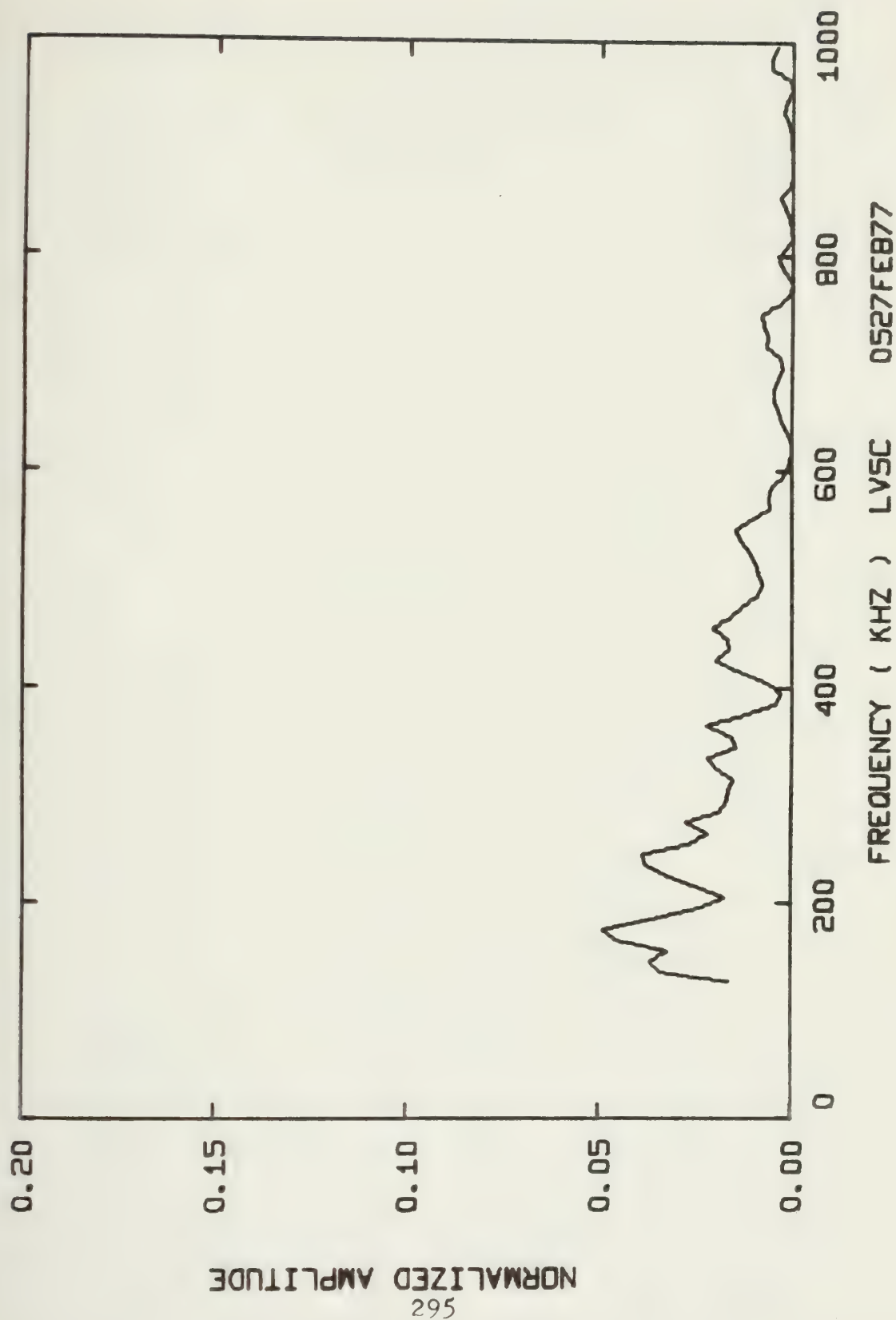




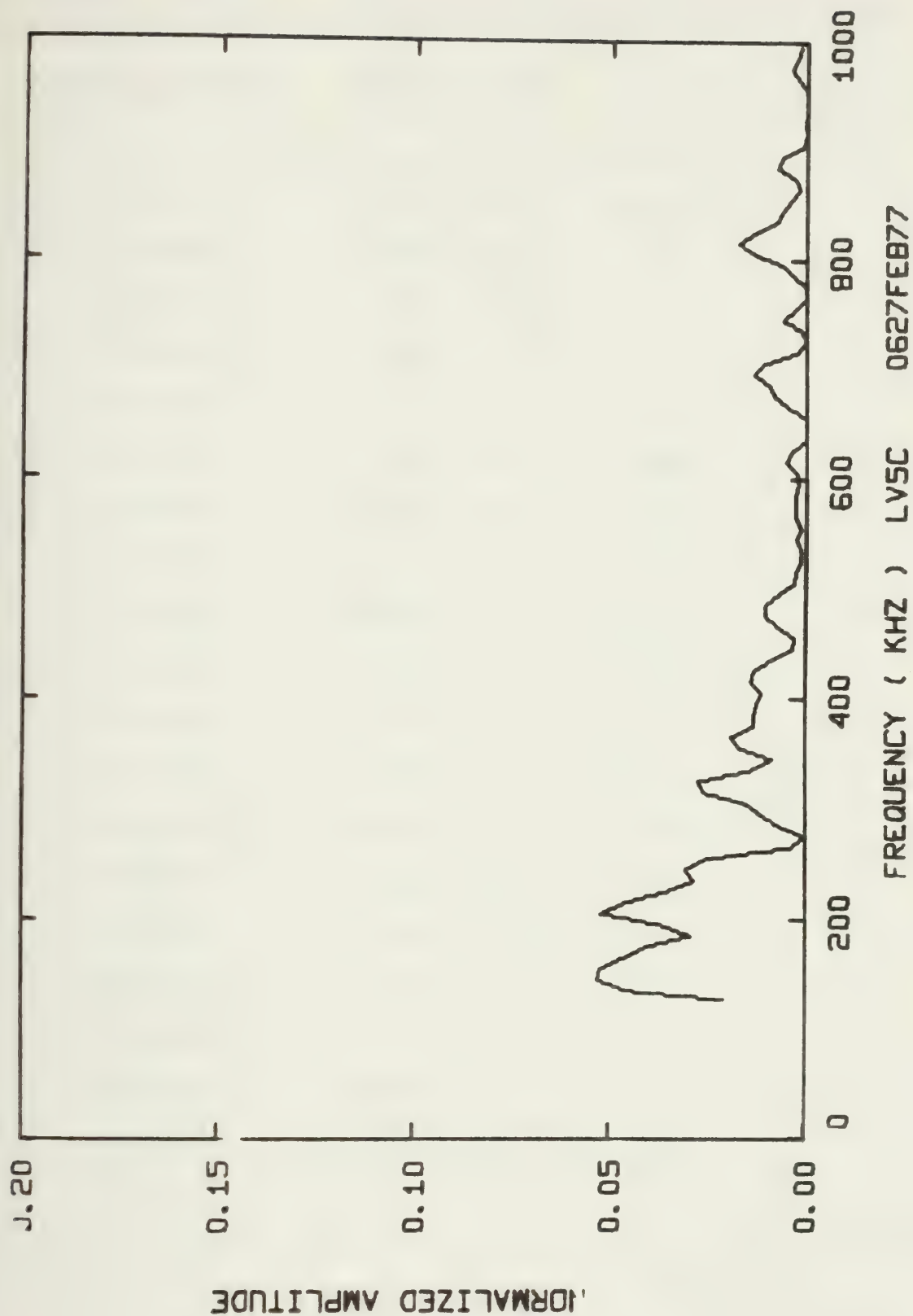












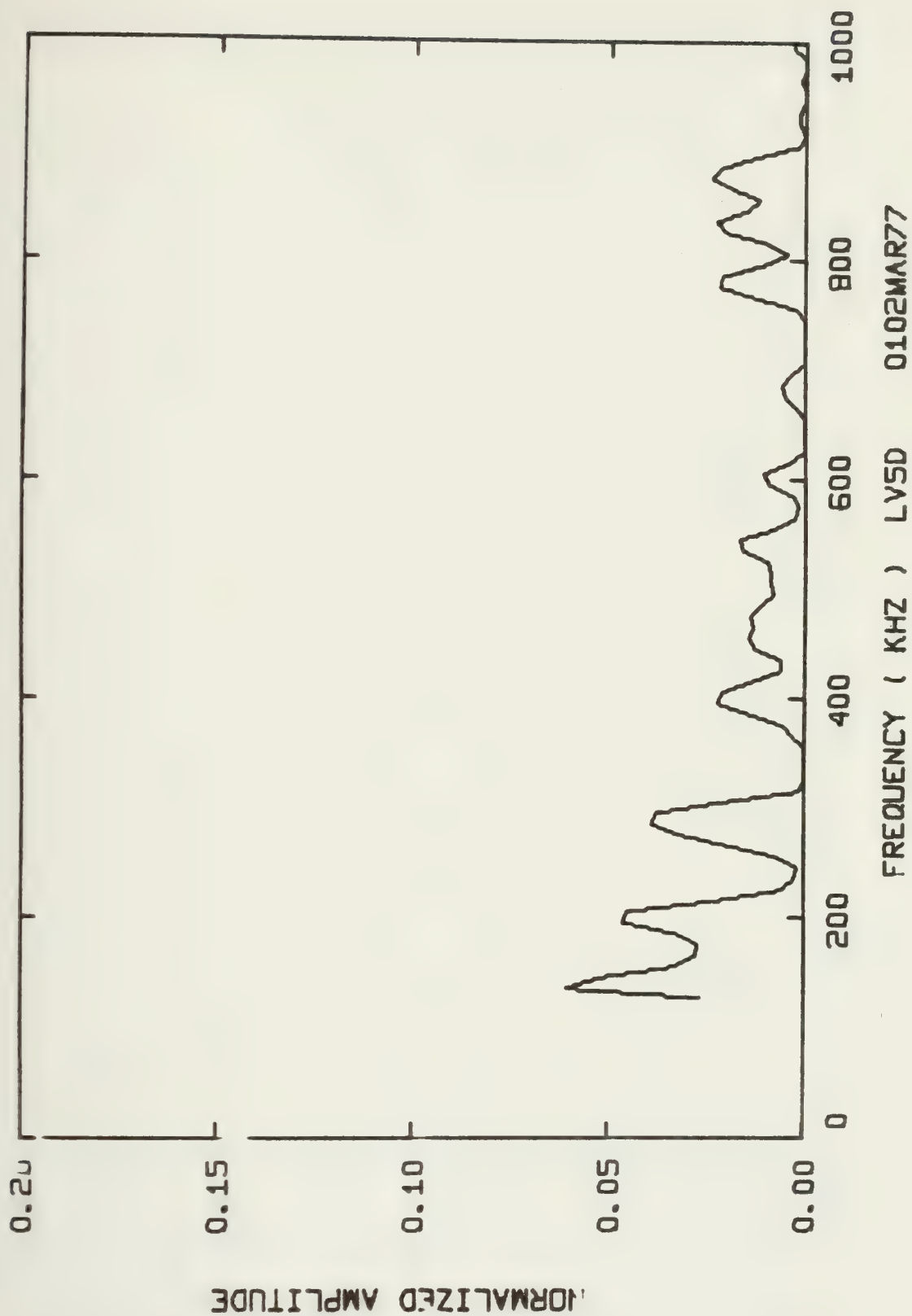




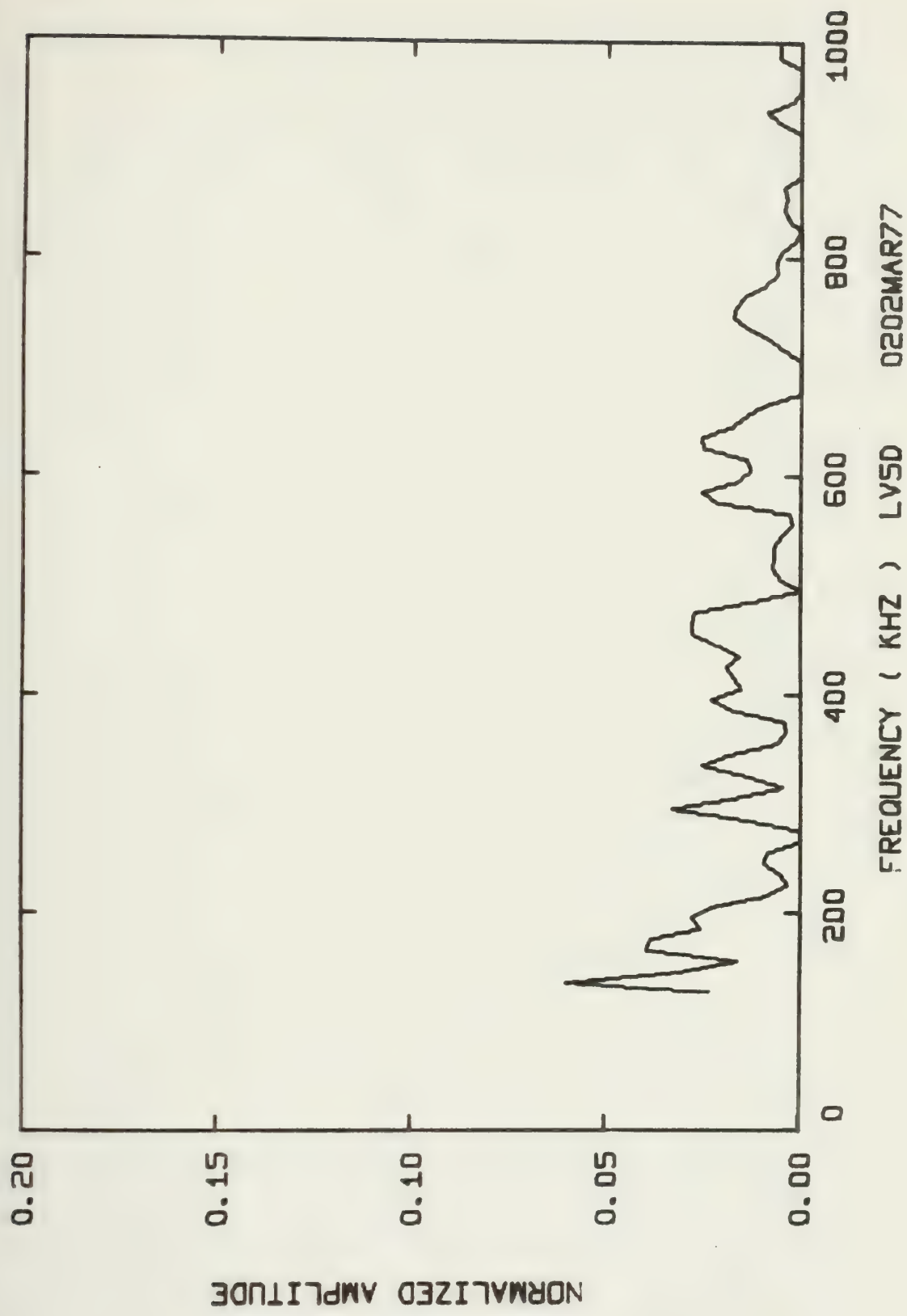
Summary of Energy per Acoustic Emission and RMS Pressure  
Across the Transducer's Face for Each Spectra

Spectral Distrib. Graph Code Number	Energy per AE (Joules)	RMS Pressure Across Face of Transducer (Pa x 10 <sup>5</sup> )
LV5D 0102MAR77	36.426 x 10 <sup>-9</sup>	58.32
0202MAR77	59.885 x 10 <sup>-9</sup>	59.12
0302MAR77	31.864 x 10 <sup>-9</sup>	49.38
0402MAR77	13.352 x 10 <sup>-9</sup>	38.30
0502MAR77	23.099 x 10 <sup>-9</sup>	50.37
0702MAR77	25.069 x 10 <sup>-9</sup>	52.48
0802MAR77	14.559 x 10 <sup>-9</sup>	39.99
0902MAR77	57.959 x 10 <sup>-9</sup>	68.01
1002MAR77	346.82 x 10 <sup>-9</sup>	101.39
0103MAR77	63.885 x 10 <sup>-9</sup>	61.25
0203MAR77	97.099 x 10 <sup>-9</sup>	75.51
0303MAR77	39.826 x 10 <sup>-9</sup>	64.28
0403MAR77	20.661 x 10 <sup>-9</sup>	47.64
0503MAR77	25.322 x 10 <sup>-9</sup>	52.74
0603MAR77	15.500 x 10 <sup>-9</sup>	38.04
0703MAR77	7.5272 x 10 <sup>-9</sup>	32.88
0803MAR77	13.384 x 10 <sup>-9</sup>	43.85
0903MAR77	30.972 x 10 <sup>-9</sup>	51.99
1003MAR77	409.50 x 10 <sup>-9</sup>	108.47

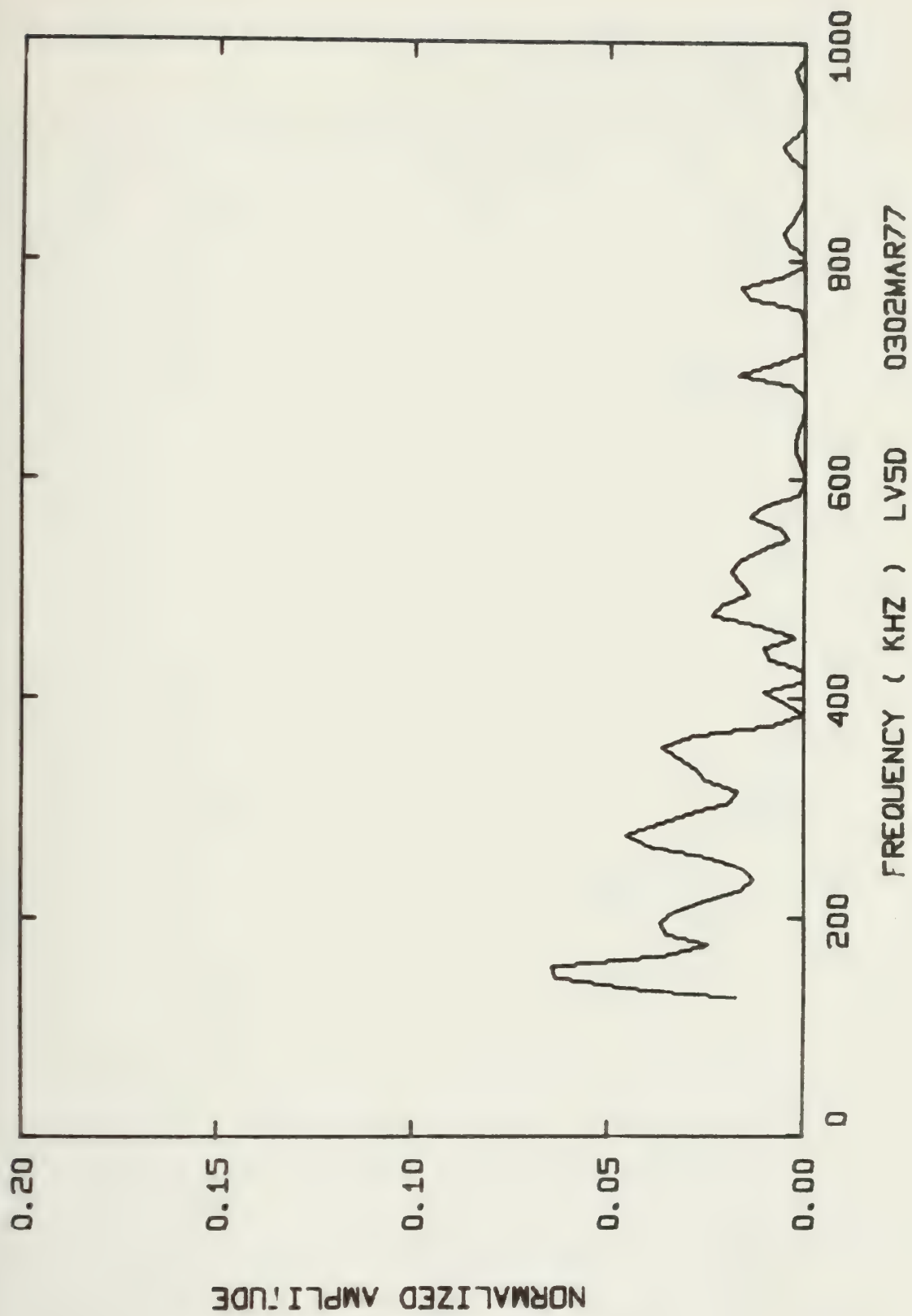






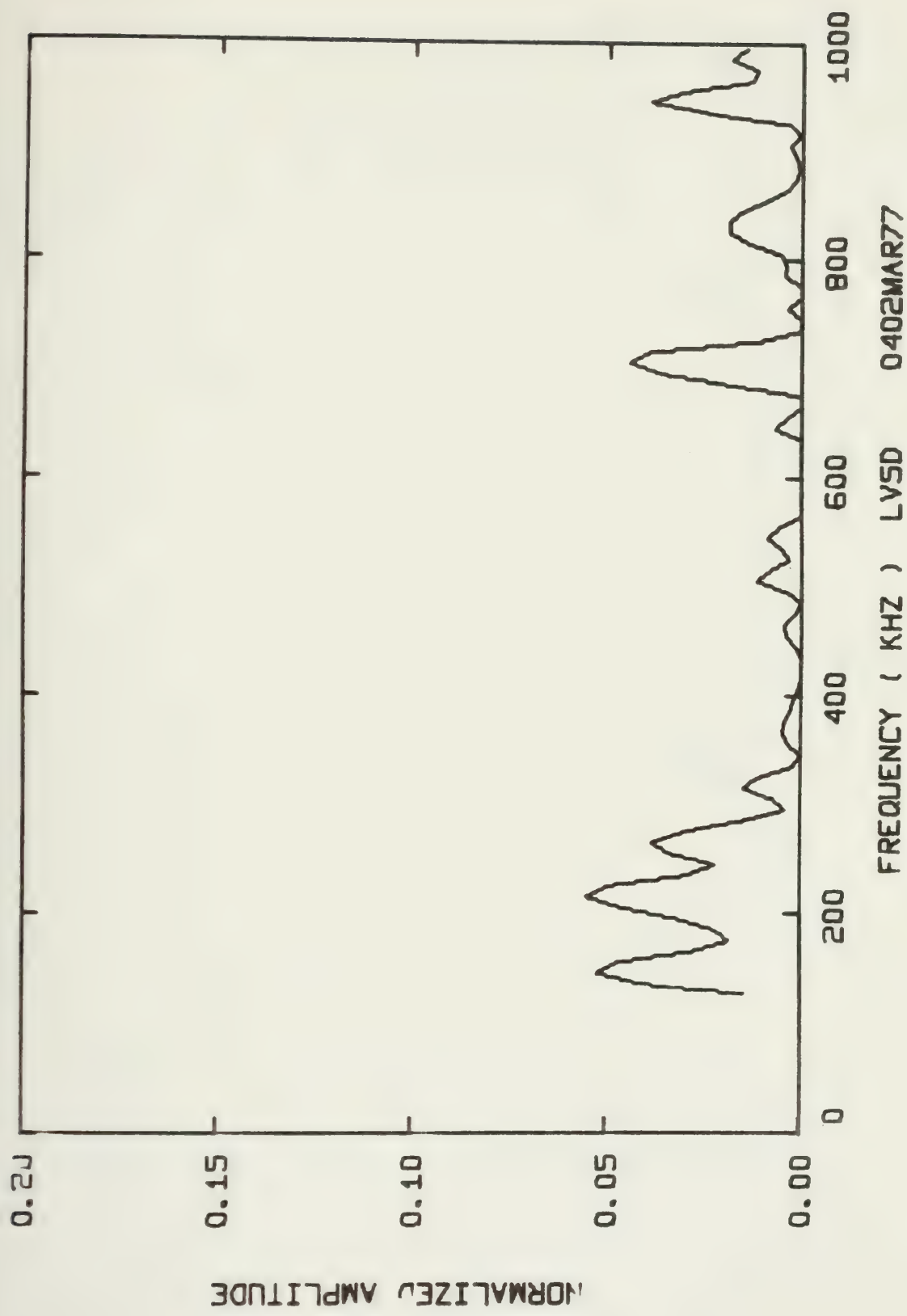




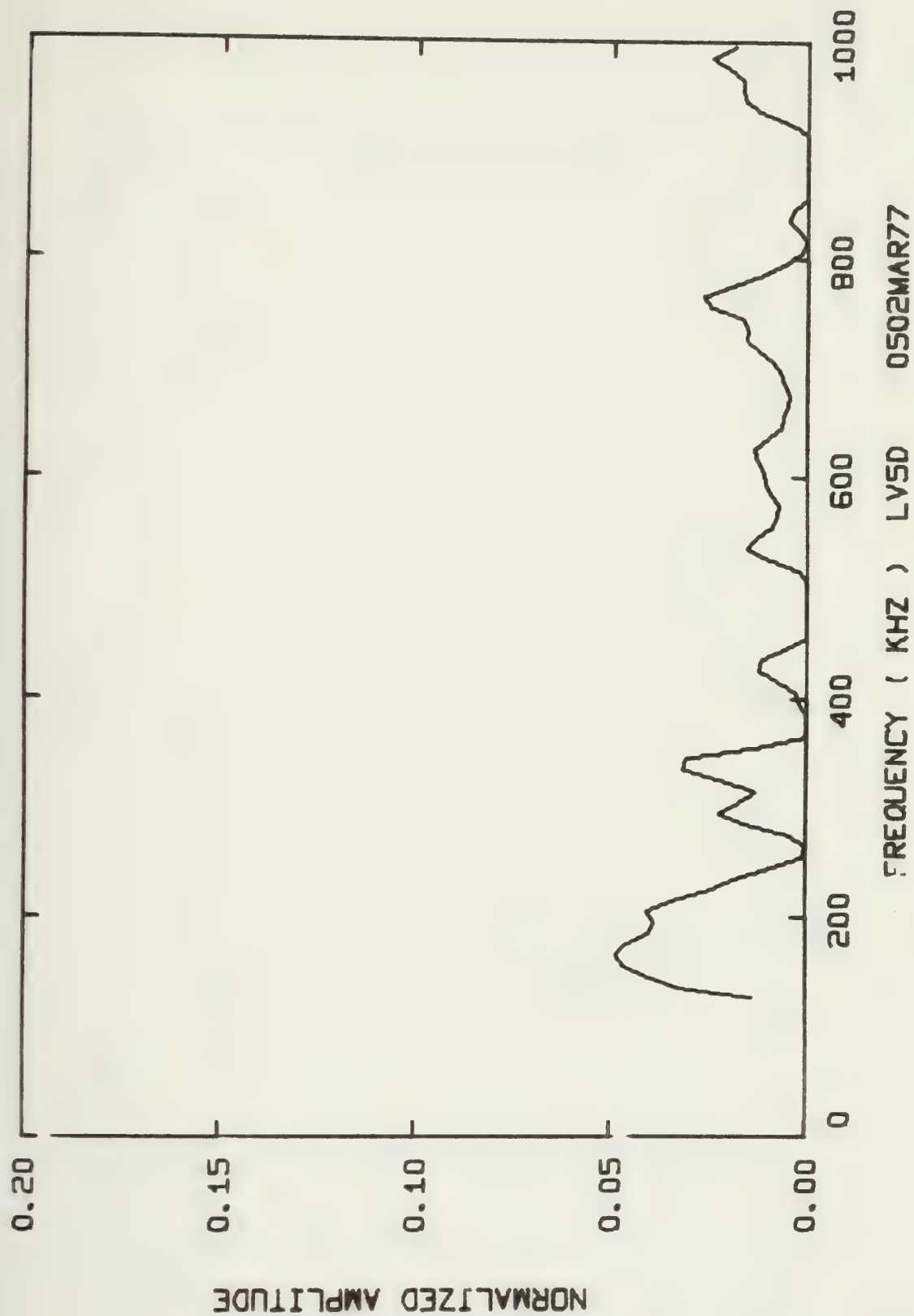




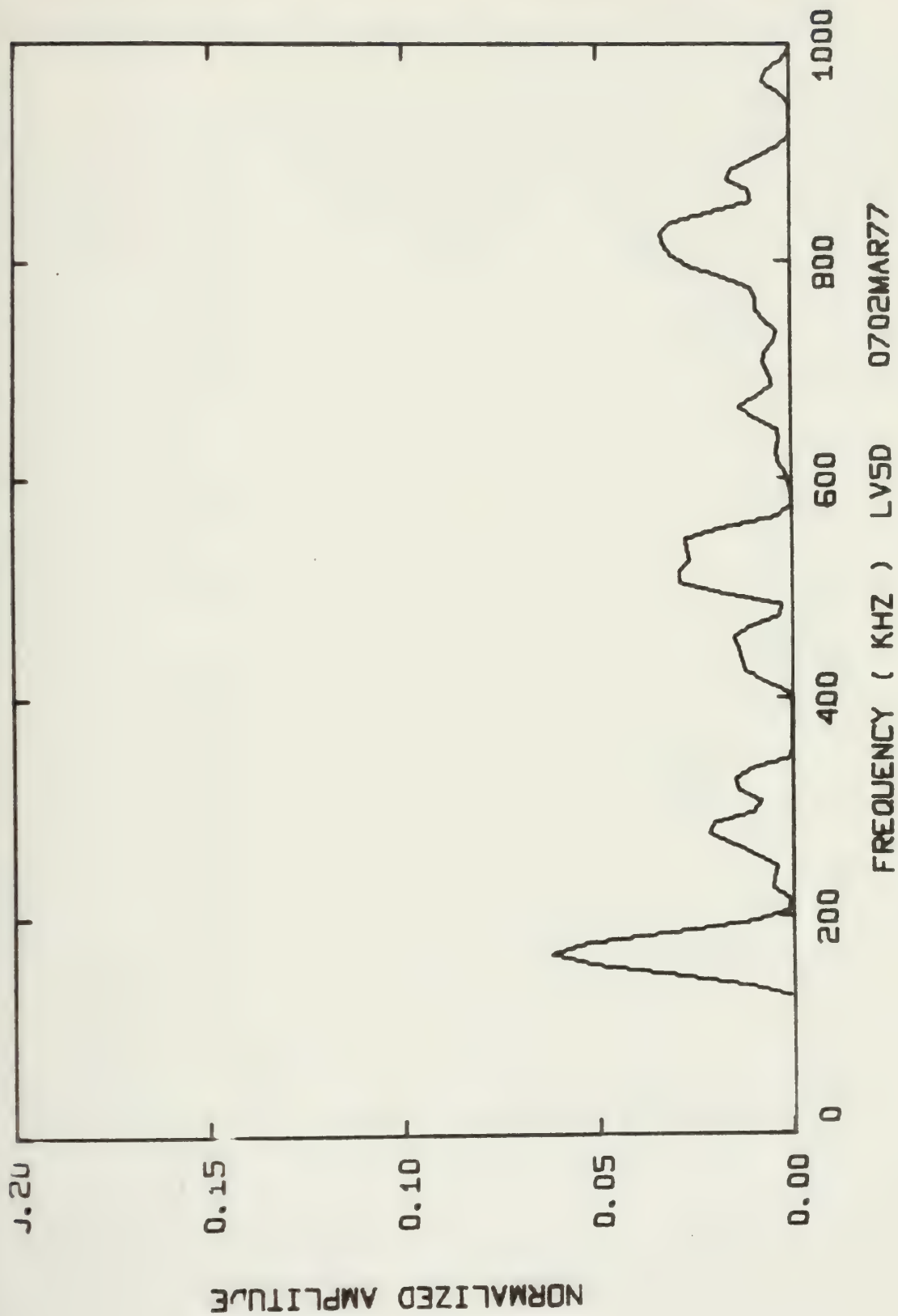




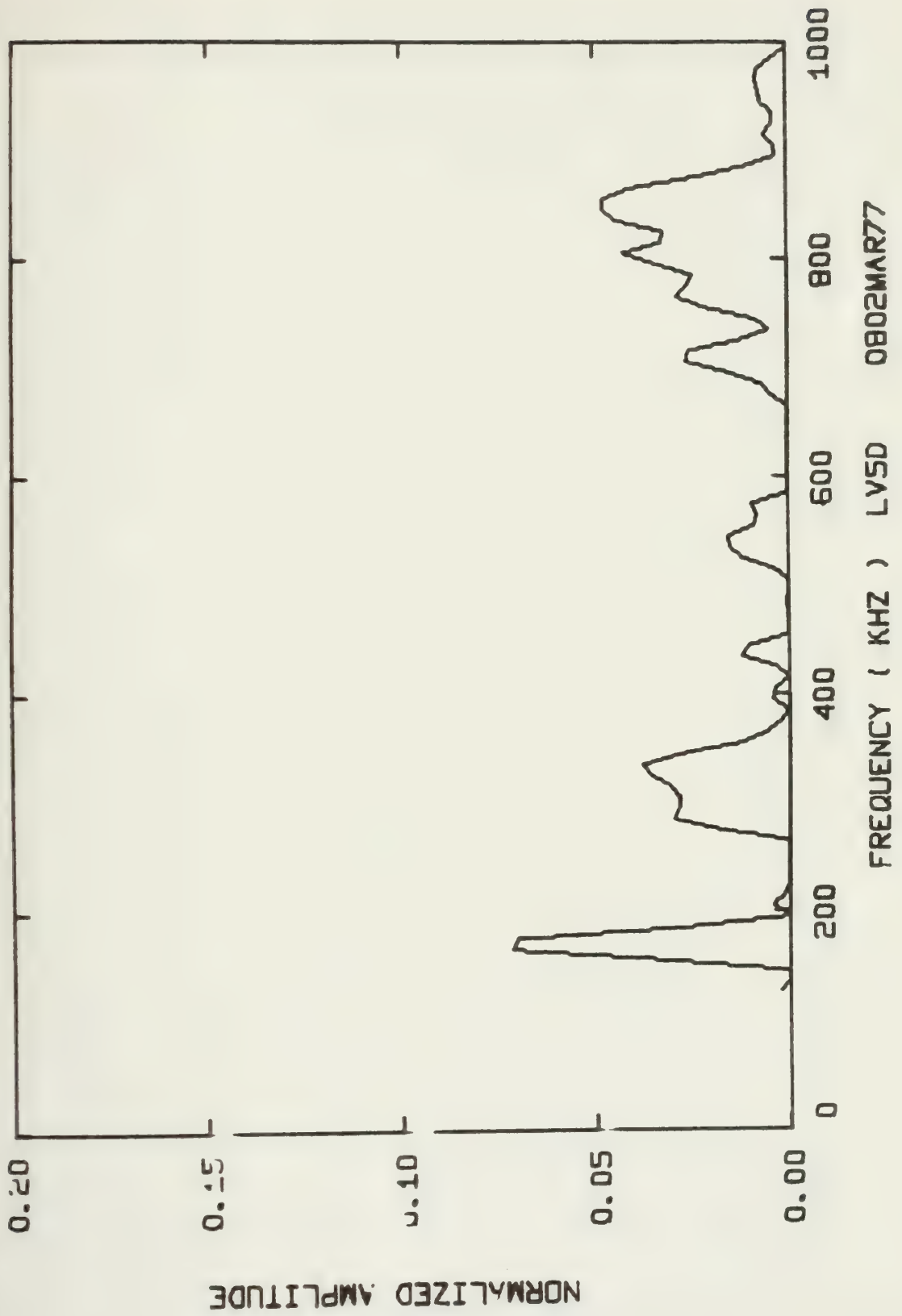






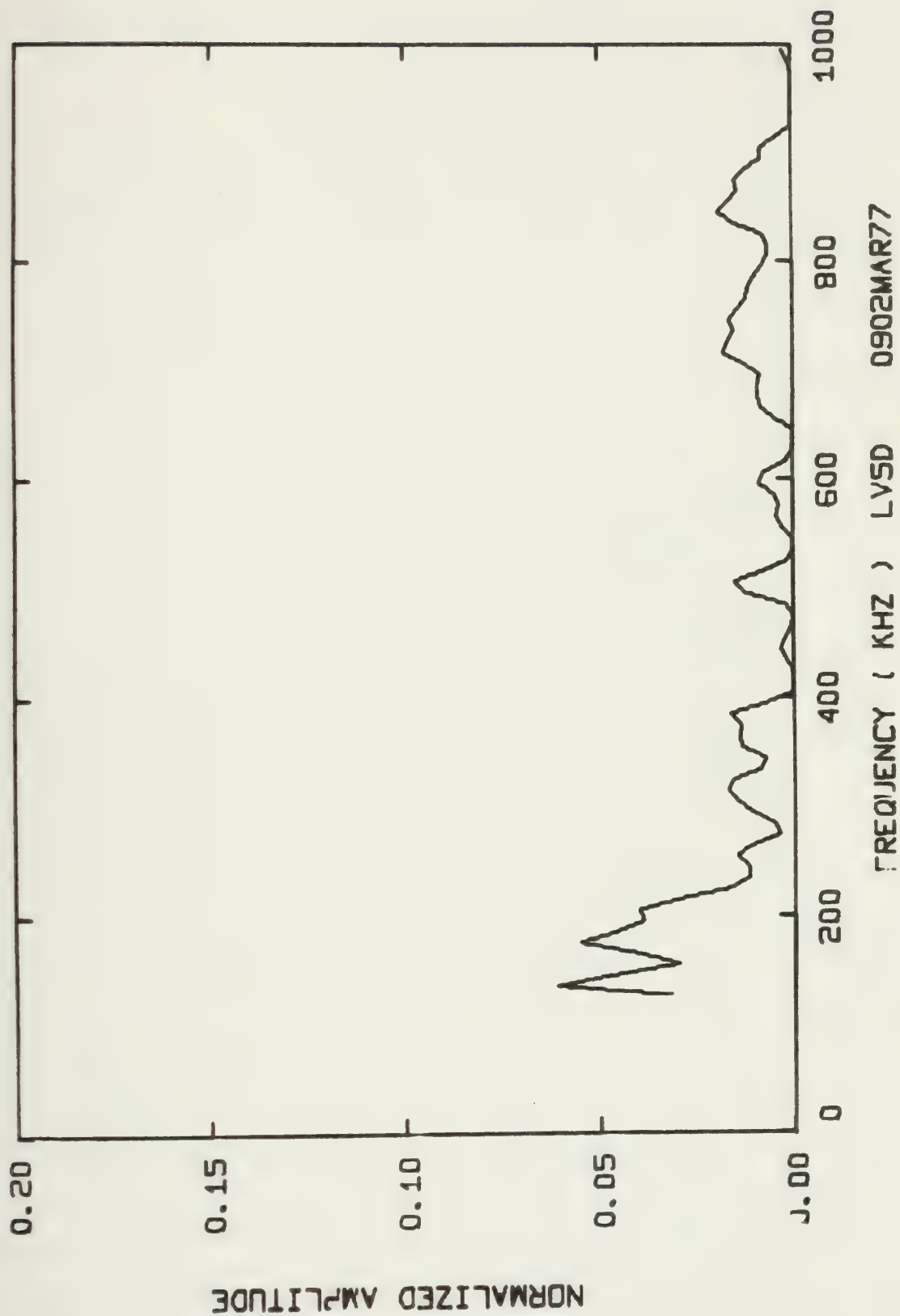




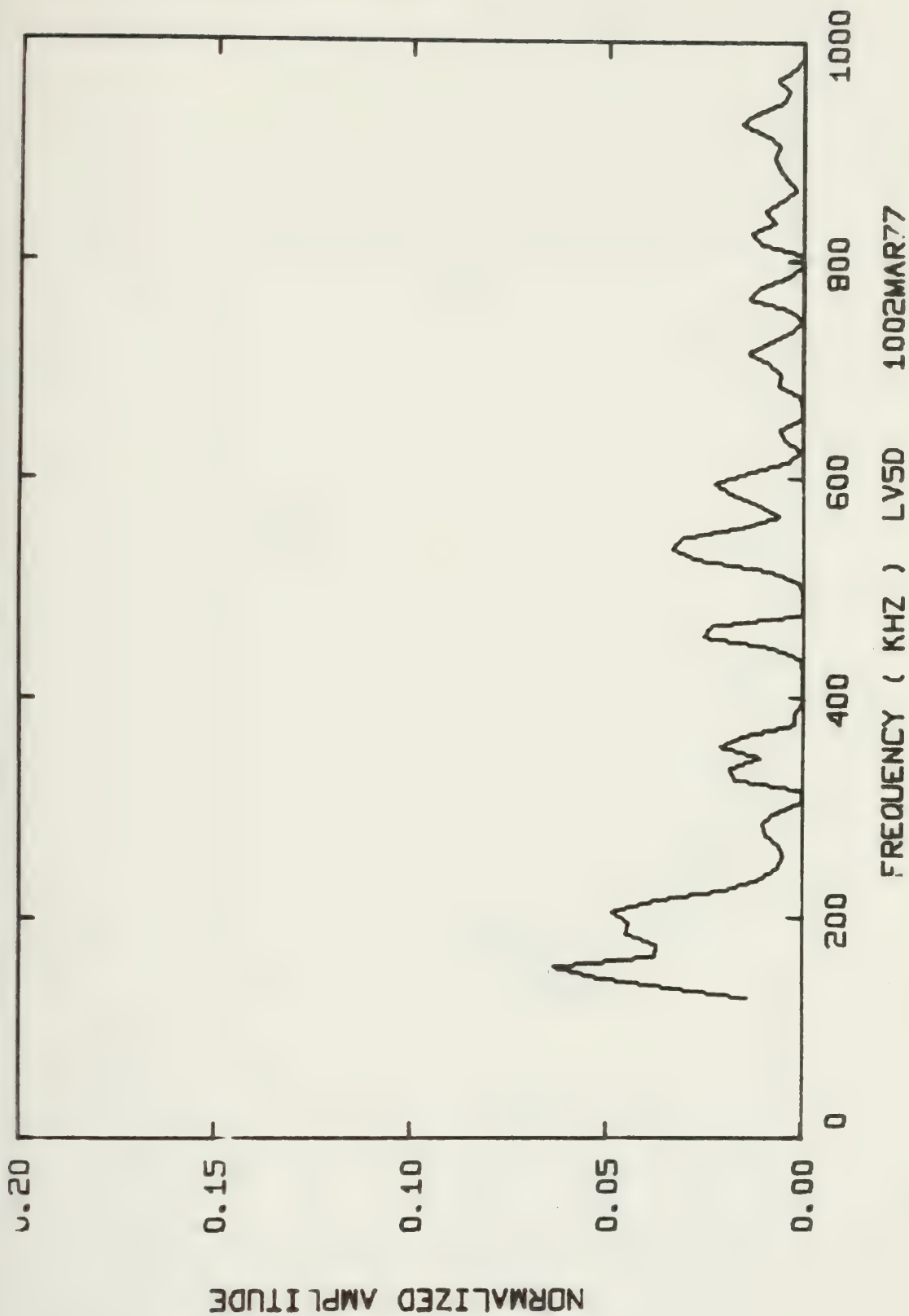




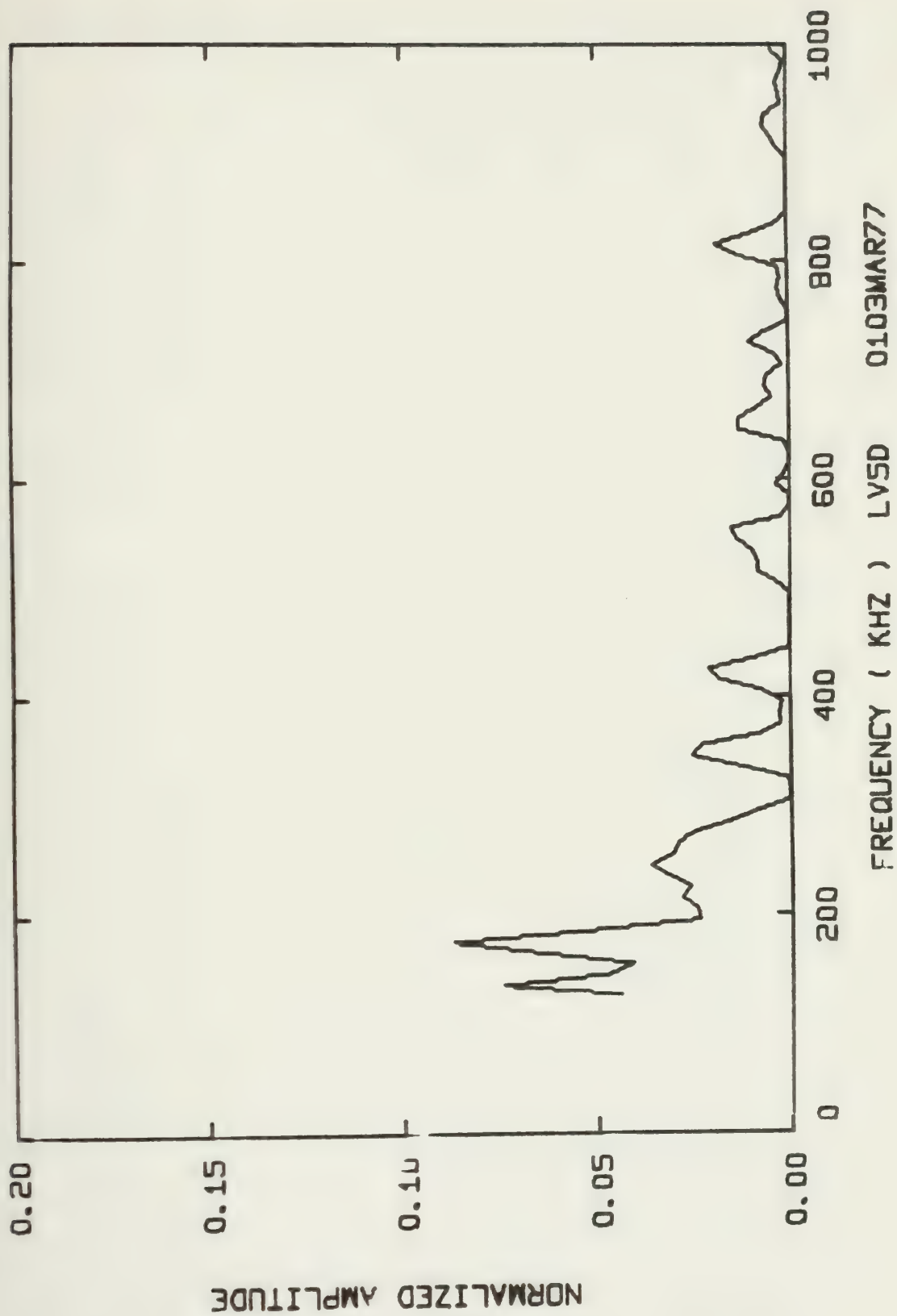




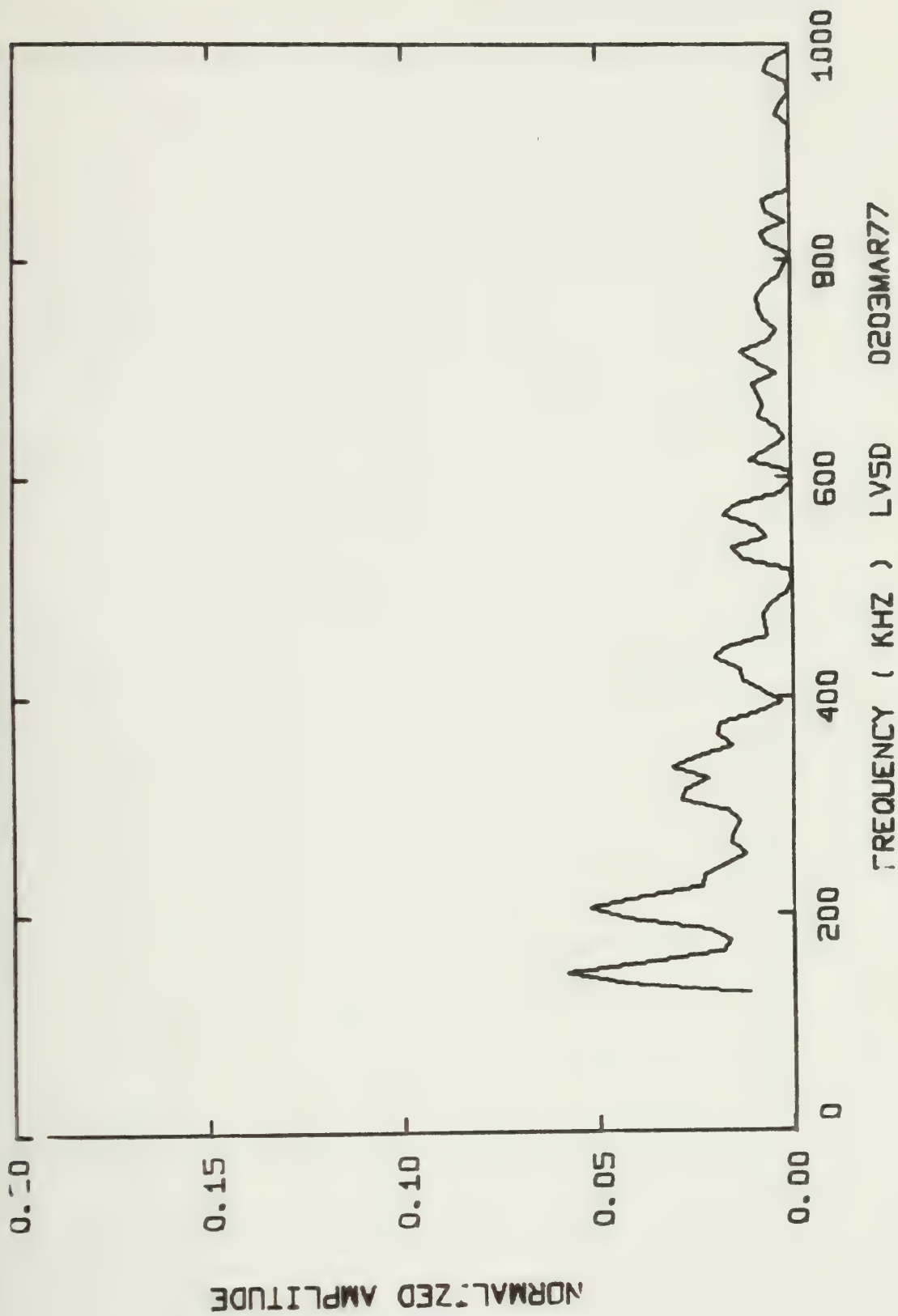






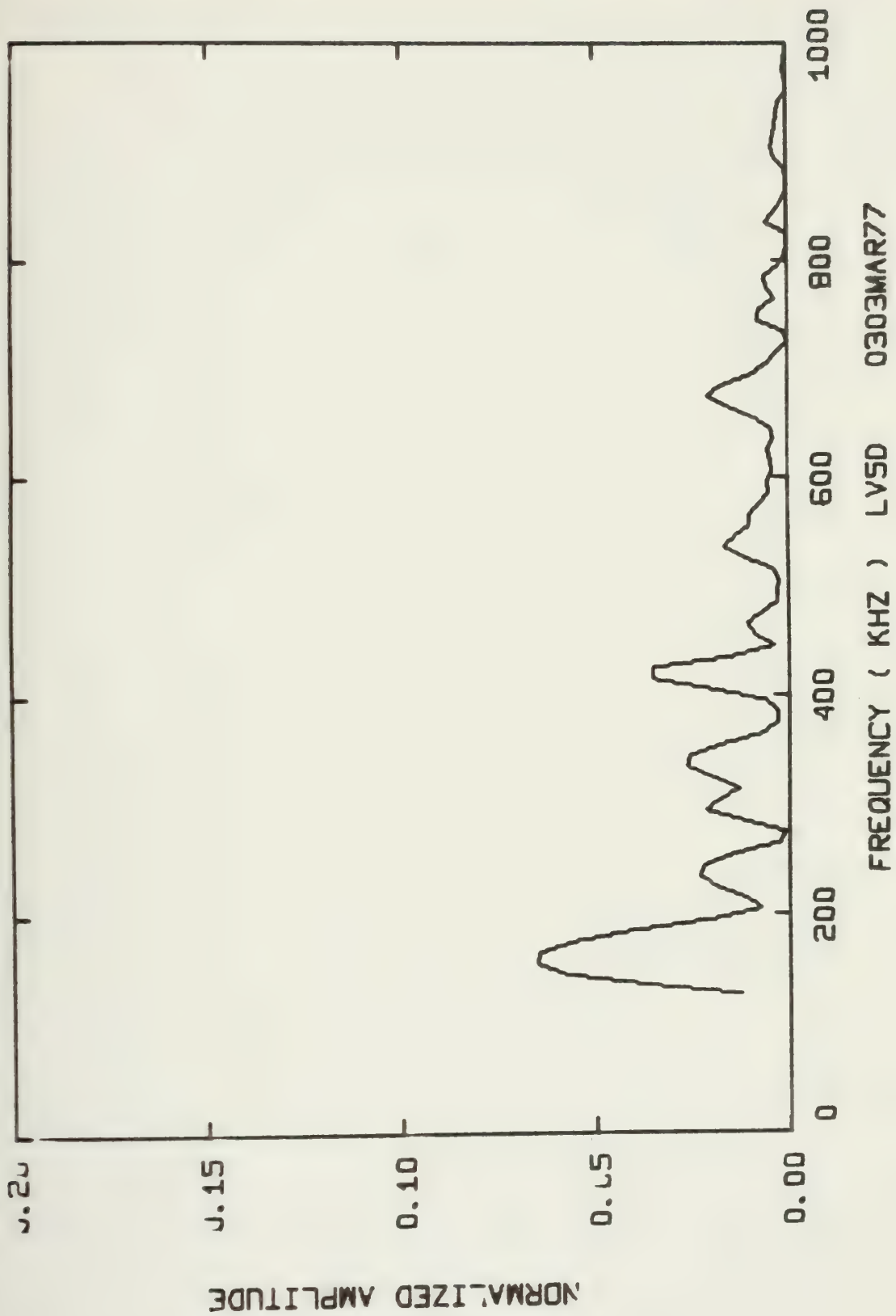




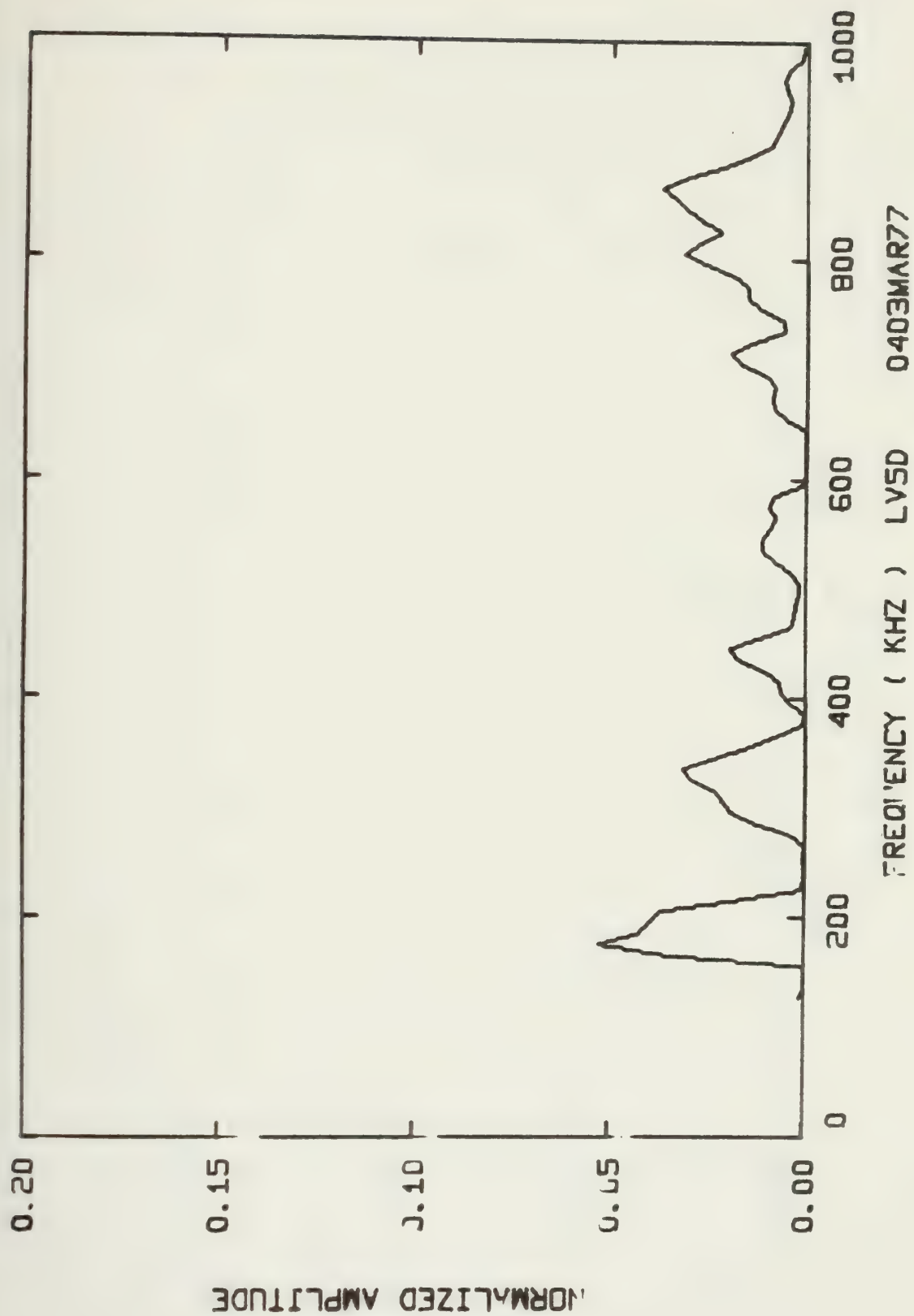




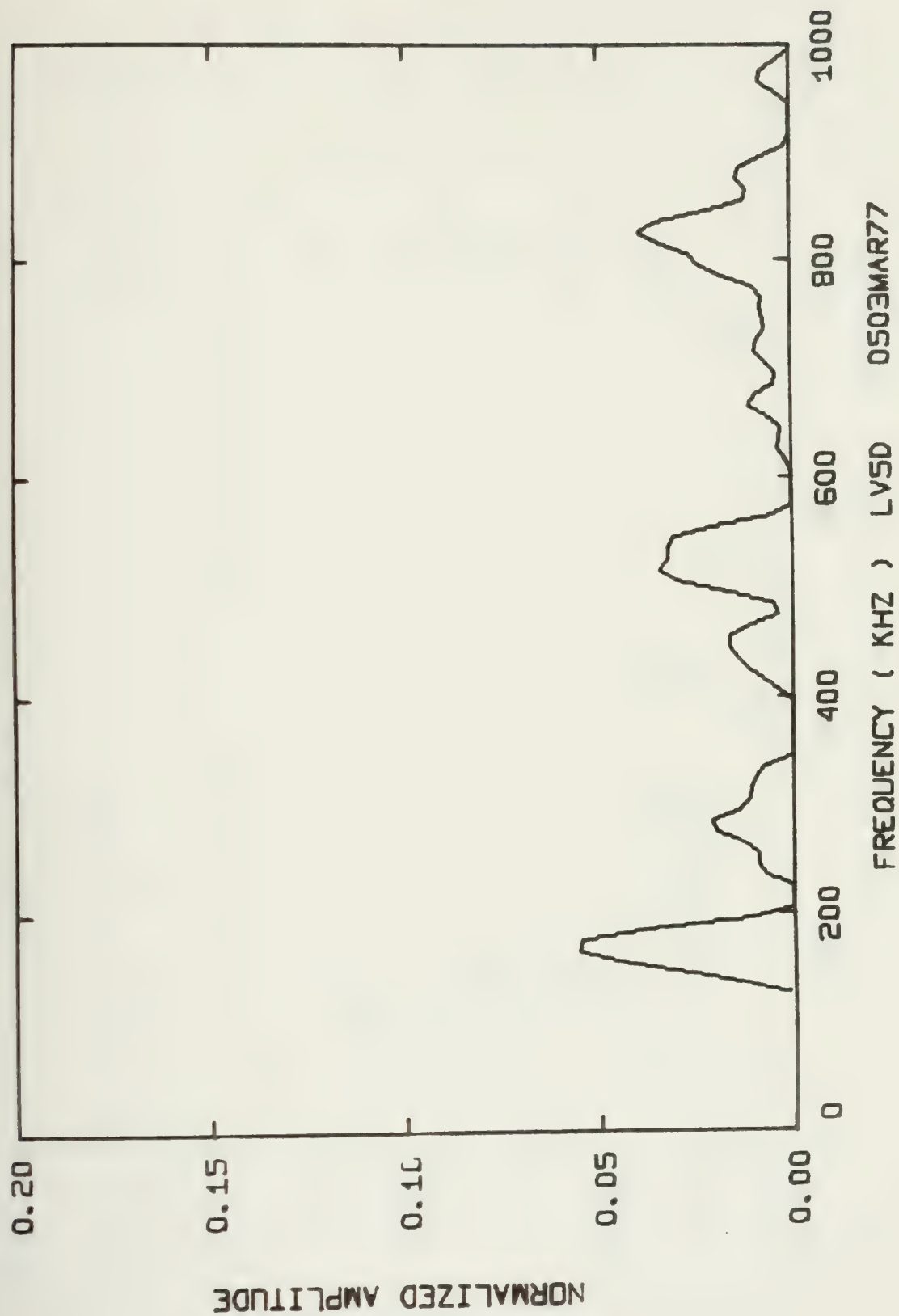




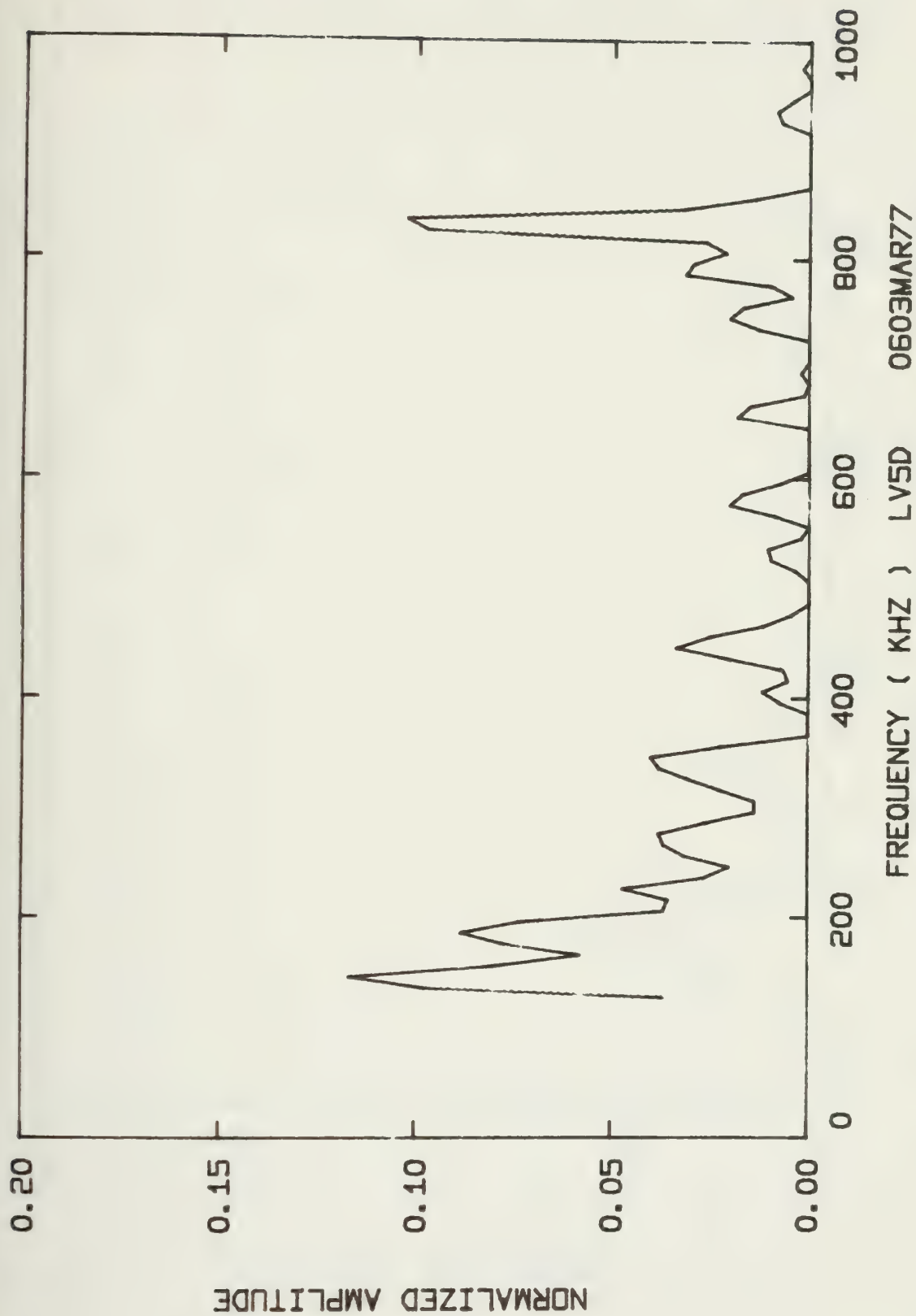






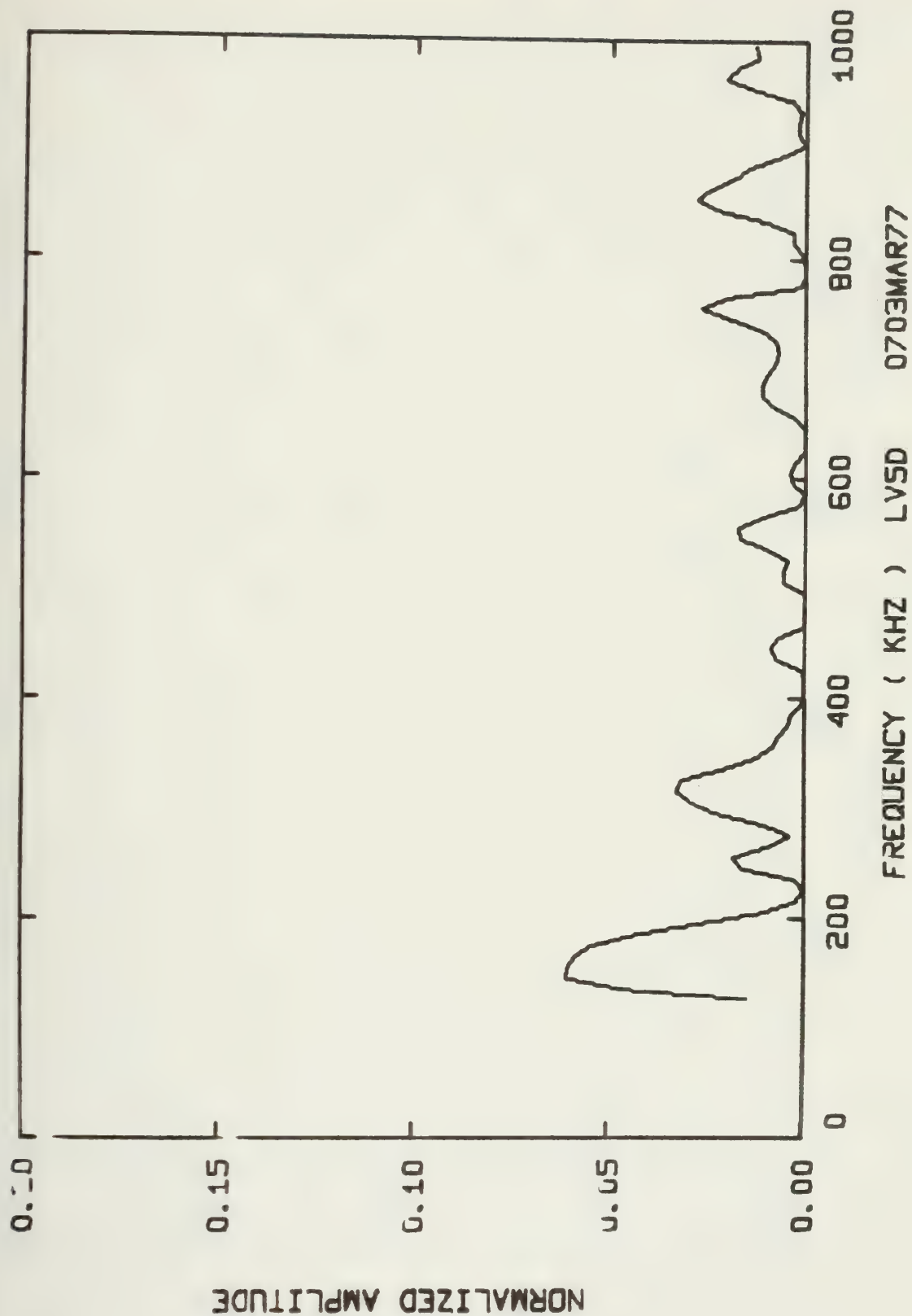




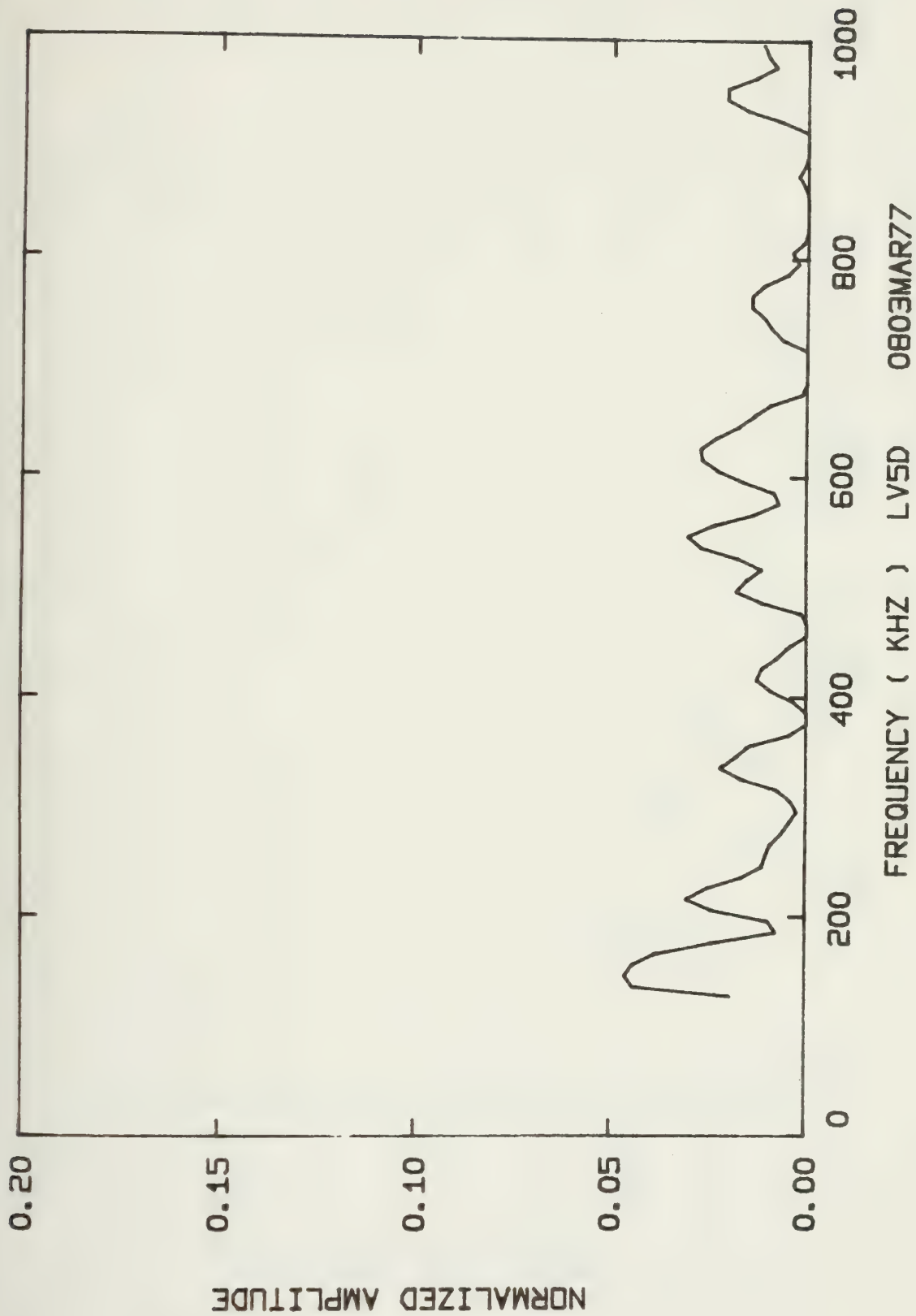




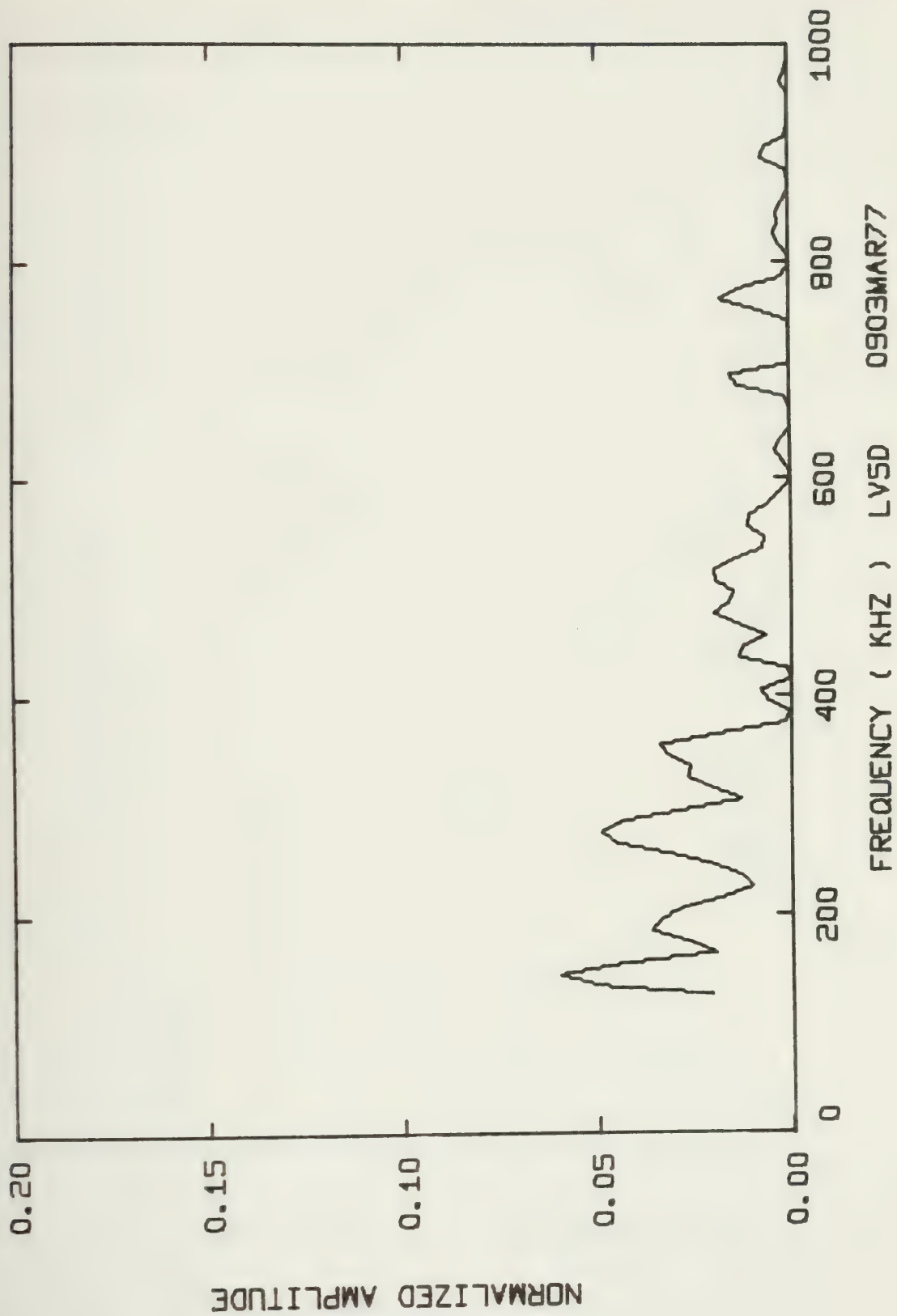




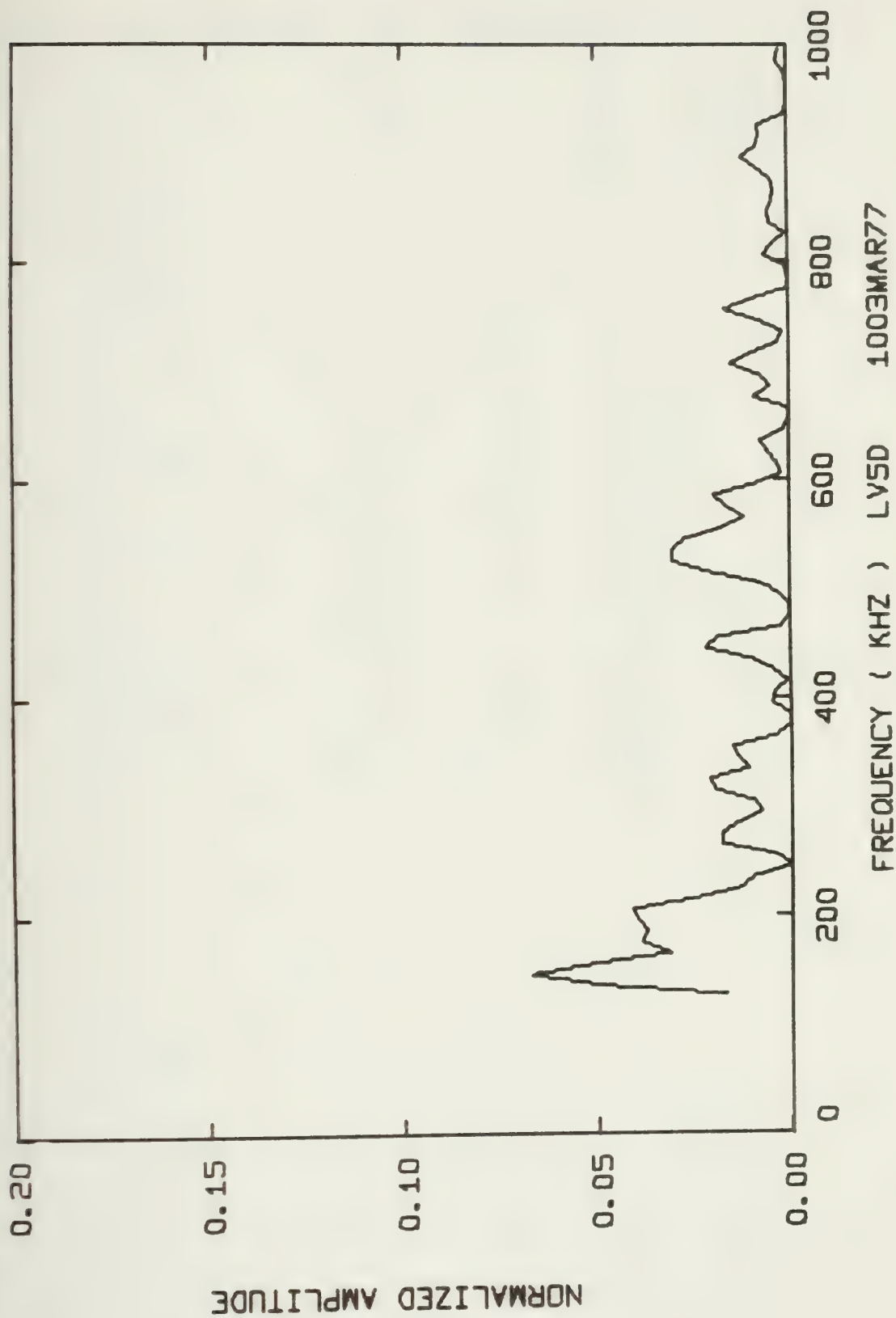












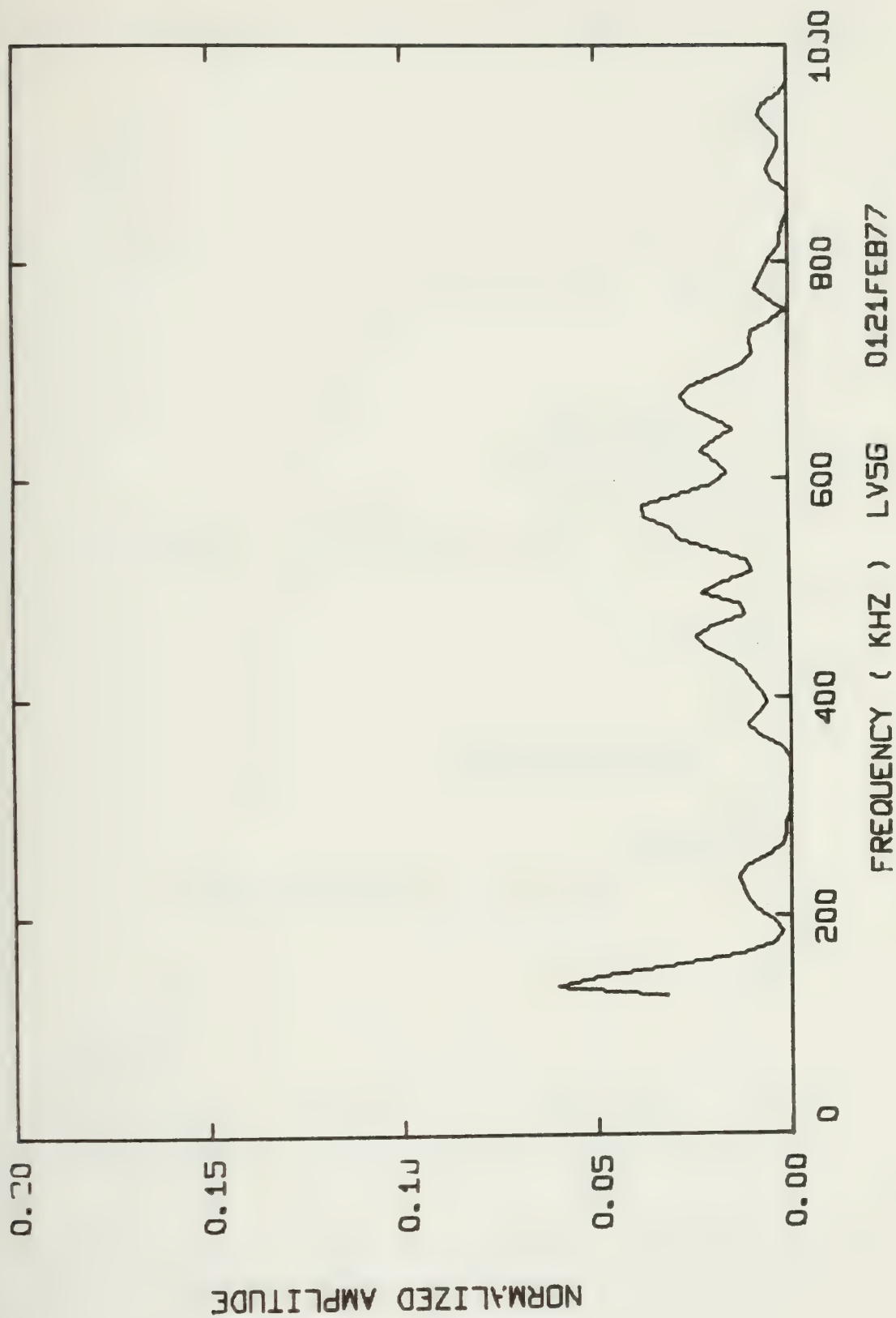




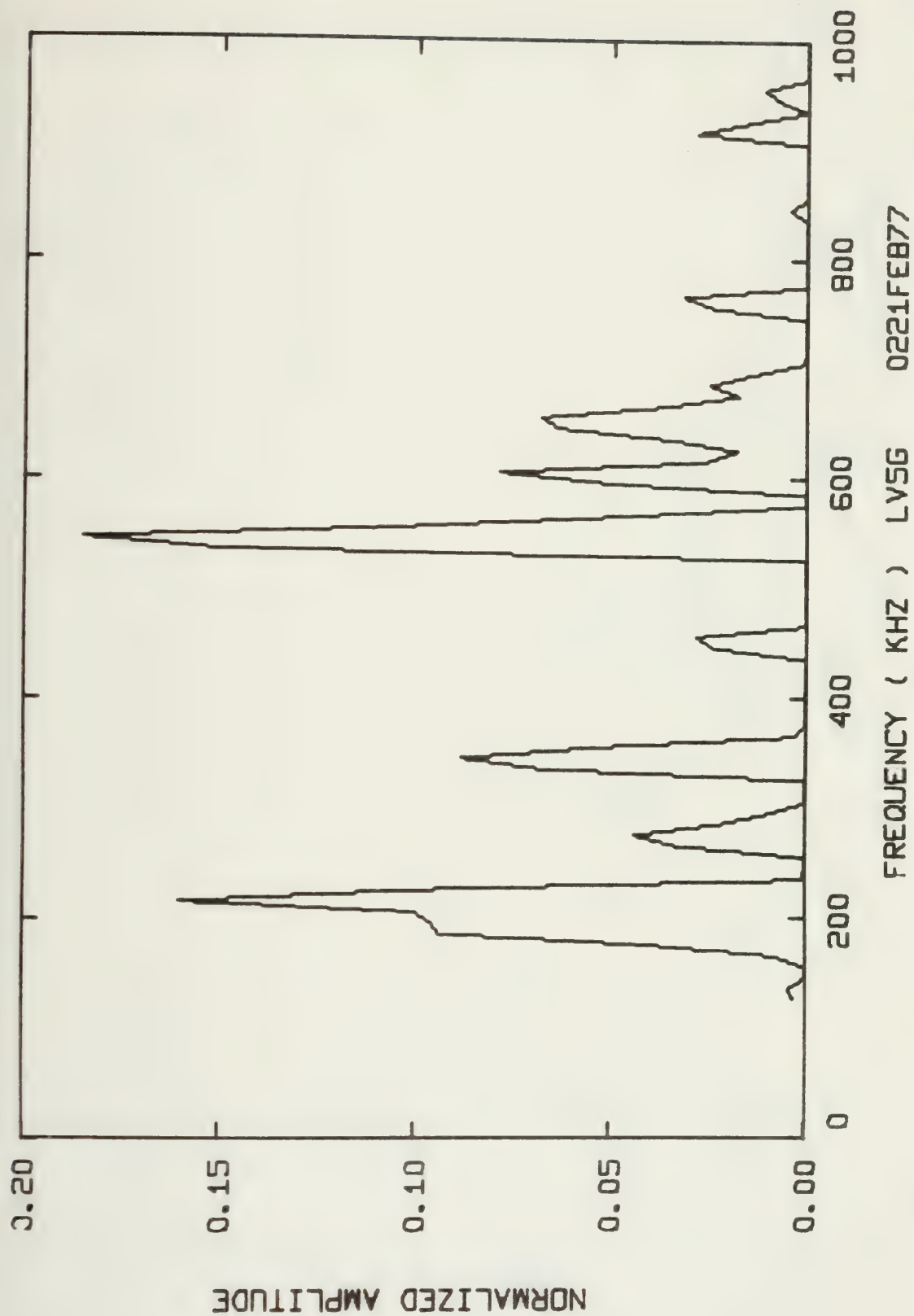
Summary of Energy per Acoustic Emission and RMS Pressure  
Across the Transducer's Face for Each Spectra

Spectral Distrib. Graph Code Number	Energy per AE (Joules)	RMS Pressure Across Face of Transducer (Pa x 10 <sup>5</sup> )
LV5G 0121FEB77	15.358 x 10 <sup>-9</sup>	46.97
0221FEB77	26.557 x 10 <sup>-9</sup>	31.49
0321FEB77	106.74 x 10 <sup>-9</sup>	66.56
0421FEB77	27.987 x 10 <sup>-9</sup>	52.45
0124FEB77	34.576 x 10 <sup>-9</sup>	49.45
0224FEB77	3.7373 x 10 <sup>-9</sup>	22.33
0324FEB77	45.547 x 10 <sup>-9</sup>	56.76
0424FEB77	42.060 x 10 <sup>-9</sup>	52.96
0524FEB77	215.36 x 10 <sup>-9</sup>	81.87
0624FEB77	50.140 x 10 <sup>-9</sup>	54.09
0724FEB77	36.707 x 10 <sup>-9</sup>	58.54
0824FEB77	513.01 x 10 <sup>-9</sup>	98.87

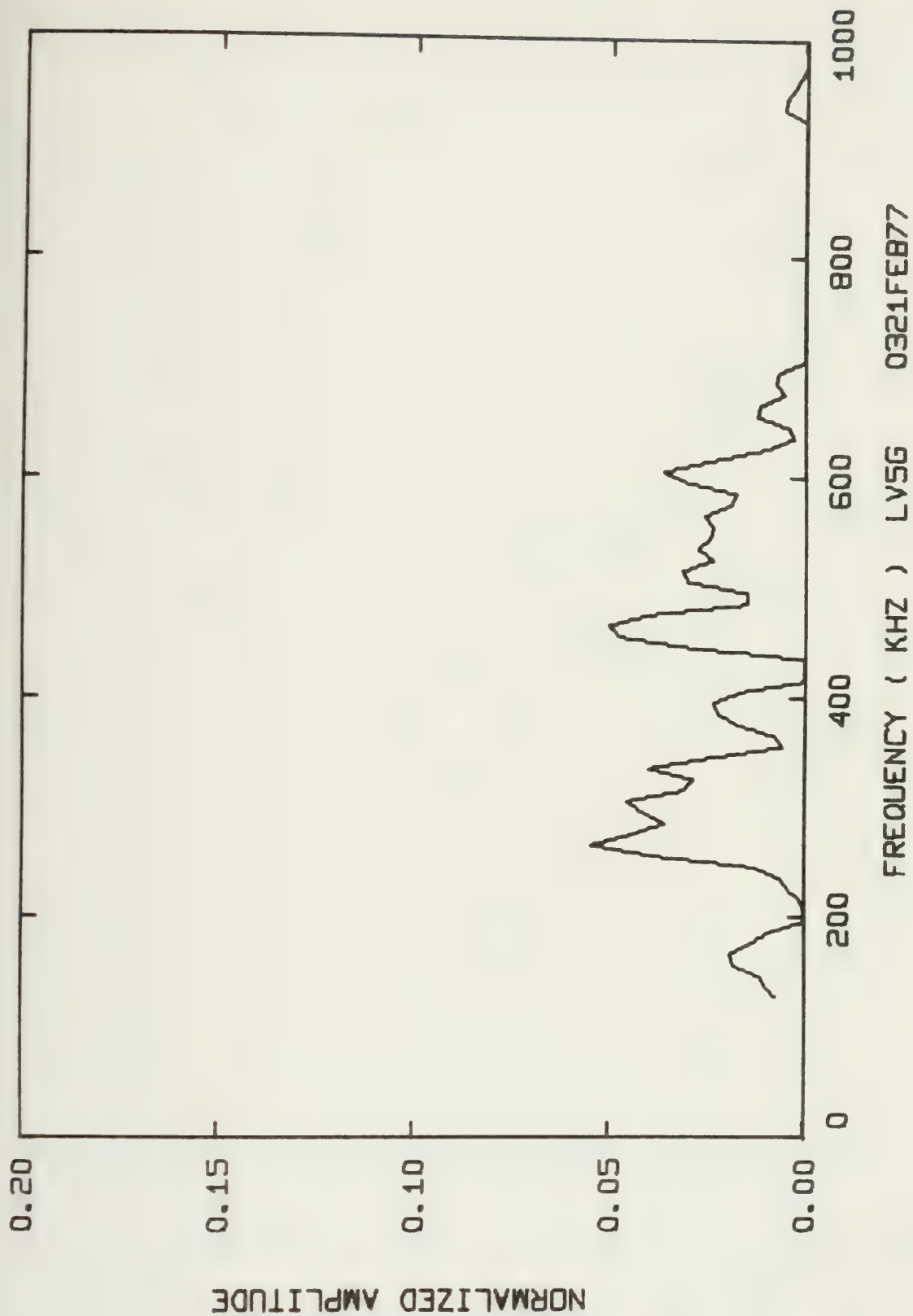






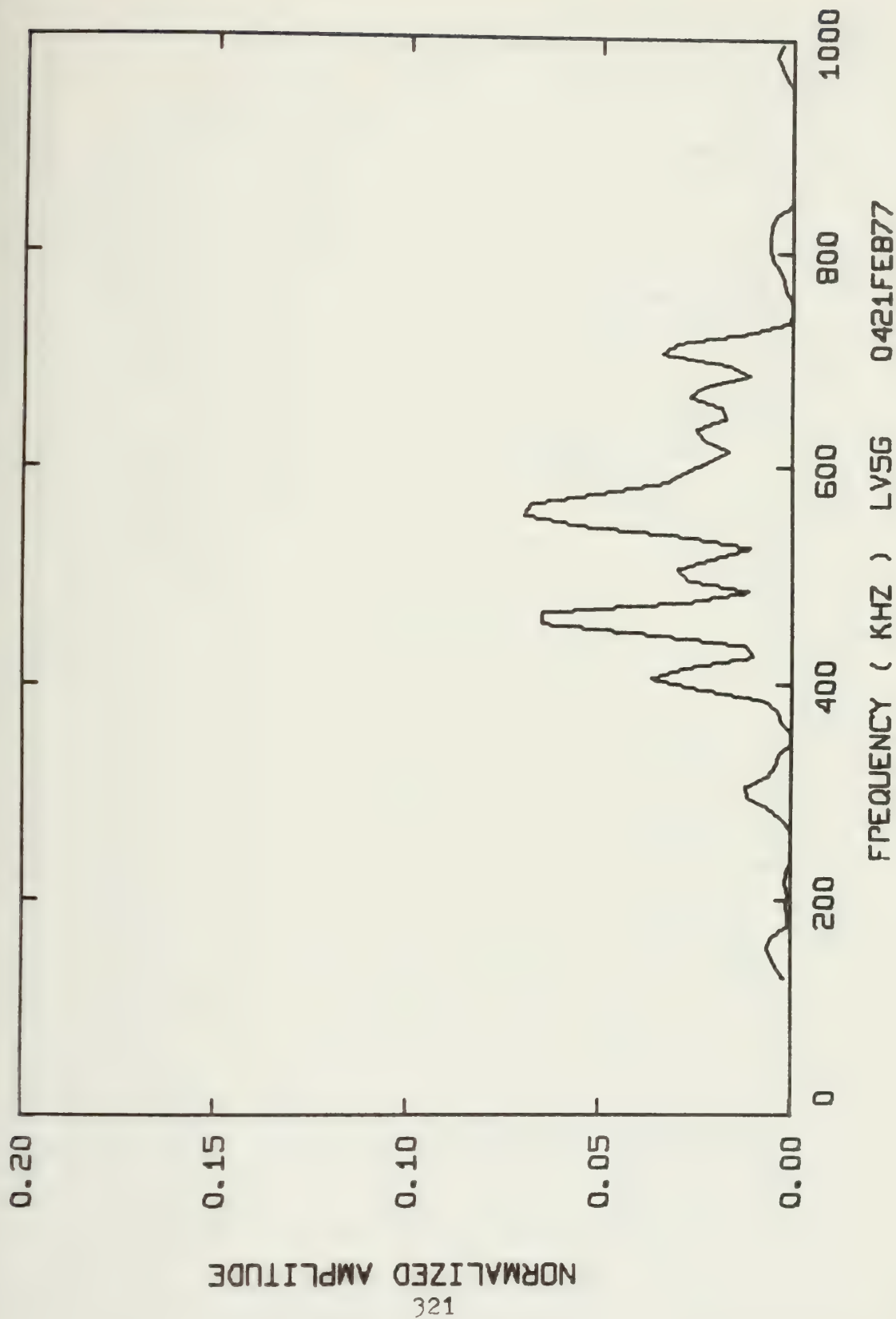




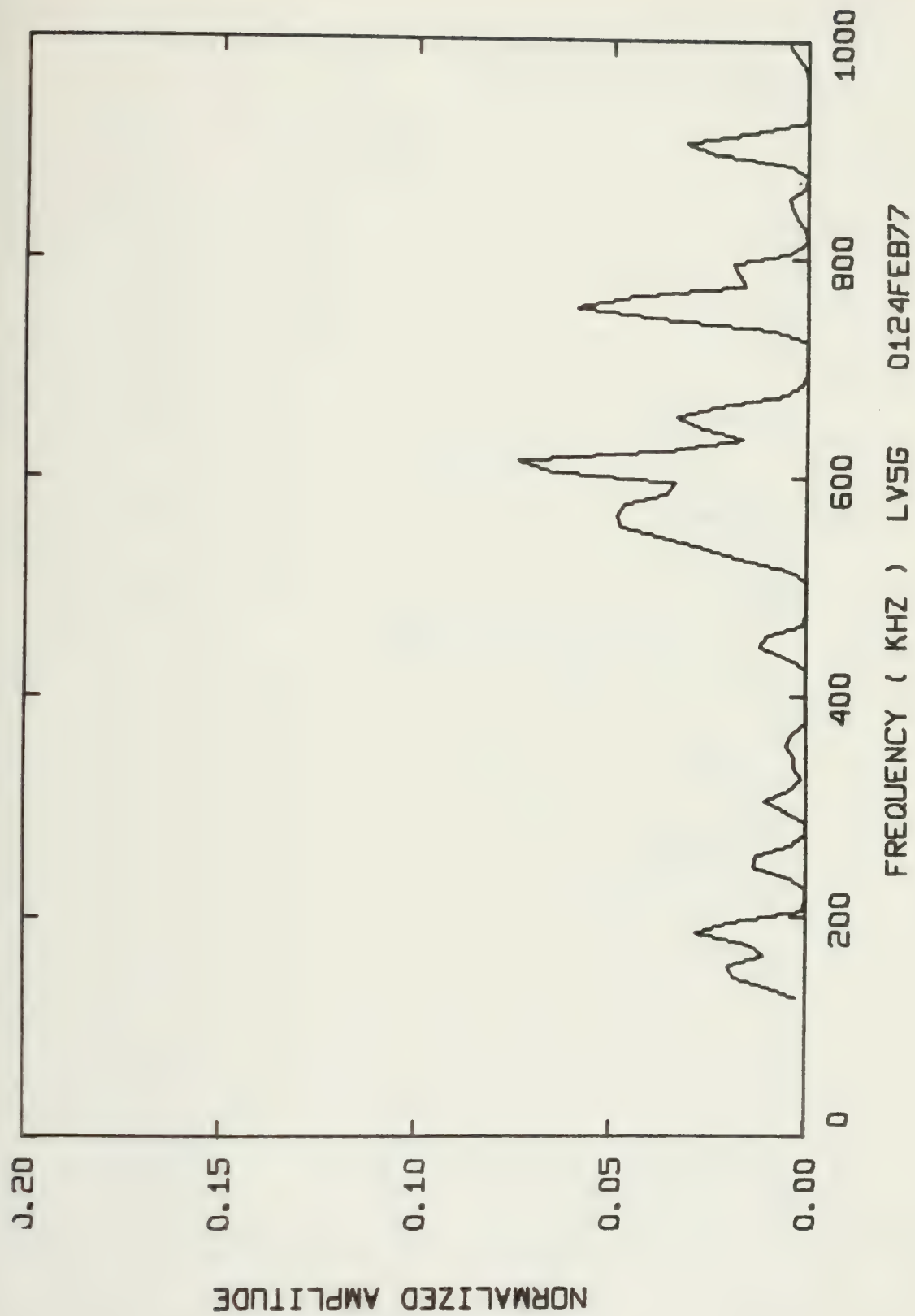




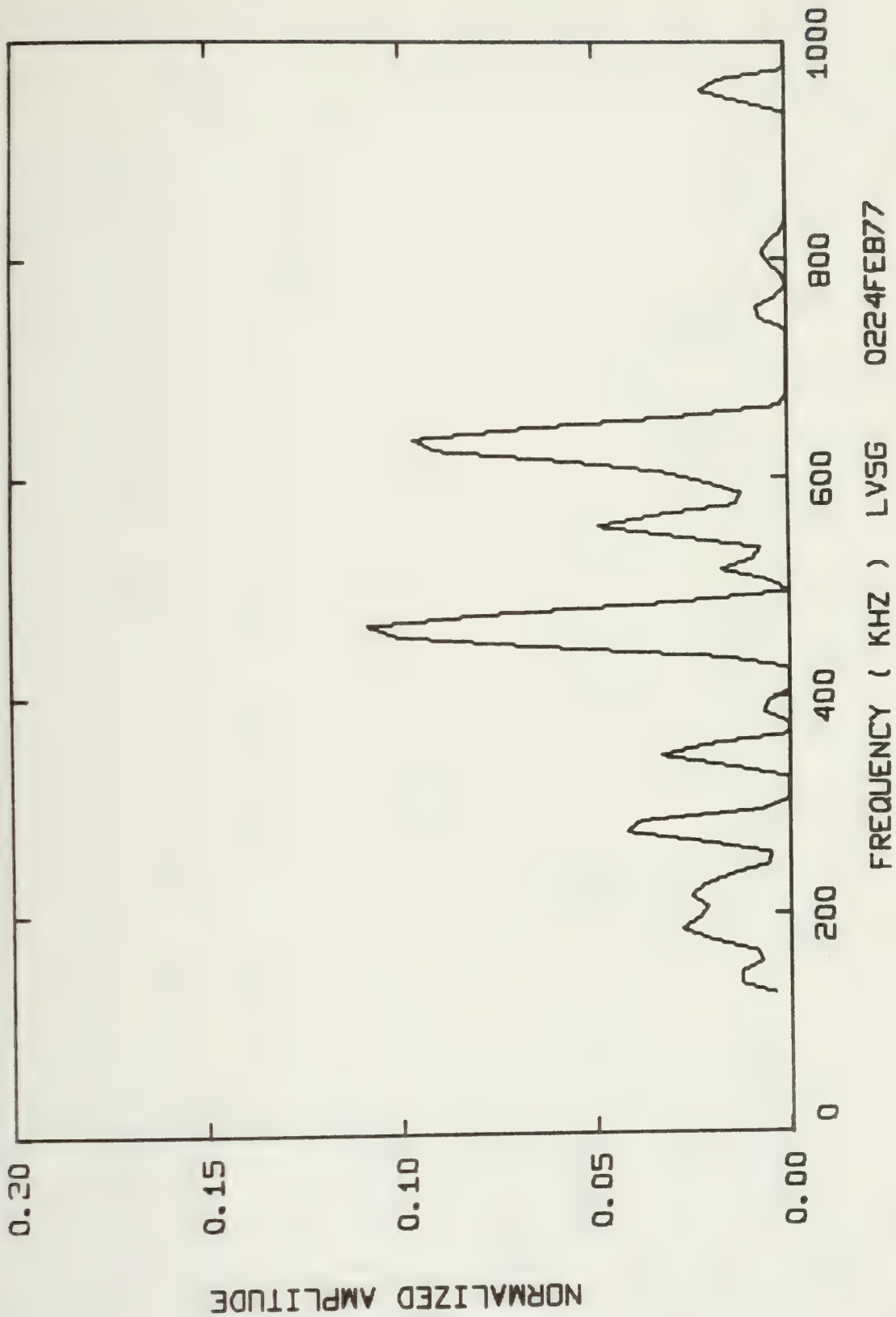




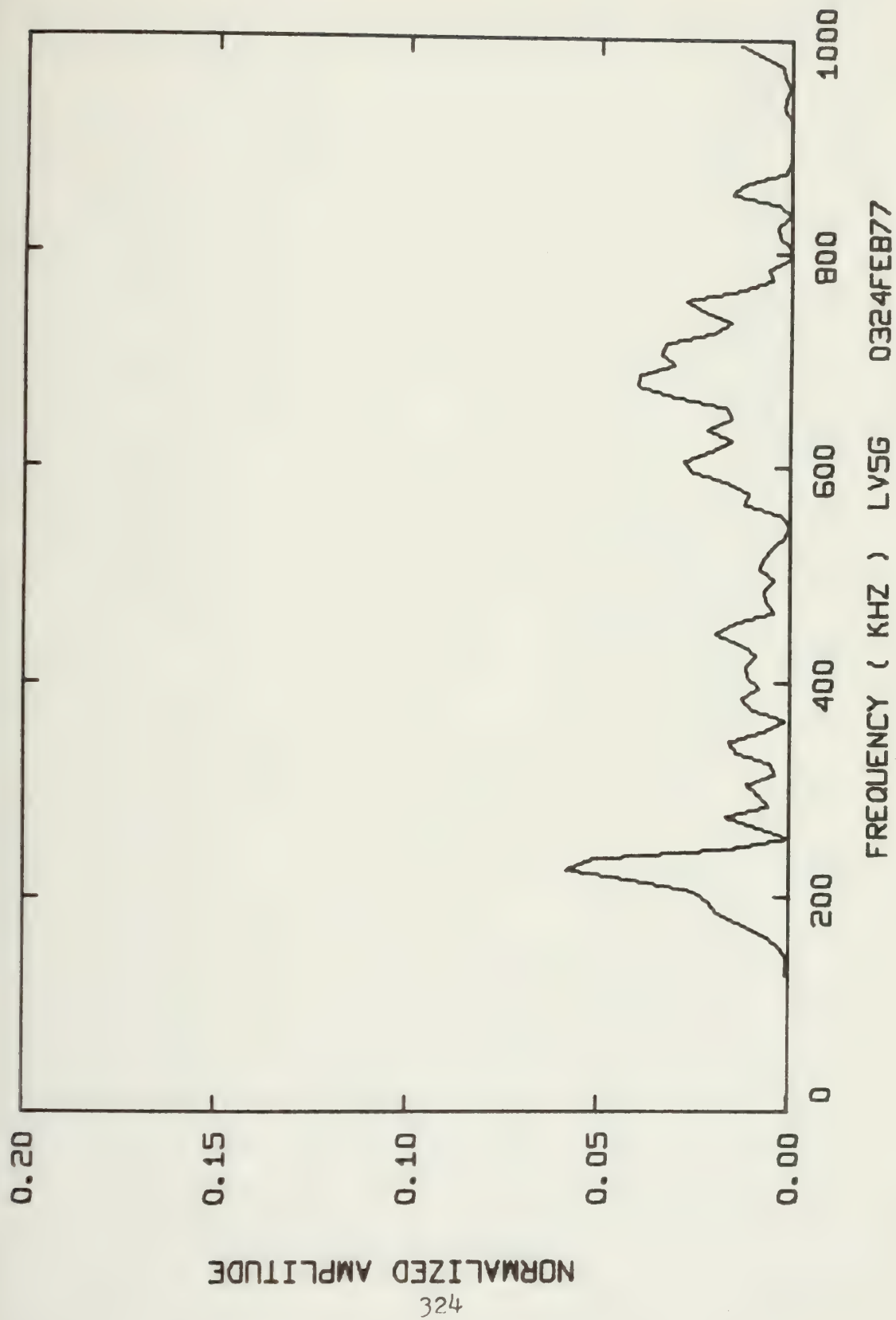






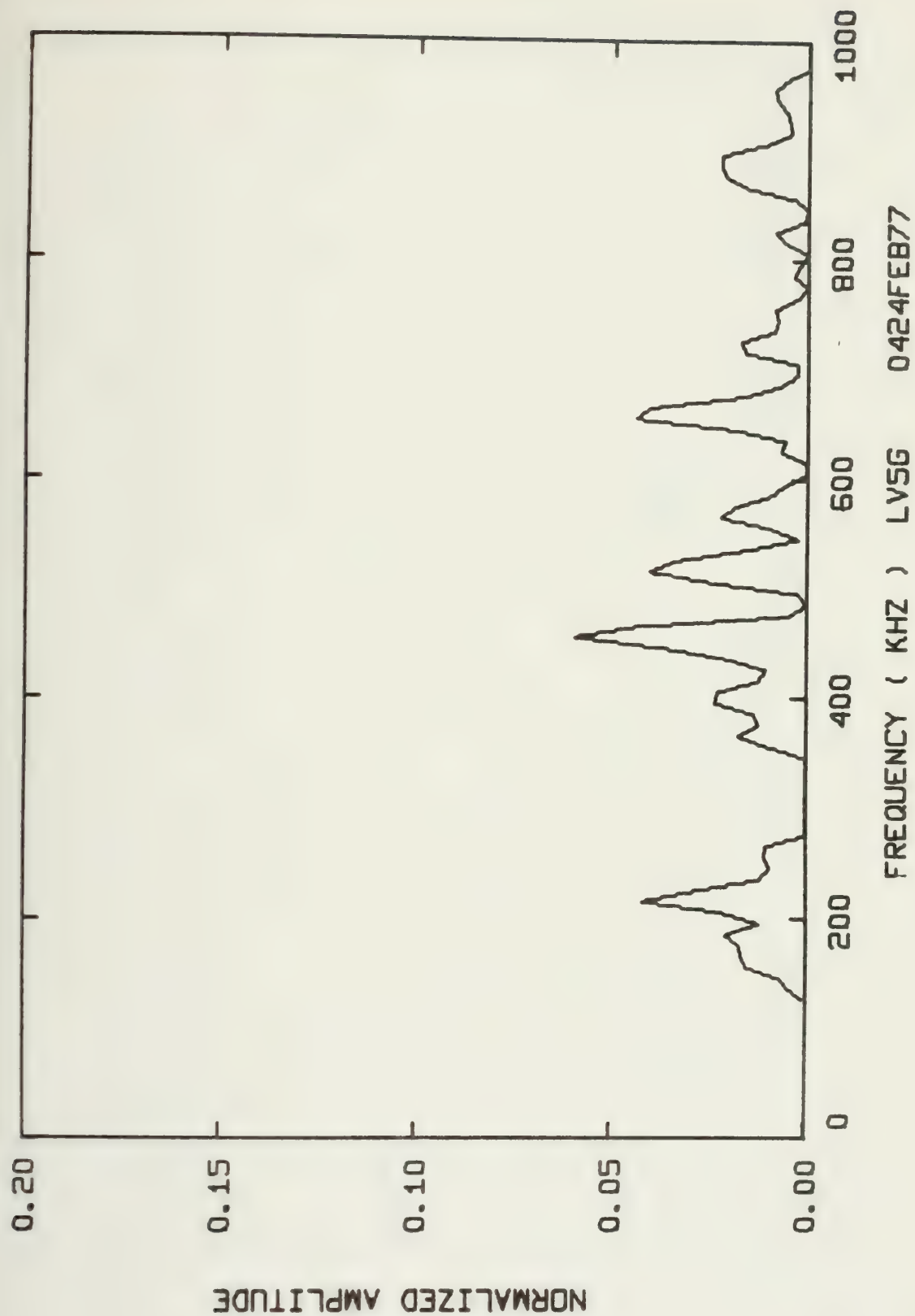




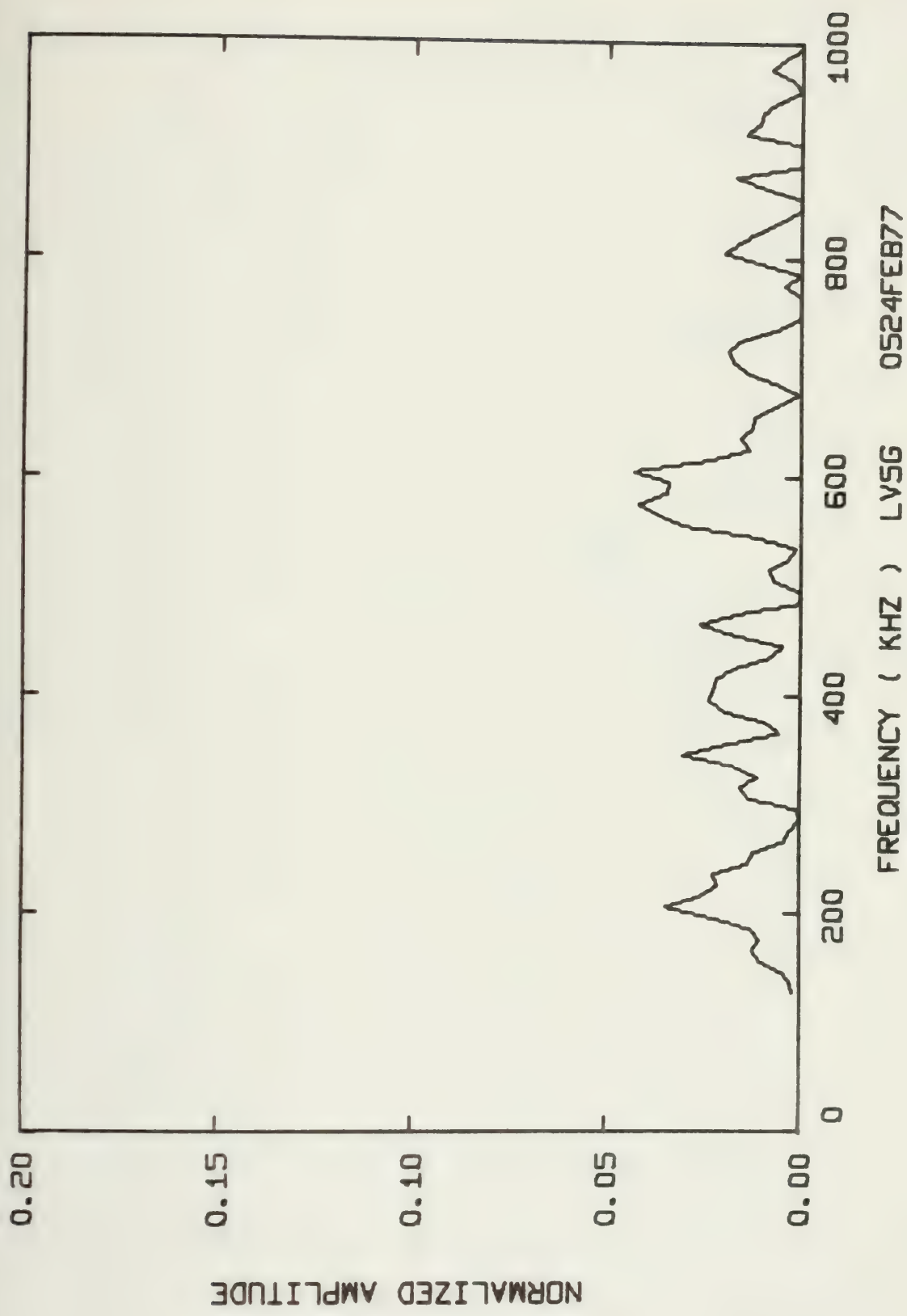




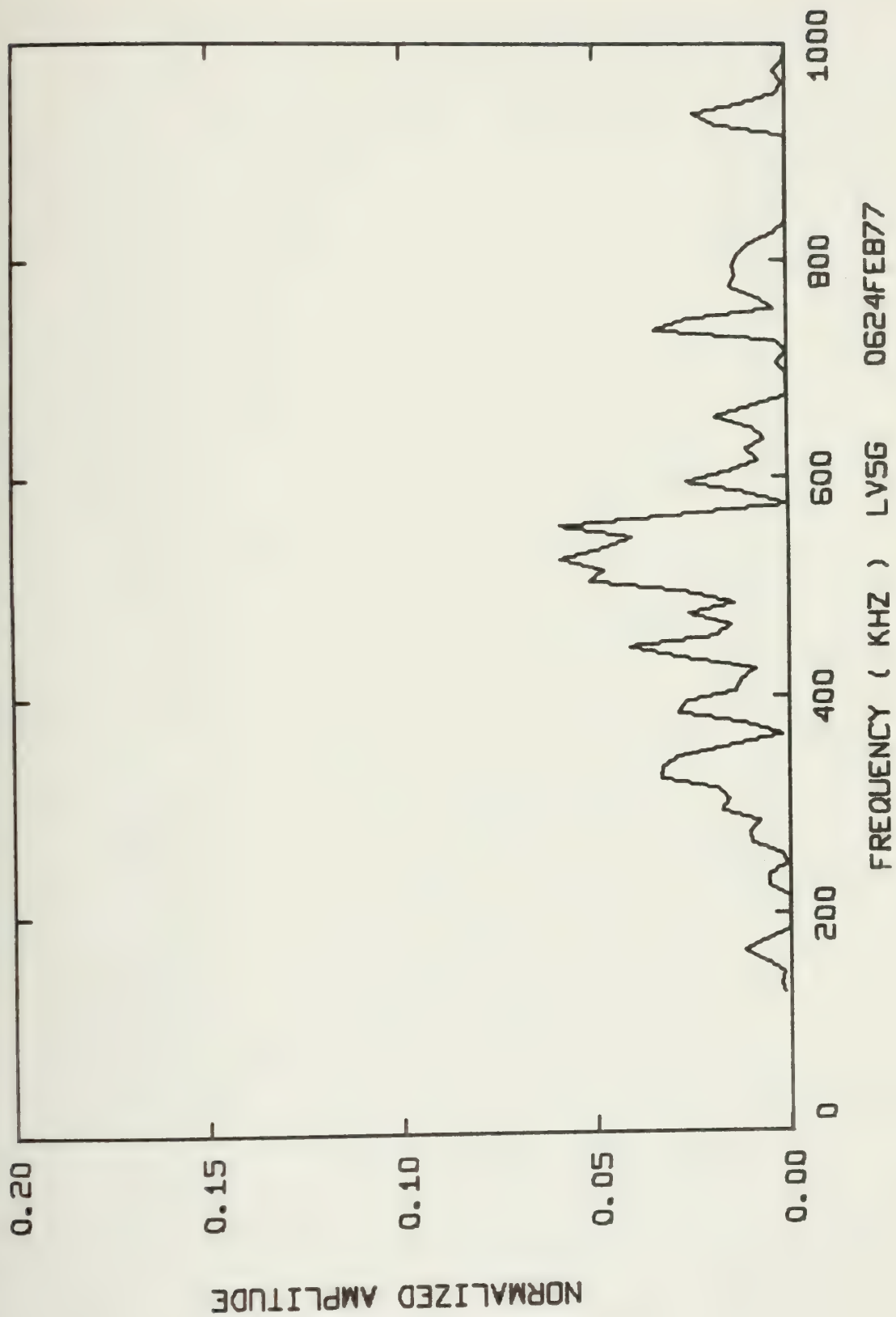




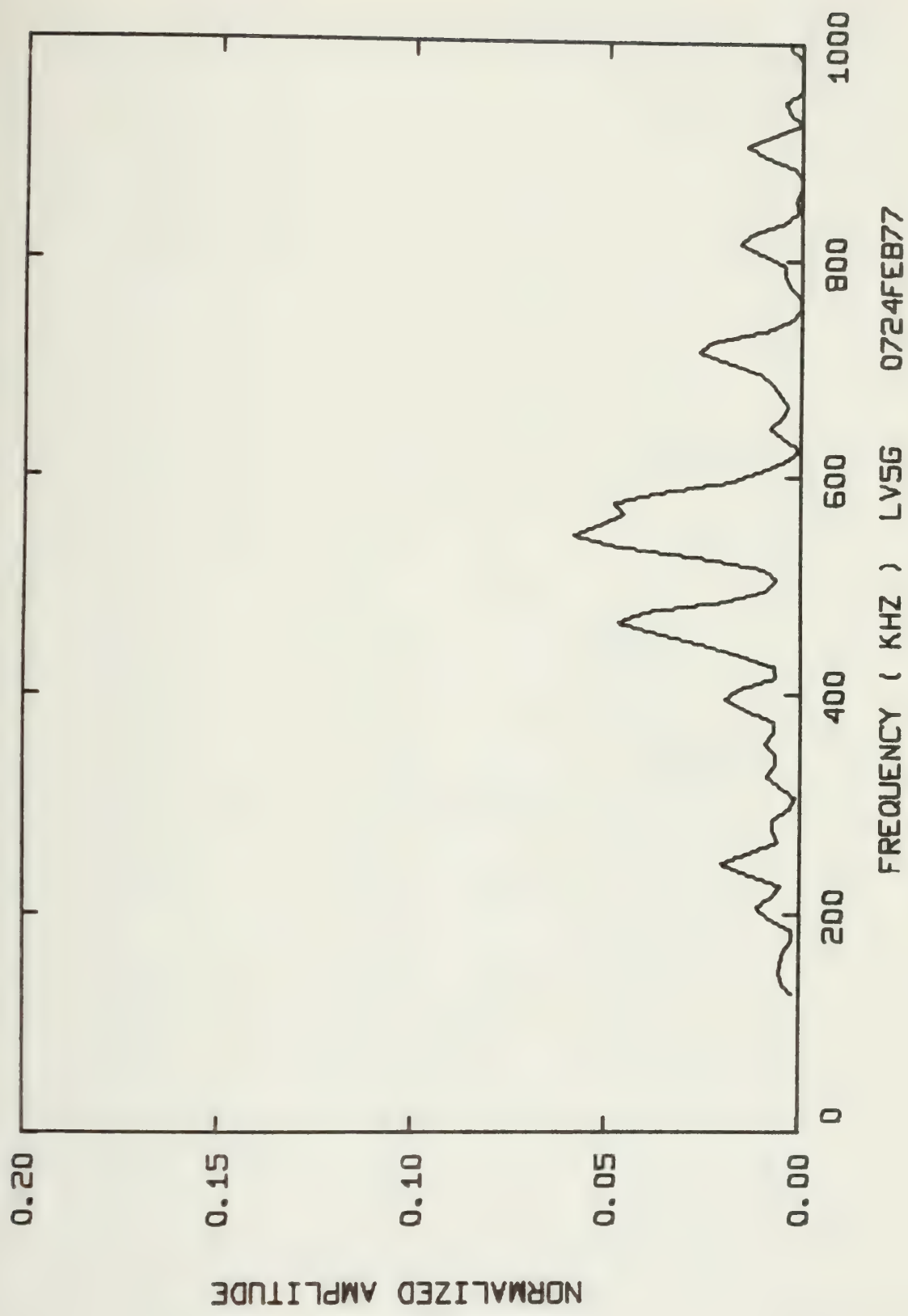






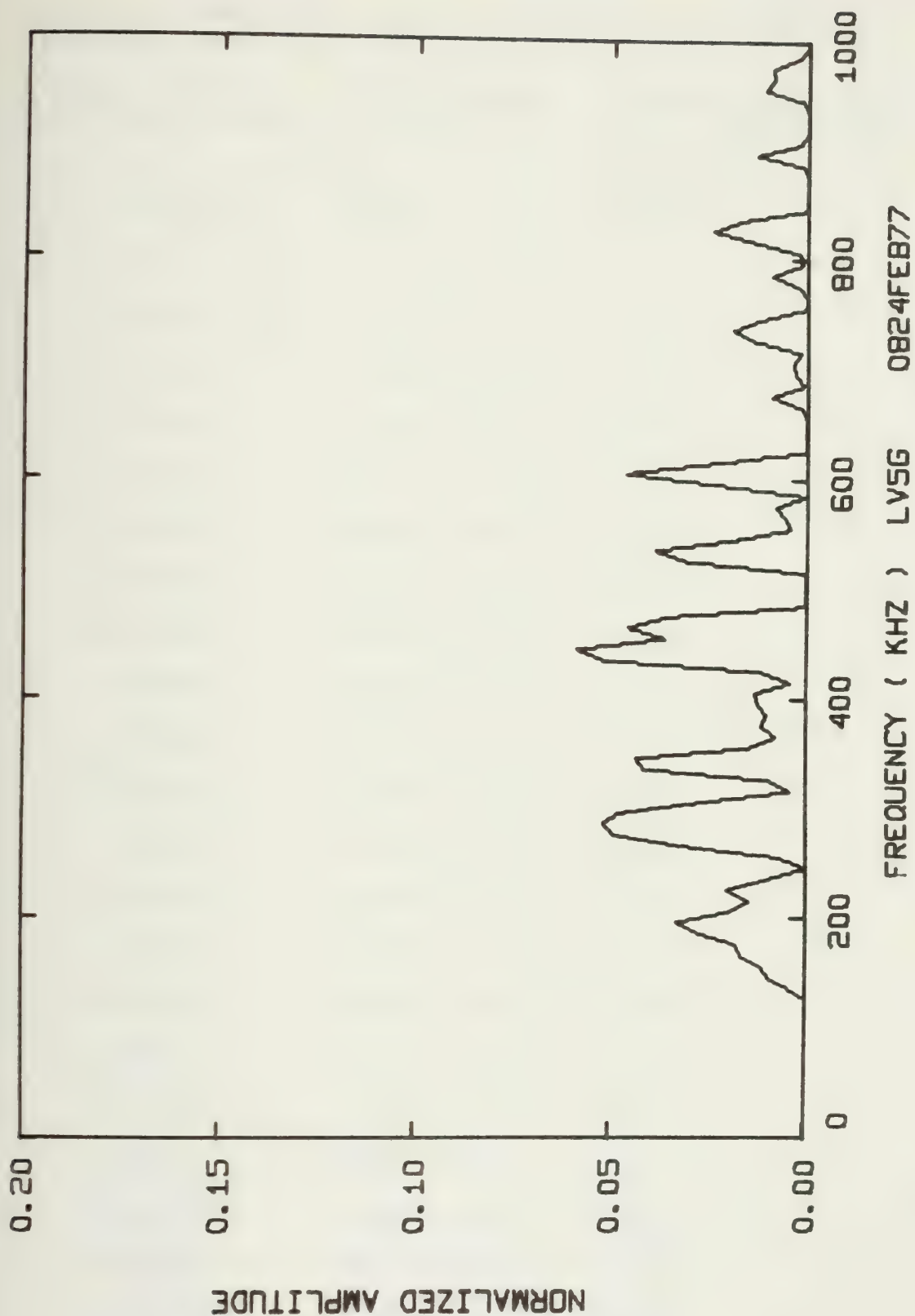














Summary of Energy per Acoustic Emission and RMS Pressure  
Across the Transducer's Face for Each Spectra

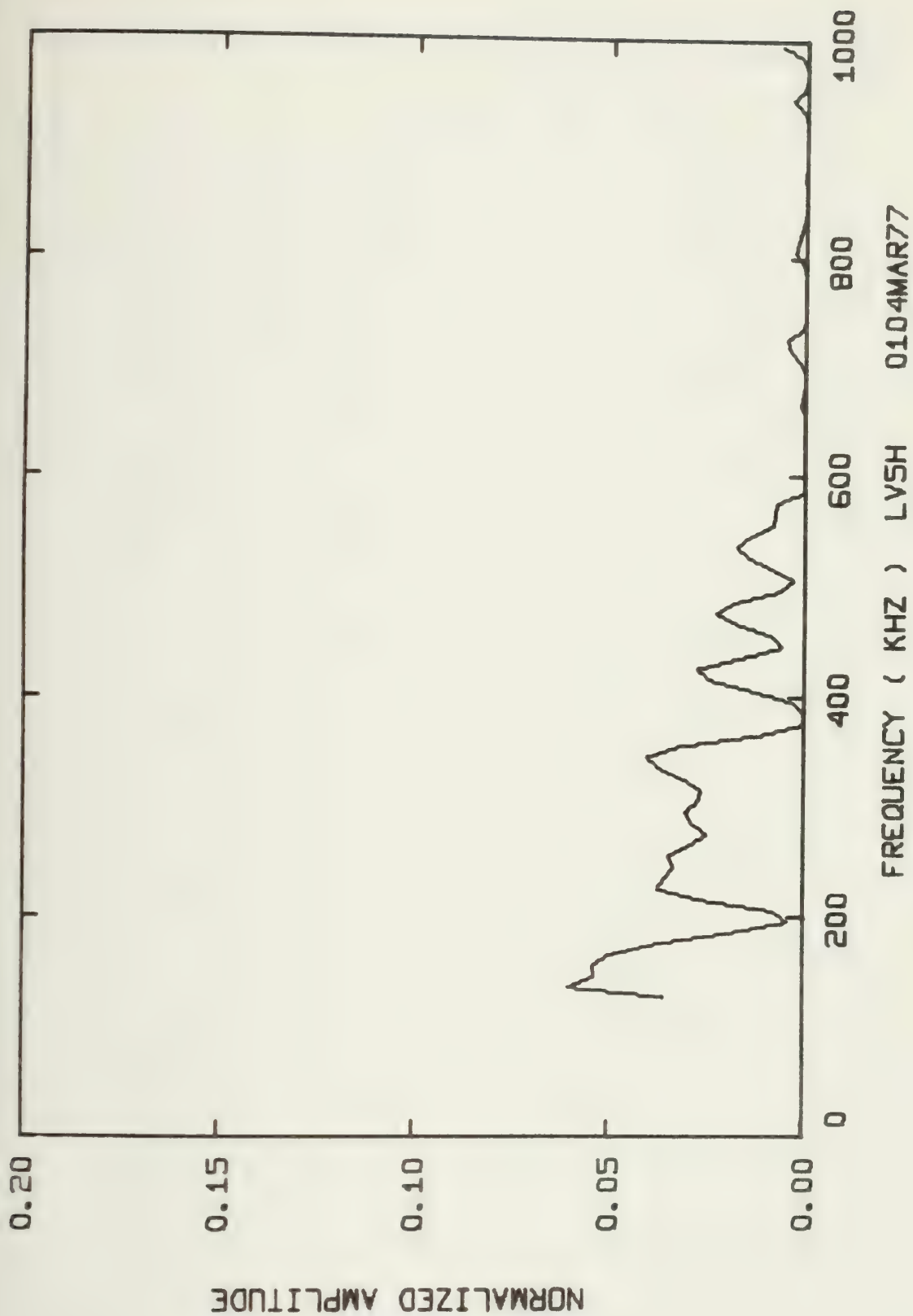
Spectral Distrib. Graph Code Number	Energy per AE (Joules)	RMS Pressure Across Face of Transducer (Pa x 10 <sup>5</sup> )
LV5H 0104MAR77	26.764 x 10 <sup>-9</sup>	54.22
0204MAR77	31.657 x 10 <sup>-9</sup>	59.32
0304MAR77	31.408 x 10 <sup>-9</sup>	60.54
0404MAR77	8.4216 x 10 <sup>-9</sup>	33.52
0504MAR77	23.627 x 10 <sup>-9</sup>	50.94
0604MAR77	38.571 x 10 <sup>-9</sup>	65.09
0704MAR77	10.352 x 10 <sup>-9</sup>	37.16
0804MAR77	14.012 x 10 <sup>-9</sup>	43.23
0904MAR77	16.728 x 10 <sup>-9</sup>	47.24
1004MAR77	84.079 x 10 <sup>-9</sup>	67.17
1104MAR77	41.115 x 10 <sup>-9</sup>	67.20
1204MAR77	19.924 x 10 <sup>-9</sup>	58.16
1304MAR77	39.082 x 10 <sup>-9</sup>	65.14
0108MAR77	26.854 x 10 <sup>-9</sup>	52.78
0208MAR77	19.545 x 10 <sup>-9</sup>	45.03
0308MAR77	29.020 x 10 <sup>-9</sup>	53.41
0408MAR77	14.253 x 10 <sup>-9</sup>	40.79
0508MAR77	17.506 x 10 <sup>-9</sup>	48.67
0608MAR77	16.465 x 10 <sup>-9</sup>	47.20
0708MAR77	16.016 x 10 <sup>-9</sup>	44.65
0808MAR77	27.133 x 10 <sup>-9</sup>	54.92
0908MAR77	28.643 x 10 <sup>-9</sup>	44.02



Summary of Energy per Acoustic Emission and RMS Pressure  
Across the Transducer's Face for Each Spectra

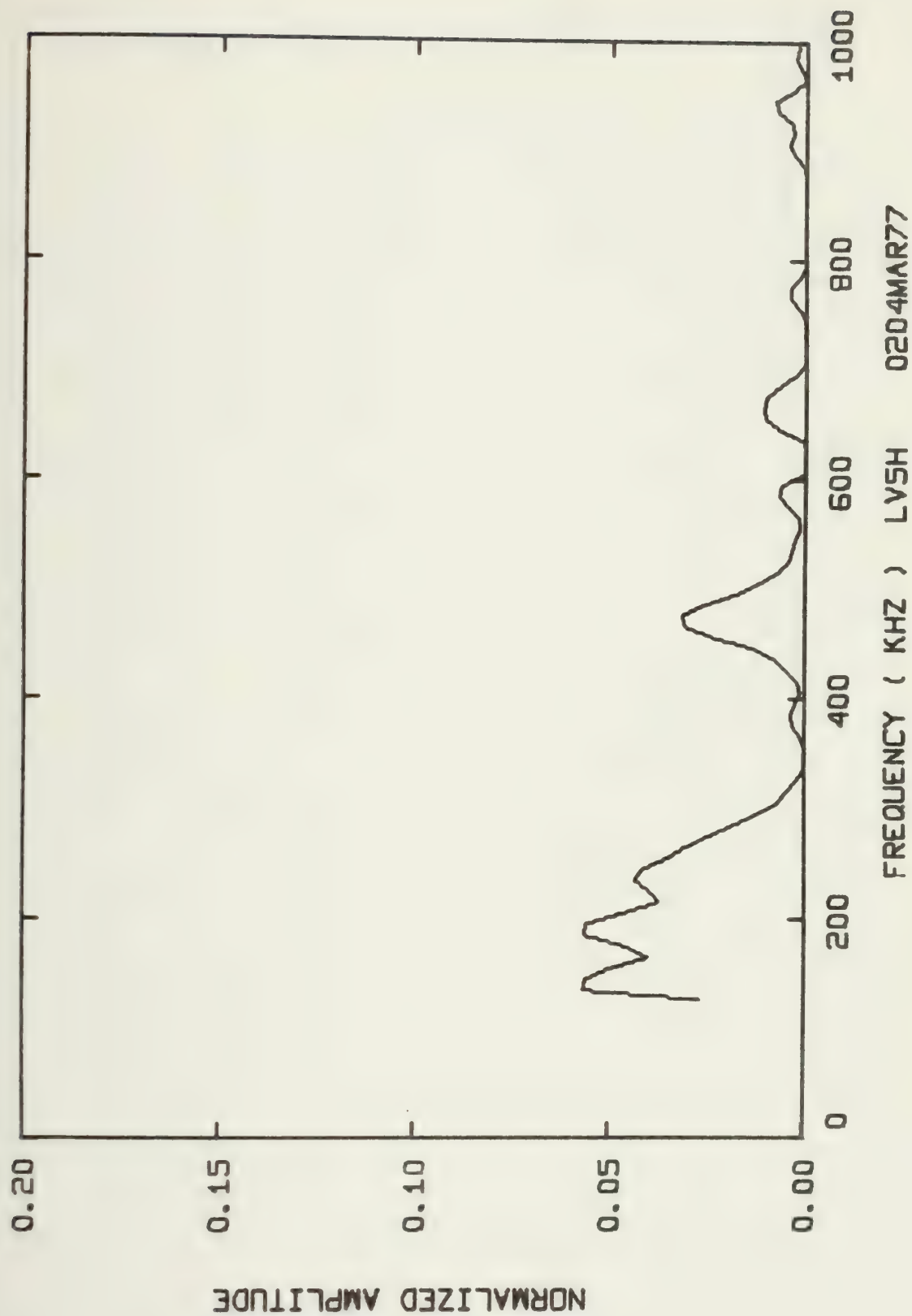
Spectral Distrib. Graph Code Number	Energy per AE (Joules)	RMS Pressure Across Face of Transducer (Pa x 10 <sup>5</sup> )
LV5H 1008MAR77	36.255 x 10 <sup>-9</sup>	61.33



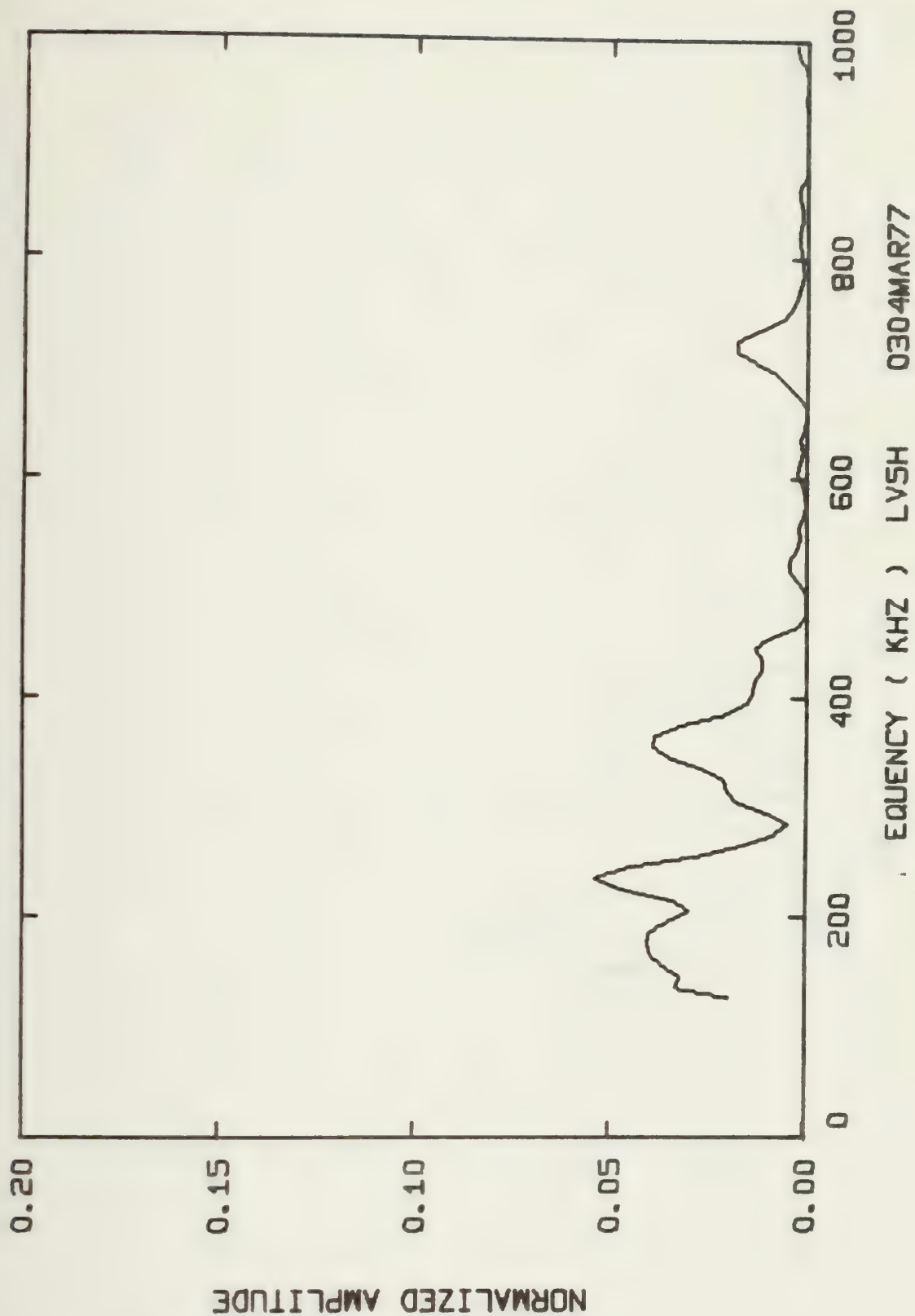




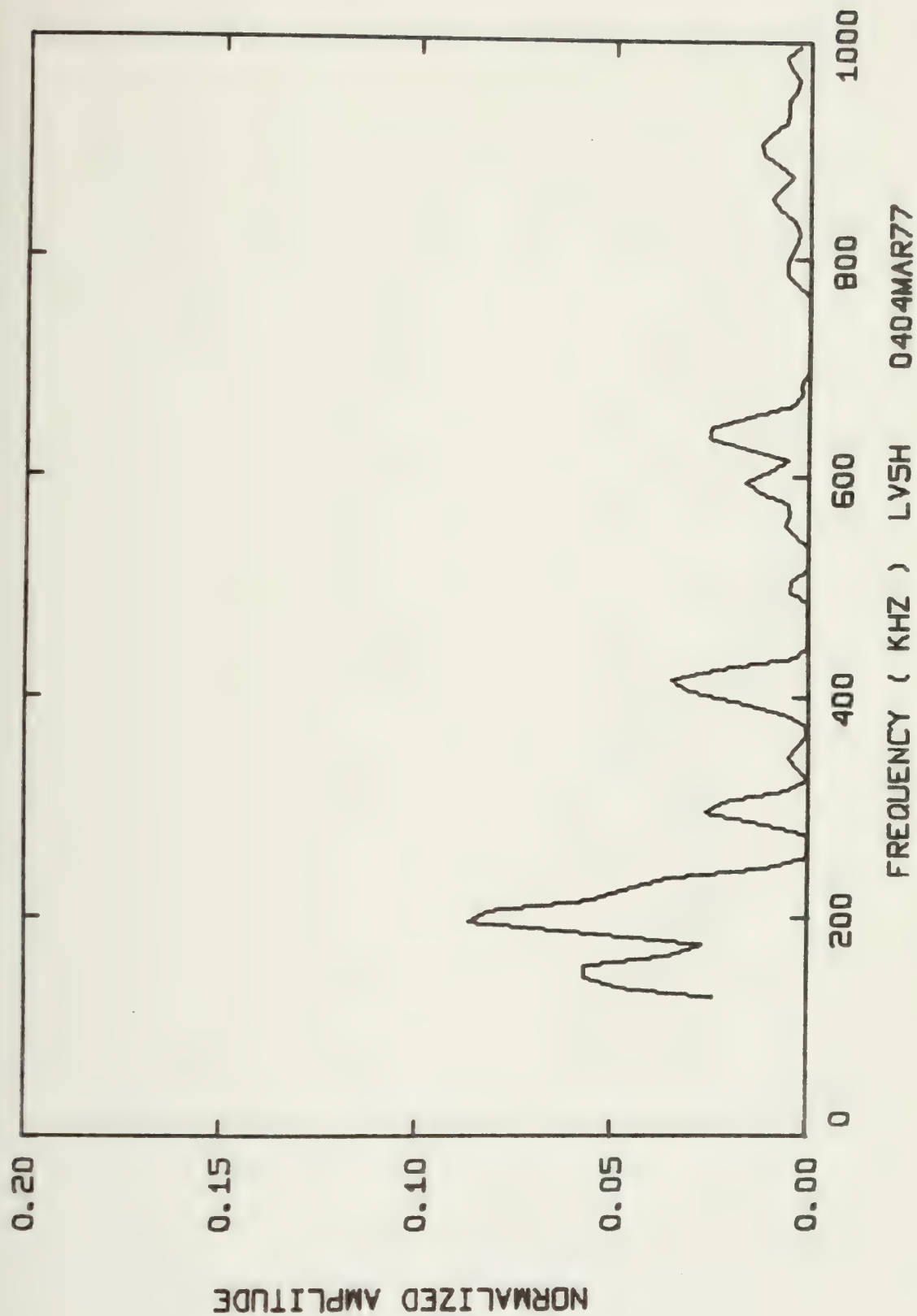




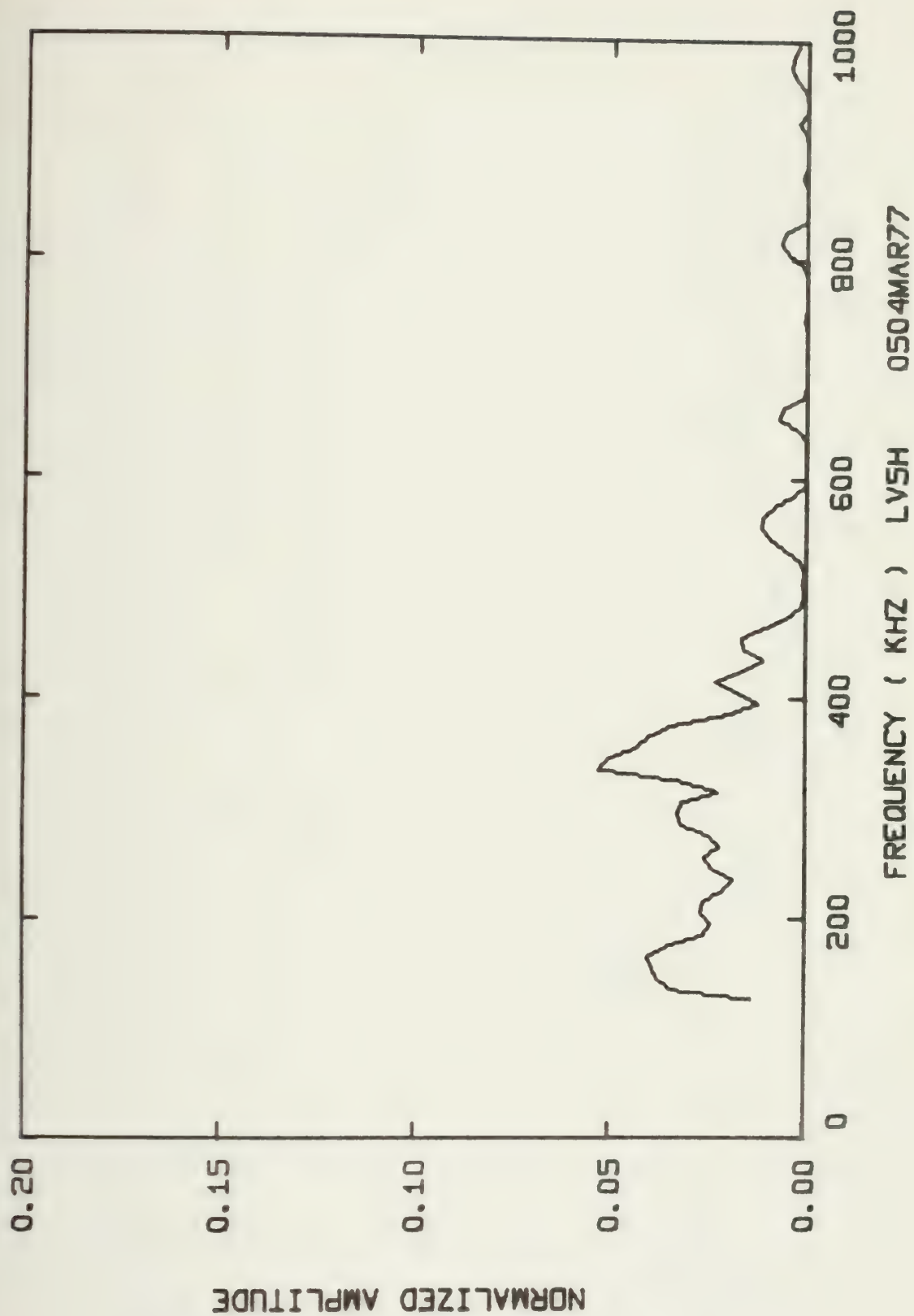






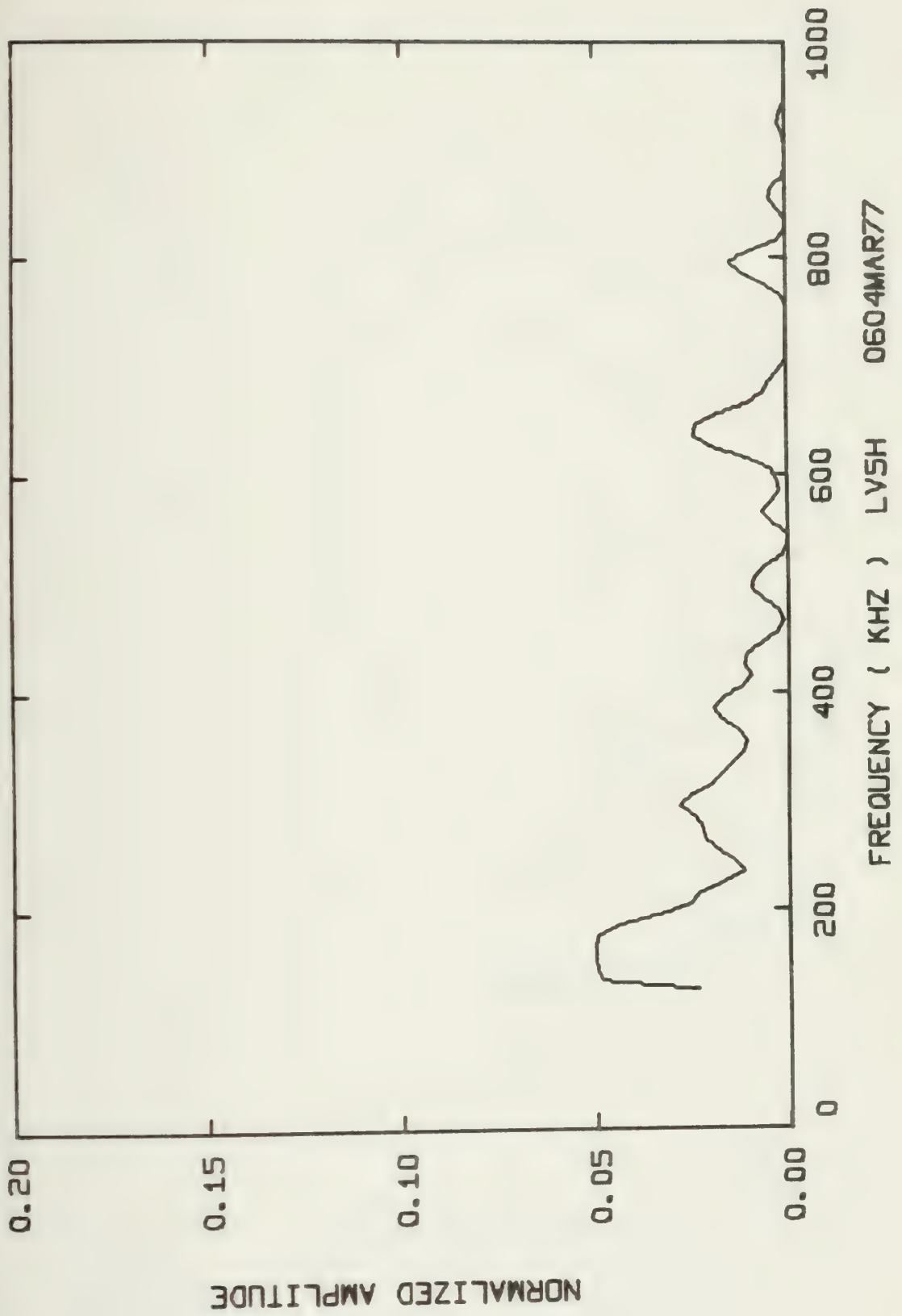




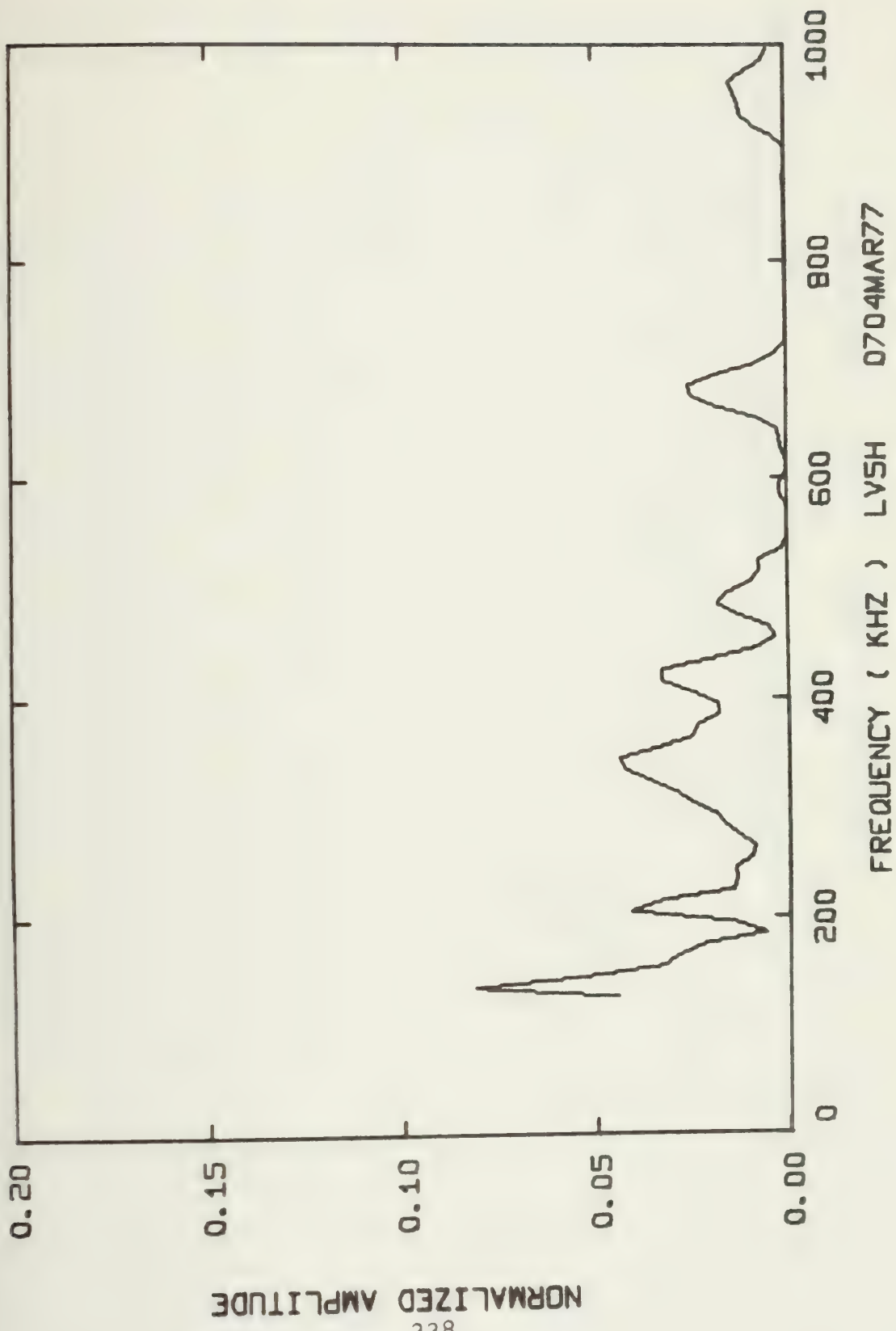




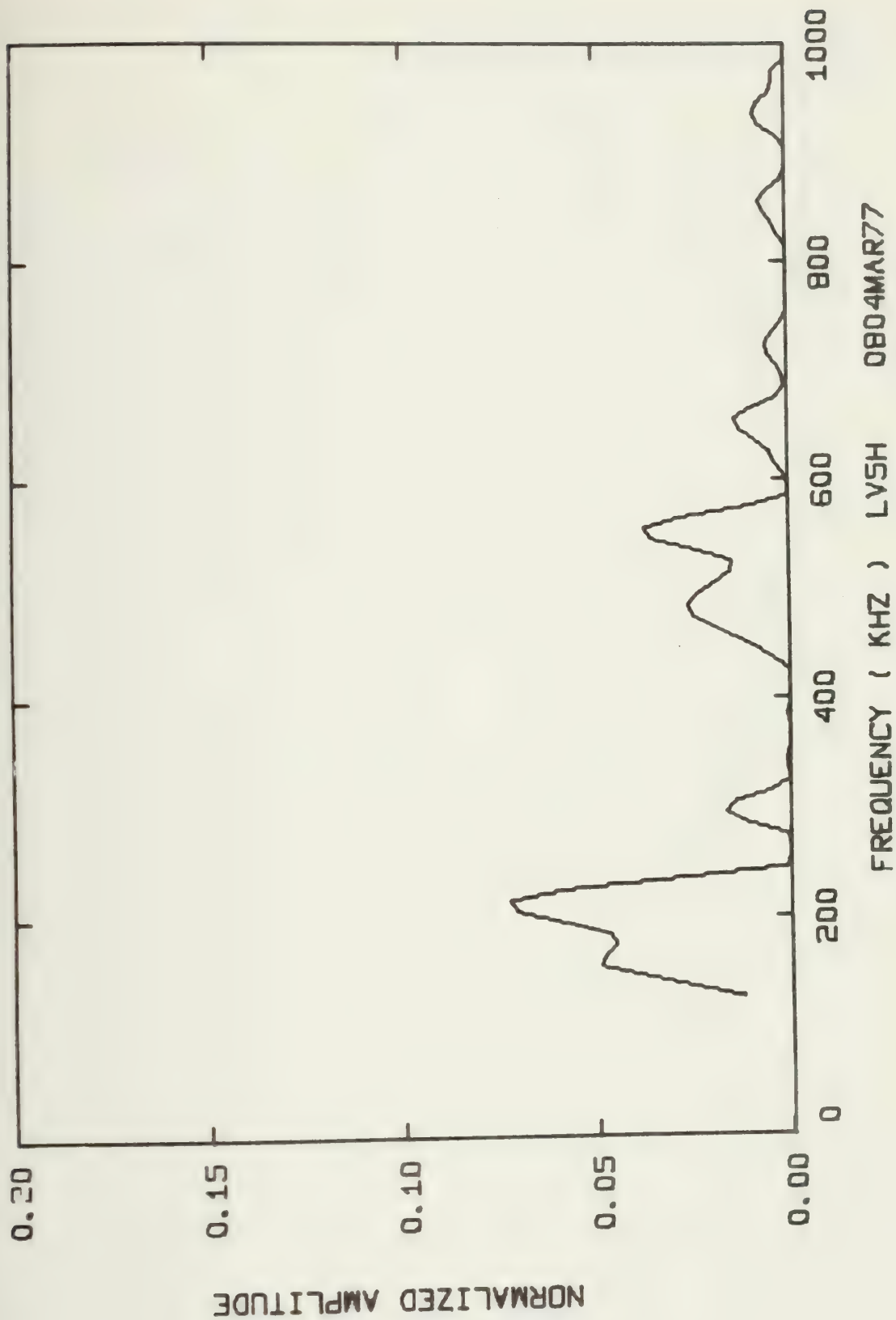




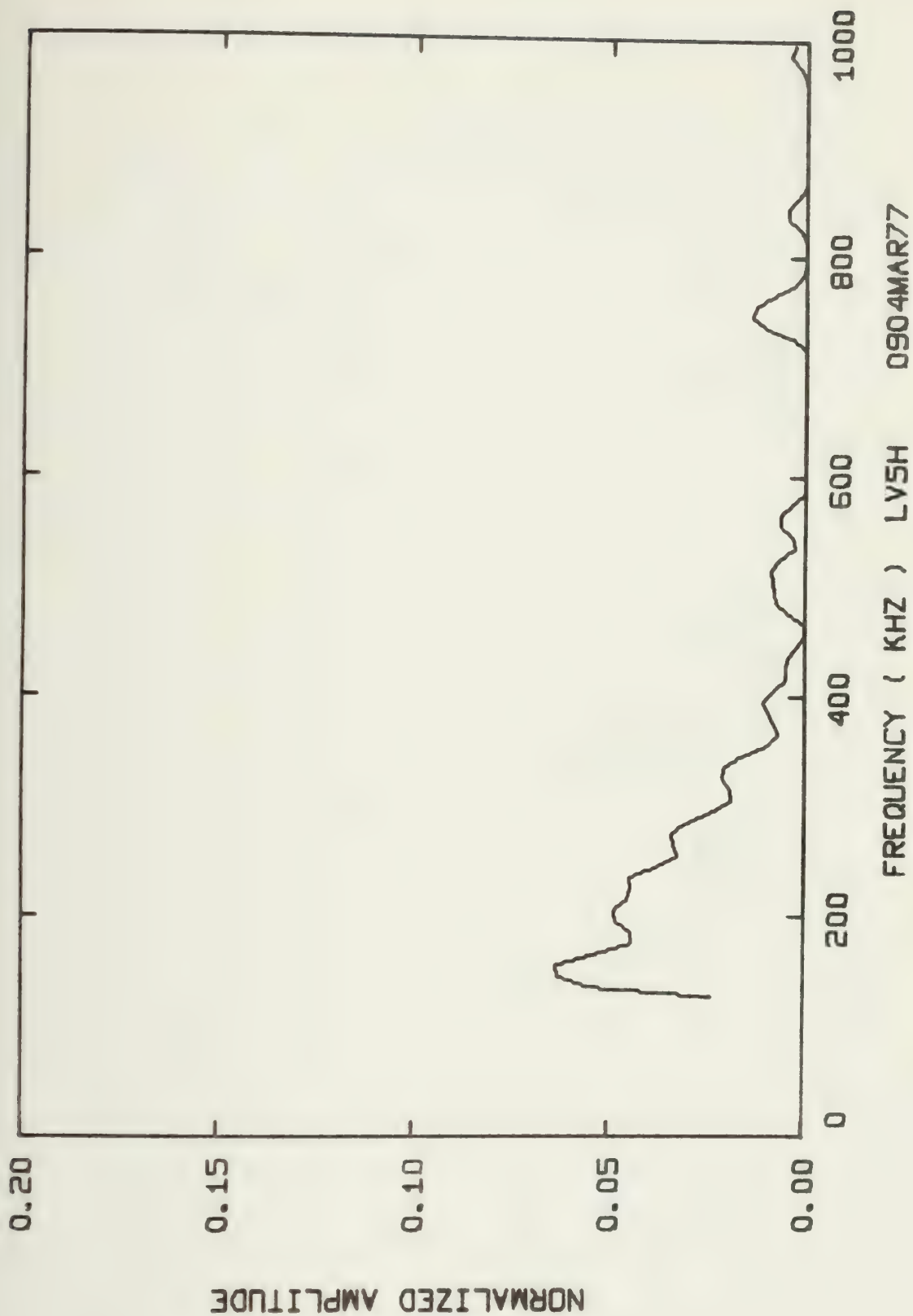






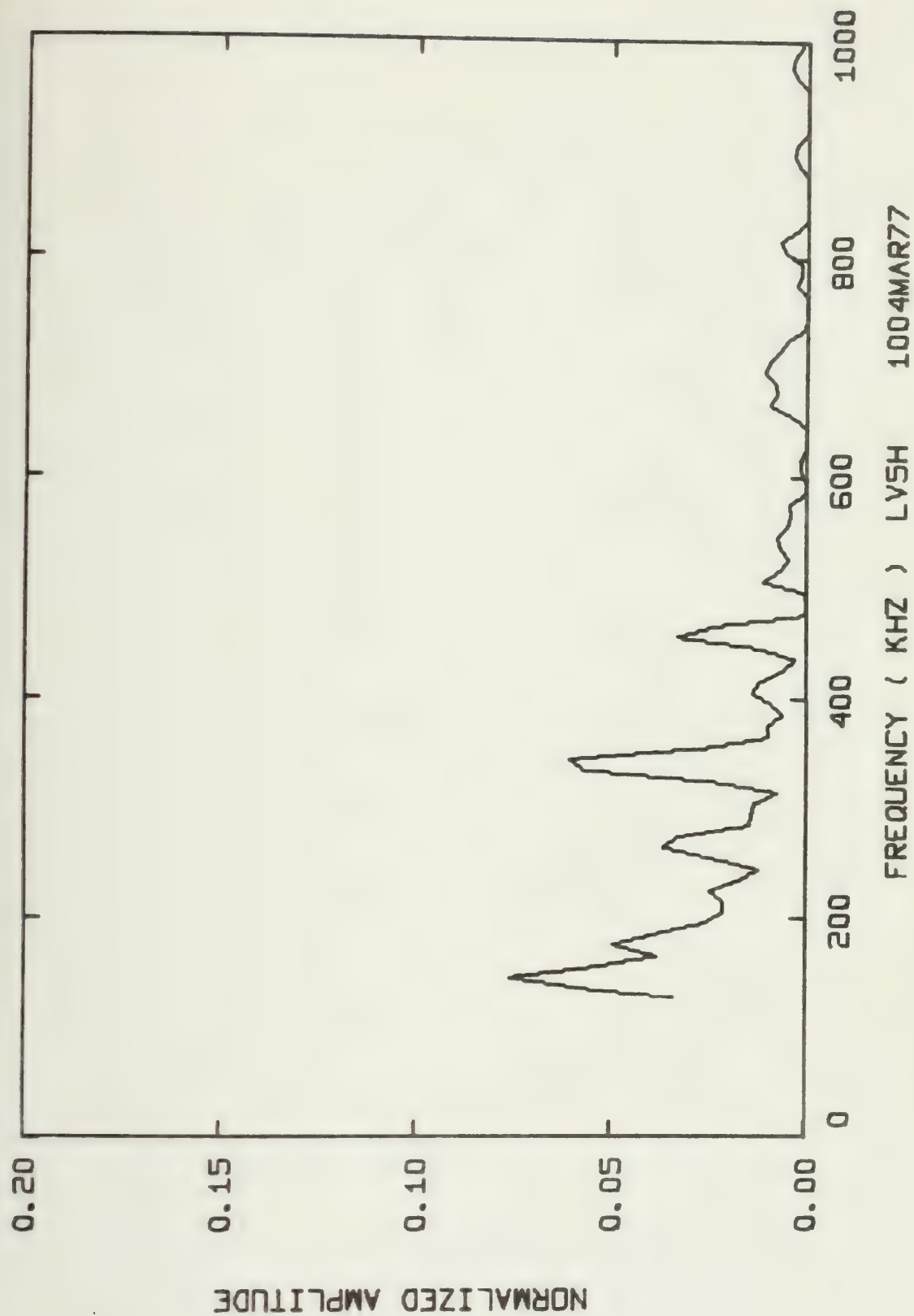




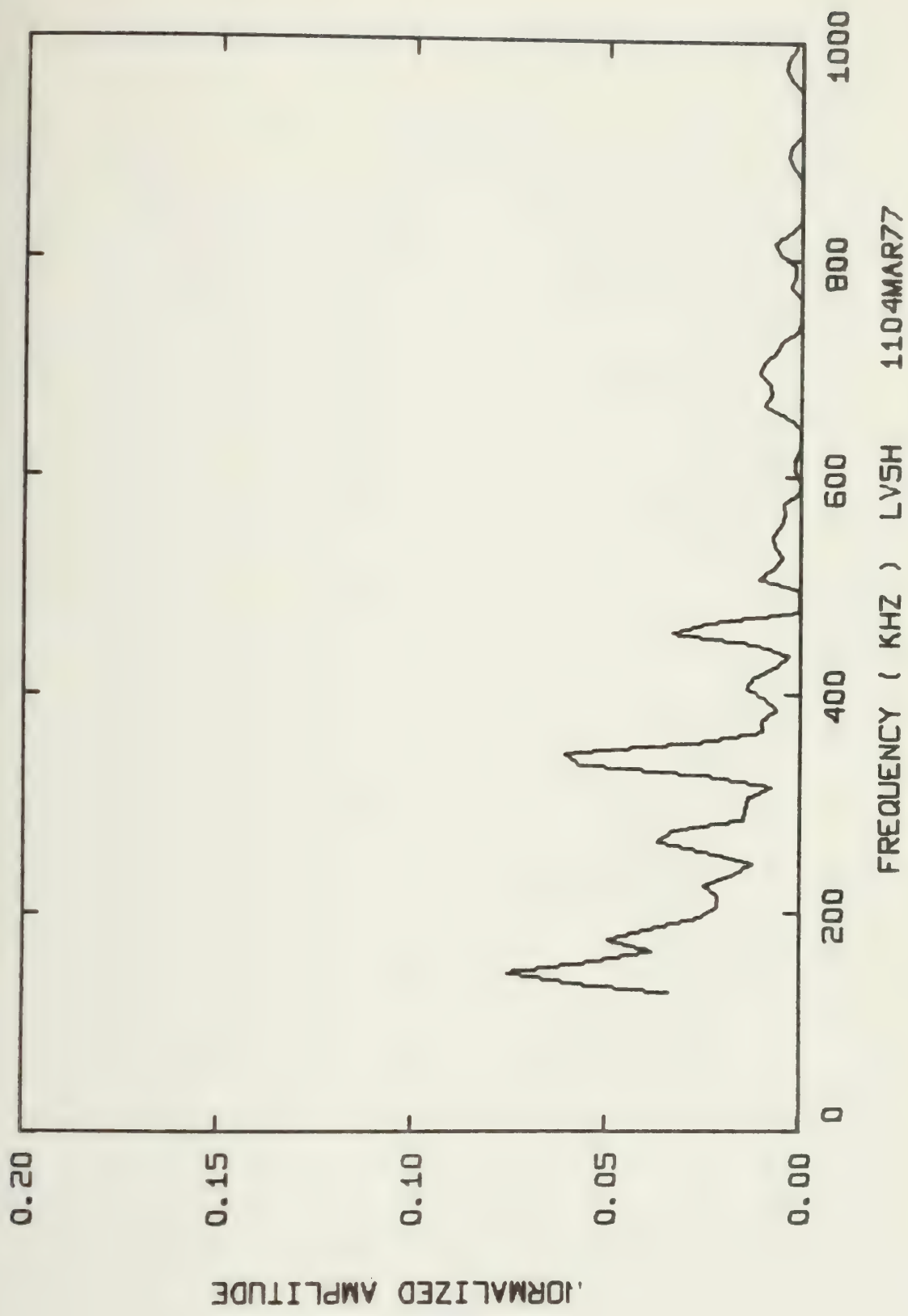




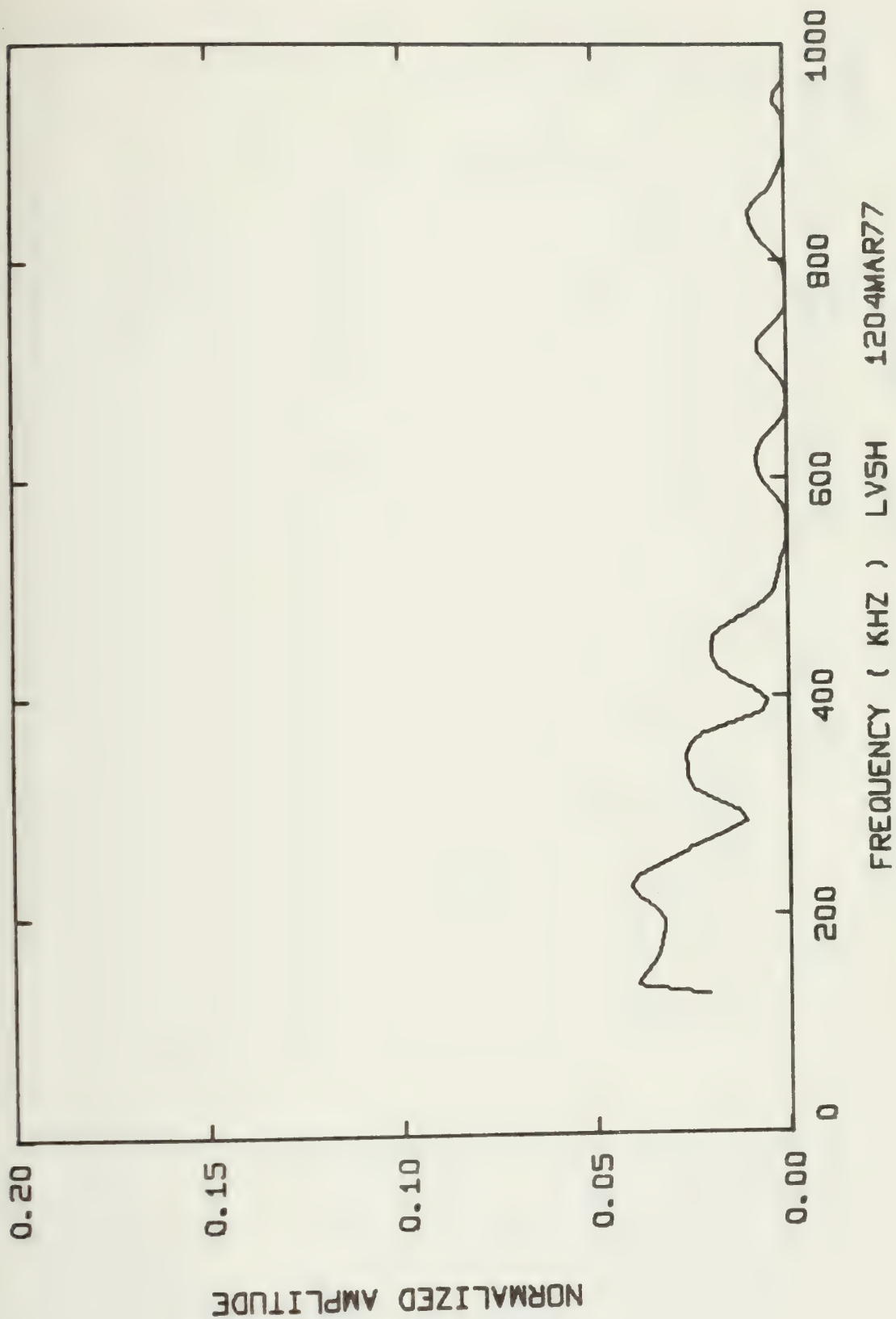




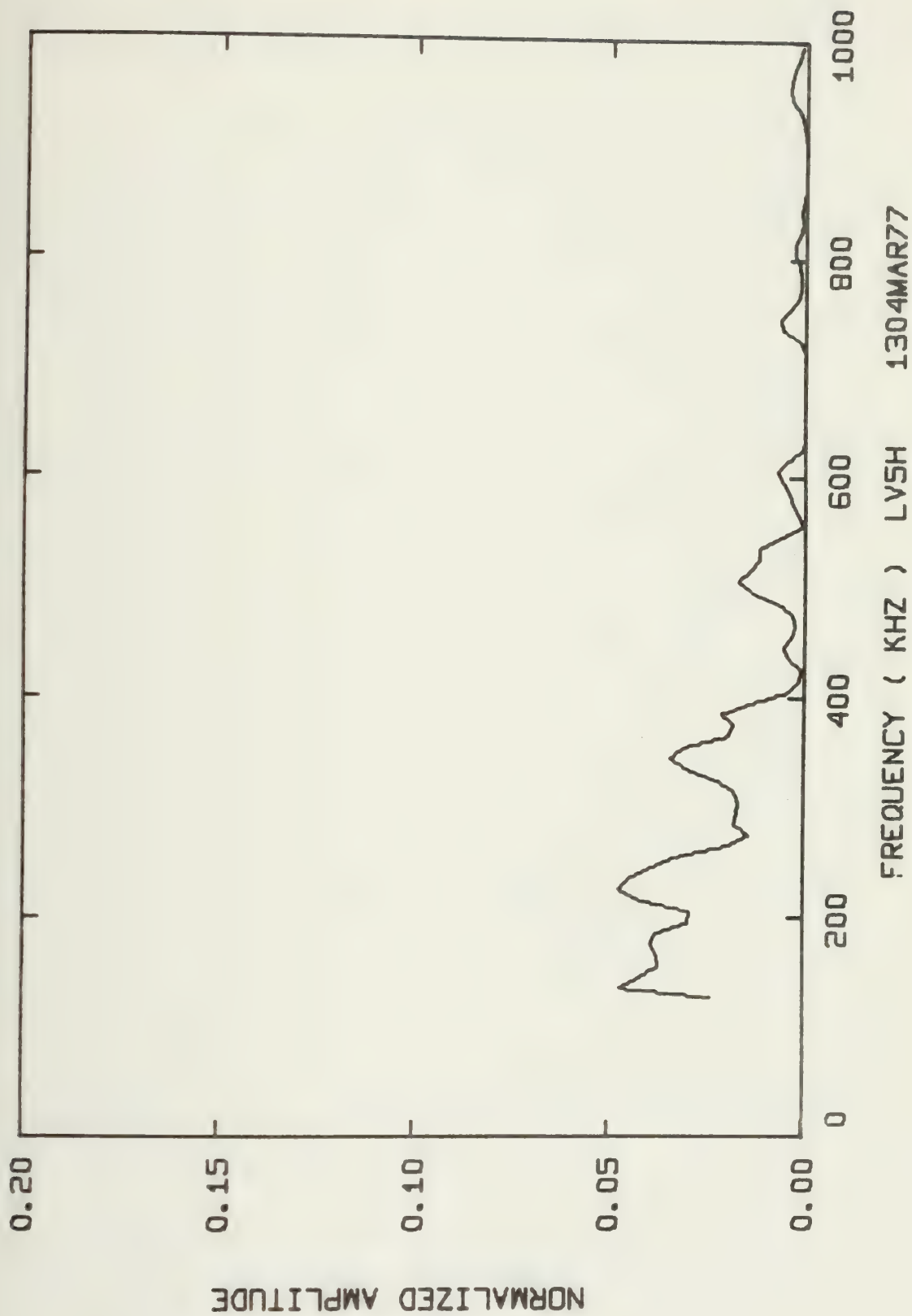






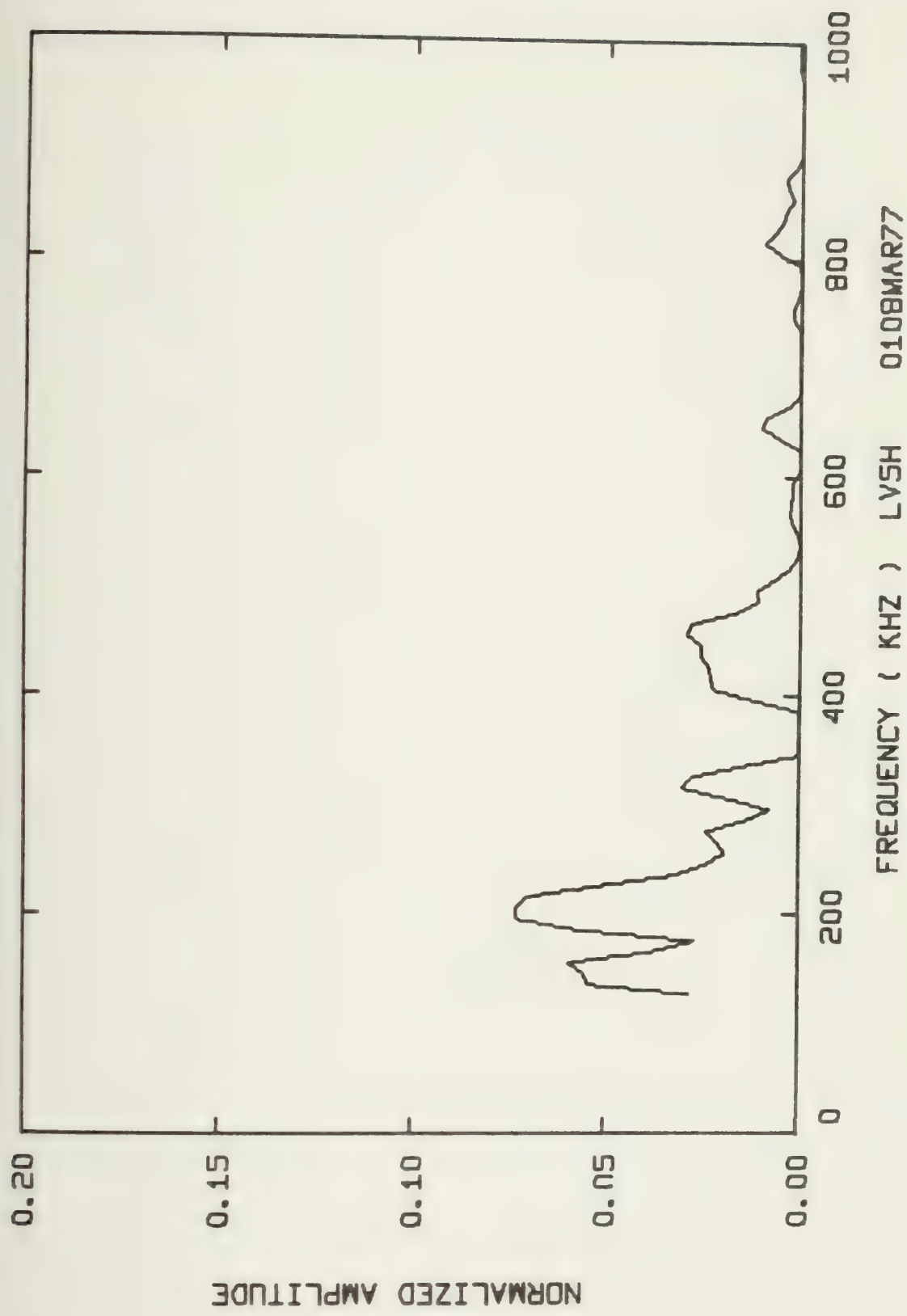




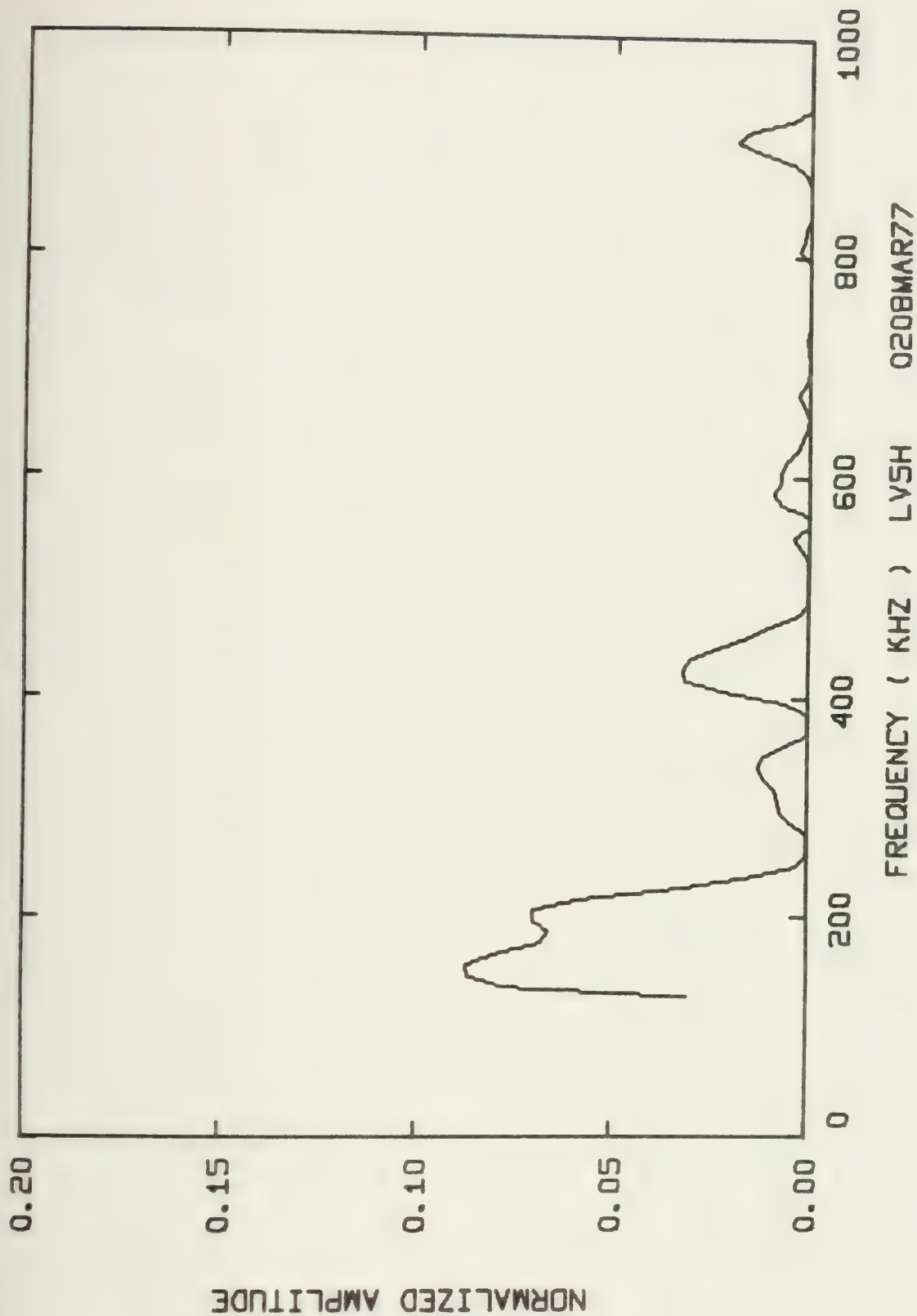




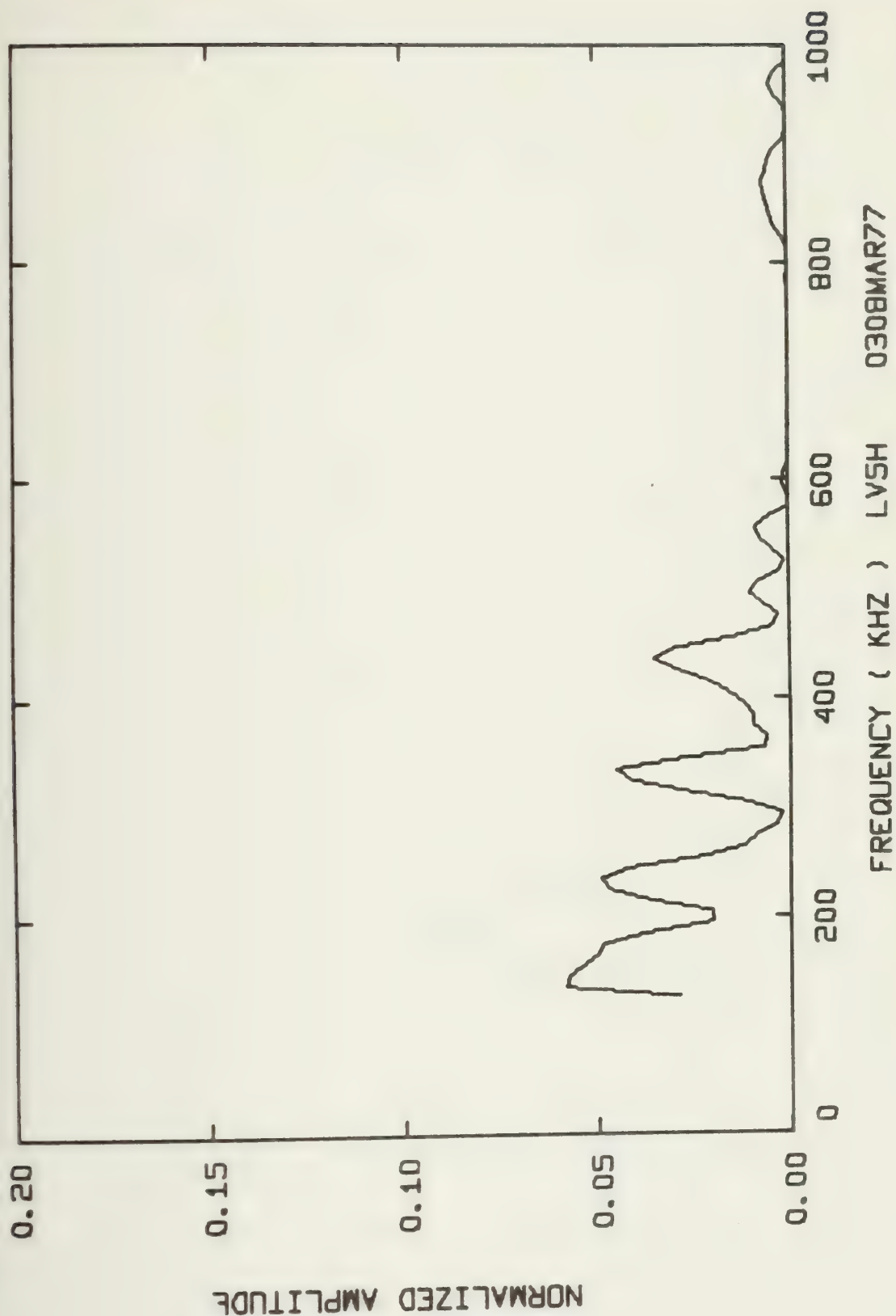




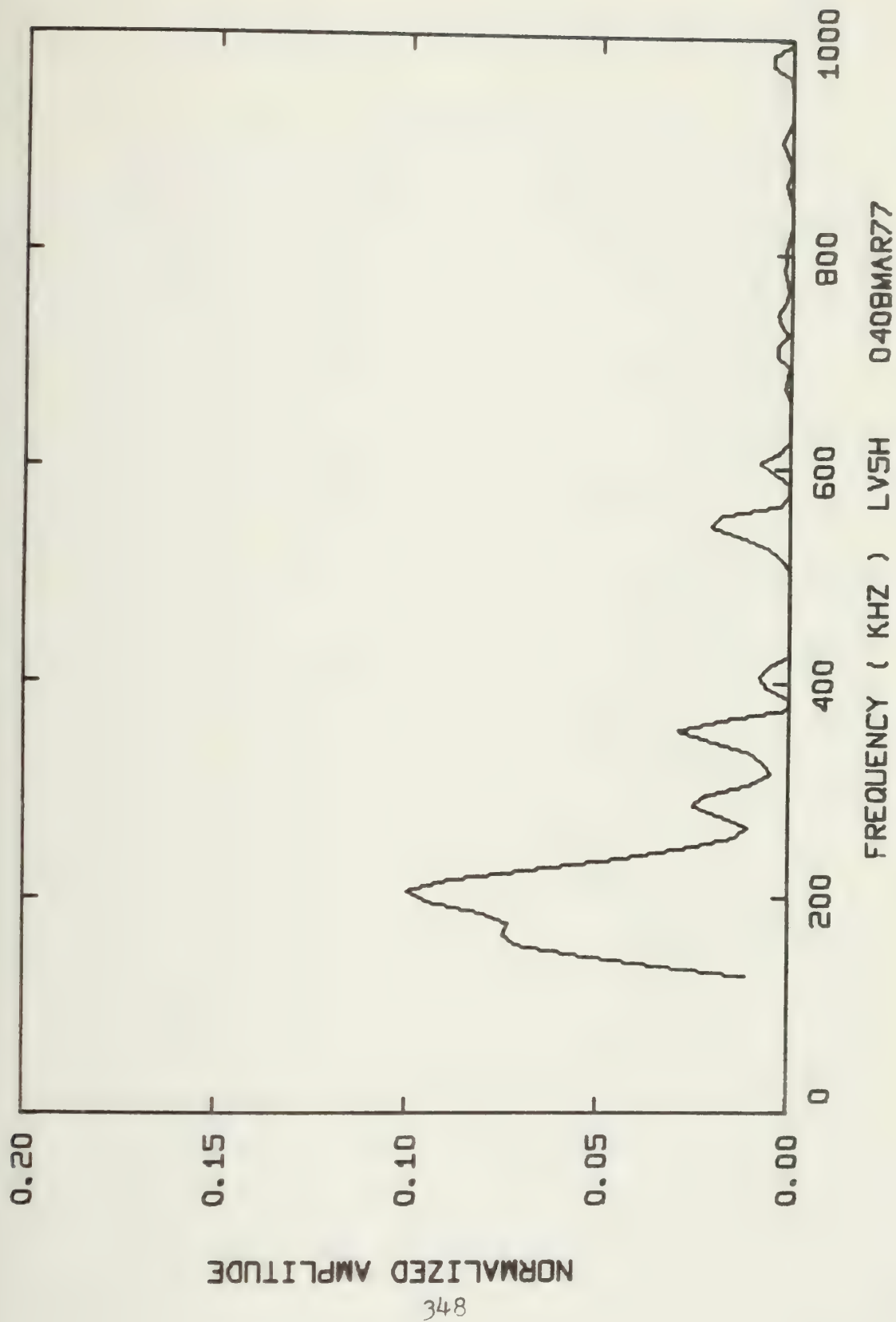






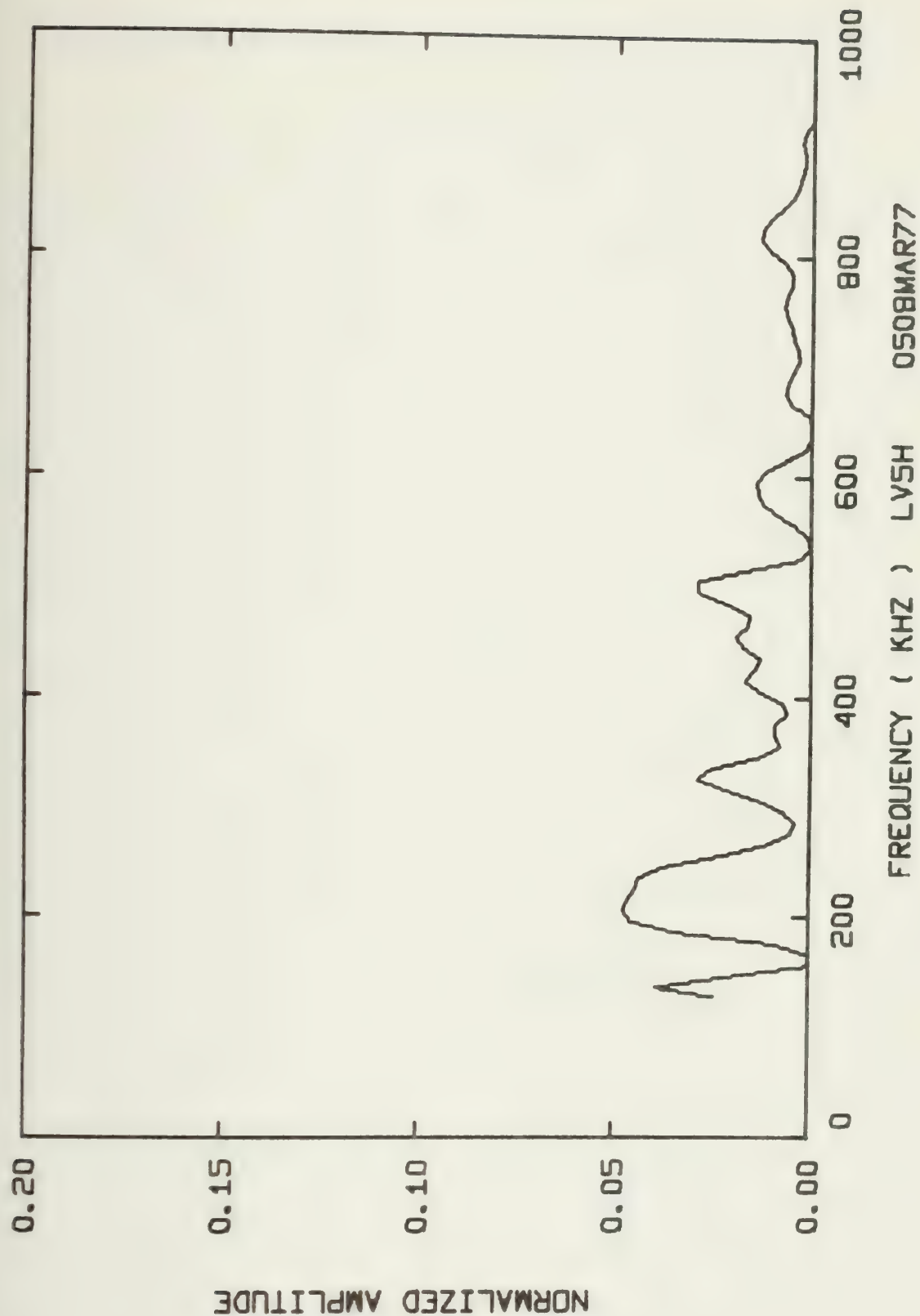




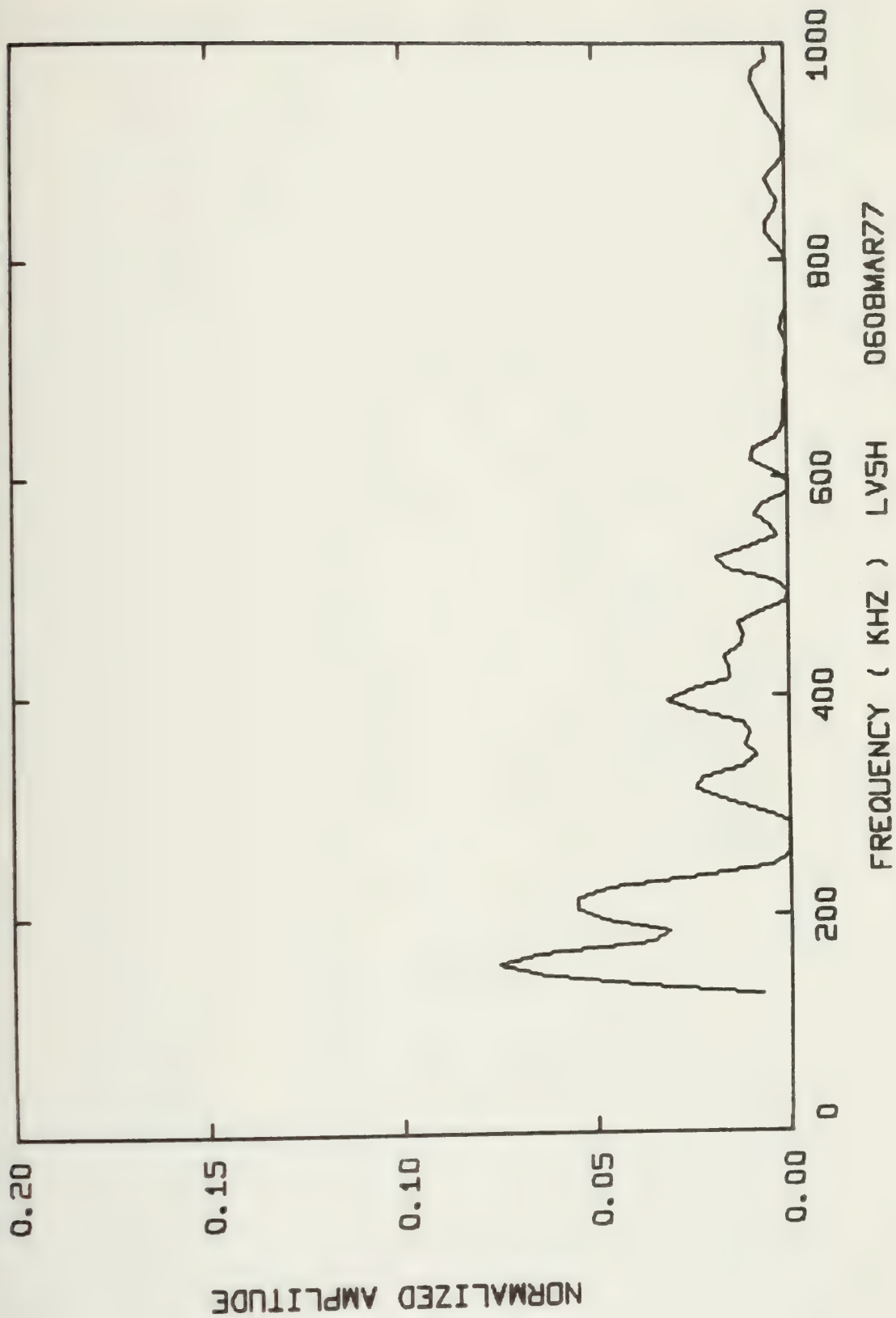




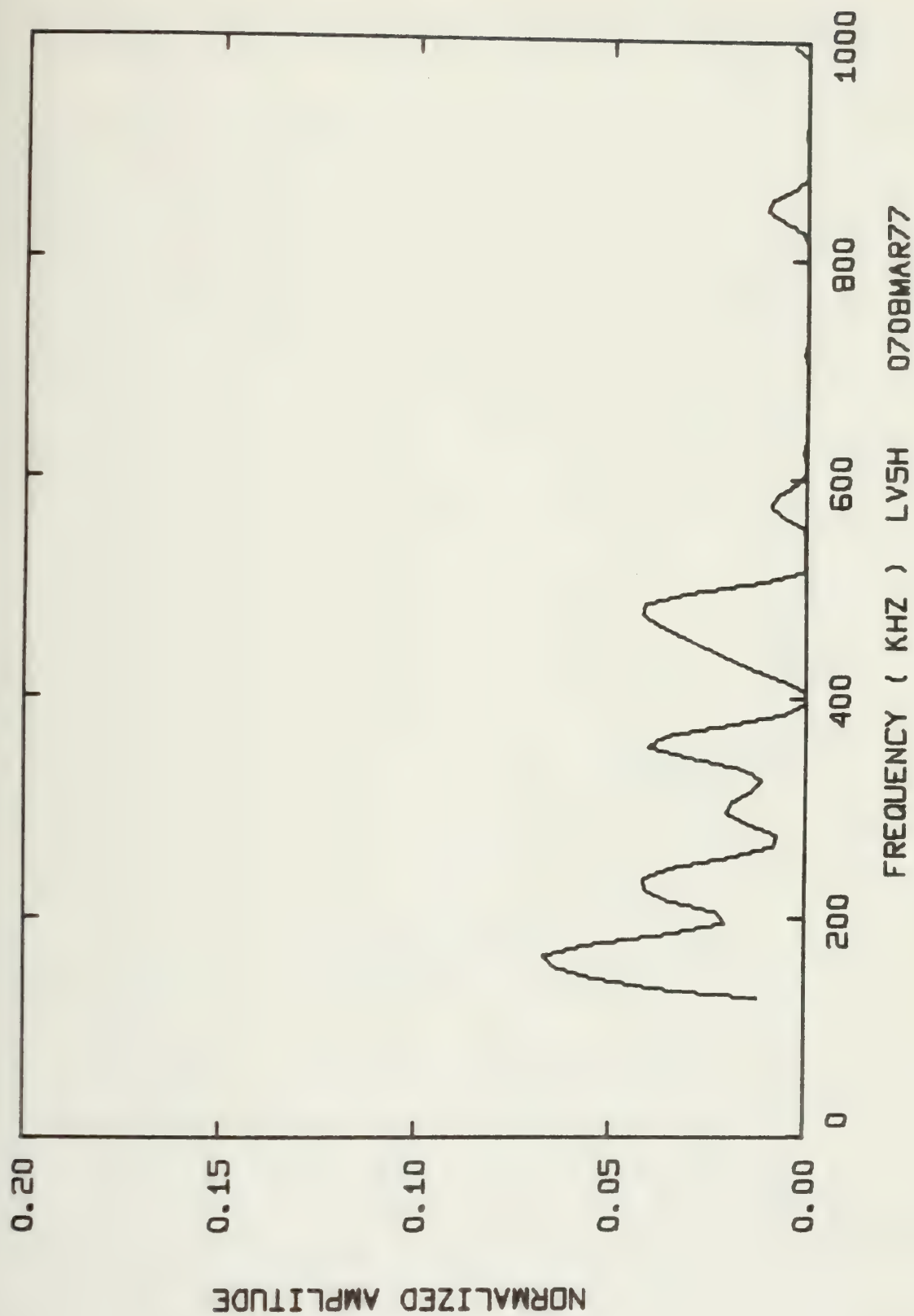




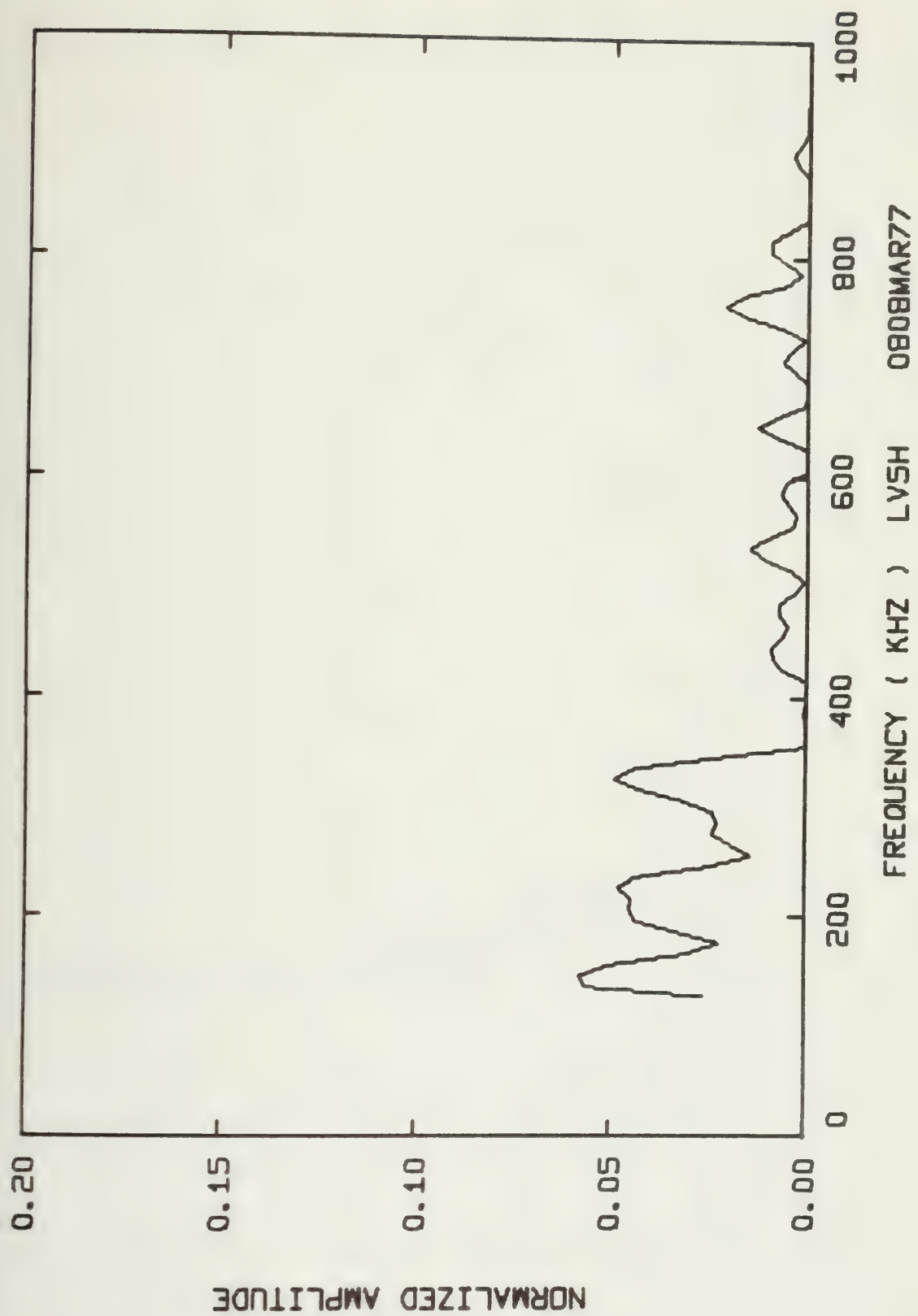






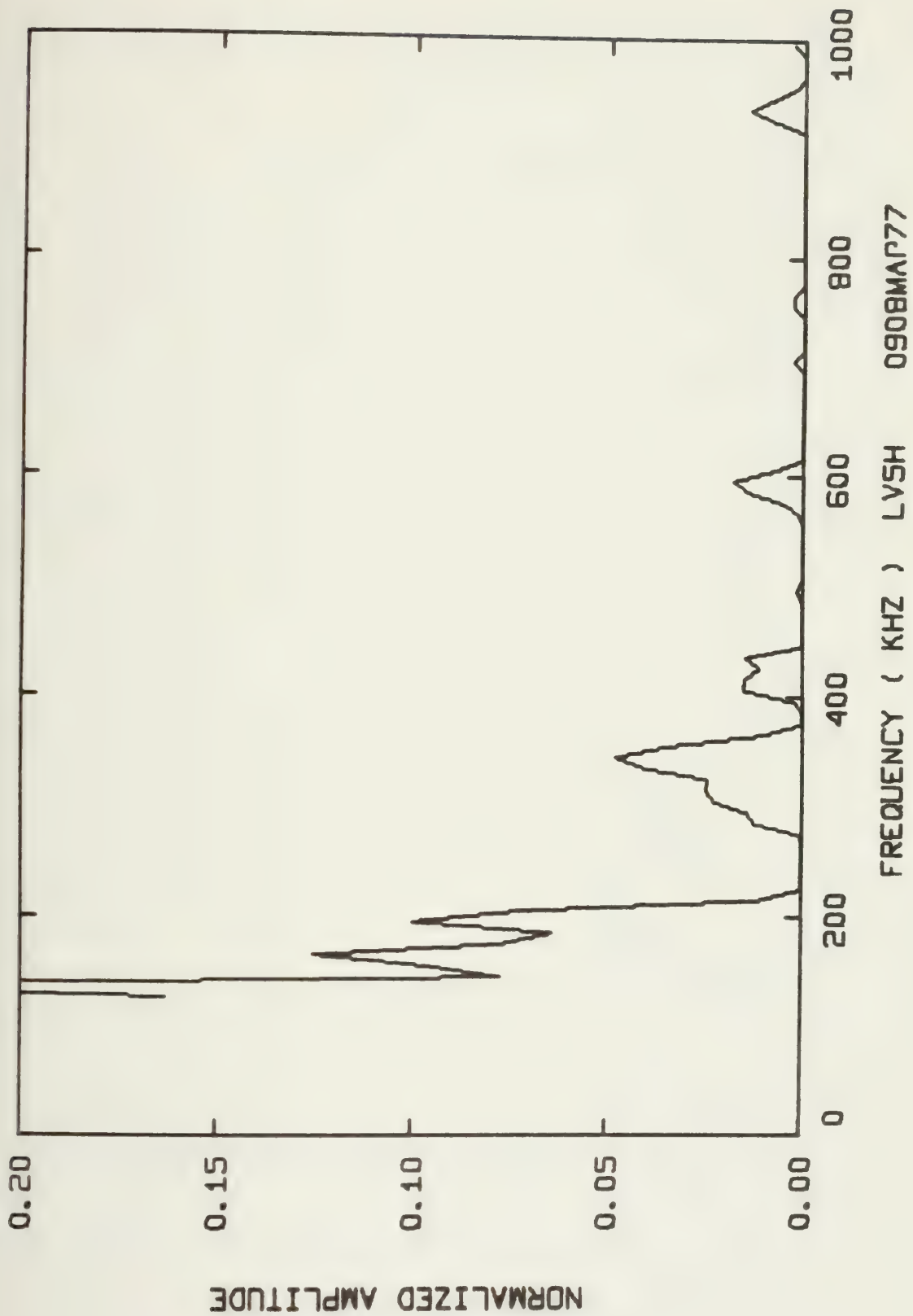




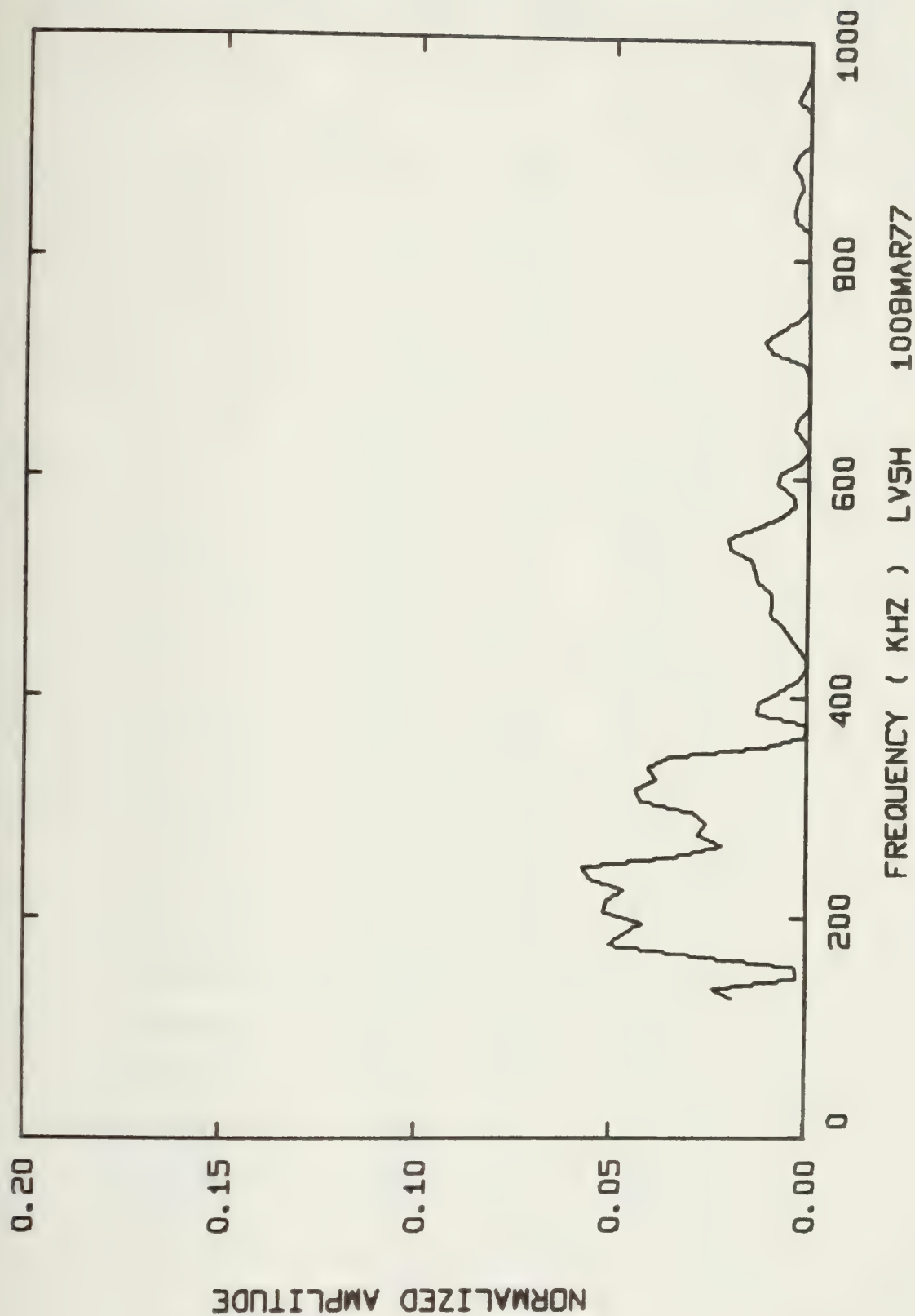










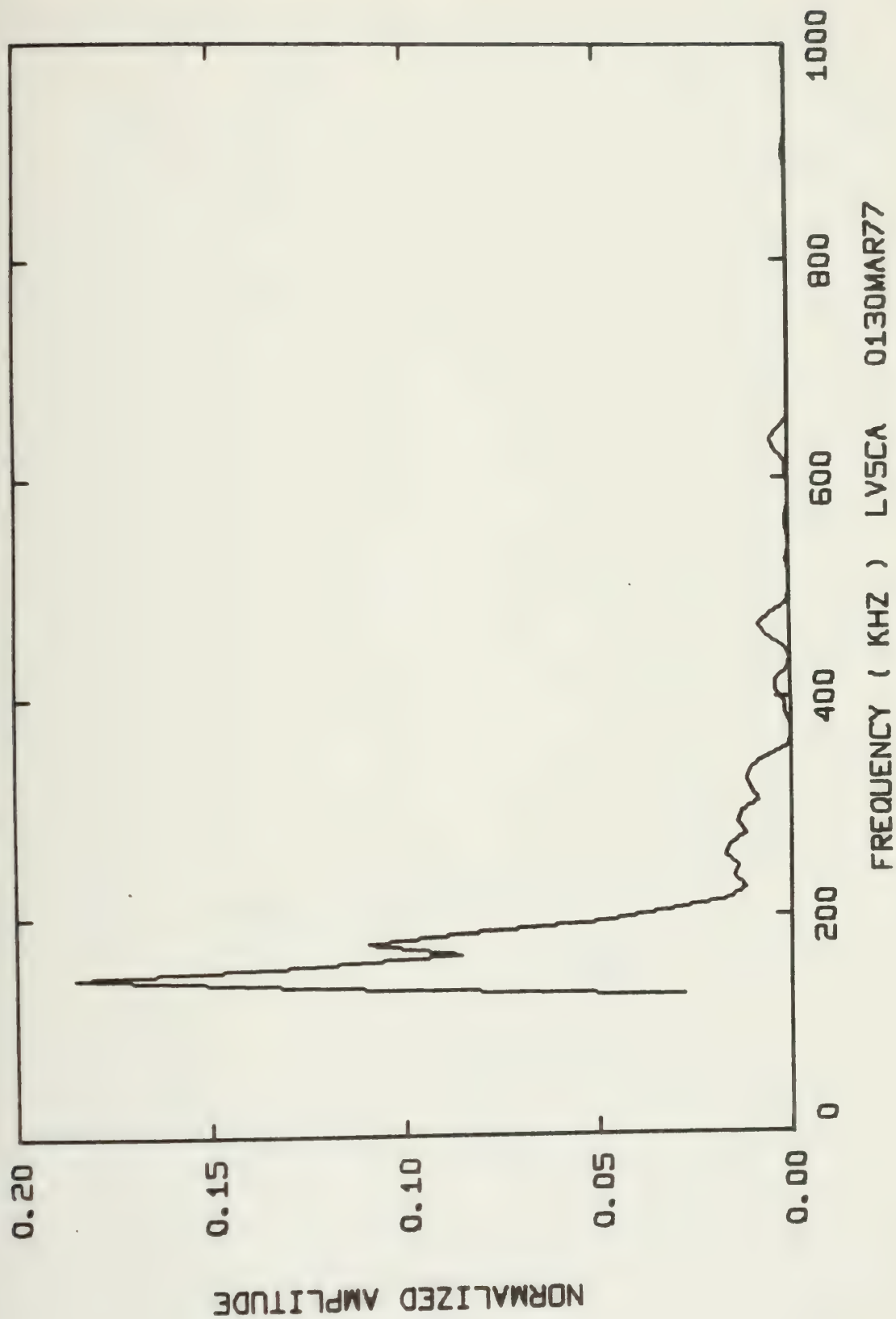




Summary of Energy per Acoustic Emission and RMS Pressure  
Across the Transducer's Face for Each Spectra

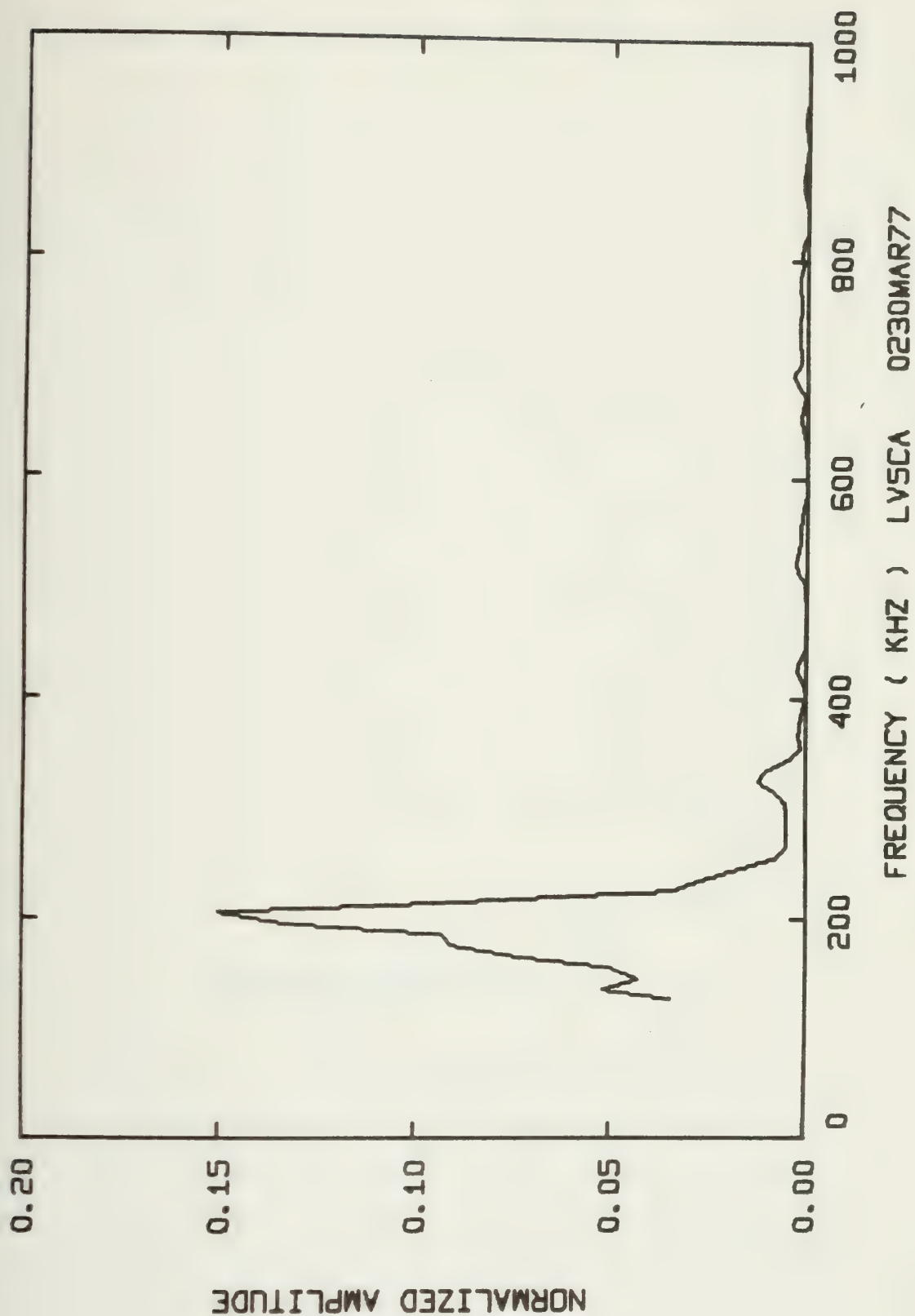
Spectral Distrib. Graph Code Number	Energy per AE (Joules)	RMS Pressure Across Face of Transducer (Pa x 10 <sup>5</sup> )
LV5CA 0130MAR77	1.7888 x 10 <sup>-6</sup>	218.45
0230MAR77	6.7522 x 10 <sup>-6</sup>	324.17
0330MAR77	19.319 x 10 <sup>-6</sup>	557.67
0430MAR77	5.4721 x 10 <sup>-6</sup>	316.51
0530MAR77	16.676 x 10 <sup>-6</sup>	524.97
0630MAR77	69.977 x 10 <sup>-6</sup>	842.27
0730MAR77	27.469 x 10 <sup>-6</sup>	623.38
0830MAR77	5.3556 x 10 <sup>-6</sup>	302.91
0930MAR77	7.1864 x 10 <sup>-6</sup>	338.68
1030MAR77	6.1334 x 10 <sup>-6</sup>	306.15
1130MAR77	4.7946 x 10 <sup>-6</sup>	328.85
1230MAR77	48.688 x 10 <sup>-6</sup>	724.95
1430MAR77	15.673 x 10 <sup>-6</sup>	447.11
1530MAR77	48.649 x 10 <sup>-6</sup>	842.46
1630MAR77	13.237 x 10 <sup>-6</sup>	482.91
1730MAR77	7.5903 x 10 <sup>-6</sup>	403.63
1830MAR77	9.3117 x 10 <sup>-6</sup>	405.02
1930MAR77	15.569 x 10 <sup>-6</sup>	523.74
2030MAR77	23.857 x 10 <sup>-6</sup>	543.18
1330MAR77	12.697 x 10 <sup>-6</sup>	447.12



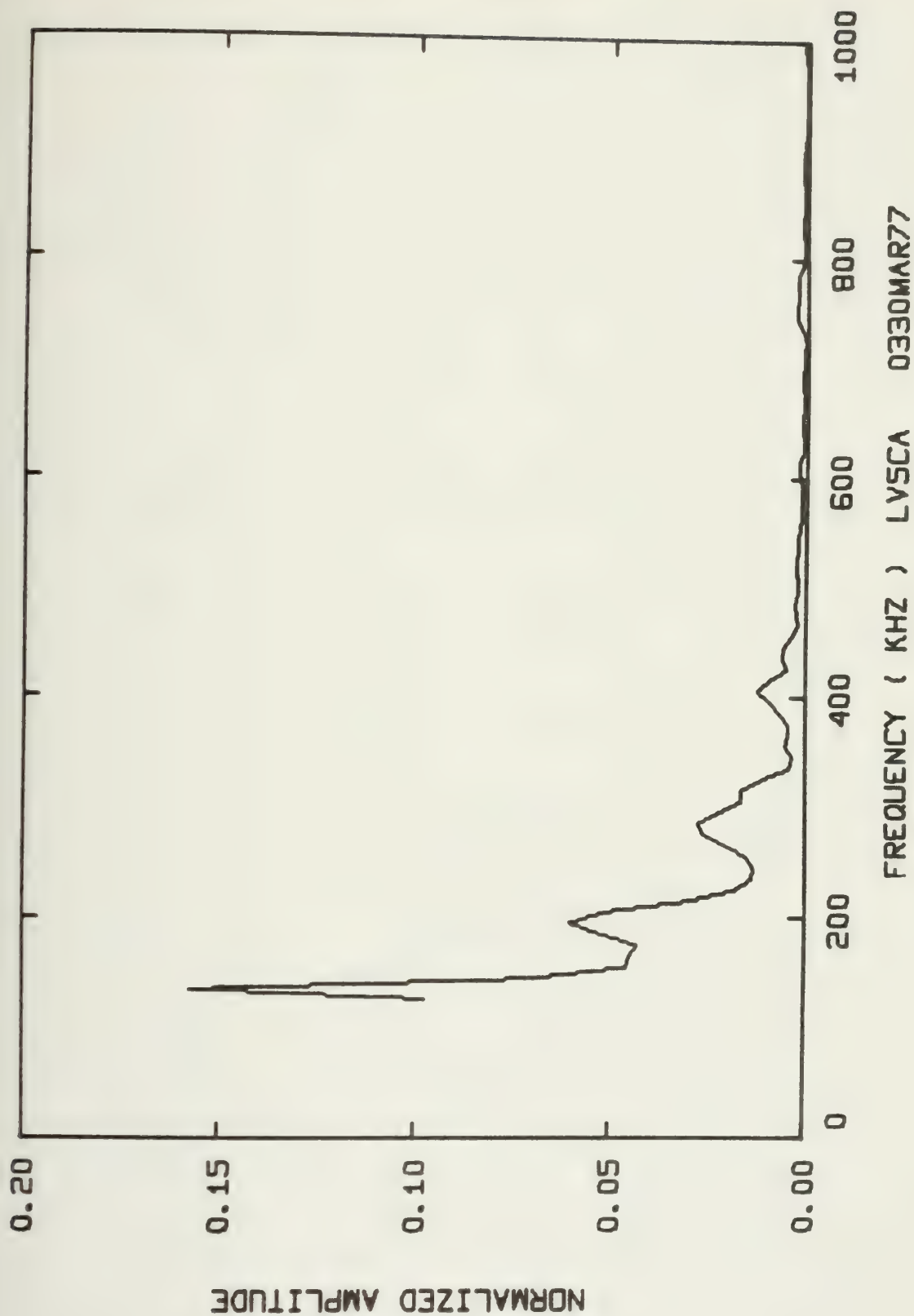




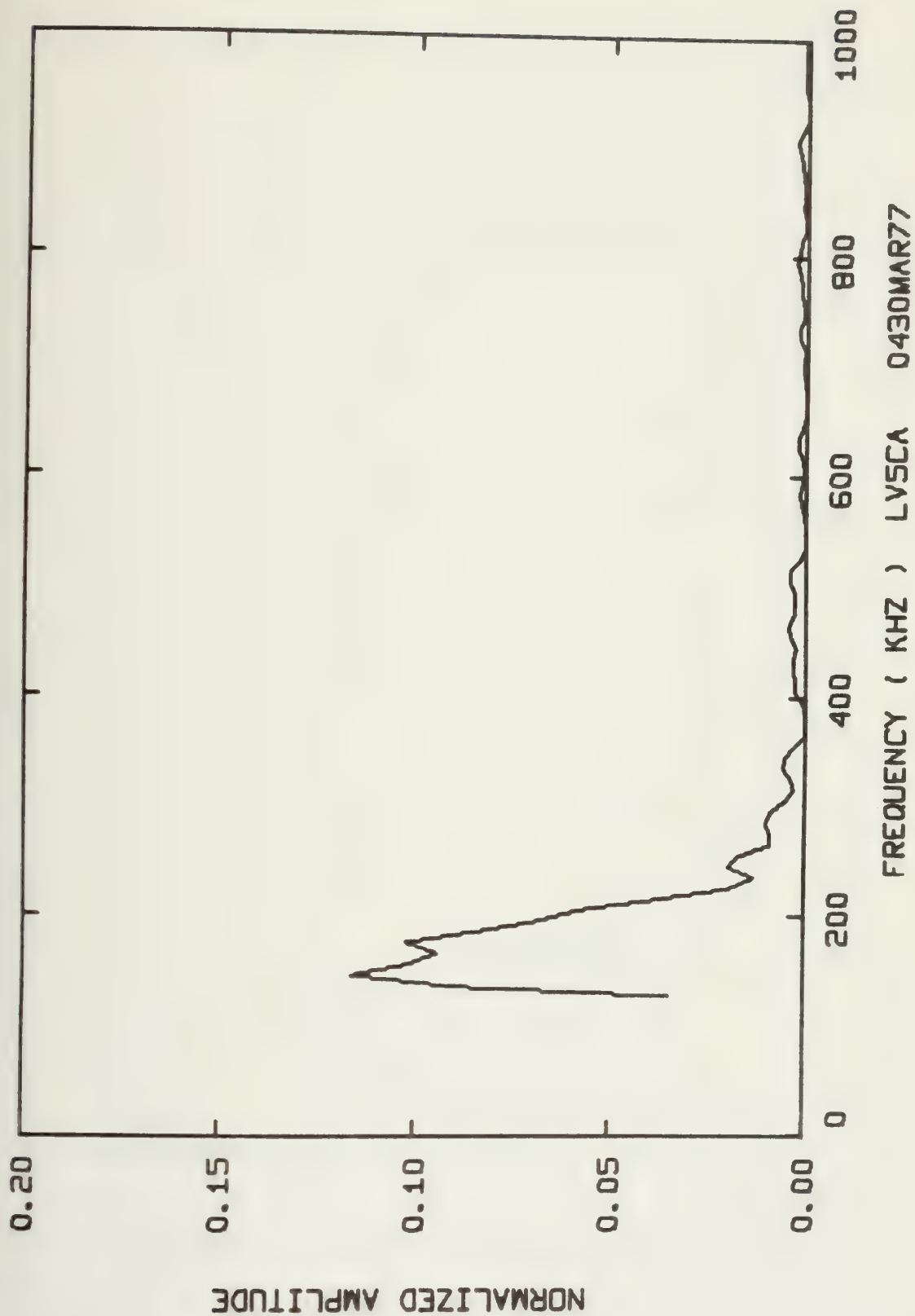




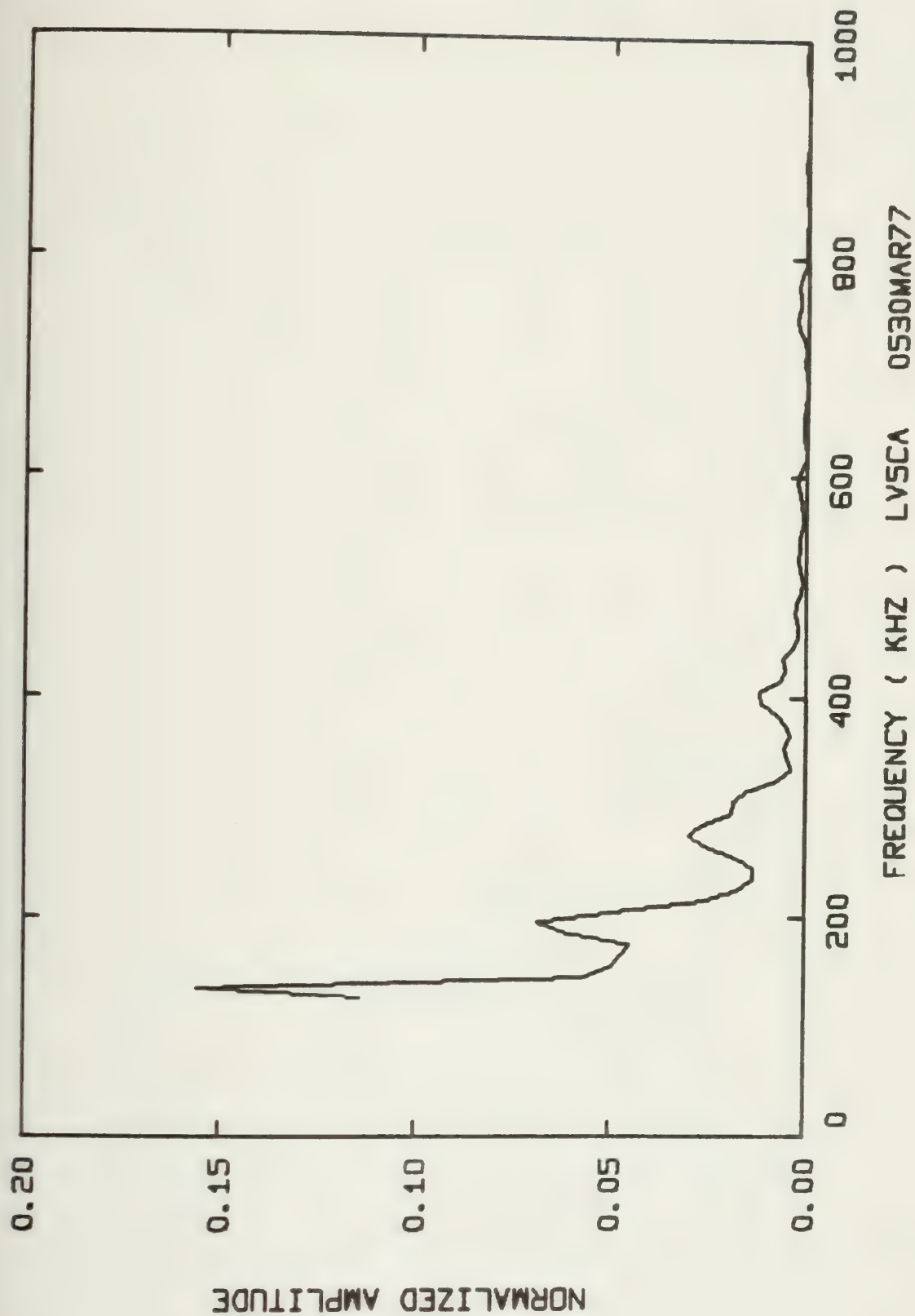






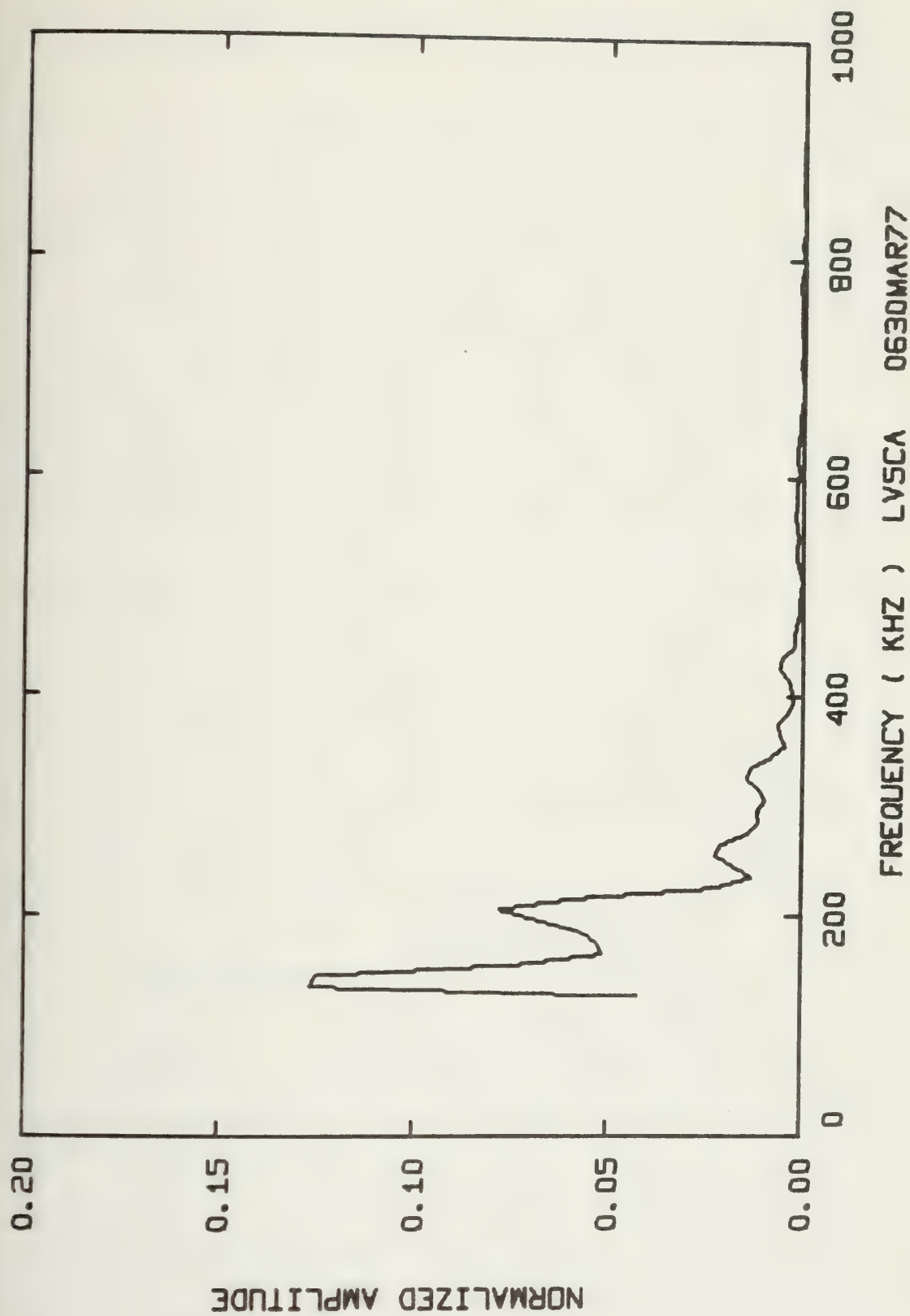




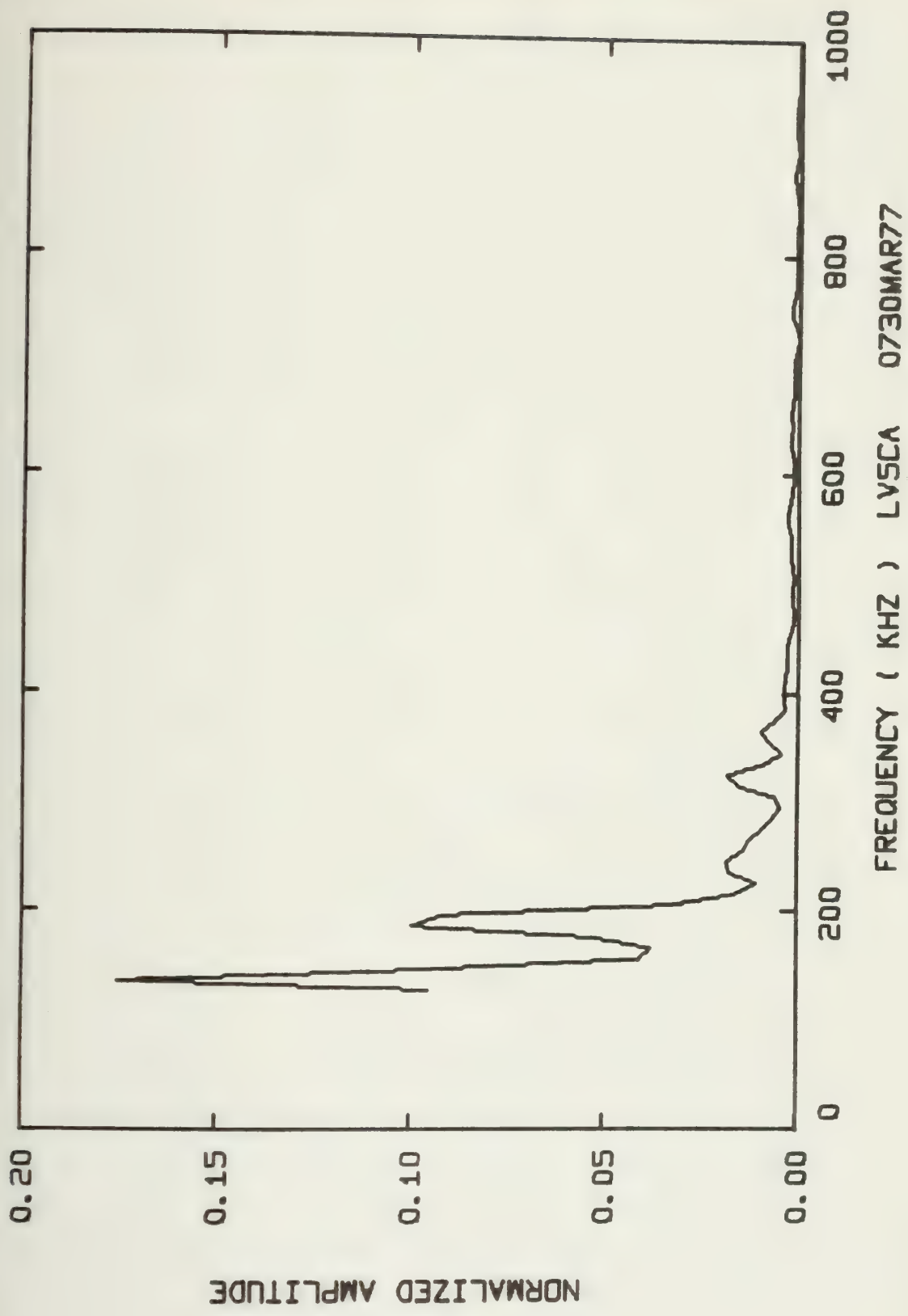




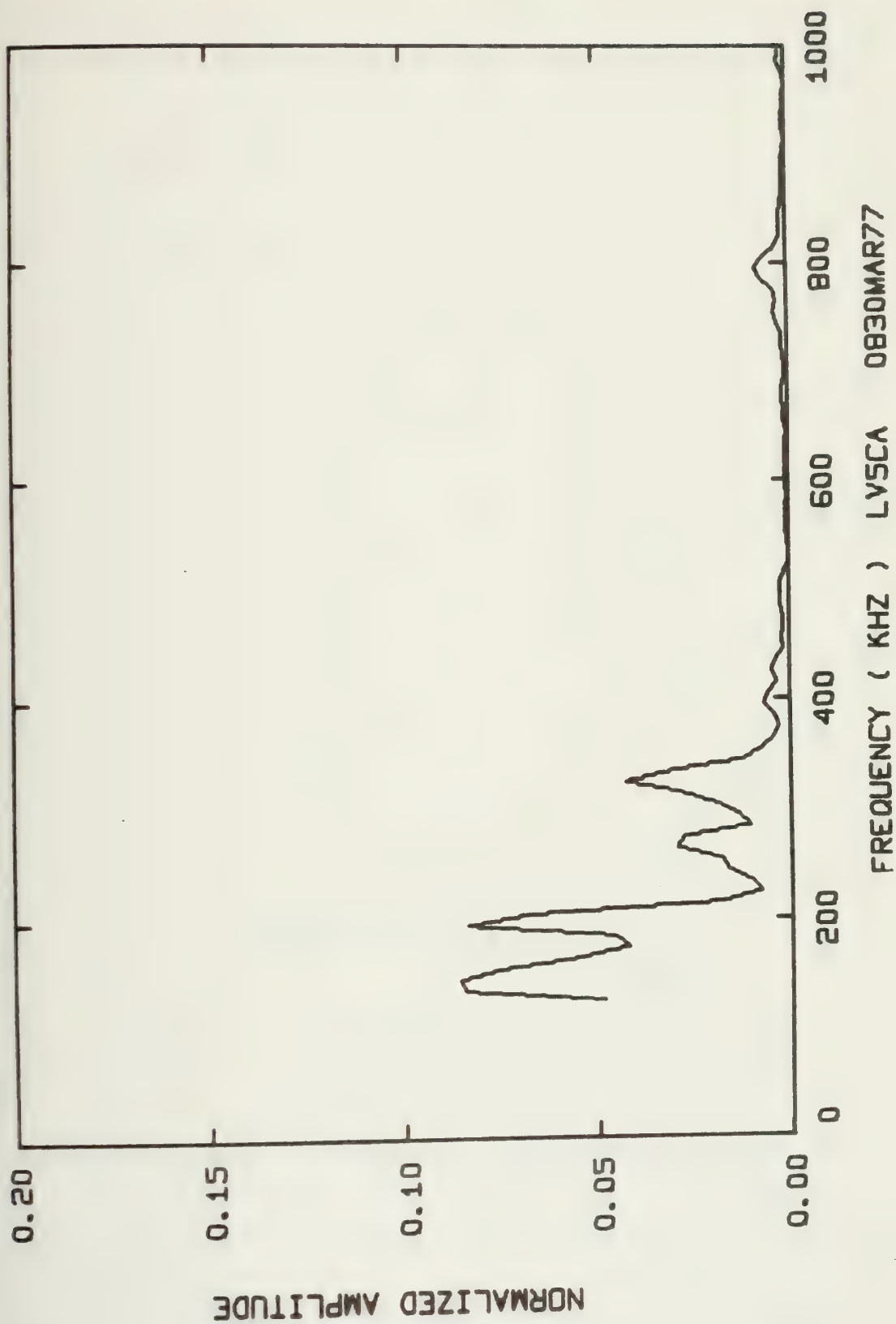




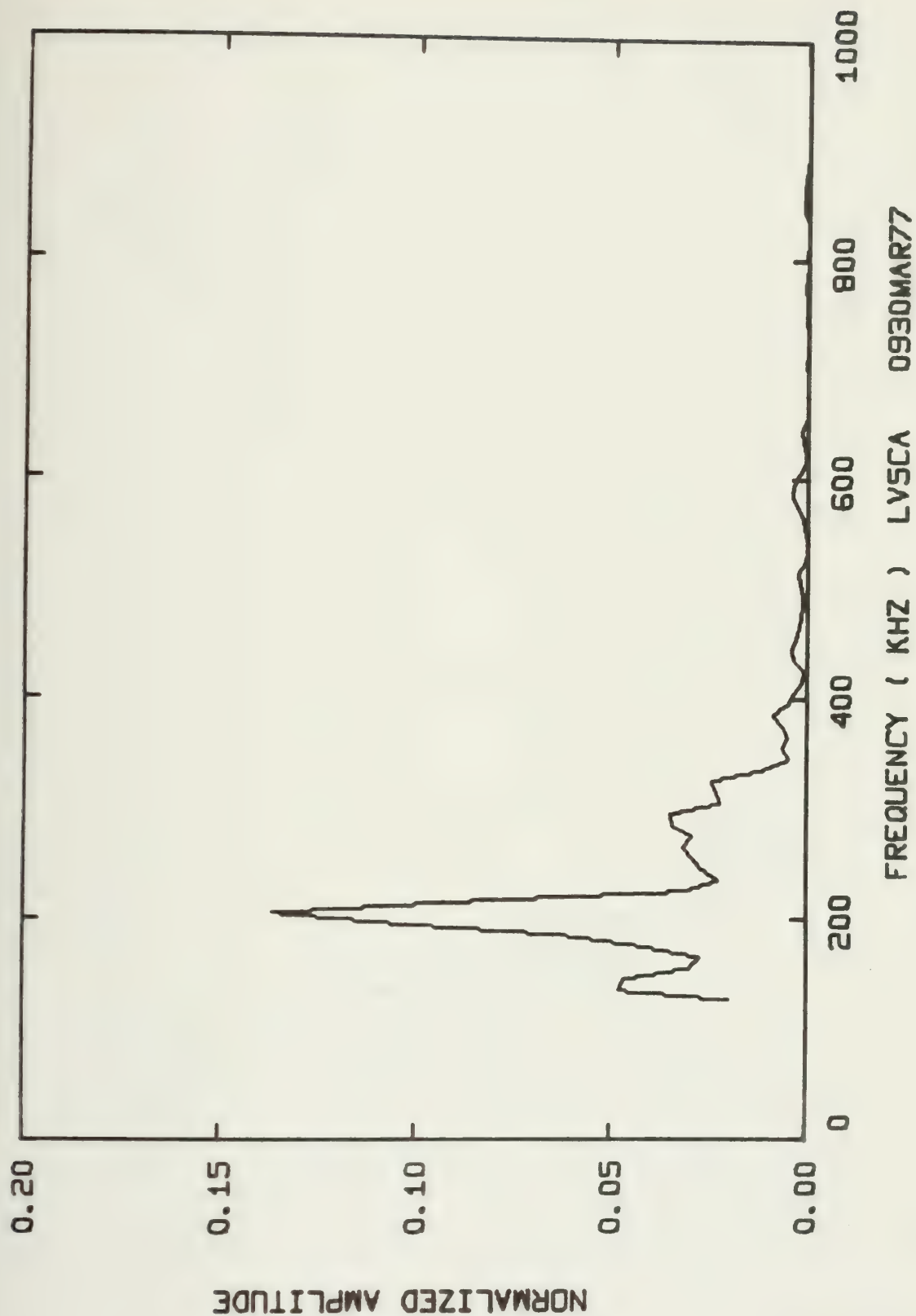






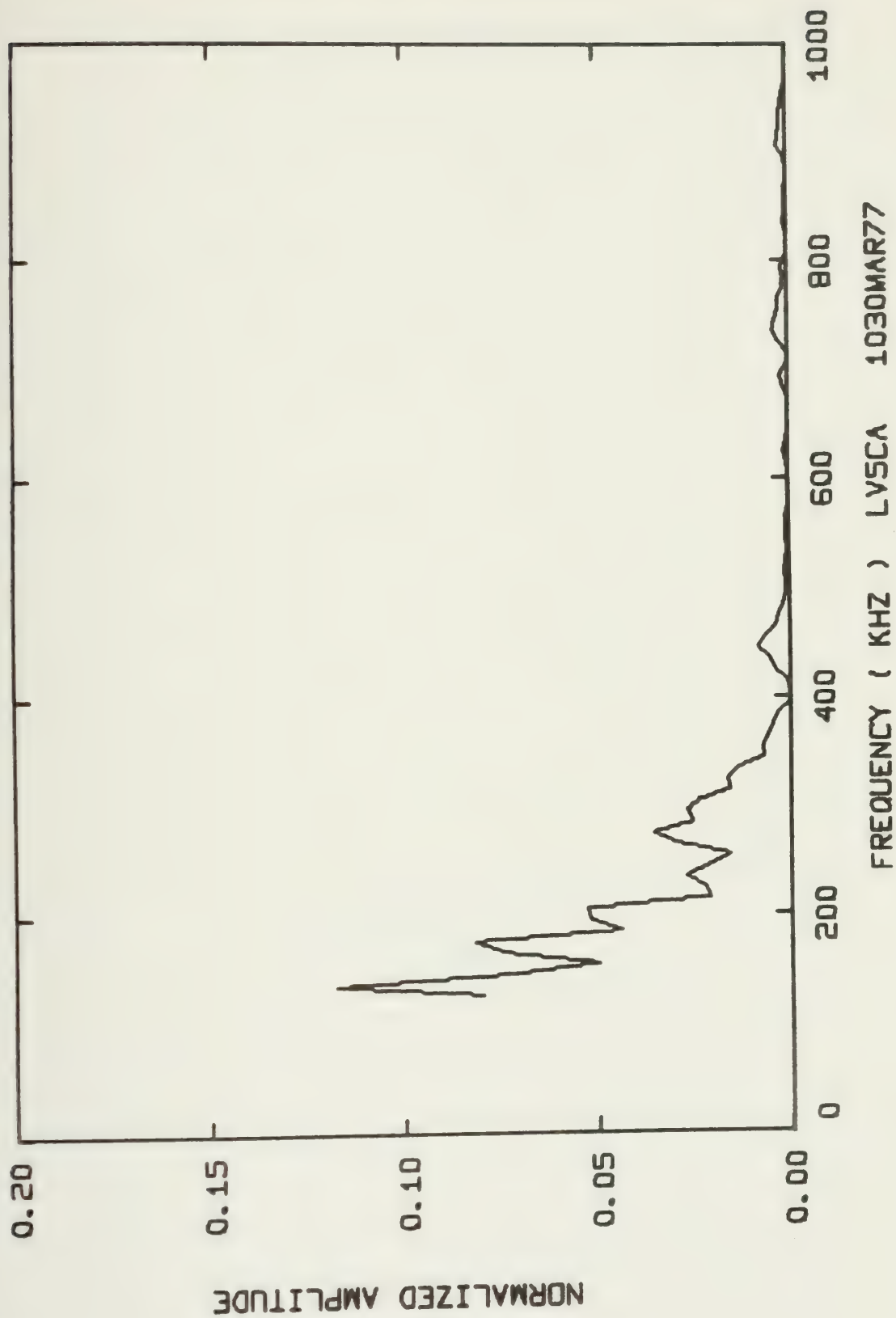




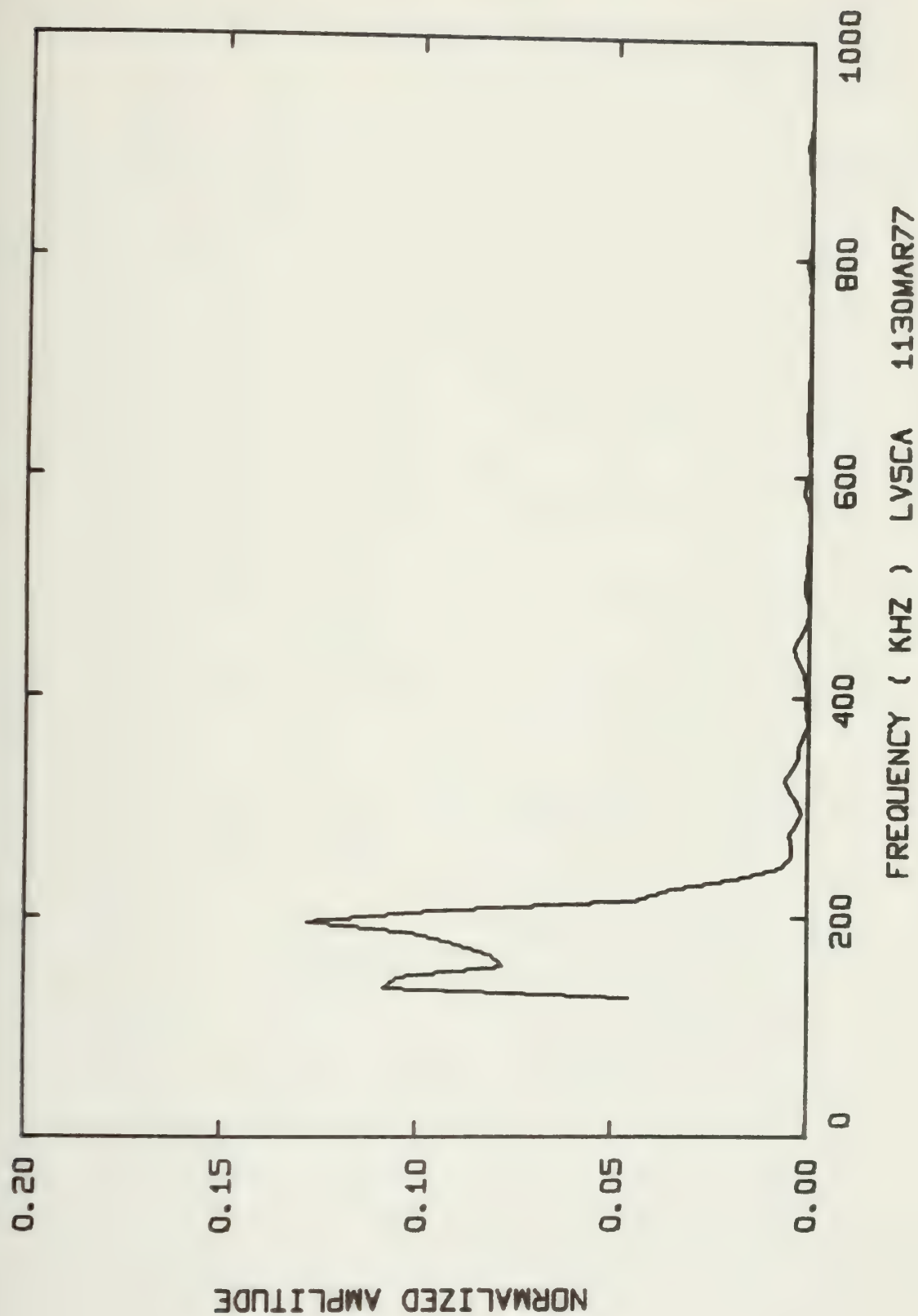




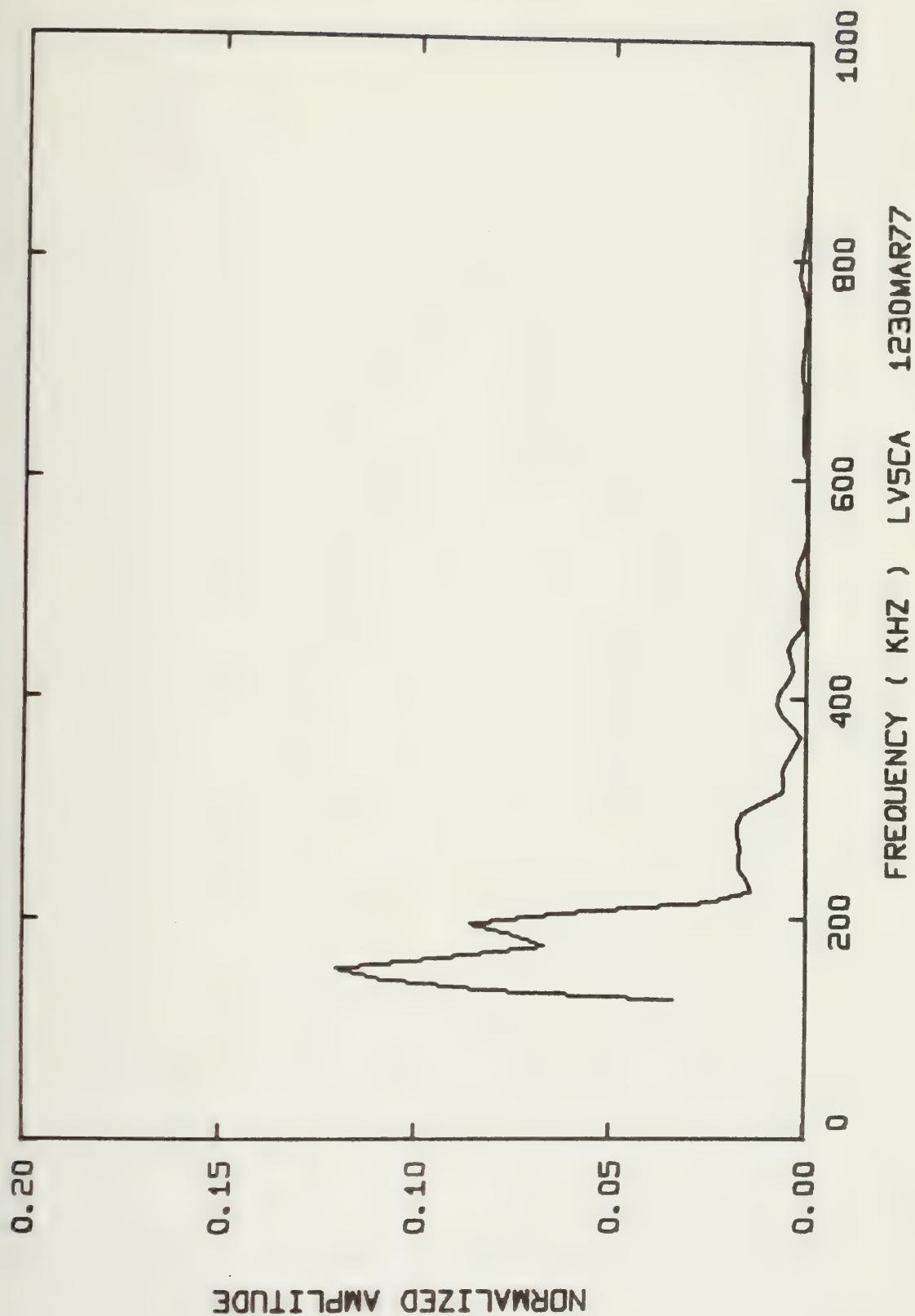




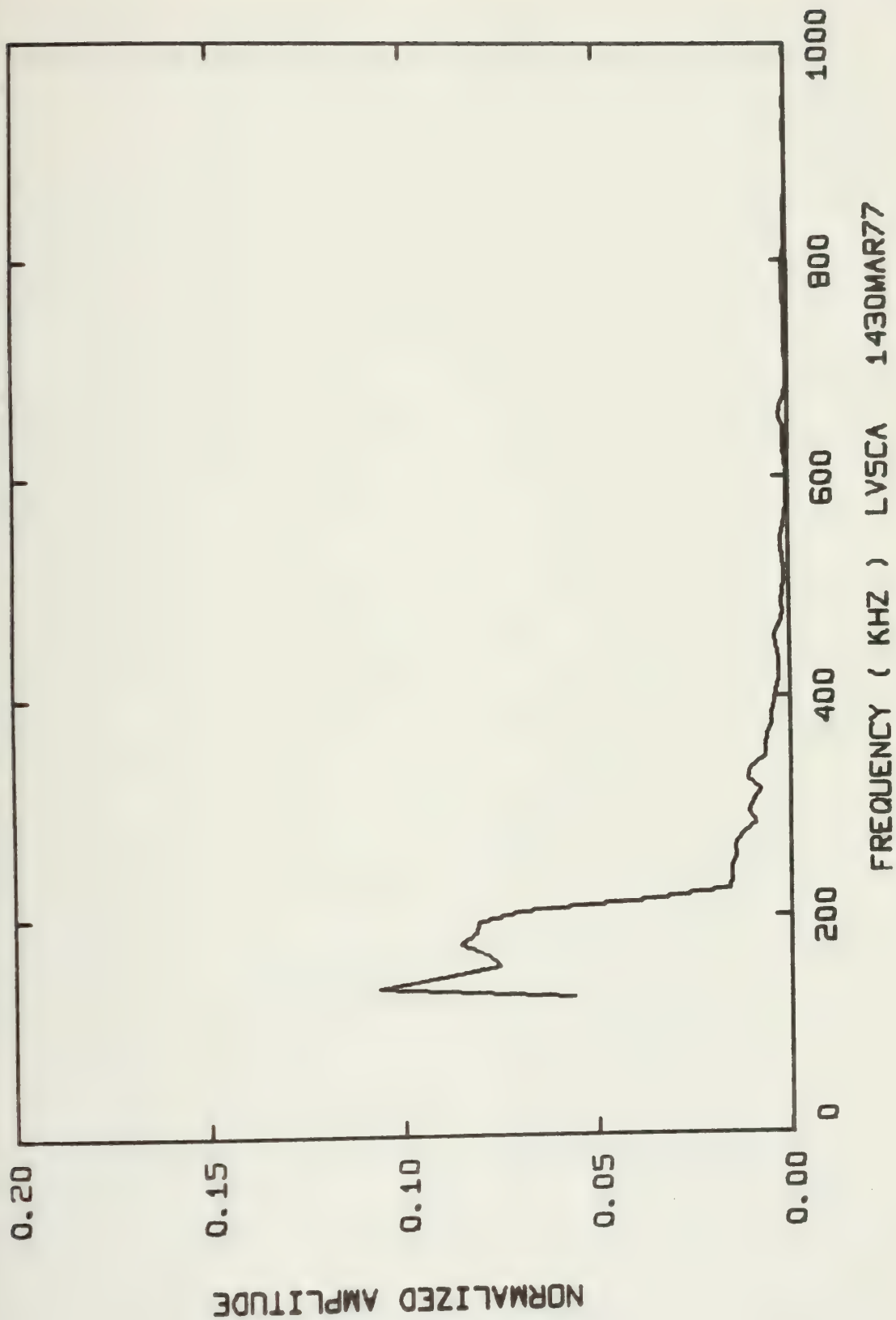






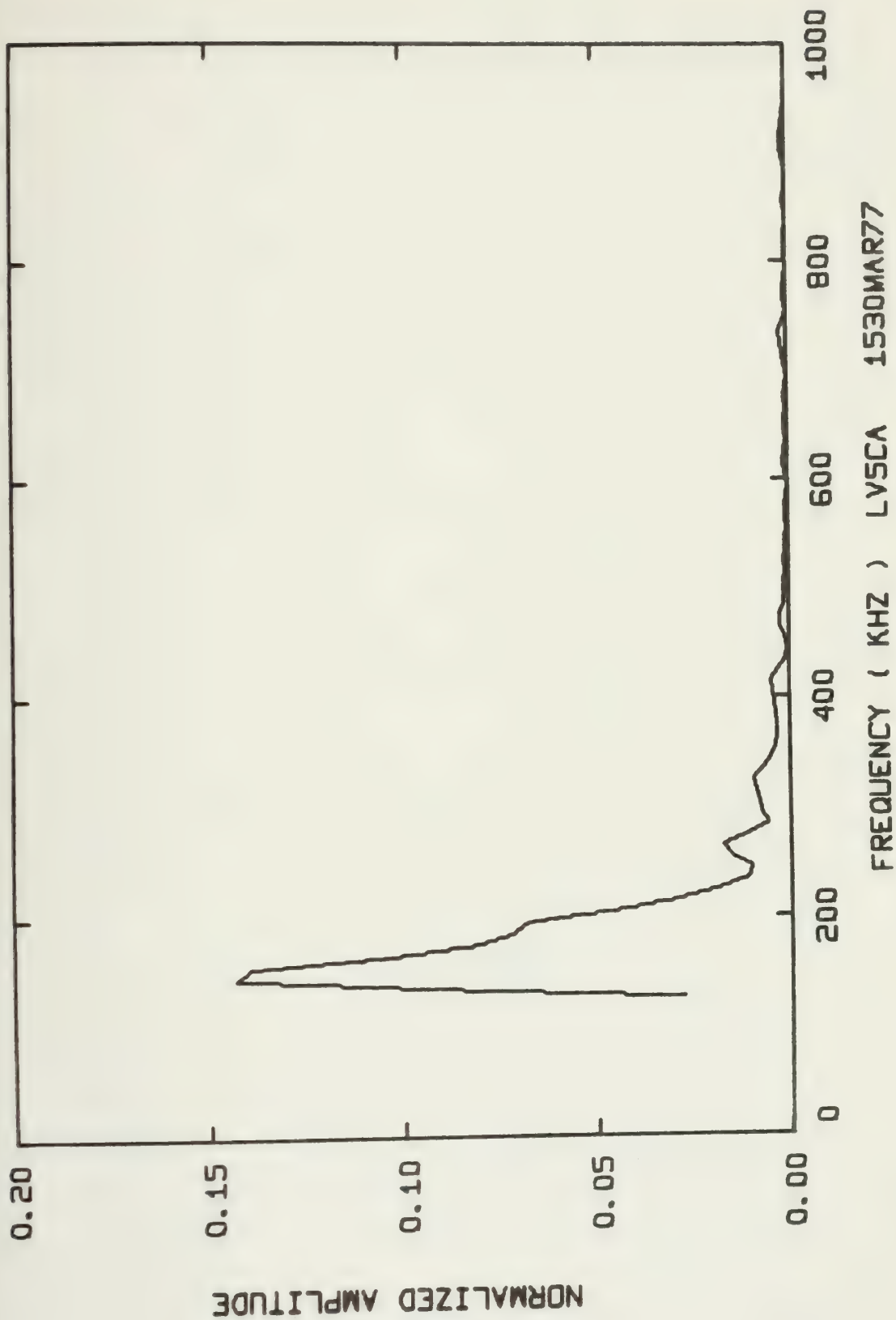




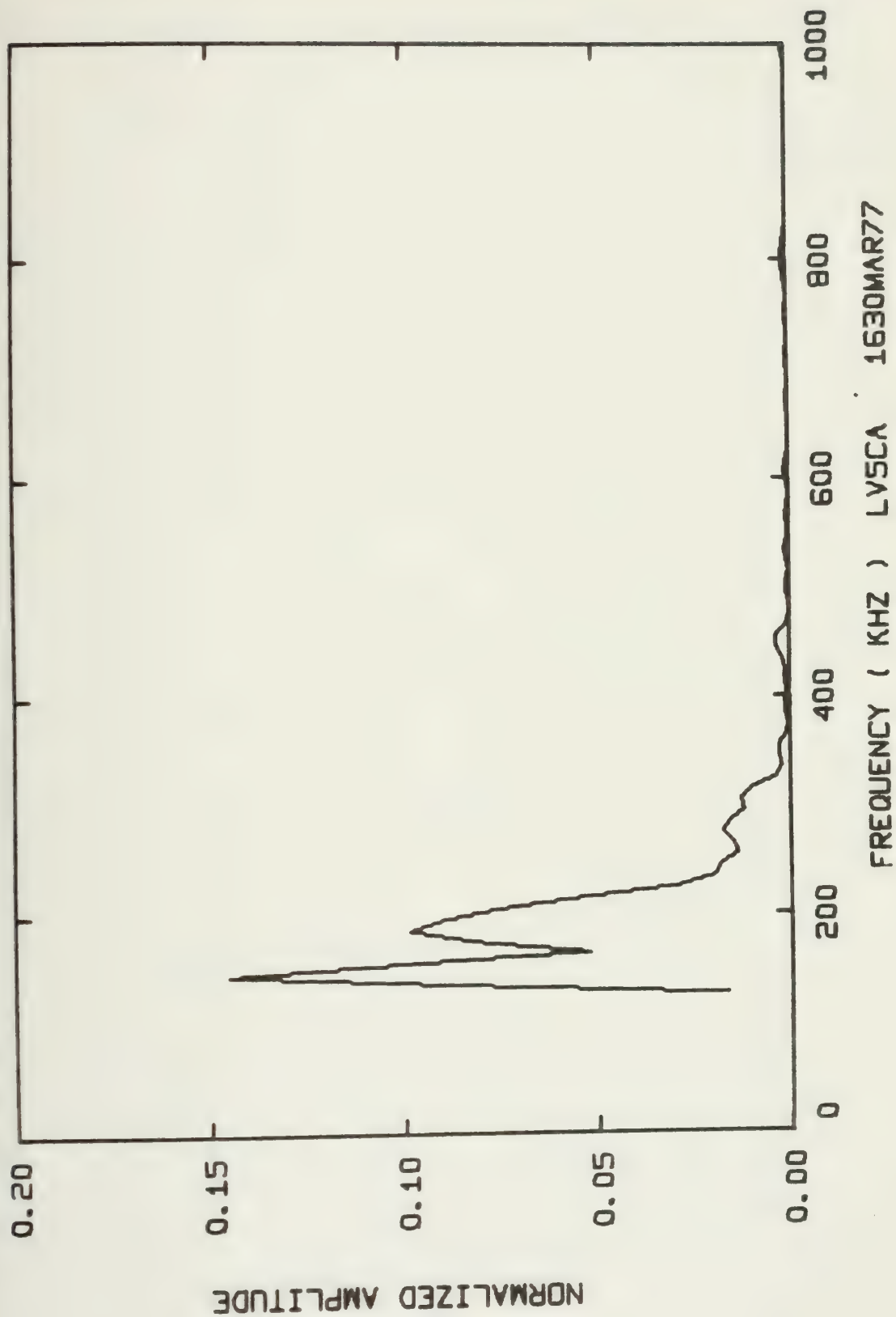




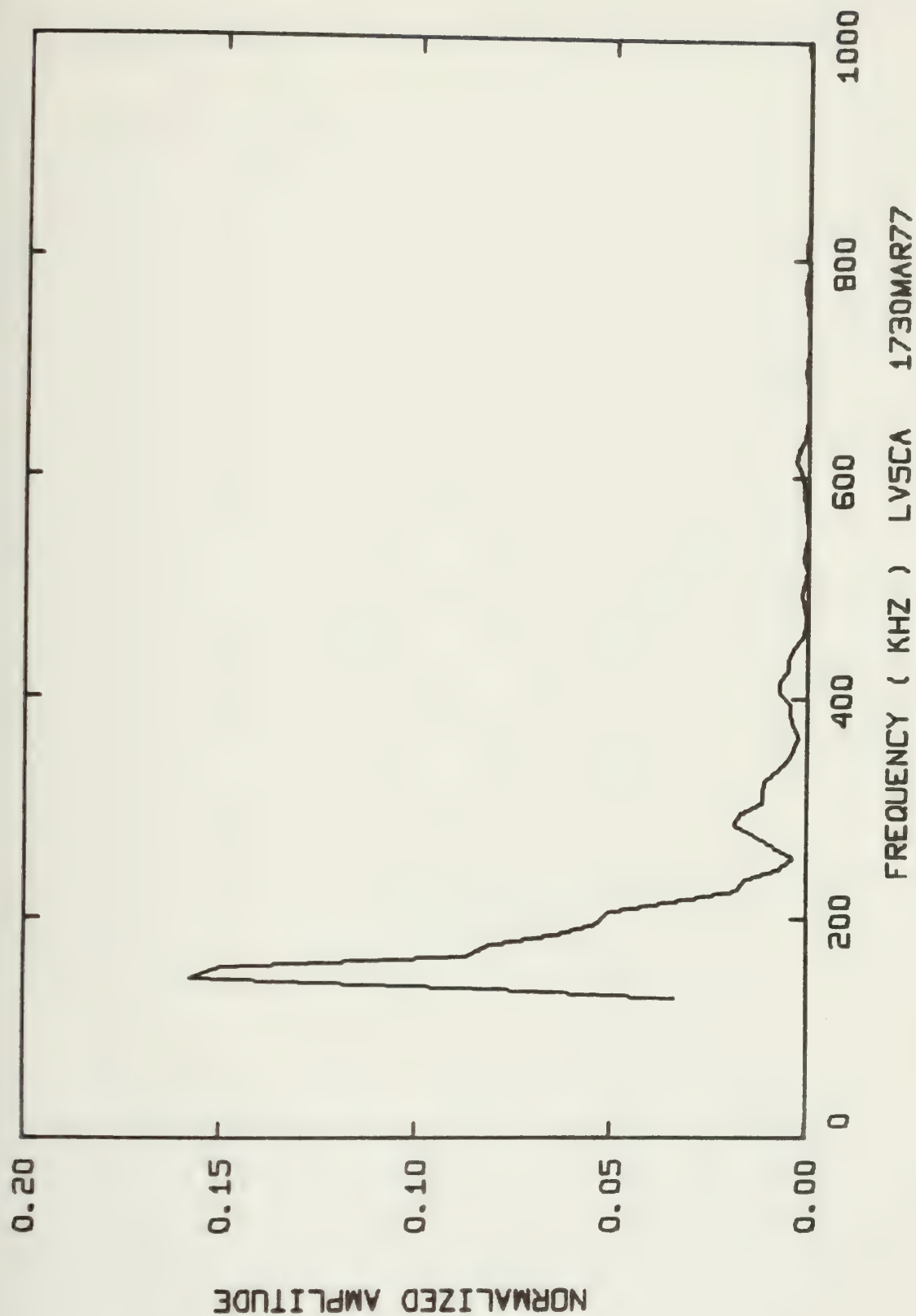




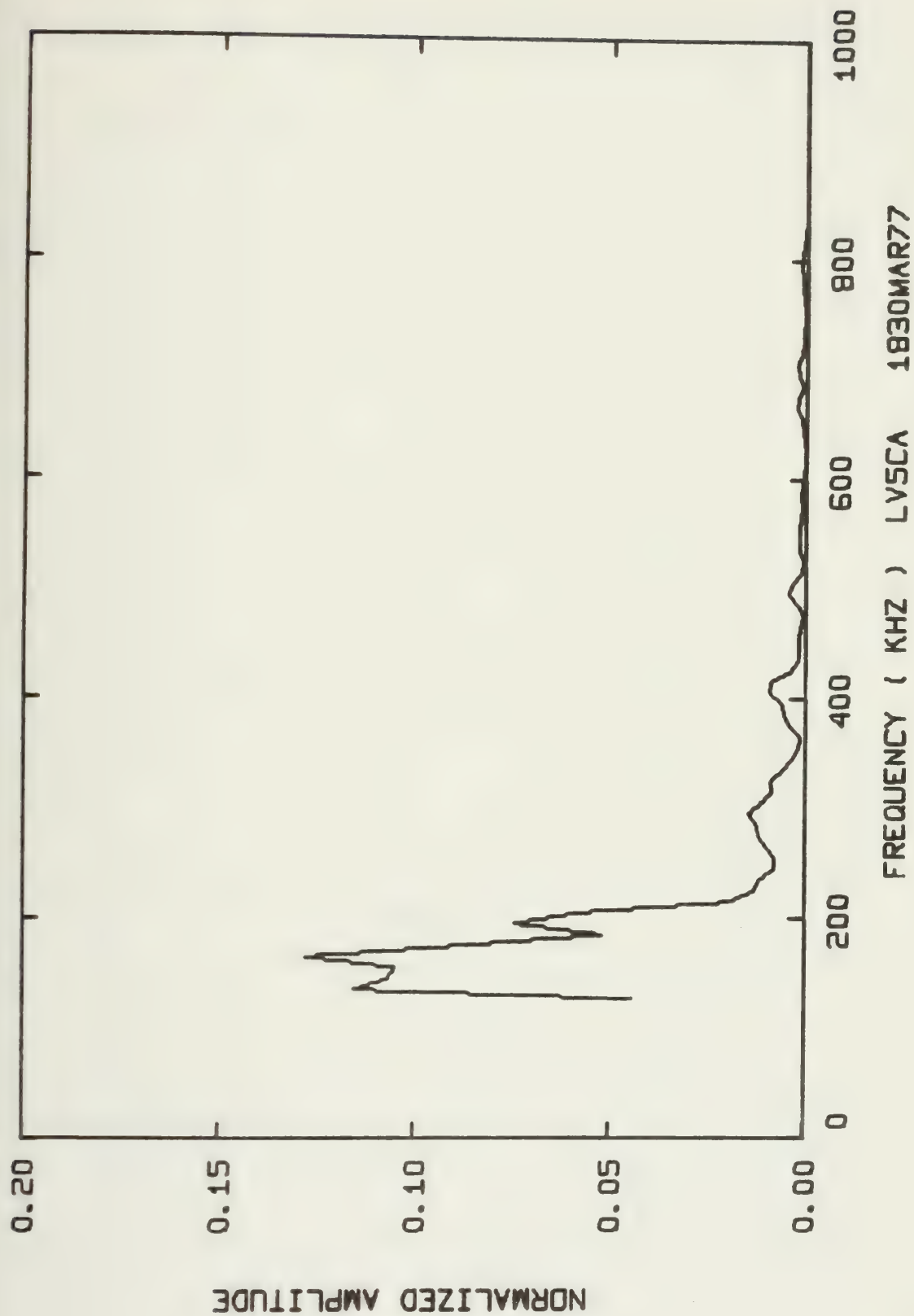






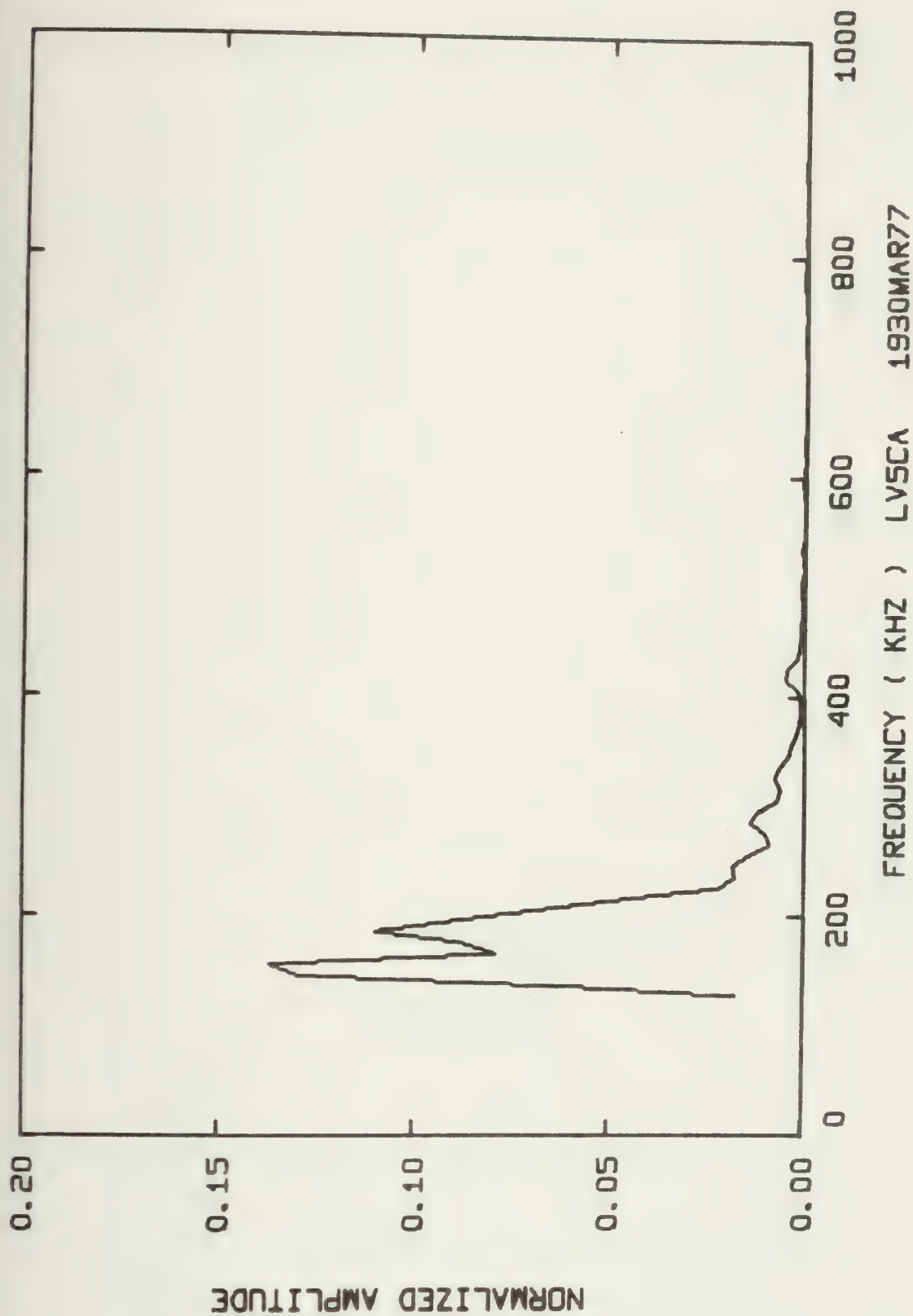




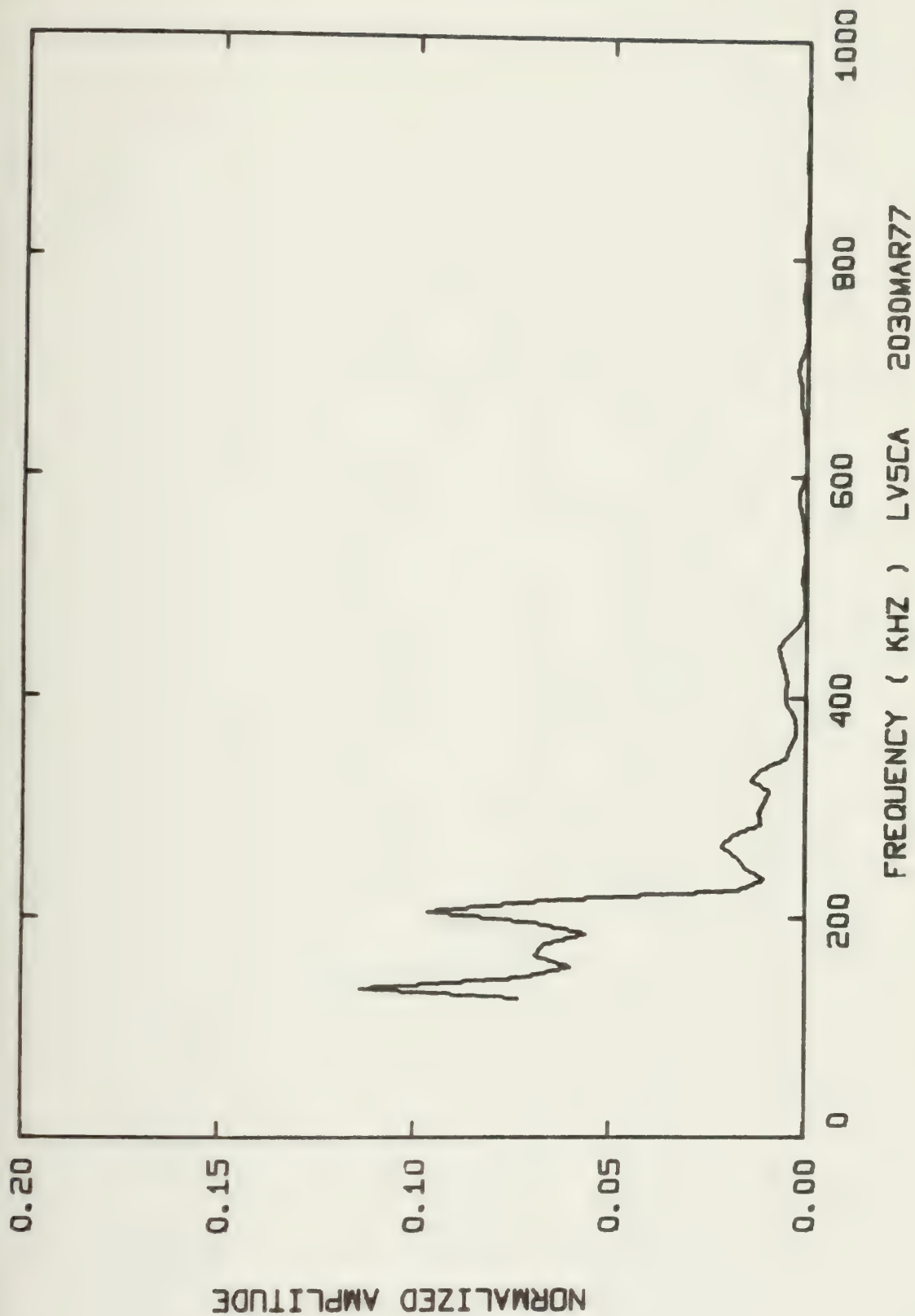




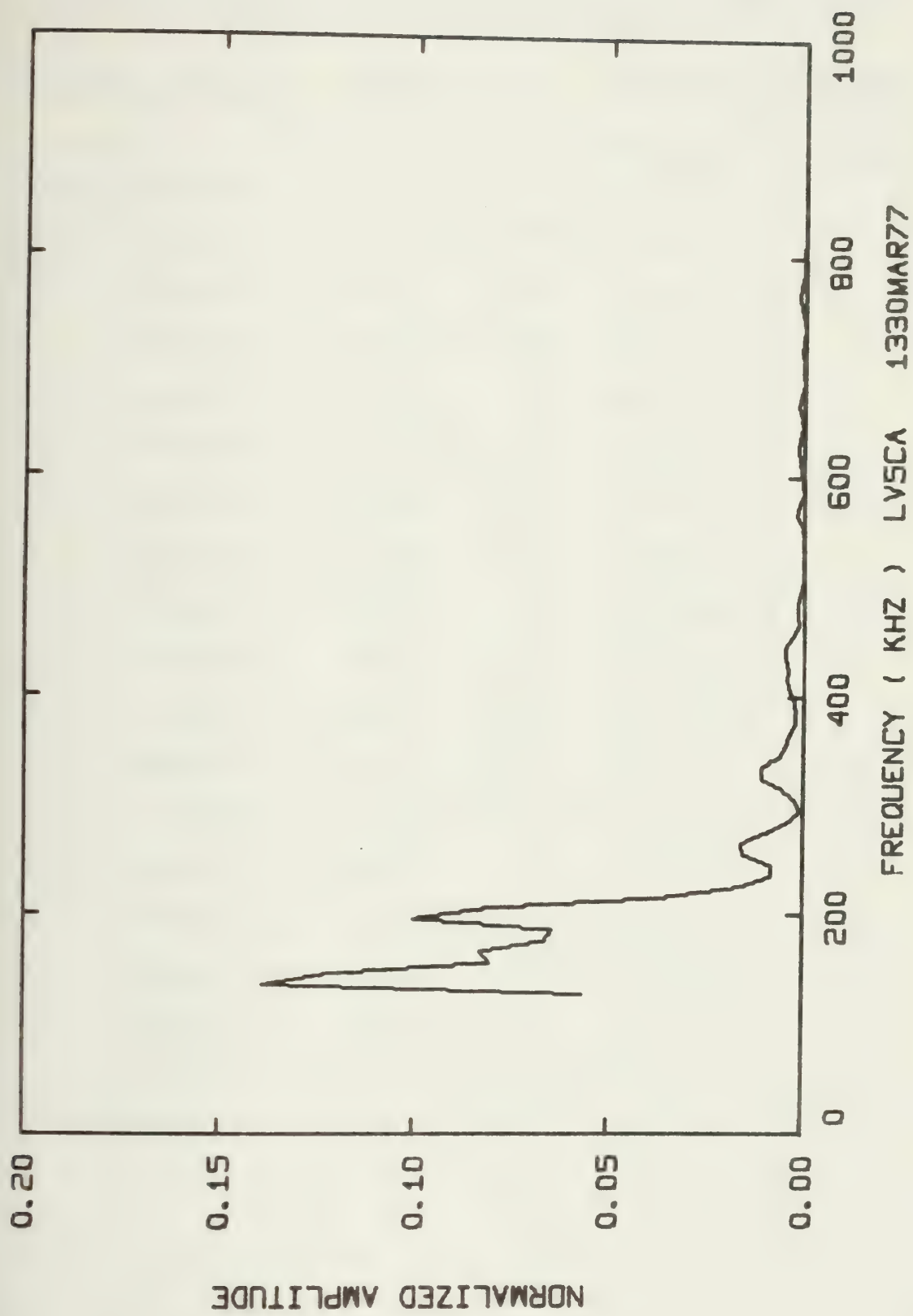












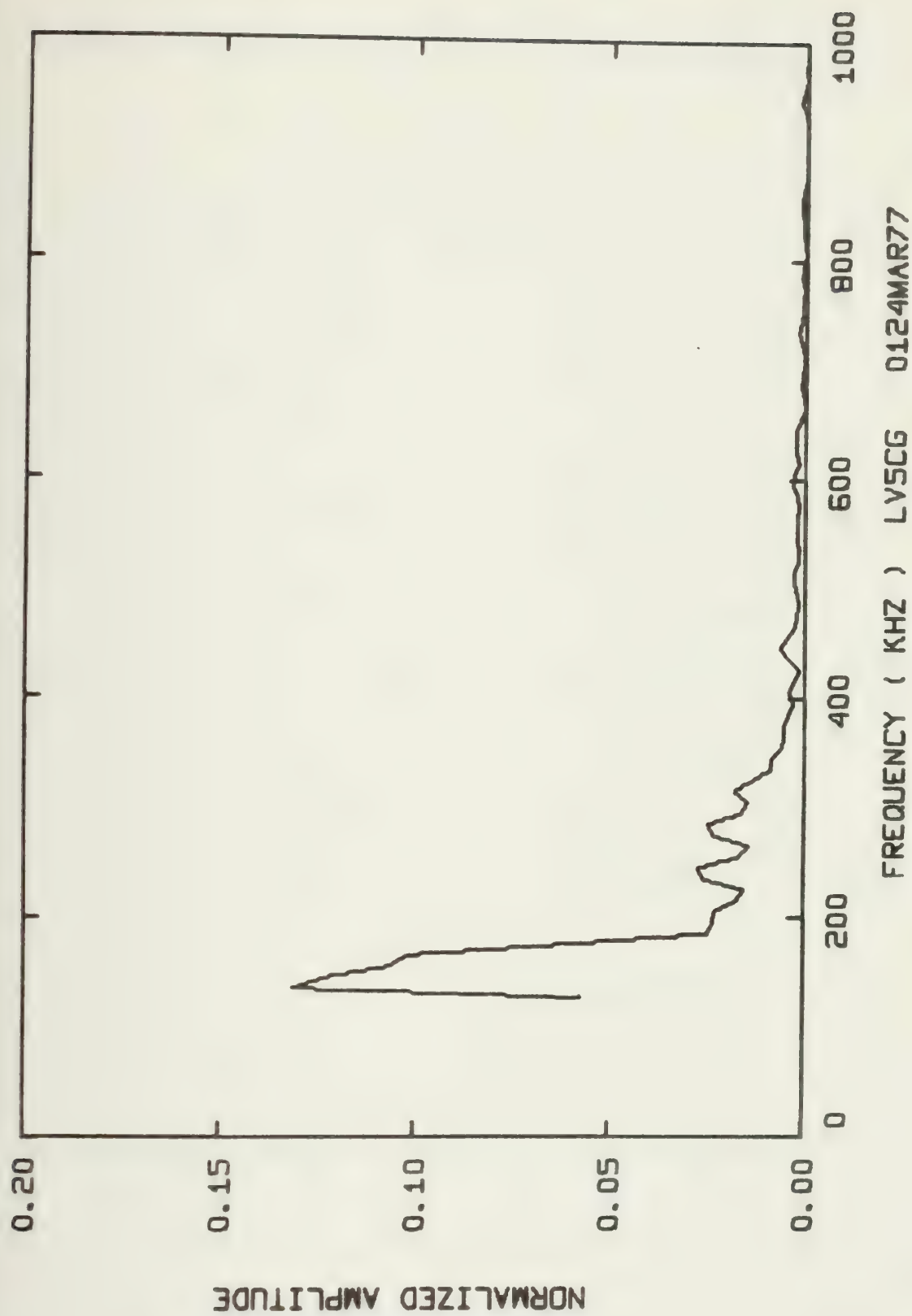


Summary of Energy per Acoustic Emission and RMS Pressure  
Across the Transducer's Face for Each Spectra

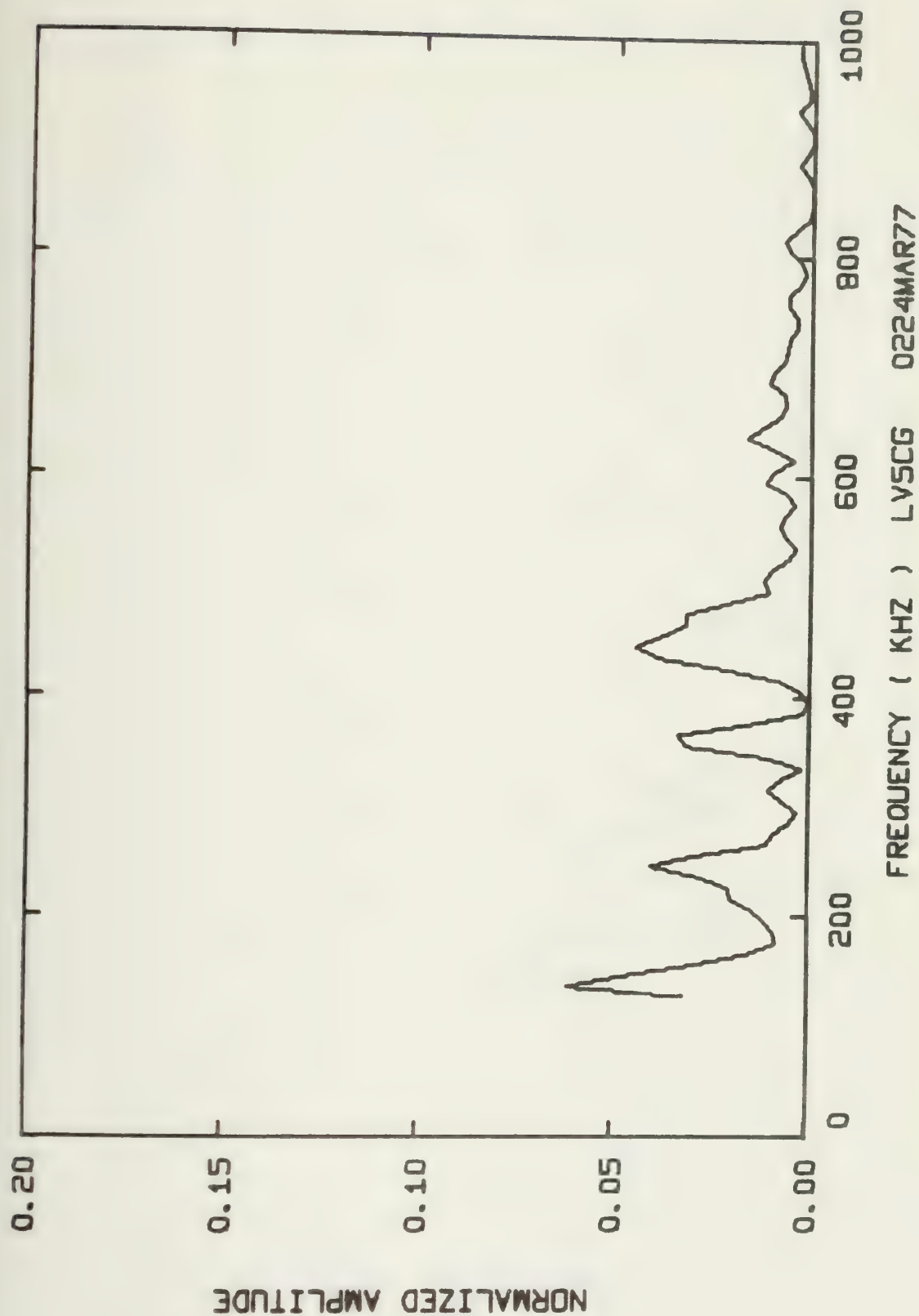
Spectral Distrib. Graph Code Number	Energy per AE (Joules)	RMS Pressure Across Face of Transducer (Pa x 10 <sup>5</sup> )
LV5CG 0124MAR77	16.920 x 10 <sup>-6</sup>	460.49
0224MAR77	34.423 x 10 <sup>-9</sup>	52.87
0324MAR77	44.677 x 10 <sup>-9</sup>	50.28
0424MAR77	398.86 x 10 <sup>-9</sup>	103.60
0524MAR77	91.554 x 10 <sup>-9</sup>	64.58
0127MAR77	341.48 x 10 <sup>-9</sup>	106.15
0227MAR77	65.203 x 10 <sup>-6</sup>	720.34
0327MAR77	32.347 x 10 <sup>-6</sup>	578.48
0427MAR77	6.8735 x 10 <sup>-6</sup>	1121.79
0128MAR77	298.29 x 10 <sup>-6</sup>	1347.32
0228MAR77	533.58 x 10 <sup>-9</sup>	112.17
0328MAR77	294.27 x 10 <sup>-9</sup>	91.95
0428MAR77	12.702 x 10 <sup>-6</sup>	414.01
0628MAR77	28.713 x 10 <sup>-9</sup>	39.14
0728MAR77	85.000 x 10 <sup>-9</sup>	58.74
0828MAR77	529.42 x 10 <sup>-6</sup>	1532.09
0928MAR77	616.46 x 10 <sup>-9</sup>	118.49
1028MAR77	90.121 x 10 <sup>-9</sup>	64.86
1128MAR77	334.82 x 10 <sup>-6</sup>	1413.66



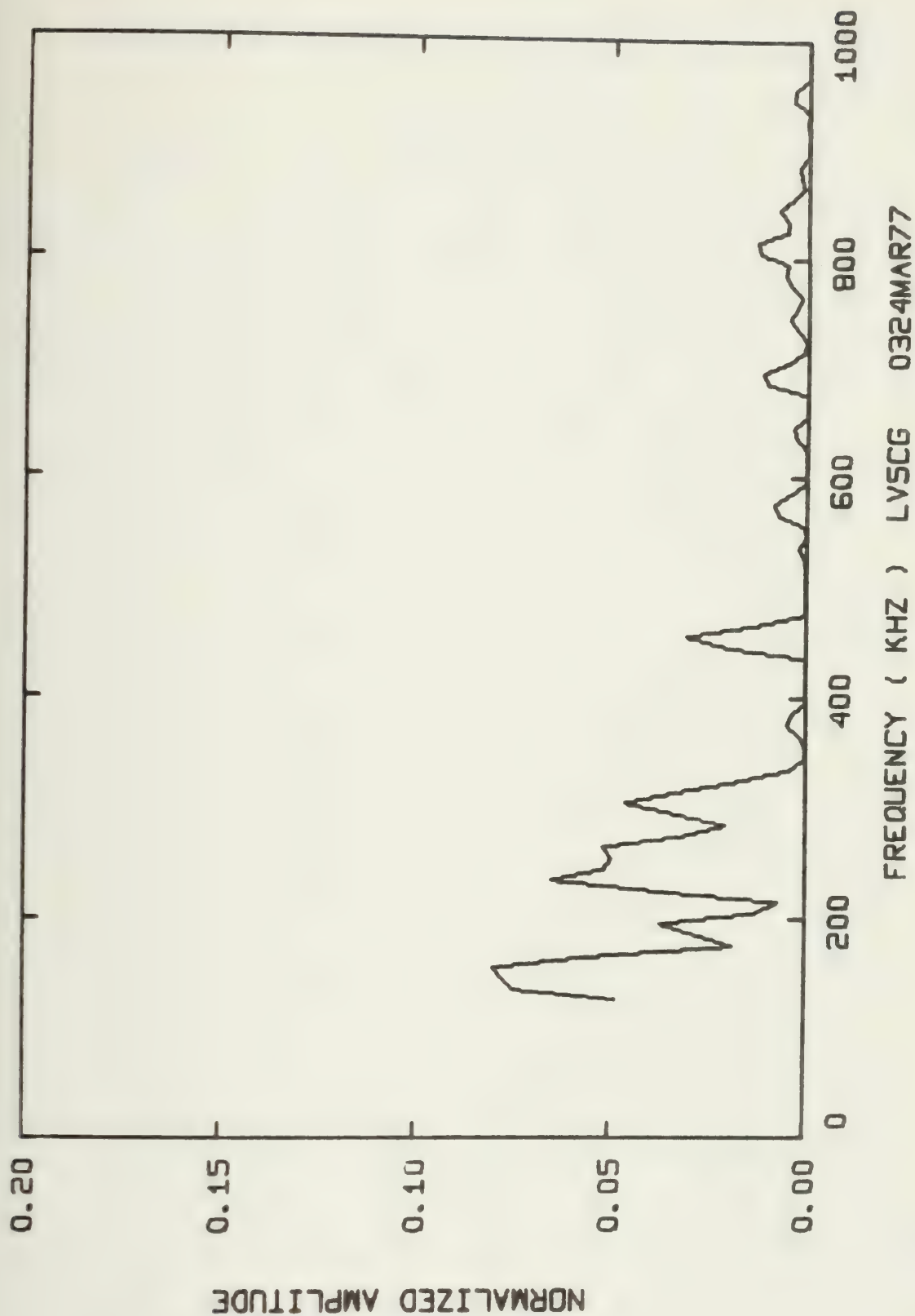




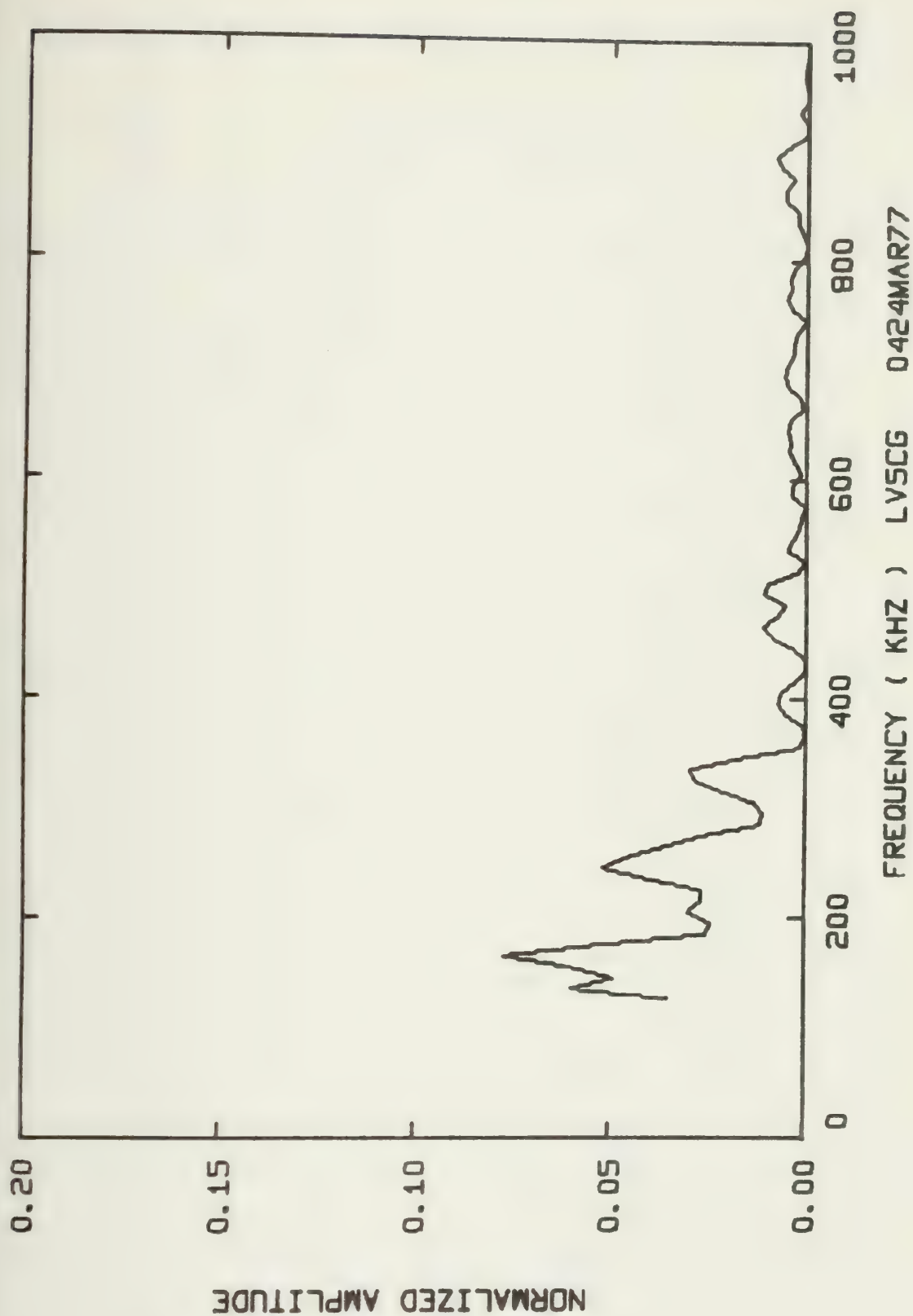






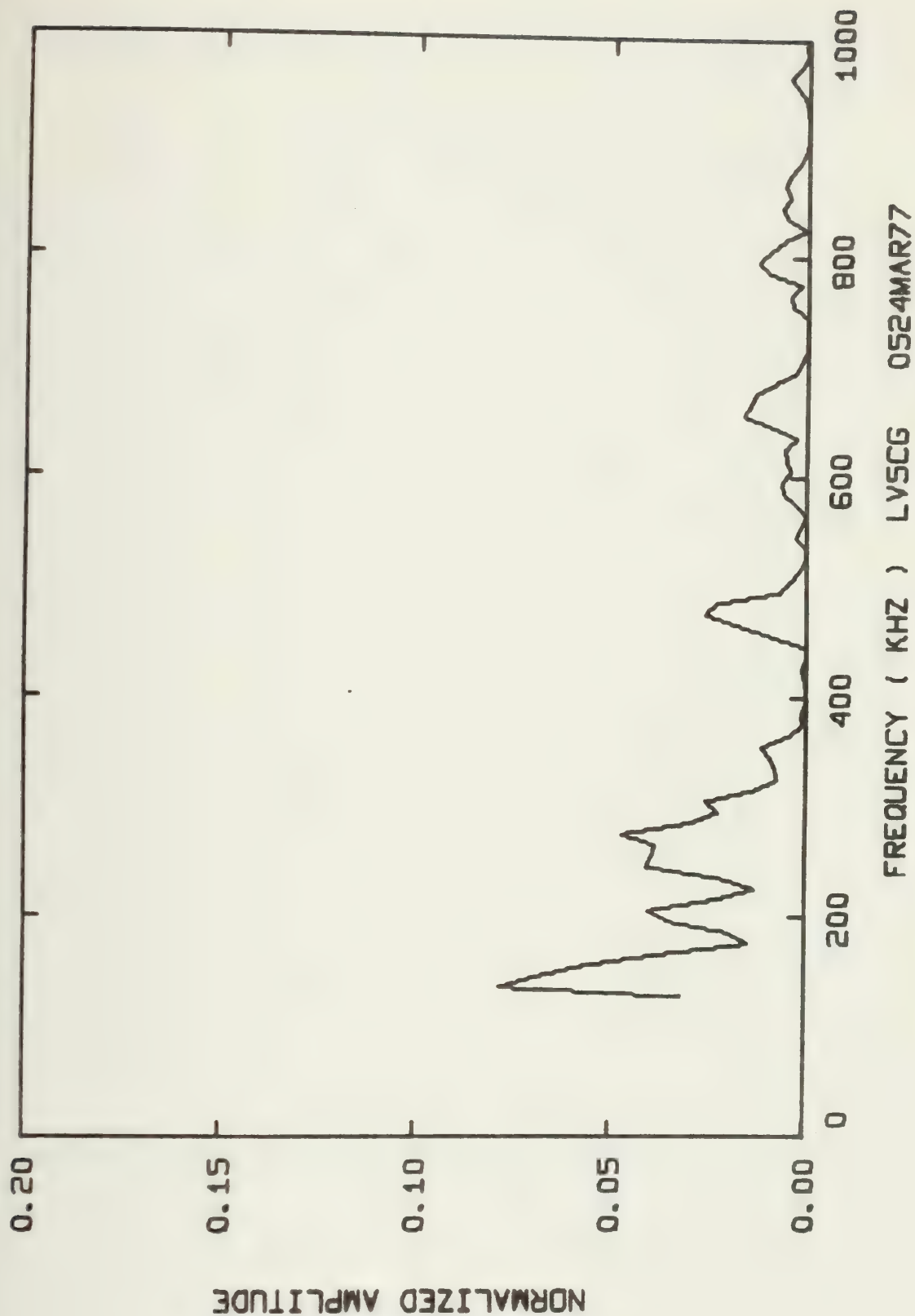




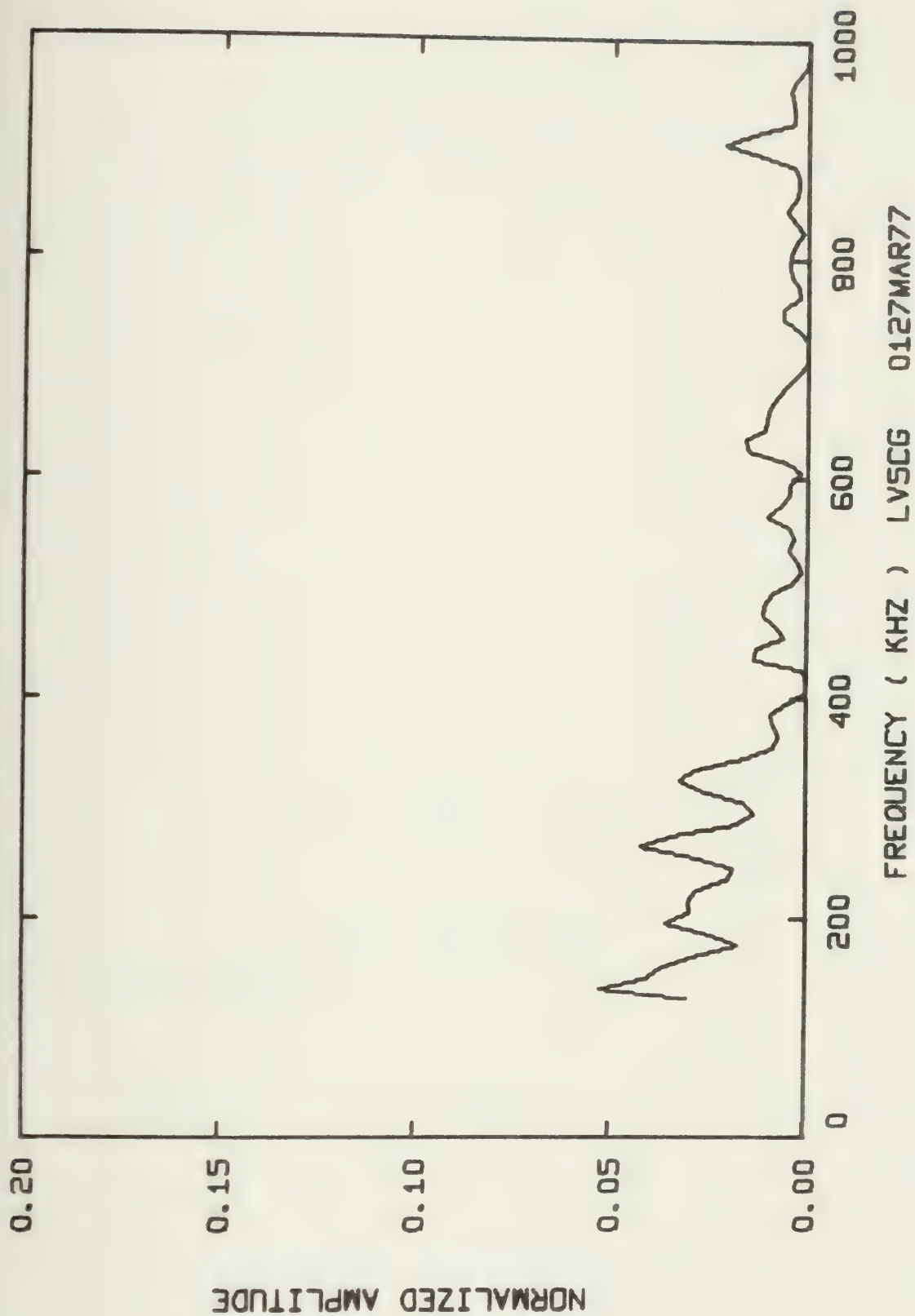




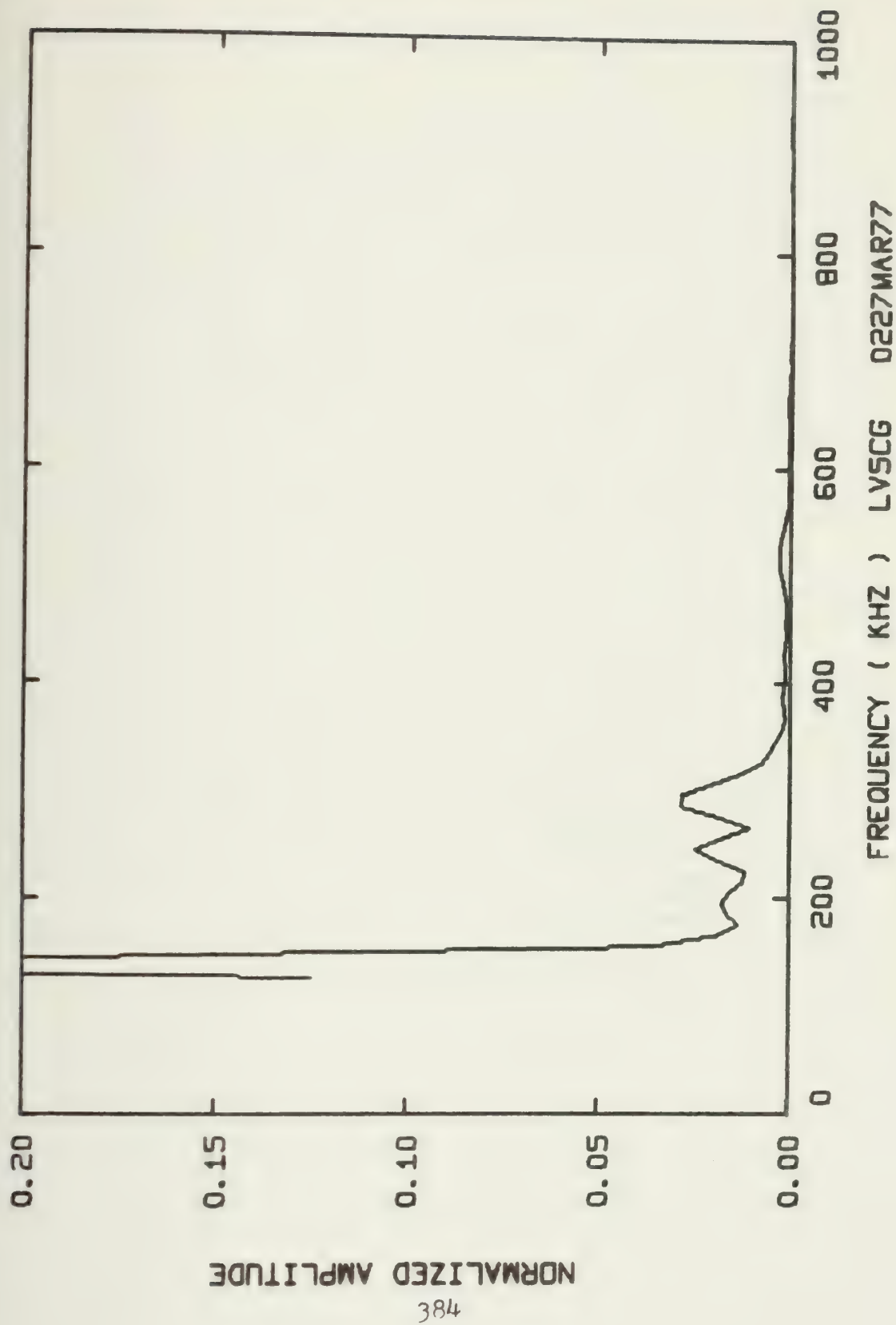




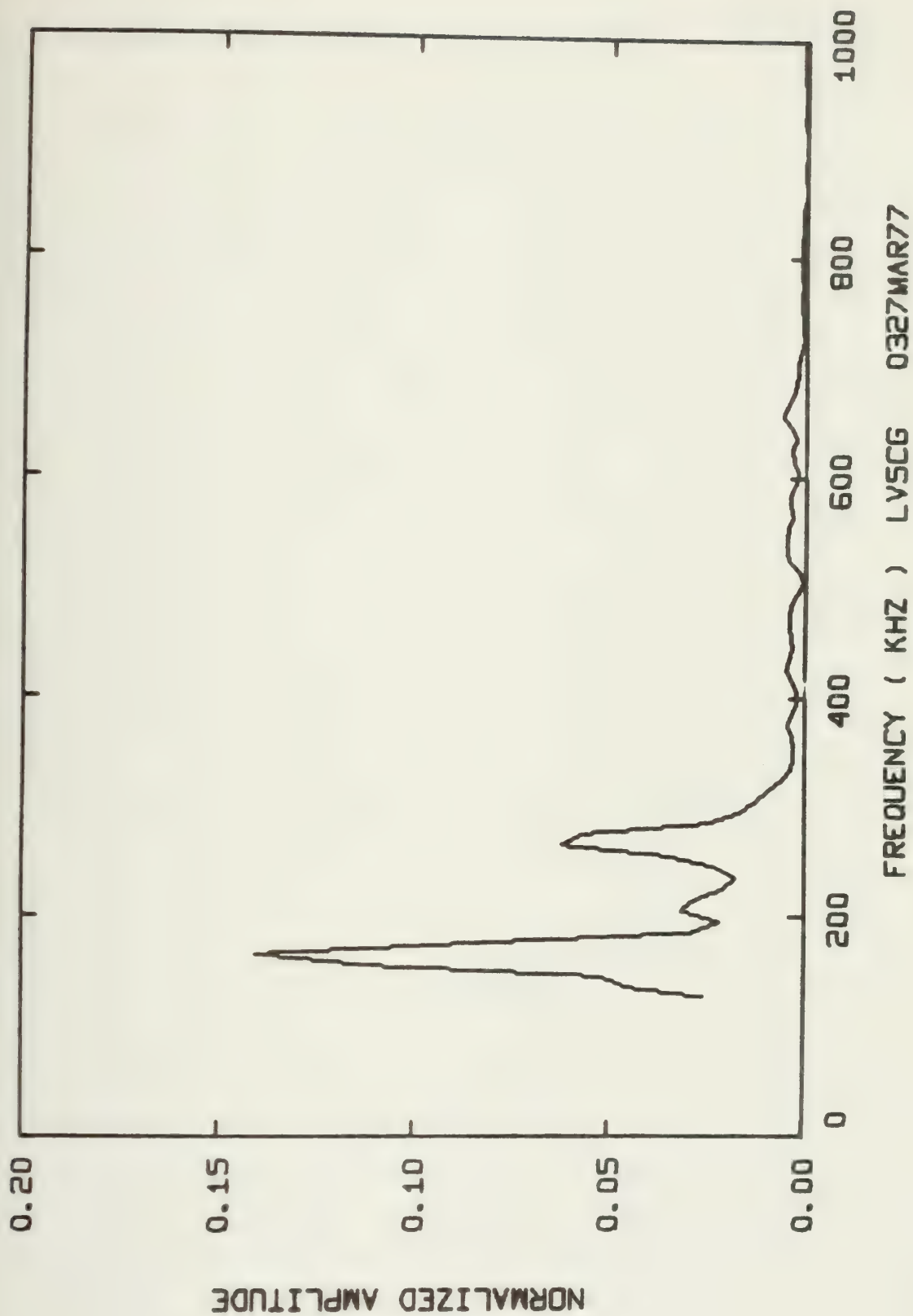








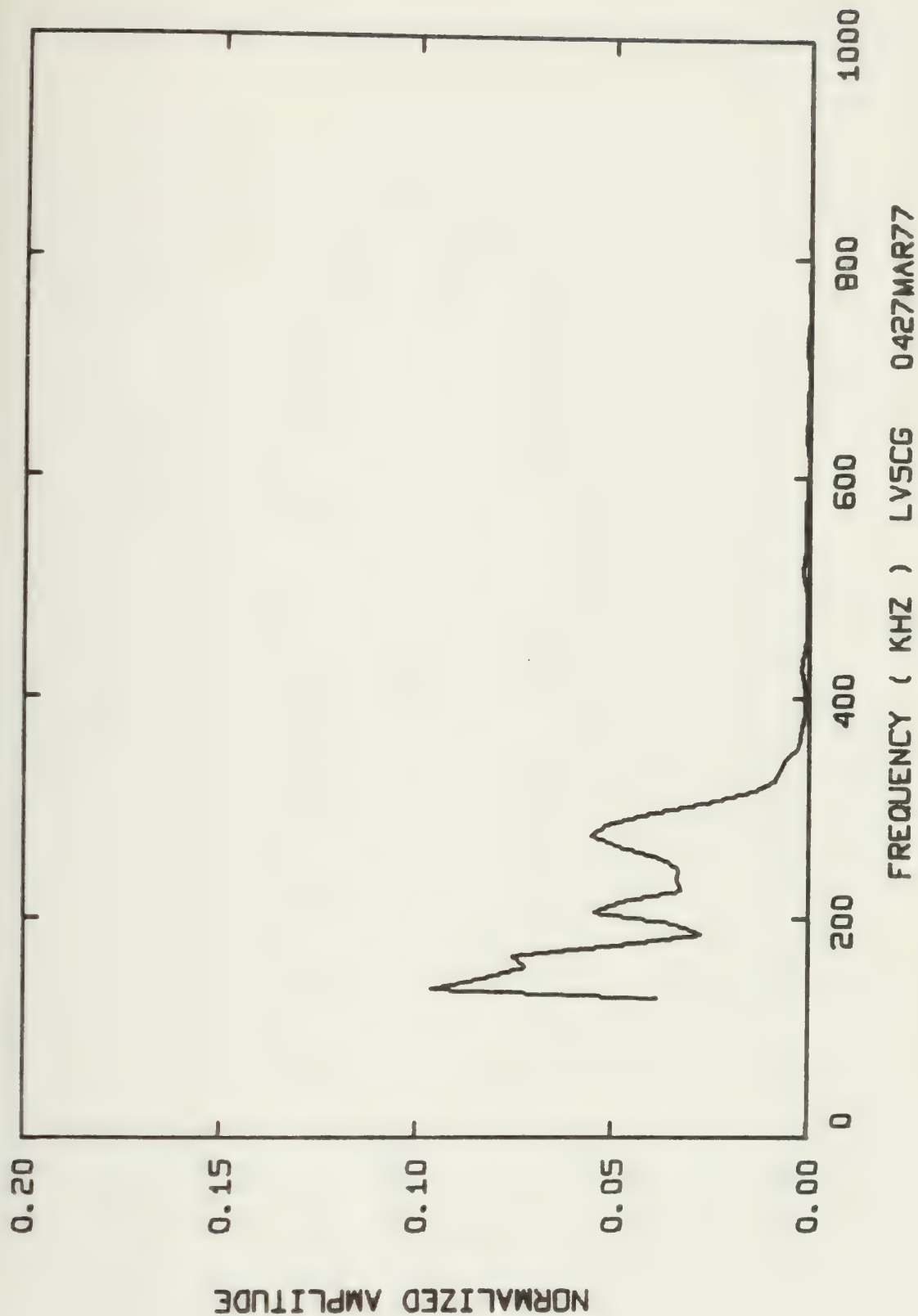




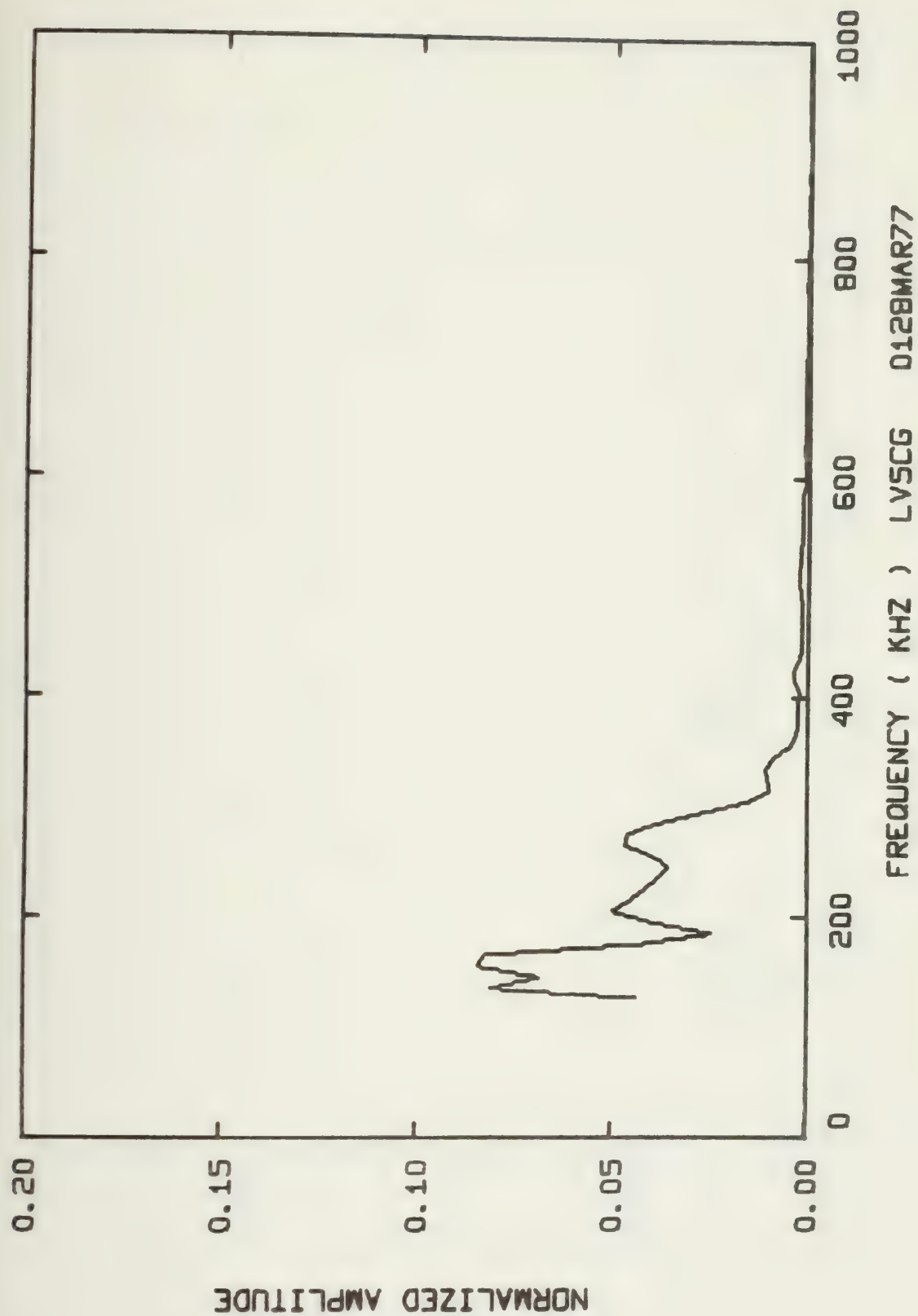
FREQUENCY ( KHZ ) LVSCG 0327MAR77



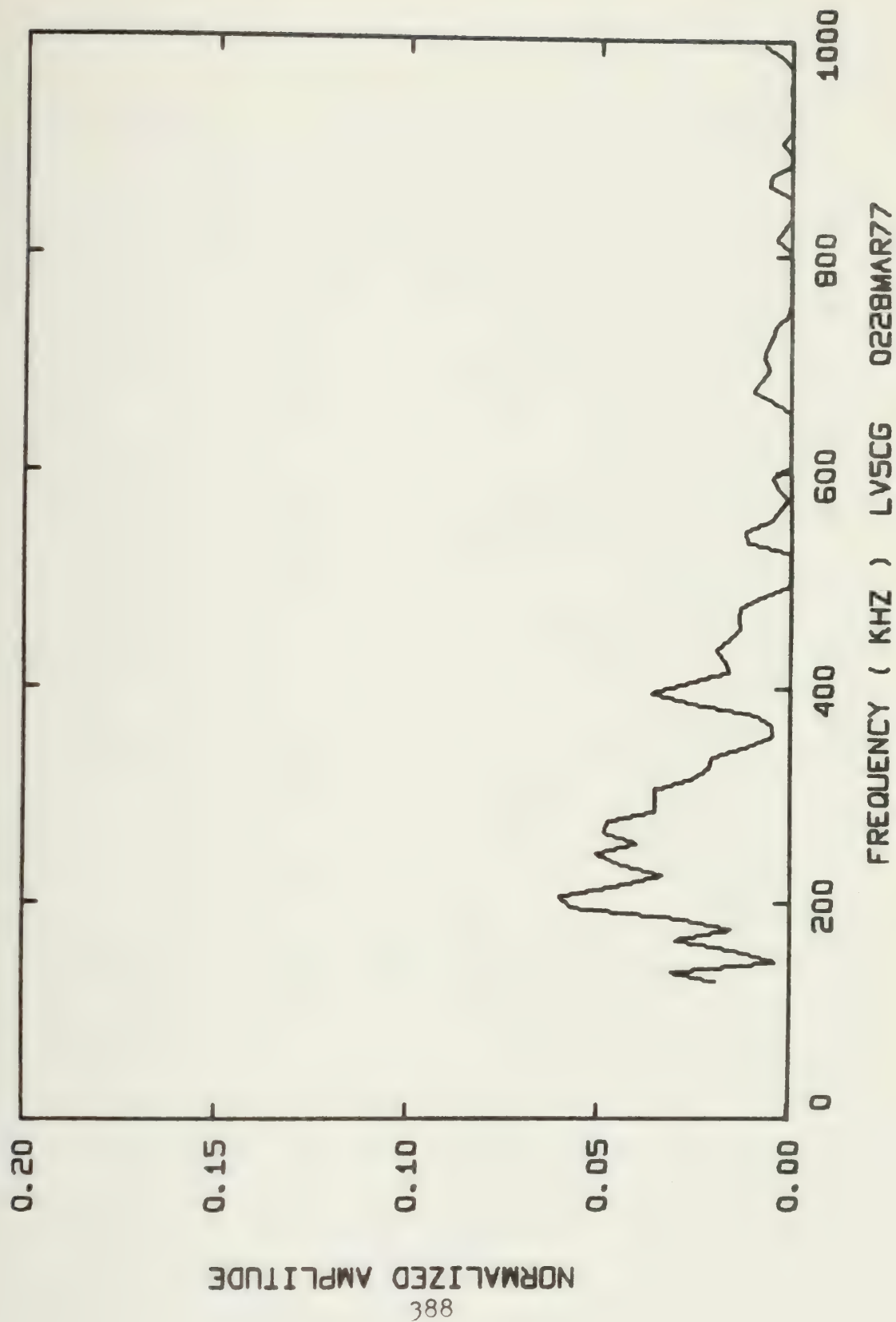




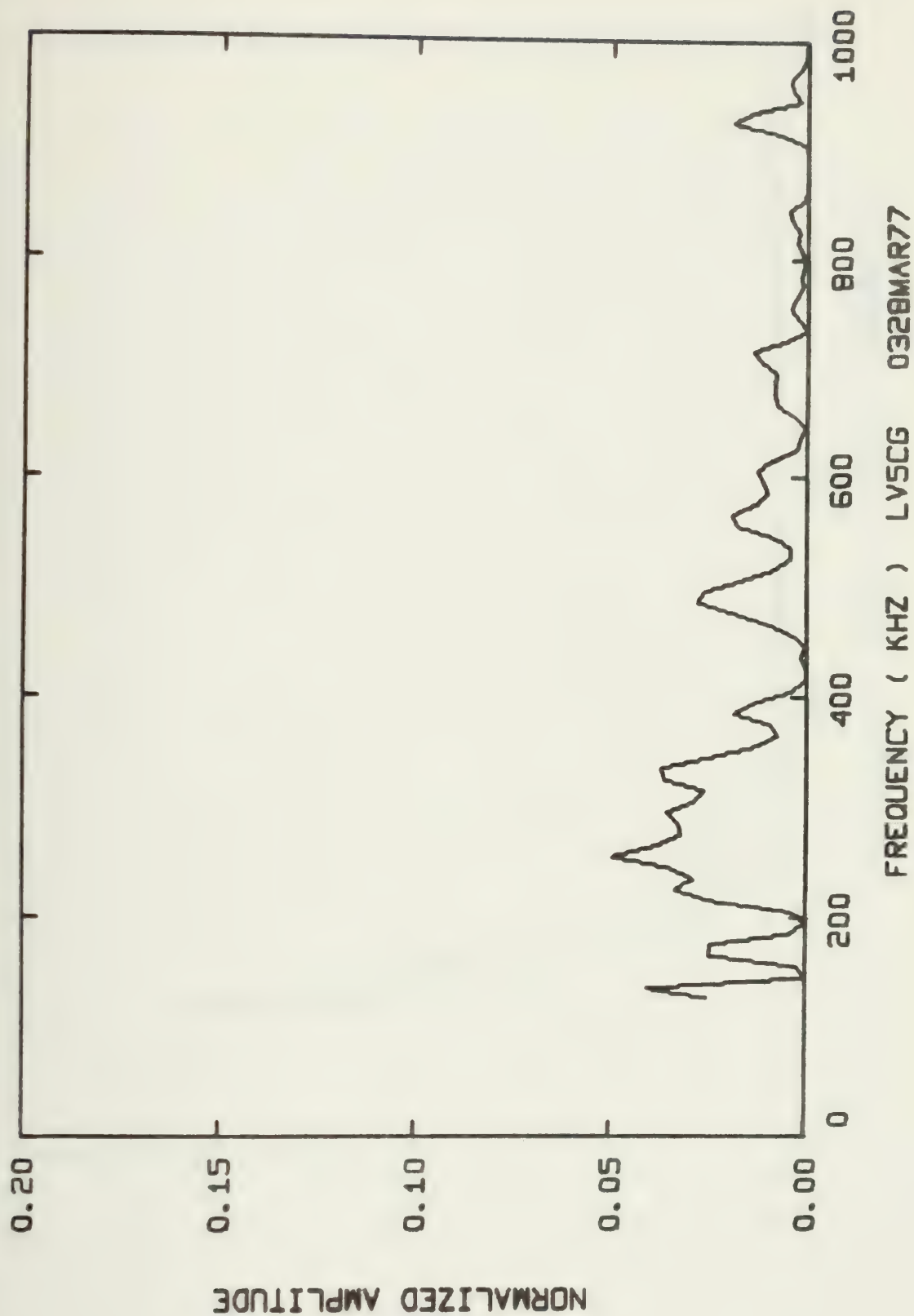






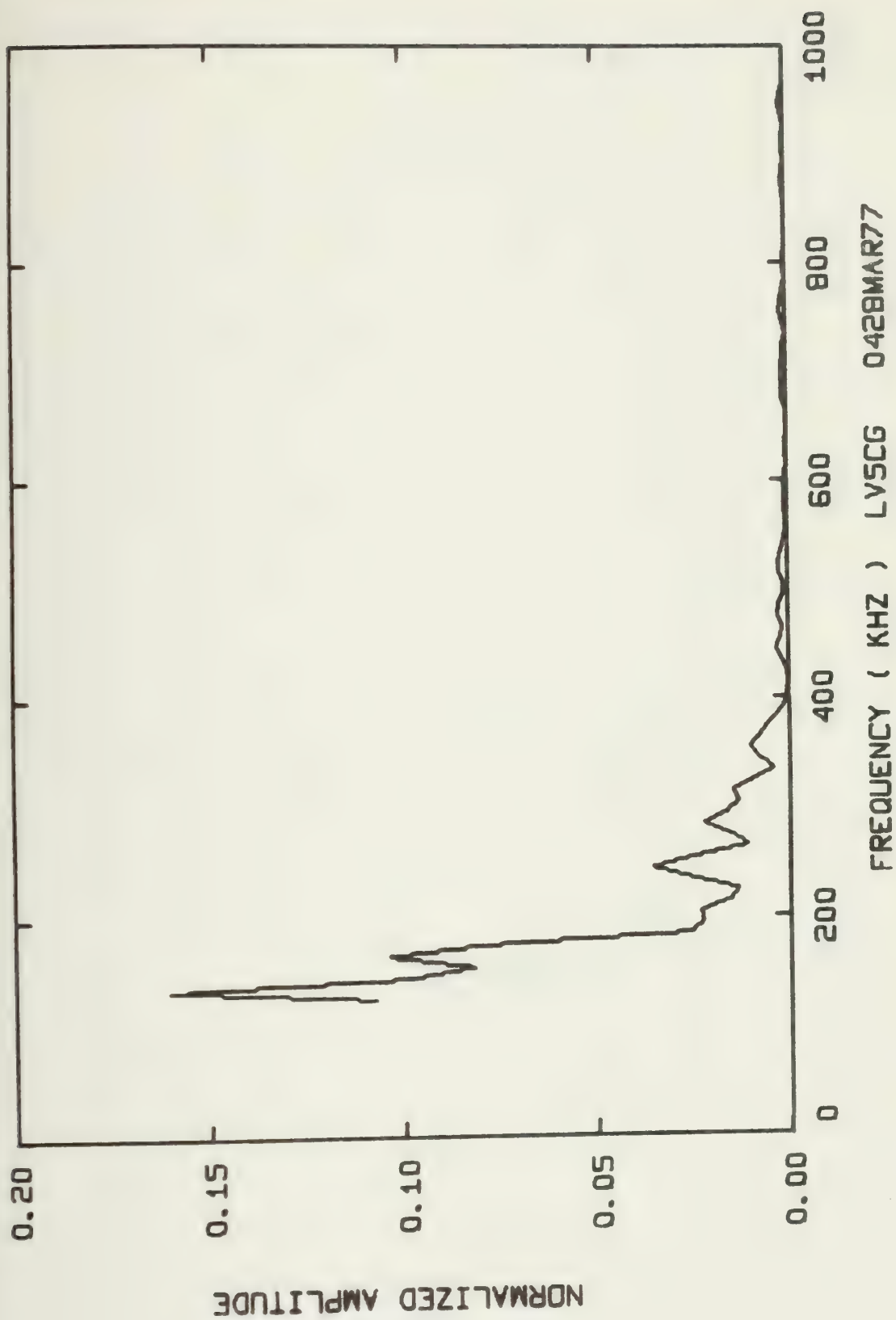




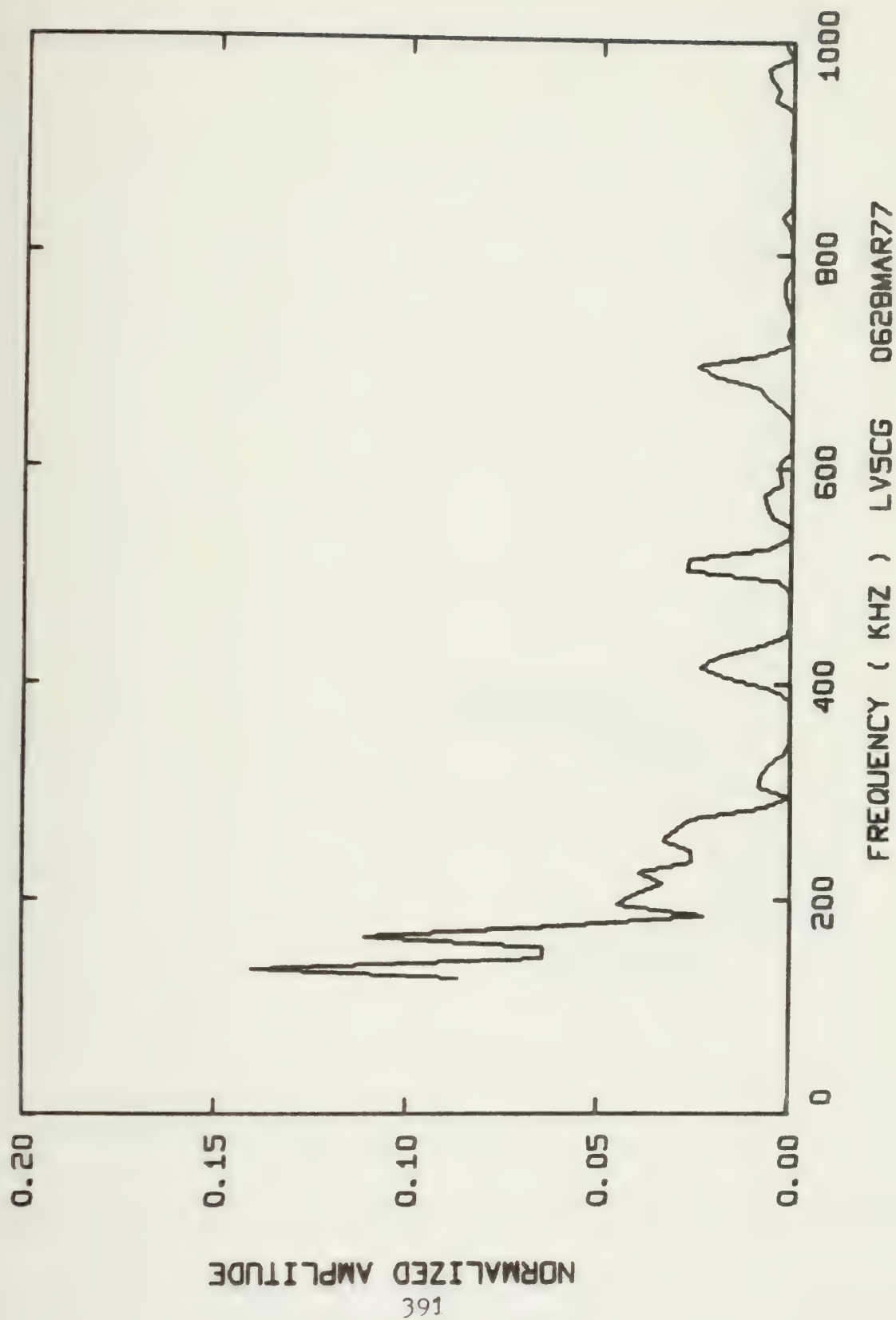




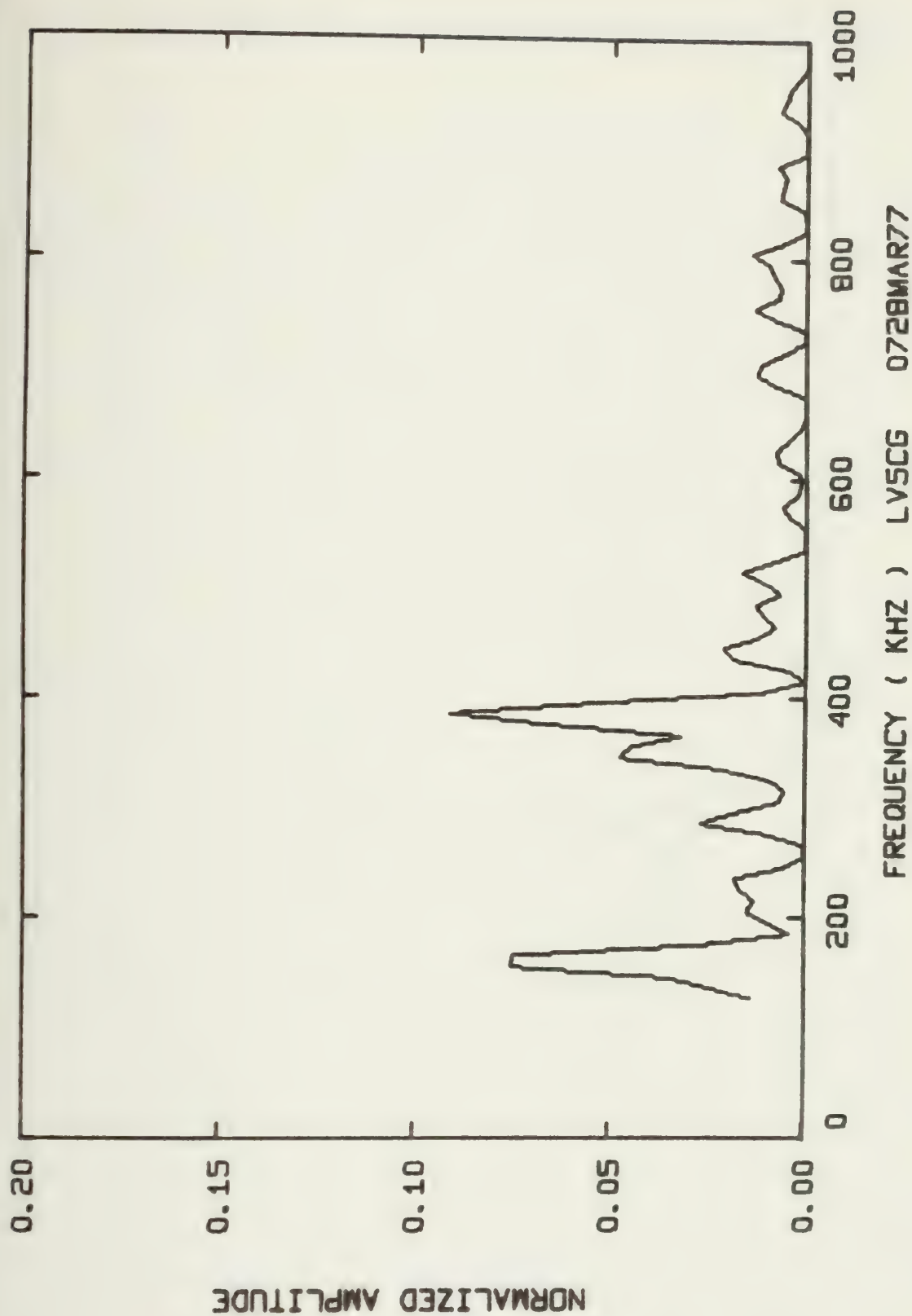




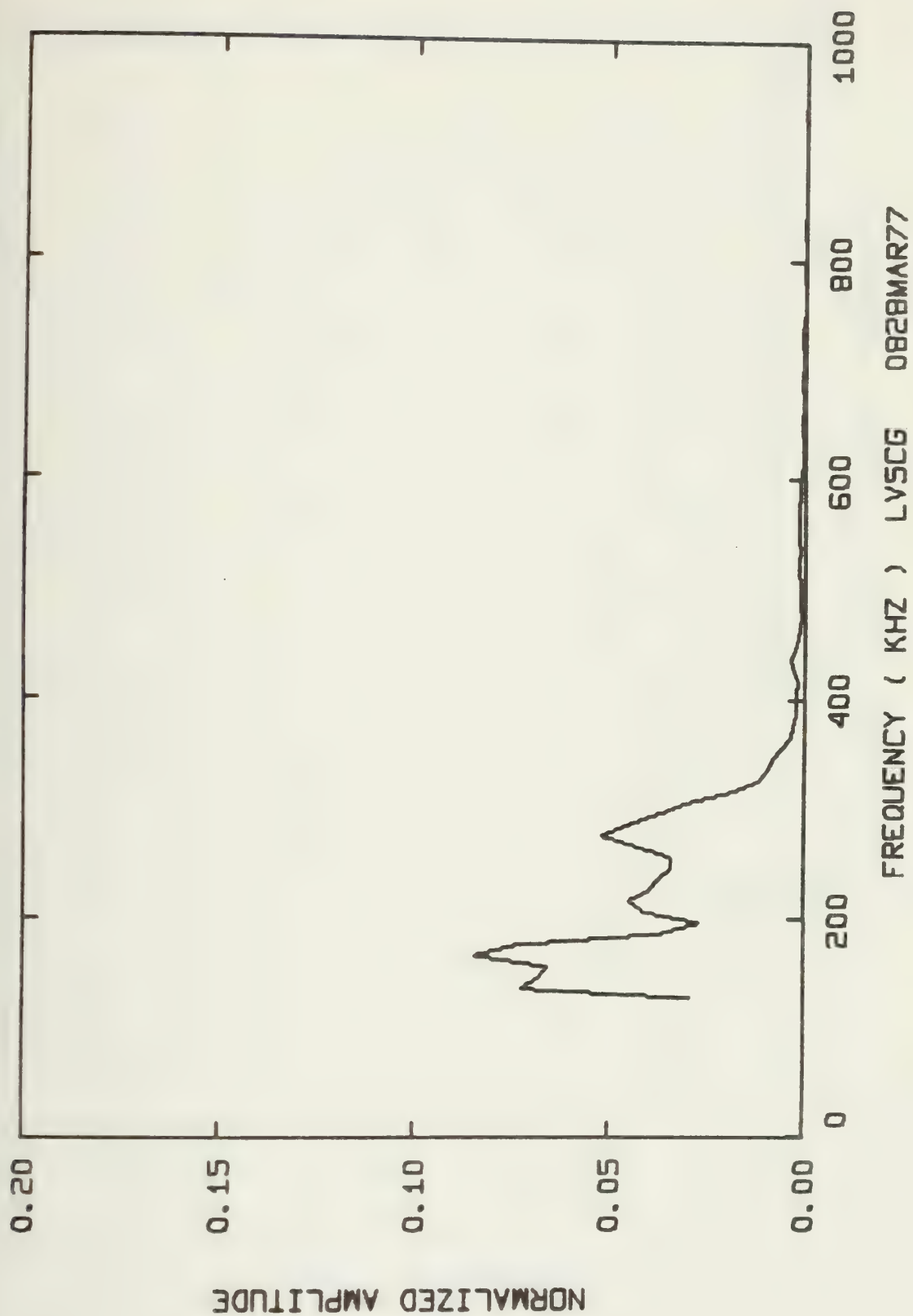






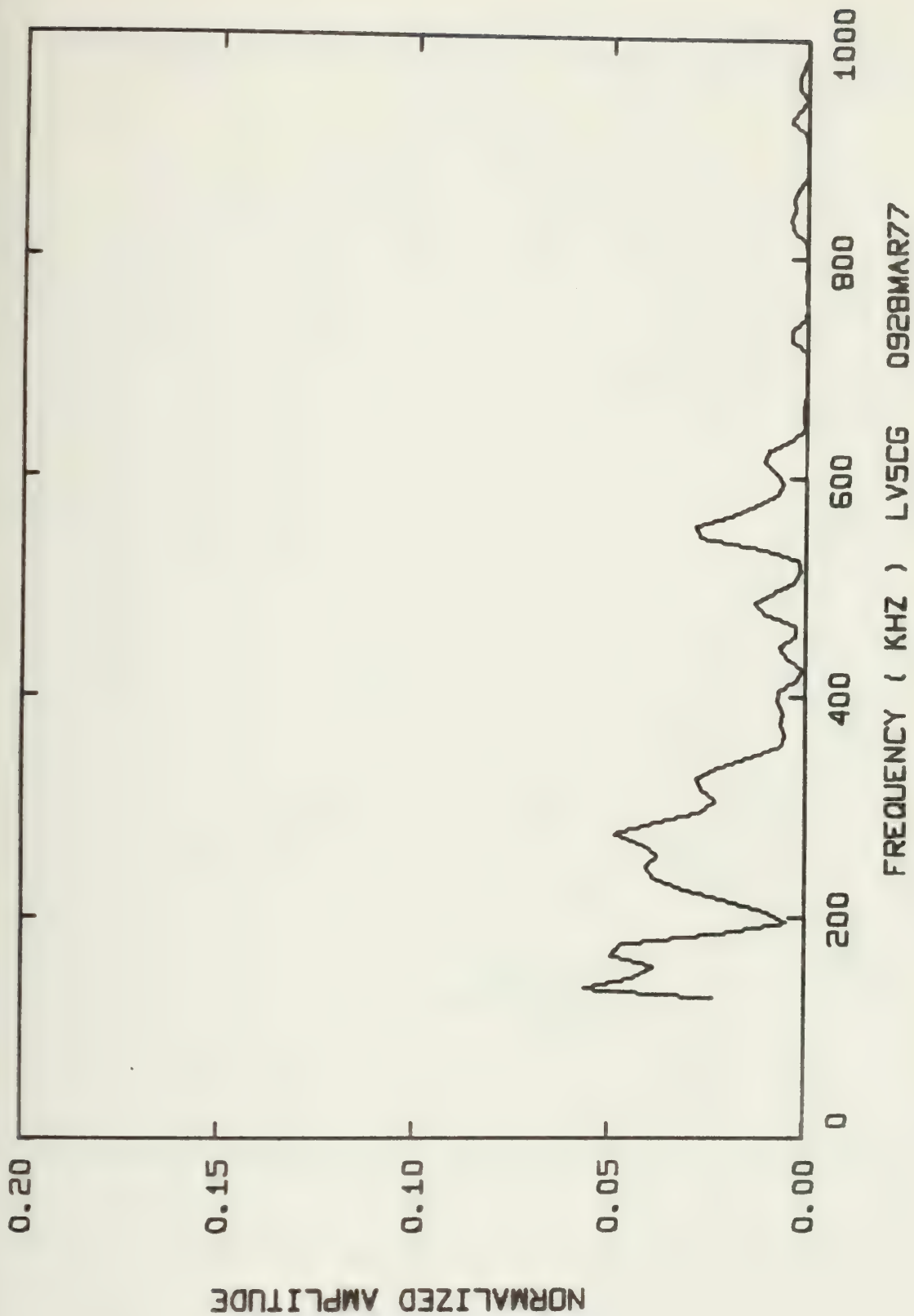




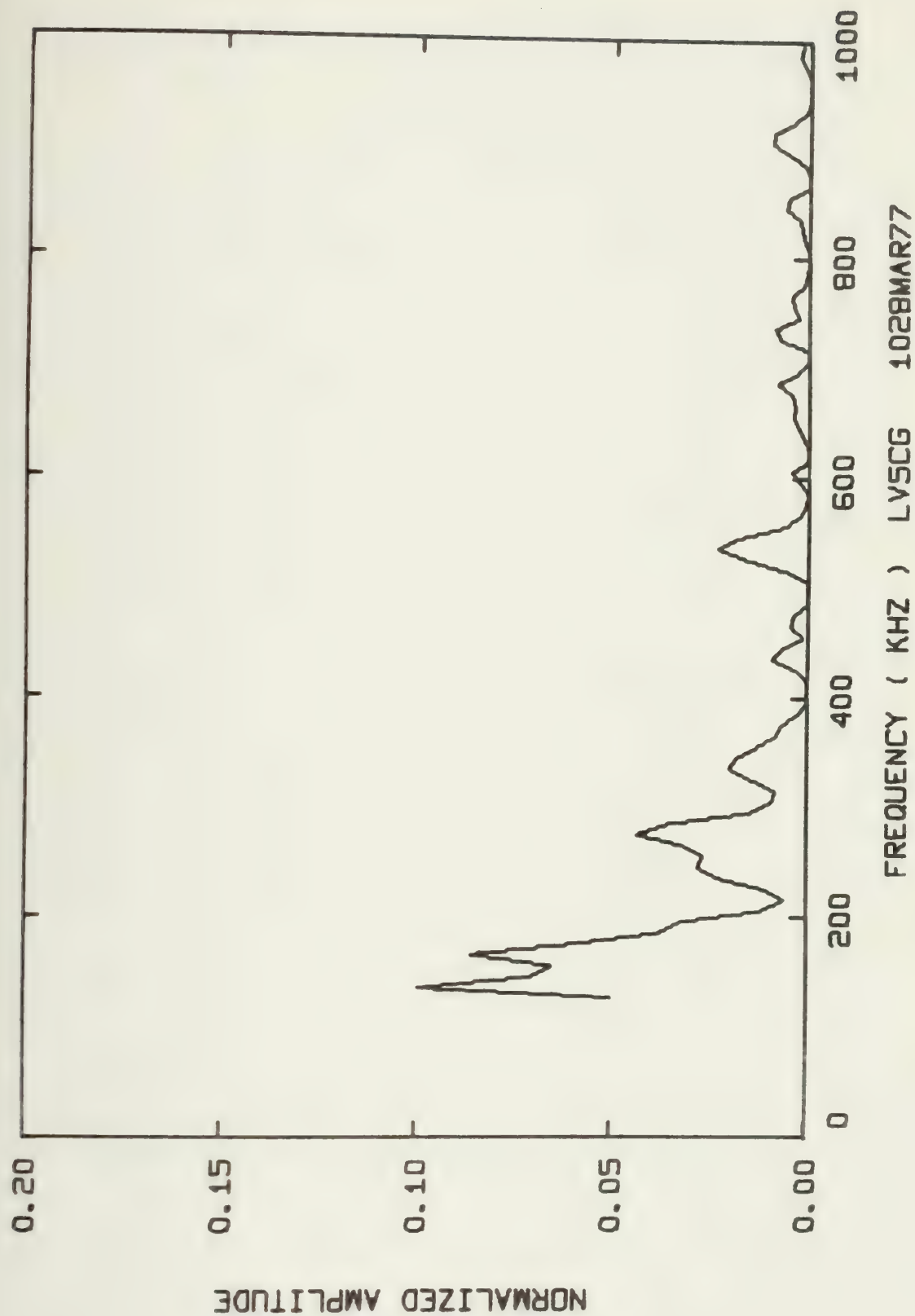




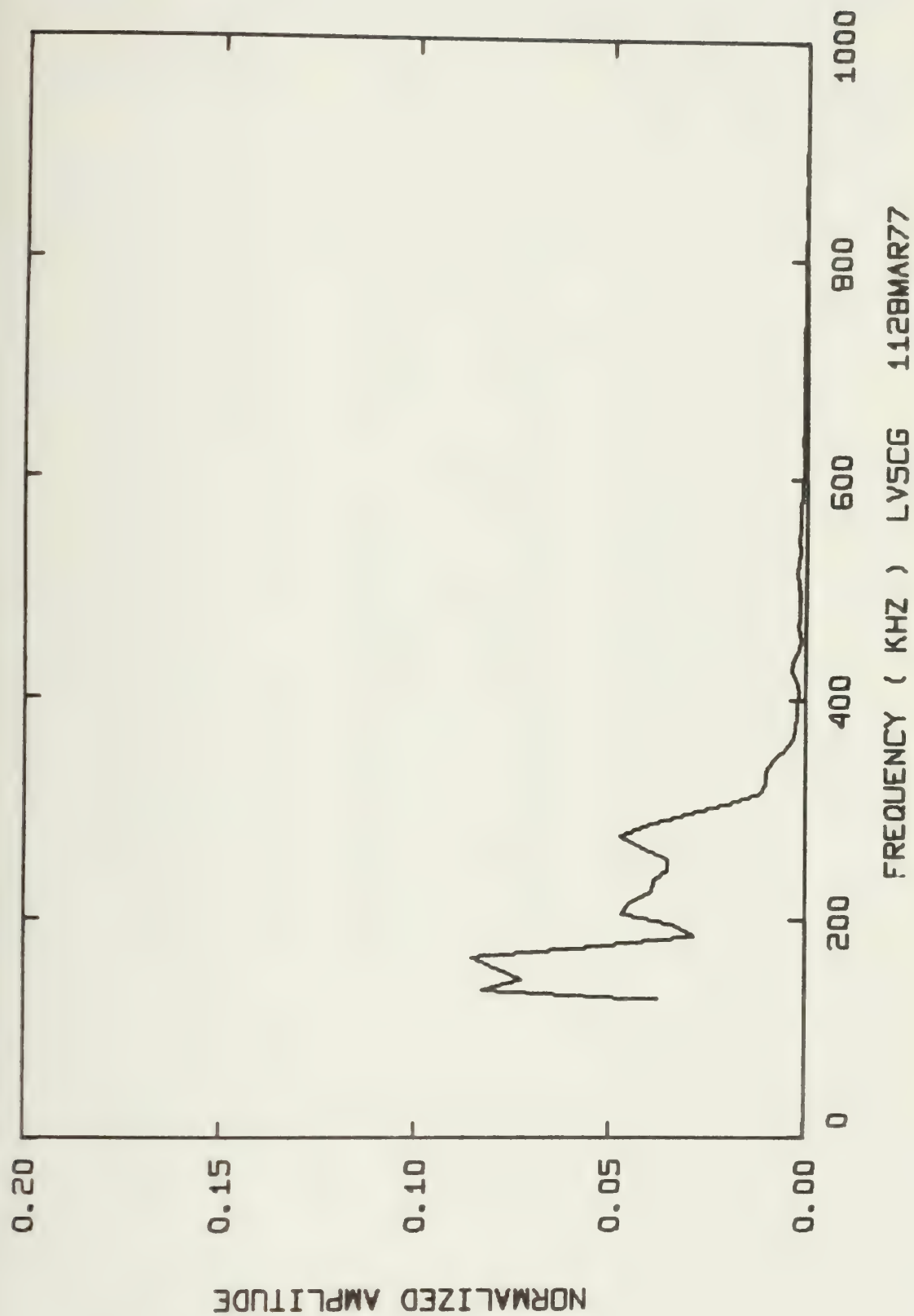












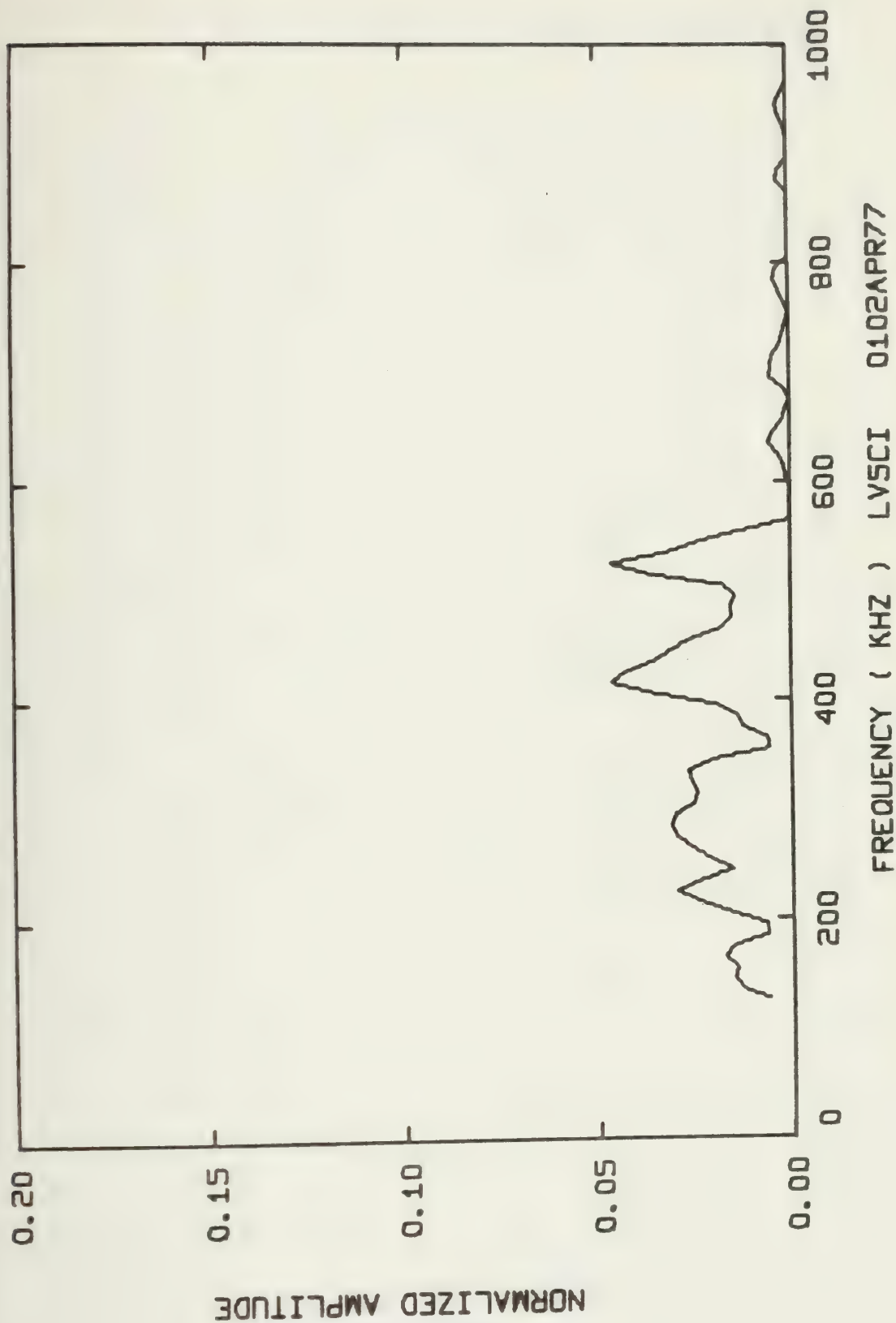


Summary of Energy per Acoustic Emission and RMS Pressure  
Across the Transducer's Face for Each Spectra

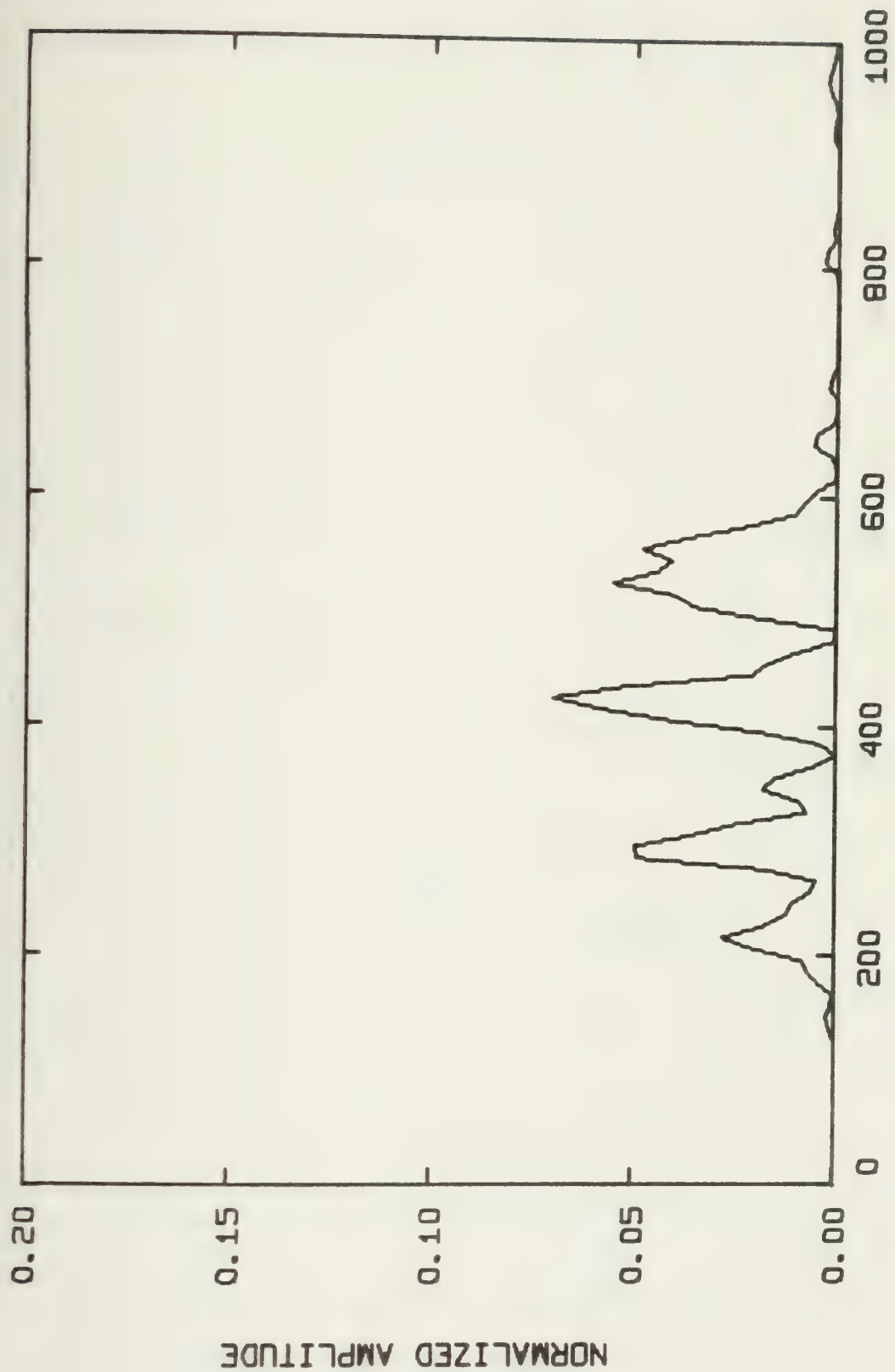
Spectral Distrib. Graph Code Number	Energy per AE (Joules)	RMS Pressure Across Face of Transducer (Pa x 10 <sup>-5</sup> )
LV5CI 0102APR77	761.34 x 10 <sup>-9</sup>	128.73
0202APR77	63.556 x 10 <sup>-9</sup>	60.90
0302APR77	281.42 x 10 <sup>-9</sup>	89.78
0402APR77	399.57 x 10 <sup>-9</sup>	84.54
0502APR77	1.8440 x 10 <sup>-6</sup>	185.38
0101APR77	668.69 x 10 <sup>-9</sup>	113.58
0201APR77	233.00 x 10 <sup>-9</sup>	80.59
0301APR77	167.29 x 10 <sup>-9</sup>	82.41
0401APR77	234.84 x 10 <sup>-9</sup>	79.61
0127MAR77	493.99 x 10 <sup>-9</sup>	114.47
0227MAR77	42.145 x 10 <sup>-9</sup>	46.76
0327MAR77	128.95 x 10 <sup>-9</sup>	75.14
0427MAR77	72.113 x 10 <sup>-9</sup>	65.91
0527MAR77	298.64 x 10 <sup>-9</sup>	81.00
0627MAR77	324.11 x 10 <sup>-9</sup>	89.48





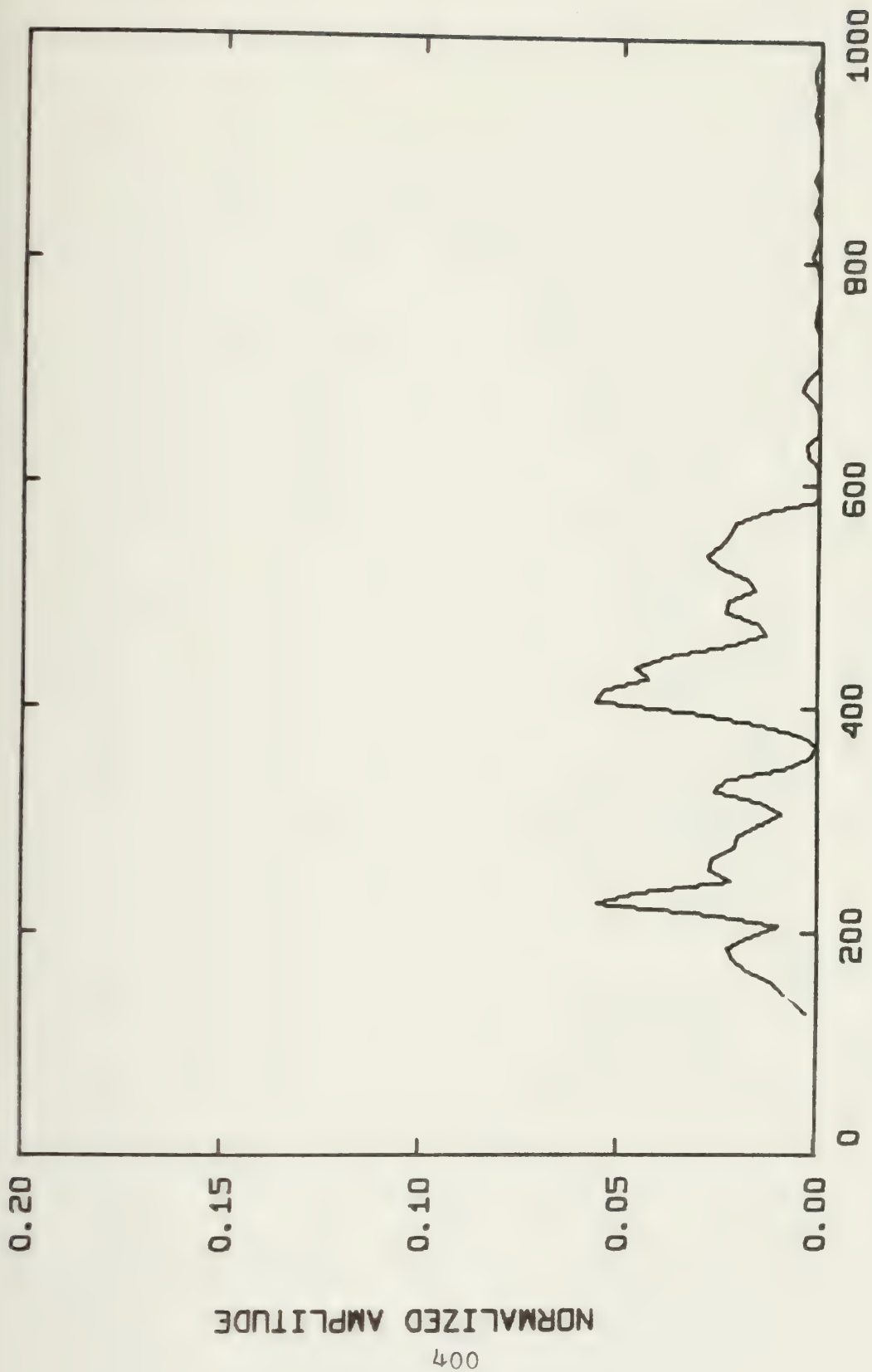






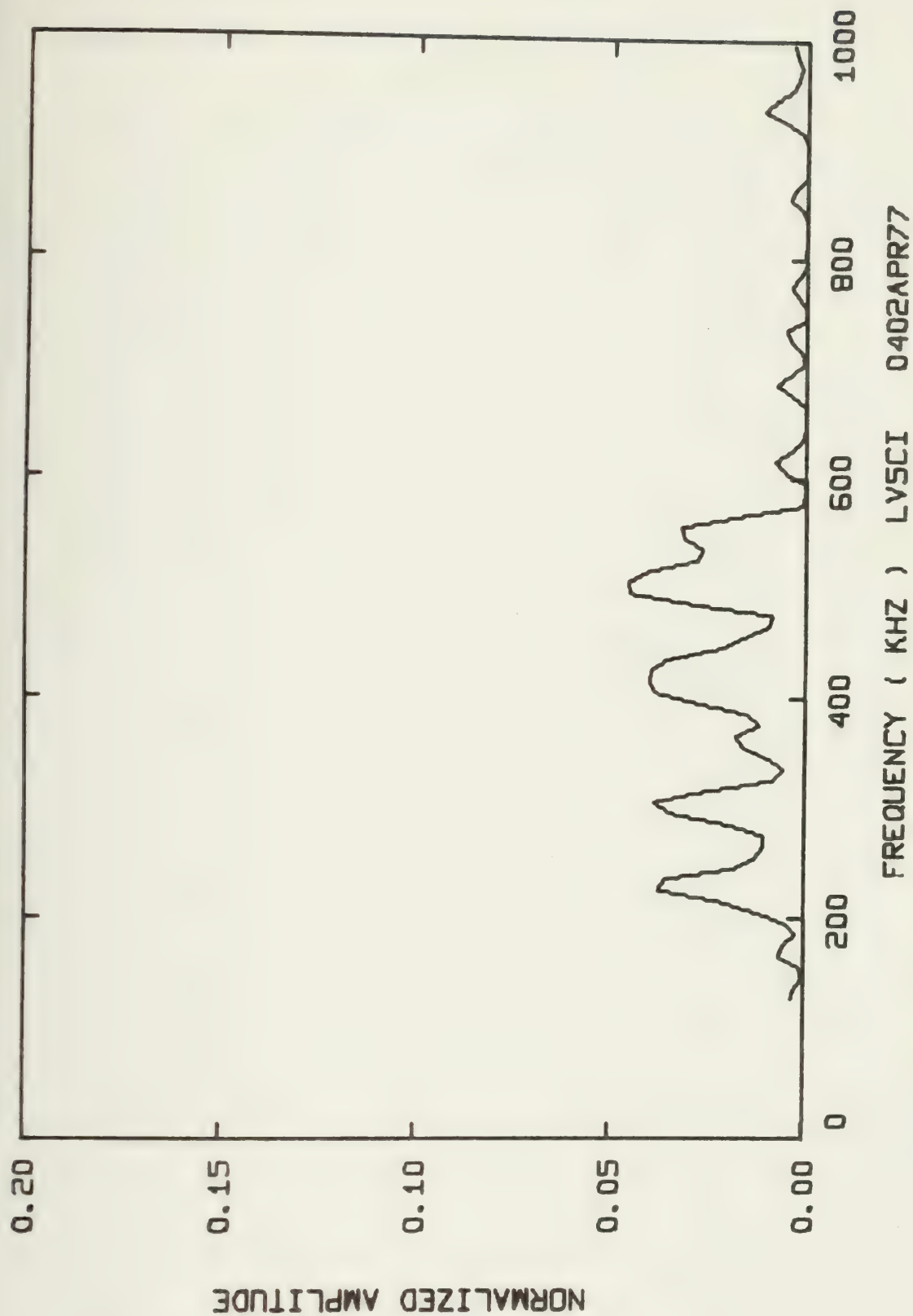
FREQUENCY ( KHZ ) LVSCI 0202APR77





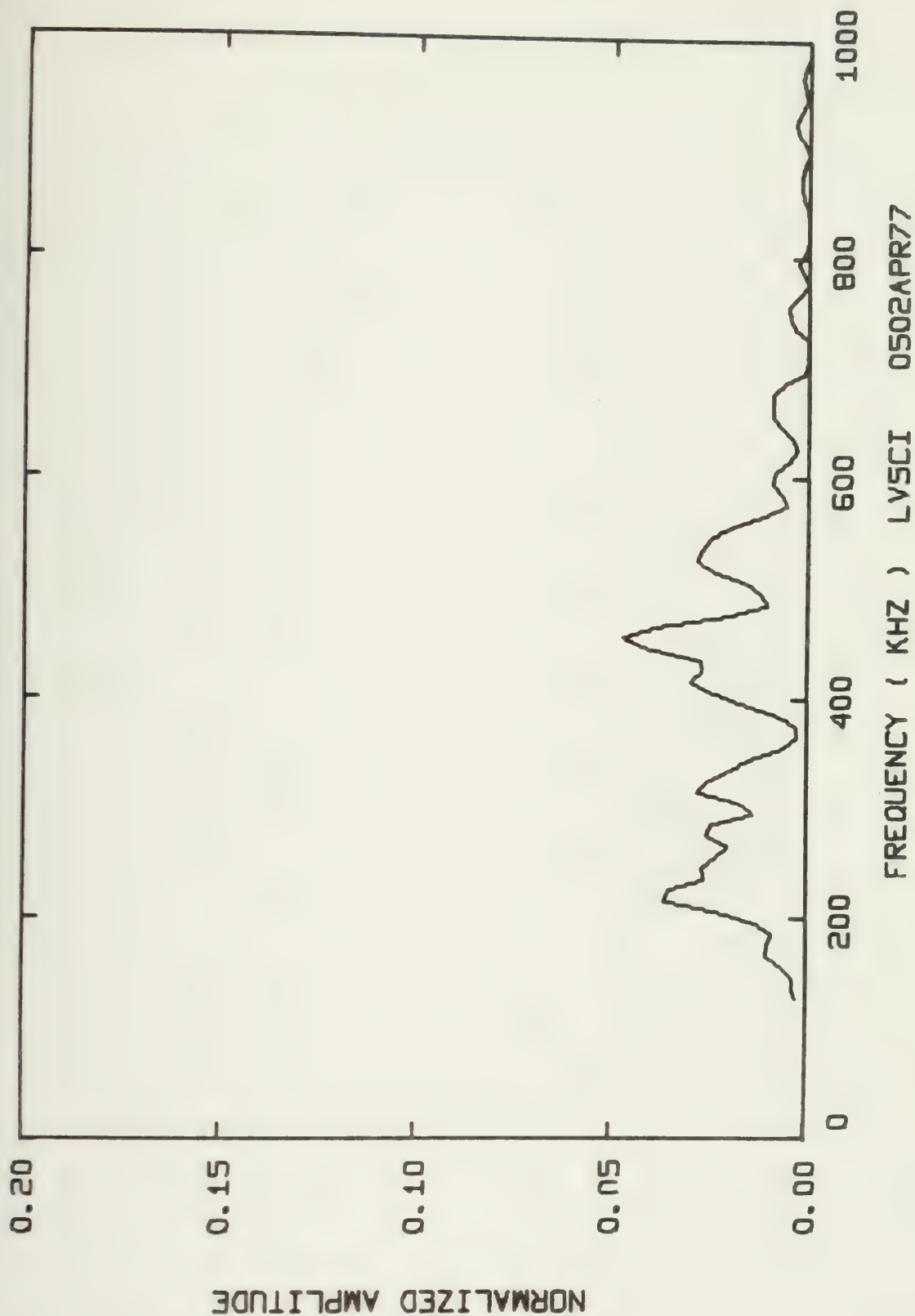
LVSCI 0302APR77



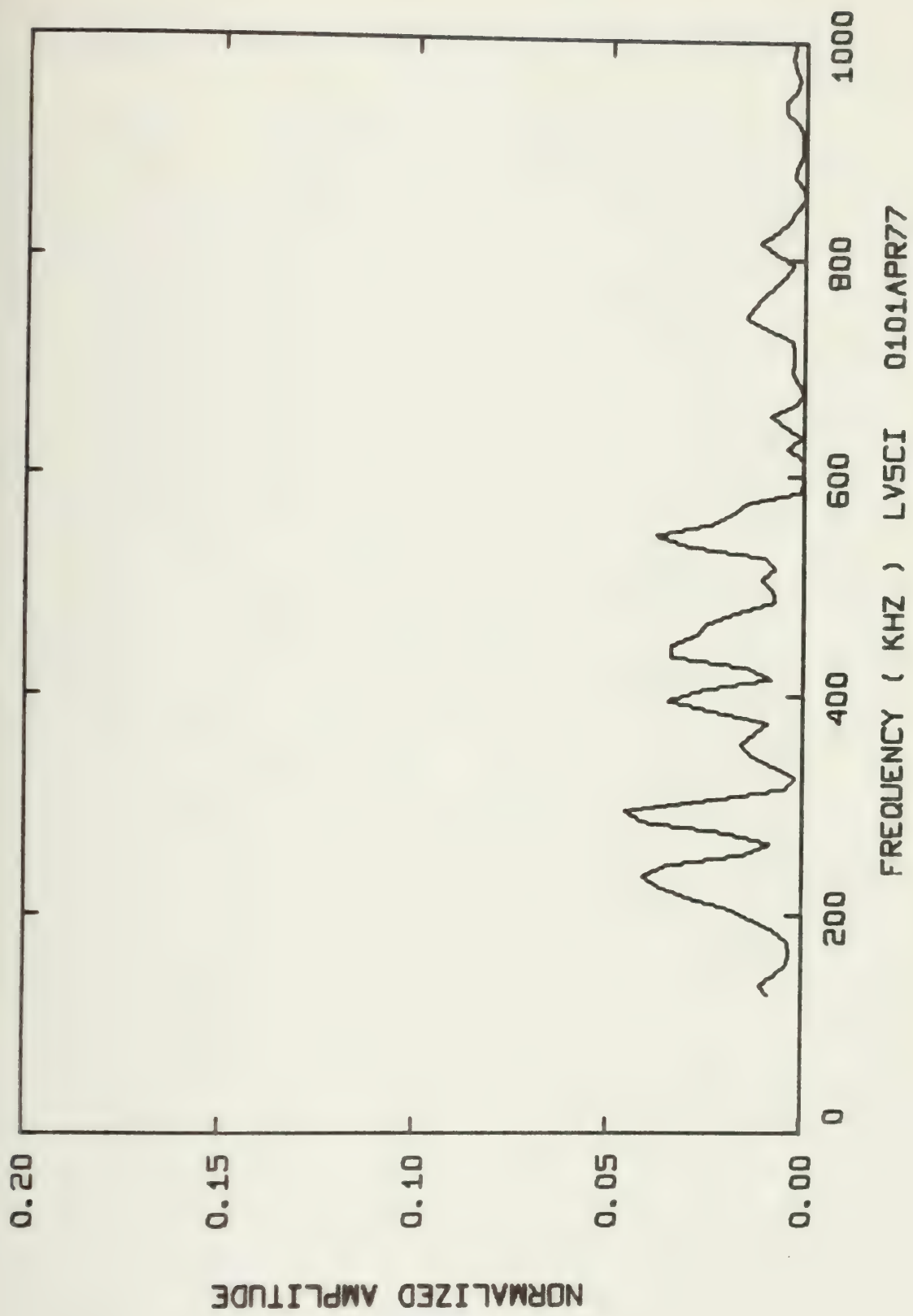




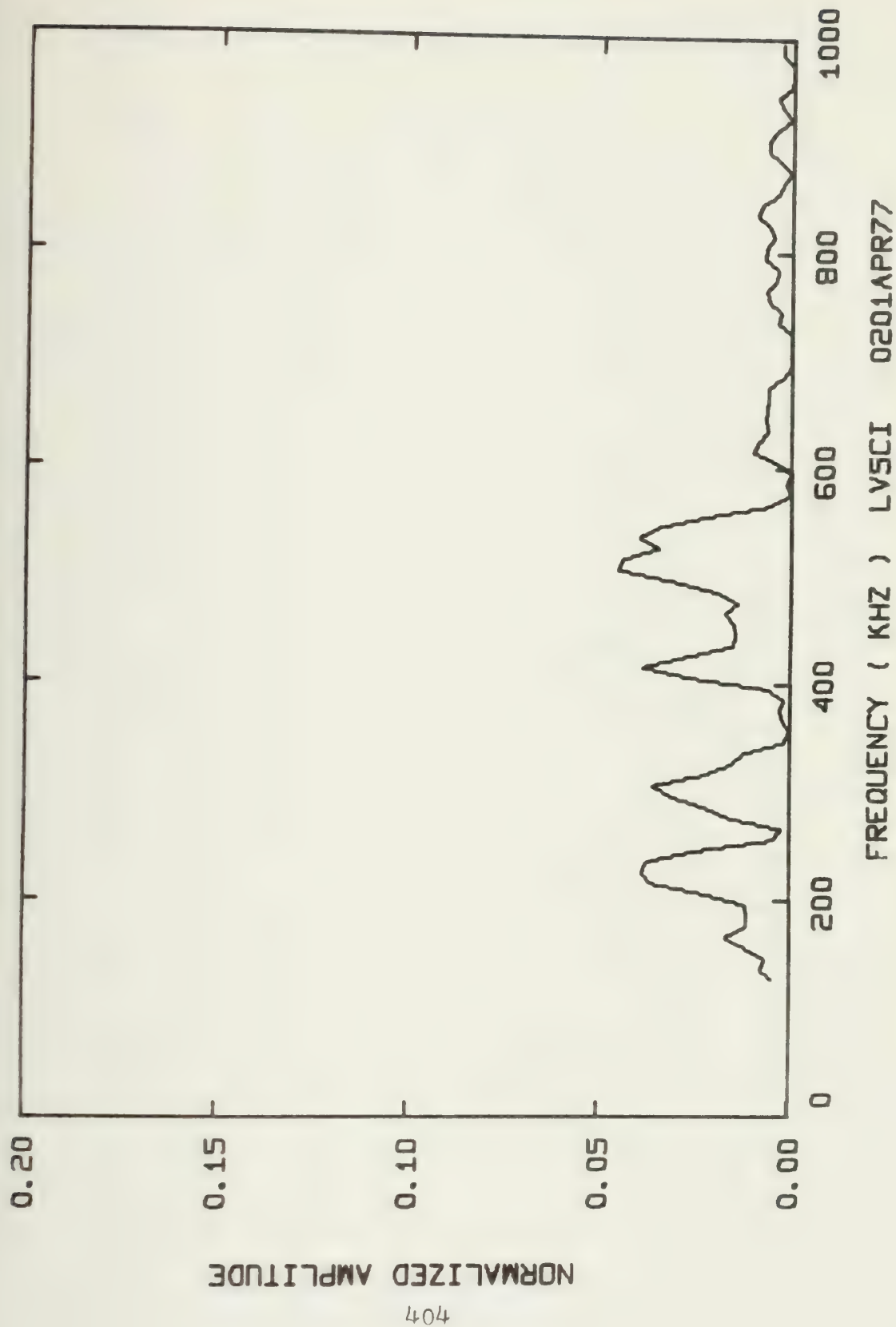




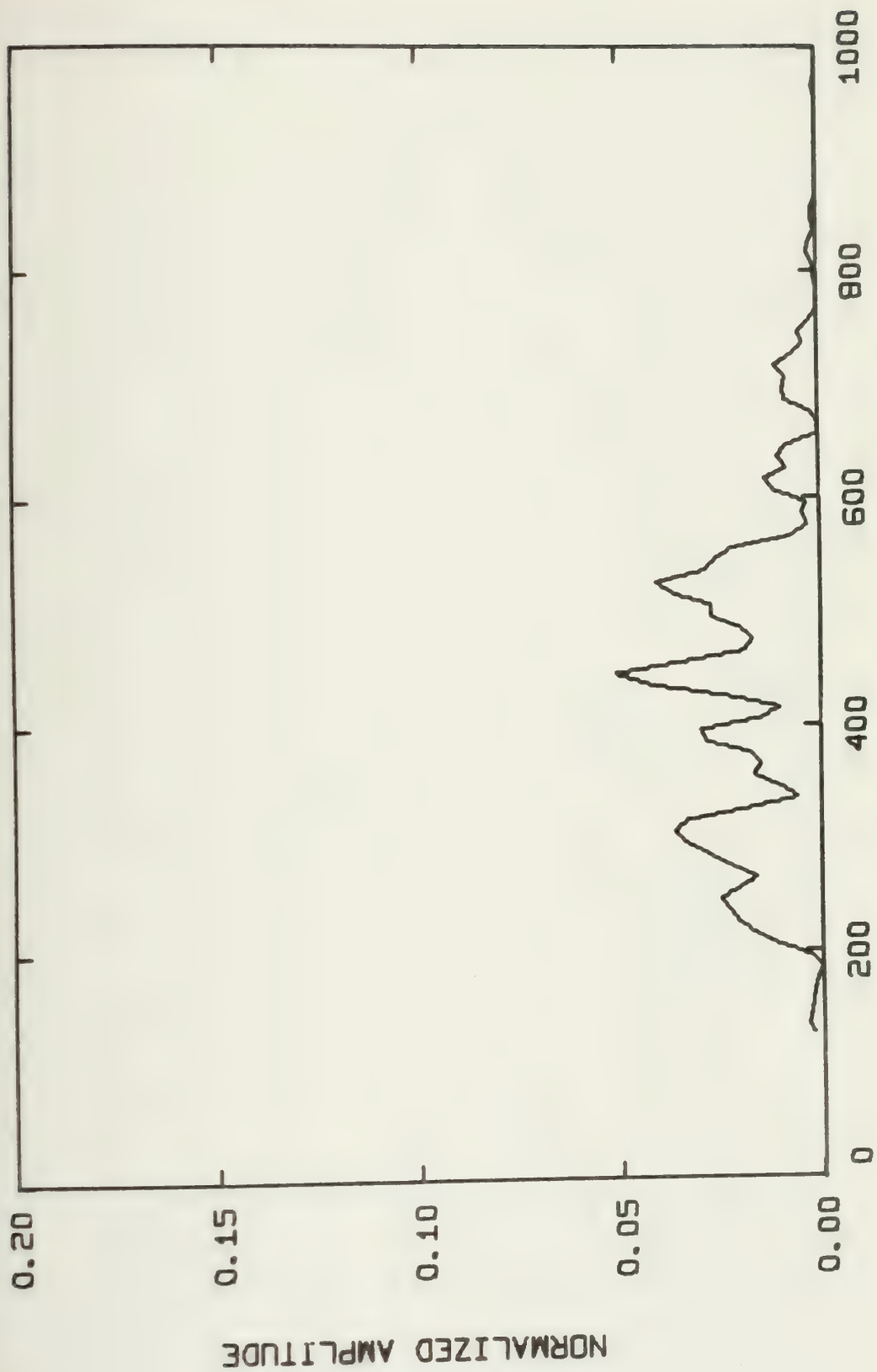








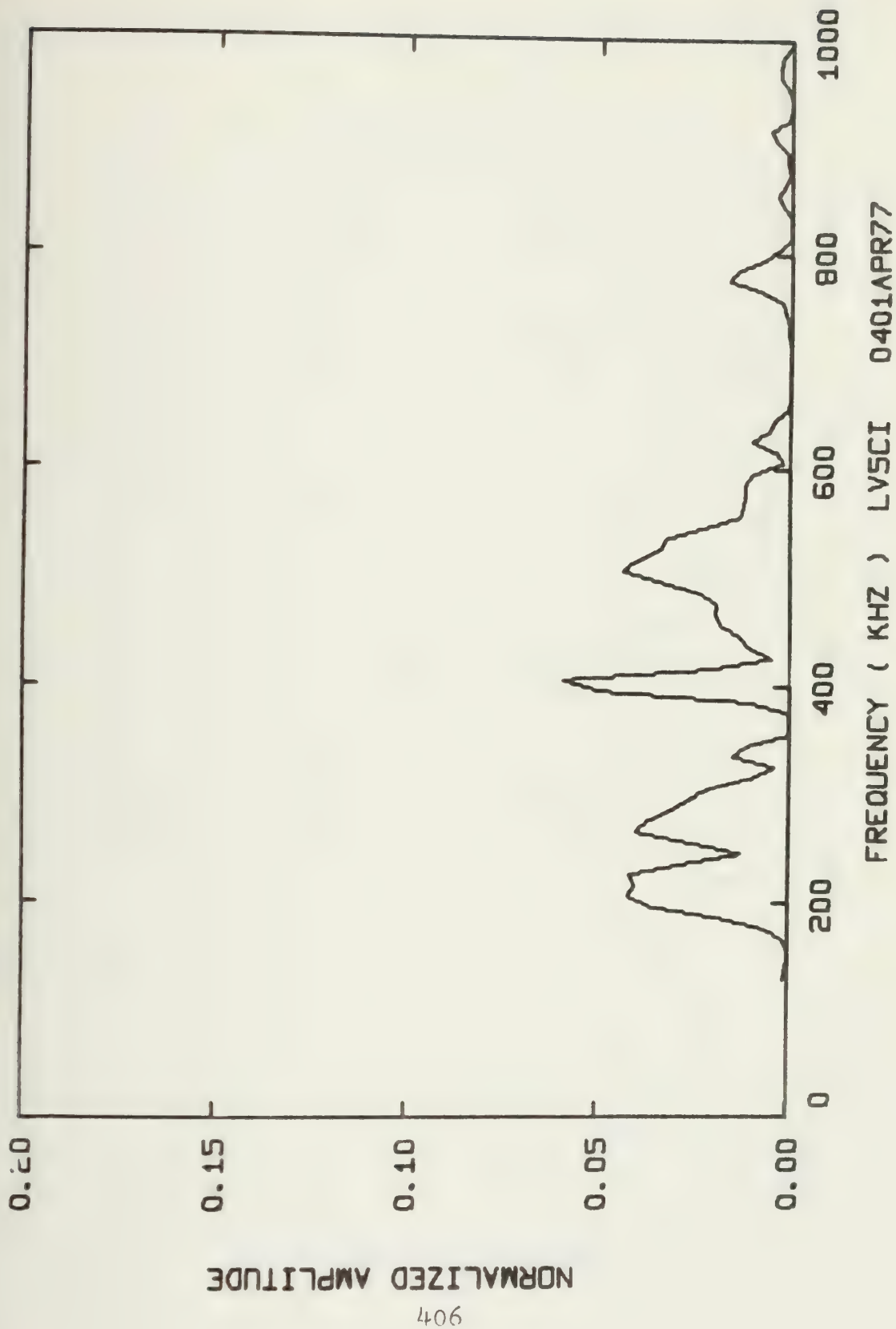




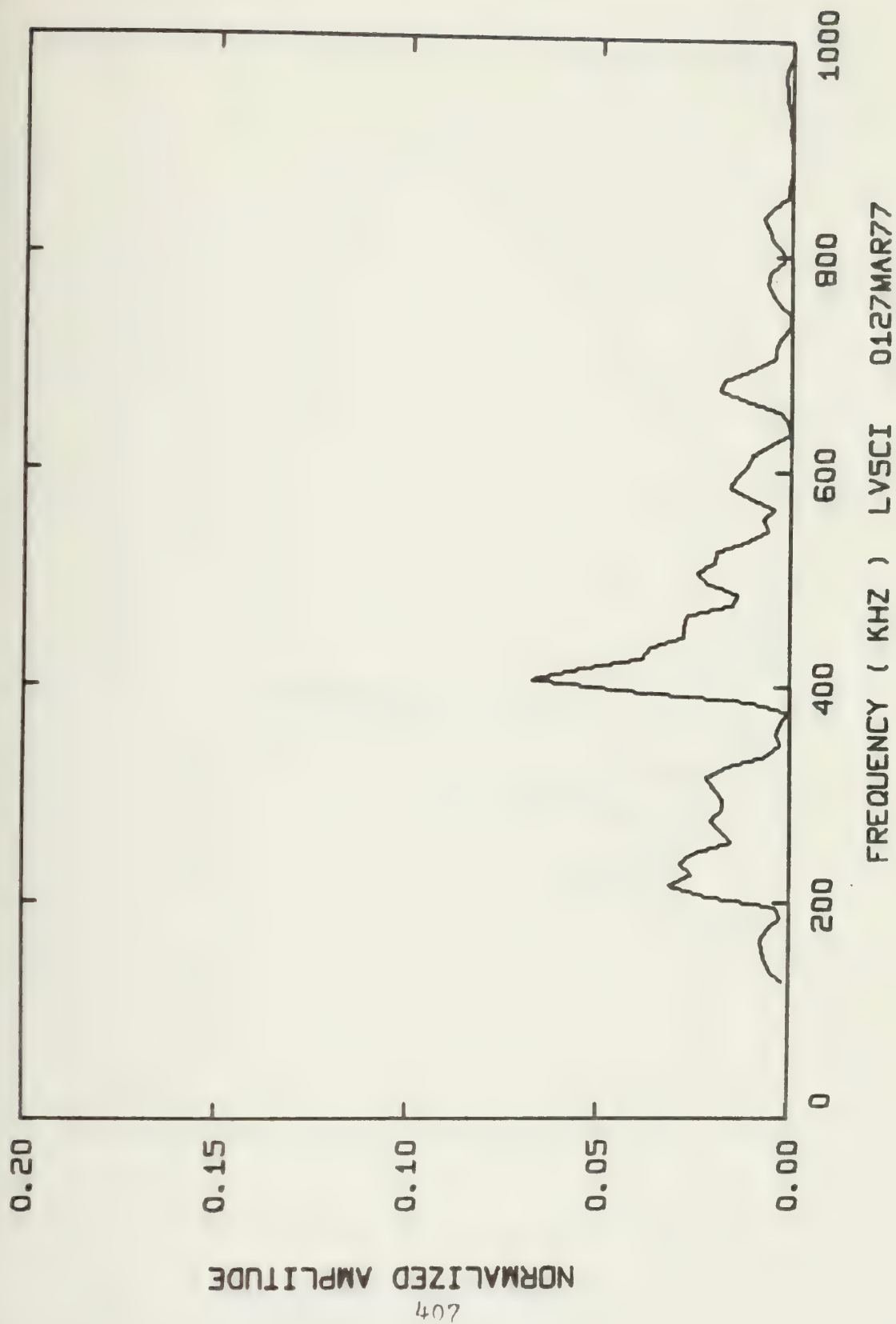
LVSCI 0301APR77



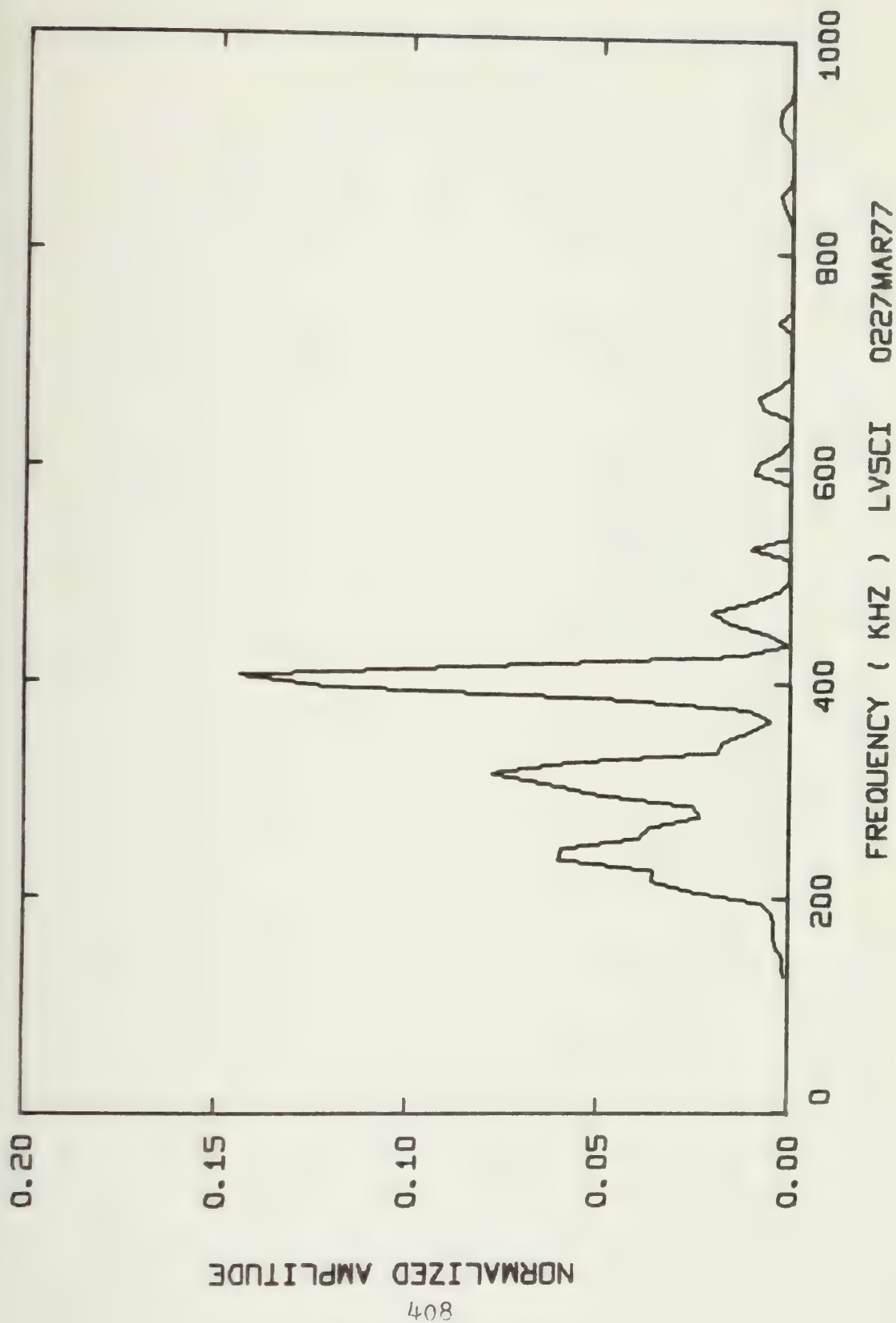




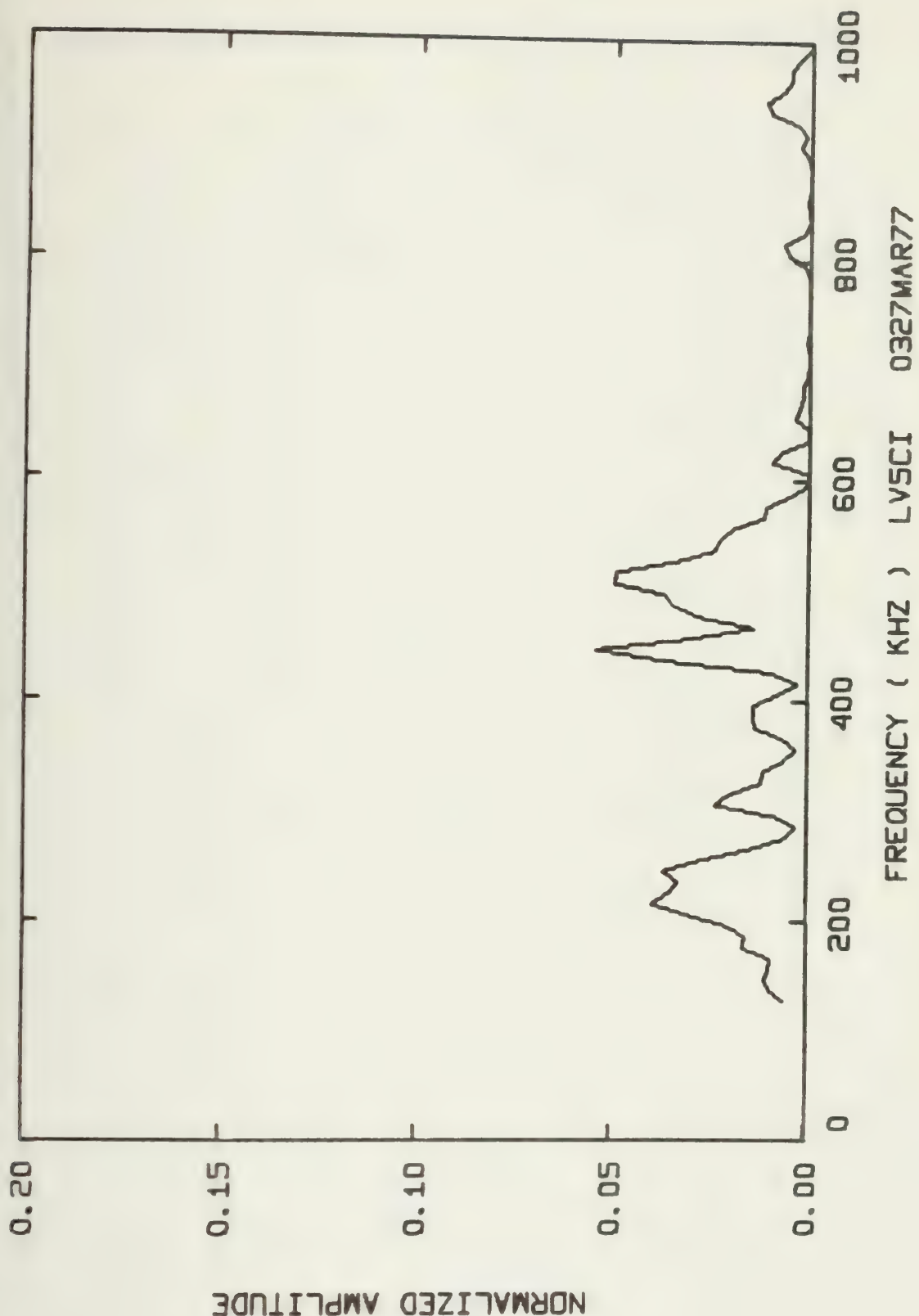










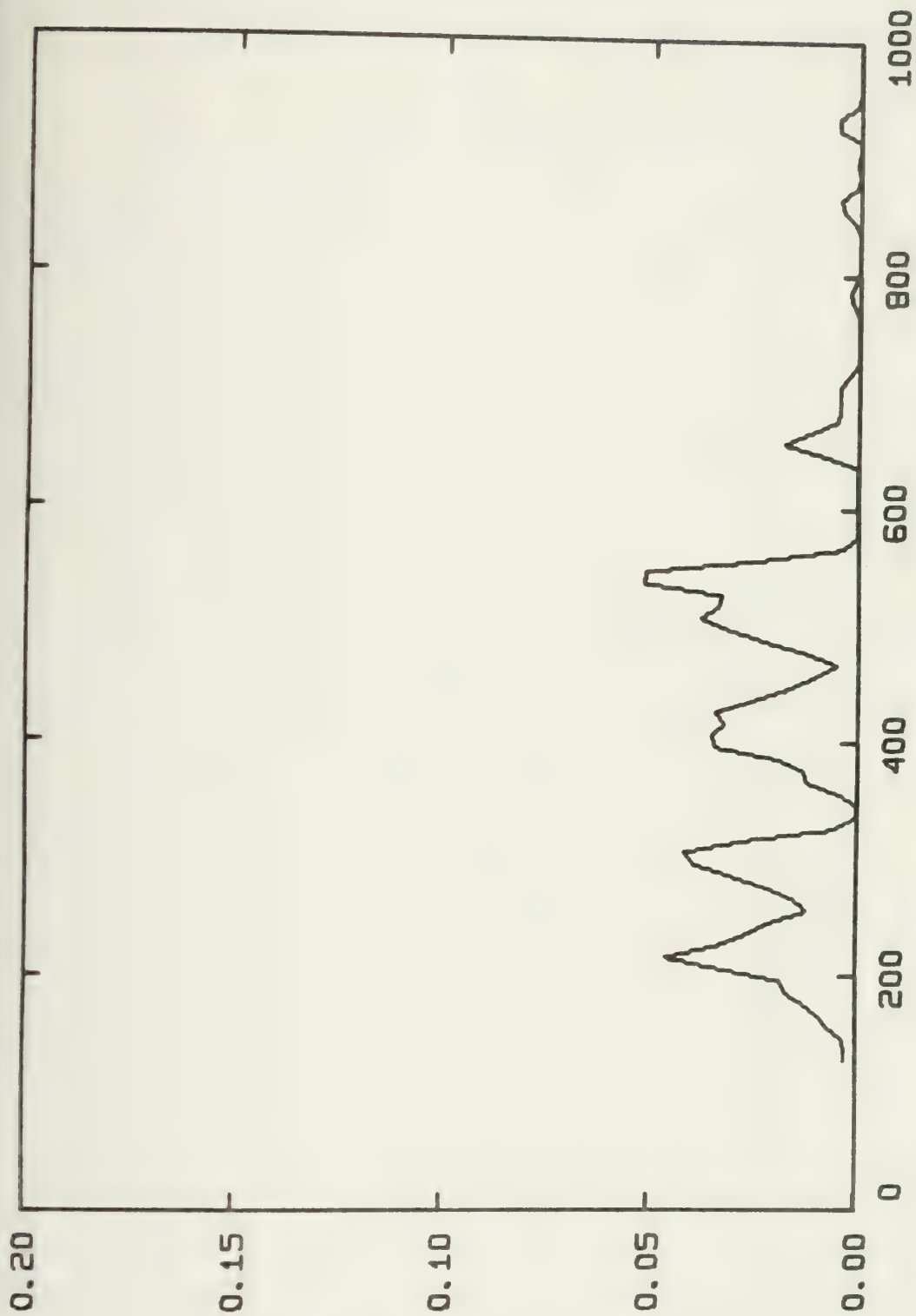


NORMALIZED AMPLITUDE

FREQUENCY ( KHZ ) LV5CI 0327MAR77



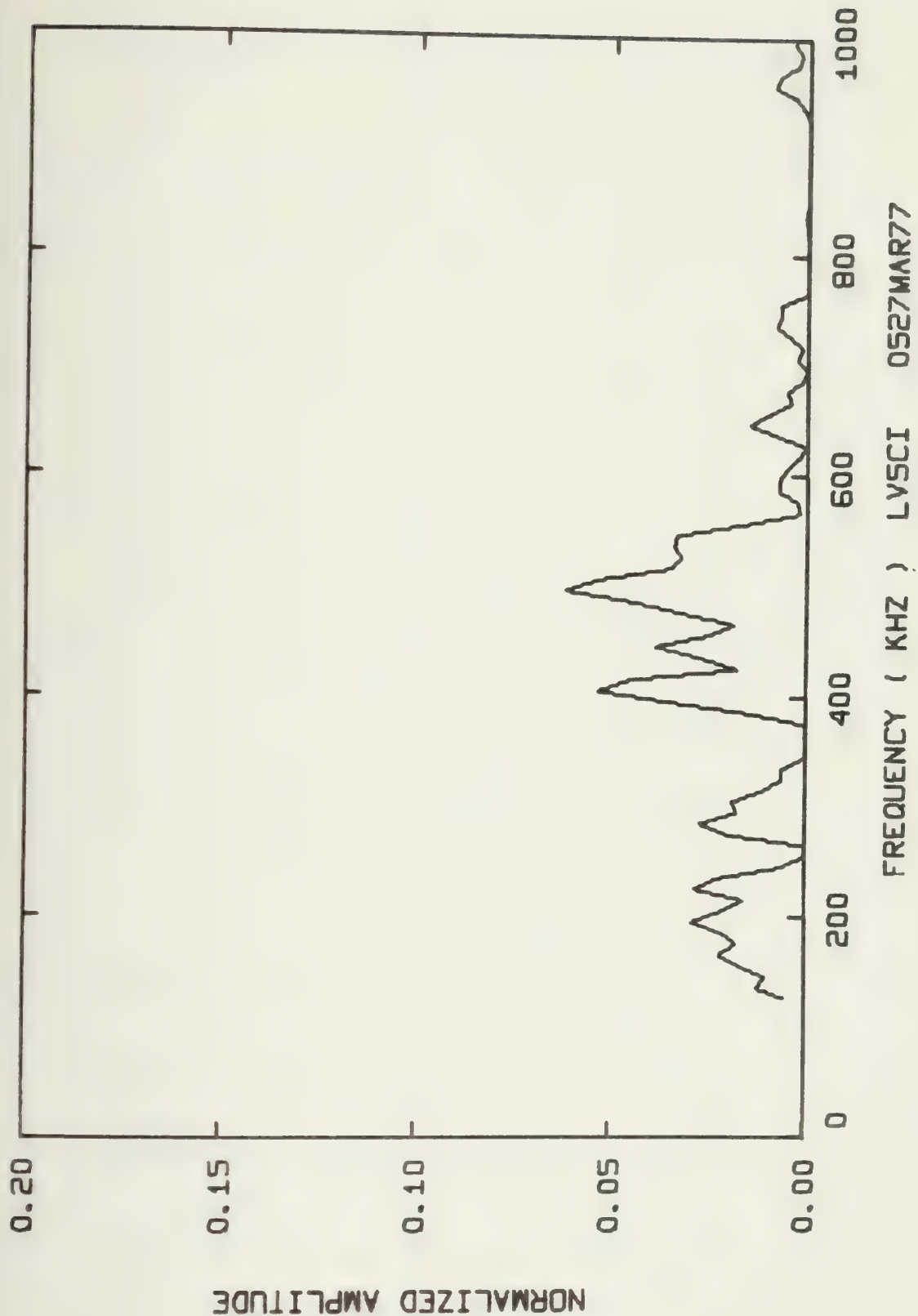




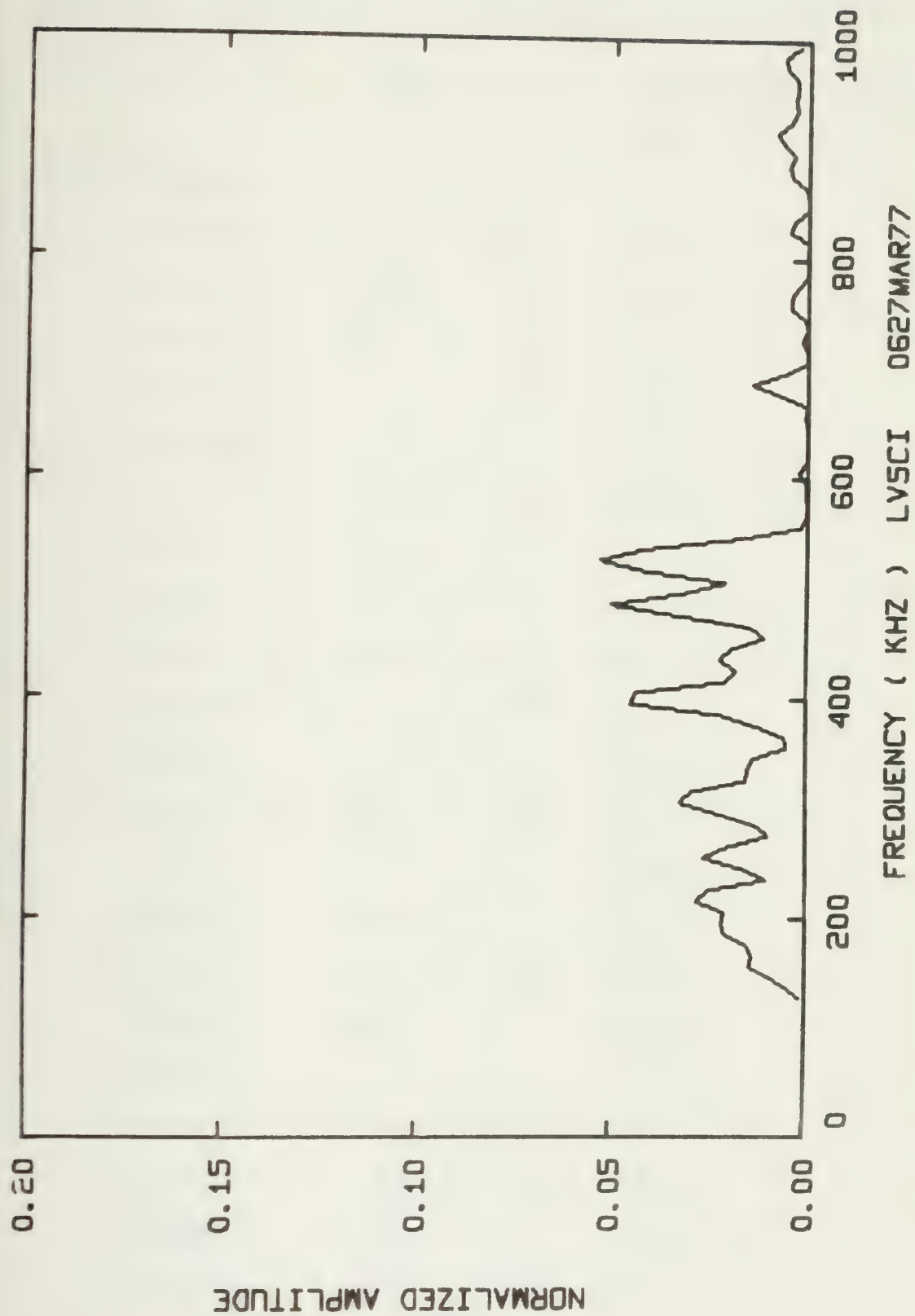
FREQUENCY ( KHZ ) LV5CI 0427MAR77

NORMALIZED AMPLITUDE









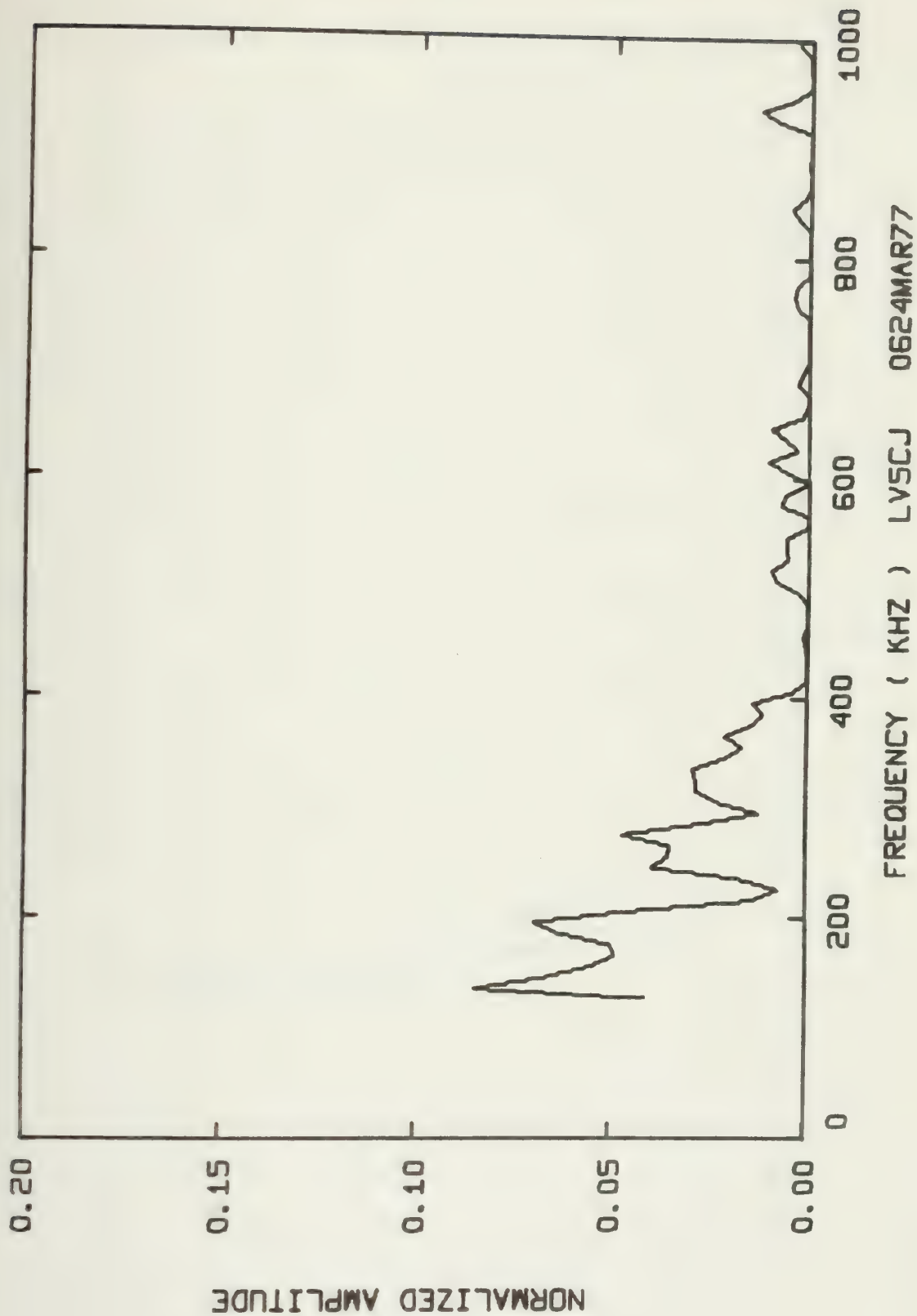


Summary of Energy per Acoustic Emission and RMS Pressure  
Across the Transducer's Face for Each Spectra

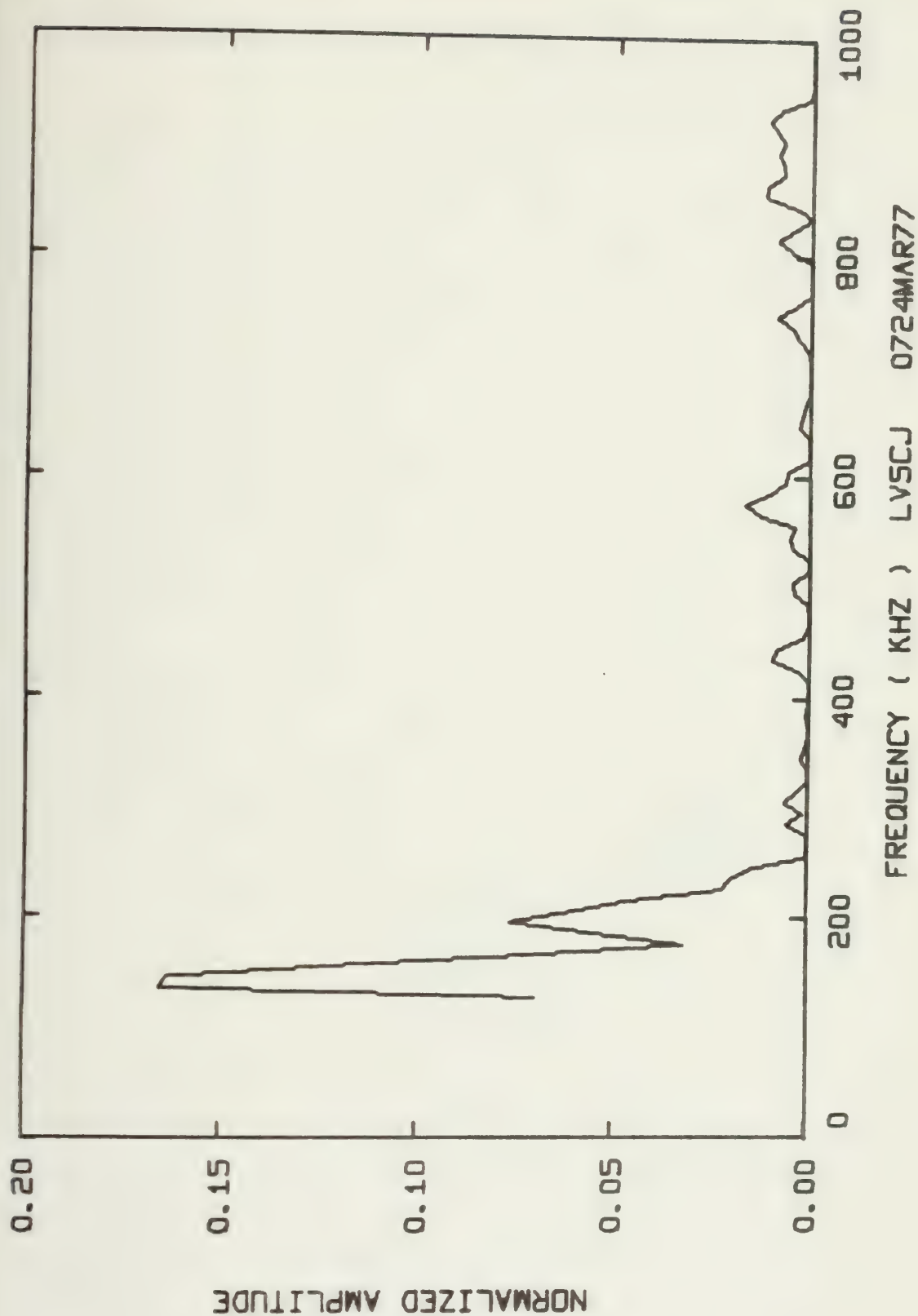
Spectral Distrib. Graph Code Number	Energy per AE (Joules)	RMS Pressure Across Face of Transducer (Pa x 10 <sup>5</sup> )
LV5CJ 0624MAR77	517.28 x 10 <sup>-9</sup>	109.20
0724MAR77	12.377 x 10 <sup>-9</sup>	38.49
0824MAR77	23.492 x 10 <sup>-9</sup>	45.71
0924MAR77	180.25 x 10 <sup>-9</sup>	82.54
1024MAR77	756.61 x 10 <sup>-9</sup>	128.78
1124MAR77	31.122 x 10 <sup>-9</sup>	46.39
1224MAR77	1.4247 x 10 <sup>-6</sup>	529.76
1324MAR77	117.68 x 10 <sup>-9</sup>	61.238
1424MAR77	979.95 x 10 <sup>-9</sup>	143.06
1524MAR77	217.47 x 10 <sup>-9</sup>	81.327
1624MAR77	1.1596 x 10 <sup>-6</sup>	143.06
1724MAR77	533.24 x 10 <sup>-9</sup>	109.80
0127MAR77	925.68 x 10 <sup>-9</sup>	131.48
0227MAR77	171.64 x 10 <sup>-9</sup>	80.714
0327MAR77	230.49 x 10 <sup>-9</sup>	90.631
0427MAR77	323.26 x 10 <sup>-9</sup>	96.370
0527MAR77	348.48 x 10 <sup>-9</sup>	100.84
0627MAR77	21.155 x 10 <sup>-9</sup>	37.562
0727MAR77	91.498 x 10 <sup>-9</sup>	60.947
0827MAR77	567.39 x 10 <sup>-9</sup>	113.67
0927MAR77	26.342 x 10 <sup>-9</sup>	41.916
1027MAR77	1.0189 x 10 <sup>-6</sup>	137.53



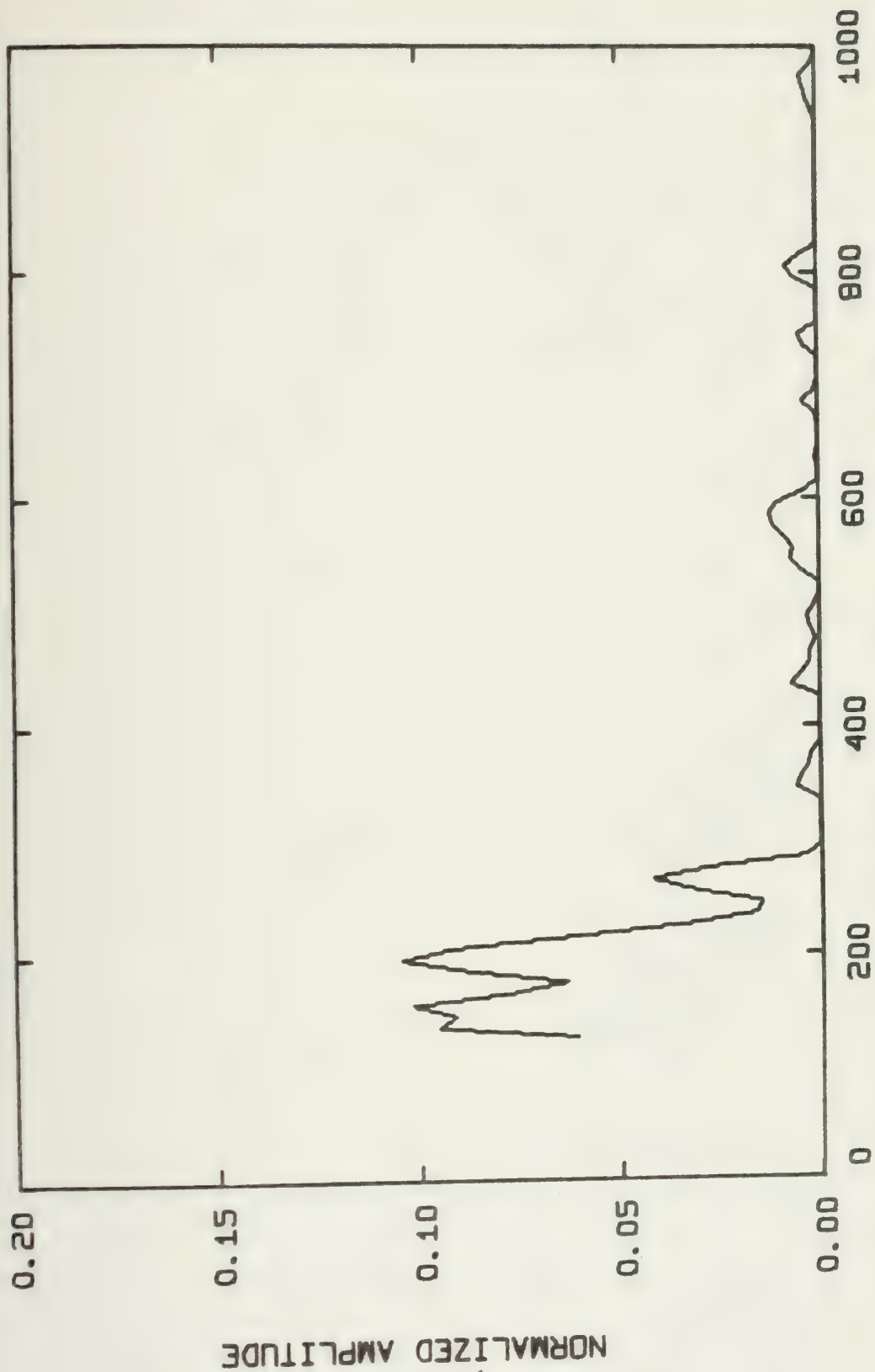






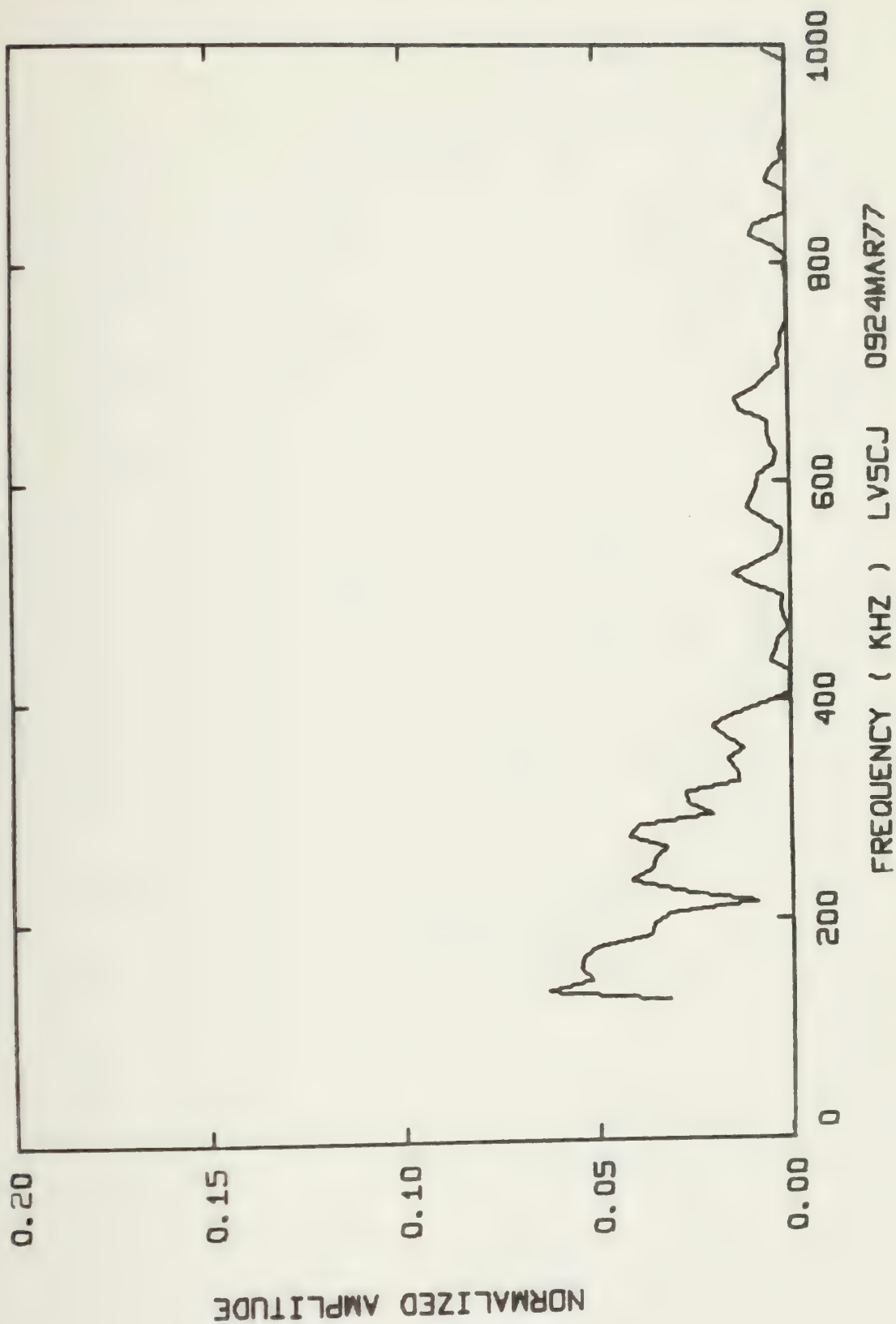






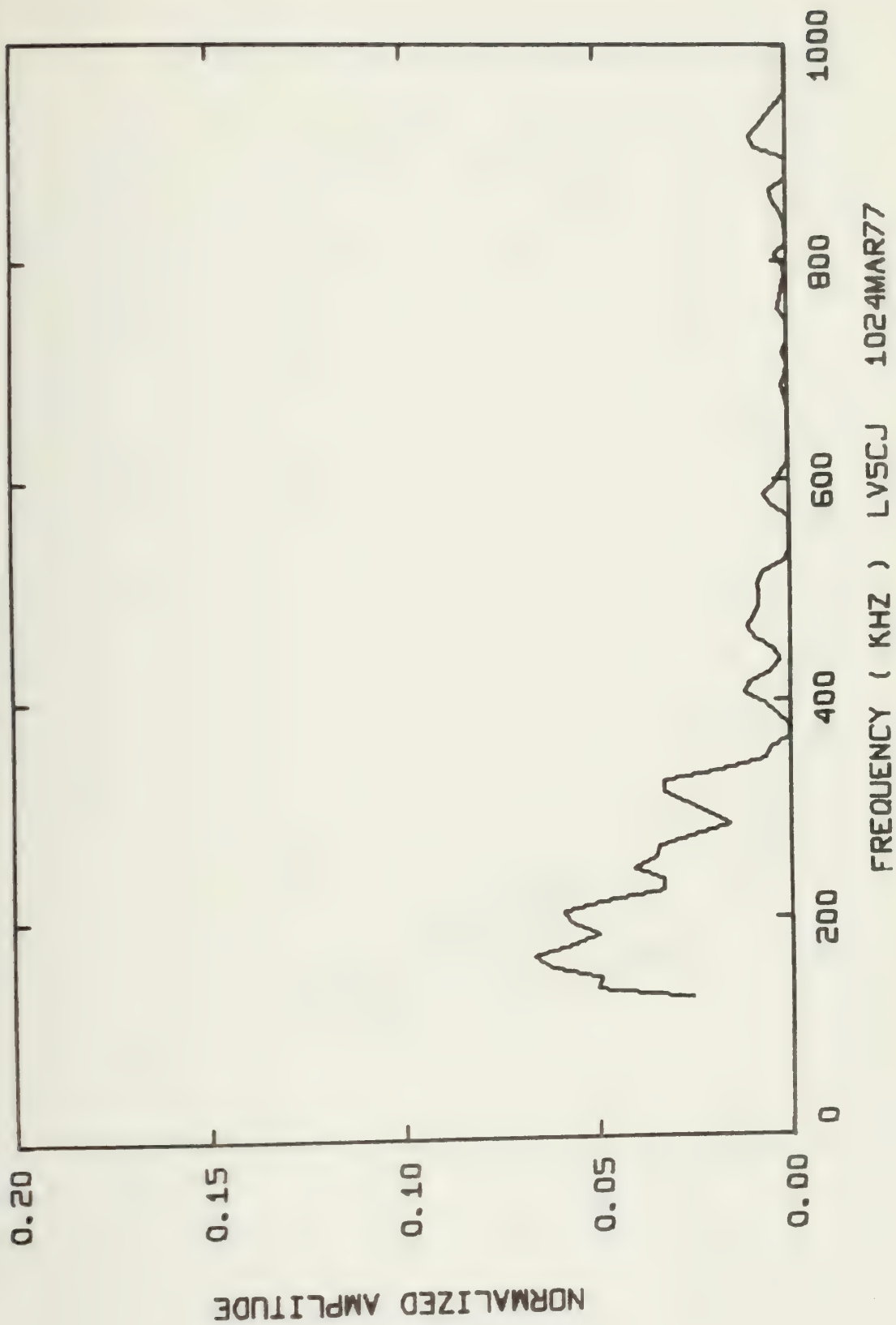
LV5CJ 0824MAR77



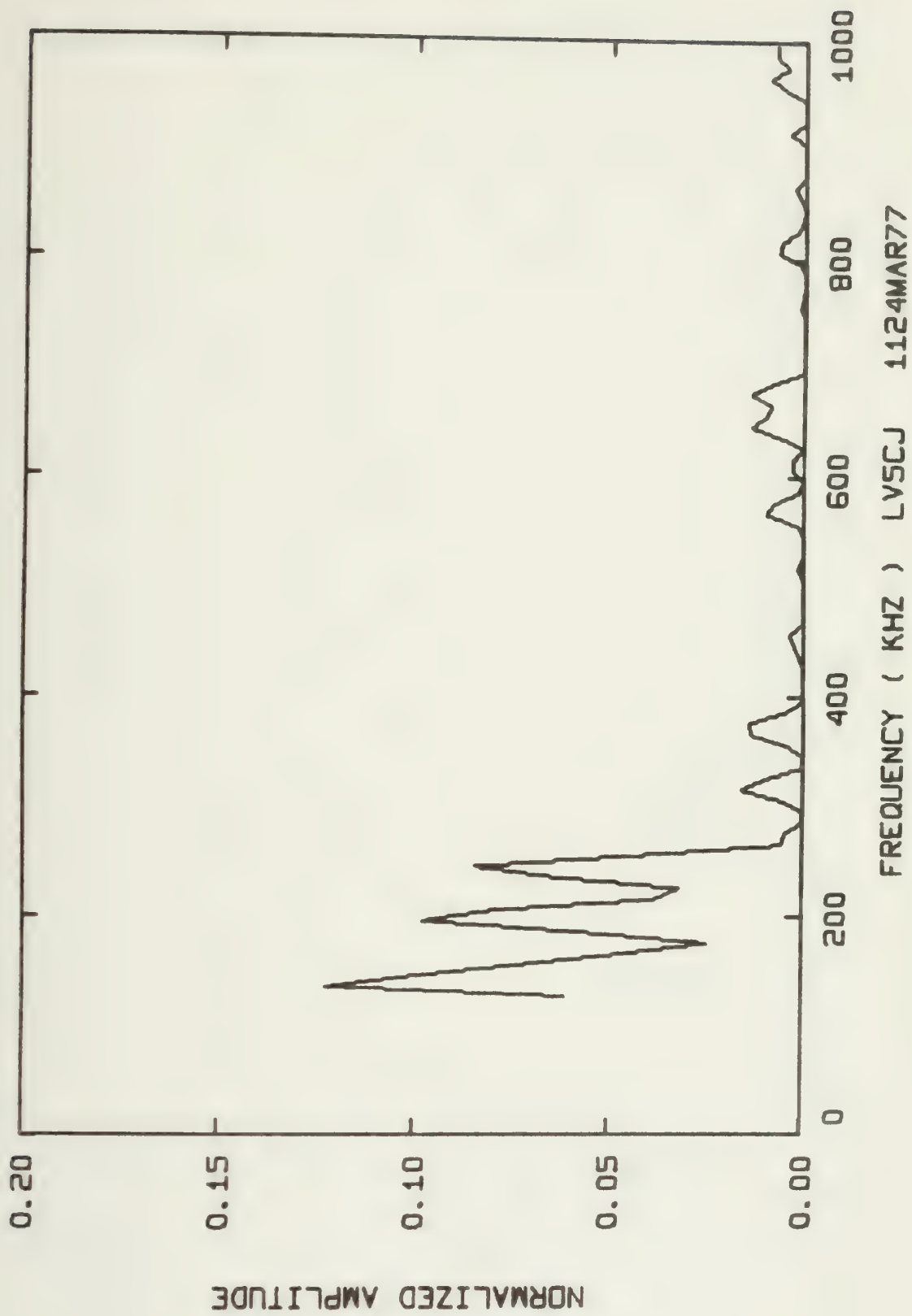




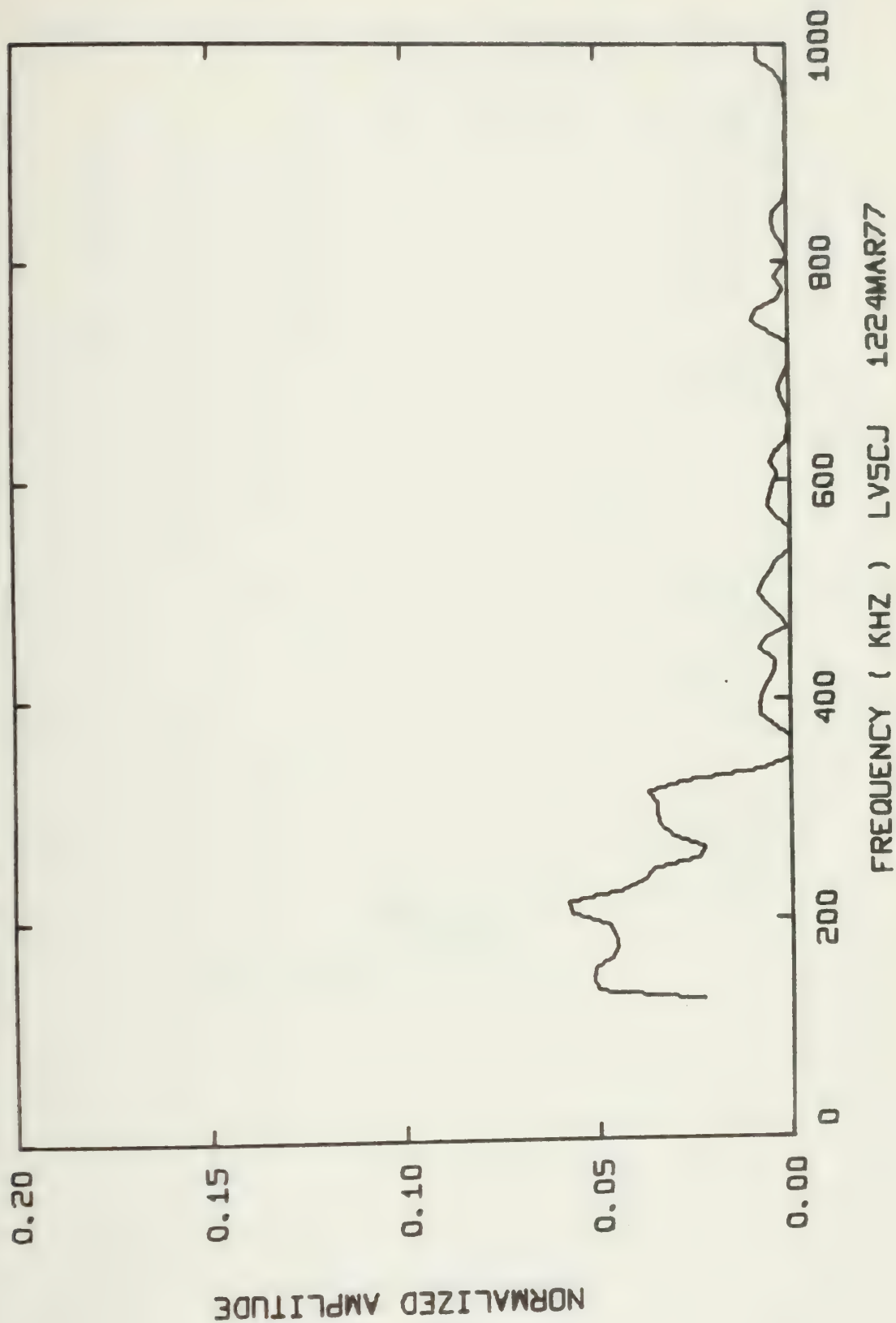




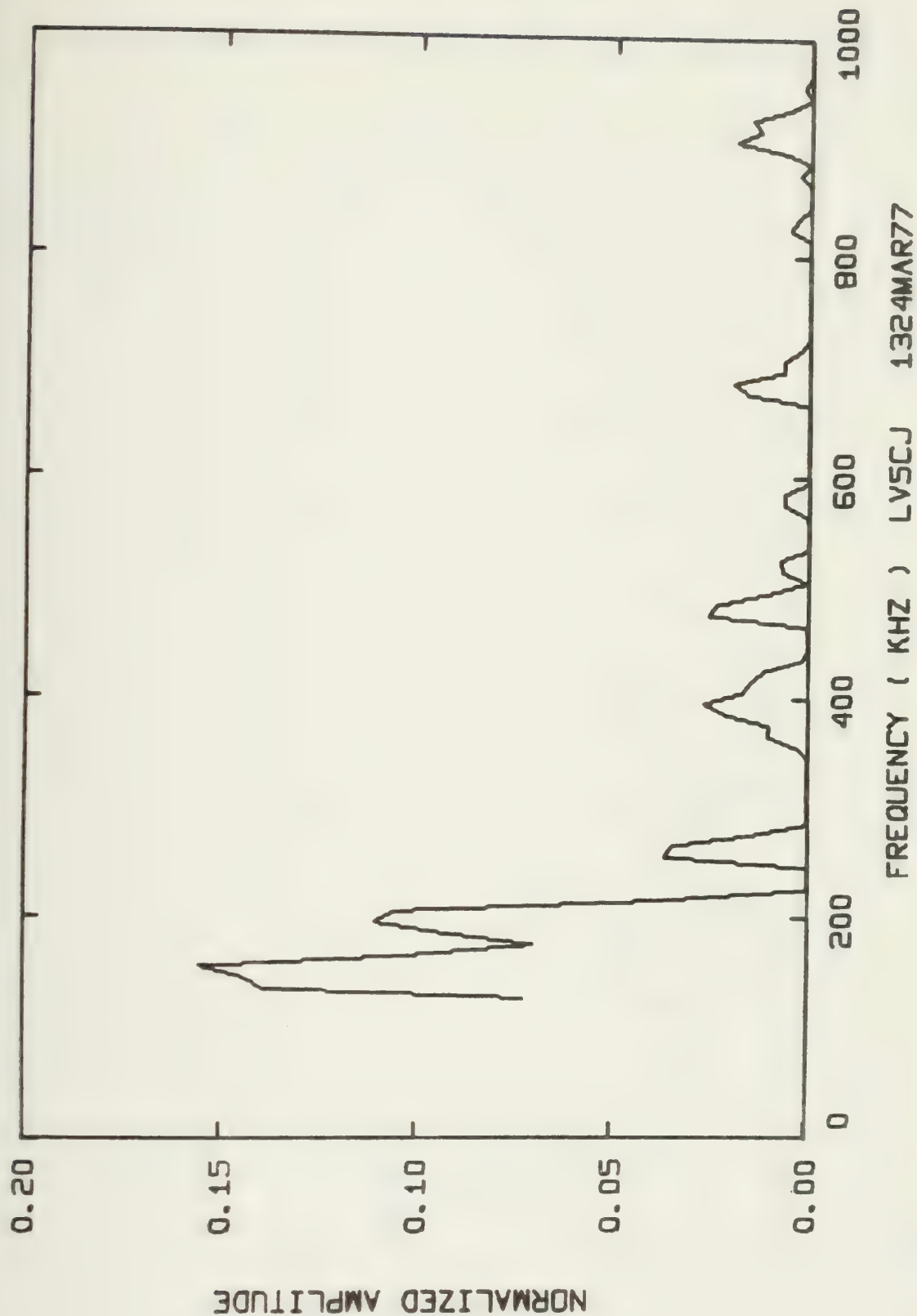






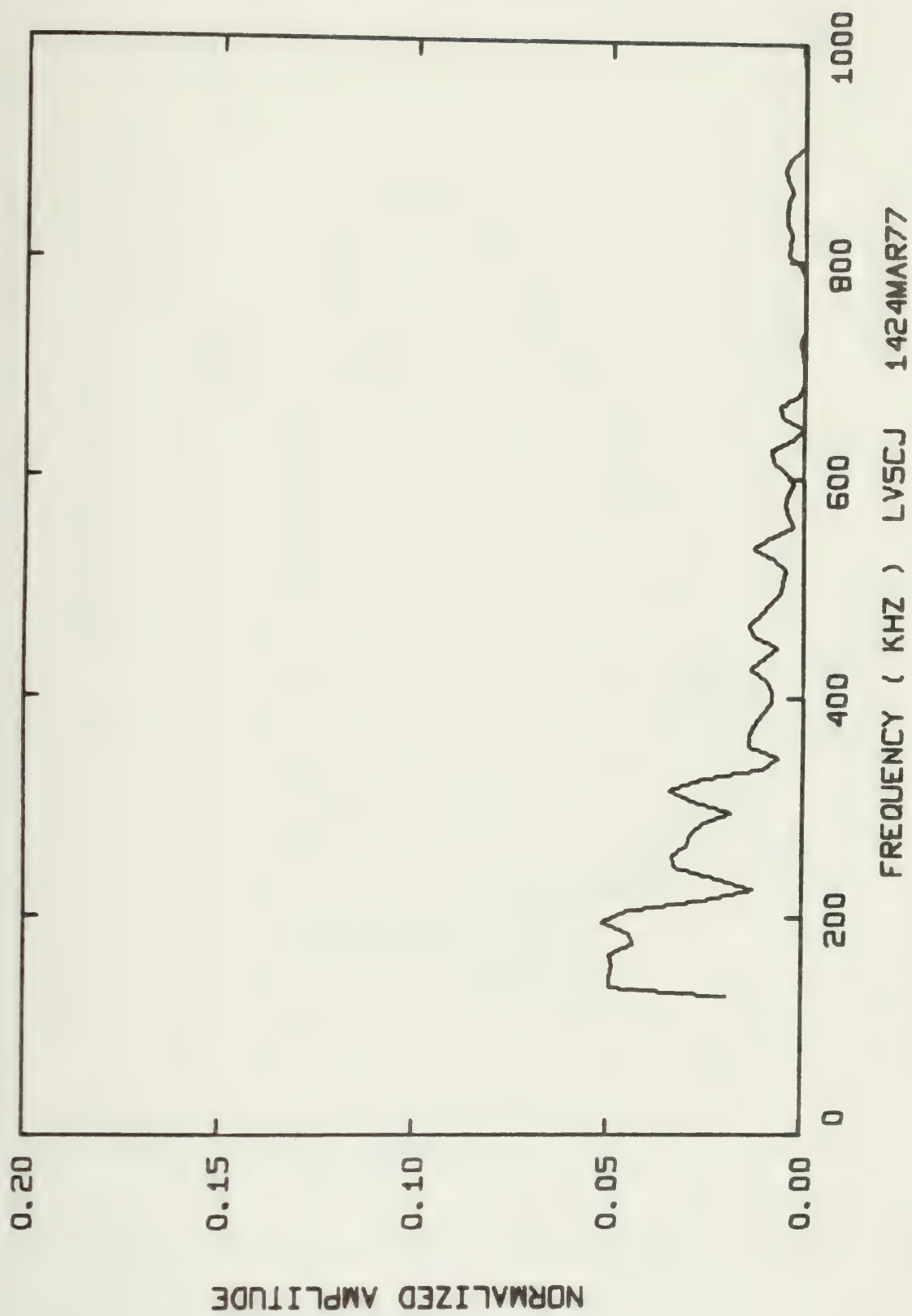




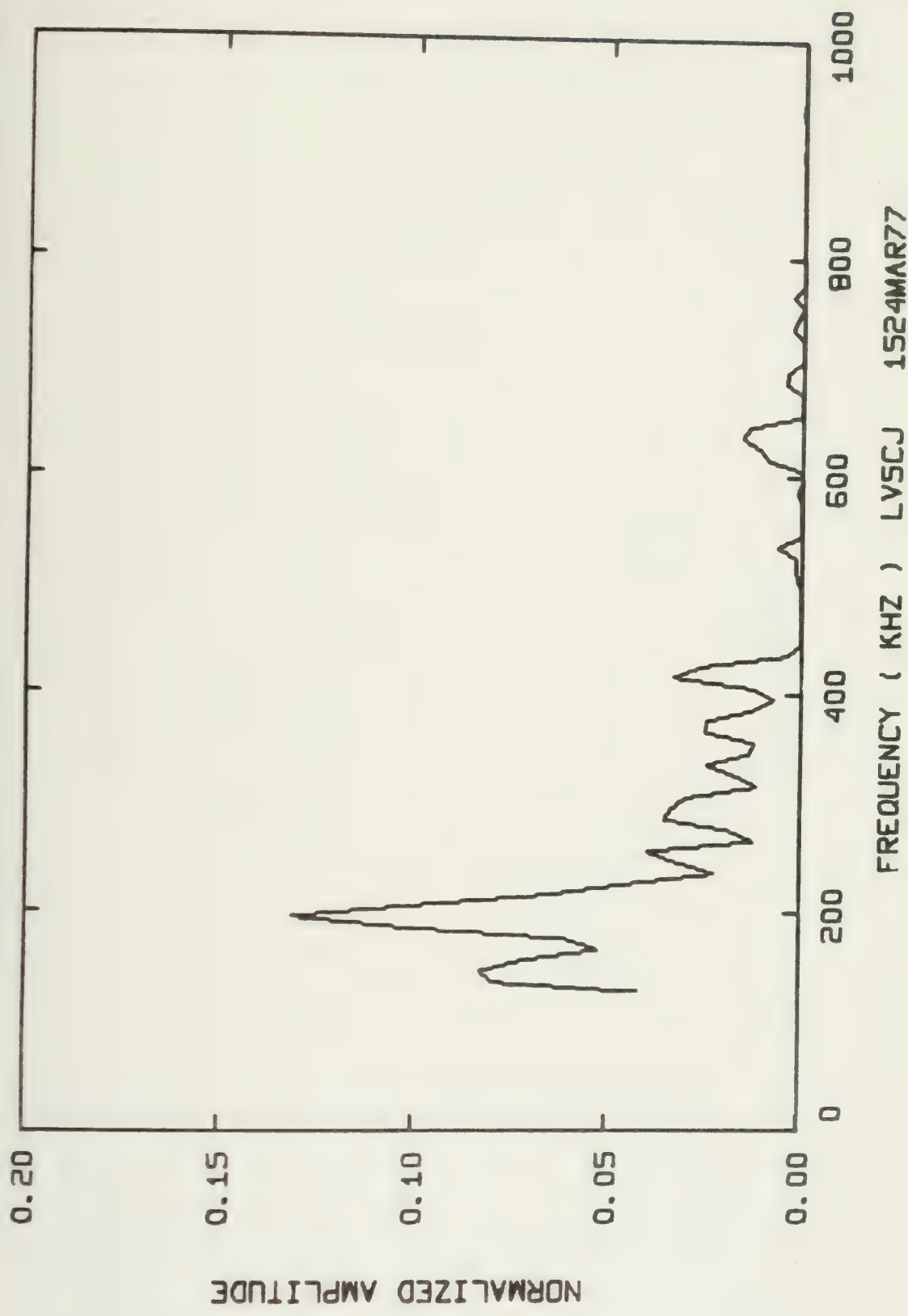




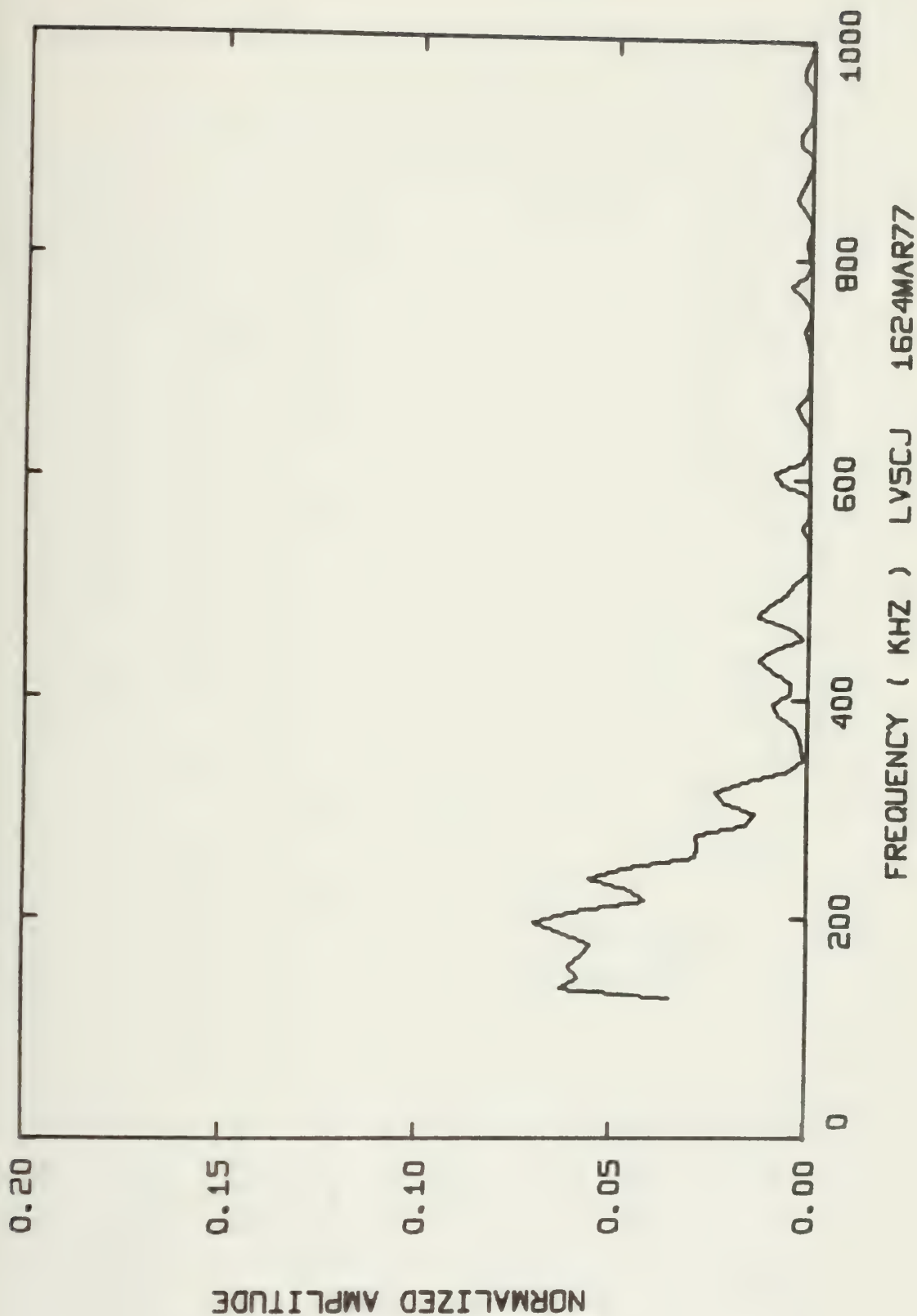




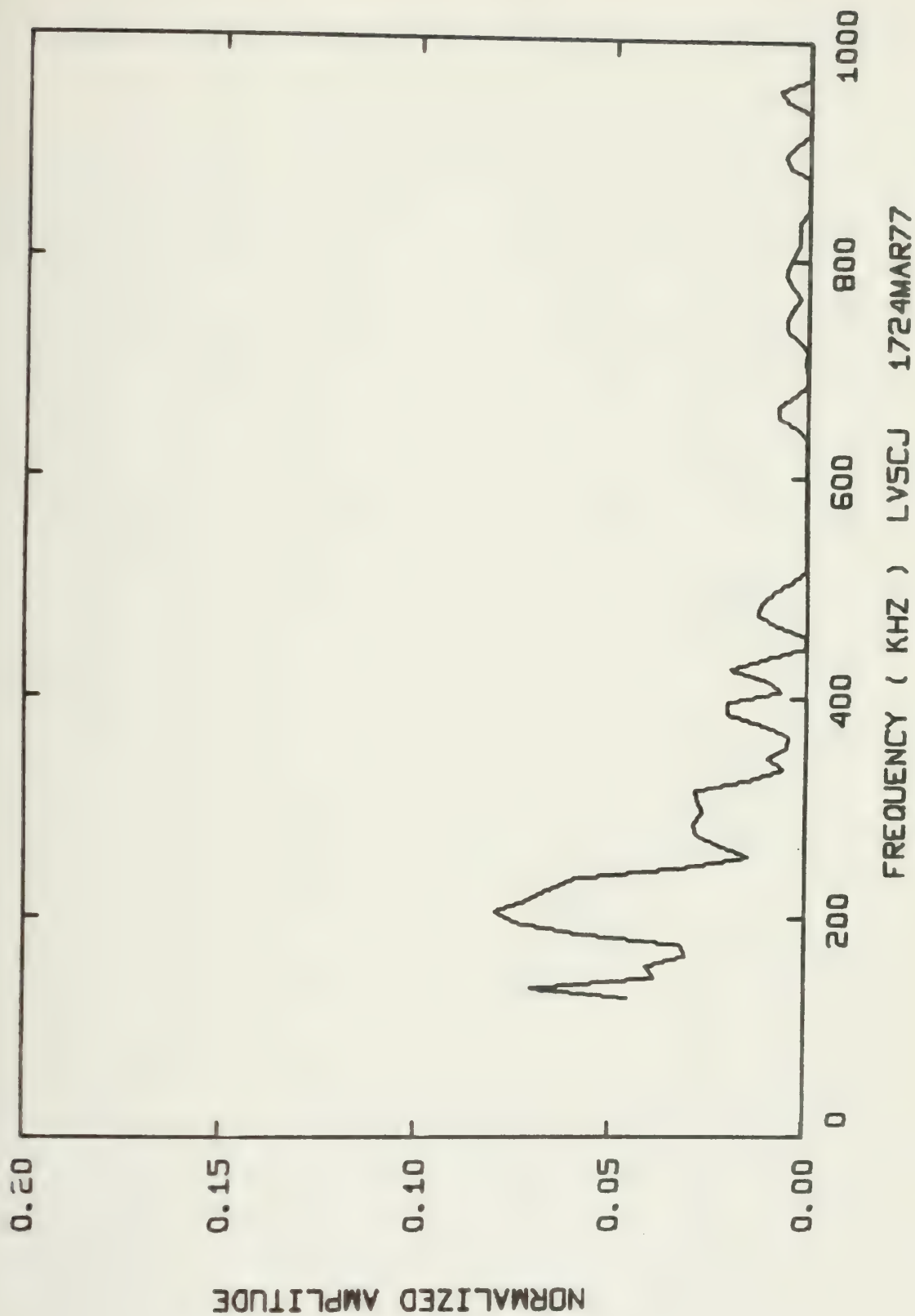






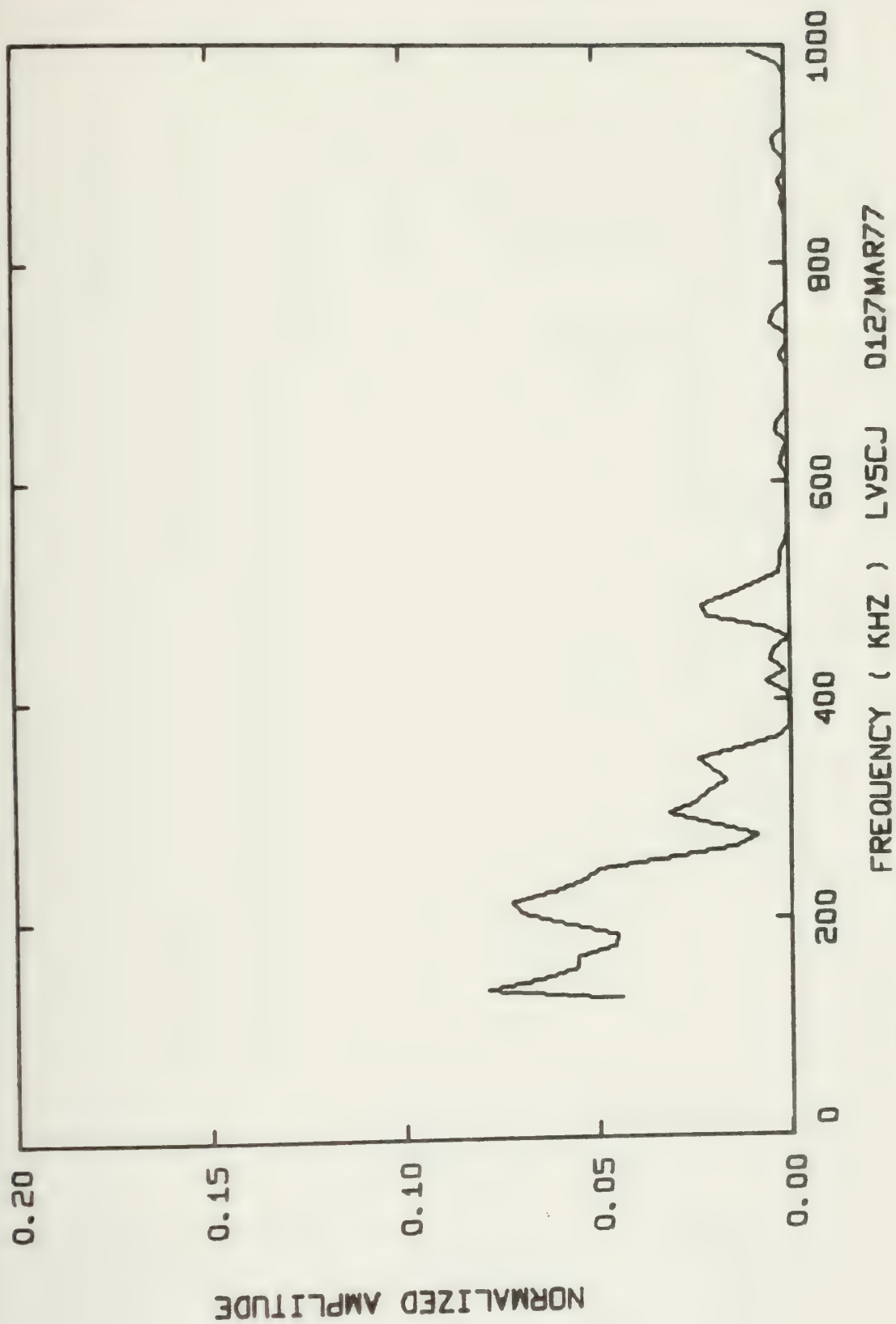




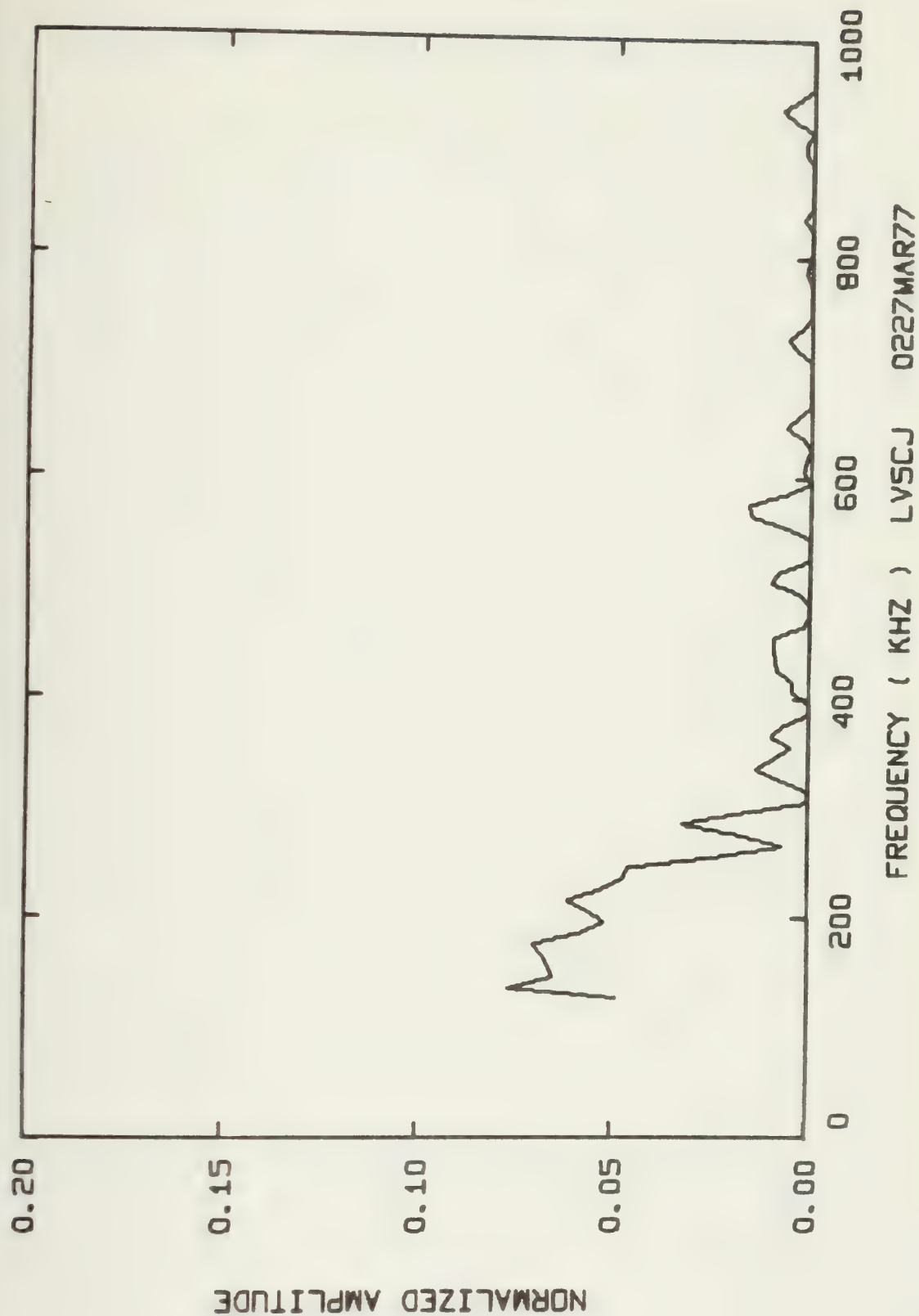




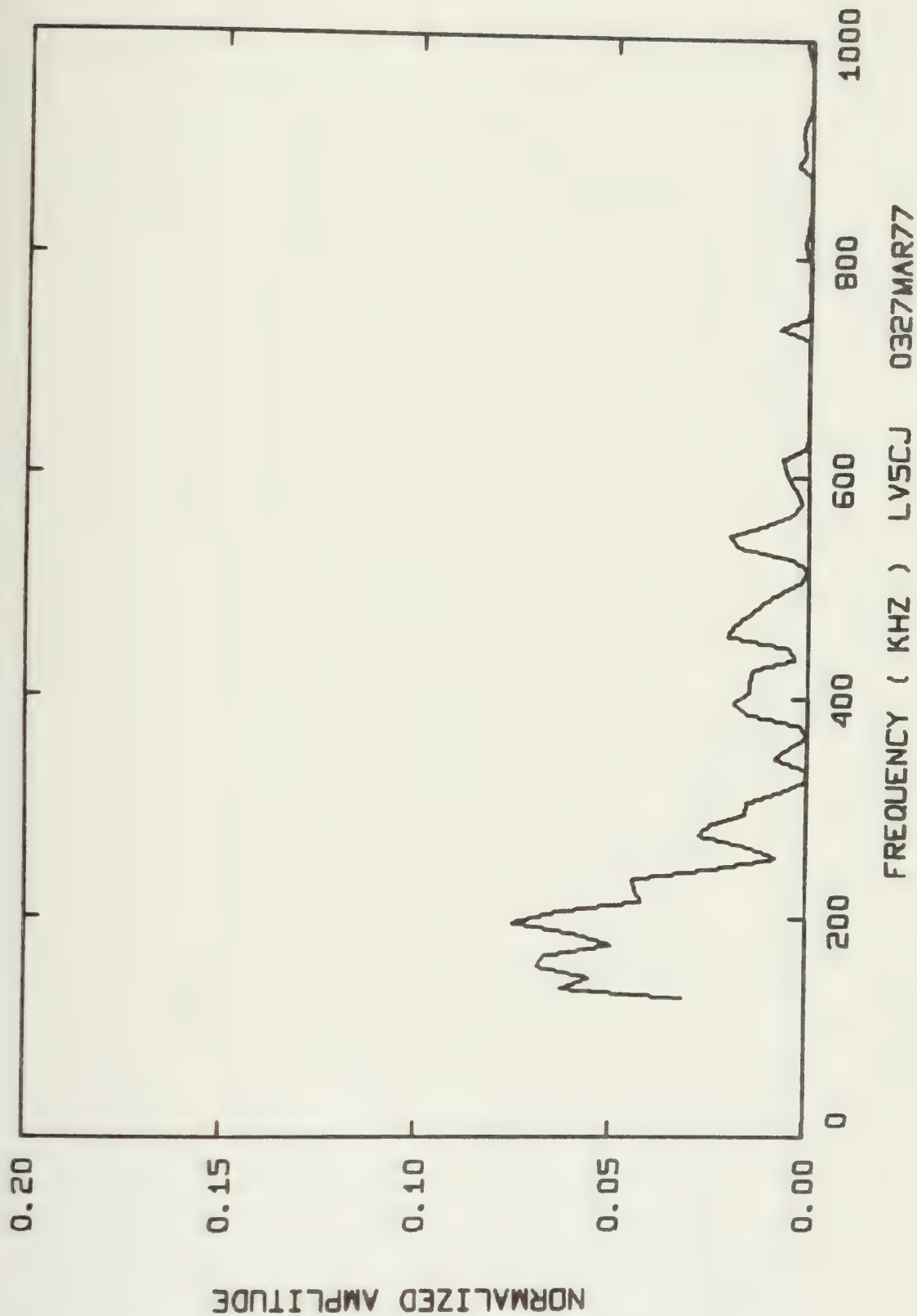




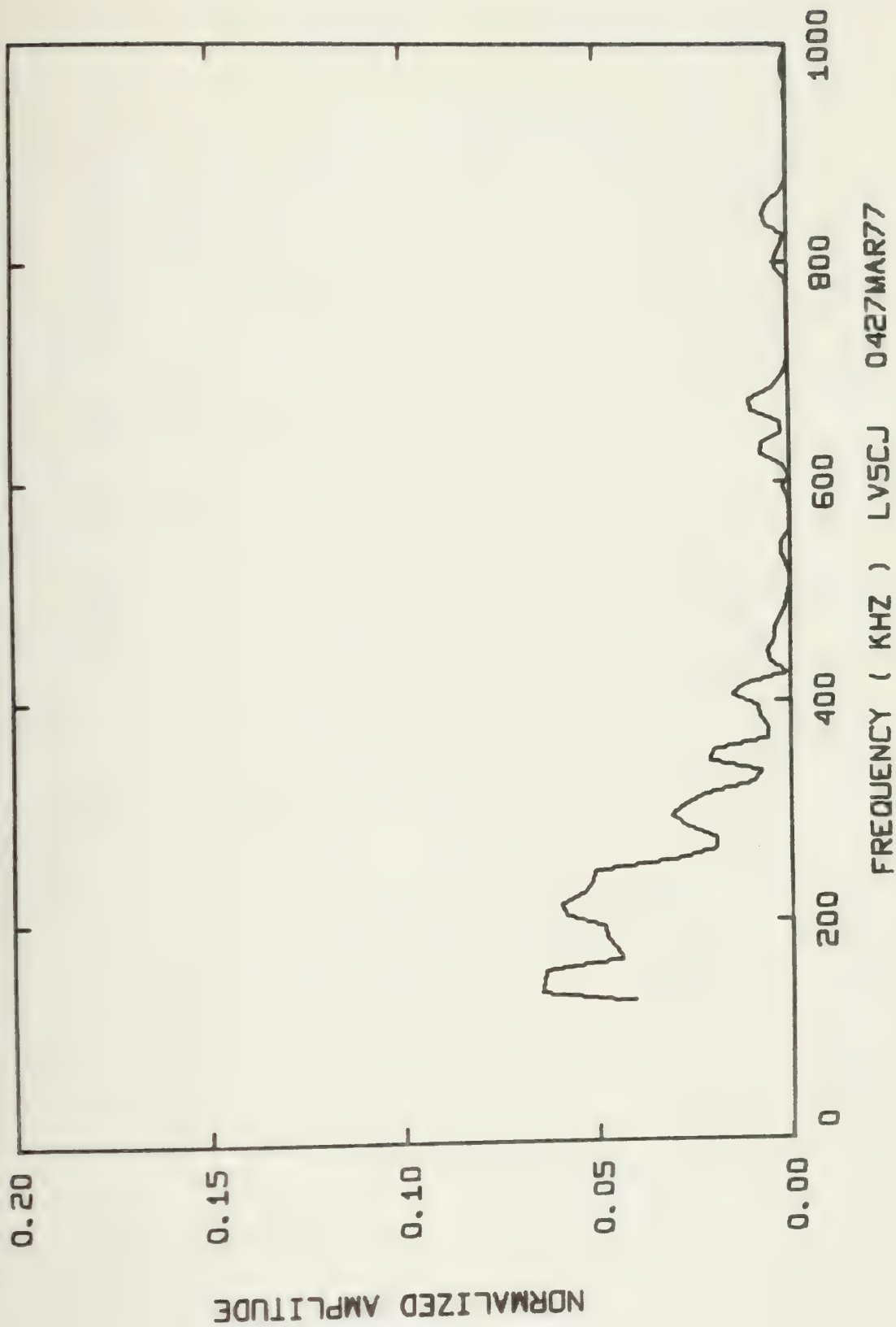






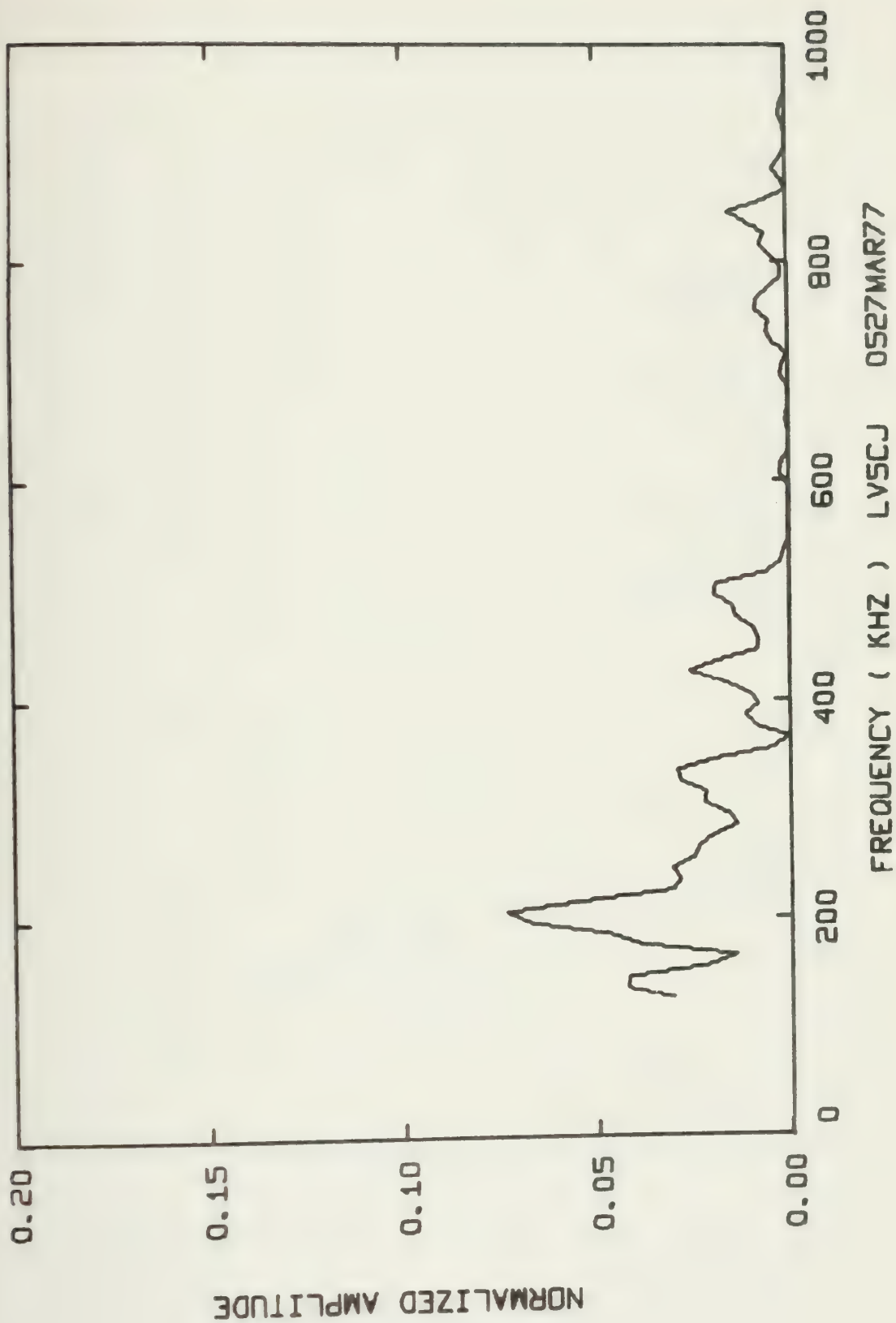




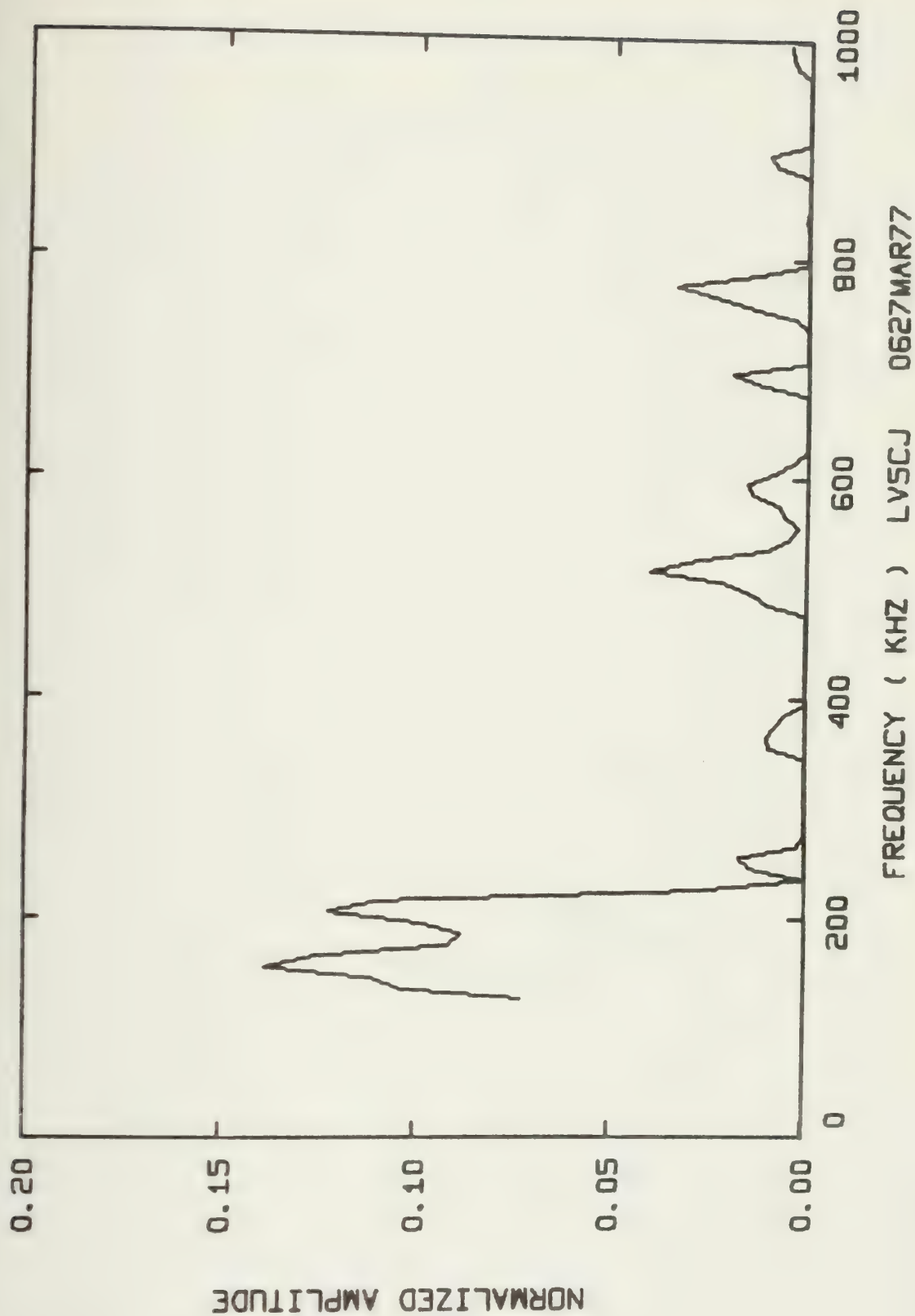




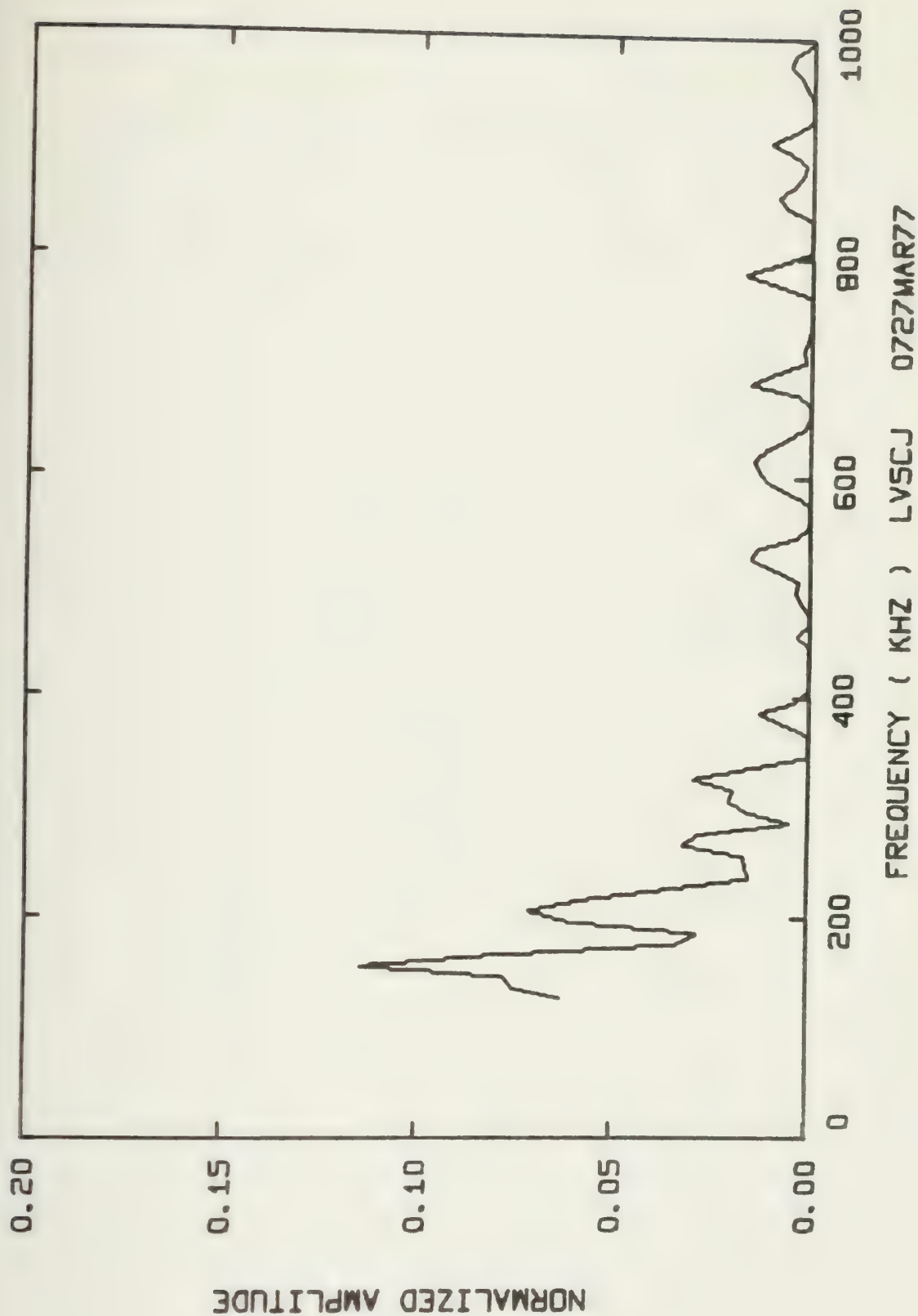




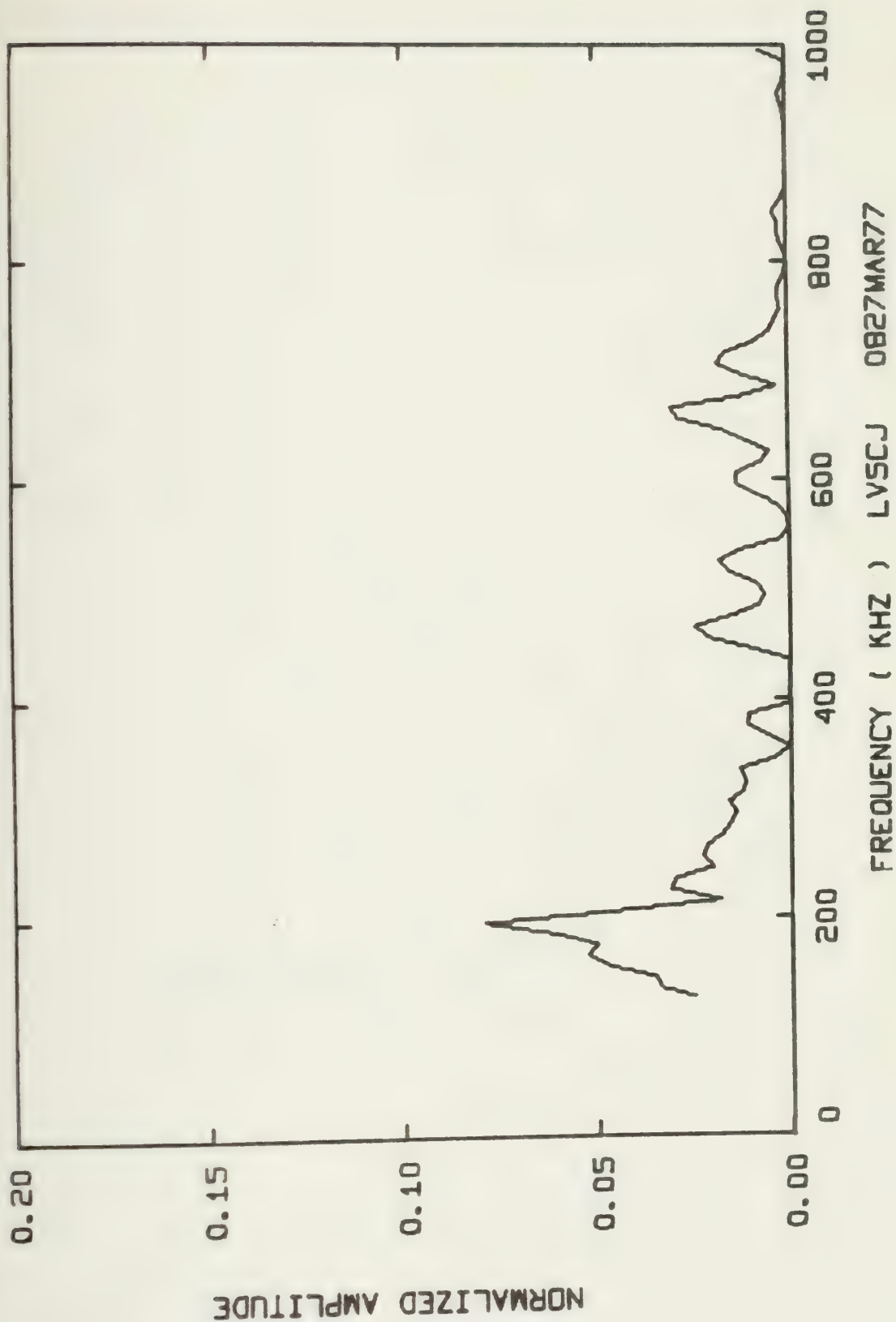






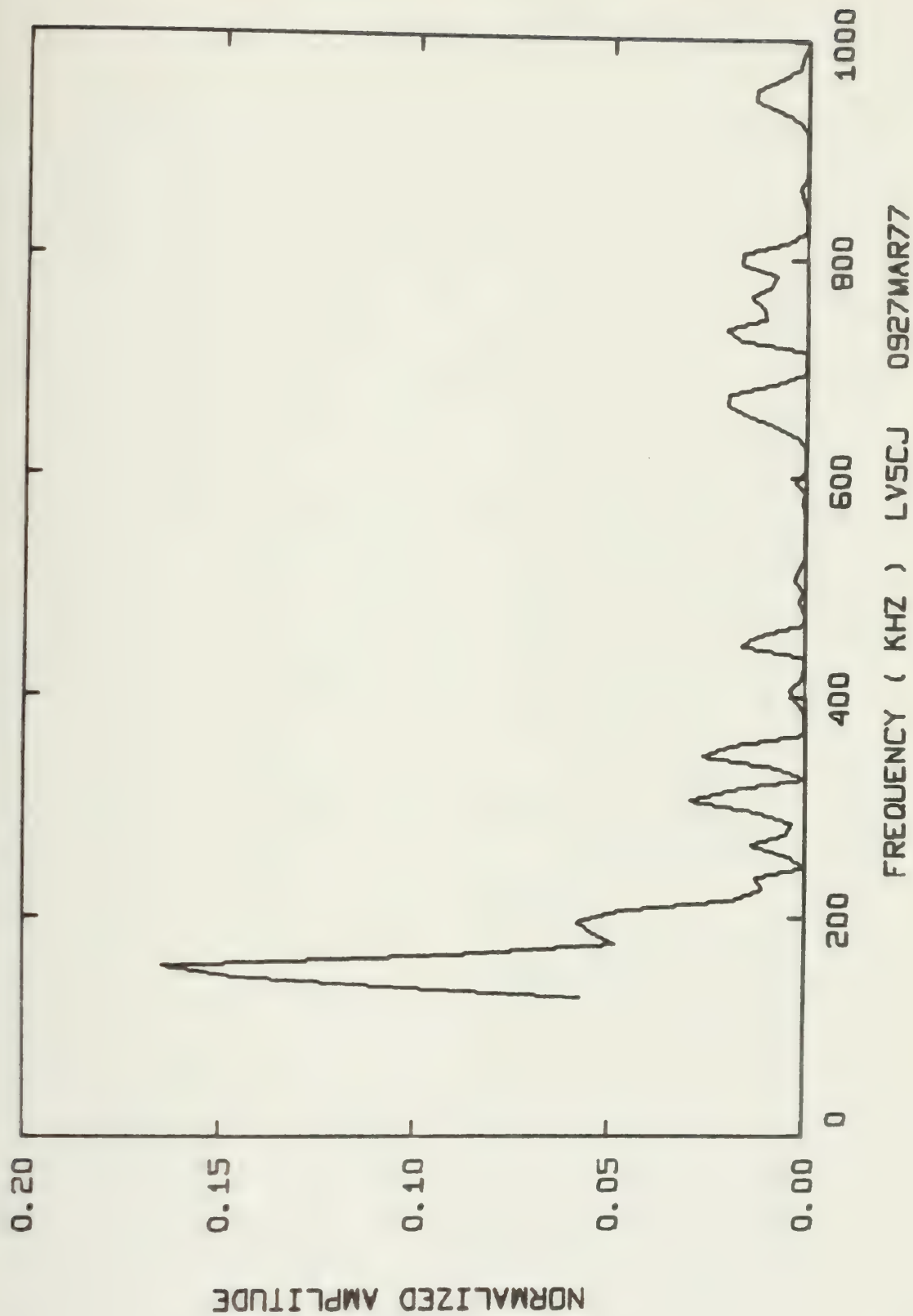




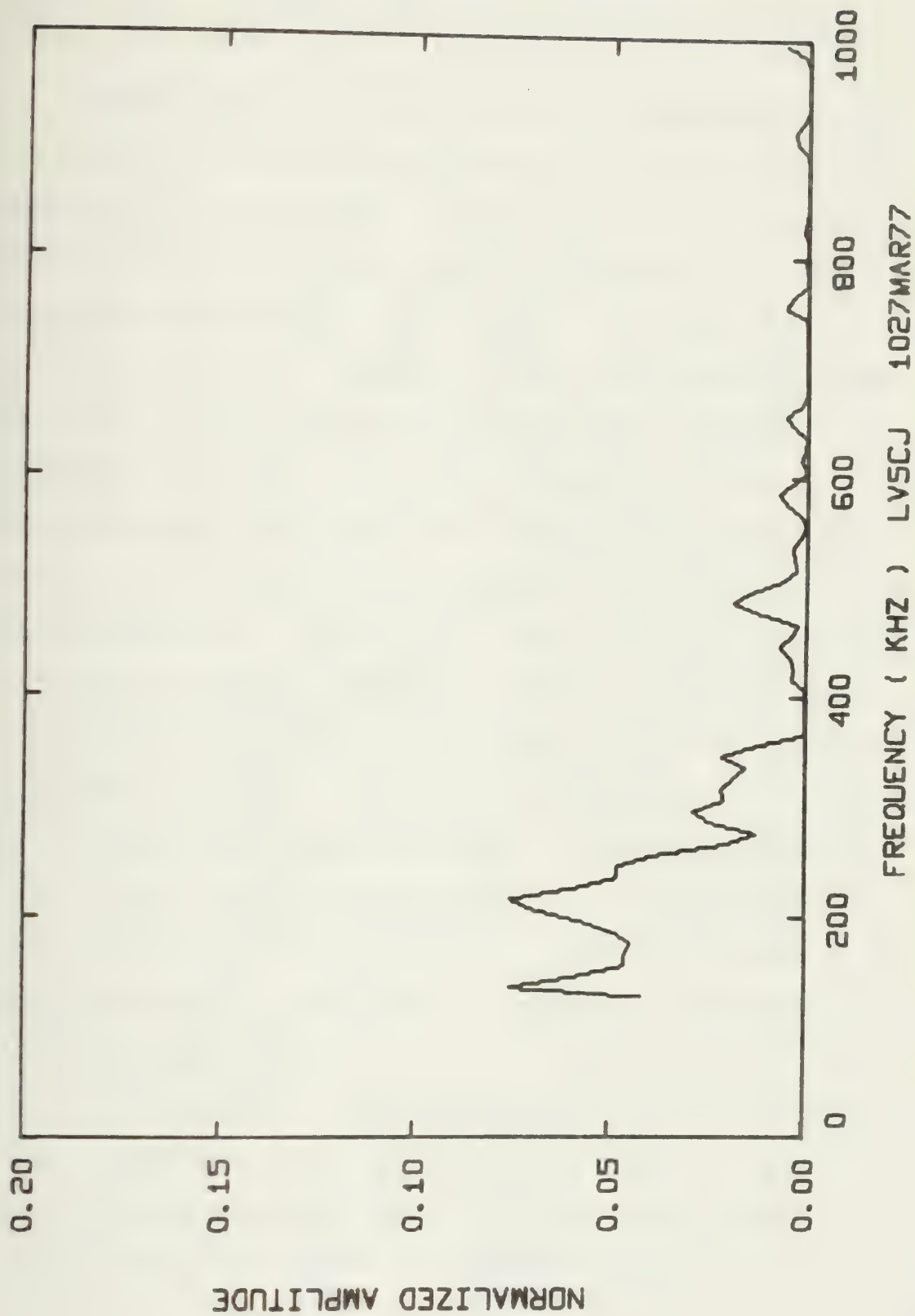














## Appendix D. The Paired-Sample t Statistic

If the difference between sample variances is large or if it is otherwise unreasonable to treat the population variances as being equal, several alternative methods can be used which do not require the assumption of equal population variances. One of these, the paired-sample t statistical test, applies to two random samples of the same size, which need not be independent. Briefly, the procedure is to work with the differences of paired observations, where the first member of each pair comes from the first sample and the second member comes from the second sample and then use what is called a one-sample t test to determine whether the mean of the differences is significantly different from zero. Two examinations can be made at each of " n " different frequencies in the case of spectral energy distributions. In many other applications, the pairing can be random. The major assumption made by the paired-sample t test is that all samples come from normal populations ( to within a reasonable degree of approximation ).

The one-sample t test can be described as follows: If  $\bar{x}$  is the mean of a random sample of size " n " taken from a normal population having a mean of zero and an unknown variance, then  $t = \frac{\bar{x} (n)^{\frac{1}{2}}}{S}$  is the value of a



random variable having the Student  $t$  distribution where  $n$  is the number of samples and  $S$  is the sample's standard deviation. This statistic carries a specification of its " degree of freedom "( which is simply  $n-1$  ). The shape of a "  $t$  " distribution is similar to that of a normal distribution. Like the standard normal distribution, the  $t$  distribution has a mean which is equal to zero, but its variance depends upon the number of degrees of freedom. For large numbers of degrees of freedom (  $n$  greater than 30 ) the  $t$  distribution can be approximated by the standard normal distribution.

Once the value of  $t$  has been calculated it will very rarely be zero ( this would imply that the mean value of the sampled differences between two spectral distributions is zero ). However, as the value of  $t$  approaches zero, the probability or confidence increases that the mean value of each spectral distribution is the same, which could imply that both sample normalized spectral energy distributions come from the same "master" or true distribution.

To initiate a test to either reject the hypothesis that the true mean of both spectral distributions is the same or to make no rejection decision and tacitly accept the hypothesis, requires the selection of a " level of significance ". The level of significance ranges from values between 0 and 1. The higher the level of





significance the more "picky" the test becomes, allowing less and less variation between spectral distributions. The level of significance must be carefully selected, particularly in a group of spectral energy distributions exhibiting a great deal of variation. An inordinately rigid or high level of significance will result in a large number of erroneous rejections of sample spectra which actually come from a population having the same "master" spectral energy distribution. Consequently, the level of significance should be chosen only after examining its impact upon sample spectra which are known or assumed to be generated by the same predominant mechanism. The ideal level of significance will allow acceptance of most of the sample spectra which are generated by the same predominant mechanism, and will reject those sample spectra which are generated by different predominant mechanisms.

Once the level of significance is chosen, the test proceeds as follows:

1. Divide the level of significance by 2.
2. Refer to either "t statistic tables" or, if the differences between the two spectral distributions are sampled at more than 30 different frequencies, to tables of the "normal distribution function."
3. If the t statistic tables are used, read the value of t directly off of the table after entering with one half of the level of significance and the number



of degrees of freedom ( where the number of degrees of freedom is equal to the number of sampled frequencies minus one ). If the normal distribution function tables are used, locate the value (  $1 - \frac{1}{2}(\text{level of significance})$  ) and read the value of  $t$  off of the chart's axis.

4. If the absolute value of  $t$  computed from the comparison of the two spectral energy distributions is greater than the value of  $t$  arrived at in step #3, the hypothesis that " both spectra have the same master spectral energy distribution " is rejected. If the absolute computed value of  $t$  is less than that which was arrived at in step #3, no rejection decision is made and the hypothesis being tested is tacitly accepted.

The fact that frequencies may be sampled at intervals to within the limit of spectral resolution capabilities of the test instrumentation, and that spectra may be compared over any frequency band of interest, makes the paired-sample  $t$  test a particularly flexible one. It is most productive when applied over frequencies having a significant spectral energy content.

As an application of the paired-sample  $t$  test, the mean normalized spectral energy distribution was computed for each specimen from a sampling of AE spectra taken just prior to specimen failure. Each specimen's mean normalized spectral energy distribution was then compared to all other specimens' mean spectral energy



distributions using the paired-sample t test between the frequencies 125 kHz to 800 kHz. The differences between spectra were computed at 10 kHz intervals ( the limiting resolution of the spectral analyzer ) at a total of 68 different frequencies. A level of significance of 0.74 was used. Table 9 lists the specific specimen pairs which were rejected by the test, having been judged to have statistically significant differences exhibited in their spectra. Table 10 gives the value of the t statistic which resulted from the comparison of each pair of specimens.

For instance, Table 9 indicates that at a level of significance of 0.741, if the absolute value of t computed in the paired-sample t test is greater than 0.331, the specimens comprising that pair will be declared " statistically different ". The first pair declared statistically different is found in the first row of Table 9, LV2B and LV1B. Table 10 designates specimen LV2B as #1 and specimen LV1B as #5. Table 10 indicates that the t statistic is 0.4897 for the pair comprised of specimen #1 and specimen #5. Since .4897 is greater than .331, the specimens in this pair are declared statistically different. On the other hand, Table 10 indicates that the t statistic is 0.1940 for the pair comprised of specimen #1 (LV2B) and specimen #2 (LV2C). Since .1940 is less than .331, this pair is not declared



statistically different and consequently does not appear in Table 9.





Table 2

Rejection Table for Paired-Sample t Test

Level of significance = 0.741.

Reject the tested hypothesis that "both specimens have the same master mean normalized spectral energy distribution if  $|t|$  is greater than 0.331.

Rejections

LV2B: LV1B, LV4A, LV5D, LV5G, LV5H, LV5CA, LV5CG, LV5CJ  
LV2C: LV2H, LV4A, LV5D, LV5G, LV5H, LV5CA, LV5CG, LV5CJ  
LV2G: LV2H, LV4A, LV5D, LV5G, LV5H, LV5CJ  
LV2H: LV2C, LV2G, LV1B, LV4A, LV5C, LV5D  
LV1B: LV2B, LV2H, LV5D, LV5G, LV5H, LV5CA, LV5CG  
LV4A: LV2B, LV2C, LV2G, LV2H, LV4C, LV5C, LV5D, LV5G,  
LV5H, LV5CA, LV5CG, LV5CI, LV5CJ  
LV4C: LV4A, LV5D, LV5G  
LV5C: LV2H, LV4A, LV5D, LV5G, LV5H, LV5CG, LV5CJ  
LV5D: LV2B, LV2C, LV2G, LV2H, LV1B, LV4A, LV4C, LV5C,  
LV5G, LV5H, LV5CA, LV5CG, LV5CI, LV5CJ  
LV5G: LV2B, LV2C, LV2G, LV1B, LV4A, LV4C, LV5C, LV5D  
LV5H: LV2B, LV2C, LV2G, LV1B, LV4A, LV5C, LV5D, LV5CJ  
LV5CA: LV2B, LV2C, LV1B, LV4A, LV5D  
LV5CG: LV2B, LV2C, LV1B, LV4A, LV5C, LV5D, LV5CJ  
LV5CI: LV4A, LV5D  
LV5CJ: LV2B, LV2C, LV2G, LV4A, LV5C, LV5D, LV5H, LV5CG



Table 10

## t Statistic Values for Specimen Pair Comparisons

Note: Each specimen number is indicated on the left hand column of the first 15 rows. These specimen number designations are then used for identification later in the table, as the value of the statistic "t" is presented for each pair of compared specimens.

#1	LV2H	MEAN	NORMALIZED	AMPLITUDE
#2	LV2C	MEAN	NORMALIZED	AMPLITUDE
#3	LV2G	MEAN	NORMALIZED	AMPLITUDE
#4	LV2F	MEAN	NORMALIZED	AMPLITUDE
#5	LV1F	MEAN	NORMALIZED	AMPLITUDE
#6	LV4A	MEAN	NORMALIZED	AMPLITUDE
#7	LV4C	MEAN	NORMALIZED	AMPLITUDE
#8	LV5C	MEAN	NORMALIZED	AMPLITUDE
#9	LV5F	MEAN	NORMALIZED	AMPLITUDE
#10	LV5B	MEAN	NORMALIZED	AMPLITUDE
#11	LV5H	MEAN	NORMALIZED	AMPLITUDE
#12	LV5G	MEAN	NORMALIZED	AMPLITUDE
#13	LV5CC	MEAN	NORMALIZED	AMPLITUDE
#14	LV5BC	MEAN	NORMALIZED	AMPLITUDE
#15	LV5CG	MEAN	NORMALIZED	AMPLITUDE

STATISTIC IS	0.1940853E 00	FOR SPECIMEN	1 AND SPECIMEN	2
STATISTIC IS	-0.1582856E 00	FOR SPECIMEN	2 AND SPECIMEN	3
STATISTIC IS	-0.5027013E 00	FOR SPECIMEN	3 AND SPECIMEN	4
STATISTIC IS	0.5846528E 00	FOR SPECIMEN	4 AND SPECIMEN	5
STATISTIC IS	0.1652167E 00	FOR SPECIMEN	5 AND SPECIMEN	6
STATISTIC IS	-0.8130833E 00	FOR SPECIMEN	6 AND SPECIMEN	7
STATISTIC IS	0.1920020E 00	FOR SPECIMEN	7 AND SPECIMEN	8
STATISTIC IS	0.1495876E 01	FOR SPECIMEN	8 AND SPECIMEN	9
STATISTIC IS	-0.1178123E 01	FOR SPECIMEN	9 AND SPECIMEN	10
STATISTIC IS	0.1877377E 10	FOR SPECIMEN	10 AND SPECIMEN	11
STATISTIC IS	-0.1302579E 00	FOR SPECIMEN	11 AND SPECIMEN	12
STATISTIC IS	0.1532381E 00	FOR SPECIMEN	12 AND SPECIMEN	13
STATISTIC IS	-0.1816140E -02	FOR SPECIMEN	13 AND SPECIMEN	14
STATISTIC IS	-0.1249401E 01	FOR SPECIMEN	14 AND SPECIMEN	15
STATISTIC IS	0.142303E -01	FOR SPECIMEN	1 AND SPECIMEN	3



Table 10 - cont.

STATISTIC IS	-	.4021107E-00	FOR SPECIMEN	2	AND SPECIMEN	4
STATISTIC IS	-	.31427117E-01	FOR SPECIMEN	3	AND SPECIMEN	5
STATISTIC IS	-	.3803300E-01	FOR SPECIMEN	4	AND SPECIMEN	6
STATISTIC IS	-	.2627553E-01	FOR SPECIMEN	5	AND SPECIMEN	7
STATISTIC IS	-	.4238686E-00	FOR SPECIMEN	6	AND SPECIMEN	8
STATISTIC IS	-	.1048003E-01	FOR SPECIMEN	7	AND SPECIMEN	9
STATISTIC IS	-	.5077505E-00	FOR SPECIMEN	8	AND SPECIMEN	10
STATISTIC IS	-	.1075336E-01	FOR SPECIMEN	9	AND SPECIMEN	11
STATISTIC IS	-	.1058839E-01	FOR SPECIMEN	10	AND SPECIMEN	12
STATISTIC IS	-	.4740707E-01	FOR SPECIMEN	11	AND SPECIMEN	13
STATISTIC IS	-	.6652376E-01	FOR SPECIMEN	12	AND SPECIMEN	14
STATISTIC IS	-	.1039007E-00	FOR SPECIMEN	13	AND SPECIMEN	15
STATISTIC IS	-	.3356677E-00	FOR SPECIMEN	1	AND SPECIMEN	4
STATISTIC IS	-	.2105362E-00	FOR SPECIMEN	2	AND SPECIMEN	5
STATISTIC IS	-	.6007990E-00	FOR SPECIMEN	3	AND SPECIMEN	6
STATISTIC IS	-	.1026692E-00	FOR SPECIMEN	4	AND SPECIMEN	7
STATISTIC IS	-	.0014275E-00	FOR SPECIMEN	5	AND SPECIMEN	8
STATISTIC IS	-	.0047170E-00	FOR SPECIMEN	6	AND SPECIMEN	9
STATISTIC IS	-	.004171238E-00	FOR SPECIMEN	7	AND SPECIMEN	10
STATISTIC IS	-	.000481429E-00	FOR SPECIMEN	8	AND SPECIMEN	11
STATISTIC IS	-	.000668410E-00	FOR SPECIMEN	9	AND SPECIMEN	12
STATISTIC IS	-	.00000541E-00	FOR SPECIMEN	10	AND SPECIMEN	13
STATISTIC IS	-	.00007701E-01	FOR SPECIMEN	11	AND SPECIMEN	14
STATISTIC IS	-	.001219102E-00	FOR SPECIMEN	12	AND SPECIMEN	15
STATISTIC IS	-	.00007205E-00	FOR SPECIMEN	1	AND SPECIMEN	5
STATISTIC IS	-	.0022853E-00	FOR SPECIMEN	2	AND SPECIMEN	6
STATISTIC IS	-	.00173502E-00	FOR SPECIMEN	3	AND SPECIMEN	7
STATISTIC IS	-	.00379651E-00	FOR SPECIMEN	4	AND SPECIMEN	8
STATISTIC IS	-	.00757036E-00	FOR SPECIMEN	5	AND SPECIMEN	9
STATISTIC IS	-	.00752814E-00	FOR SPECIMEN	6	AND SPECIMEN	10
STATISTIC IS	-	.0002906E-01	FOR SPECIMEN	7	AND SPECIMEN	11
STATISTIC IS	-	.003105393E-00	FOR SPECIMEN	8	AND SPECIMEN	12
STATISTIC IS	-	.001052077E-01	FOR SPECIMEN	9	AND SPECIMEN	13
STATISTIC IS	-	.00040729E-00	FOR SPECIMEN	10	AND SPECIMEN	14
STATISTIC IS	-	.000453376E-00	FOR SPECIMEN	11	AND SPECIMEN	15
STATISTIC IS	-	.004677400E-00	FOR SPECIMEN	1	AND SPECIMEN	6
STATISTIC IS	-	.003143635E-00	FOR SPECIMEN	2	AND SPECIMEN	7
STATISTIC IS	-	.001360569E-00	FOR SPECIMEN	3	AND SPECIMEN	8
STATISTIC IS	-	.001728478E-01	FOR SPECIMEN	4	AND SPECIMEN	9
STATISTIC IS	-	.000016619E-00	FOR SPECIMEN	5	AND SPECIMEN	10
STATISTIC IS	-	.002211041E-01	FOR SPECIMEN	6	AND SPECIMEN	11
STATISTIC IS	-	.001086047E-00	FOR SPECIMEN	7	AND SPECIMEN	12
STATISTIC IS	-	.000052632E-01	FOR SPECIMEN	8	AND SPECIMEN	13
STATISTIC IS	-	.00733733E-00	FOR SPECIMEN	9	AND SPECIMEN	14
STATISTIC IS	-	.001004055E-01	FOR SPECIMEN	10	AND SPECIMEN	15
STATISTIC IS	-	.001179196E-01	FOR SPECIMEN	1	AND SPECIMEN	7
STATISTIC IS	-	.000640479E-01	FOR SPECIMEN	2	AND SPECIMEN	8





Table 10 - cont.

STATISTIC	IS	-0.1036412E-01	FOR SPECIMEN	3 AND SPECIMEN	9
STATISTIC	IS	-0.2131301E-00	FOR SPECIMEN	4 AND SPECIMEN	10
STATISTIC	IS	-0.125703E-00	FOR SPECIMEN	5 AND SPECIMEN	11
STATISTIC	IS	-0.4560941E-00	FOR SPECIMEN	6 AND SPECIMEN	12
STATISTIC	IS	-0.4104873E-01	FOR SPECIMEN	7 AND SPECIMEN	13
STATISTIC	IS	-0.1959893E-00	FOR SPECIMEN	8 AND SPECIMEN	14
STATISTIC	IS	-0.1214524E-01	FOR SPECIMEN	3 AND SPECIMEN	15
STATISTIC	IS	-0.1799667E-00	FOR SPECIMEN	1 AND SPECIMEN	8
STATISTIC	IS	-0.1590877E-01	FOR SPECIMEN	2 AND SPECIMEN	9
STATISTIC	IS	-0.4547452E-00	FOR SPECIMEN	3 AND SPECIMEN	10
STATISTIC	IS	-0.1306982E-01	FOR SPECIMEN	4 AND SPECIMEN	11
STATISTIC	IS	-0.7337793E-00	FOR SPECIMEN	5 AND SPECIMEN	12
STATISTIC	IS	-0.5069309E-00	FOR SPECIMEN	6 AND SPECIMEN	13
STATISTIC	IS	-0.1819439E-00	FOR SPECIMEN	7 AND SPECIMEN	14
STATISTIC	IS	-0.5431589E-00	FOR SPECIMEN	8 AND SPECIMEN	15
STATISTIC	IS	-0.1311239E-01	FOR SPECIMEN	1 AND SPECIMEN	9
STATISTIC	IS	-0.5411333E-00	FOR SPECIMEN	2 AND SPECIMEN	10
STATISTIC	IS	-0.127933E-00	FOR SPECIMEN	3 AND SPECIMEN	11
STATISTIC	IS	-0.1550072E-01	FOR SPECIMEN	4 AND SPECIMEN	12
STATISTIC	IS	-0.3545326E-00	FOR SPECIMEN	5 AND SPECIMEN	13
STATISTIC	IS	-0.6265116E-00	FOR SPECIMEN	6 AND SPECIMEN	14
STATISTIC	IS	-0.1805096E-00	FOR SPECIMEN	7 AND SPECIMEN	15
STATISTIC	IS	-0.3354938E-00	FOR SPECIMEN	1 AND SPECIMEN	10
STATISTIC	IS	-0.5003518E-00	FOR SPECIMEN	2 AND SPECIMEN	11
STATISTIC	IS	-0.2981674E-00	FOR SPECIMEN	3 AND SPECIMEN	12
STATISTIC	IS	-0.3360220E-01	FOR SPECIMEN	4 AND SPECIMEN	13
STATISTIC	IS	-0.1543226E-00	FOR SPECIMEN	5 AND SPECIMEN	14
STATISTIC	IS	-0.1450198E-00	FOR SPECIMEN	6 AND SPECIMEN	15
STATISTIC	IS	-0.5304309E-00	FOR SPECIMEN	1 AND SPECIMEN	11
STATISTIC	IS	-0.3422086E-00	FOR SPECIMEN	2 AND SPECIMEN	12
STATISTIC	IS	-0.3002102E-00	FOR SPECIMEN	3 AND SPECIMEN	13
STATISTIC	IS	-0.170147E-01	FOR SPECIMEN	4 AND SPECIMEN	14
STATISTIC	IS	-0.1009072E-01	FOR SPECIMEN	5 AND SPECIMEN	15
STATISTIC	IS	-0.3305425E-00	FOR SPECIMEN	1 AND SPECIMEN	12
STATISTIC	IS	-0.3047157E-00	FOR SPECIMEN	2 AND SPECIMEN	13
STATISTIC	IS	-0.2074201E-00	FOR SPECIMEN	3 AND SPECIMEN	14
STATISTIC	IS	-0.1048610E-00	FOR SPECIMEN	4 AND SPECIMEN	15
STATISTIC	IS	-0.4190636E-00	FOR SPECIMEN	1 AND SPECIMEN	13
STATISTIC	IS	-0.3075530E-00	FOR SPECIMEN	2 AND SPECIMEN	14
STATISTIC	IS	-0.5004531E-00	FOR SPECIMEN	3 AND SPECIMEN	15
STATISTIC	IS	-0.1519448E-00	FOR SPECIMEN	1 AND SPECIMEN	14
STATISTIC	IS	-0.1635407E-00	FOR SPECIMEN	2 AND SPECIMEN	15
STATISTIC	IS	-0.1009209E-00	FOR SPECIMEN	1 AND SPECIMEN	15





Appendix E. AE Spectral Energy, AE Pressure, and  
Normalized AE Energy Distribution from ( $\pm 45^\circ$ ,  $\pm 45^\circ$ )<sub>s</sub>  
Specimens at Various Ascending Loads

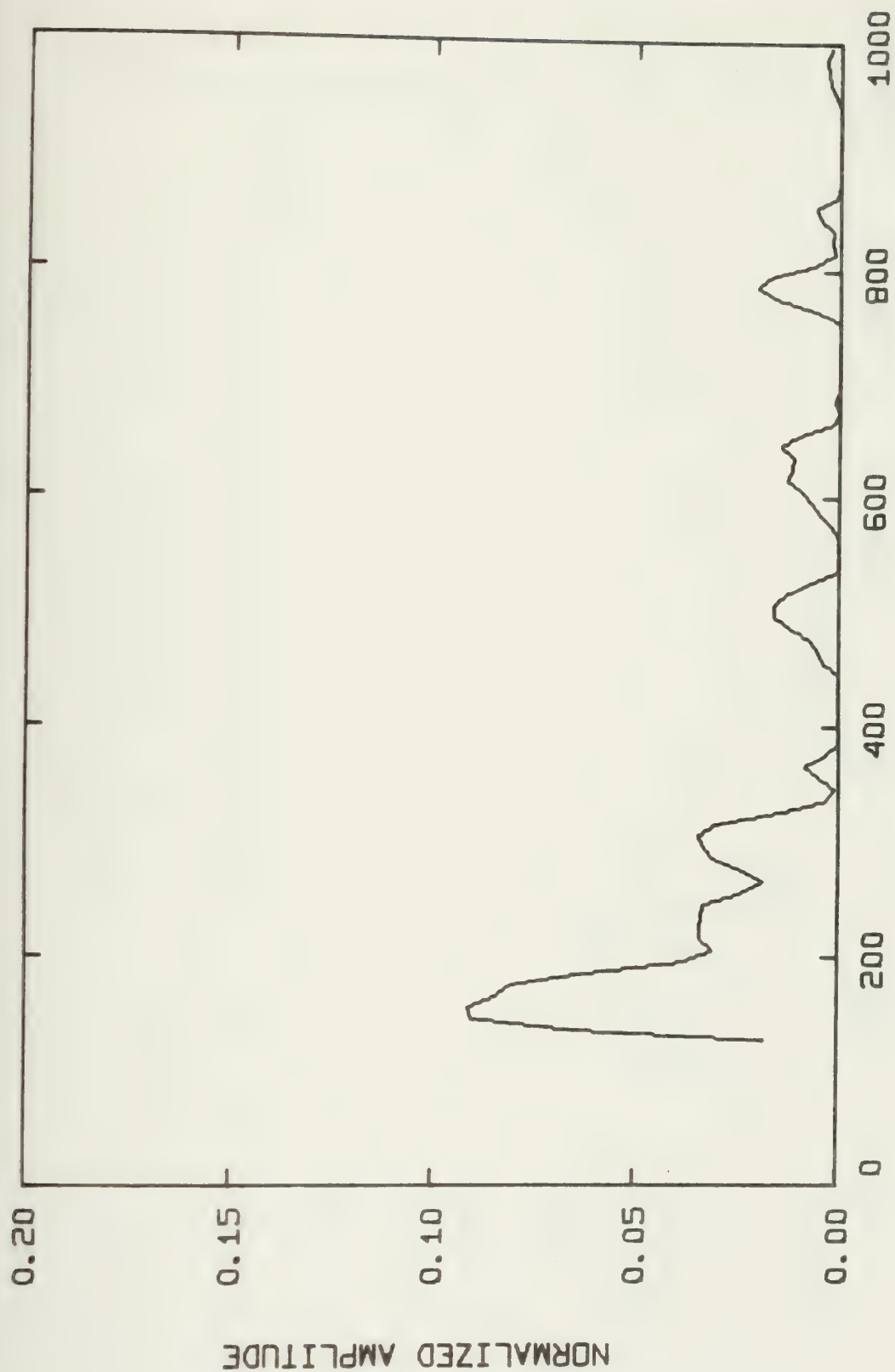
1. Normalized AE energy distributions from specimens LV5CA, LV5CG, and LV5CJ are presented.
2. The spectral distributions for each specimen are preceded by a summary sheet listing the graph code number, the energy used to normalize the graph, RMS pressure of AE excitation, and the specimen's load at the time the AE sample was taken.
3. Y axis values are dimensionless.



Summary of Energy per AE and RMS Pressure for Ascending Loads

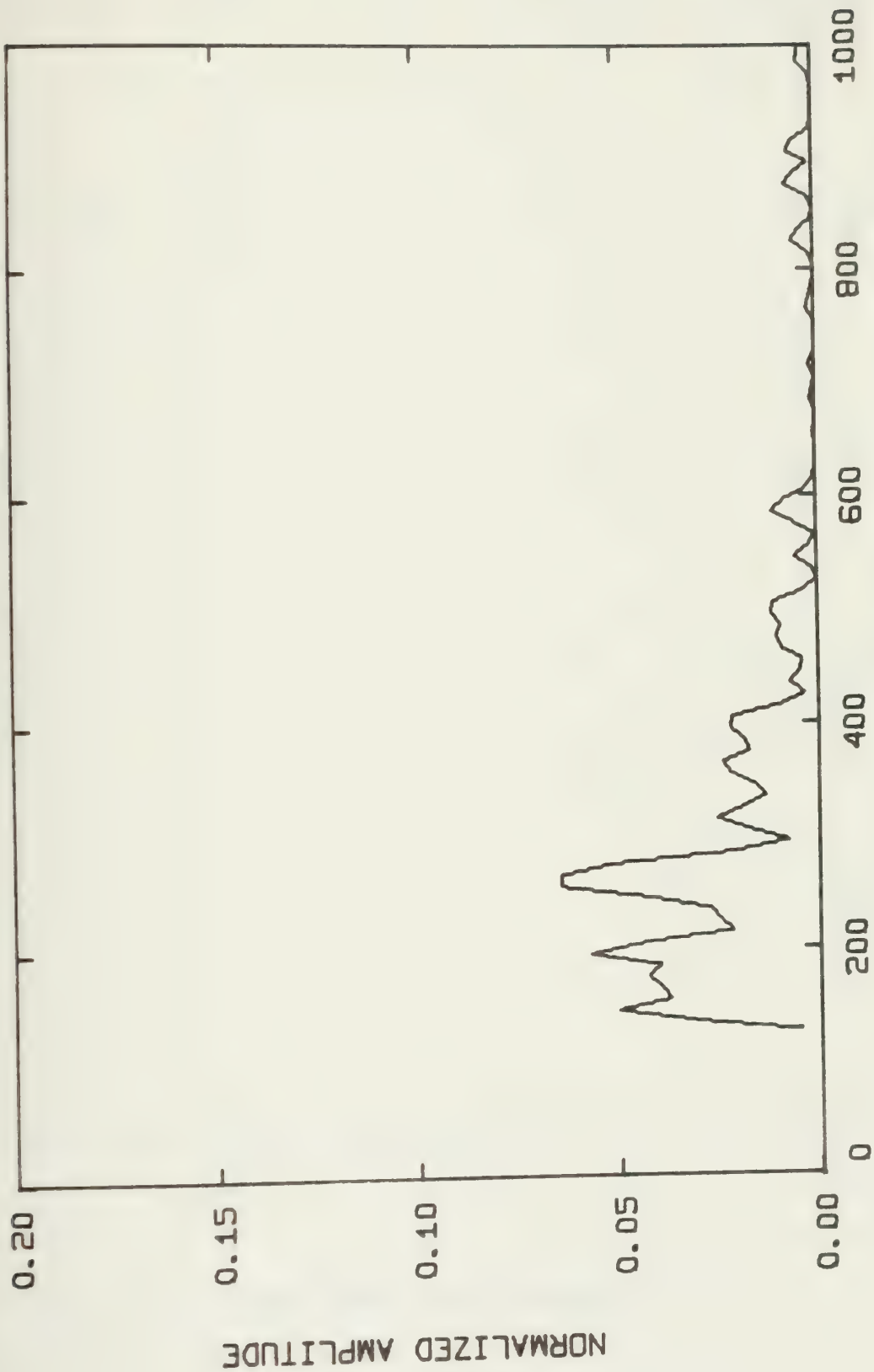
Spectral Distribution Graph Code Number	Energy per AE (Joules x $10^9$ )	RMS Pressure Across Face of Transducer (Pa x $10^6$ )	Load kN
LV5CA			
1812APR77	10.032	353.40	1.33
1712APR77	106.08	767.84	1.33
1612APR77	22.157	479.44	1.33
1512APR77	27.992	538.89	1.56
1412APR77	23.451	493.24	1.56
1312APR77	43.405	511.34	1.56
1212APR77	39.421	487.31	1.82
1112ARP77	138.39	661.83	1.82
1012APR77	69.992	683.23	1.82
0912APR77	66.233	664.63	1.82
0812APR77	242.24	981.07	2.00
0712APR77	96.000	705.68	2.00
0612APR77	179.04	963.71	2.00
0512APR77	1007.0	1453.6	2.22
0412APR77	1322.9	1675.5	2.22
0312APR77	1114.5	1894.3	2.22
0212APR77	19,802.0	5771.8	2.14
0112APR77	54,891.0	8054.5	2.14





FREQ (KHZ) LV5CA 1812APR77 LOAD 1.33 KN

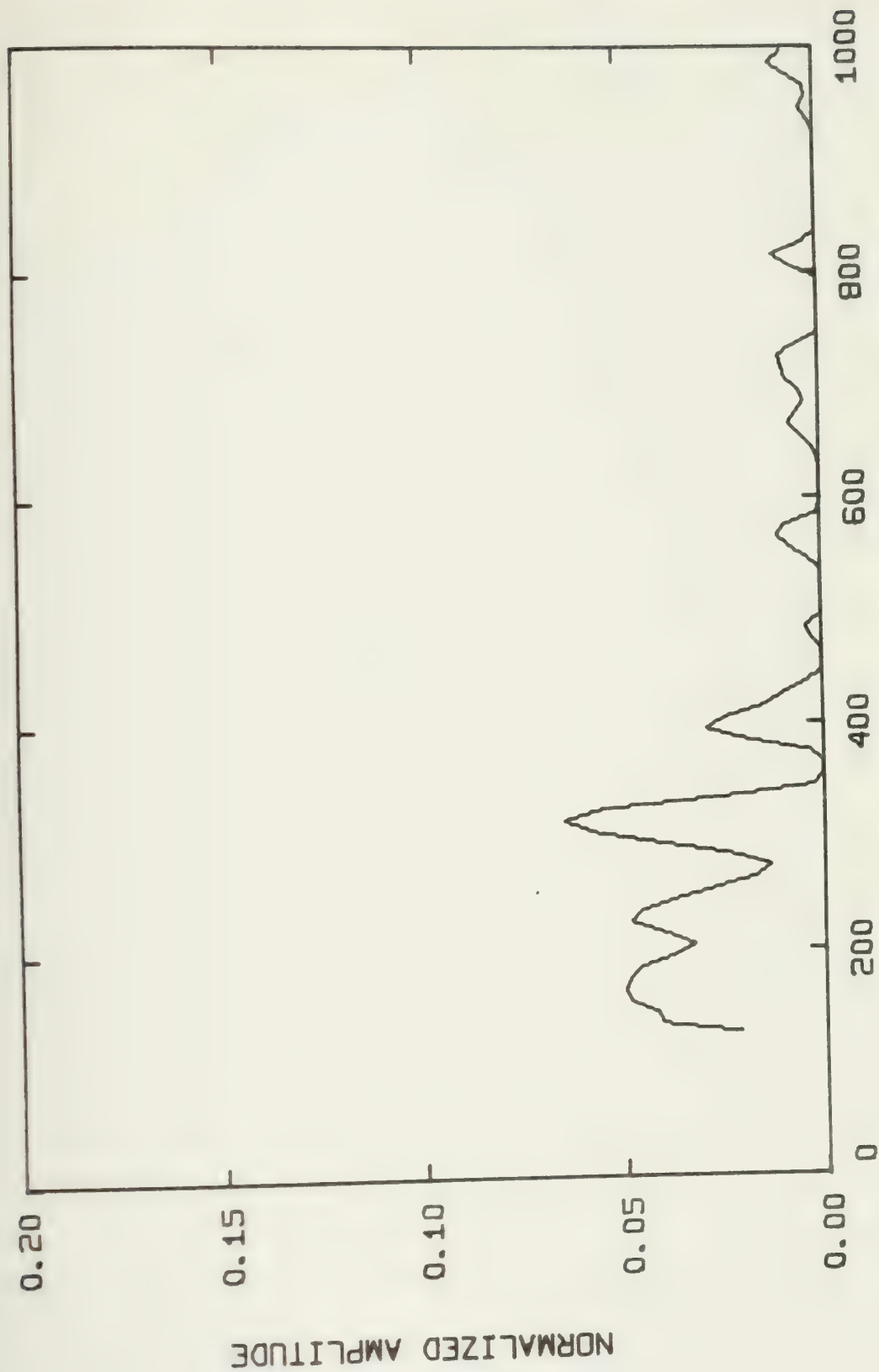




FREQ (KHZ) LVSCA 1712APR77 LOAD 1.33 KN

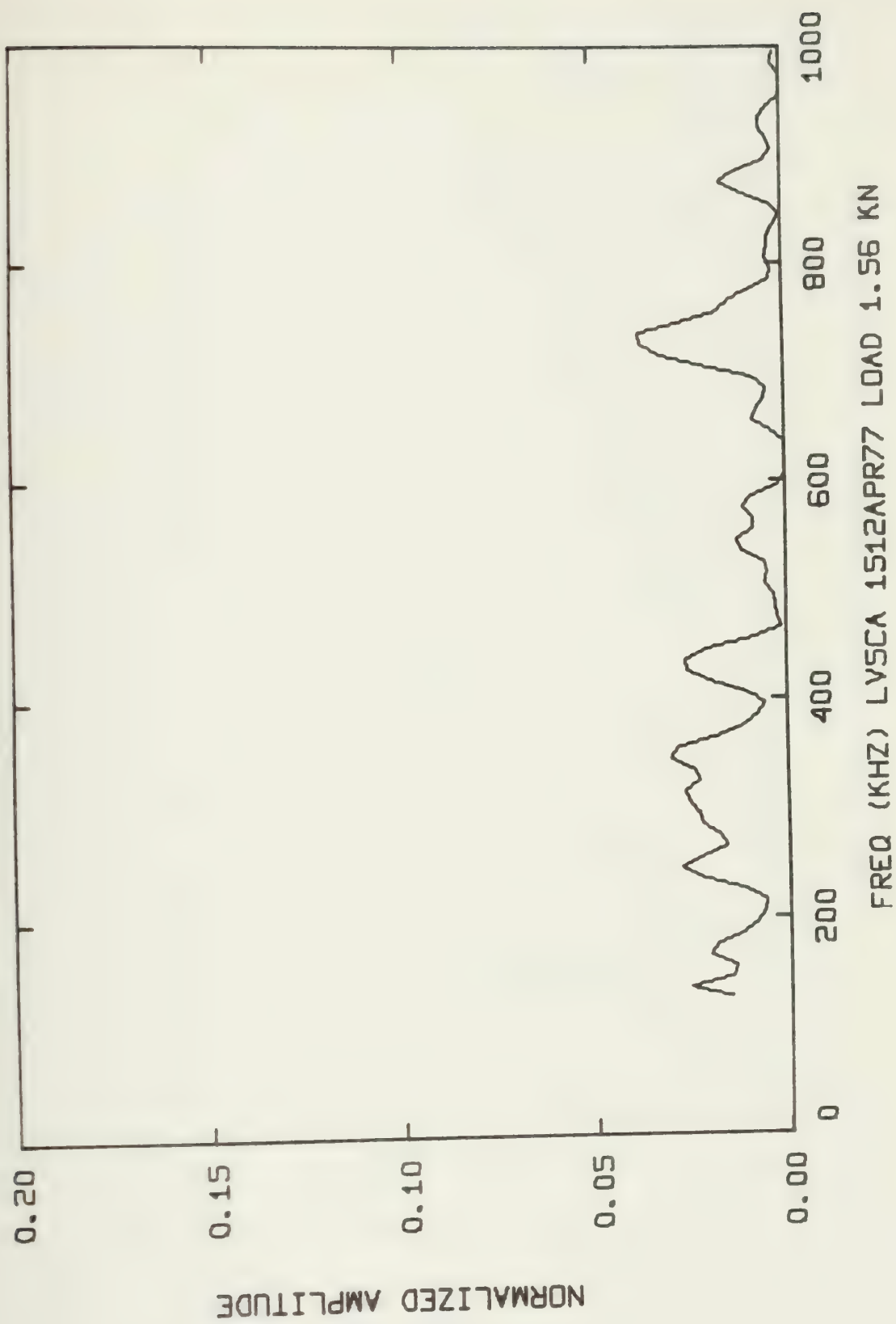




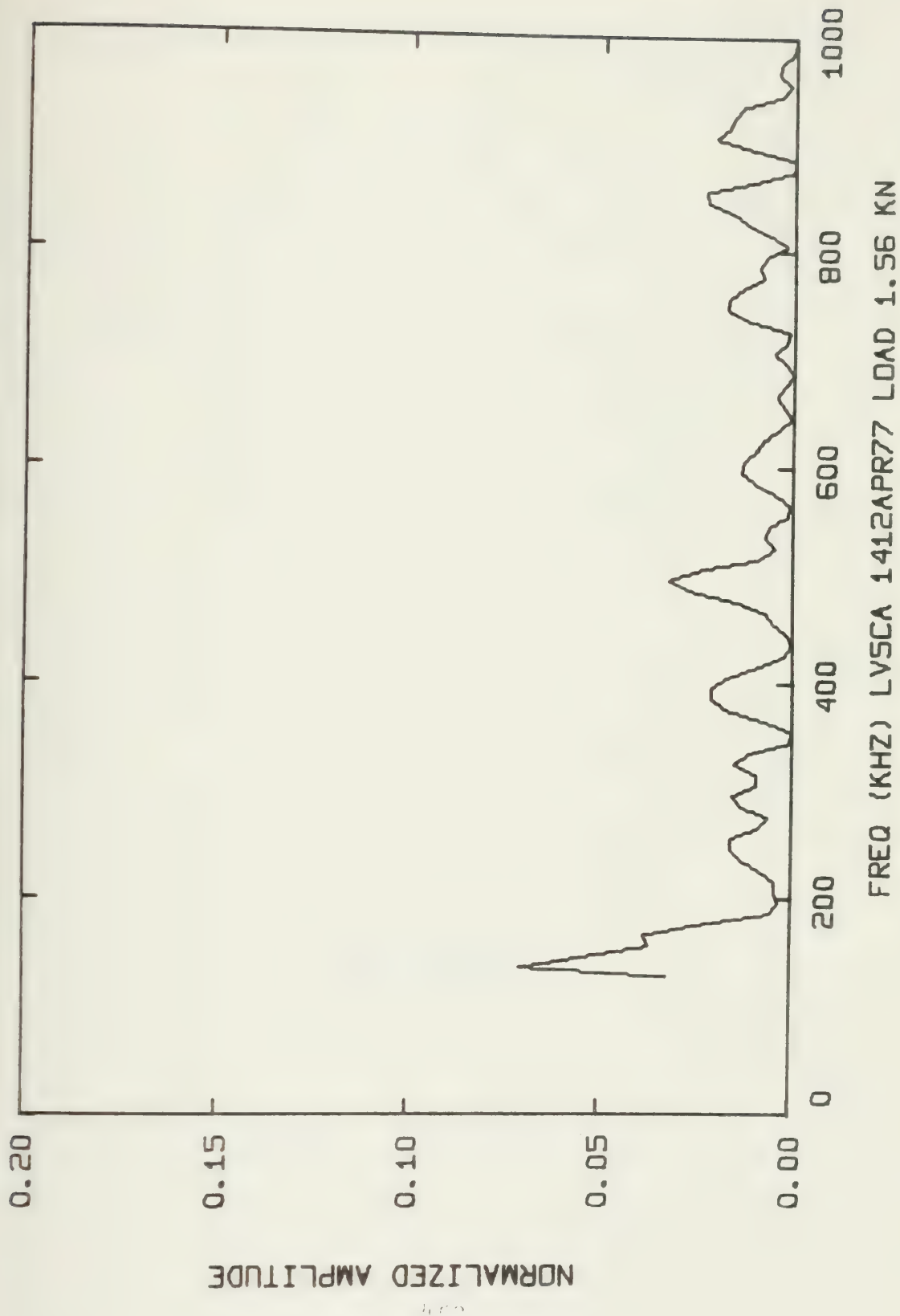


LV5CA 1612APR77 LOAD 1.33 KN

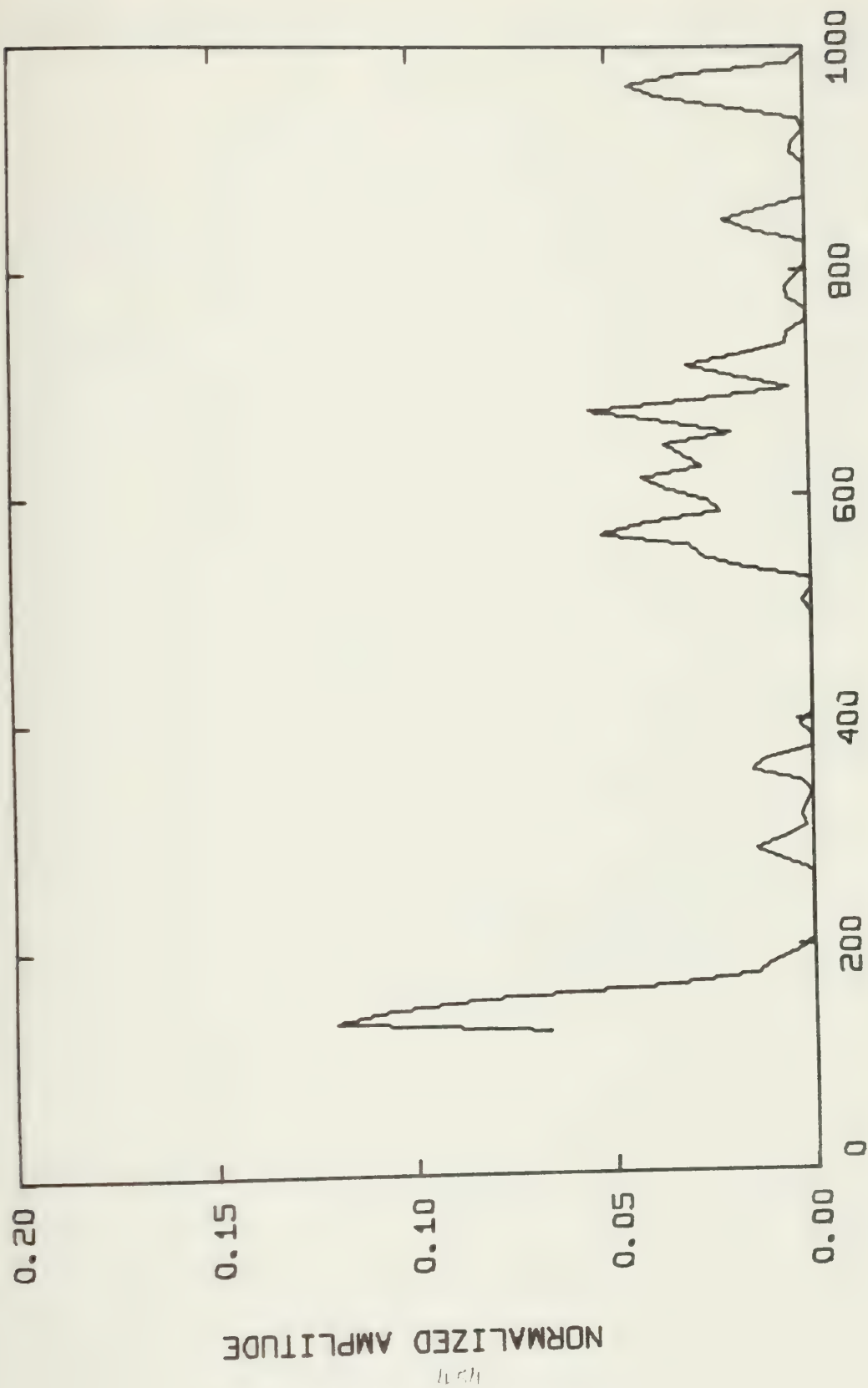






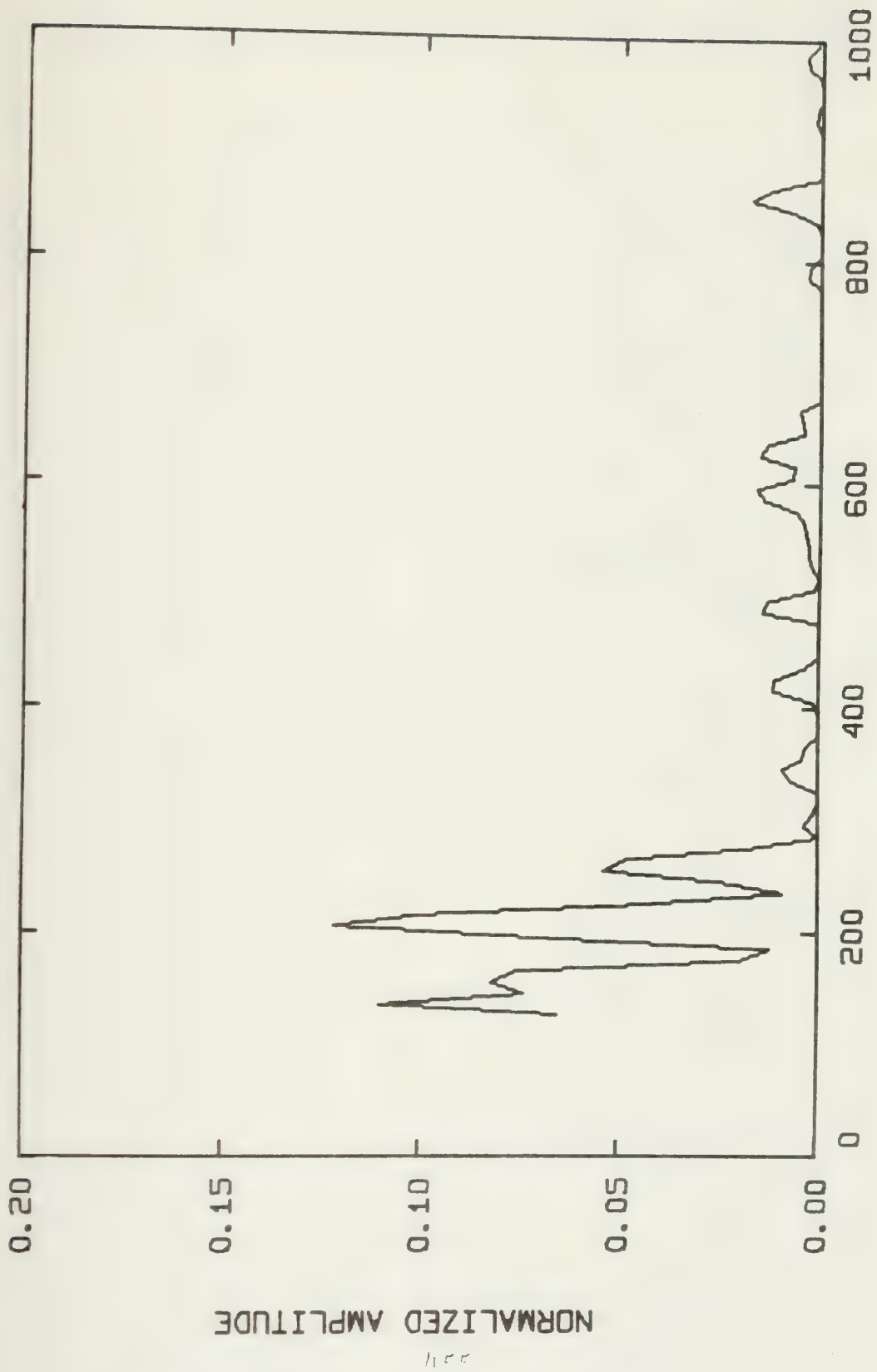






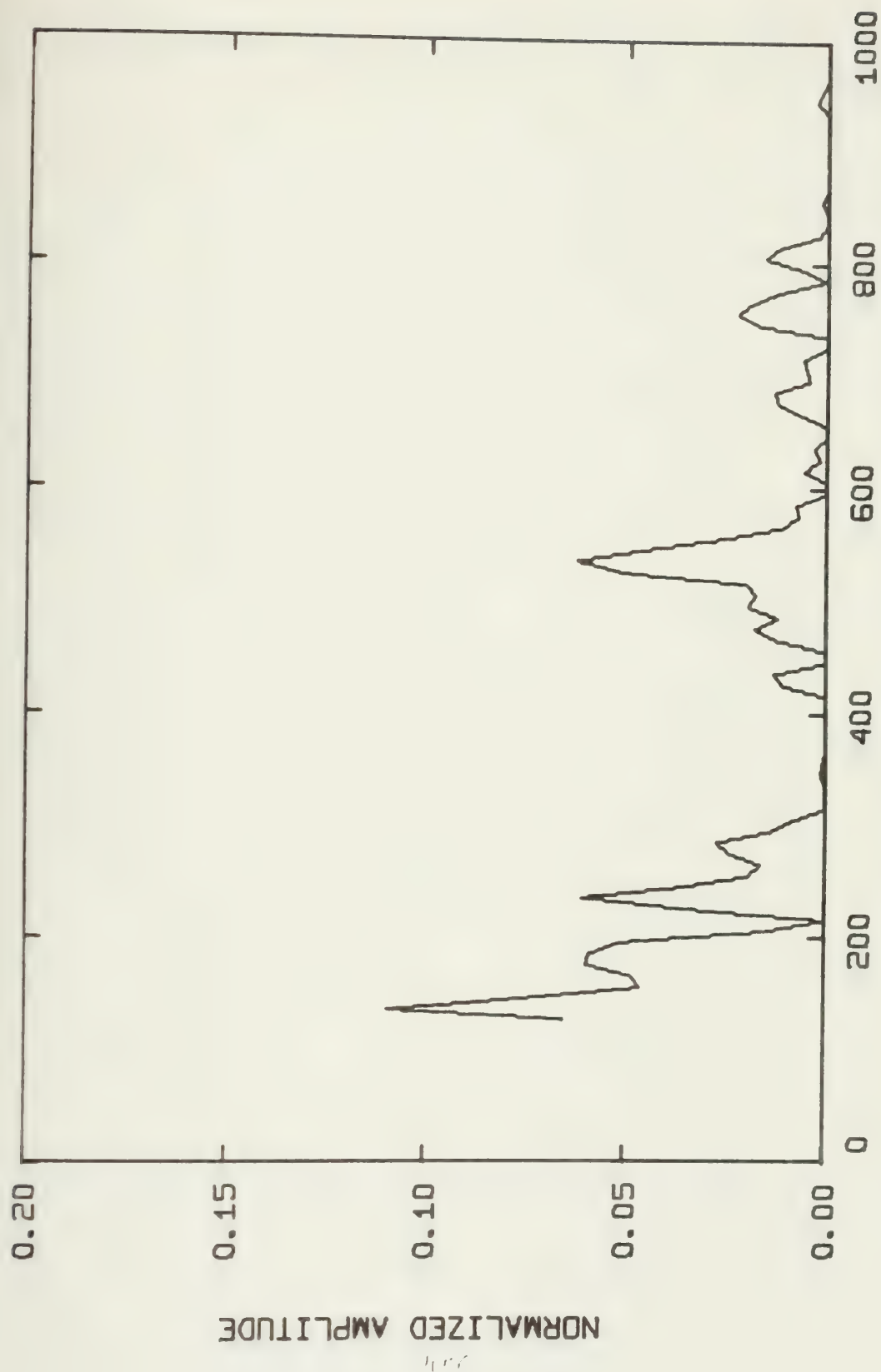






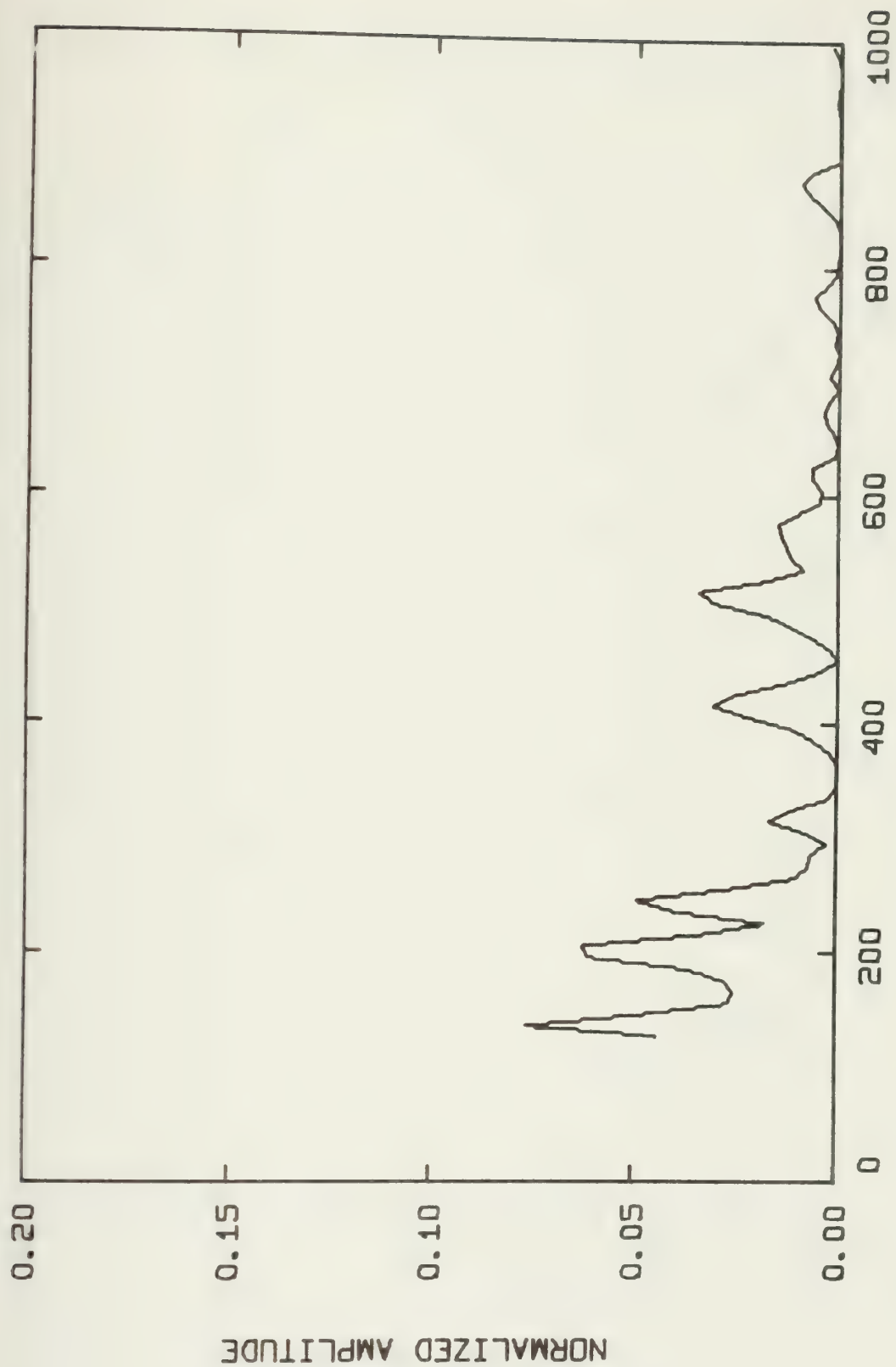
FREQ (KHZ) LVSCA 1212APR77 LOAD 1.82 KN





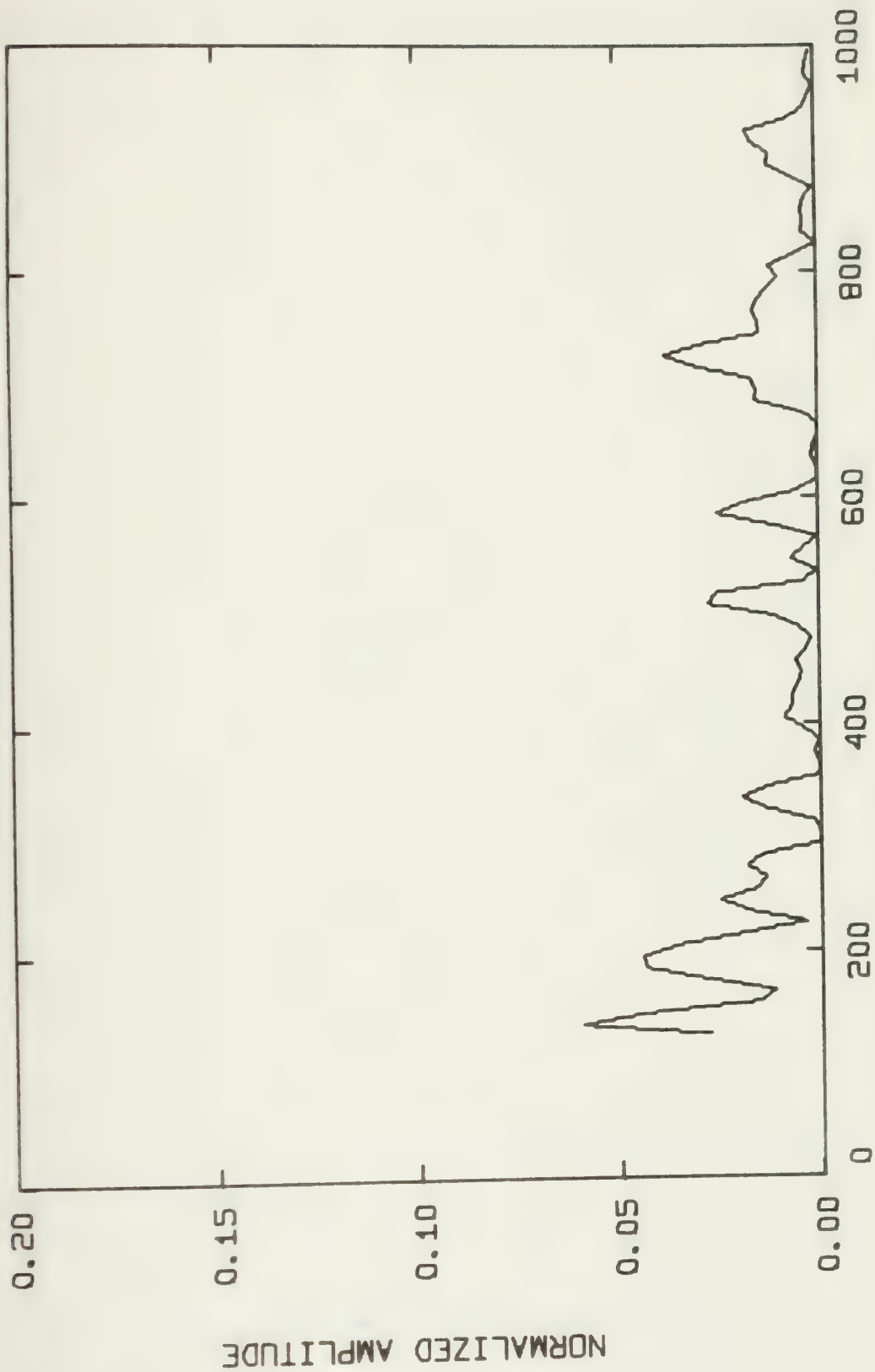
FREQ (KHZ) LVSCA 1112APR77 LOAD 1.82 KN





LVSCA 1012APR77 LOAD 1.82 KN

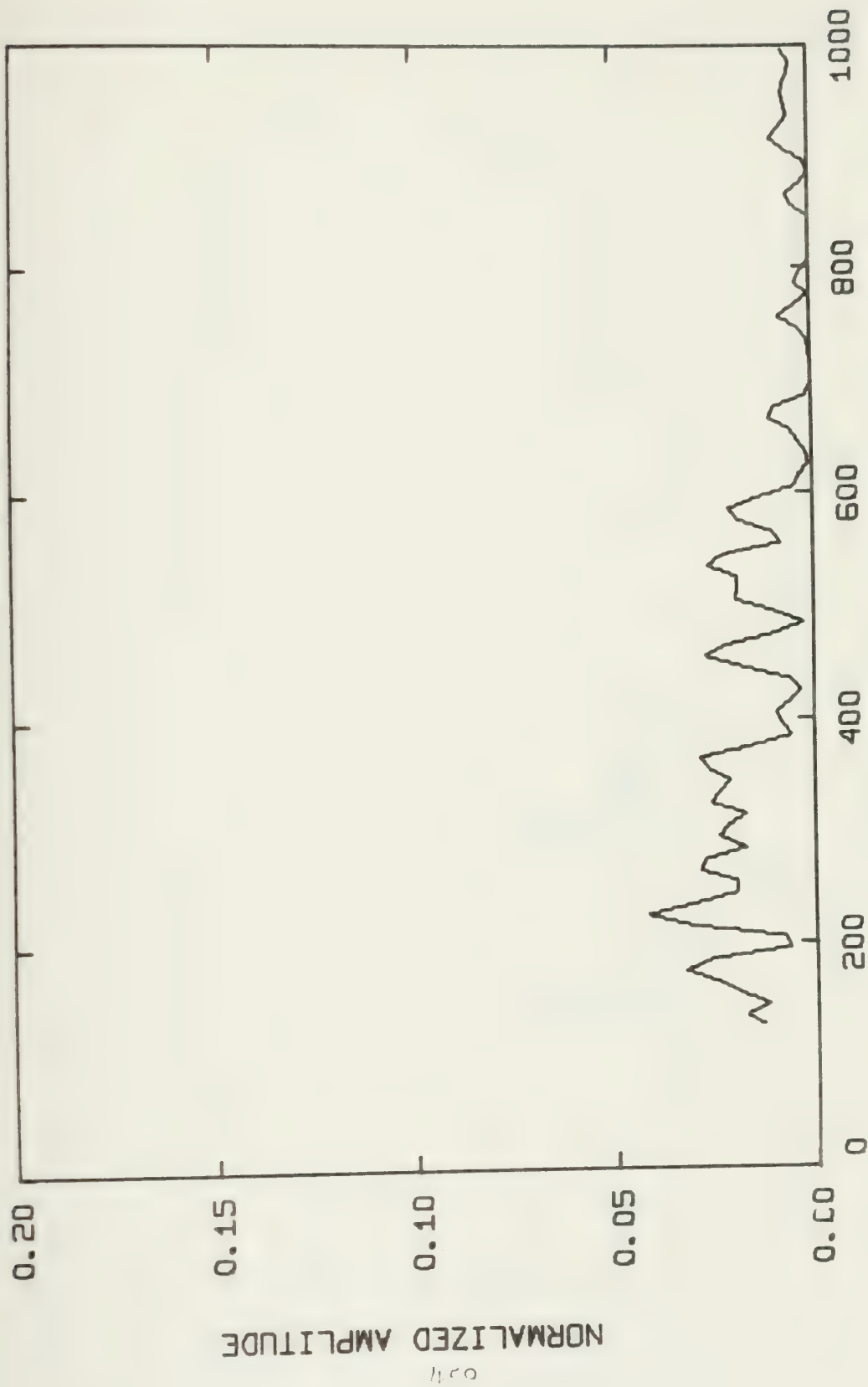




LVSCA 0912APR77 LOAD 1.82 KN

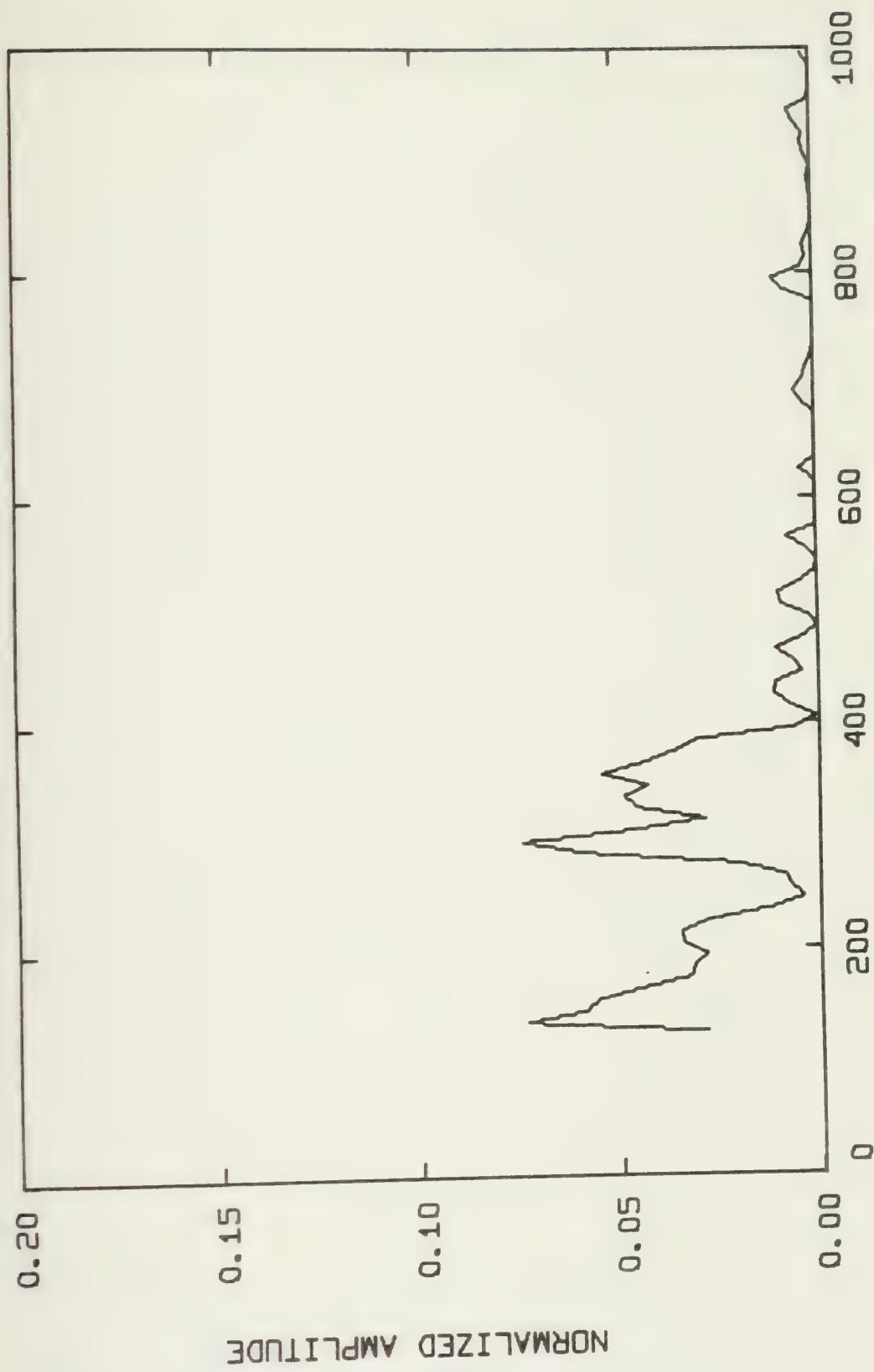






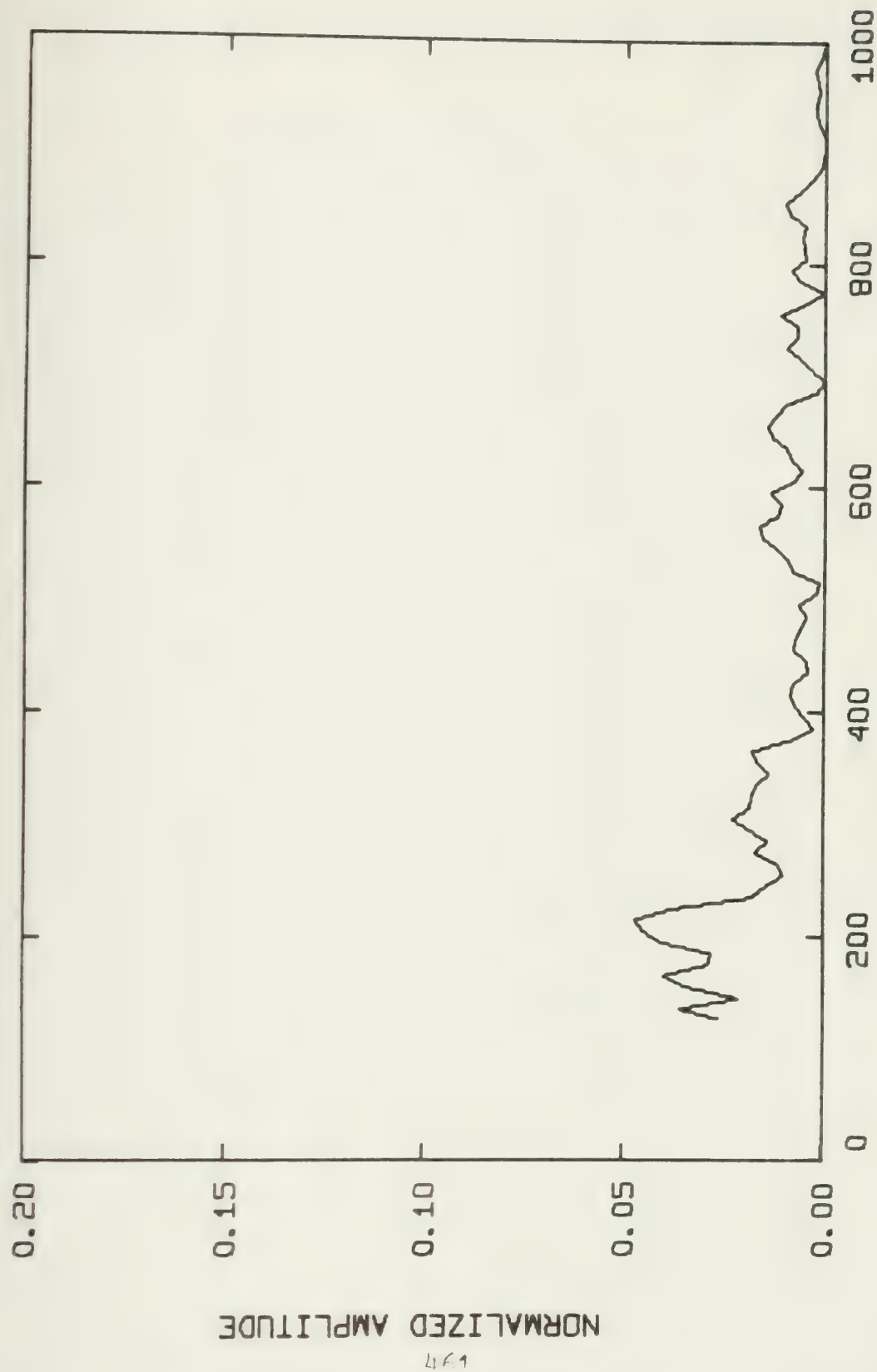
LVSCA 0812APR77 LOAD 2.00 KN





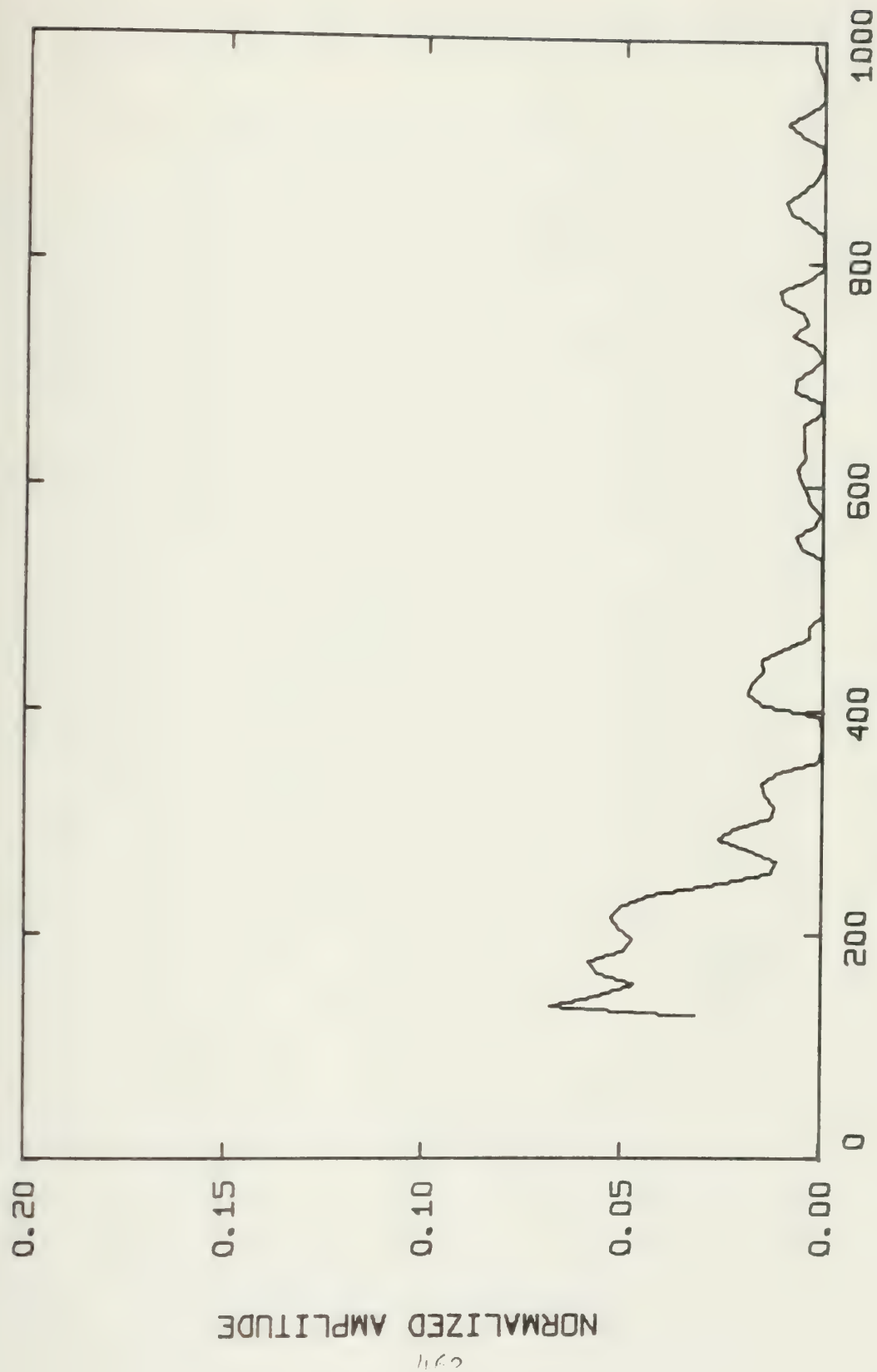
FREQ (KHZ) LV5CA 0712APR77 LOAD 2.00 KN





LV5CA 0612APR77 LOAD 2.00 KN

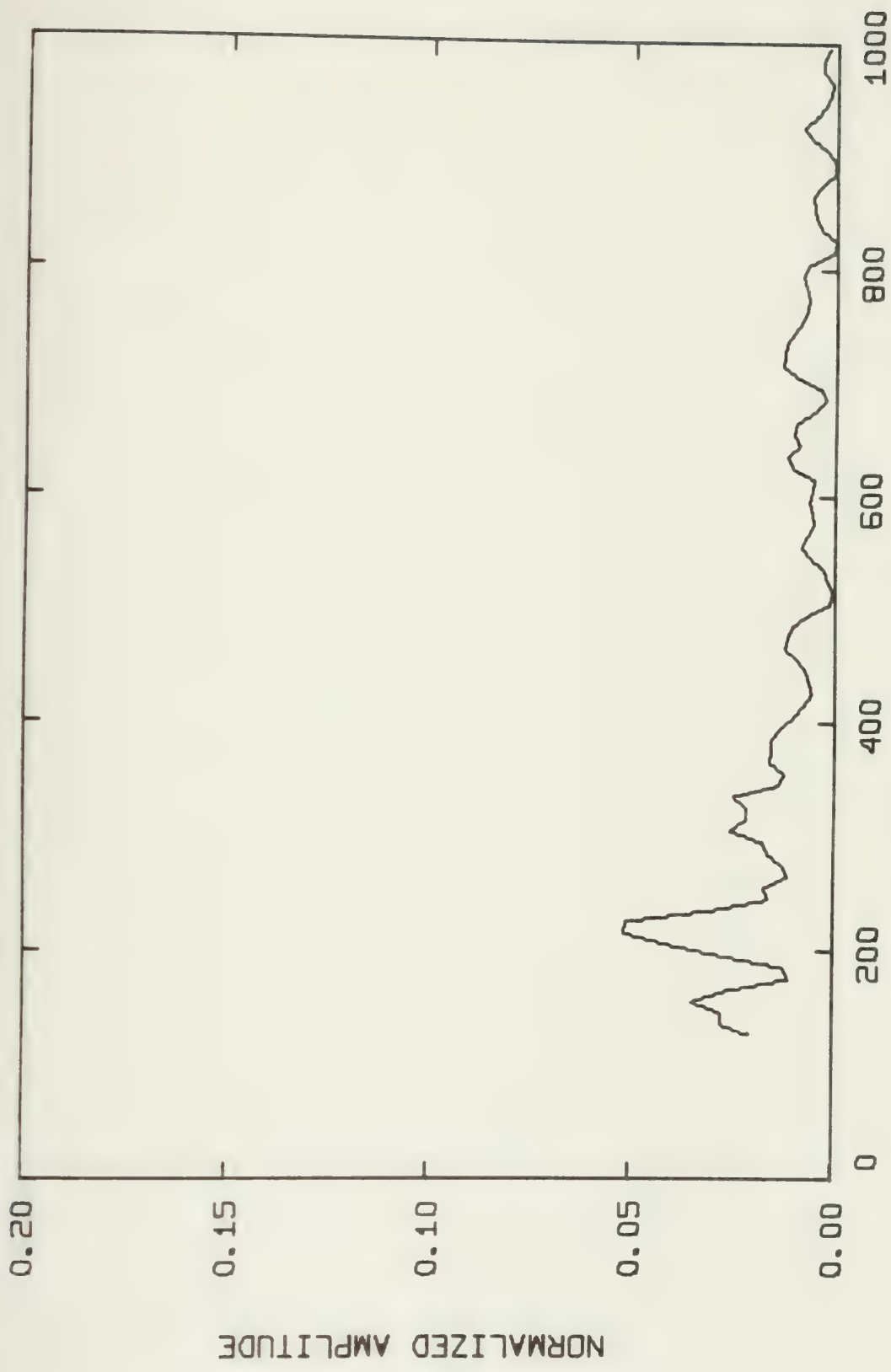




FREQ (KHZ) LV5CA 0512APR77 LOAD 2.22 KN

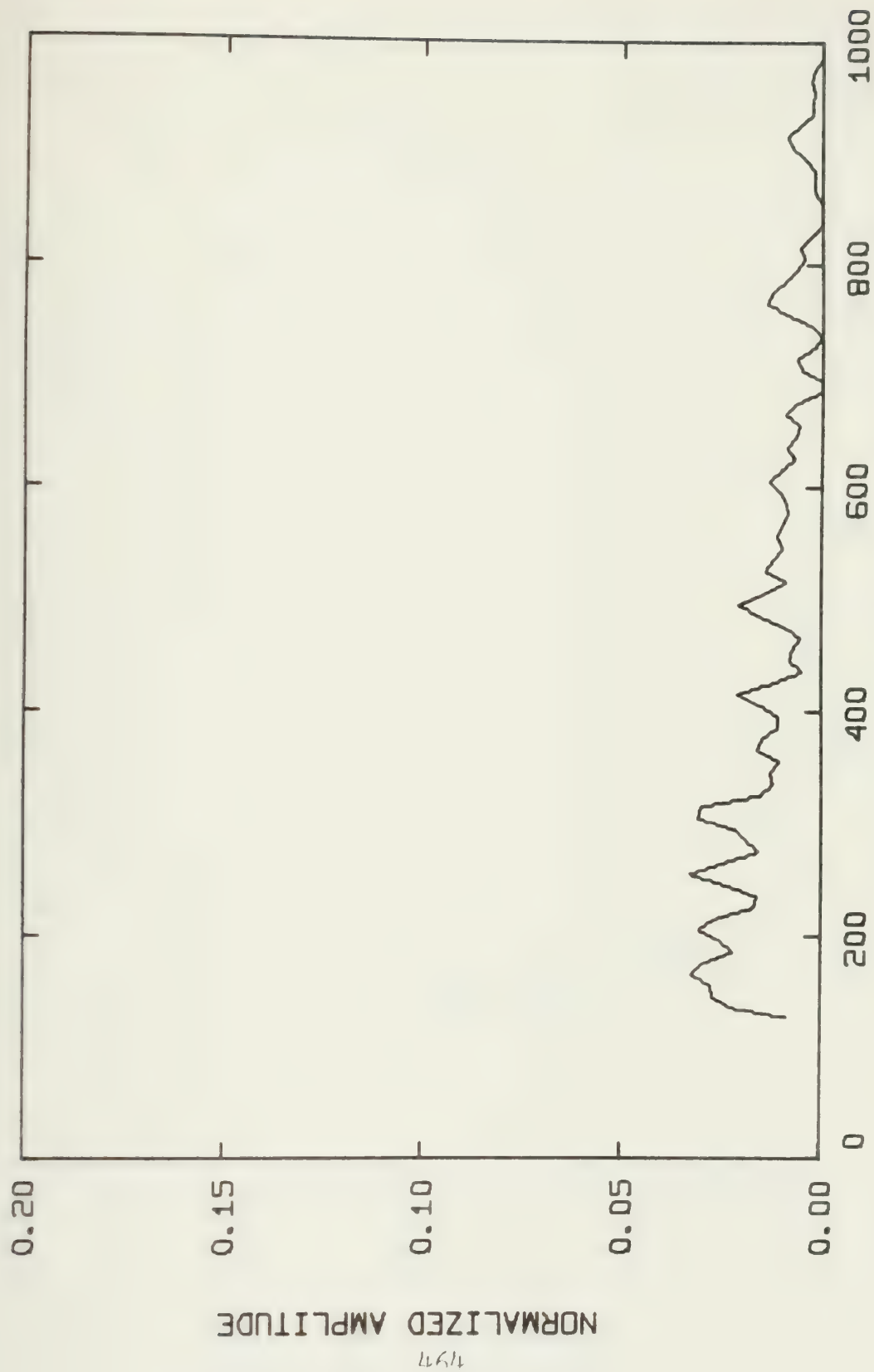




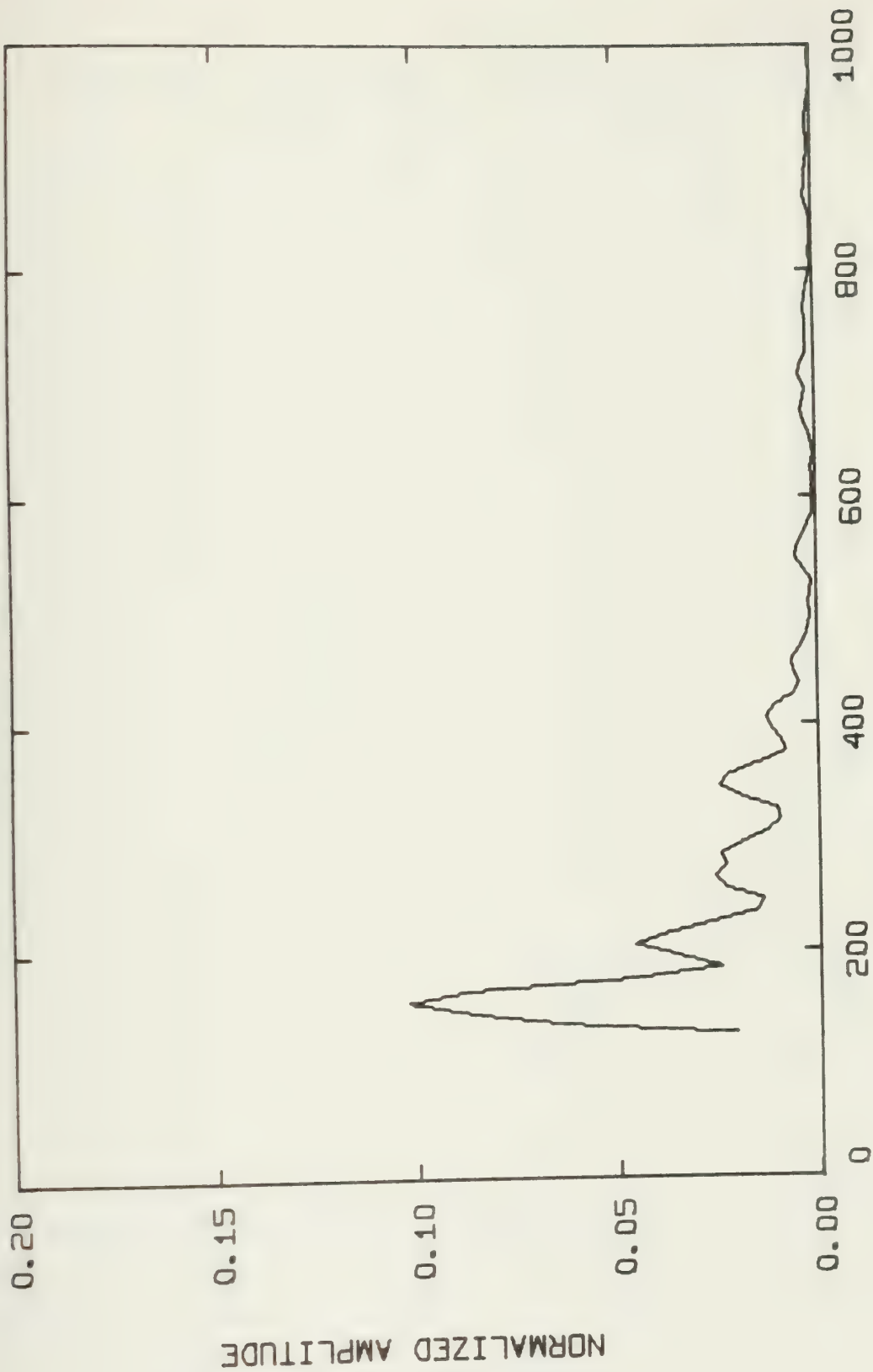


FREQ (KHZ) LV5CA 0412APR77 LOAD 2.22 KN



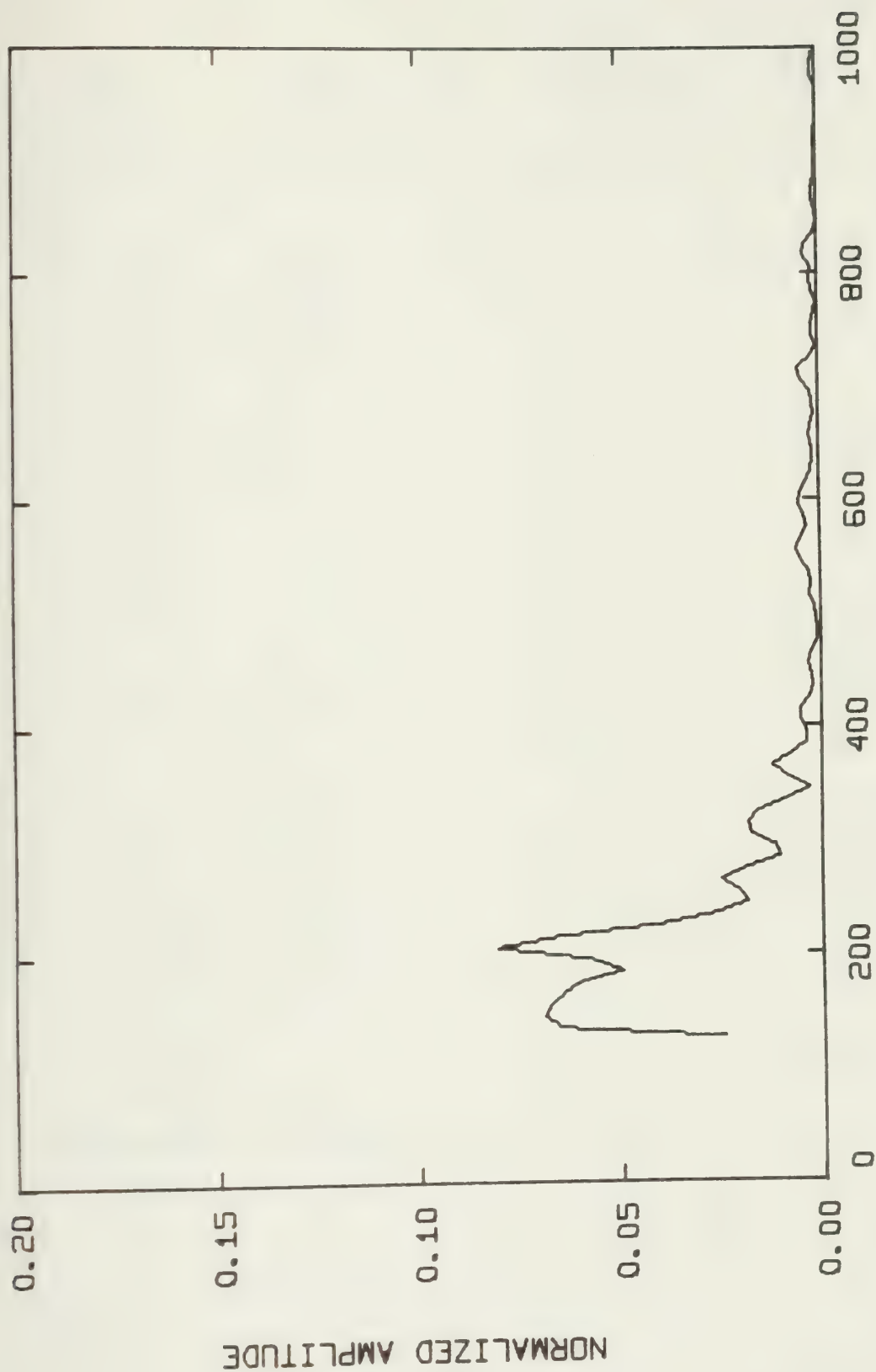






LV5CA 0212APR77 LOAD 2.14 KN





LVSCA 0112APR77 LOAD 2.14 KN

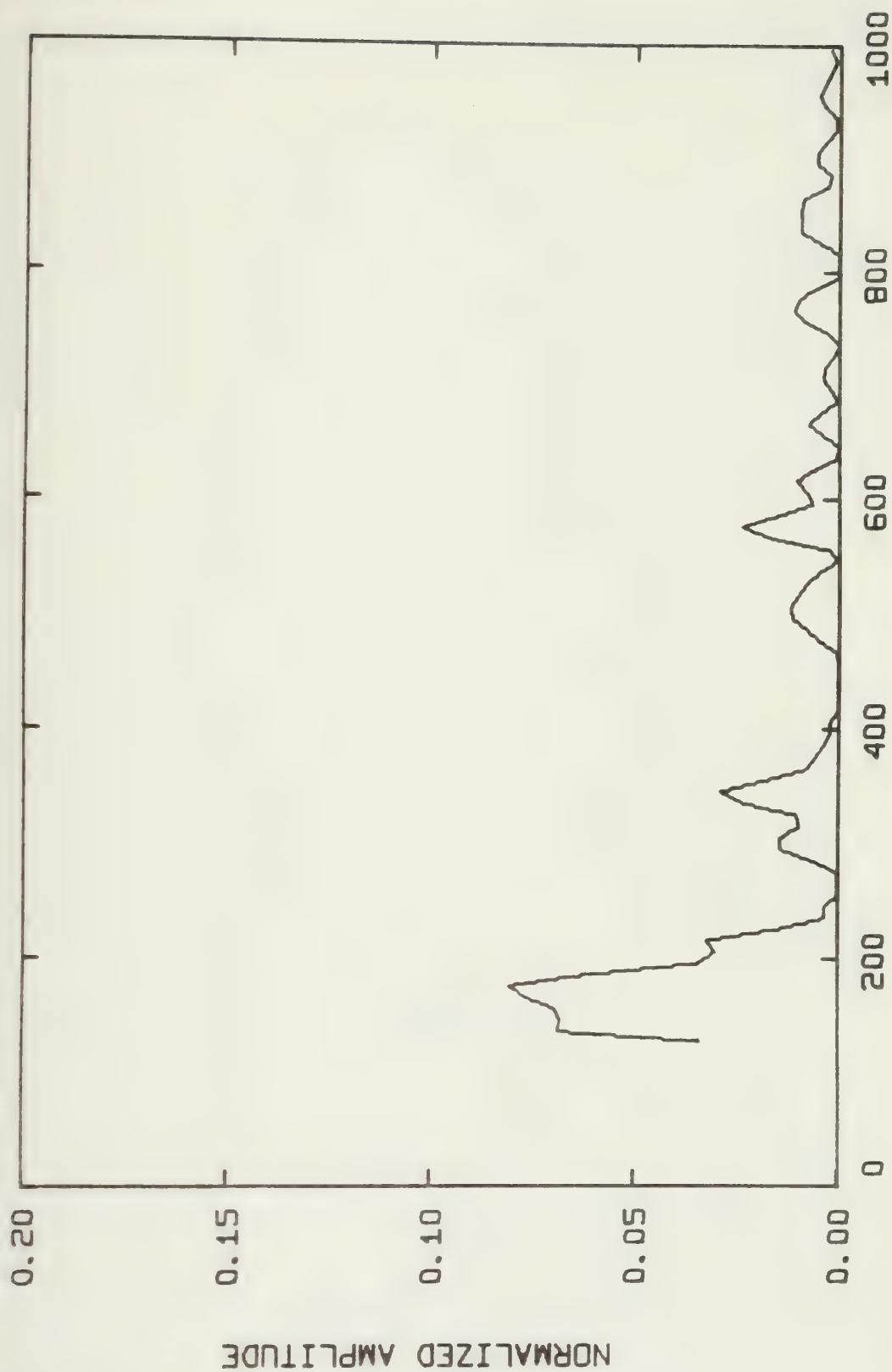




Summary of Energy per AE and RMS Pressure for Ascending Loads

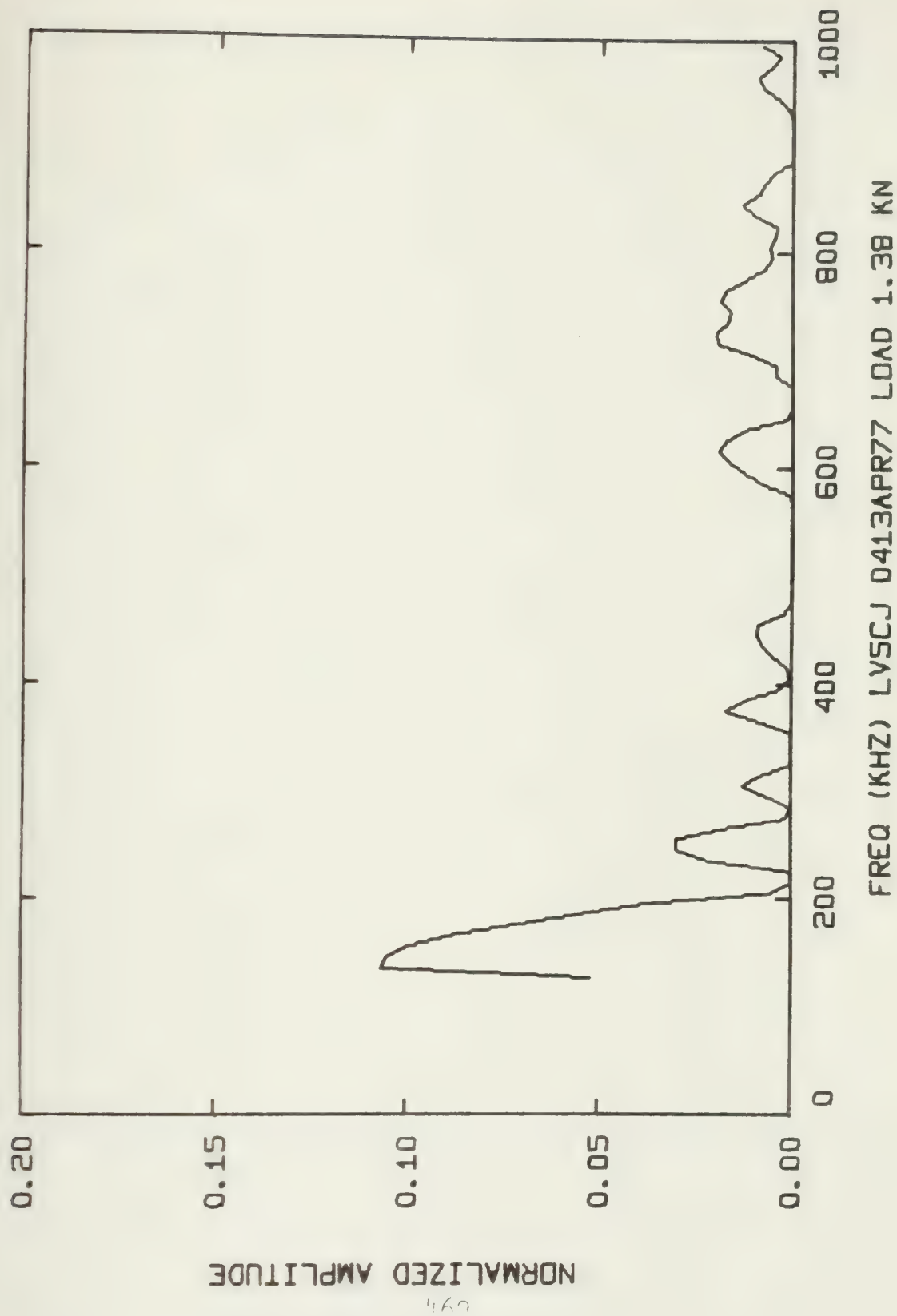
Spectral Distribution Graph Code Number	Energy per AE (Joules x $10^9$ )	RMS Pressure Across Face of Transducer (Pa x $10^6$ )	Load kN
IV50J			
1413APR77	18.642	439.78	1.38
0413APR77	12.441	369.68	1.38
1013APR77	26.974	529.00	1.38
0313APR77	203.56	884.41	1.56
1213APR77	326.69	1053.2	1.56
1313APR77	194.12	920.30	1.56
0213APR77	52.174	719.89	1.78
0513APR77	46.045	596.08	1.78
0613APR77	78.835	705.23	1.78
0113APR77	116.25	749.96	2.00
1113APR77	37.981	512.53	2.00
1213APR77	114.49	804.92	2.00
0713APR77	440.04	1006.0	2.22
0813APR77	524.04	1099.2	2.22
0913APR77	262.91	936.33	2.22
1513APR77	27.601	606.76	2.22
1813APR77	233.40	852.30	2.27
1613APR77	21.549	409.47	2.27



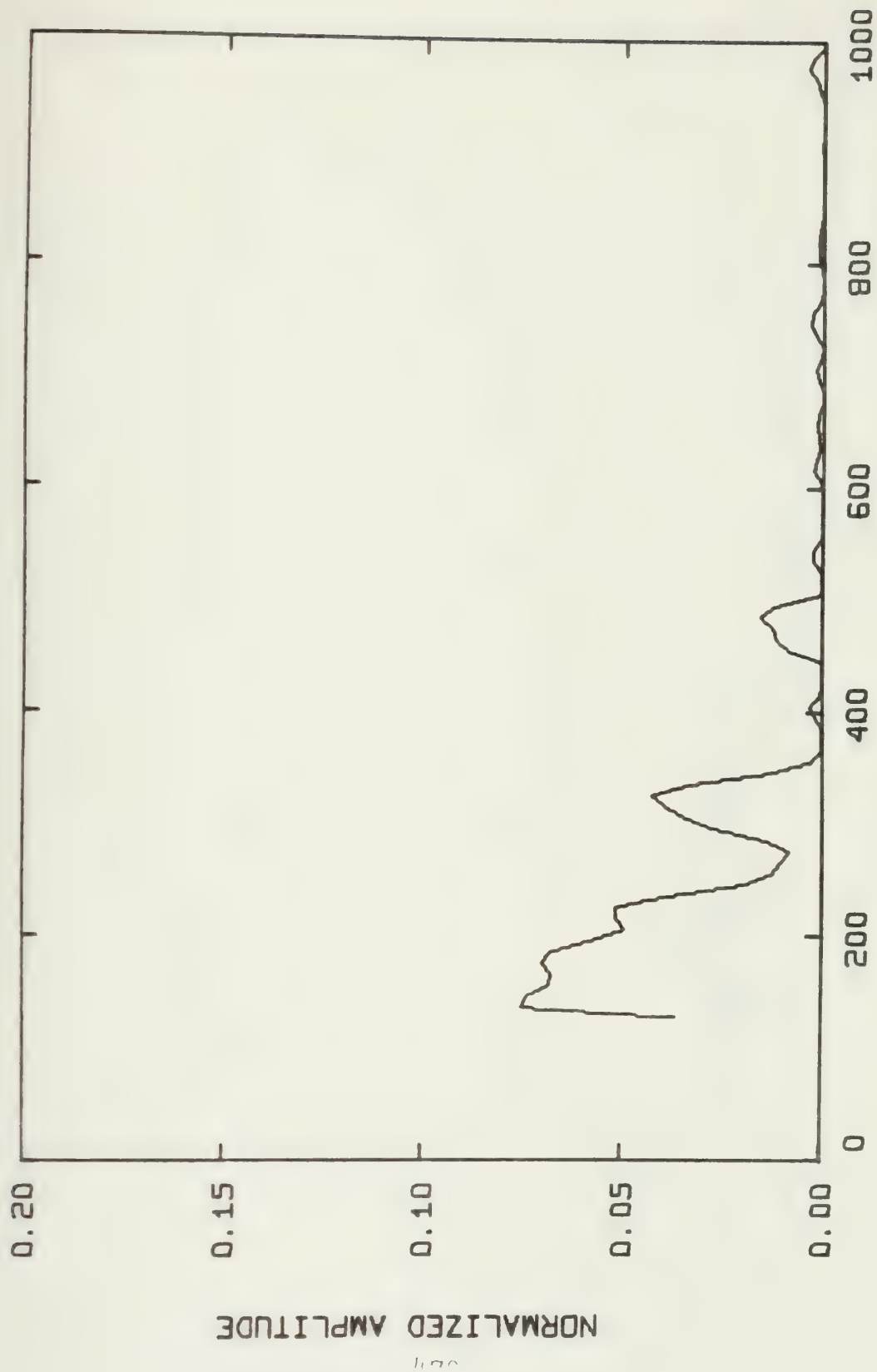


LV5CJ 1413APR77 LOAD 1.38 KN





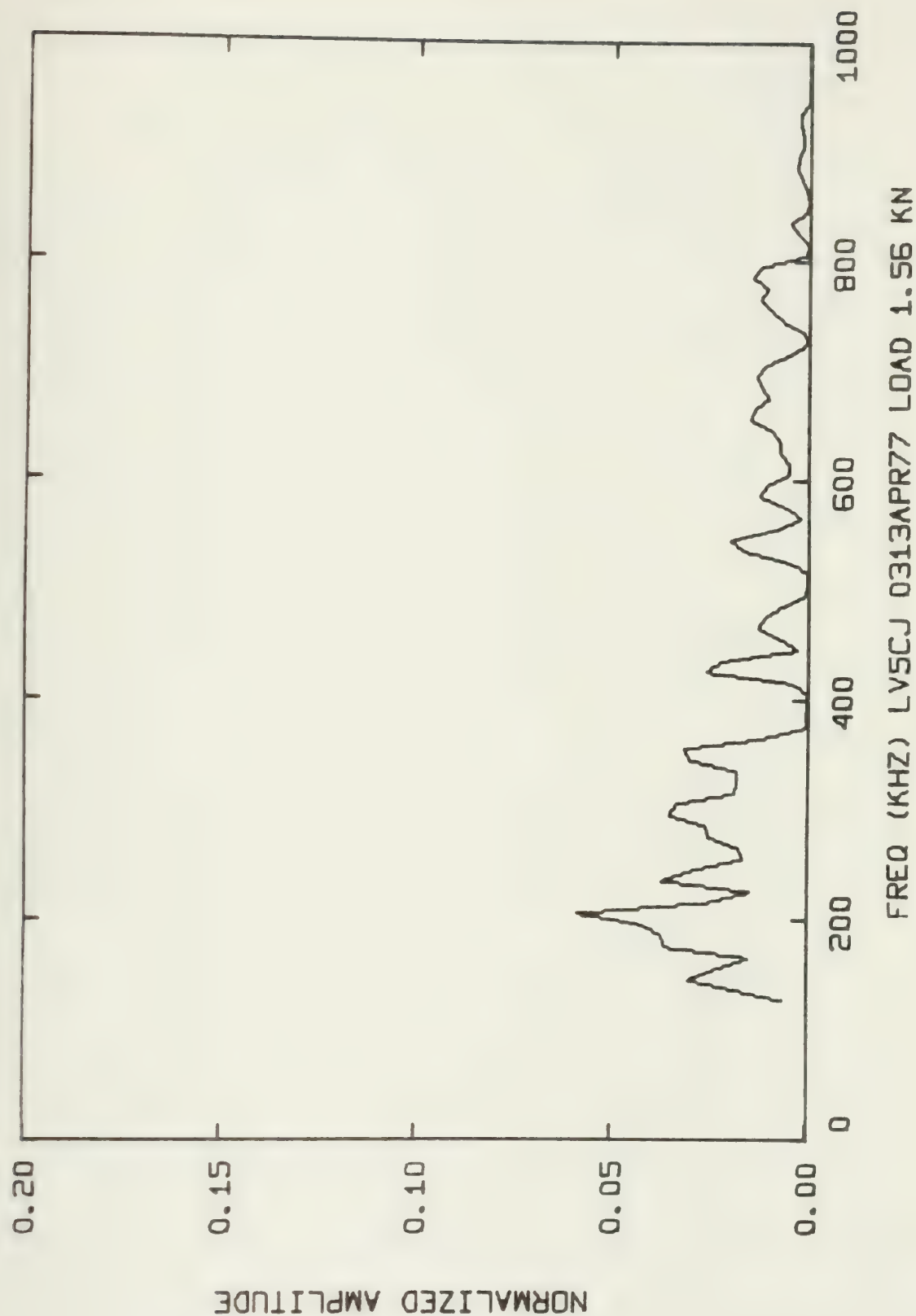




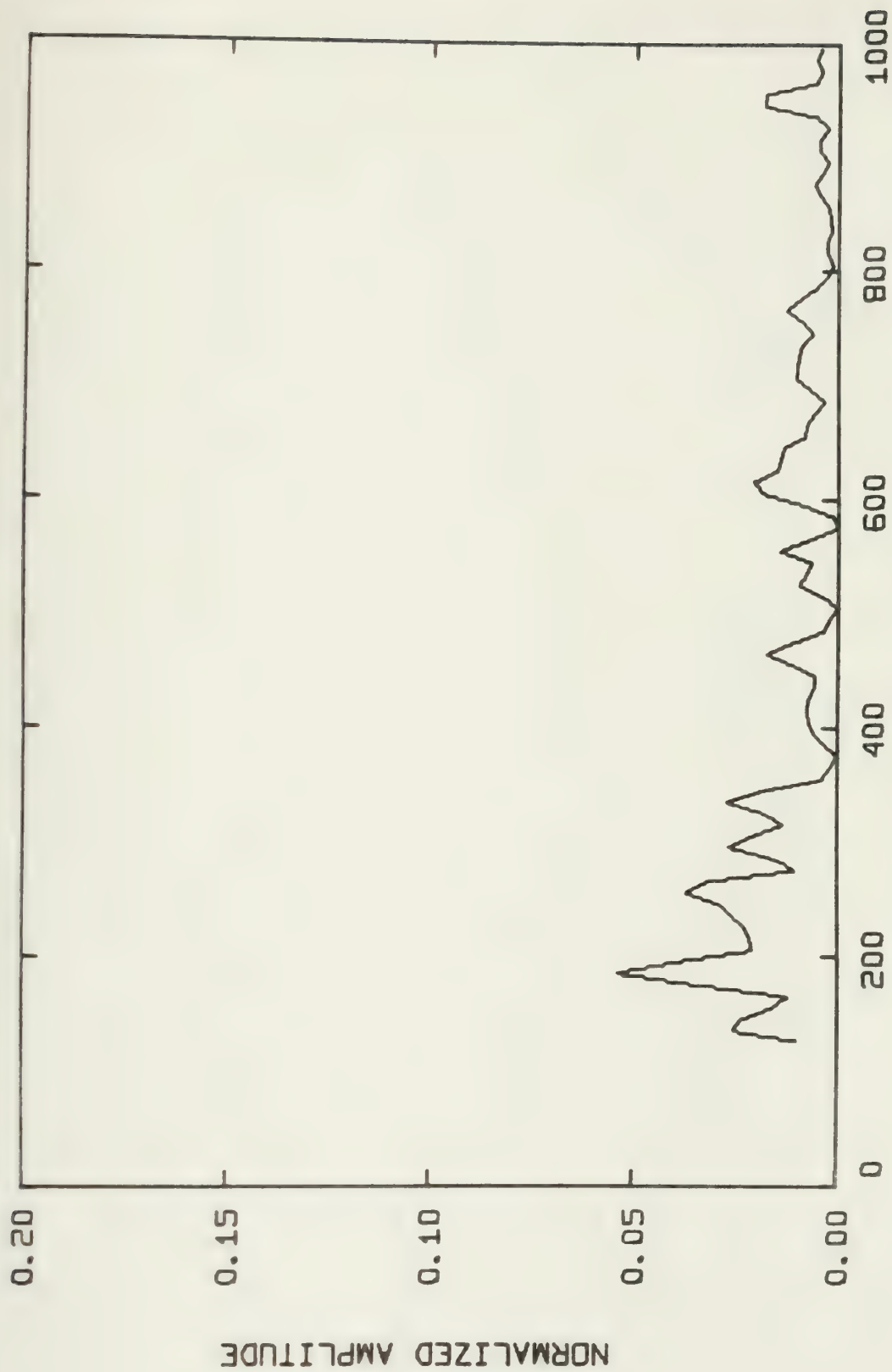
FREQ (KHZ) LV5CJ 1013APR77 LOAD 1.38 KN





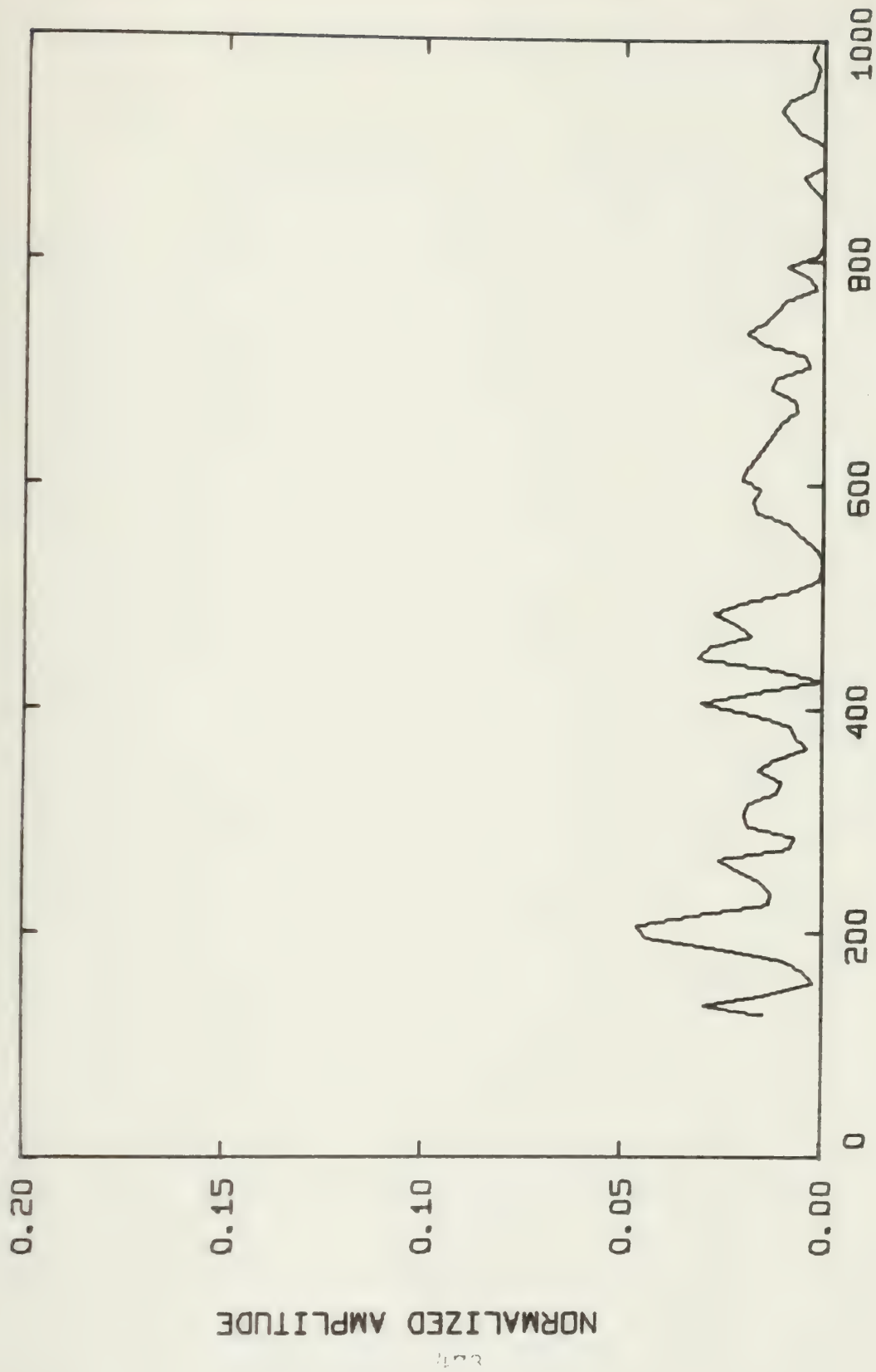






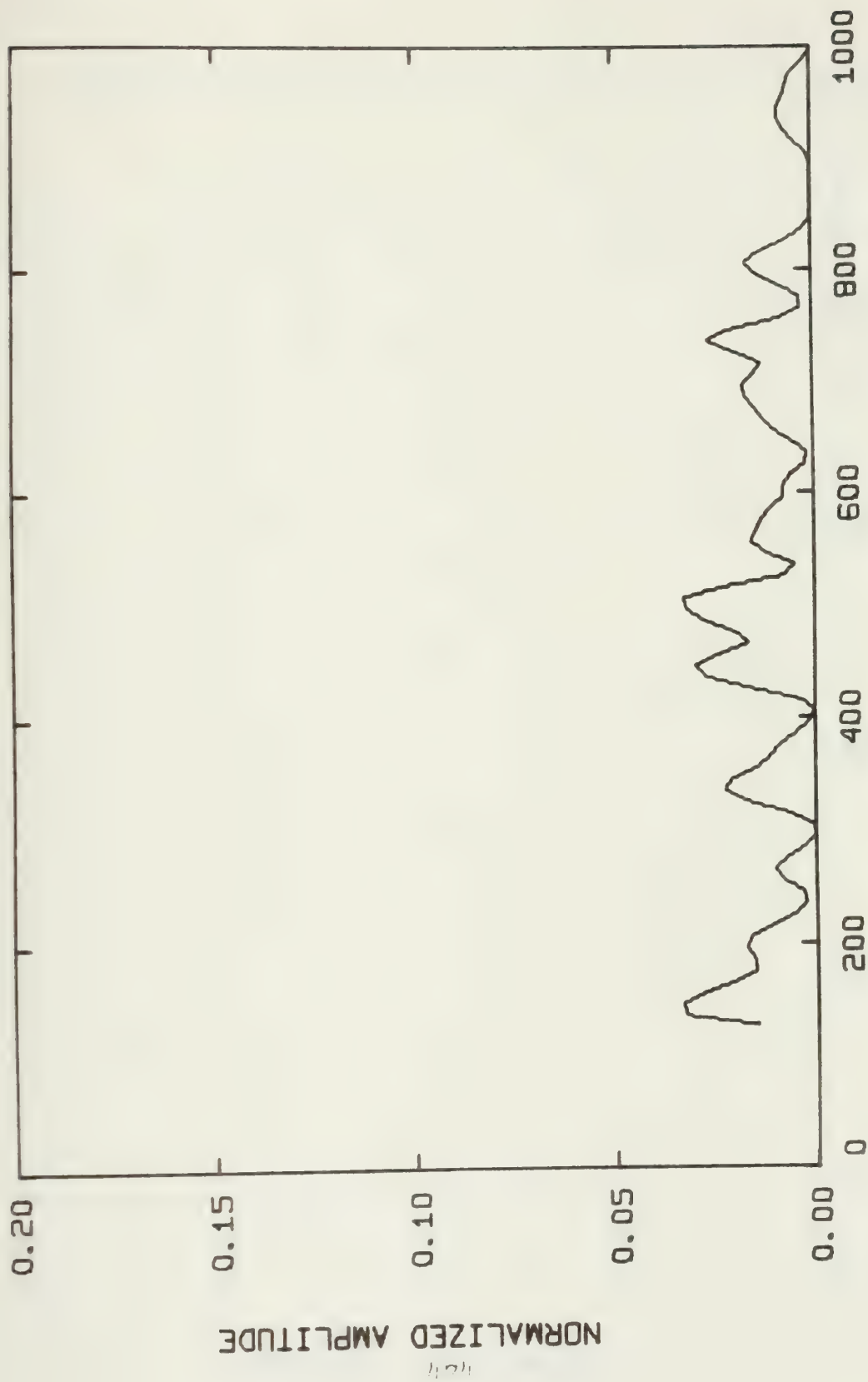
LVSCJ 1213APR77 LOAD 1.56 KN





FREQ (KHZ) LV5CJ 1313APR77 LOAD 1.56 KN

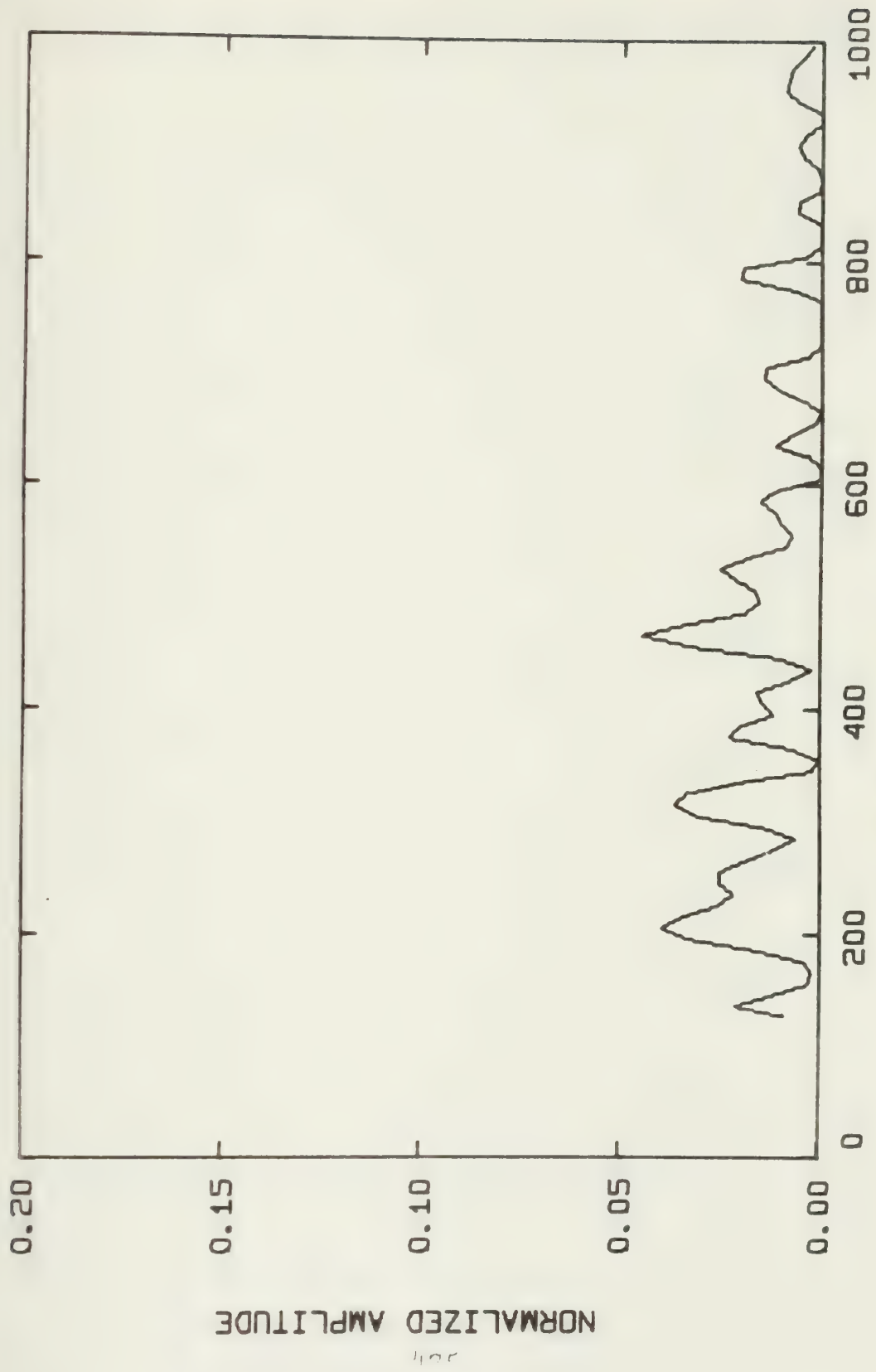




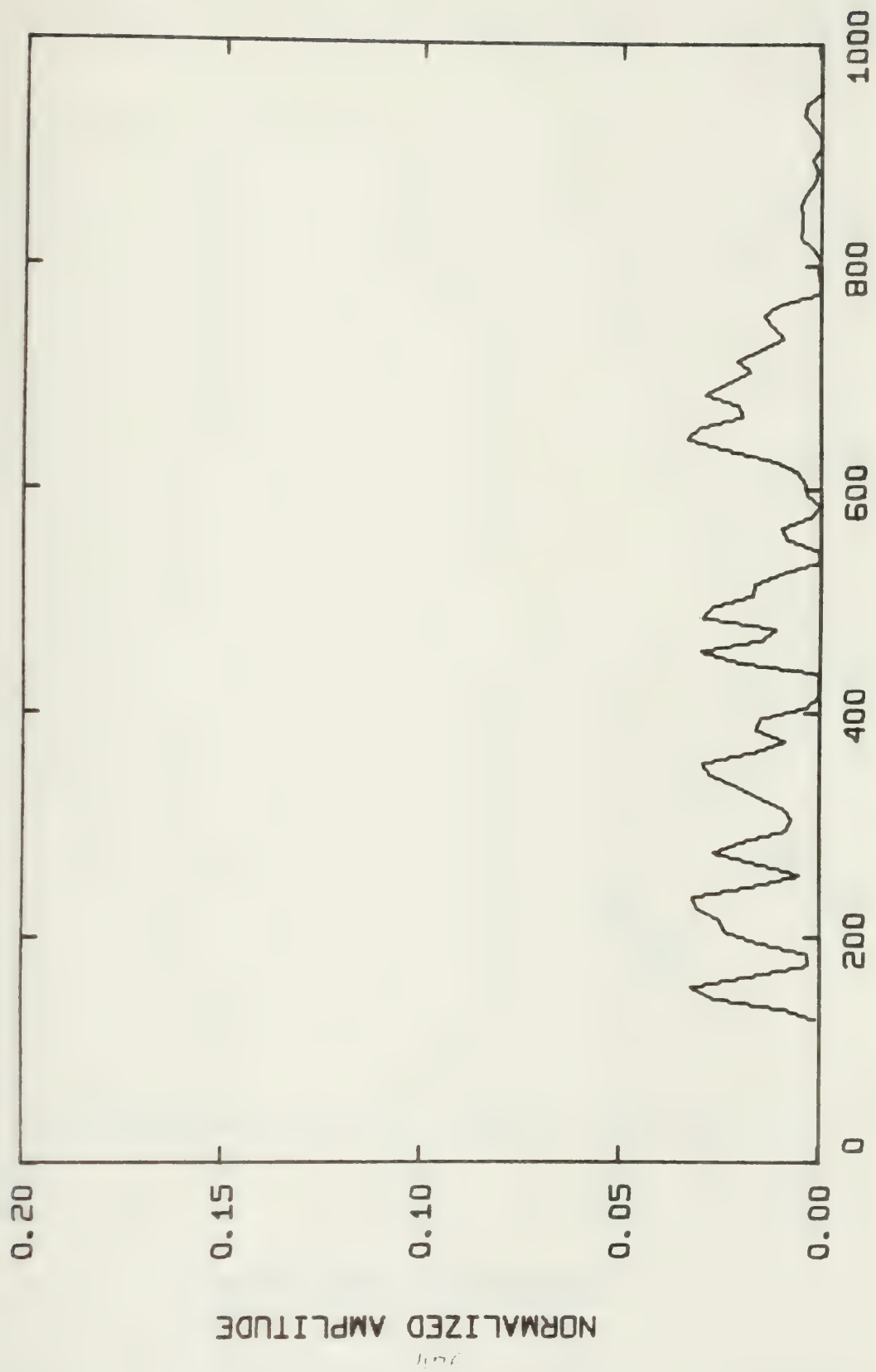
FREQ (KHZ) LVSCJ 0213APR77 LOAD 1.78 KN





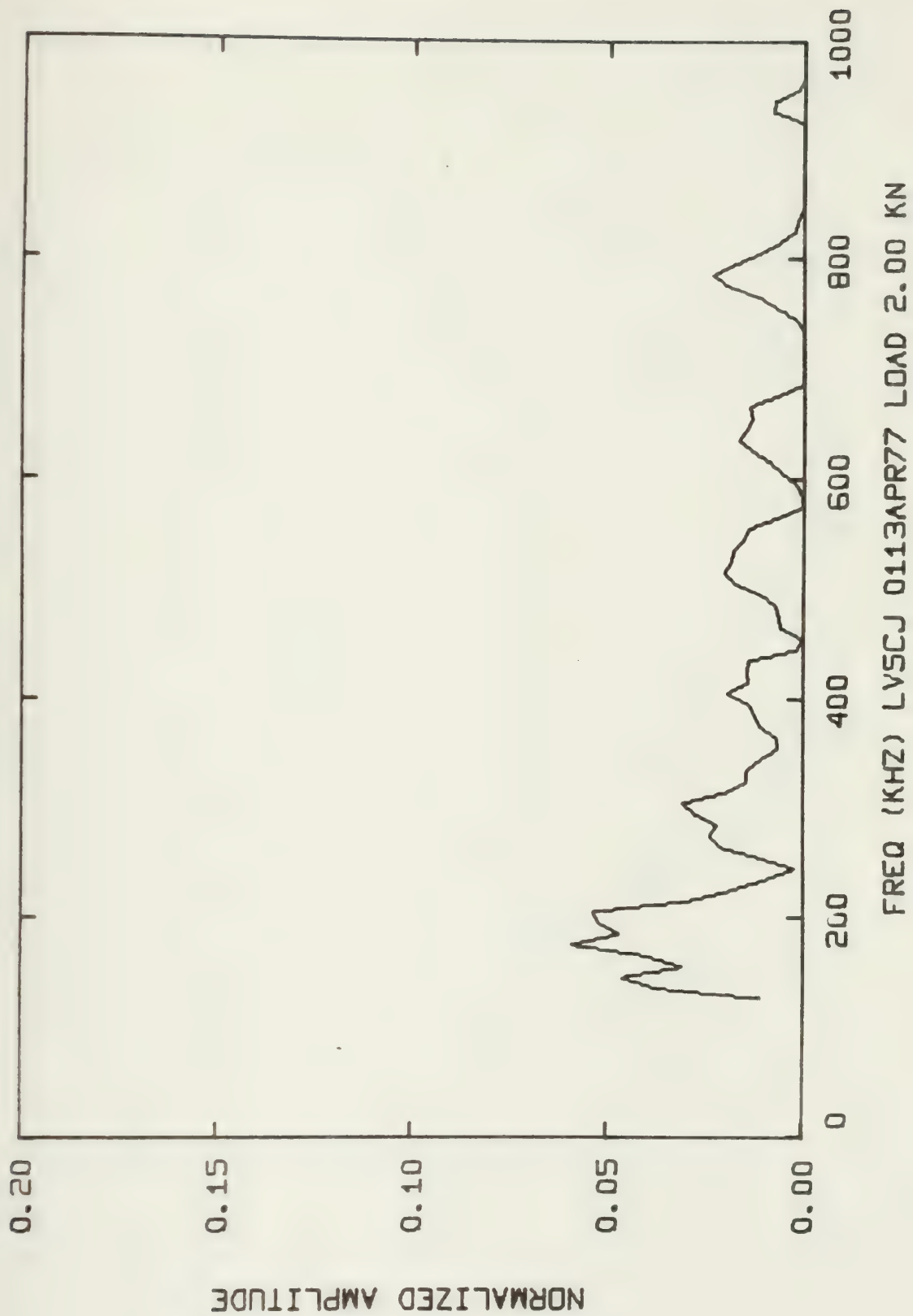




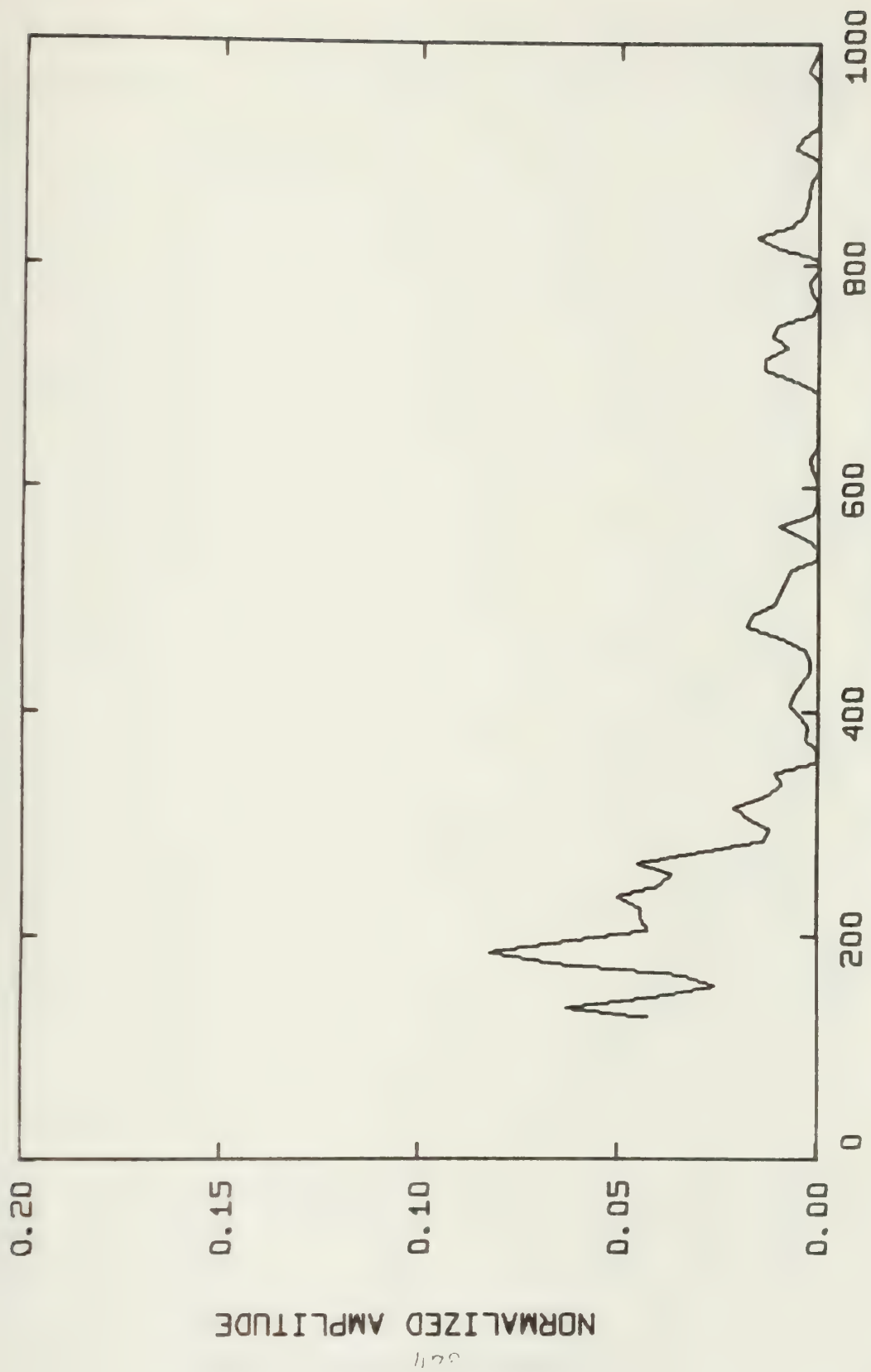


FREQ (KHZ) LVSCJ 0613APR77 LOAD 1.78 KN





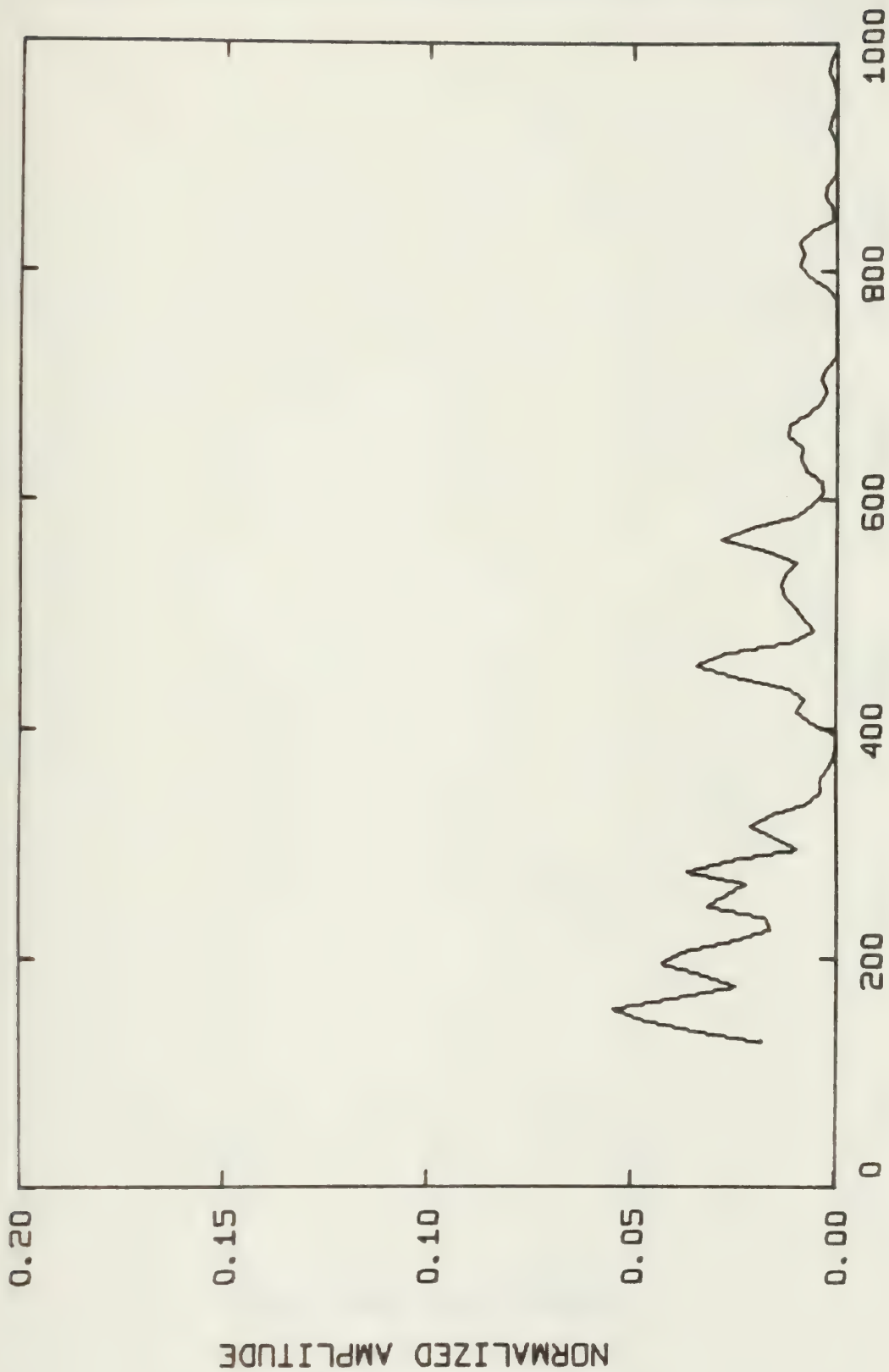




LV5CJ 1113APR77 LOAD 2.00 KN

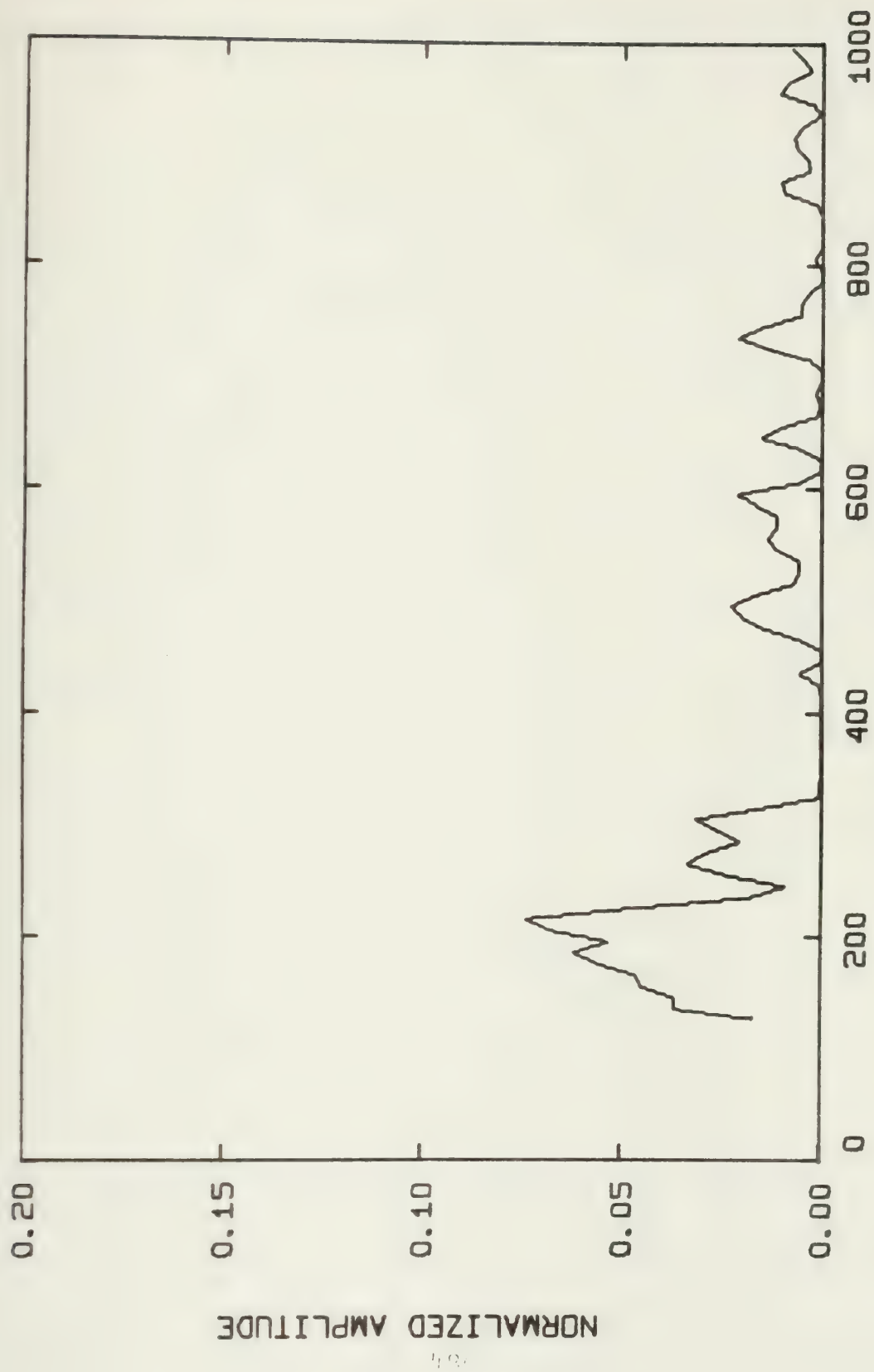






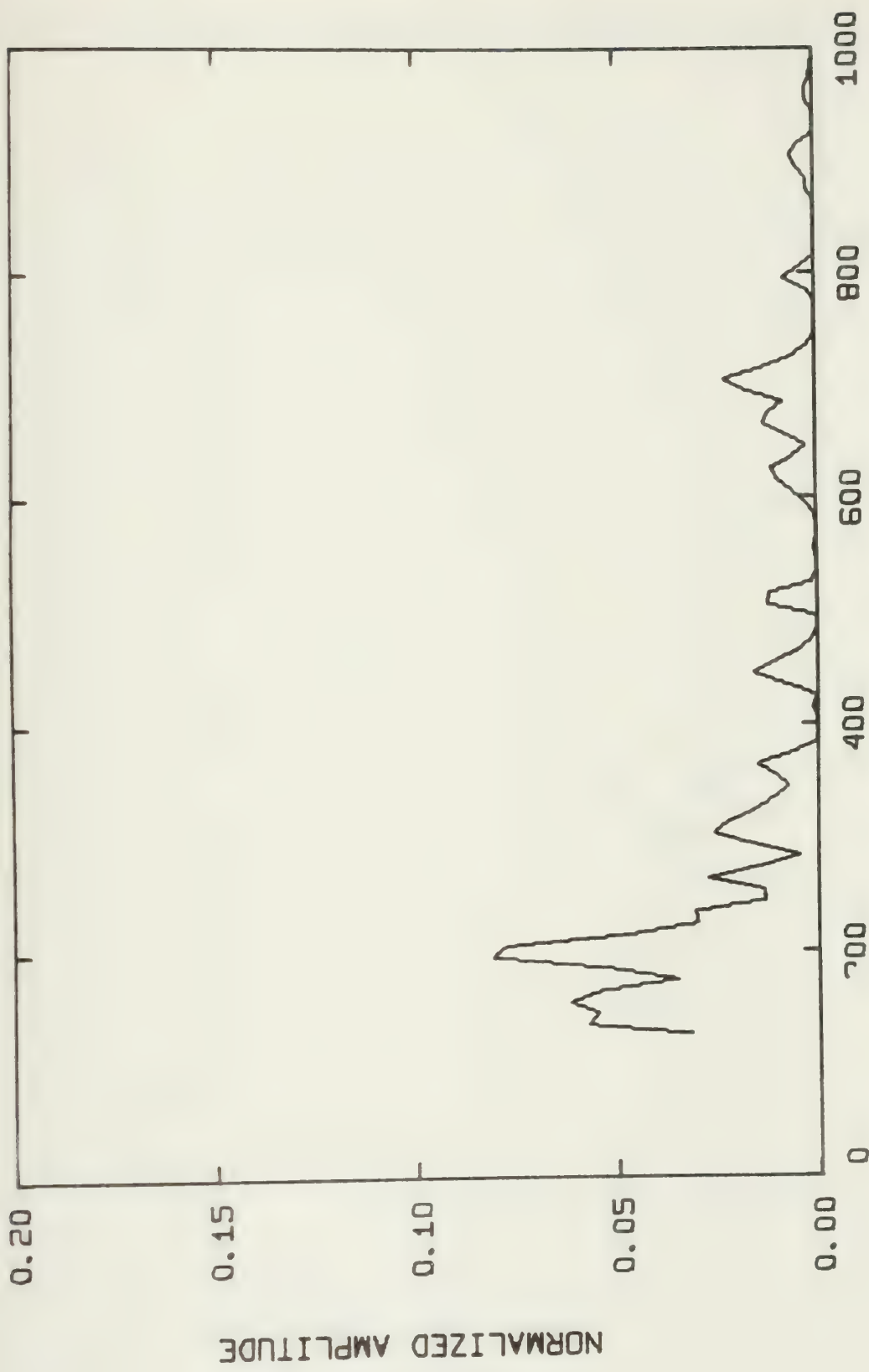
LV5CJ 1713APR77 LOAD 2.00 KN





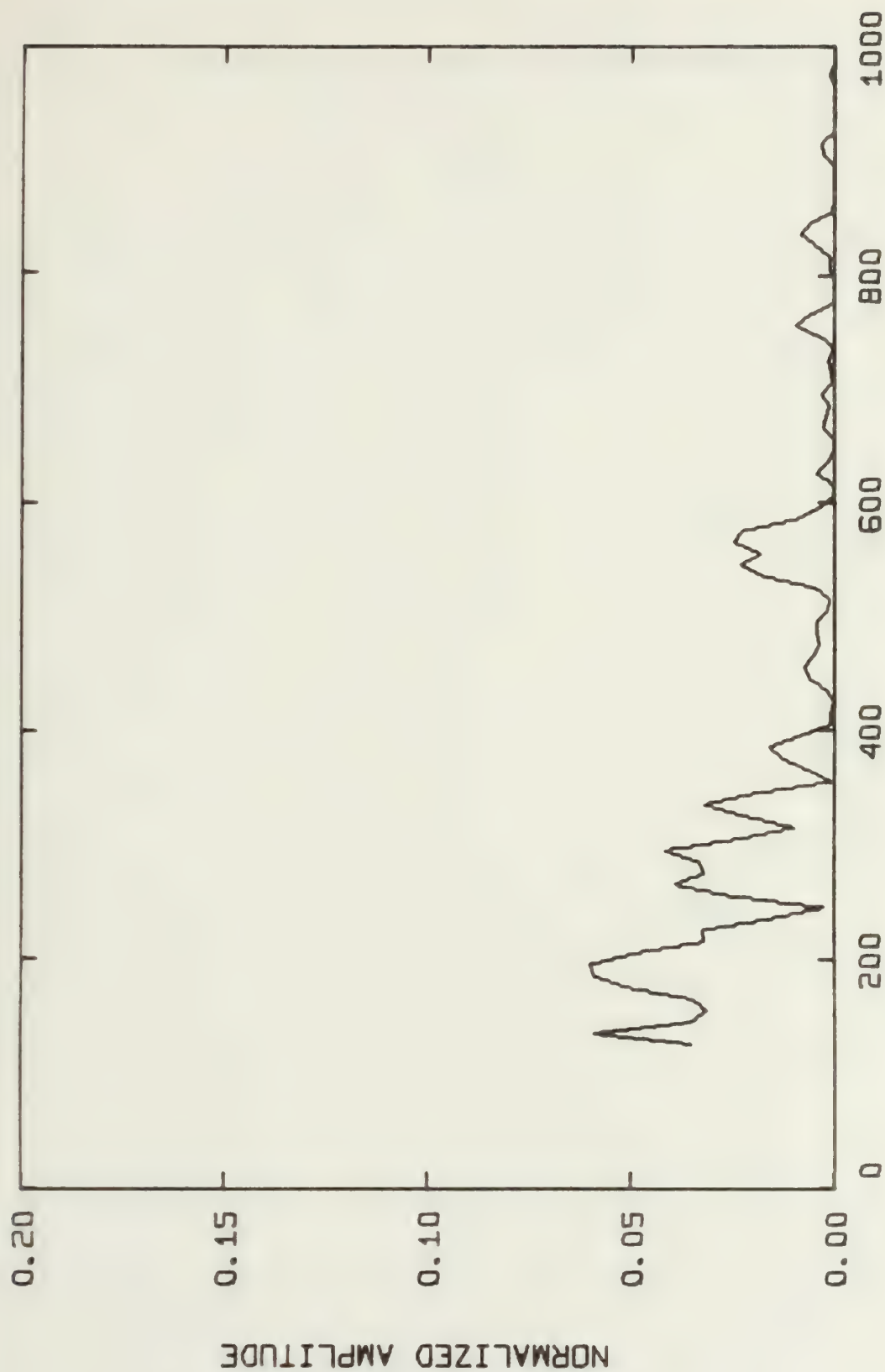
FREQ (KHZ) LVSCJ 0713APR77 LOAD 2.22 KN





FREQ (KHZ) LV5CJ 0813APR77 LOAD 2.22 KN

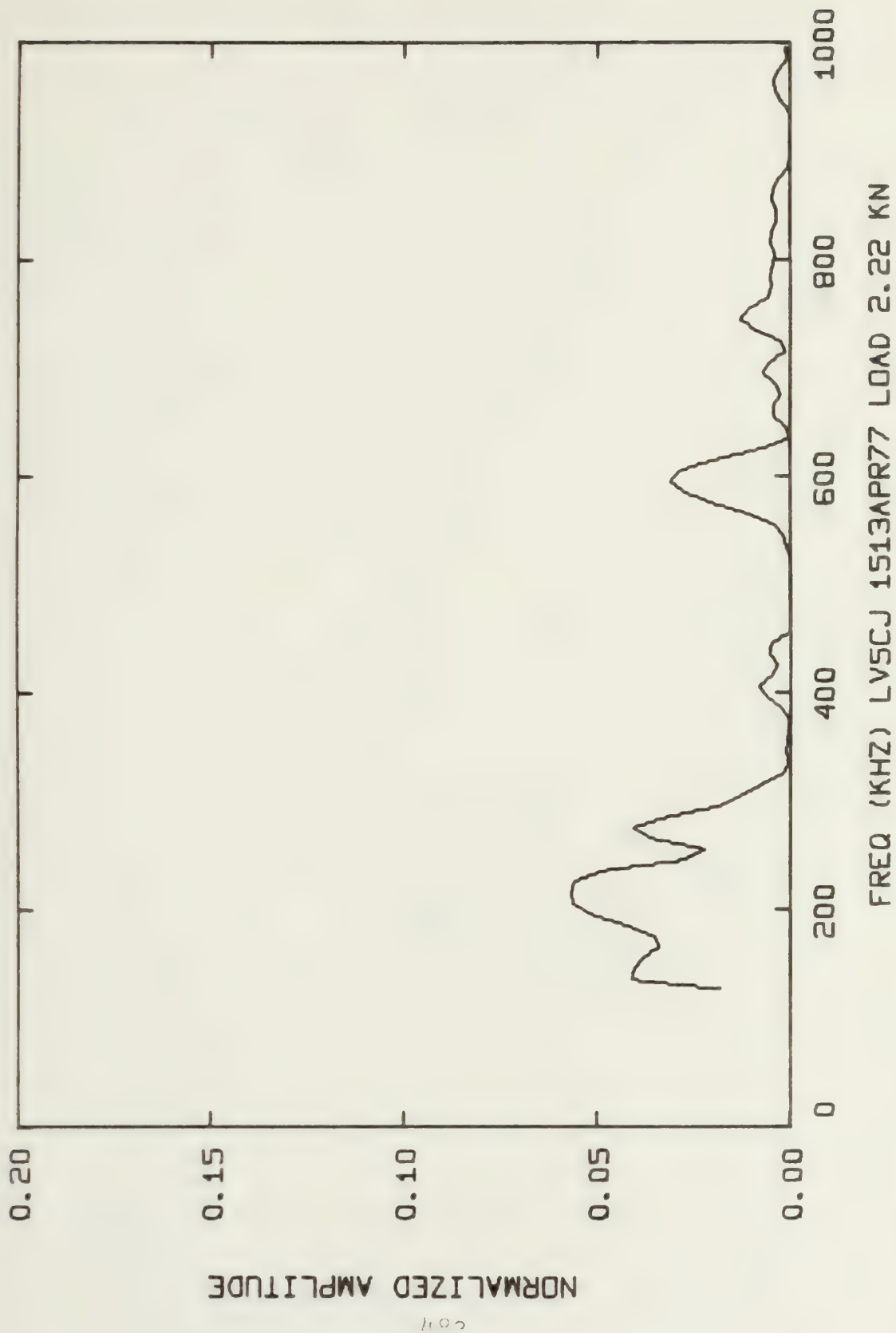




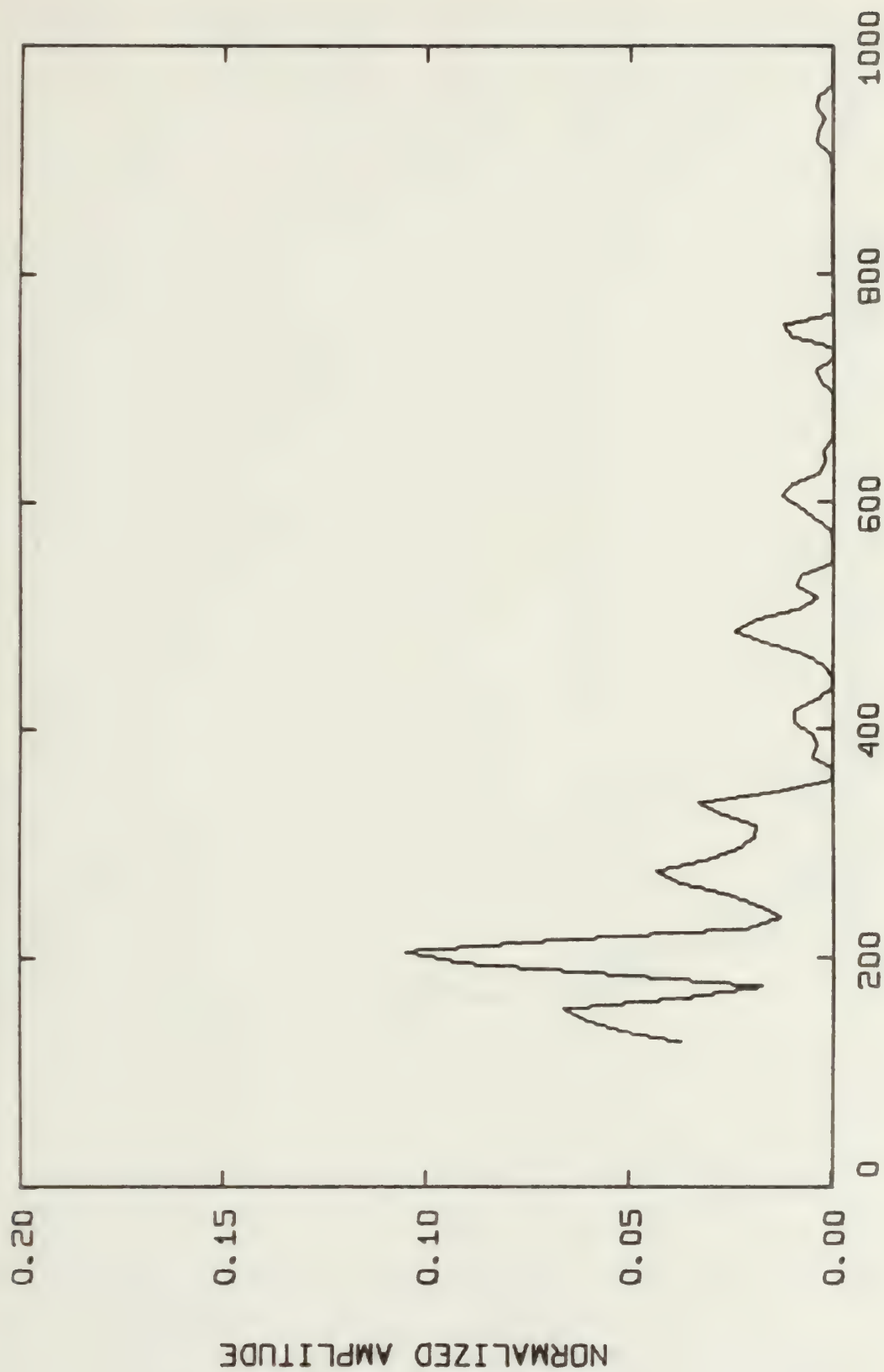
FREQ (KHZ) LVSCJ 0913APR77 LOAD 2.22 KN





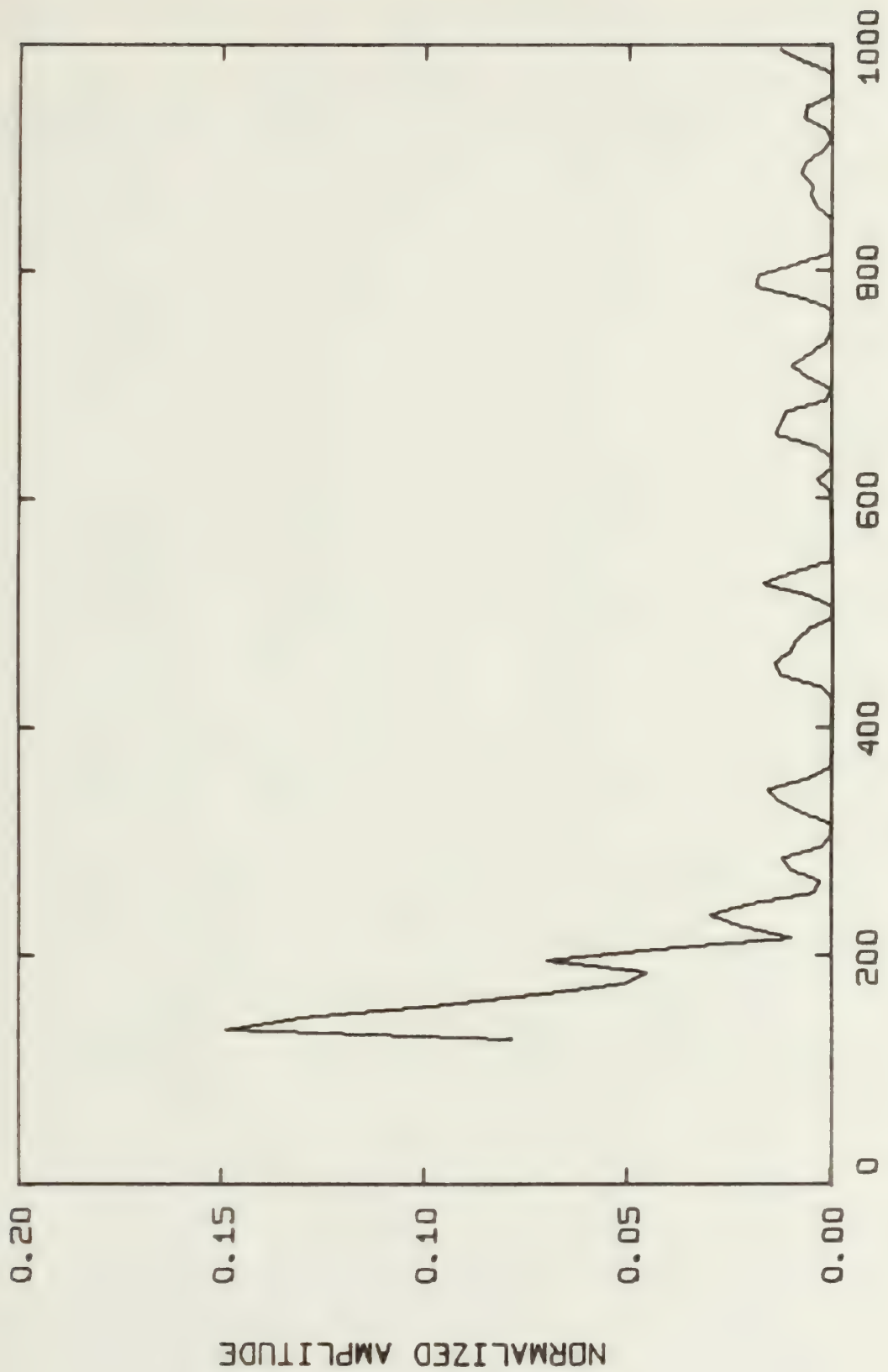






FREQ (KHZ) LVSCJ 1813APR77 LOAD 2.27 KN





FREQ (KHZ) LV5CJ 1613APR77 LOAD 2.27 KN



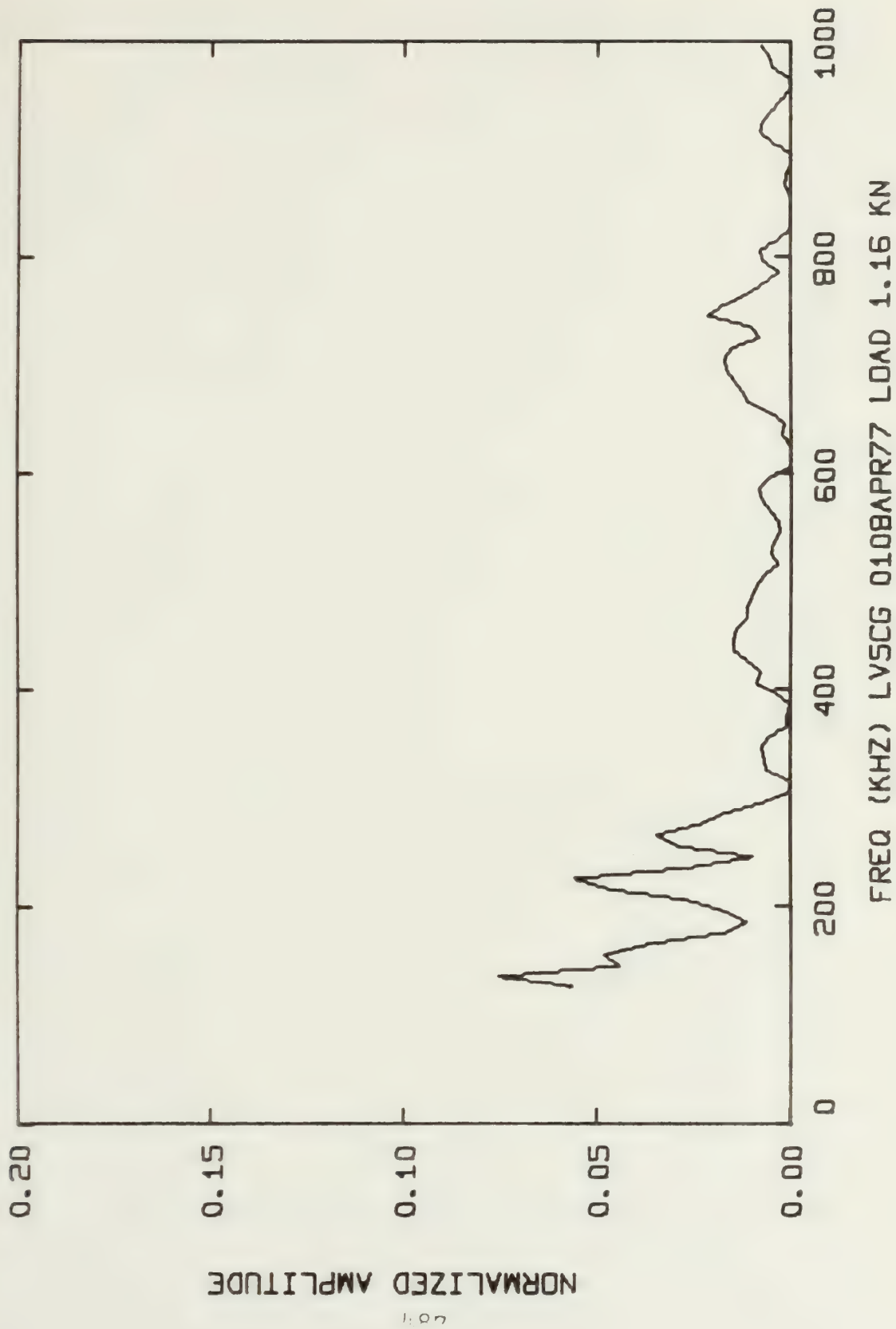
# Summary of Energy per AE and RMS Pressure for Ascending Loads

Spectral Distribution Graph Code Number	Energy per AE (Joules $\times 10^9$ )	RMS Pressure Across Face of Transducer (Pa $\times 10^6$ )	Load kN
IV50G			
0108APR77	22.254	669.6	1.16
0208APR77	191.85	853.3	2.22
0308APR77	243.55	961.5	2.22
0408APR77	1141.9	1612.6	2.36
0508APR77	4509.0	3204.4	2.36
0608APR77	10,406.0	3794.1	2.36
1008APR77	12,943.0	4488.0	2.38
0808APR77	27,689.0	4579.0	2.38
0708APR77	129,750.0	6163.7	2.38
0908APR77	153,020.0	6633.1	2.38

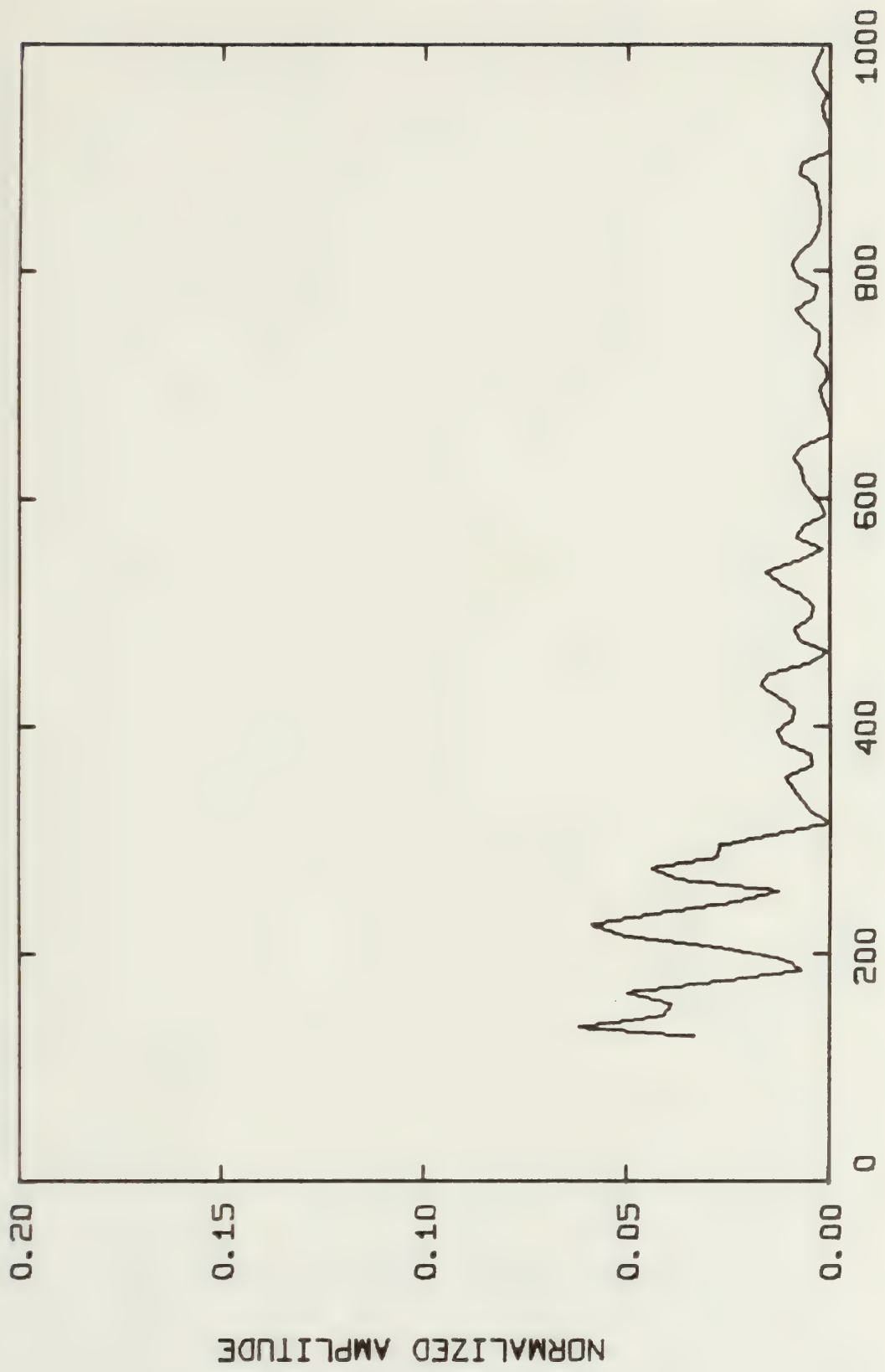
Note: Specimen IV50G was loaded to 2.42 kN during the third cycle of loading. AE spectra were sampled during the fourth (and final) cycle at loads substantially less than the specimen's maximum "historical" load.





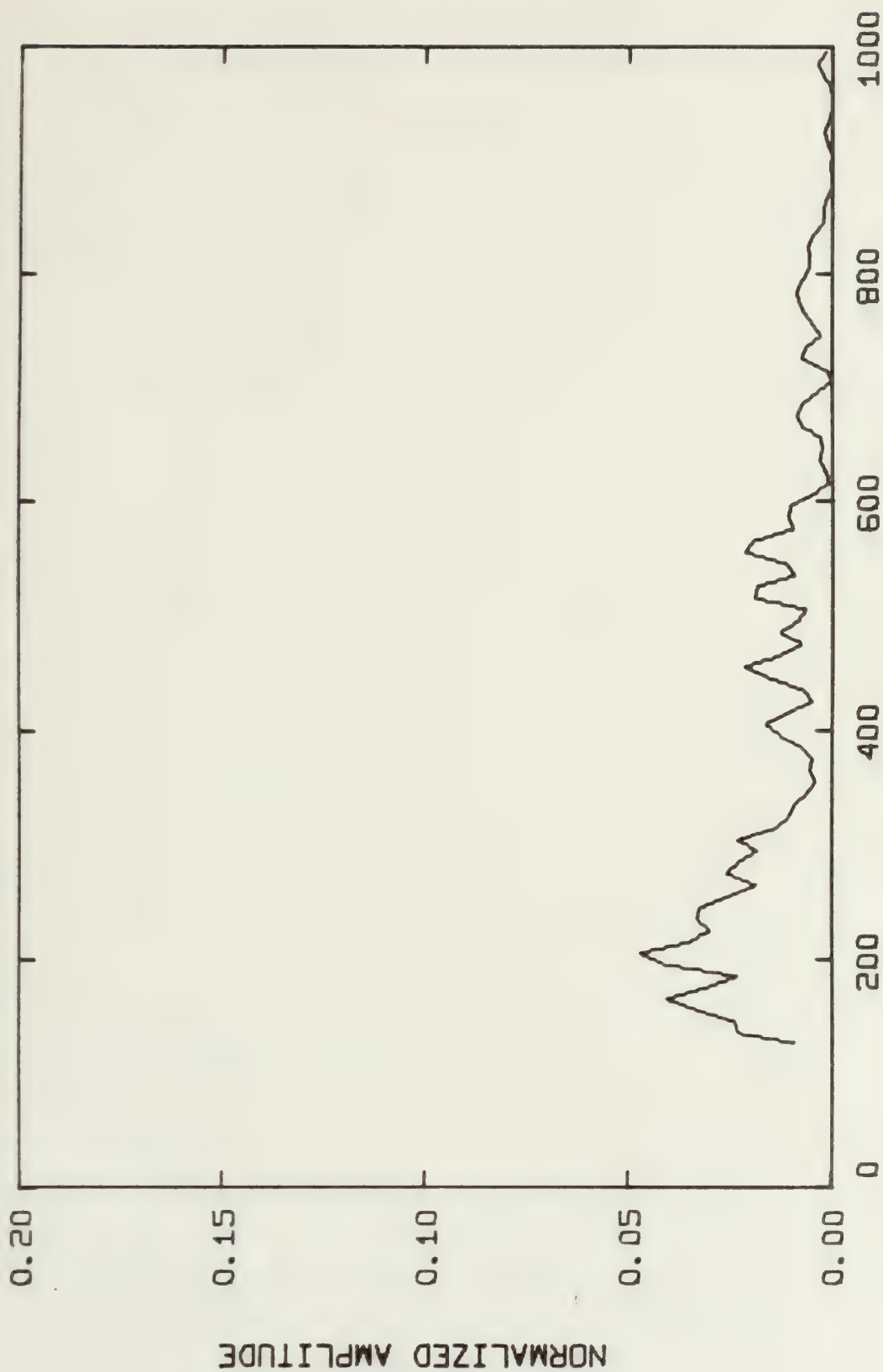






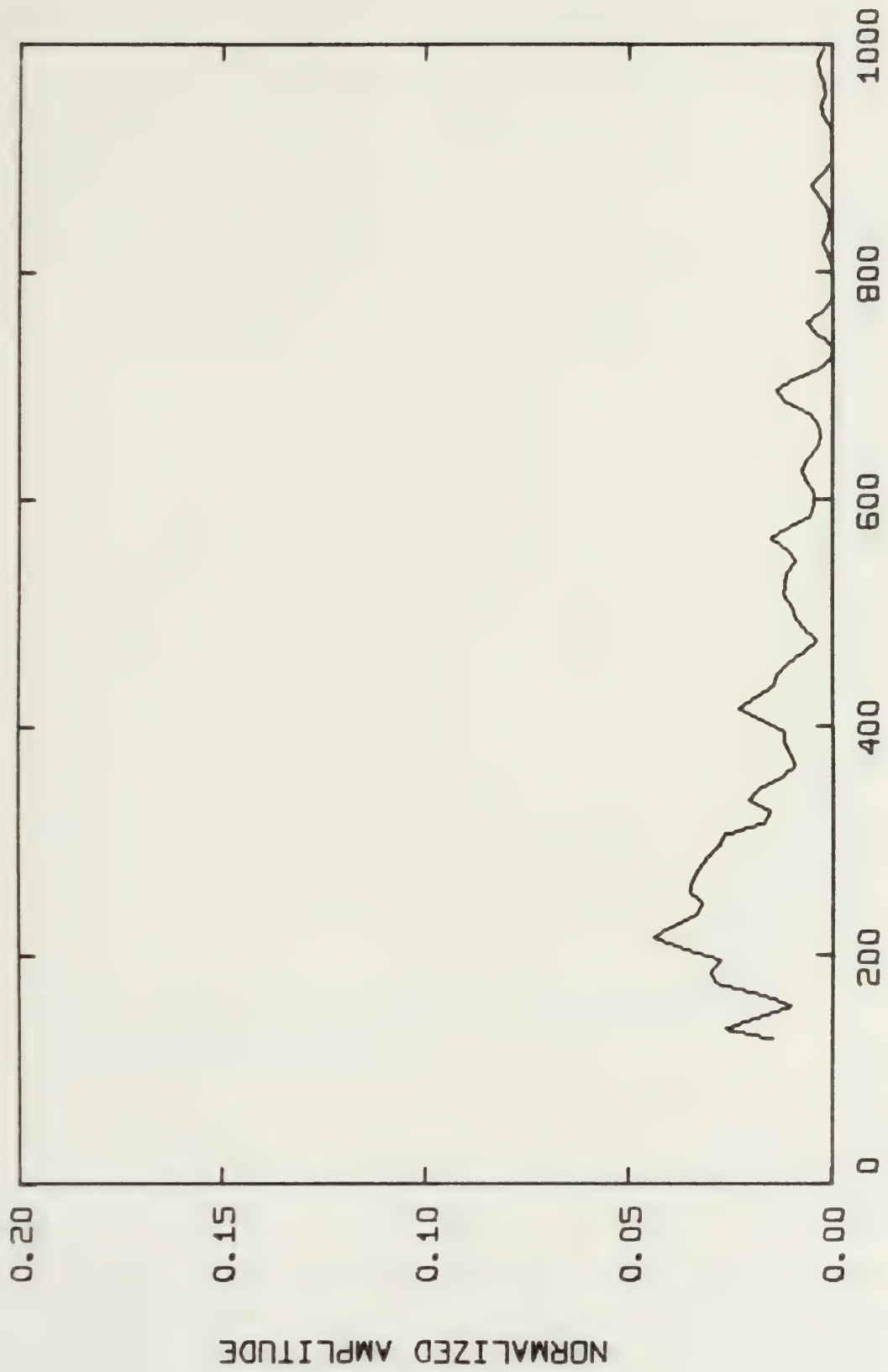
FREQ (KHZ) LV5CG 0208APR77 LOAD 2.22 KN





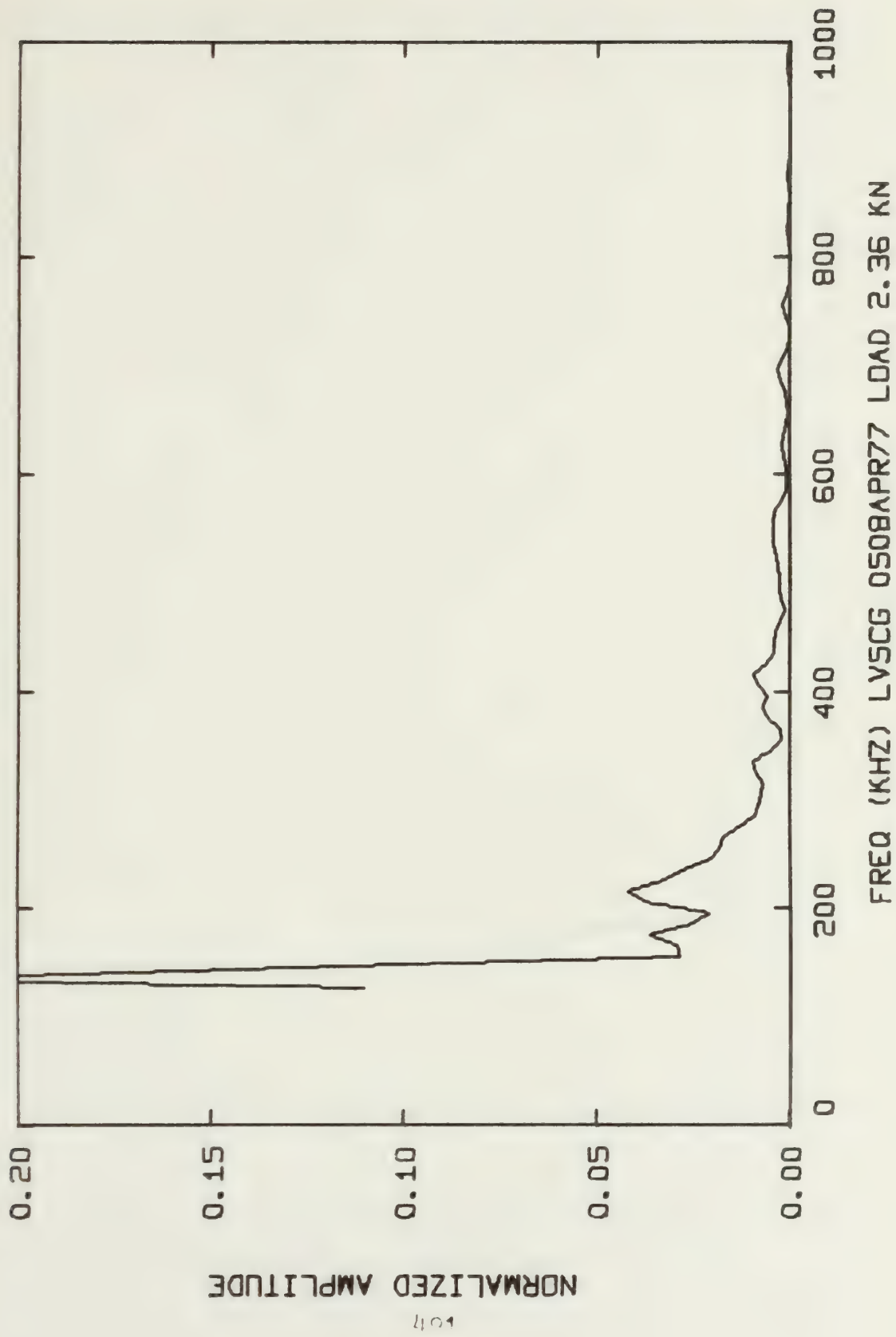
LVSCG 0308APR77 LOAD 2.22 KN



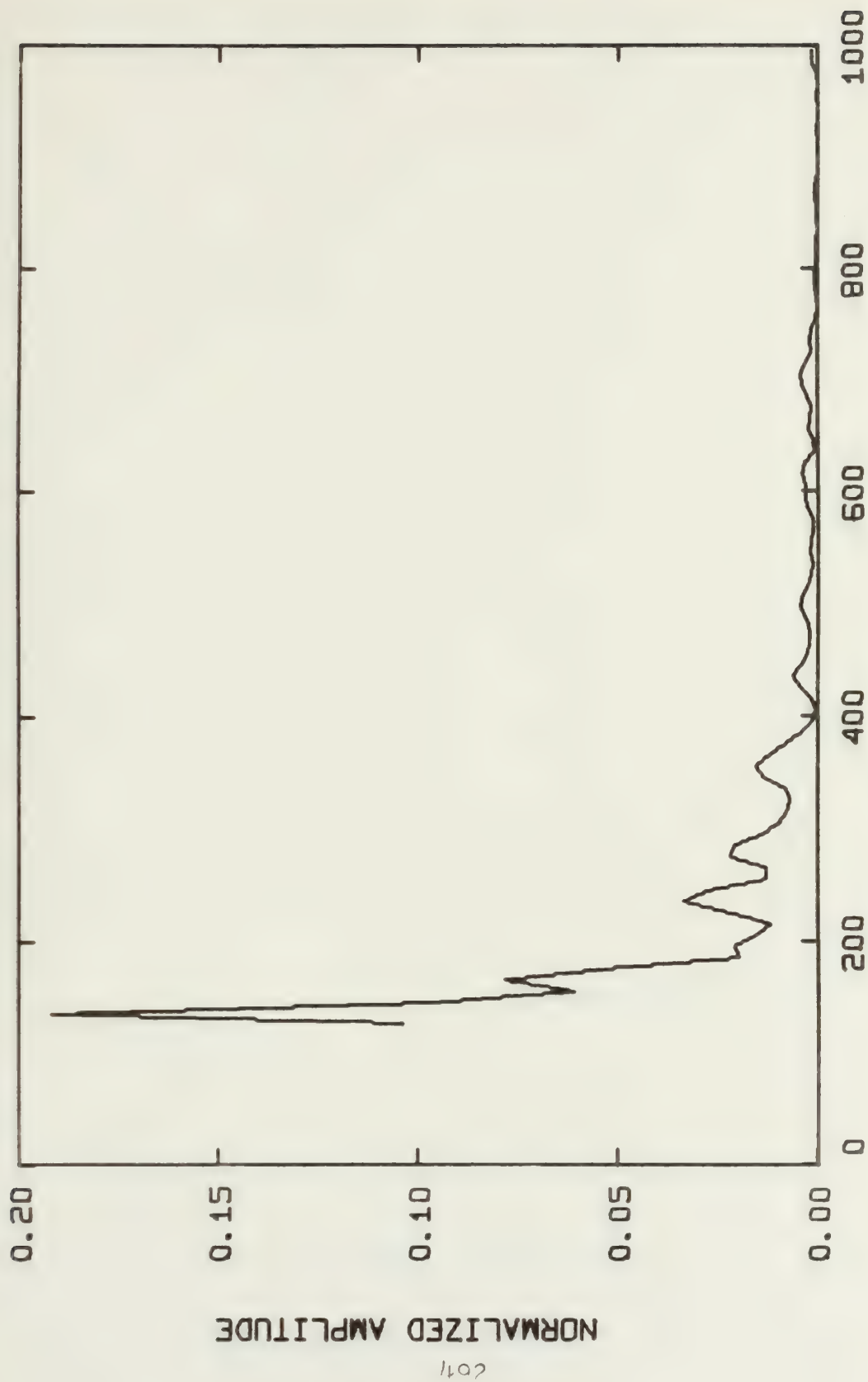






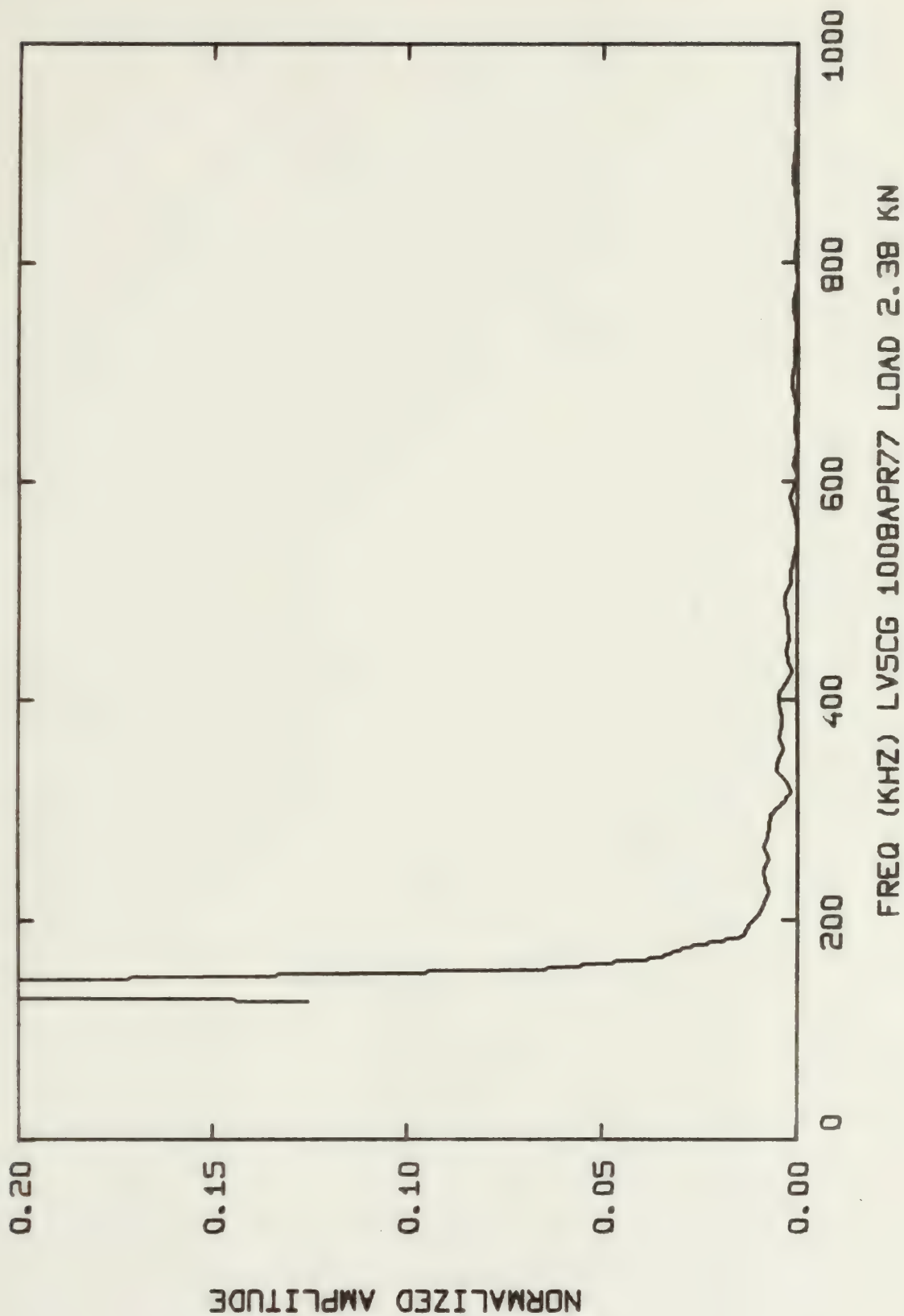




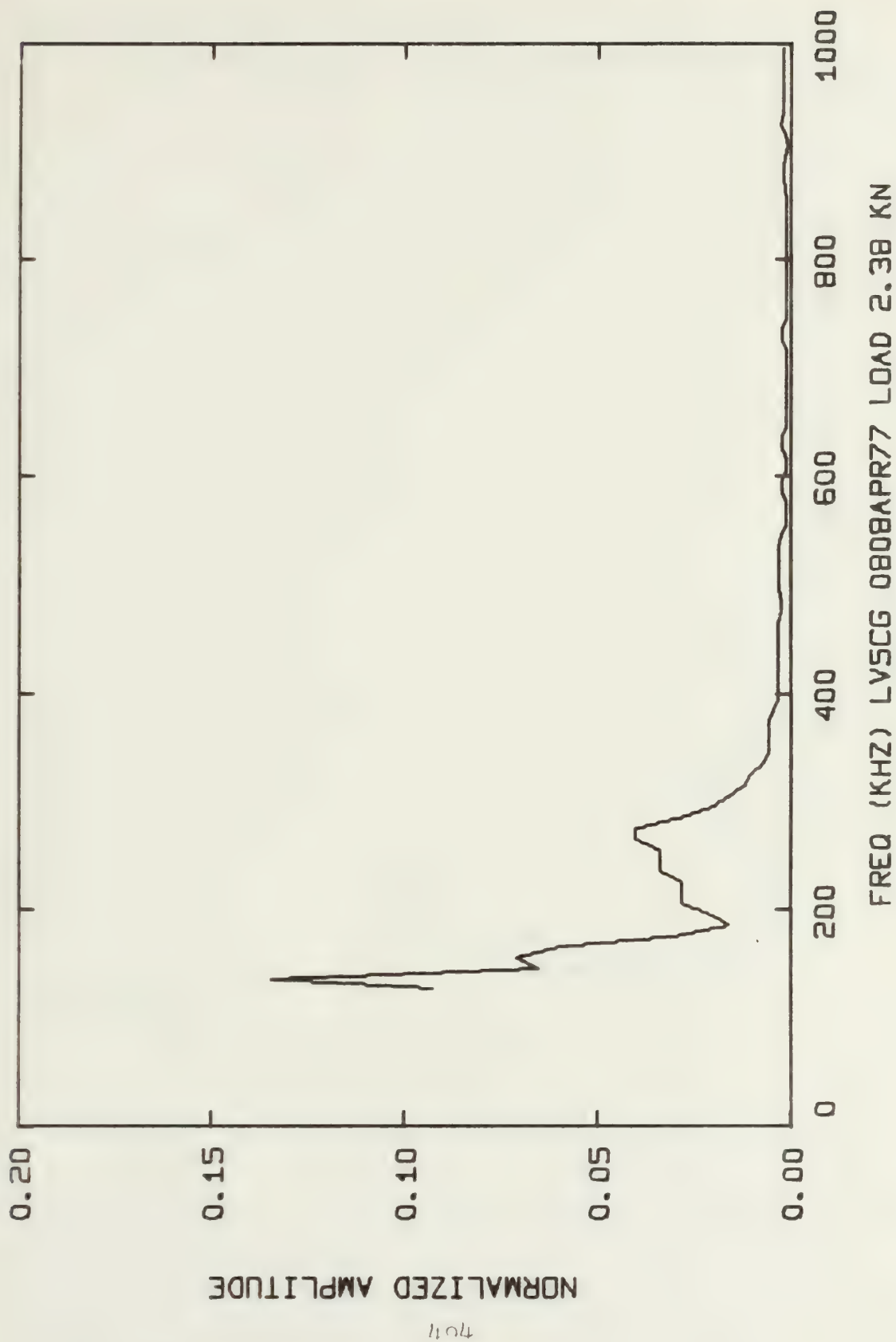


FREQ (KHZ) LVSCG 0608APR77 LOAD 2.36 KN



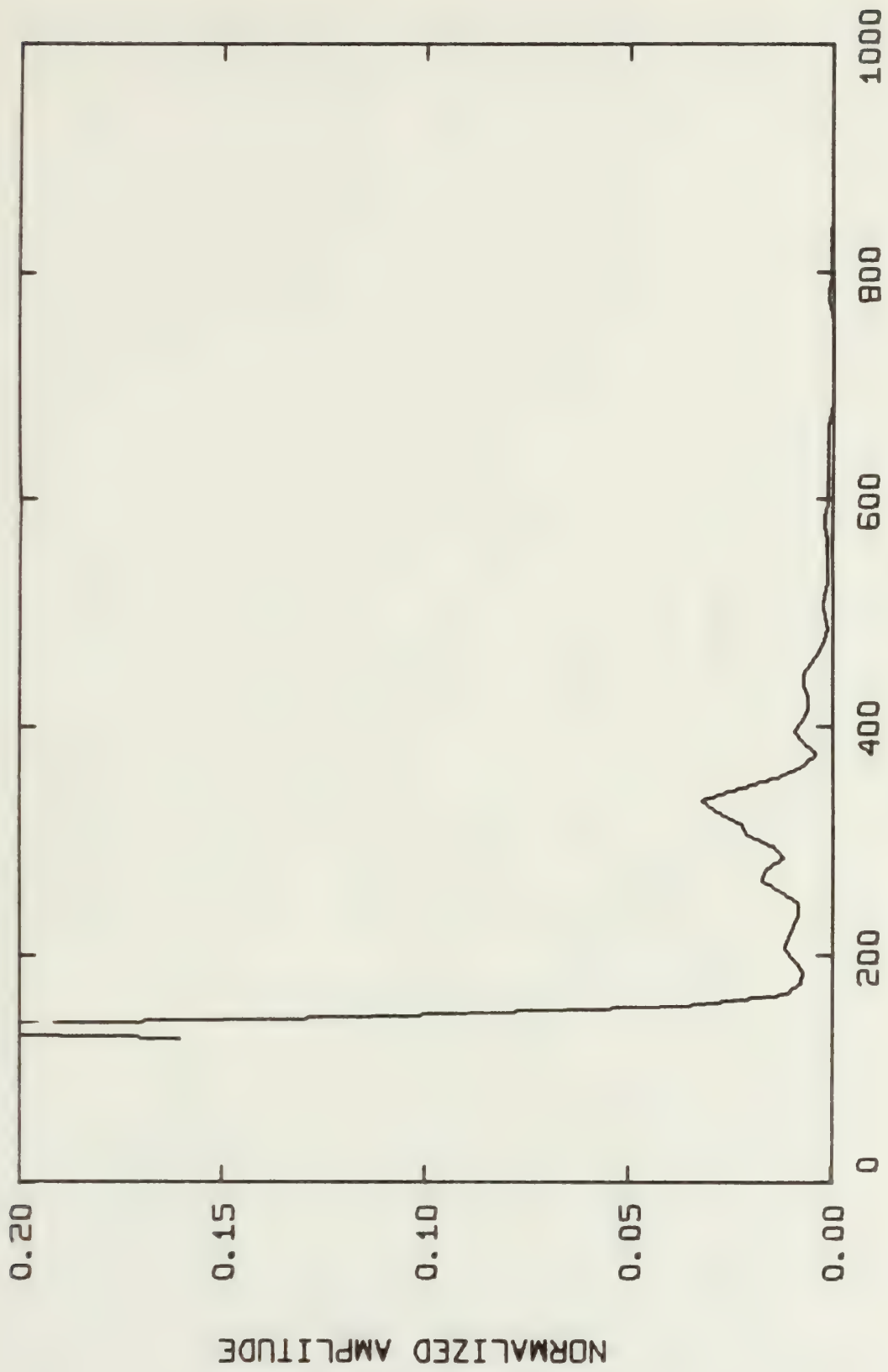






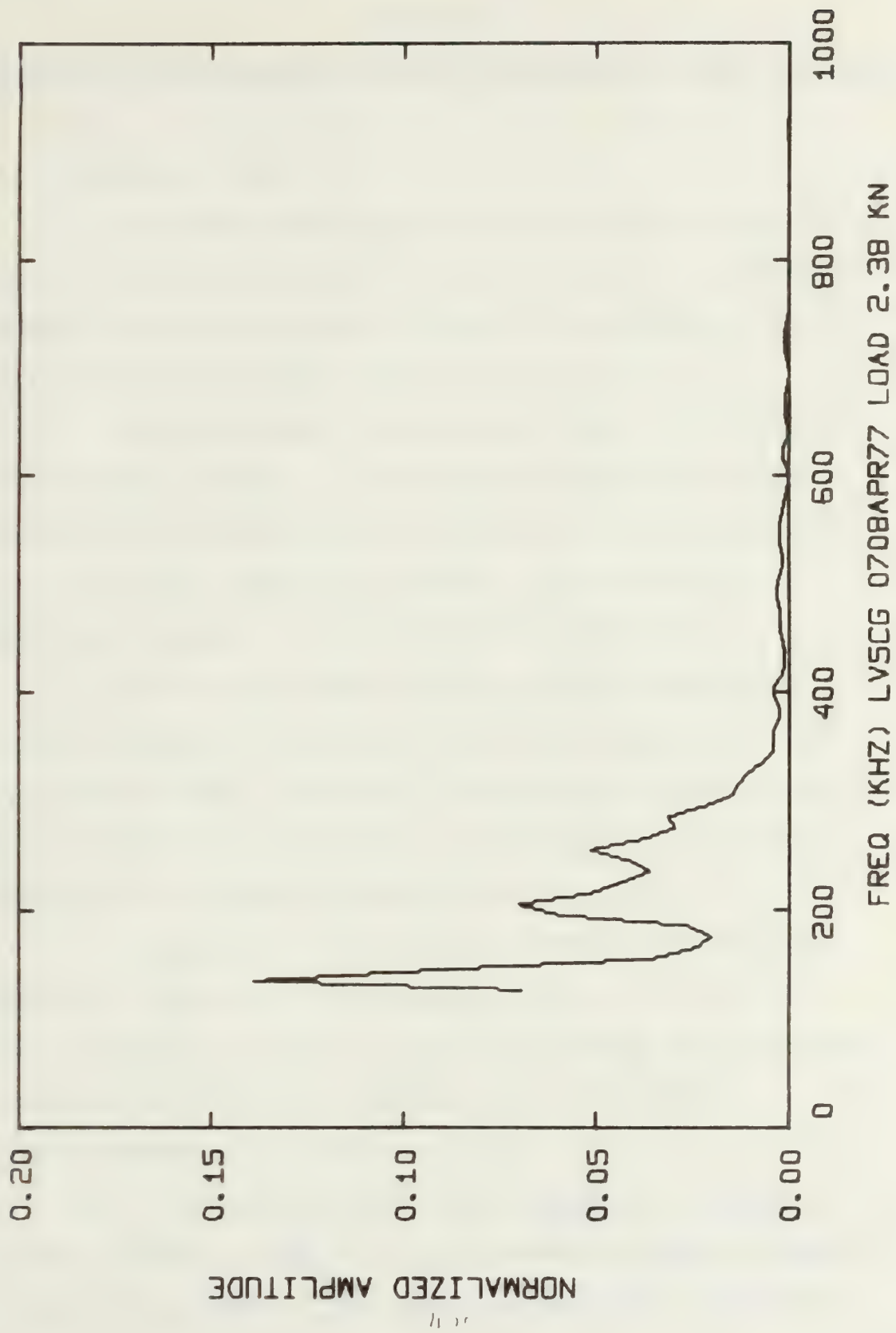






FREQ (KHZ) LVSCG 0908APR77 LOAD 2.38 KN







## Appendix F

### Notes on Operational Procedure for Tests and Data Analysis

#### A. During the Test

1. Insulate grips and loading pins with electrical tape. This is necessary to prevent spurious electrical signals generated by the Instron testing machine from saturating the acoustic emission equipment.

2. Make sure that the grips are tightly bolted onto the specimen endtabs. Securing the upper grip before placing the specimen in the test machine and securing the lower grip after the specimen has been placed in the test machine is the recommended procedure.

3. Remove the cotter pin in the test machine's upper fixture to allow for freedom of rotation in the horizontal plane. This will reduce any cross coupling torque which might otherwise be introduced in off-axis multi-ply specimens during the tensile test.

4. Electrically ground the specimen to the common ground of the acoustic emission system. This may be done with wire or aluminum foil connecting the specimen's grips to the AE system ground. This will reduce electromagnetic interference (EMI).

5. To further prevent EMI, shield all transducer leads and the preamplifier with several layers of heavy duty aluminum foil. This shield should be connected to



the transducer case.

6. Some trials and tribulation are necessary before locating the optimum path for the cable from the preamplifier to the amplifier. Proper positioning of the cable in the testing room will reduce EMI.

7. Take the AE output from the model 201 signal processor to the spectral analyzer. Spectral analyzer settings should be -20 dB reference and -20 dBm optimum input. Spectral analyzer should be run at 200 kHz per division in the auto-sweep mode. Video filter should be on full and the analyzer's oscilloscope should be in the linear presentation mode. If EMI is a problem, the oscilloscope will exhibit spikes superposed onto an otherwise flat spectrum. Review steps (4-6) if this is the case. Check electrical continuity between the specimen and the Instron testing machine with an ohmmeter. The meter should indicate an infinite resistance between them. If it doesn't, remove the specimen from the test fixture and adjust the electrical tape insulation as necessary.

8. The transducer can be attached after the specimen is secured in the test fixture. Two size 12 rubber bands with viscous resin (SC-6) couplant work quite well with 12.7 mm. wide specimens. Balancing the transducer with a dummy transducer on the opposite side of the specimen will minimize any bending moments induced by the weight of the





transducer. (This is particularly important with the 90° specimens) However, both transducers must share a common ground, even though the dummy transducer is not energized, if EMI is to be effectively eliminated.

9. Make sure that none of the aluminum foil shielding touches the Instron test machine.

10. Prepare the video tape recorder prior to testing by carefully cleaning the helical scan heads. Use the procedure in the operator's manual.

11. Make sure that the tape recorder is on line synchronization.

12. Follow the tape recorder operator's instructions to insure that all controls are set to their proper positions.

13. If it is desired to measure AE-RMS on the X-Y recorder, calibrate the RMS background noise floor and establish that value as a zero baseline. Increase the sensitivity of the X-Y recorder and run the zero control down so that accurate RMS measurements may be made above the noise floor.

14. Proper selection of scales on the time axis and Y axis of the X-Y recorder will greatly reduce later required data analysis effort.

15. Make sure that all leads to the X-Y recorder are securely connected. Loose leads will result in severe EMI problems.



## B. Data Analysis

1. Clean the tape recorder's heads carefully before any playback of data. Use the operator's manual as necessary to gain facility with the use of slow action/stop action and audio controls.

2. The tape recorder output is taken to the synchronized gate box via a shielded cable. Take the "normal trigger" from the gate box to the external trigger input of an oscilloscope. Run the oscilloscope in the external trigger mode. Take the AE output from the gate box to the oscilloscope's Y axis input. Adept use of the gate, X axis multiplier, and horizontal position controls is essential for rapid data review. The gate should generally be operated in the "a+b heads" mode. Use of the high or low width control settings on the gate box are dependent upon the duration of the signal. Verniers for gate width and position may be adjusted to accept only the data of interest.

3. The reels on the tape recorder may be manually positioned while the tape recorder is in the stop action mode. Sweep time settings on the oscilloscope should be adjusted so that one sweep corresponds to one frame from the video tape recorder. The edges of the frame can be easily located due to the presence of high spurious noise in their immediate vicinity. Position these off the edges of the oscilloscope by adjusting both the reels and the





oscilloscope's sweep rate control.

4. After an AE event of interest is located and gated, the spectral analysis procedure may commence.

5. Connections between the spectral analyzer and the X-Y recorder are available on the back of the analyzer. Use the vertical output for the Y axis and horizontal output for the X axis inputs to the X-Y recorder. Switch the X-Y recorder servo to on. Adjust the horizontal calibration control on the X-Y recorder so that one sweep of the analyzer's oscilloscope corresponds to ten horizontal chart divisions on the X-Y recorder. Then complete the operator's check and calibration procedure, as listed in the operator's manual, while the X-Y recorder is in the stand-by mode.

6. Connect "cal" output to 50 ohm input.

7. Set "optimum input" to 0 dBm and oscilloscope presentation to linear.

8. Set "reference level" and "reference level fine" to zero.

9. Set "freq span/div" to "F" and "time/div" to manual. Turn the video filter control fully clockwise.

10. With manual control, set the peak of the calibration signal at 7.08 on X-Y recorder chart, taking care to adjust the X-Y recorder's zero level.

11. Iterate between "zero" and "cal" controls on X-Y recorder until the calibration signal produces 7.08



divisions of deflection on the Y axis of the chart.

Calibration is now complete.

12. Pen "up". Adjust X-Y recorder "zero" control so the pen is positioned on the horizontal baseline of the chart. Position the spectral analyzer's sweep manually so that it is near (but not on) the calibration signal's spike on the oscilloscope. Switch X-Y recorder from "standby" to "on". Adjust the recorder's X axis "zero" control so that the pen is aligned slightly to the left of the intended vertical axis on the chart.

13. Pen "down". Manually run the sweep through the 250 MHz calibration signal's spike on the oscilloscope. The pen should follow and trace the spike to the left of the chart's intended vertical axis as a calibration mark. Pen "up", servo on "standby".

14. Change "freq span/div" to 100 kHz, "time/div" to one second and "resolution" to the lower of the 10 kHz settings (arrows together). This will give an oscilloscope presentation from 0 to 1 MHz. Remove "cal" input from spectral analyzer.

15. Now turn horizontal axis "zero" control on X-Y recorder at least two full turns clockwise. Adjust "freq zero" on the spectral analyzer, using procedures given in the operator's manual. Analyzer's sweep mode should be reset to "single sweep".





16. Turn X-Y recorder servo to "on", and, after the sweep is completed, adjust the horizontal zero of the recorder so that the pen is approximately located over the vertical axis on the chart. Press the "zero check" button on the vertical controls of the X-Y recorder. Adjust the vertical zero control while the vertical "zero check" button is depressed so that the pen is centered over the horizontal axis. Make sure, while the vertical "zero check" button is still depressed, that the pen is centered over the vertical axis. Pen down (on the chart's origin). Remove finger from vertical "zero check" button. The pen will draw the vertical axis. Repeat several times - depress vertical "check zero" and release - to darken the vertical axis as desired. Again depress the vertical axis "zero check" button and hold it down. Pen down. Flick "single sweep trigger" on the spectral analyzer. The pen will draw the horizontal axis. Check the horizontal axis length and insure that it is ten major divisions long. Lift pen.

17. Release vertical axis "zero check" button. The pen will move to the top of the vertical axis. With no input to the spectral analyzer, trigger "single sweep" and manipulate the vertical zero control so that the sweep's asymptotic zero is on the chart's baseline horizontal axis. The system should now be both calibrated and zeroed.



18. Put the X-Y recorder servo in "standby". Now zero the frequency on the spectral analyzer using the procedure as indicated in the operator's manual. Switch analyzer's sweep mode back to "single sweep" when the frequency has been properly zeroed on the spectral analyzer.

19. Find an AE event on the video tape using the procedures discussed previously. Initiate a "dry run"; with pen up and gated AE signal connected to the spectral analyzer's "50 ohm input". Set the X-Y recorder's servo on, analyzer sweep rate to "10 sec/div" and trigger the "single sweep." Adjust the gain on the reference level of the spectral analyzer until the desired Y axis excursion of the X-Y recorder is obtained. To compute the Y axis calibration, divide all Y axis values on the chart (originally  $1\text{mV}_{\text{RMS}}/\text{div}$ ) by the "ref dB" gain setting. (for instance, an analyzer "-20dB ref" setting means that the Y axis on the chart is calibrated at 1 mv/10 per division or, more properly, 100 microvolts (RMS) per division per unit frequency.)

20. Re-zero the frequency on the spectral analyzer using standard procedures. Re-zero the chart's asymptotic zero (with no input to the spectral analyzer) several times. Set the sweep control at 10 sec/div; set the sweep mode in "single sweep," video filter on fully clockwise; input the gated signal; switch the servo of the X-Y recorder to on;



pen down; trigger the single sweep, and be sure to flip the pen up just before the sweep is completed.





Thesis  
E263  
v.2

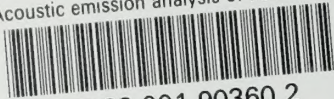
Egan

Acoustic emission  
analysis of fiber  
composite failure  
mechanisms.

171167



thesE263v.2  
Acoustic emission analysis of fiber comp



3 2768 001 90360 2  
DUDLEY KNOX LIBRARY